frontiers | Research Topics

Autophagy modulation in cancer treatment utilizing nanomaterials and nanocarriers

Edited by
Marco Cordani, Maria Condello, Stefania Meschini and Raffaele Strippoli

Published in
Frontiers in Oncology
Frontiers in Pharmacology

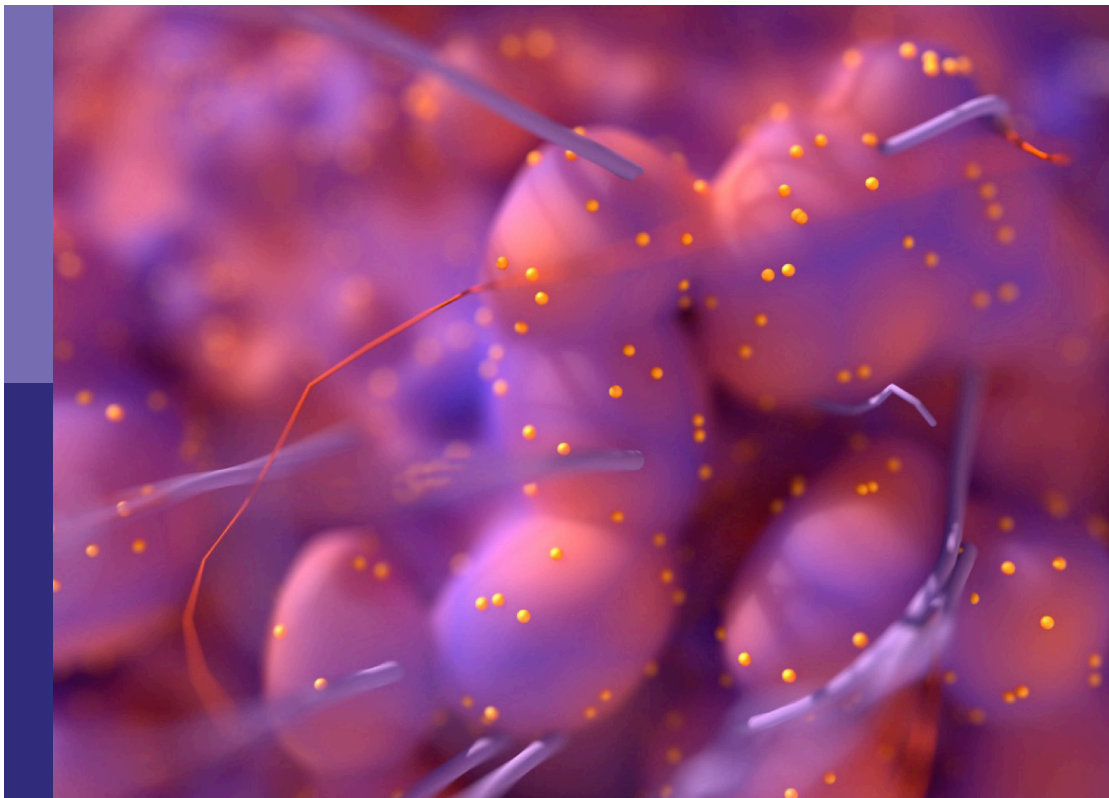

ISSN 1664-8714
ISBN 978-2-8325-2762-7
DOI 10.3389/978-2-8325-2762-7

About Frontiers

Frontiers is more than just an open access publisher of scholarly articles: it is a pioneering approach to the world of academia, radically improving the way scholarly research is managed. The grand vision of Frontiers is a world where all people have an equal opportunity to seek, share and generate knowledge. Frontiers provides immediate and permanent online open access to all its publications, but this alone is not enough to realize our grand goals.

Frontiers journal series

The Frontiers journal series is a multi-tier and interdisciplinary set of open-access, online journals, promising a paradigm shift from the current review, selection and dissemination processes in academic publishing. All Frontiers journals are driven by researchers for researchers; therefore, they constitute a service to the scholarly community. At the same time, the *Frontiers journal series* operates on a revolutionary invention, the tiered publishing system, initially addressing specific communities of scholars, and gradually climbing up to broader public understanding, thus serving the interests of the lay society, too.

Dedication to quality

Each Frontiers article is a landmark of the highest quality, thanks to genuinely collaborative interactions between authors and review editors, who include some of the world's best academicians. Research must be certified by peers before entering a stream of knowledge that may eventually reach the public - and shape society; therefore, Frontiers only applies the most rigorous and unbiased reviews. Frontiers revolutionizes research publishing by freely delivering the most outstanding research, evaluated with no bias from both the academic and social point of view. By applying the most advanced information technologies, Frontiers is catapulting scholarly publishing into a new generation.

What are Frontiers Research Topics?

Frontiers Research Topics are very popular trademarks of the *Frontiers journals series*: they are collections of at least ten articles, all centered on a particular subject. With their unique mix of varied contributions from Original Research to Review Articles, Frontiers Research Topics unify the most influential researchers, the latest key findings and historical advances in a hot research area.

Find out more on how to host your own Frontiers Research Topic or contribute to one as an author by contacting the Frontiers editorial office: frontiersin.org/about/contact

Autophagy Modulation in Cancer Treatment Utilizing Nanomaterials and Nanocarriers

Topic editors

Marco Cordani — Complutense University of Madrid, Spain
Maria Condello — National Institute of Health (ISS), Italy
Stefania Meschini — National Institute of Health (ISS), Italy
Raffaele Strippoli — Sapienza University of Rome, Italy

Citation

Cordani, M., Condello, M., Meschini, S., Strippoli, R., eds. (2023). *Autophagy modulation in cancer treatment utilizing nanomaterials and nanocarriers*. Lausanne: Frontiers Media SA. doi: 10.3389/978-2-8325-2762-7

Table of contents

frontiers | Frontiers in Oncology

TYPE Editorial
PUBLISHED 06 June 2023
DOI 10.3389/fonc.2023.1217401

OPEN ACCESS

EDITED AND REVIEWED BY
Tao Liu,
University of New South Wales, Australia

*CORRESPONDENCE
Marco Cordani
mcordani@ucm.es

RECEIVED 05 May 2023
ACCEPTED 19 May 2023
PUBLISHED 06 June 2023

CITATION
Cordani M, Condello M, Meschini S and Strippoli R (2023) Editorial: Autophagy modulation in cancer treatment utilizing nanomaterials and nanocarriers. *Front. Oncol.* 13:1217401. doi: 10.3389/fonc.2023.1217401

Editorial: Autophagy modulation in cancer treatment utilizing nanomaterials and nanocarriers

Marco Cordani[1,2]*, Maria Condello[3], Stefania Meschini[3] and Raffaele Strippoli[4,5]

[1]Department of Biochemistry and Molecular Biology, School of Biology, Complutense University, Madrid, Spain, [2]Instituto de Investigaciones Sanitarias San Carlos (IdISSC), Madrid, Spain, [3]National Center for Drug Research and Evaluation, National Institute of Health, Rome, Italy, [4]Department of Molecular Medicine, Sapienza University of Rome, Rome, Italy, [5]National Institute for Infectious Diseases L. Spallanzani IRCCS, Rome, Italy

KEYWORDS

nanomaterials, nanocarriers, drug delivery, cancer therapy, autophagy

Editorial on the Research Topic
Autophagy modulation in cancer treatment utilizing nanomaterials and nanocarriers

Autophagy is a cellular self-degradation process which plays an important role in cellular homeostasis by eliminating malfunctioning proteins and damaged organelles favoring cellular regeneration (1). In cancers, this process may maintain genetic stability and favor cell survival promoting drug resistance. However, in some contexts, autophagy can also induce tumor suppressor mechanisms by activating cell death after exposure to several environmental stresses, including treatment with anti-cancer agents (2). Thus, since autophagy has a dual role in cancer, its pharmacological modulation can, depending by tumor tissue, stage, and metabolic/environmental context, either suppress or promote cancer cell survival.

Recent advances in the modern field of nanotechnology make possible to counteract human diseases with effective bioactive compounds, overcoming the obstacles of traditional drugs such as biodistribution, biocompatibility and degradation or stability (3). Interestingly, nanomaterials have been explored as potent modulators of autophagy through multiple mechanisms and have been exploited as therapeutic agents against cancer (4). The relevance of nanomedicine for autophagy modulation is remarked by several clinical trials that have been set up in the last years (5). This suggests that the application of encapsulated drugs active in autophagy is effective in clinical practice and it would acquire more clinical relevance in the near future, as a complementary therapy for the treatment of cancers.

This Research Topic gathers original research and review papers on novel drugs in cancer treatments based on autophagy modulation as well as the application of novel nanomedicines capable of modulating autophagy, and/or new discoveries in autophagy-related signaling pathways in cancer. The 9 accepted articles consist of 5 Original Research articles, 3 Reviews and 1 Brief Research article. Overall, these studies demonstrate that inhibition or enhancement of the autophagy pathway may serve as an effective tool to counteract cancer.

In the last years, many herbal medicines and bioactive natural products have been explored for their antitumoral efficacy through modulation of key cellular signaling routes involving autophagy (6). In this regard, the Review Article by Wang et al. and Chavda et al. focused on the therapeutic effects and mechanisms of plant-derived natural products as well as combination therapy on cancer disease. The authors discussed the tumor suppressor role of several natural compounds in autophagy modulation and the recent strategies of their encapsulation to generate effective nano-delivery tools for targeted therapies in cancer. The translational potential of such nanoformulations in the clinic is also discussed. This review aims to elicit the interest of the community for developing anticancer strategies in both cellular and animal models, with high efficacy and low side effects.

Nazir et al. described the synthesis of 3-O-prenyl glycyrrhetinic acid (NPC-402), a derivative of glycyrrhetinic acid, and reported its cytotoxic activity in melanoma in *in vitro* and *in vivo* models. They showed that NPC-402 induces endoplasmic reticulum stress-mediated autophagy through modulation of an ERK/AKT signaling pathway in melanoma cells and reduces the tumor size and weight without any toxic side effects in C57BL/6J mice. Since methods to encapsulate NPC-402 in nanoformulations have been previously described (7), NCP-402 has the potential to become a nanomedicine for autophagy modulation for melanoma treatment. Hepatocellular carcinoma (HCC) is the third most common cause of cancer-related death globally (8). Despite many efforts made to find effective therapeutic strategies, HCC often becomes resistant to Sorafenib, the first-line chemotherapy, and only 15% of liver cancer patients survive at 5 years from diagnosis. In a study led by Sun et al. the effect of 5-chloro-N′-(2,4-dimethoxybenzylidene)-1H-indole-2-carbohydrazide (IHZ-1/ZJQ-24), a novel indole hydrazide derivative with bioactive proprieties for the management of liver cancer, has been evaluated. The authors showed that treatment with IHZ-1 in HCC cell lines increases the generation of intracellular reactive oxygen species (ROS) and induces autophagy through the activation of a ROS/JNK pathway. Interestingly, an indole hydrazide derivative has been encapsulated in different types of nanomaterials, such as hydrogels, pH-controlled biopolymers, or metal oxide nanoparticles, for their efficient delivery in cancer cells (9–11). Paclitaxel (PTX) and norcantharidin (NCTD) are anticancer compounds that have been described to be active in autophagy mechanisms (12–14). Xie et al. have generated PTX/NCTD-loaded core–shell lipid nanoparticles modified with a tumor neovasculature-targeted peptide, APRPG and investigated their anti-tumor effects in HCC. These functionalized nanostructures were reported to alter a complex network of signaling pathways involved in the migration and proliferation of liver cancer cells and reduced the volume and growth of HCC in animal models without side effects in healthy tissues. The antitumor activity of zinc-oxide nanospheres (ZnO-NS) has been explored for liver cancer treatment. In this regard, Hassan et al. showed that ZnO-NS synthesized by the Sol-gel method induced strong cytotoxic stress, ROS accumulation and lipid peroxidation in HuH7 cell line. They also reported lipid droplets accumulation and alterations in mitochondria leading to cell death. On the other side, the biochemical and mechanical proprieties of tumor microenvironment may affect drug distribution and release at the tumor site. To overcome this barrier, Yeow et al. produced a recombinant fusion protein consisting in tumor necrosis factor-α (TNF-α) and CSG peptide (CSGRRSSKC) to deplete extracellular matrix in liver cancer generated in mice models. This treatment was able to enhance an intra-tumoral accumulation of iron-oxide nanoparticles (IO-NPs) as determined by magnetic resonance imaging analysis. Since IO-NPs have been extensively studied as autophagy modulators in cancer therapy (15, 16) this study may set the basis for combined therapies based on the modulation of tumor microenvironment in combination with metal-oxide nanostructures to intervene on cancer autophagy.

Breast cancer is the most common cancer that affect women worldwide. Despite significant progress, breast cancer remains the tumor with the highest mortality. Autophagy plays an important role during breast cancer genesis and progression participating in many phenotypic traits such as migration, invasion, and therapy resistance (17). Nanomedicine is a promising strategy for breast cancer treatment. Products such as Doxil® and Abraxane® have already been used for breast cancer treatment as adjuvant therapy with favorable clinical outcomes (18). The review article authored by Gharoonpour et al. summarizes the advantages and disadvantages of nanoparticles-based therapy in breast cancer through autophagy modulation. The authors thoroughly discuss the translational potential of several nanoformulations combined with traditional chemotherapy, and the different phases of clinical trials involving nanomedicine that have been set up for breast cancer treatment. Moreover, Zhang et al. explored the therapeutic potential of chitosan/alginate nanoparticles for co-delivery of anti-autophagy drugs doxorubicin and hydroxychloroquine in breast cancer cells. This nanodelivery system was able to efficiently encapsulate these anti-autophagy drugs and allow their pH-sensitive release in the tumoral site.

Hence, the importance of the knowledge of the regulatory mechanisms of autophagy, along with the potential opportunities presented by newly emerging nanocarriers and nanomaterials suitable for bypassing developed cellular resistance, makes this topic particularly interesting. We believe that these advances will inspire basic and clinical scientists working in related fields to further investigate molecular mechanisms and to perform translational studies.

Author contributions

MCor wrote the original draft and revised the manuscript. The other authors revised the manuscript and provided valuable suggestions. All authors listed have approved this manuscript for publication.

Funding

MCor was funded by Spanish Ministry of Science and Innovation (MCIN/AEI: 10.13039/501100011033) and European Union NextGeneration (EU/PRTR), funding reference: RYC2021-

031003-I. RS was supported by Ministry for Health of Italy (Ricerca Corrente).

Conflict of interest

The authors declare that the research was conducted in the absence of any commercial or financial relationships that could be construed as a potential conflict of interest.

Publisher's note

References

1. Aman Y, Schmauck-Medina T, Hansen M, Morimoto RI, Simon AK, Bjedov I, et al. Autophagy in healthy aging and disease. *Nat Aging* (2021) 1:634–50. doi: 10.1038/s43587-021-00098-4

2. Singh SS, Vats S, Chia AYQ, Tan TZ, Deng S, Ong MS, et al. Dual role of autophagy in hallmarks of cancer. *Oncogene* (2018) 37:1142–58. doi: 10.1038/s41388-017-0046-6

3. Patra JK, Das G, Fraceto LF, Campos EVR, Rodriguez-Torres MDP, Acosta-Torres LS, et al. Nano based drug delivery systems: recent developments and future prospects. *J Nanobiotechnol* (2018) 16:71. doi: 10.1186/s12951-018-0392-8

4. Cordani M, Somoza Á Targeting autophagy using metallic nanoparticles: a promising strategy for cancer treatment. *Cell Mol Life Sci* (2019) 76:1215–42 doi: 10.1007/s00018-018-2973-y

5. López-Méndez TB, Sánchez-Álvarez M, Trionfetti F, Pedraz JL, Tripodi M, Cordani M, et al. Nanomedicine for autophagy modulation in cancer therapy: a clinical perspective. *Cell Biosci* (2023) 13:44. doi: 10.1186/s13578-023-00986-9

6. Al-Bari MAA, Ito Y, Ahmed S, Radwan N, Ahmed HS, Eid N. Targeting autophagy with natural products as a potential therapeutic approach for cancer. *Int J Mol Sci* (2021) 22:9807. doi: 10.3390/ijms22189807

7. Zhou Q, Wu J, Lian B, Zhang B, Zhang P, Pan R. Glycyrrhetinic acid-modified sulfated hyaluronic acid nanoparticles coencapsulating doxorubicin and magnolol for the synergistic treatment of hepatocellular carcinoma. *ACS Appl Nano Mater* (2022) 5:15070–82. doi: 10.1021/acsanm.2c03245

8. Bruix J, Raoul JL, Sherman M, Mazzaferro V, Bolondi L, Craxi A, et al. Efficacy and safety of sorafenib in patients with advanced hepatocellular carcinoma: subanalyses of a phase III trial. *J Hepatol* (2012) 57:821–9. doi: 10.1016/j.jhep.2012.06.014

9. Chitra G, Selvi MS, Franklin DS, Sudarsan S, Sakthivel M, Guhanathan S. pH-sensitive biopolymeric hydrogel-based on indole-3-acetic acid for wound healing and anti-cancer applications. *SN Appl Sci* (2019) 1:1641. doi: 10.1007/s42452-019-1339-x

10. Panichikkal J, Mohanan DP, Koramkulam S, Krishnankutty RE. Chitosan nanoparticles augmented indole-3-acetic acid production by rhizospheric pseudomonas monteilii. *J Basic Microbiol* (2022) 62:1467–74. doi: 10.1002/jobm.202100358

11. Karakeçili A, Korpayev S, Dumanoğlu H, Alizadeh S. Synthesis of indole-3-acetic acid and indole-3-butyric acid loaded zinc oxide nanoparticles: effects on rhizogenesis. *J Biotechnol* (2019) 303:8–15. doi: 10.1016/j.jbiotec.2019.07.004

12. Zamora A, Alves M, Chollet C, Therville N, Fougeray T, Tatin F, et al. Paclitaxel induces lymphatic endothelial cells autophagy to promote metastasis. *Cell Death Dis* (2019) 10:956. doi: 10.1038/s41419-019-2181-1

13. Khing TM, Choi WS, Kim DM, Po WW, Thein W, Shin CY, et al. The effect of paclitaxel on apoptosis, autophagy and mitotic catastrophe in AGS cells. *Sci Rep* (2021) 11:23490. doi: 10.1038/s41598-021-02503-9

14. Liu Z, Li B, Cao M, Jiang J. Norcantharidin triggers apoptotic cell death in non-small cell lung cancer *via* a mitophagy-mediated autophagy pathway. *Ann Transl Med* (2021) 9:971. doi: 10.21037/atm-21-2360

15. Mundekkad D, Cho WC. Mitophagy induced by metal nanoparticles for cancer treatment. *Pharmaceutics* (2022) 14:2275. doi: 10.3390/pharmaceutics14112275

16. Uzhytchak M, Smolková B, Lunova M, Jirsa M, Frtús A, Kubinová Š, et al. Iron oxide nanoparticle-induced autophagic flux is regulated by interplay between p53-mTOR axis and bcl-2 signaling in hepatic cells. *Cells.* (2020) 9:1015. doi: 10.3390/cells9041015

17. Niklaus NJ, Tokarchuk I, Zbinden M, Schläfli AM, Maycotte P, Tschan MP. The multifaceted functions of autophagy in breast cancer development and treatment. *Cells.* (2021) 10:1447. doi: 10.3390/cells10061447

18. Wu D, Si M, Xue H, Wong HL. Nanomedicine applications in the treatment of breast cancer: current state of the art. *Int J Nanomedicine.* (2017) 12:5879–92. doi: 10.2147/IJN.S123437

frontiers in Oncology

ORIGINAL RESEARCH
published: 07 February 2022
doi: 10.3389/fonc.2022.811747

Indole Hydrazide Compound IHZ-1 Induces Apoptosis and Autophagy *via* Activation of ROS/JNK Pathway in Hepatocellular Carcinoma

Manting Sun[1†], *Dan Liu*[1†], *Yang Yuan*[1], *Juhua Dan*[1], *Shuting Jia*[1], *Ying Luo*[1,2*] *and Jing Liu*[1*]

[1] *Laboratory of Molecular Genetics of Aging and Tumor, Medical School, Kunming University of Science and Technology, Kunming, China,* [2] *Guizhou Provincial Key Laboratory of Pathogenesis & Drug Development on Common Chronic Diseases, School of Basic Medicine, Guizhou Medical University, Guiyang, China*

OPEN ACCESS

Edited by:
Shiv K. Gupta,
Mayo Clinic, United States

Reviewed by:
Kamini Singh,
Albert Einstein College of Medicine, United States
Min Li,
Sun Yat-Sen University Cancer Center (SYSUCC), China

***Correspondence:**
Jing Liu
jingliu1437@163.com
Ying Luo
luoying@gmc.edu.cn

[†]*These authors have contributed equally to this work*

Specialty section:
This article was submitted to Cancer Molecular Targets and Therapeutics, a section of the journal Frontiers in Oncology

Received: *09 November 2021*
Accepted: *10 January 2022*
Published: *07 February 2022*

Citation:
Sun M, Liu D, Yuan Y, Dan J, Jia S, Luo Y and Liu J (2022) Indole Hydrazide Compound IHZ-1 Induces Apoptosis and Autophagy via Activation of ROS/JNK Pathway in Hepatocellular Carcinoma. Front. Oncol. 12:811747. doi: 10.3389/fonc.2022.811747

Hepatocellular carcinoma is one of the most common primary malignant tumors of the digestive system. Compound 5-chloro-*N*′-(2,4-dimethoxybenzylidene)-1*H*-indole-2-carbohydrazide (IHZ-1/ZJQ-24) is a novel indole hydrazide derivative. In a recent study, we demonstrated that IHZ-1 inhibits tumor growth and induces cell apoptosis through inhibiting the kinase activity of mTORC1 without activation of AKT, which is associated with JNK/IRS-1 activation. However, the impact and mechanisms of JNK activation by IHZ-1 in hepatocellular carcinoma remains entirely unknown. Here, we find that IHZ-1 increases the generation of intracellular ROS and enhances autophagy. The phosphorylation of JNK induced by IHZ-1 was reversed by the decreased ROS level. Moreover, inhibition of ROS/JNK or autophagy equally attenuated apoptotic effect induced by IHZ-1. Our findings suggest that the activation of JNK by IHZ-1 treatment is dependent on the generation of ROS that mediates apoptosis and autophagy in hepatocellular carcinoma.

Keywords: IHZ-1, JNK/ROS, autophagy, apoptosis, hepatic cellular carcinoma (HCC)

INTRODUCTION

Primary carcinoma of the liver [hepatocellular carcinoma (HCC)] is one of the familiar digestive system neoplasms (1). Current treatments for HCC include surgery, radiation therapy, and drug therapy, but the overall outlook for most patients has not improved significantly, with 5-year survival rates below 20% (2). Therefore, the development of novel therapies for the management of HCC is especially urgent.

Our previous study reported that IHZ-1 has also been named ZJQ-24 (5-chloro-*N*′-(2,4-dimethoxybenzylidene)-1H-indole-2-carbohydrazide) (**Figure 1A**) induced cell apoptosis by inhibiting the mTORC1 activity without activation of AKT *via* phosphorylation of c-Jun N-terminal kinase (JNK) (3). Although the inhibition of AKT/mTOR by IHZ-1 has positive correlation with antitumor effect, the mechanisms of JNK activation remain unclear. Also, whether the activation of JNK by IHZ-1 can result in apoptosis or autophagy has not been investigated yet.

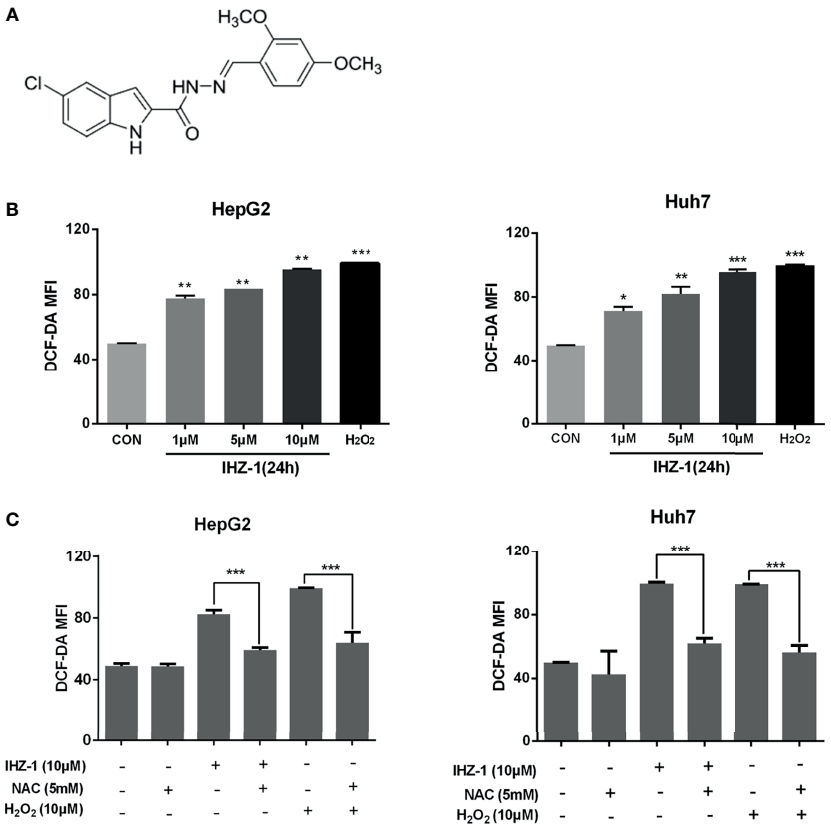

FIGURE 1 | IHZ-1 induced ROS generation in HCC cells. **(A)** Structural formula of compound IHZ-1. **(B)** Intracellular ROS level were measured by fluorescence microscope with DCFH-DA staining after IHZ-1 treatment **(C)** or pretreated with NAC and analyzed by flow cytometer. *p < 0.05, **p < 0.01, and ***p < 0.001.

JNK is a type of serine/threonine kinase which belongs to one of the mitogen-activated protein kinases (MAPK), and its activation regulates many cellular progresses, such as apoptosis and autophagy which are two main types of programmed cell death (PCD) (4). In the early transient phase of JNK activation, JNK serves to promote autophagy and cell survival because of upstream protein kinase of Bcl-2 family proteins (5). Whereas in the later and more sustained phase of JNK activation, JNK serves to induce apoptosis (6). For several decades, apoptosis has been considered the pivotal mechanism of cell death in tumor cells *via* mitochondria-dependent pathway (7), and enhancing cell apoptosis is also a main strategy of cancer therapy. However, many studies have reported that the mechanisms of anticancer treatment are not only confined to apoptosis but also involved autophagy. Autophagy has been identified as a "self-eating" process of organelles and cytosolic macromolecules (8). It plays an important role in cell death, normal physiology, and cellular homeostasis. However, autophagy is defined as type II programmed cell death and has a dual role including prodeath or prosurvival which depends on the cell type and the level of stress (9). Although, the crosstalk between autophagy and apoptosis is very complicated and remains controversial. They may be triggered by common upstream stressor reactive oxygen species (ROS) which is known as a mediator for the activation of MAPK (10). In cancer research, increasing studies suggest that different levels of ROS results in autophagy and apoptosis (11). Hence, targeted activation on the ROS/JNK pathway might be beneficial in antitumor treatment. Here, we found the activation of JNK by IHZ-1 was dependent on ROS generation and induced cell apoptosis. Furthermore, we investigated the IHZ-1-induced cell apoptosis and autophagy regulated by the ROS/JNK signaling pathway.

MATERIALS AND METHODS

Chemicals

IHZ-1 compound was identified and provided by the Key Laboratory of Medicinal Chemistry for Natural Resource (Yunnan University). The compound was prepared as 100 mM stock solutions in DMSO and aliquots stored at −20°C, protected from light. Reagents, unless specified otherwise, were purchased from Sigma-Aldrich Ltd. (Shanghai, China).

Cell Lines and Culture Conditions

The cell lines (HepG2, HUH-7) were obtained from the American Type Culture Collection (ATCC, Manassas, VA, USA). Cells were cultured in DMEM medium (Gibco,

Invitrogen, New York, NY, USA) supplemented with 10% FBS (Gibco) at 37°C in a humidified atmosphere of 5% CO_2.

ROS Detection

ROS level was measured by 2,7-dichlorofluo-rescein diacetate (DCFH-DA). Cells on a 96-well plate were allowed to attach overnight, then treated with IHZ-1 (1, 5, and 10 μM) for 24 h. The medium was removed and washed 3 times with PBS, then incubated with DCFH-DA at 37°C for 30 min, measuring the ROS levels through fluorescence microplate reader with 488 nm excitation wavelength and 525 nm emission wavelength.

Polymerase Chain Reaction (Real-Time PCR)

Real-time PCR analysis was performed as described previously (12). Total RNA was extracted using TRIzol reagent (Invitrogen), then 500 ng total RNA was reversely transcribed into cDNA by High-Capacity cDNA Reverse Transcription Kit (Applied Biosystems, Waltham, MA, USA). The mRNA expression was detected using SYBR Green assay in 7300 Real-Time PCR System (Applied Biosystems). The following primers were used: *Atg5* forward 5′-CACTTTGTCAGTTACCAACGTCA-3′ and *Atg5* reverse 5′-AAAGATGTGCTTCGAGATGTGT-3′; *ULK1* forward 5′-CGACCTCCAAATCGTGCTTCT-3′ and *ULK1* reverse 5′-GGCAAGTTCGAGTTCTCCCG-3′; and *Beclin1* forward 5′-GAATCTGCGAGAGACACCATC-3′ and *Beclin1* reverse 5′-CCATGCAGGTGAGCTTCGT-3′. The program of real-time system is 95°C for 10 min, then 40 cycles of 95°C for 15 s and 60°C for 1 min. Data analysis was performed using the following equations: $\triangle$C=Ct(sample)−Ct(endogenous control); $\triangle\triangle$ Ct=$\triangle$Ct(sample)−Ct(untreated); and fold change = $2^{-\triangle\triangle Ct}$.

GFP-LC3-II Transfection

HepG2 and Huh7 cells were seeded onto cover slips in 6-well plates at a density of 1×10^5 cells/well and left overnight, then transfected with 3 μg GFP-LC3-II plasmid using Lipo2000 (Invitrogen Corporation) according to manufacturer's instructions. After 24 h, cells were treated with IHZ-1 (1, 5, and 10 μM) and vehicle. After 24 h, cells were fixed with 4% paraformaldehyde in PBS at 4°C for 30 min, and GFP-LC3-II fluorescence was examined under a fluorescence microscope. For each slide, 100 cells were analyzed and mean numbers of punctate GFP-LC3-II spots/cell were calculated.

Western Blot Analysis

For each sample, all the cells were lysed for 30 min in lyses buffer on 4°C; after ultrasound, the cell debris was centrifuged at 12,000 rpm for 20 min at 4°C, protein concentration was detected by BCA (Beyotime, Haimen, China), using 12% sodium dodecyl sulfate-polyacrylamide gel electrophoresis (SDS-PAGE) to separate the proteins, the separated proteins were blotted onto PVDF membrane, blocking 2 h at room temperature with 5% nonfat dry milk in TBST, incubating the antibody for 16 h at 4°C with 1:1,000 concentration, washing PVDF membrane 3 times for 10 min in TBST, incubating secondary antibody at 25°C for 2 h with the 1:10,000 concentration, washing membranes 3 times for 10 min in TBST. Finally, the membranes were visualized with the enhanced chemiluminescence (ECL) detection system (GE Healthcare, Piscataway, NJ, USA). All of the primary antibodies (p-JNK, JNK, P62, LC3-II, GAPDH) were purchased from Cell Signaling Technology, Inc. (Danvers, MA, USA).

Annexin-V/PI Assay

Apoptotic cells were identified using Annexin-V/PI staining analyses. Briefly, cells were respectively seeded into 6-well plates and treated with IHZ-1 in different concentrations (1, 5, and 10 μM) or IHZ-1combine with chloroquine (10 μM) for 24 h. Cells were then harvested and washed using PBS. The surface levels of phosphatidylserine were quantitatively detected using Annexin V-FITC and PI apoptosis kit according to the manufacturer's instructions (BD Biosciences, San Jose, CA, USA). The stained cell number were analyzed by flow cytometry (Accuri C6, BD Biosciences, Franklin Lakes, NJ, USA) within 1 h.

Quantification of Acidic Vesicular Organelles With Acridine Orange

HepG2 and Huh7 cells were seeded into 6-well plates and allowed to attach overnight before treatment with IHZ-1(1, 5, and 10 μM) and vehicle. Cells were stained with acridine orange (AO) (1 mg/ml) for 15 min. Media were removed and cells washed with PBS and analyzed by flow cytometry, green (510–530 nm, FL1-H channel) and red (>650 nm, FL3-H channel). The bar for FL3-H in the control sample was set so that the acidic vesicular organelle (AVO)-positive cells represented approximately 5% of the population. Compound-treated samples were measured under the same conditions.

Statistical Analysis

The results were expressed as mean ± standard deviation (SD). Statistical differences were evaluated using the two-tailed Student's *t*-test and analysis of variance (ANOVA) followed by *q*-test, considered significant at $^{*}p < 0.05$, $^{**}p < 0.01$, or $^{***}p < 0.001$.

RESULTS

IHZ-1 Activation of JNK *via* ROS Generation To Induce Cell Apoptosis

For research if whether IHZ-1 induces the upregulation of ROS, we used 2,7-dichlorodihydro-fluorescein diacetate (DCFH-DA) staining followed by flow cytometry; H_2O_2 was included as a positive control. As shown in **Figure 1B**, IHZ-1 induced ROS generation in a dose-dependent manner, as reflected by the increase of fluorescence intensity. To further verify that IHZ-1 induces the generation of ROS, we used *N*-acetylcysteine (NAC) to clear ROS and detect changes in ROS levels. The data showed that the high ROS levels dropped after NAC treatment (**Figure 1C**).

It is reported that JNK can be regulated by ROS (13). The production of ROS easily activates JNK, which usually plays a very important role for cell survival (14, 15). So we treated cells

with NAC and JNK inhibitor (SP600125) and tested the expression of JNK in HCC cells. Our result showed that IHZ-1 increased the expression level of p-JNK and the upregulation of p-JNK was inhibited by NAC and SP600125 (**Figure 2A**). To demonstrate the effect of ROS-induced JNK activation on cell survival, we used flow cytometry to detect apoptosis by Annexin-V/PI double staining. When ROS and JNK were inhibited, the number of apoptotic cells was reduced (**Figure 2B**). Collectively, we demonstrated that IHZ-1 caused JNK upregulation in ROS-dependent HCC cells, which is required for IHZ-1-induced apoptosis.

IHZ-1 Triggers Autophagy

Recent studies have shown that ROS-mediated autophagy has two opposing functions in a variety of HCC treatments: promoting cell survival or inducing cell death (16). Therefore, we first used AO staining to evaluate the number of acidic organelles in HepG2 and Huh7 cells. As shown in **Figure 3A**, the number of acidic organelles increased especially in HepG2 cells. In addition, the real-time PCR showed that the mRNA expression levels of *Beclin1*, *Atg5*, and *ULK1* increased after IHZ-1 treatment (**Figure 3B**). To further determine the activation of autophagy, the GFP-LC3II lentivirus was transfected in HepG2 cells to detect the fluorescent puncta formation of autophafosomes. After treatment with IHZ-1 for 24 h, green puncta formation presented a significant increase in a dose-dependent manner (**Figure 3C**). Next, Western blotting assay was used to test the LC3-II and p62 which are the main marker proteins of autophagy. It showed that IHZ-1 treatment upregulated the LC3-II in HCC cells. However, the amount of

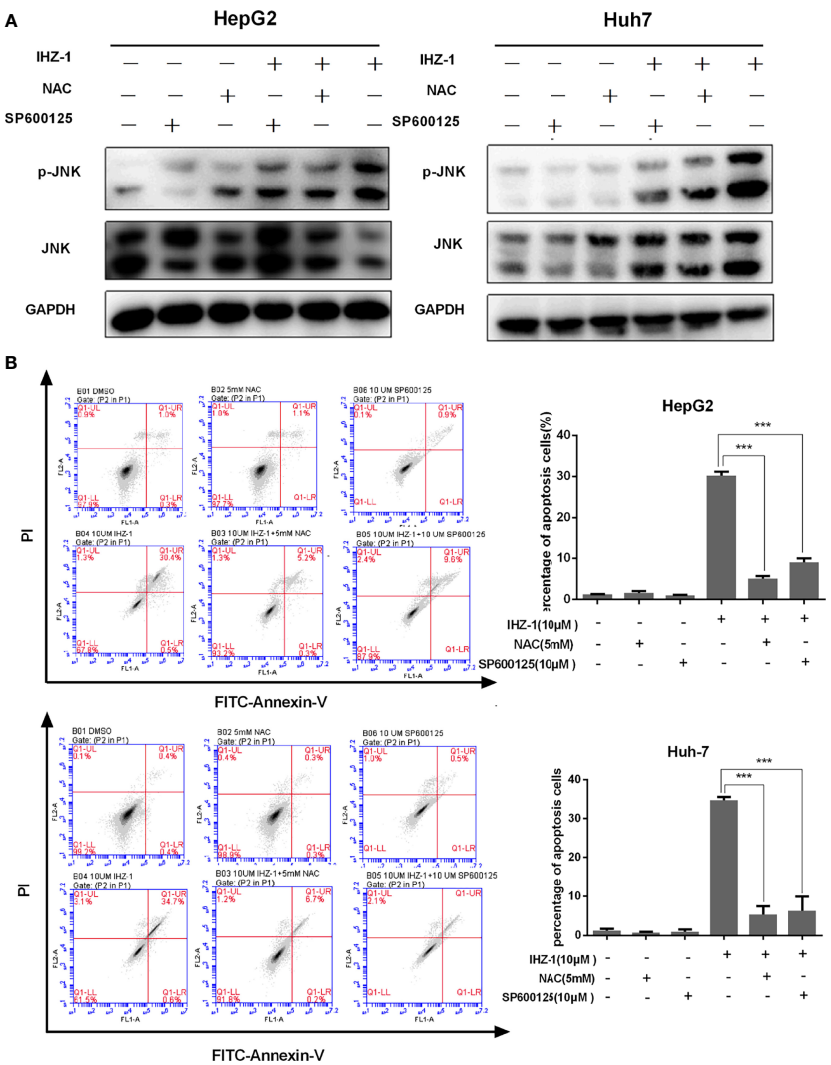

FIGURE 2 | IHZ-1 caused apoptosis through activating ROS/JNK cascade in HCC cells. **(A)** Cells were incubated with IHZ-1 and pretreated with NAC or SP600125. Immunoblots of p-JNK and JNK protein expression was quantified. **(B)** The apoptosis cells were evaluated by flow cytometry using Annexin-V/PI double staining. ***p < 0.001.

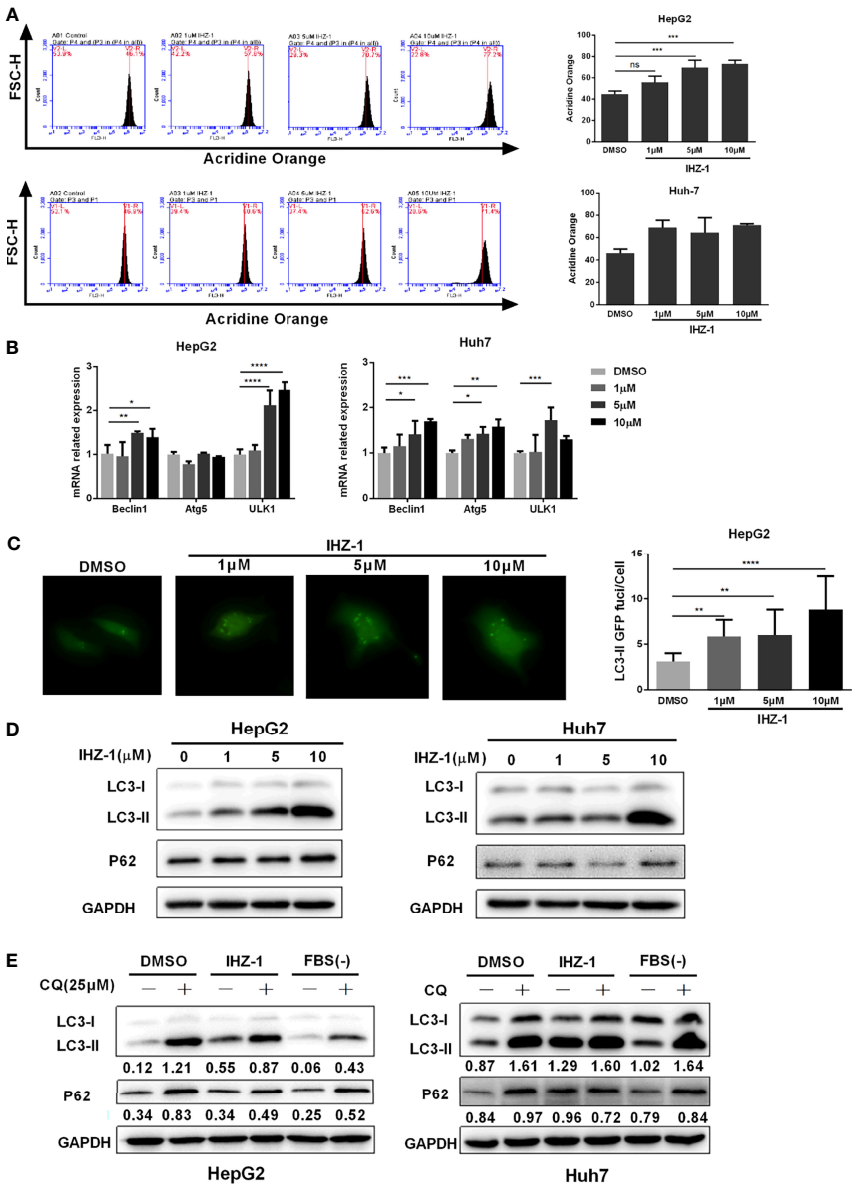

FIGURE 3 | IHZ-1 triggers autophagy. **(A)** The number of acidic organelles were evaluated by acridine orange staining and analyzed by flow cytometry. **(B)** The autophagy-related mRNAs were determined by real-time PCR. **(C)** Representative images of HCC cells steadily articulating GFP-LC3 after IHZ-1 treatment. **(D)** The autophagy-related proteins were determined by western blotting. **(E)** The autophagic flux was determined by immunoblot analysis of LC3-II and P62 levels in HCC cells incubated with IHZ-1 in the presence or absence of CQ. As indicated below each lane, the LC3-II/GAPDH and P62/GAPDH ratios were determined using the ImageJ software. *$p < 0.05$, **$p < 0.01$, ***$p < 0.001$, and ****$p < 0.0001$. no significance (ns).

p62 that was delivered to the lysosomes for degradation did not decrease after IHZ-1 treatment (**Figure 3D**). This result seems to suggest that IHZ-1 impairs the autophagic degradation process. In order to obtain a better evaluation of autophagic flux, we carried out Western blotting to detect the p62 expression using the cells treated with autophagy inhibitor chloroquine (CQ, 25 μM) as control (17). We also used the starvation medium as a positive control to induce the autophagic flux. As shown in **Figure 3E**, IHZ-1 decreased the level of p62 in the presence of CQ. These results suggested that IHZ-1 caused autophagy through activating ROS/JNK in HCC cells.

Suppression of the Autophagy Flux Enhanced by IHZ-1 Promotes Apoptosis

Autophagy has opposite roles for therapeutic purposes in tumor, including the effect of promoting or preventing apoptotic cell death. We further used CQ to inhibit IHZ-1-induced autophagy in HCC cells. Flow cytometric analysis results showed that the

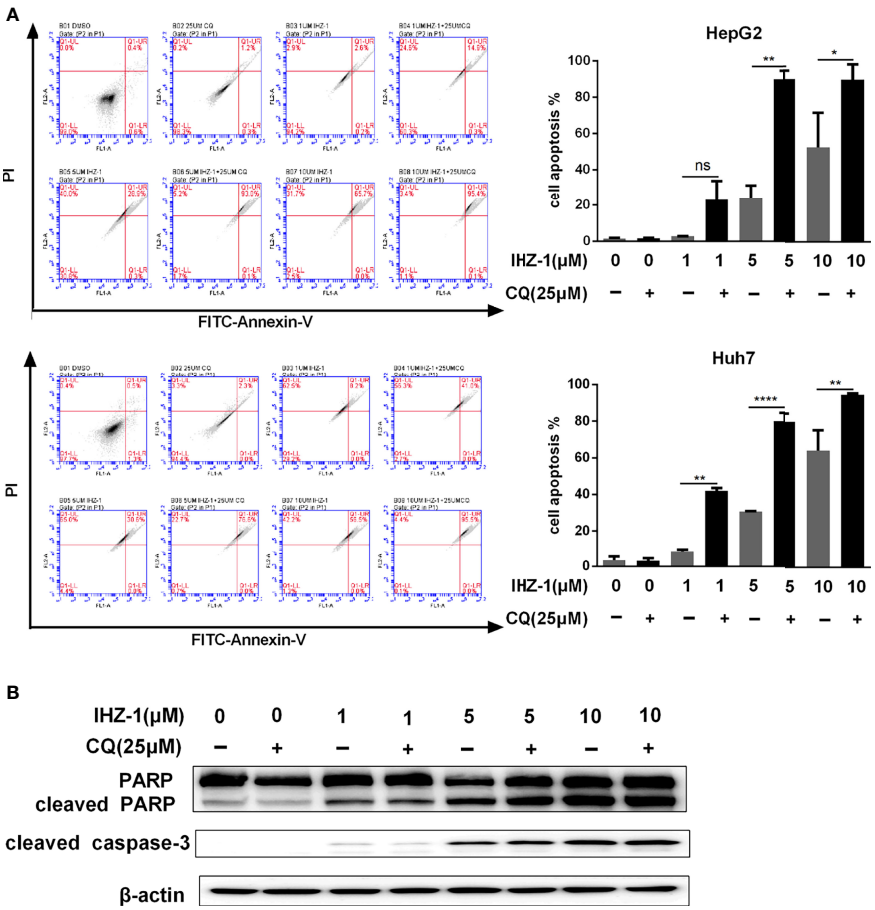

FIGURE 4 | Suppression the autophagy flux enhanced by IHZ-1 promote apoptosis. **(A)** The autophagic flux induced by IHZ-1 was inhibited by CQ. The apoptotic cells were then evaluated by flow cytometry with Annexin-V/PI staining. **(B)** The apoptosis-related protein levels were determined by Western blotting. *p < 0.05, **p < 0.01, and ****p < 0.0001. no significance (ns).

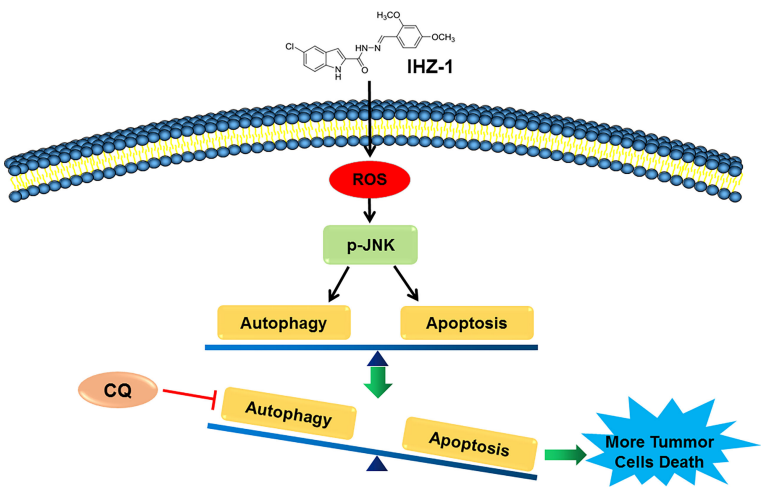

FIGURE 5 | The mechanism of IHZ-1 induced apoptosis and autophagy in HCC cells. IHZ-1 could accumulate ROS and induce autophagy in HCC cells, while inhibiting autophagy could enhance the apoptosis induced by IHZ-1.

administration with CQ significantly enhance the apoptosis effect induced by IHZ-1 (**Figure 4A**). In addition, Western blotting results revealed that treatment with CQ also strengthened apoptosis-associated protein expression induced by IHZ-1, such as cleaved PARP and cleaved caspase3 (**Figure 4B**). The above results indicated that IHZ-1 triggered autophagy of HCC in a dose-dependent manner. The autophagy triggered by IHZ-1 may be antiapoptosis.

DISCUSSION

Our previous study has reported that IHZ-1 (ZJQ-24) effectively suppressed HCC proliferation *via* G_2/M phase arrest and caspase-dependent apoptosis. IHZ-1 induced cell apoptosis by inhibiting the mTORC1 activity without activation of AKT *via* phosphorylation of JNK (3). However, the mechanisms of JNK activation remain unclear. Here, we have detected that JNK activation by IHZ-1 is ROS dependent which results in cell apoptosis. Further experiments indicated that the ROS generation by IHZ-1 also induces autophagy. In addition, CQ could strengthen the power of IHZ-1-induced apoptosis, which suggested that the autophagy induced by IHZ-1 may support cell survival (**Figure 5**).

Accumulated evidence has indicated that JNK activation could transduce oxidative stress and induce cell apoptosis (18, 19). This guided us to believe that the JNK activation by IHZ-1 was ROS dependent. A high level of ROS after IHZ-1 treatment in HCC cells was found during the research of apoptosis. In addition, we found that accumulation of ROS could trigger the activation of JNK, whereas pretreatment with NAC could attenuate the phosphorylation of JNK. Our data specified that IHZ-1 may active the JNK by induction of the high level of ROS. In this study, we also found that the apoptosis induced by IHZ-1 was attenuated by pretreatment with NAC and SP600125, a JNK inhibitor. Taken together, these results showed that IHZ-1 induces apoptosis by triggering the ROS/JNK-dependent pathway.

Besides apoptosis, ROS/JNK pathway activation could also induce autophagy, which also has a vital role in regulating cell death. During the process of autophagy, the cytoplasmatic vesicles and intracellular organelles were transported into autophagodomes, then decomposed and digested in the lysosome (20). Accumulated studies indicates that autophagy critically regulates cellular homeostasis and has two-edged sword effects, providing protection or causing cell damage (21). In our study, we first identified that IHZ-1 could induce autophagy with the results that the number of acidic organelles was increased and the expression levels of autophagy genes and LC3-II were enhanced. To further determine the autophagic flux, we tested the LC3-II and p62 levels by immunoblotting in the presence of CQ. Our data demonstrated that IHZ-1 attenuated the expression of p62 after CQ treatment, suggesting the activation of autophagic flux. Our results also indicated that the autophagy inhibitor CQ could enhance the power of IHZ-1-induced apoptosis, which suggested that autophagy triggered by IHZ-1 may support survival during the death of HCC cells.

Some evidence has demonstrated that ROS was a signaling molecule; it could induce apoptosis and/or activate autophagy, depending on the cellular components (22). Meanwhile, apoptosis and autophagy share many signaling pathways, such as the MAPK pathway including JNK, p38 MAPK, and ERK (23). However, the molecular mechanisms of ROS/JNK-mediated apoptosis and autophagy with IHZ-1 treatment are still not clear. It is worthy to note in our study that IHZ-1 could increase generation of ROS and activate ROS-dependent JNK signaling pathway, while the cell fate of IHZ-1 on cell apoptosis and autophagy was opposite. It suggested that autophagy could be a self-protective reaction of tumor cells with IHZ-1 treatment. Hence, we speculated that triggering apoptosis and autophagy by IHZ-1 was associated with the level of ROS.

In conclusion, our results showed that IHZ-1 could significantly induce apoptosis and autophagy through activation of ROS-dependent JNK signaling pathways. Furthermore, inhibition autophagy enhanced IHZ-1-induced apoptosis, suggesting that IHZ-1-induced autophagy played a protective role in HCC cells. These findings not only indicated that IHZ-1 induced apoptosis through ROS/JNK pathways but also offer an alternate approach of combining IHZ-1 with autophagy inhibitor together for human HCC treatment as well.

DATA AVAILABILITY STATEMENT

The original contributions presented in the study are included in the article/supplementary material. Further inquiries can be directed to the corresponding authors.

AUTHOR CONTRIBUTIONS

All the authors confirmed that they have reviewed the manuscript entitled "Indole Hydrazide Compound IHZ-1 Induces Apoptosis and Autophagy *via* Activation of ROS/JNK Pathway in Hepatocellular Carcinoma" and approved its submission to the journal of "Frontiers in Oncology". The specific work of each author in this study was as follows: SJ, YL, and JL: perception and design and final approval of the version to be published. MS, DL, YY, and JD: participation in the whole work, drafting of the article, and data analysis.

FUNDING

This study was supported by grants from the National Natural Science Foundation of China (No. 82060660) and Yunnan Fundamental Research Project (grant No. 202101AT070086, 2019FB109).

REFERENCES

1. Bray F, Ferlay J, Soerjomataram I, Siegel RL, Torre LA, Jemal A. Global Cancer Statistics 2018: GLOBOCAN Estimates of Incidence and Mortality Worldwide for 36 Cancers in 185 Countries. *CA Cancer J Clin* (2018) 68:394–424. doi: 10.3322/caac.21492
2. Allemani C, Matsuda T, Di Carlo V, Harewood R, Matz M, Niksic M, et al. Global Surveillance of Trends in Cancer Survival 2000-14 (CONCORD-3): Analysis of Individual Records for 37 513 025 Patients Diagnosed With One of 18 Cancers From 322 Population-Based Registries in 71 Countries. *Lancet* (2018) 391:1023–75. doi: 10.1016/S0140-6736(17)33326-3
3. Liu J, Liu Y, Zhang J, Liu D, Bao Y, Chen T, et al. Indole Hydrazide Compound ZJQ-24 Inhibits Angiogenesis and Induces Apoptosis Cell Death Through Abrogation of AKT/mTOR Pathway in Hepatocellular Carcinoma. *Cell Death Dis* (2020) 11:926. doi: 10.1038/s41419-020-03108-2
4. Huang KM, Chen YY, Zhang R, Wu YZ, Ma Y, Fang XQ, et al. Honokiol Induces Apoptosis and Autophagy *via* the ROS/ERK1/2 Signaling Pathway in Human Osteosarcoma Cells *In Vitro* and *In Vivo*. *Cell Death Dis* (2018) 9:157–73. doi: 10.1038/s41419-017-0166-5
5. Wei YJ, Sinha S, Levine B. Dual Role of JNK1-Mediated Phosphorylation of Bcl-2 in Autophagy and Apoptosis Regulation. *Autophagy* (2008) 4:949–51. doi: 10.4161/auto.6788
6. Ventura JJ, Hubner A, Zhang C, Flavel RA, Shokat KM, Davis RJ. Chemical Genetic Analysis of the Time Course of Signal Transduction by JNK. *Mol Cell* (2006) 21:701–10. doi: 10.1016/j.molcel.2006.01.018
7. Sinha K, Das J, Pal PB, Sil PC. Oxidative Stress: The Mitochondria-Dependent and Mitochondria-Independent Pathways of Apoptosis. *Arch Toxicol* (2013) 87:1157–80. doi: 10.1007/s00204-013-1034-4
8. Rosenfeldt MT, Ryan KM. The Role of Autophagy in Tumour Development and Cancer Therapy. *Expert Rev Mol Med* (2009) 11:e36. doi: 10.1017/S1462399409001306
9. Janku F, McConkey DJ, Hong DS, Kurzrock R. Autophagy as a Target for Anticancer Therapy. *Nat Rev Clin Oncol* (2011) 8:528–39. doi: 10.1038/nrclinonc.2011.71
10. Chio IIC, Tuveson DA. ROS in Cancer: The Burning Question. *Trends Mol Med* (2017) 23:411–29. doi: 10.1016/j.molmed.2017.03.004
11. Tang Z, Zhao L, Yang Z, Liu Z, Gu J, Bai B, et al. Mechanisms of Oxidative Stress, Apoptosis, and Autophagy Involved in Graphene Oxide Nanomaterial Anti-Osteosarcoma Effect. *Int J Nanomed* (2018) 13:2907–19. doi: 10.2147/IJN.S159388
12. Xiang ZL, Zeng ZC, Fan J, Tang ZY, Zeng HY, Gao DM. Gene Expression Profiling of Fixed Tissues Identified Hypoxia-Inducible Factor-1alpha, VEGF, and Matrix Metalloproteinase-2 as Biomarkers of Lymph Node Metastasis in Hepatocellular Carcinoma. *Clin Cancer Res* (2011) 17:5463–72. doi: 10.1158/1078-0432.CCR-10-3096
13. Zeng KW, Song FJ, Wang YH, Li N, Yu Q, Liao LX, et al. Induction of Hepatoma Carcinoma Cell Apoptosis Through Activation of the JNK-Nicotinamide Adenine Dinucleotide Phosphate (NADPH) Oxidase-ROS Self-Driven Death Signal Circuit. *Cancer Lett* (2014) 353:220–31. doi: 10.1016/j.canlet.2014.07.022
14. Ueda S, Masutani H, Nakamura H, Tanaka T, Ueno M, Yodoi J. Redox Control of Cell Death. *Antioxid Redox Signal* (2002) 4:405–14. doi: 10.1089/15230860260196209
15. Ding M, Li J, Leonard SS, Shi X, Costa M, Castranova V, et al. Differential Role of Hydrogen Peroxide in UV-Induced Signal Transduction. *Mol Cell Biochem* (2002) 234-235:81–90. doi: 10.1007/978-1-4615-1087-1_9
16. Yuan X, Wang B, Yang L, Zhang Y. The Role of ROS-Induced Autophagy in Hepatocellular Carcinoma. *Clinics Res Hepatol Gastroenterol* (2018) 42:306–12. doi: 10.1016/j.clinre.2018.01.005
17. Yue W, Hamai A, Tonelli G, Bauvy C, Nicolas V, Tharinger H, et al. Inhibition of the Autophagic Flux by Salinomycin in Breast Cancer Stem-Like/Progenitor Cells Interferes With Their Maintenance. *Autophagy* (2013) 9:714–29. doi: 10.4161/auto.23997
18. Wang G, Zhang T, Sun W, Wang H, Yin F, Wang Z, et al. Arsenic Sulfide Induces Apoptosis and Autophagy Through the Activation of ROS/JNK and Suppression of Akt/mTOR Signaling Pathways in Osteosarcoma. *Free Radic Biol Med* (2017) 106:24–37. doi: 10.1016/j.freeradbiomed.2017.02.015
19. Dhanasekaran DN, Reddy EP. JNK-Signaling: A Multiplexing Hub in Programmed Cell Death. *Genes Cancer* (2017) 8:682–94. doi: 10.18632/genesandcancer.155
20. Denton D, Kumar S. Autophagy-Dependent Cell Death. *Cell Death Differ* (2019) 26:605–16. doi: 10.1038/s41418-018-0252-y
21. Onorati AV, Dyczynski M, Ojha R, Amaravadi RK. Targeting Autophagy in Cancer. *Cancer* (2018) 124:3307–18. doi: 10.1002/cncr.31335
22. Gao L, Loveless J, Shay C, Teng Y. Targeting ROS-Mediated Crosstalk Between Autophagy and Apoptosis in Cancer. *Adv Exp Med Biol* (2020) 1260:1–12. doi: 10.1007/978-3-030-42667-5_1
23. Sui X, Kong N, Ye L, Han W, Zhou J, Zhang Q, et al. P38 and JNK MAPK Pathways Control the Balance of Apoptosis and Autophagy in Response to Chemotherapeutic Agents. *Cancer Lett* (2014) 344:174–9. doi: 10.1016/j.canlet.2013.11.019

Conflict of Interest: The authors declare that the research was conducted in the absence of any commercial or financial relationships that could be construed as a potential conflict of interest.

frontiers in Oncology

BRIEF RESEARCH REPORT
published: 22 February 2022
doi: 10.3389/fonc.2022.837234

ECM Depletion Is Required to Improve the Intratumoral Uptake of Iron Oxide Nanoparticles in Poorly Perfused Hepatocellular Carcinoma

*Yen Ling Yeow[1], Jiansha Wu[1], Xiao Wang[1], Louise Winteringham[1], Kirk W. Feindel[2], Janina E. E. Tirnitz-Parker[3], Peter J. Leedman[1], Ruth Ganss[1] and Juliana Hamzah[1,3]**

[1] Harry Perkins Institute of Medical Research, Centre for Medical Research, QEII Medical Centre, The University of Western Australia, Nedlands, WA, Australia, [2] Centre for Microscopy, Characterisation and Analysis, The University of Western Australia, Nedlands, WA, Australia, [3] Curtin Medical School and Curtin Health Innovation Research Institute, Curtin University, Bentley, WA, Australia

OPEN ACCESS

Edited by:
Massimo Broggini,
Mario Negri Pharmacological Research Institute (IRCCS), Italy

Reviewed by:
Phei Er Saw,
Sun Yat-sen Memorial Hospital, China
Junhua Mai,
Houston Methodist Research Institute, United States

***Correspondence:**
Juliana Hamzah
juliana.hamzah@perkins.org.au

Specialty section:
This article was submitted to Cancer Molecular Targets and Therapeutics, a section of the journal Frontiers in Oncology

Received: 16 December 2021
Accepted: 20 January 2022
Published: 22 February 2022

Citation:
Yeow YL, Wu J, Wang X, Winteringham L, Feindel KW, Tirnitz-Parker JEE, Leedman PJ, Ganss R and Hamzah J (2022) ECM Depletion Is Required to Improve the Intratumoral Uptake of Iron Oxide Nanoparticles in Poorly Perfused Hepatocellular Carcinoma. Front. Oncol. 12:837234. doi: 10.3389/fonc.2022.837234

Improving tumor access for drug delivery is challenging, particularly in poorly perfused tumors. The availability of functional tumor blood vessels for systemic access is vital to allow drugs or imaging agents to accumulate in the tumor parenchyma. We subjected mice engineered to develop hepatocellular carcinoma (HCC), to treatment with tumor necrosis factor alpha (TNFα) conjugated to a CSG peptide (CSGRRSSKC). CSG binds to the laminin-nidogen-1 complex of the extracellular matrix (ECM) in HCC. When produced as a recombinant fusion protein, the TNFα-CSG functions as an ECM depletion agent *via* an immune-mediated mechanism to improve tumor perfusion. Tumor perfusion in HCC was dramatically improved after daily intravenous (i.v.) injection of 5 µg TNFα-CSG for five consecutive days. Following treatment, we assessed the tumor accessibility to accumulate an imaging agent, superparamagnetic iron-oxide nanoparticles (IO-NP). Here, we compared the passive delivery of an i.v. dose of IO-NP in HCC following ECM depletion after TNFα-CSG treatment, to the intratumoral accumulation of a comparable dose of CSG-targeted IO-NP in HCC with intact ECM. Magnetic resonance imaging (MRI) T_2-weighted scans and T_2 relaxation times indicate that when the tumor ECM is intact, HCC was resistant to the intratumoral uptake of IO-NP, even when the particles were tagged with CSG peptide. In contrast, pre-treatment with TNFα-CSG resulted in the highest IO-NP accumulation in tumors. These findings suggest poorly perfused HCC may be resistant to molecular-targeted imaging agents including CSG-IO-NP. We demonstrate that specific ECM depletion using TNFα-CSG improves nanoparticle delivery into poorly perfused tumors such as HCC.

Keywords: extracellular matrix, peptide targeting, hepatocellular carcinoma, nanoparticles, tumor necrosis factor, immune cells, perfusion, magnetic resonance imaging

INTRODUCTION

Systemic delivery of therapeutics and imaging agents in tumors relies primarily on accessibility *via* tumor blood vessels (1). The passive delivery of non-targeted agents in tumors is based on the enhanced permeability and retention (EPR) effect of leaky tumor vasculature, resulting in higher accumulation in tumors than in normal tissues (2). However, this passive delivery *via* the EPR effect is insufficient to allow macromolecules and nanoparticles to extravasate and accumulate in the parenchyma of solid tumors (3). More recently, ligands with specific binding affinity to unique molecular tumor targets have been developed for the delivery of therapeutic and imaging payloads including nanoparticle-based contrast agents (4). We have previously reported a tumor extracellular matrix (ECM)-targeting peptide, CSG, that specifically binds to the aberrant network of laminin-nidogen-1 complex in a number of mouse and human solid tumors including breast, pancreatic and liver cancers (5). When CSG is linked to superparamagnetic iron-oxide nanoparticles (IO-NP), CSG-IO-NP accumulate selectively in the stromal ECM, for instance in pancreatic neuroendocrine tumors (PNET) (6).

However, intratumoral binding to specific molecular targets relies on a functional circulation *via* tumor blood vessels. This remains a challenge for clinical and experimental tumors that are heterogeneously perfused and thus represents a significant barrier to drug delivery (7–11). In particular, tumors that develop in the liver, including hepatocellular carcinoma (HCC) are difficult to target for nanoparticle delivery (8–13). Whilst the normal liver is very well-perfused through hepatic arterial and portal venous blood flows, HCC nodules are fed primarily *via* arterial blood supply (8, 13–15). Hence, intravenously injected nanoparticles accumulate preferentially in the normal liver (10, 13). Furthermore, the heterogeneity of blood perfusion in HCC can impede intratumoral uptake of nanoparticles. Dysplastic nodules and early-stage HCC are hyper-vascularized and well-perfused but late-stage and poorly differentiated HCC showed significant decrease in arterial blood supply. Injection of imaging materials detectable by contrast-enhanced computed tomography, ultrasonography and magnetic resonance imaging (MRI) revealed a perfusion defect in advanced-staged HCC compared to the non-cancerous regions (8, 10, 11). Therefore, the use of nanoparticle-based imaging contrast enhancement in HCC diagnosis is often based on non-specific accumulation in the hepatic tissues and small peritumoral vessels surrounding the tumors (16, 17).

We have previously shown that CSG-IO-NP targets the stromal ECM in a PNET tumor model and is a contrast agent superior to untargeted IO-NP in detecting tumor stroma by MRI (6). In addition, we have developed a therapeutic approach to improve tumor perfusion in PNET and breast cancer models using an immune modulating cytokine tagged to CSG peptide, TNFα-CSG. TNFα-CSG treatment induces immune-mediated ECM depletion, which alleviates the compression on the tumor blood vessels and enhances tumor perfusion. TNFα-CSG-treated tumors are then more accessible for systemic uptake of nanoparticles (5).

In this study, we assessed the accumulation of CSG-IO-NP and untargeted IO-NP in poorly perfused HCC with intact ECM, and the passive uptake of IO-NP following ECM-depletion by TNFα-CSG treatment. Our findings indicate that IO-NP have poor access to HCC, even when the particles were targeted with CSG peptide. However, IO-NP accumulation in HCC is significantly improved following pre-treatment with TNFα-CSG. Thus, we demonstrate that TNFα-CSG is a useful ECM-depletion agent that can significantly improve HCC perfusion and facilitate the passive delivery of IO-NP.

METHODS

Animal Models

ALB-Tag mice (on a C3H background) express the oncogene SV40 Large T antigen (Tag) under the control of the mouse albumin gene promoter (ALB), and develop spontaneous HCC as previously described (18). RIP1-Tag5 mice express Tag under the control of the rat insulin gene promoter (RIP) in pancreatic β cells, and develop spontaneous PNET as previously described (19). ALB-Tag or RIP1-Tag5 mice with advanced tumor nodules were used at ≈10–12 or ≈29–30 weeks of age, respectively. All mice were kept under pathogen-free and temperature-controlled conditions in individually ventilated cages, exposed to a 12-hour day-to-night cycle. A minimum of n = 3 mice per group were used in each study. All animal experiments were performed in accordance with the Australian code for the care and use of animals for scientific purposes at the University of Western Australia (UWA) Animal Facility with approval from the UWA Animal Ethics Committee.

In Vivo Lectin Perfusion

Mice were intravenously (i.v., tail vein) injected with 1 μg/μL of tomato lectin (Lycopersicon esculentum conjugated to either FITC or DyLight® 594; Vector). After 10 min of circulation, the mice were heart-perfused with 2% neutral-buffered formalin (w/v) and tumors with surrounding normal tissue were frozen in the O.C.T. compound (Tissue-Tek®).

CSG Peptide and TNFα-CSG Synthesis

Synthetic carboxyfluorescein (FAM)-labelled CSG (molecular weight=1,612.17) was kindly provided by Dr. Vankata Ramana Kotamraju (Sanford Burnham Prebys Medical Discovery Institute, La Jolla, CA, USA). Recombinant murine TNFα-CSG (18.9 kDa) was produced as described previously (5, 20).

In Vivo Peptide and TNFα-CSG Binding

Tumor-bearing mice were injected i.v. with 100 μL of either 1 mM FAM-CSG, FITC-TNFα-CSG or FITC-TNFα in phosphate buffered saline (PBS). After 1 h, animals were euthanised and subjected to transcardial perfusion with sterile PBS to remove unbound peptides or proteins. Tissues, including tumor, heart, liver, spleen, kidney, vertebrae, lung and pancreas were excised and imaged under a UV illuminator (Illumatool, Lightools Research, CA, USA) for assessment of green fluorescence intensity.

Tissues were embedded in O.C.T. (Tissue-Tek®) and stored at -80° C for histology analysis.

TNFα-CSG Treatment

Tumor-bearing mice were i.v. injected once per day with PBS, CSG (0.8 μg), or TNFα-CSG (5 μg) for 4 to 5 consecutive doses. Tumors were analyzed for immune cell infiltration, lectin perfusion and IO-NP uptake within 48 h after final treatment, unless stated otherwise.

Analysis of Intratumoral Nanoparticle Uptake by Magnetic Resonance Imaging

Superparamagnetic iron oxide nanoparticles (IO-NP) with and without CSG conjugation were prepared and analyzed as previously published (6, 21–23). Untargeted IO-NP (6) were injected i.v. (100 μL, 5 mg/kg Fe) in tumor-bearing mice within 24 h after final treatment with TNFα-CSG or CSG peptide. In parallel, untreated tumor-bearing mice received an i.v. dose of CSG-IO-NP as described previously (6). After 4 h circulation, mice were perfused with sterile PBS. Tissues were collected, fixed in 2% formalin for 2 h and embedded in 2% agarose. *Ex vivo* MRI scans were performed at 9.4 T with a Bruker BioSpec 94/30 magnet, Avance III HD console and ParaVision 6.0.1 acquisition software as described previously (5, 6). T2* and T2 parameter maps were calculated from the MGE and MSME datasets, respectively, using the ParaVision 6.0.1 macro *fitinlsa*, which fits the signal for each pixel according to a mono-exponential decay. Image analysis was performed using ImageJ. Tumor volume and IO-NP-induced changes in MRI signal level were measured by using the *Image Display and Processing Tool*. Regions of interest (ROI) for each tumor was manually defined using the *track* tool, based on the MSME image with TE = 8 ms. Statistical analyses for tumor volumes were obtained by combining the ROI statistics on an image slice by slice.

Flow Cytometry Analysis

Tumors and normal liver tissues were excised from PBS-control and TNFα-CSG-treated C3H and ALB-Tag mice, minced and incubated in Dulbecco's Modified Eagle Medium (DMEM) high-glucose medium containing 0.1 mg/ml DNase I (Sigma) and 0.5 mg/ml collagenase IV (Sigma) for 1 h at 37°C under gentle rotation. The cell suspension was passed through a 70-μm membrane filter and subsequently washed with FACS buffer [1% BSA (w/v, Sigma) in PBS]. For analysis of immune cells, viable cells were stained with the following antibodies: CD11b-A488 (M1/70, BD Pharmingen, 1:100), CD68-A647 (FA-11, Biolegend, 1:100), CD8-FITC (53-6.7, eBioscience, 1:100), CD4-FITC (GK1.5, eBioscience, 1:100) and CD45-A700 (30-F11, eBioscience, 1:100). Cells were imaged on a BD SORP Fortessa and analyzed on BD FACSDiva software version 8.0.1 (BD Biosciences, USA).

Histology Analysis

Tissue distribution of bound lectin, FAM-CSG and FITC-TNFα-CSG was detected on 8 μm tissue sections based on their fluorescence intensity. The intensity of FITC-TNFα-CSG and FITC-TNFα in tissues were amplified with anti-fluorescein antibody (polyclonal, LifeTechnologies). For co-staining analysis, the following antibodies were used: anti-SV40 Large T antigen antibody (polyclonal, Santa Cruz, 1:100) anti-CD31 (390; ebioscience, 1:100), anti-laminin (polyclonal; Millipore, 1:200) and anti-nidogen-1 (polyclonal; Millipore, 1:100), CD11b (M1/70, BD Pharmingen), CD68 (FA-11, Abcam), CD8 (53-6.7, eBioscience, 1:100) and CD4 (GK1.5, eBioscience, 1:100). For secondary detection, fluorescence-labelled 488-, 594- or 647-conjugated anti-rat, rabbit or goat IgG (LifeTechnologies) were used. Images were captured on a Nikon Ti-E microscope (Nikon Instrument Inc., NY, USA) or 3DHISTECH Slide Scanner (3DHISTECH, Budapest, Hungary). Image analysis and quantification were performed using NIS software modules (version 4.0).

Statistical Analysis

Statistical analyses were performed using GraphPad Prism 7 (GraphPad Prism Software, San Diego, CA, USA). Data were analyzed by the Student's t-test (two-tailed) or one-way analysis of variance (ANOVA) as indicated. A p value < 0.05 was considered statistically significant. Error bars indicate standard error of the mean (SEM). Experiments were carried out in an unblinded fashion.

RESULTS

Accessibility of ALB-Tag HCC to Lectin, CSG Peptide and TNFα-CSG

Intratumoral perfusion requires functional blood vessels. We first evaluated blood vessel functionality in ALB-Tag HCC in comparison with PNET in RIP1-Tag5 mice using i.v.-injected lectin binding to blood vessels as a surrogate marker for tumor perfusion. **Figure 1A** compares the ALB-Tag and RIP1-Tag5 tumors that were positive for SV40 T antigen. Whilst all vessels in the surrounding normal liver were positive for lectin, ALB-Tag HCC showed only weak traces of lectin-painted blood vessels. In contrast, RIP1-Tag5 tumors visibly displayed lectin-painted blood vessels. This finding suggests that the ALB-Tag HCC is more difficult to access systemically than RIP1-Tag5 tumors.

However, as shown in **Figure 1B**, i.v.-injected fluorescein-conjugated CSG peptide (FAM-CSG), homed specifically into HCC but not other normal tissues including liver. In HCC, FAM-CSG colocalized with its target receptor, the laminin and nidogen-1 complex, which is expressed in tumor ECM (**Figure 1C**). As indicated by nidogen-1 staining in **Figure 1D**, HCC expressed CSG receptor at levels 25-fold higher than the normal liver. In addition, the i.v.-injected FITC-labeled TNFα-CSG also accumulated strongly in HCC compared to the liver tissue (**Figure 1E**). The unconjugated TNFα showed limited tumor uptake (**Figure 1E**). These data demonstrate that CSG-tagged molecules accumulate in HCC tumor parenchyma, and when conjugated to TNFα, have the potential to influence the ECM perfusion barrier.

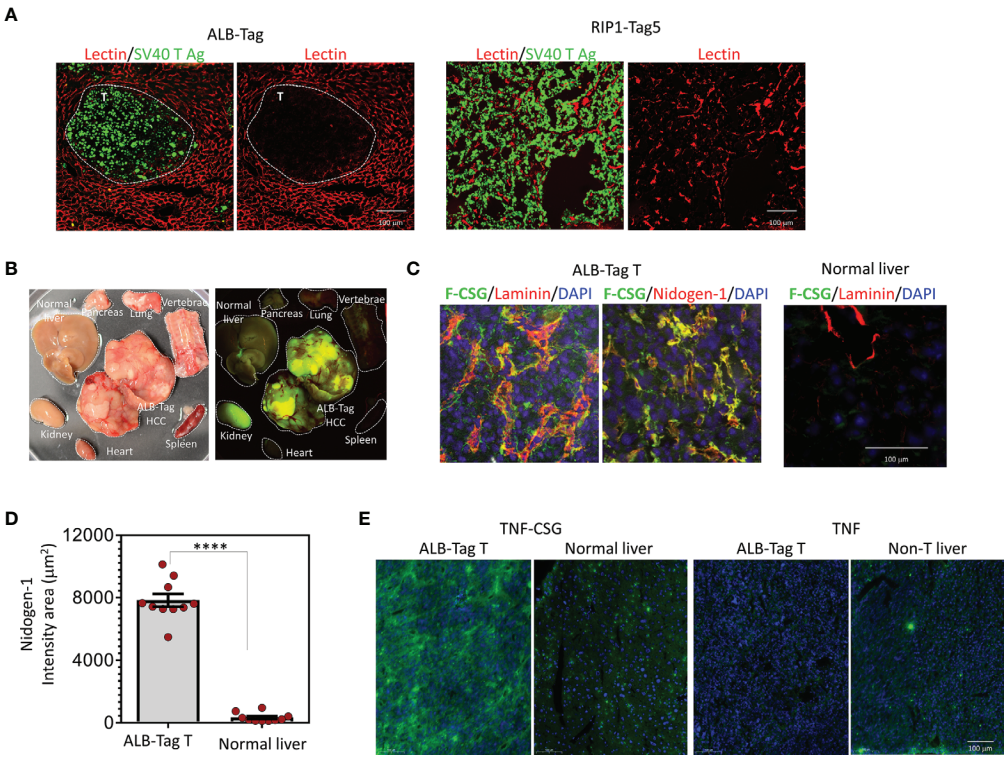

FIGURE 1 | HCC accessibility to lectin and binding specificity to CSG peptide and TNFα-CSG. **(A)** Lycopersicon Esculentum (Tomato) Lectin DyLight® 594 was injected i.v. in mice bearing ALB-Tag HCC or RIP1-Tag5 tumors. Representative micrographs on indicated tissues show lectin-painted vessels (red) in tumors (T) stained with anti-SV40 Large T antigen antibody (green). **(B)** Mice bearing ALB-Tag HCC were i.v. injected with 0.1 mmol of FAM-CSG, and tissues were collected after 1 h of circulation. Photographic image of collected tissues under bright light (left) and UV illuminator (right) are shown. Peptide binding is shown in tumors (green) but not in normal tissues. The kidney is the clearance organ. **(C)** HCC tumors from ALB-Tag mice and normal liver from C3H mice were co-stained for laminin and nidogen-1. Representative micrographs show FAM-CSG binding (green) and laminin or nidogen-1 expression (red). Co-localisation is indicated in yellow. Scale bar 100 µm. **(D)** Quantitative analysis of nidogen-1 staining per field of each tumor or normal liver, as shown in panel **(C)** and mean ± SEM (****P < 0.0001 by Student's *t*-test). **(E)** Analysis of FITC-TNFα-CSG and FITC-TNFα binding *in vivo* detected with anti-FITC antibody (green) and nuclear staining (DAPI) in indicated tissues. Scale bars: 25 µm.

Immune-Mediated Effects of TNFα-CSG in Improving HCC Perfusion

We have previously demonstrated that directing TNFα-CSG to tumor ECM triggers immune cell infiltration which in turn delivers a cocktail of ECM-degrading proteases leading to specific tumor ECM breakdown (5). To assess the intratumoral effect of TNFα-CSG in HCC, ALB-Tag mice and age-matched wild-type C3H mice were treated with an i.v. dose of 5 µg TNFα-CSG per day for five consecutive days. Tumors from ALB-Tag mice and normal liver from C3H mice were analyzed two days after the final treatment for immune infiltrates, ECM content and lectin binding (**Figure 2**). ALB-Tag HCC tumors treated with TNFα-CSG showed significantly higher infiltration of macrophages ($CD68^+/CD11b^+$), $CD8^+$ and $CD4^+$ T cells compared to PBS-treated tumors (gating strategy and FACS plots are shown in **Supplementary Figure S1**). The TNFα-CSG-induced immune cell infiltration was specific to tumors as the immune cell status in normal liver tissue remained unaffected by the TNFα-CSG treatment (**Figures 2A, B**). Intratumorally, the immune infiltrates accumulated mainly in ECM areas positive for nidogen-1 expression (**Figure 2B**).

Next, we assessed changes to the tumor ECM content in response to TNFα-CSG treatment. Data in **Figure 2C** highlight that nidogen-1 staining in TNFα-CSG-treated tumors was significantly lower than in the control PBS-treated tumors. This ECM-depletion effect is consistent with our previous data in other tumor models (5). To determine the effect of ECM reduction on tumor perfusion, lectin binding to tumor blood vessels was compared in TNFα-CSG- treated versus control tumors. **Figure 2D** shows representative tumors with lectin-painted blood vessels co-stained for the blood vessel marker CD31. The indicated micrographs show a lack of lectin-staining in HCC with intact ECM, even though the tumors were positive for vessel staining (CD31). TNFα-CSG-treated tumors show visible lectin-painted blood vessels ($lectin^+/CD31^+$). The quantitative analysis showed a 6-fold increase in lectin-painted tumor blood vessels in TNFα-CSG-treated HCC (**Figure 2D**). These data demonstrate that TNFα-CSG improves blood vessel function in HCC.

Accessibility of IO-NP in Intact and ECM-Depleted HCC

Next, we assessed the intratumoral uptake of CSG-IO-NP in HCC by performing *ex vivo* MRI scans of the ALB-Tag HCC tumors following 4 h *in vivo* circulation of CSG-IO-NP. In parallel, we include the MRI scans of ALB-Tag HCC injected with untargeted IO-NPs, following TNFα-CSG or CSG-peptide control treatment at doses and dosing frequencies as described in **Figure 2**. **Figure 3A** illustrates T2* and T2 relaxation images of scanned HCC based on their small (diameter < 5 mm) and large (diameter > 5 mm) sizes. Based on changes in the T2 relaxation time which indicate the relative amount of IO-NP in tumors, our data (**Figure 3B**) demonstrate that CSG-IO-NP did not effectively accumulate in HCC, unlike previously reported in the RIP1-Tag5 tumors (6). There was no significant difference between CSG-IO-NP and the untargeted IO-NP in HCC with intact ECM. However, our data showed that TNFα-CSG pretreatment induced significantly higher IO-NP accumulation in HCC, when compared to control tumors treated with either CSG-targeted or untargeted IO-NP.

We further confirmed the distribution of IO-NP in HCC by immunofluorescence analysis. **Figure 4** shows micrographs of HCC with and without ECM depletion, immunologically stained for traces of FAM-labelled CSG-IO-NP and FAM-IO-NP and distribution of infiltrating macrophages ($CD68^+$). The micrographs depict higher traces of IO-NP in TNα-CSG-treated HCC compared to CSG-IO-NP in the HCC with intact ECM (**Figure 4A**). The IO-NP distribution in response to TNFα-

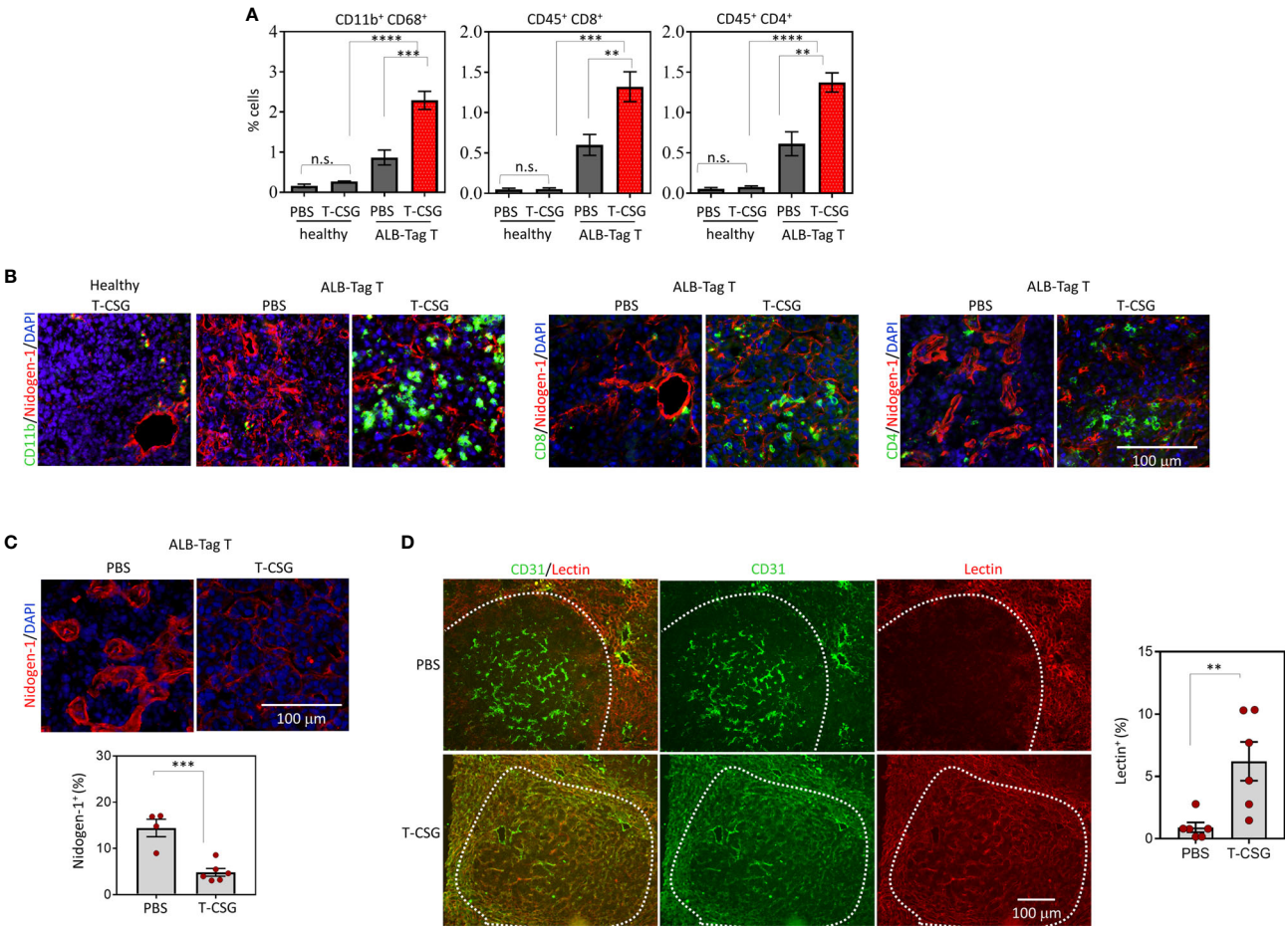

FIGURE 2 | Intratumoral effects of TNFα-CSG on immune cell infiltration, ECM content and lectin perfusion. **(A)** Quantification of immune cells in HCC and normal liver in ALB-Tag and C3H mice treated with daily i.v. injection of PBS or 5 µg TNFα-CSG for five consecutive days. Bar charts show mean ± SEM of cell counts for macrophages ($CD11b^+$/$CD68^+$) and T cells ($CD45^+$ $CD8^+$ or $CD45^+$ $CD4^+$) in each treatment group, **P<0.01, ***P < 0.001, ****P< 0.0001 and n.s. (not significant) when P > 0.05 (by one-way ANOVA test). **(B)** Co-staining of HCC and normal liver sections treated with five daily doses of indicated compounds, as in panel **(A)**. Micrographs depict $CD11b^+$ cells and $CD8^+$ and $CD4^+$ T-cell (green) infiltration particularly around nidogen-1(red)-positive structures. Scale bar: 100 µm. **(C)** Top: Representative tumors from indicated treatment groups indicating changes to nidogen-1 content (red). Bottom: Quantitative analysis of nidogen-1 staining/field/tumor in PBS and TNFα-CSG treatment group and mean ± SEM (***P < 0.001 by Student's *t*-test). **(D)** Co-staining of lectin-perfused HCC [following treatment as in panel **(B, C)**] with CD31 (red, blood vessels). Micrographs show co-localisation (yellow) of lectin and CD31 staining in tumors. Scale bar: 100 µm. Right: Data show the fraction of lectin-positive staining in individual tumors and mean ± SEM (**P < 0.01 by Student's *t*-test).

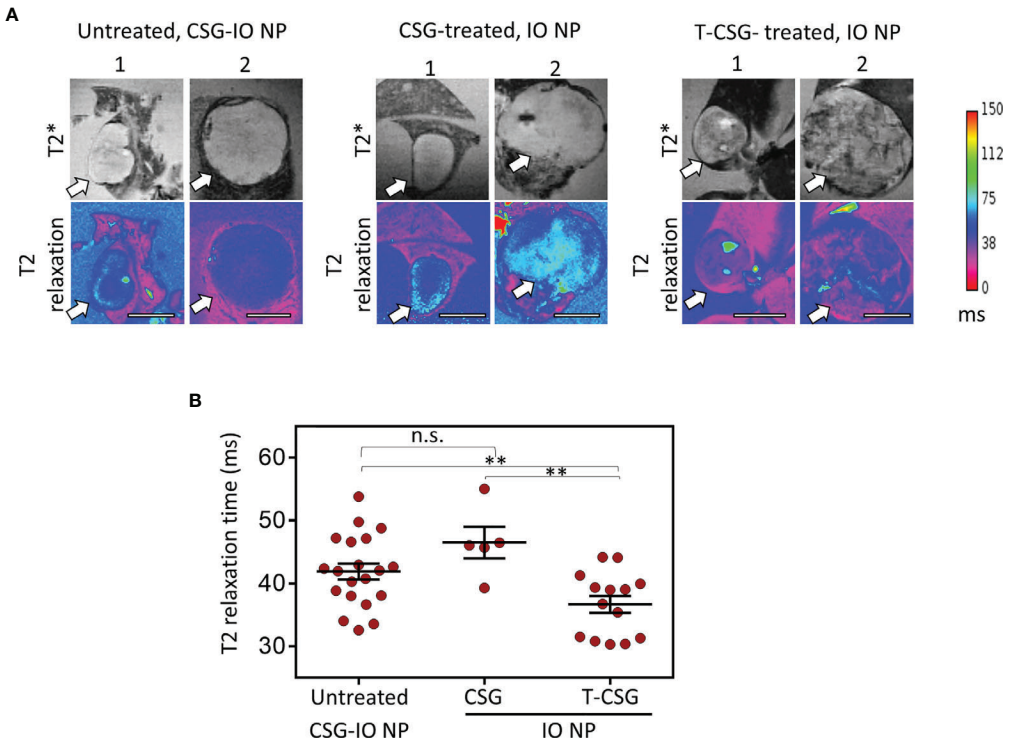

FIGURE 3 | Accumulation of CSG-IO-NP and IO-NP in HCC with intact and/or reduced ECM detected by MRI. **(A)** Representative images of T2*-weighted (top) and T2 relaxation maps (magenta, bottom) from *ex vivo* MRI scans of liver with HCC (tumor sizes, <5 mm and >5 mm in diameter, indicated by arrow). Scale bars: 4 mm. Left: HCC with intact ECM after 4 h *in vivo* circulation of CSG-IO-NP. Middle: HCC treated with 5 × 0.8 μg CSG peptide and then i.v.-injected with untargeted IO-NP. Right: HCC treated with 5 × 5 μg TNFα-CSG and then i.v.-injected with untargeted IO-NP. **(B)** Reduction in T2 relaxation time indicates the relative increase of IO-NP in individual tumors and mean ± SEM per group (**P < 0.01 and n.s. when P > 0.05 by one-way ANOVA test).

CSG treatment exceeds the number of $CD68^+$ macrophages (**Figure 4B**), suggesting that intratumoral accumulation of IO-NP was independent of phagocytic uptake of the nanoparticles by the infiltrating macrophages. Our findings suggests that pre-treatment with perfusion-promoting agents, such as TNFα-CSG, may improve the delivery of nanoparticles especially for poorly perfused tumors, such as ALB-Tag HCC.

DISCUSSION

Our study demonstrates that whilst EPR may be sufficient for some small drug molecules to penetrate solid tumors, poorly perfused tumors may remain inaccessible for larger molecules, including nanoparticles such as IO-NP. Even when IO-NP were tagged with CSG peptide, which is known to improve intratumoral uptake through CSG-specific binding to the aberrantly expressed tumor ECM (6), poorly perfused ALB-Tag HCC remained resistant to IO-NP uptake. IO-NP particles mainly accumulated in the normal liver. However, a short treatment with TNFα-CSG to increase tumor perfusion resulted in significant improvement in the accumulation of IO-NP in the otherwise impenetrable HCC. Therefore, in addition to the normal clearance activity of the liver, these findings highlight that inadequate perfusion of the tumor represents a major barrier that may significantly affect drug delivery and treatment efficacy in HCC.

Systemically injected agents, including nanoparticles, circulate in the blood until they are cleared from the circulation and eliminated from the body either by renal clearance, or by the liver *via* hepatobiliary elimination (15). The liver clearance pathway makes it particularly challenging to develop strategies for the delivery of agents for liver-associated diseases such as HCC. Hence, the drug delivery approach for HCC needs to take into consideration both passive and active mechanisms to improve intratumoral delivery and to minimize non-specific uptake and rapid elimination by the liver (14). Here, we found that HCC tissues are accessible to small molecules including CSG (<1.5 kDa) and TNFα-CSG (18.9 kDa) but less accessible to lectin conjugates (>70 kDa) and larger molecules such as IO-NP.

Our data indicate that CSG, as a free peptide, effectively escapes the rapid and non-specific liver uptake. CSG is an excellent HCC-targeting agent as it binds specifically to aberrant tumor ECM and not to the normal ECM. However, the use of CSG as HCC-targeting agent for intratumoral delivery is greatly influenced by the type and size of payloads. HCC

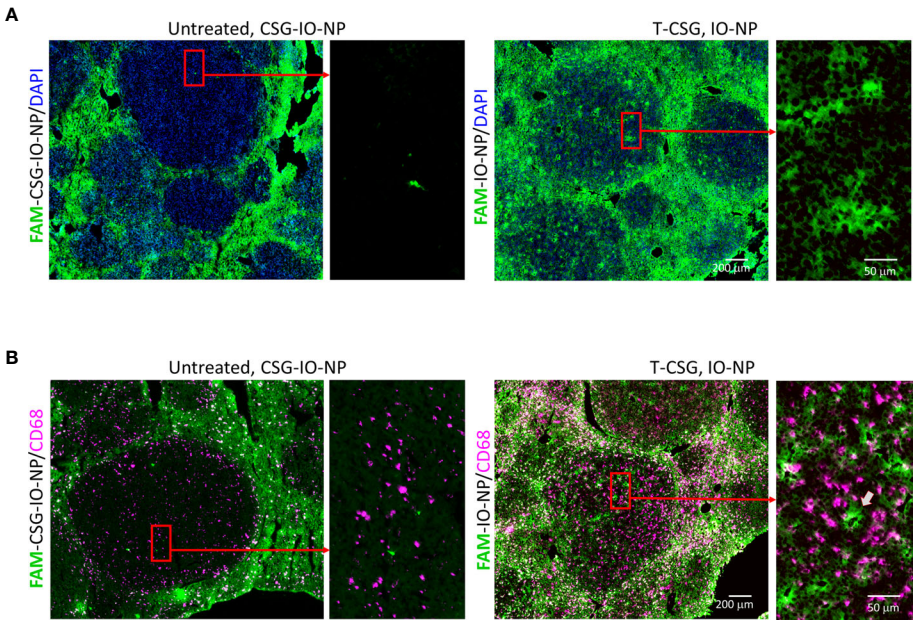

FIGURE 4 | Intratumoral localisation of IO-NP. Liver tissue sections from indicated treatment group 4 h after an i.v. injection of FAM-labelled CSG-IO-NP and IO-NP (as described in **Figure 3**) were analyzed for IO-NP distribution. **(A)** Representative micrographs show detection of FAM-labelled CSG-IO-NP and IO-NP, which were amplified by immunostaining with anti-FITC antibody (green). Rectangular box: Selected regions in HCC were compared for IO-NP accumulation at higher magnification. **(B)** Corresponding tissues in **(A)** were co-stained for $CD68^+$ cells (infiltrating macrophages, red). Arrow: An area within tumor positive for IO-NP that lacks $CD68^+$ cells. Scale bars: 200 and 50 µm.

tissues are inaccessible to the CSG targeted IO-NP, an agent that we have previously shown to be highly effective for intratumoral delivery in tumors with high ECM content such as PNET (6). Similar to the untargeted IO-NP, the CSG-IO-NP mostly accumulated in the non-malignant liver. This finding suggests that the rate of hepatic nanoparticle uptake is quicker and more efficient than CSG-IO-NP access and accumulation in tumors. Our data are consistent with previous reports that found non-specific IO-NP accumulation to be a major challenge for nanomedicines, irrespective of the physical and chemical properties of nanoparticles such as careful control over their surface coating to improve blood half-life, and incorporation of active targeting moieties with specific ligands for enhanced tumor binding (12).

Furthermore, like other treatment-resistant cancers, HCC is comprised of dense stroma with excessive production of ECM (24, 25). Since HCC develops in the setting of cirrhosis in the vast majority of cases, the excessive fibrotic changes with significant matrix deposition and disruption of the hepatic architecture make it extremely challenging for therapeutic agents to penetrate and reach the target cancer cells (26, 27). Our ALB-Tag tumors display some of these microenvironmental features, including the high ECM content and poor perfusion, despite the high level of vascularization of ALB-Tag HCC. TNFα-CSG treatment of mice bearing ALB-Tag HCC increased intratumoral immune cell infiltrates, reduced ECM content and improved tumor perfusion. The observed intratumoral effects in response to TNFα-CSG are consistent with our previous findings in other solid tumor models (5). The ECM-depletion in these tumors was triggered by the protease secretion through increased immune cell infiltration (5). Similar protease-mediated ECM breakdown is likely to occur in HCC, as the TNFα-CSG-treated ALB-Tag tumors showed reduced ECM content. Our ECM-depletion approach to improve tumor perfusion using TNFα-CSG is also consistent with other ECM-reducing strategies to enhance perfusion and increase access to solid tumors (28–31).

An important application of TNFα-CSG treatment may be to sensitize HCC for improved systemic access of nanoparticles such as IO-NP and potentially other HCC-specific therapeutics. CSG binding is conserved in human HCC (5), and thus in addition to its use to enhance diagnostic imaging, TNFα-CSG has the therapeutic potential to improve patient outcome. Currently, most patients are diagnosed with HCC at an advanced stage, when systemic therapy is the only treatment option. The commonly used systemic therapies are the tyrosine kinase inhibitors, sorafenib and lenvatinib, both of which have significant associated toxicity and provide only a marginal survival benefit (32, 33). We have shown that CSG targeting of TNFα dramatically rescued the systemic toxicity associated with untargeted TNFα (5), and therefore ECM-depletion by TNFα-CSG is viable and safe in a preclinical setting. Our data suggest that TNFα-CSG may provide a much-needed novel approach to

improve treatment efficacy by increasing systemic access to these drugs.

DATA AVAILABILITY STATEMENT

The original contributions presented in the study are included in the article/**Supplementary Material**. Further inquiries can be directed to the corresponding author.

ETHICS STATEMENT

The animal study was reviewed and approved by the University of Western Australia Animal Ethics Committee.

AUTHOR CONTRIBUTIONS

Conceptualization, JH and RG. Investigation, YY, JW, XW, and KF. Funding acquisition, JH, RG, and PL. Supervision, JH, KF, and LW. Writing, JH. Review and editing, JH, RG, LW, PL, and JT-P. All authors have read and agreed to the published version of the manuscript.

FUNDING

This research was supported by Cancer Council WA project grant, Perkins Ride to Conquer Cancer, Liver Cancer Collaboration, NHMRC project grants (APP1058073, APP1121131, APP1157240) to JH and RG, and a Cancer Research Institute Clinic and Laboratory Integration Program (CLIP) Grant to RG. JH and RG are the recipients of the Cancer Council Western Australia Research Fellowship and a Woodside Energy Cancer Research Fellowship, respectively.

ACKNOWLEDGMENTS

We thank Meenu Chopra for performing the MRI imaging studies and Ji Li for assisting with FACS analysis. The authors acknowledge the facilities, and the scientific and technical assistance of Microscopy Australia at the Centre for Microscopy, Characterisation and Analysis, The University of Western Australia, a facility funded by the University, State and Commonwealth Governments.

SUPPLEMENTARY MATERIAL

The Supplementary Material for this article can be found online at: https://www.frontiersin.org/articles/10.3389/fonc.2022.837234/full#supplementary-material

Supplementary Figure 1 | Gating strategies and flow cytometry plots of quantification of $CD11b^+/CD68^+$, $CD8^+/CD45^+$ and $CD4^+/CD45^+$ in normal liver (from C3H mice) and ALB-Tag HCC tumors following i.v. injections of PBS or TNFα-CSG (5 μg dose/day) for 5 consecutive days.

REFERENCES

1. Choi IK, Strauss R, Richter M, Yun CO, Lieber A. Strategies to Increase Drug Penetration in Solid Tumors. *Front Oncol* (2013) 3:193. doi: 10.3389/fonc.2013.00193
2. Matsumura Y, Maeda H. A New Concept for Macromolecular Therapeutics in Cancer Chemotherapy: Mechanism of Tumoritropic Accumulation of Proteins and the Antitumor Agent Smancs. *Cancer Res* (1986) 46:6387–92.
3. Prabhakar U, Maeda H, Jain RK, Sevick-Muraca EM, Zamboni W, Farokhzad OC, et al. Challenges and Key Considerations of the Enhanced Permeability and Retention Effect for Nanomedicine Drug Delivery in Oncology. *Cancer Res* (2013) 73:2412–7. doi: 10.1158/0008-5472.CAN-12-4561
4. Ruoslahti E. Peptides as Targeting Elements and Tissue Penetration Devices for Nanoparticles. *Adv Mater* (2012) 24:3747–56. doi: 10.1002/adma.201200454
5. Yeow YL, Kotamraju VR, Wang X, Chopra M, Azme N, Wu J, et al. Immune-Mediated ECM Depletion Improves Tumour Perfusion and Payload Delivery. *EMBO Mol Med* (2019) 11:e10923. doi: 10.15252/emmm.201910923
6. Chopra M, Wu J, Yeow YL, Winterinham L, Clemons TD, Saunders M, et al. Hamzah, Enhanced Detection of Desmoplasia by Targeted Delivery of Iron Oxide Nanoparticles to the Tumour-Specific Extracellular Matrix. *Pharmaceutics* (2021) 13(10):1663. doi: 10.3390/pharmaceutics13101663
7. Gillies RJ, Schornack PA, Secomb TW, Raghunand N. Causes and Effects of Heterogeneous Perfusion in Tumors. *Neoplasia* (1999) 1:197–207. doi: 10.1038/sj.neo.7900037
8. Asayama Y, Yoshimitsu K, Nishihara Y, Irie H, Aishima S, Taketomi A, et al. Arterial Blood Supply of Hepatocellular Carcinoma and Histologic Grading: Radiologic-Pathologic Correlation. *AJR Am J Roentgenol* (2008) 190:W28–34. doi: 10.2214/AJR.07.2117
9. Hectors SJ, Wagner M, Bane O, Besa C, Lewis S, Remark R, et al. Quantification of Hepatocellular Carcinoma Heterogeneity With Multiparametric Magnetic Resonance Imaging. *Sci Rep* (2017) 7:2452. doi: 10.1038/s41598-017-02706-z
10. Imai Y, Murakami T, Yoshida S, Nishikawa M, Ohsawa M, Tokunaga K, et al. Superparamagnetic Iron Oxide-Enhanced Magnetic Resonance Images of Hepatocellular Carcinoma: Correlation With Histological Grading. *Hepatology* (2000) 32:205–12. doi: 10.1053/jhep.2000.9113
11. Yang D, Li R, Zhang XH, Tang CL, Ma KS, Guo DY, et al. Perfusion Characteristics of Hepatocellular Carcinoma at Contrast-Enhanced Ultrasound: Influence of the Cellular Differentiation, the Tumor Size and the Underlying Hepatic Condition. *Sci Rep* (2018) 8:4713. doi: 10.1038/s41598-018-23007-z
12. Haute DV, Berlin JM. Challenges in Realizing Selectivity for Nanoparticle Biodistribution and Clearance: Lessons From Gold Nanoparticles. *Ther Deliv* (2017) 8:763–74. doi: 10.4155/tde-2017-0057
13. Tanimoto A, Kuribayashi S. Application of Superparamagnetic Iron Oxide to Imaging of Hepatocellular Carcinoma. *Eur J Radiol* (2006) 58:200–16. doi: 10.1016/j.ejrad.2005.11.040
14. Baboci L, Capolla S, Di Cintio F, Colombo F, Mauro P, Dal Bo M, et al. The Dual Role of the Liver in Nanomedicine as an Actor in the Elimination of Nanostructures or a Therapeutic Target. *J Oncol* (2020) 2020:4638192. doi: 10.1155/2020/4638192
15. Poon W, Zhang YN, Ouyang B, Kingston BR, Wu JLY, Wilhelm S, et al. Elimination Pathways of Nanoparticles. *ACS Nano* (2019) 13:5785–98. doi: 10.1021/acsnano.9b01383
16. Andreou C, Neuschmelting V, Tschaharganeh DF, Huang CH, Oseledchyk A, Iacono P, et al. Imaging of Liver Tumors Using Surface-Enhanced Raman Scattering Nanoparticles. *ACS Nano* (2016) 10:5015–26. doi: 10.1021/acsnano.5b07200
17. Unterrainer M, Eze C, Ilhan H, Marschner S, Roengvoraphoj O, Schmidt-Hegemann NS, et al. Recent Advances of PET Imaging in Clinical Radiation Oncology. *Radiat Oncol* (2020) 15:88. doi: 10.1186/s13014-020-01519-1
18. Ryschich E, Lizdenis P, Ittrich C, Benner A, Stahl S, Hamann A, et al. Molecular Fingerprinting and Autocrine Growth Regulation of Endothelial Cells in a Murine Model of Hepatocellular Carcinoma. *Cancer Res* (2006) 66:198–211. doi: 10.1158/0008-5472.CAN-05-1636

19. Ganss R, Hanahan D. Tumor Microenvironment can Restrict the Effectiveness of Activated Antitumor Lymphocytes. *Cancer Res* (1998) 58:4673–81.
20. Johansson A, Hamzah J, Payne CJ, Ganss R. Tumor-Targeted TNFalpha Stabilizes Tumor Vessels and Enhances Active Immunotherapy. *Proc Natl Acad Sci USA* (2012) 109:7841–6. doi: 10.1073/pnas.1118296109
21. Kang YS, Risbud S, Rabolt JF, Stroeve P. Synthesis and Characterization of Nanometer-Size Fe3O4 and γ-Fe2O3 Particles. *Chem Mater* (1996) 8:2209–11. doi: 10.1021/cm960157j
22. Starmans LW, Burdinski D, Haex NP, Moonen RP, Strijkers GJ, Nicolay K, et al. Iron Oxide Nanoparticle-Micelles (ION-Micelles) for Sensitive (Molecular) Magnetic Particle Imaging and Magnetic Resonance Imaging. *PloS One* (2013) 8:e57335. doi: 10.1371/journal.pone.0057335
23. Yu M, Huang S, Yu KJ, Clyne AM. Dextran and Polymer Polyethylene Glycol (PEG) Coating Reduce Both 5 and 30 Nm Iron Oxide Nanoparticle Cytotoxicity in 2D and 3D Cell Culture. *Int J Mol Sci* (2012) 13:5554–70. doi: 10.3390/ijms13055554
24. Henke E, Nandigama R, Ergun S. Extracellular Matrix in the Tumor Microenvironment and Its Impact on Cancer Therapy. *Front Mol Biosci* (2019) 6:160. doi: 10.3389/fmolb.2019.00160
25. Pickup MW, Mouw JK, Weaver VM. The Extracellular Matrix Modulates the Hallmarks of Cancer. *EMBO Rep* (2014) 15:1243–53. doi: 10.15252/embr.201439246
26. Forner A, Reig M, Bruix J. Hepatocellular Carcinoma. *Lancet* (2018) 391:1301–14. doi: 10.1016/S0140-6736(18)30010-2
27. Wallace MC, Friedman SL. Hepatic Fibrosis and the Microenvironment: Fertile Soil for Hepatocellular Carcinoma Development. *Gene Expr* (2014) 16:77–84. doi: 10.3727/105221614X13919976902057
28. Caruana I, Savoldo B, Hoyos V, Weber G, Liu H, Kim ES, et al. Heparanase Promotes Tumor Infiltration and Antitumor Activity of CAR-Redirected T Lymphocytes. *Nat Med* (2015) 21:524–9. doi: 10.1038/nm.3833
29. Kirtane AR, Sadhukha T, Kim H, Khanna V, Koniar B, Panyam J. Fibrinolytic Enzyme Cotherapy Improves Tumor Perfusion and Therapeutic Efficacy of Anticancer Nanomedicine. *Cancer Res* (2017) 77:1465–75. doi: 10.1158/0008-5472.CAN-16-1646
30. Provenzano PP, Cuevas C, Chang AE, Goel VK, Von Hoff DD, Hingorani SR. Enzymatic Targeting of the Stroma Ablates Physical Barriers to Treatment of Pancreatic Ductal Adenocarcinoma. *Cancer Cell* (2012) 21:418–29. doi: 10.1016/j.ccr.2012.01.007
31. Rahbari NN, Kedrin D, Incio J, Liu H, Ho WW, Nia HT, et al. Anti-VEGF Therapy Induces ECM Remodeling and Mechanical Barriers to Therapy in Colorectal Cancer Liver Metastases. *Sci Transl Med* (2016) 8:360ra135. doi: 10.1126/scitranslmed.aaf5219
32. Kudo M, Finn RS, Qin S, Han KH, Ikeda K, Piscaglia F, et al. Lenvatinib Versus Sorafenib in First-Line Treatment of Patients With Unresectable Hepatocellular Carcinoma: A Randomised Phase 3 non-Inferiority Trial. *Lancet* (2018) 391:1163–73. doi: 10.1016/S0140-6736(18)30207-1
33. Llovet JM, Ricci S, Mazzaferro V, Hilgard P, Gane E, Blanc JF, et al. Sorafenib in Advanced Hepatocellular Carcinoma. *N Engl J Med* (2008) 359:378–90. doi: 10.1056/NEJMoa0708857

Conflict of Interest: The authors declare that the research was conducted in the absence of any commercial or financial relationships that could be construed as a potential conflict of interest.

Publisher's Note: All claims expressed in this article are solely those of the authors and do not necessarily represent those of their affiliated organizations, or those of the publisher, the editors and the reviewers. Any product that may be evaluated in this article, or claim that may be made by its manufacturer, is not guaranteed or endorsed by the publisher.

frontiers in Oncology

REVIEW
published: 29 March 2022
doi: 10.3389/fonc.2022.867655

Nano-Drug Delivery Systems Entrapping Natural Bioactive Compounds for Cancer: Recent Progress and Future Challenges

Vivek P. Chavda[1†‡], Aayushi B. Patel[2†‡], Kavya J. Mistry[2†], Suresh F. Suthar[2†], Zhuo-Xun Wu[3], Zhe-Sheng Chen[3*†] and Kaijian Hou[4,5*†]*

[1] Department of Pharmaceutics and Pharmaceutical Technology, L.M. College of Pharmacy, Ahmedabad, India, [2] Pharmacy Section, L.M. College of Pharmacy, Ahmedabad, India, [3] Department of Pharmaceutical Science, College of Pharmacy and Health Sciences, St. John's University, New York, NY, United States, [4] Department of Preventive Medicine, Shantou University Medical College, Shantou, China, [5] Department of Endocrine and Metabolic Diseases, Longhu Hospital, The First Afliated Hospital of Shantou University Medical College, Shantou, China

Cancer is a prominent cause of mortality globally, and it becomes fatal and incurable if it is delayed in diagnosis. Chemotherapy is a type of treatment that is used to eliminate, diminish, or restrict tumor progression. Chemotherapeutic medicines are available in various formulations. Some tumors require just one type of chemotherapy medication, while others may require a combination of surgery and/or radiotherapy. Treatments might last from a few minutes to many hours to several days. Each medication has potential adverse effects associated with it. Researchers have recently become interested in the use of natural bioactive compounds in anticancer therapy. Some phytochemicals have effects on cellular processes and signaling pathways with potential antitumor properties. Beneficial anticancer effects of phytochemicals were observed in both *in vivo* and *in vitro* investigations. Encapsulating natural bioactive compounds in different drug delivery methods may improve their anticancer efficacy. Greater *in vivo* stability and bioavailability, as well as a reduction in undesirable effects and an enhancement in target-specific activity, will increase the effectiveness of bioactive compounds. This review work focuses on a novel drug delivery system that entraps natural bioactive substances. It also provides an idea of the bioavailability of phytochemicals, challenges and limitations of standard cancer therapy. It also encompasses recent patents on nanoparticle formulations containing a natural anti-cancer molecule.

Keywords: cancer, chemotherapy, drug delivery system, natural bioactive compound, phytochemical, nanomedicine

OPEN ACCESS

Edited by:
Peixin Dong,
Hokkaido University, Japan

Reviewed by:
Jianxiang Li,
Soochow University Medical College, China
Shanzhi Wang,
University of Arkansas at Little Rock, United States
Zhaoliang Li,
University of Utah, United States

***Correspondence:**
Vivek P. Chavda
Vivek7chavda@gmail.com
Zhe-Sheng Chen
Chenz@stjohns.edu
Kaijian Hou
kaijianhou@126.com

***ORCID:**
Vivek P. Chavda
orcid.org/0000-0002-7701-8597
Zhe-Sheng Chen
orcid.org/0000-0002-8289-097X
Kaijian Hou
orcid.org/0000-0003-1733-0068
Aayushi B. Patel
orcid.org/0000-0002-1086-4369
Kavya J. Mistry
orcid.org/0000-0003-0710-3144
Suresh F. Suthar
orcid.org/0000-0002-3588-880X

These authors have contributed equally to this work and share first authorship

Specialty section:
This article was submitted to Pharmacology of Anti-Cancer Drugs, a section of the journal Frontiers in Oncology

Received: *01 February 2022*
Accepted: *24 February 2022*
Published: *29 March 2022*

HIGHLIGHTS

- Traditional medicines hold a significant role in many healthcare systems around the world.
- According to a World Health Organization (WHO) assessment, conventional medicine meets and/or supplements the fundamental health needs of around 80% of the community in underdeveloped nations.

- Plant-derived anticancer medicines are highly sought after because they are effective inhibitors of cancer cells.
- Although the development of nano drugs is fraught with uncertainty, and the development of potent bioactive chemicals from natural origin is not a popular alternative today, improving the effectiveness of known natural bioactive substances using nanotechnology has become a typical aspect.
- Different drug delivery systems entrapping natural bioactive compounds for cancer treatment are summarized.
- Application of Nano drug-delivery systems for natural anticancer agents can improve bioavailability, biodistribution, therapeutic activity, drug targetting, and stability.

INTRODUCTION

Cancer is an abnormal and autonomous cell proliferation caused by a lack of replication control (1, 2). Delayed assessment and non-responsive treatments are the leading reasons for elevated death rates in cancer patients. Knowledge of the principles underlying tumor biology has resulted in substantial advances in cancer control, diagnosis, and therapy in recent years. Surgery, immunotherapy, radiation therapy, chemotherapy, and targeted hormone medications are all traditional ways of cancer management (3). These strategies are often restricted due to their inadequate specificity, since they might also influence healthy cells and the host immune system, resulting in undesirable adverse effects. Furthermore, except for surgery, all medicines employed in cancer management can generate drug resistance in tumor cells. Therefore, anticancer medication research continues for new and better ways to treat tumors. Medication tolerance remains a major issue in cancer care (3). When there is a poor or no reaction to anticancer medication at the start or throughout therapy, resistance might be innate or inherited. Multidrug resistance (MDR) occurs when a patient develops resistance to one treatment and becomes tolerant to additional unrelated drugs (4). Tumors are made of two fundamental components, replicating neoplastic cells and supporting stroma of connective tissues with blood vessels. Mixed tumors, tumors of parenchyma cells, mesenchymal tumors, and tumors of more than one germ cell layer are all different forms of cancer (5, 6). Exogenous carcinogens might be physical, chemical, or biological (7). Biological carcinogens comprise viruses, bacteria, and parasites. Endogenous chemicals of anabolic and catabolic processes, and cells carrying a dormant virus, are the foundation of carcinogenesis (8). Prevention of carcinogen production, reduction of their activation, and enhancement of their elimination can aid in the prevention of cancers (9). Cancer risk factors in humans involve alcohol use, cigarette use, nutritional inadequacy, insufficient physical activity, pollution, and noncommunicable diseases. Chronic diseases including *H. pylori, hepatitis B, hepatitis C, human papillomavirus*, and *Epstein-Barr virus* are also considered risk factors for cancer (10). Diagnosis of cancer is carried out by tissue sample analysis, blood test, Computed Tomography (CT) scan, endoscopy, and many more such methods. Radiotherapy, chemotherapy, and surgery are the most common cancer treatments; however, novel technologies are also underway (11). Most radiation therapy is used for the treatment of glioblastoma, breast cancer, cervical cancer, laryngeal cancer, and others. Radiation includes high-energy ionizing radiation like X-ray and gamma rays which target the tumor cells and damage DNA directly or through the generation of free radicals (12).

Chemotherapy is a term that refers to a medication that involves the use of synthetic chemicals. Anticancer drugs can be used alone or in combination to damage cancer cells or prevent the growth of a tumor. The main issue with chemotherapy is the side effects associated with anticancer drugs. Side effects result from a lack of specificity towards tumor-causing cells. Anticancer drugs can also affect our normal cells, which may lead to side effects (13, 14). Vinca alkaloids, taxanes, epipodophyllotoxins, camptothecins, genistein, and quercetin or rutin are some plant products associated with cancer treatment. Such herbal medications have a lower index of side effects than allopathic medications that are effective in cancer treatment. Some hormonal treatments are also available for the treatment of tumors. Hormones such as glucocorticoids, estrogen, progesterone, and gonadotropin-releasing hormone (GRH) analogs are effective against some cancers. Radioactive isotopes also have a place in chemotherapy, for example, radioactive iodine ^{131}I is used to treat thyroid cancer (15). Recent developments of plant-based medicines and research associated with them describe that herbal medications for cancer treatment may replace chemotherapy and can be more effective against tumors (16).

THE ROLE OF AYURVEDA IN CANCER THERAPY

Ayurveda is one of the ancient medicinal plant systems (6000 years old) utilized in the current time for curing or suppressing numerous cancers using natural drugs and their extracts (17, 18). The objective of Ayurveda therapy in cancer treatment is to supplement the mind's self-healing powers. It aids in the diagnosis of cancers and provides information on herbs and alternative treatments (19). Cancer-like diseases not only affect physical health but also affect mental health. Discordances between the mind and the body cause a variety of symptoms such as lethargy, anxiety, restlessness, and depression (20). When cancer strikes, it causes disorders in the body and affects the *Tamas* (it is the energy that holds all things together over time) and the *Kapha*. Ayurveda offers a significant psychotherapy technique that has been utilized and is currently being implemented in various nations. Plants are an important resource for medication. Plants like vinca, shattering, guduchi, triphala, and tulsi have been utilized as anticancer agents (21). Ayurveda's goal in treating cancer is to provide preventive, curative, therapeutic, and prophylactic care. Cachexia is a tumor-induced metabolic alteration that triggers an immune response, for which several ayurvedic herbs are used. Ayurvedic medications may not only promote full recovery but also minimize adverse effects in cancer therapy (20). The first goal of Ayurvedic cancer therapy is to regulate and manage *Tridosha* [Vata (wind), Pitta (bile), and Kapha (phlegm), corresponding to the three elements of the universe: air, fire, and water] and *Triguna* (Sattva, Rajas, and Tamas - integral components of the mind). As per Charaka and Sushruta Samhitas, cancer can be

classified as *Arbuda* (major neoplasm), and *Granthi* cancers (minor neoplasm) which fall under group 1 cancer as per Ayurveda that includes *Raktarbuda* (leukemia), *Mamsarbuda* (melanoma), and *Mukharbuda* (oral tumor) (22, 23). Group 2 cancer comprises tumors that are *Tridosaj Gulmas* (tumor of stomach and liver). Group 3 diseases include *Asadhya Kamala* (jaundice) and *Nadi Varna* (sinusitis) (22, 24).

Triguna has an important role in health research fields which contains guna (energy), sattva (quality of reality and purity), rajas (enthusiasm), and tamas (quality of dullness) (25). Triguna is available to everyone and variations in that indicate the health status and nature of a person (26). Ayurvedic treatment of cancer (**Figure 1**) involves i) cleaning and removal of doshas (Sodhna Chikitsa using Panchkarma), ii) serenity of doshas (Somana Chikitsa), iii) rectification of defects (Dhatwangi Chikitsa), iv) immunotherapy (Rasayana Proyaga), v) antineoplastic drugs (Vyadhipratyanika Chikitsa), vi) symptomatic therapy (Lakshanika Chikitsa), vii) surgery (Sastra Chikitsa), viii) maintenance of patient health (Prakritisthapani Chikitsa), ix) restoring the body from disease condition (Rognashini Chikitsa), and x) spiritual treatment (Naishthiki Chikitsa) (26, 27). The general ayurvedic treatment includes maintenance of healthy lifestyle, maintenance of fit digestive power, removal of toxins from the body by *Panchkarma* (method of cleansing the body of all the unwanted waste after lubricating it), revivification by use of Rasayana. Ayurvedic treatment can also be used along with chemotherapy or radiotherapy (28).

HERBAL PLANTS EXHIBITING ANTICANCER ACTIVITIES

Human bodies are made of millions of cells, each of which is a self-contained living organism in and of itself. Ordinary body cells proliferate and replicate for a short amount of time before ceasing to do so. Afterward, they only proliferate when they need to rebuild damaged or dead cells. When this cellular replication mechanism becomes uncontrollable, a tumor develops. Cancer cells' aberrant expansion and division are triggered by DNA destruction in these cells (20).

Traditional medicines hold a significant role in many healthcare systems around the world. Plants' medical and economic advantages are being more widely recognized and developed in both developing and developed countries. A plant or plant component utilized for its aroma, flavor, and/or medicinal characteristics is known as the herb. Herbal medications and phytomedicines are all terms for products manufactured from herbs that are used to preserve or promote wellbeing (29, 30). Plant-based medications make up around a quarter of the current Indian pharmacopeia, according to estimates. Conventional medicinal herbs are organically existing plant-derived drugs that have been utilized to alleviate disease in local or regional healing traditions with little or no chemical modification (31). Preventive care, disease control, serious adverse effects associated with synthetic medicines, and inadequate therapeutic choices for critical diseases are some of the factors for using herbal

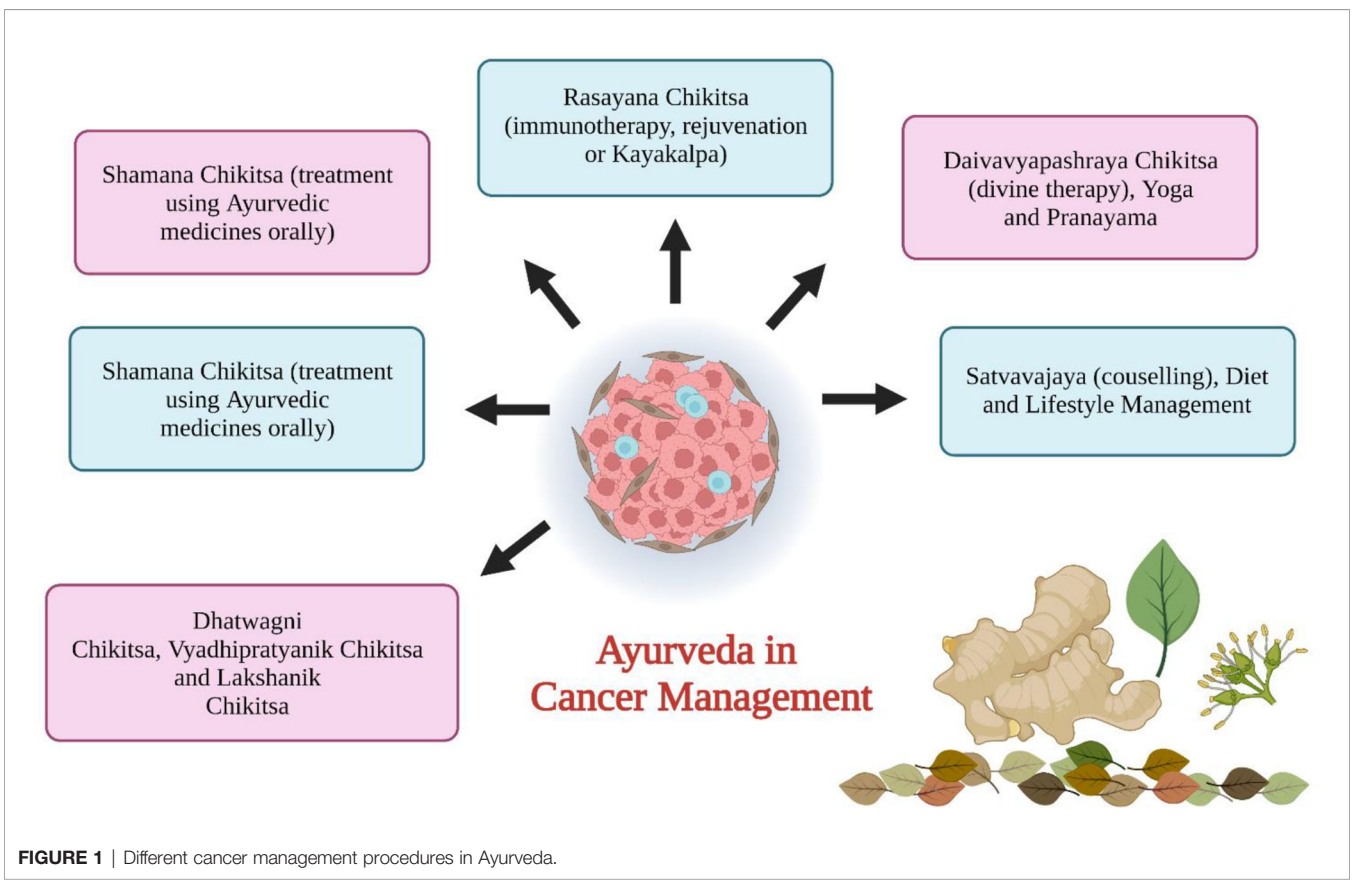

FIGURE 1 | Different cancer management procedures in Ayurveda.

pharmaceuticals (22, 30). Tibetan traditional medicine is still somewhat localized in their nation of origin, while others, like Ayurvedic and Chinese traditional medicines, are becoming more widely utilized across the world. Plants filled with chemicals that may have chemoprotective properties are undergoing clinical studies (32). **Table 1** summarized and describes several plant species based on their common mechanism of action and anticancer therapeutic activities.

BIOAVAILABILITY OF PHYTOCHEMICALS

Food-derived chemicals reach the circulatory system and are transported to certain tissues where they exert physiological properties. Nutritional phytochemicals are metabolized and carried by the gastrointestinal epithelium before entering the circulatory system (111). The complexity of the biological system include:

- Food material variety and human subject (digestion difference in infants, adults, and the elderly, even there is difference between female and male digestion)
- Complex interactions occur between food/chemicals throughout storage, processing, digestion, and absorption that potentially alter health benefits.
- The process pathways such as compound solubility, gut pH, gut microbiota metabolism, penetration through the intestinal wall, efficient efflux mechanism, and metabolic activities in the first pass may alter the bioavailability of phytochemicals (112, 113).

As per Meyskens and Szabo, the majority of studies recognize one nutrient as the potential cause while ignoring the impact of other phytonutrients or biological factors. As a consequence, in clinical investigations for a certain molecule, the entire diet must be considered (114). According to Lipinski's rule of five, a substance will be more effective if it contains not more than (NMT) 5 hydrogen-bond donors, NMT 10 hydrogen-bond acceptors, a molecular mass of NMT 500 daltons, a partition coefficient (log P-value) of NMT 5, and NMT 10 rotatable bonds (115). The exceptions include polyphenols like curcumin and green tea. The lymphatic system, instead of the circulatory system, provides phenols with better bioavailability. Molecular forms of phenolics, including glycone or aglycone, can affect absorption that results in variations in bioavailability.

Through uptake and efflux channels on the epithelial cell surface, the intestinal epithelium tissue provides a significant impact on bioavailability. P-glycoprotein, breast cancer resistance protein, and multidrug resistance protein 2 are the primary chemopreventive drug transporters (116). The ATP-binding cassette transporter family has the transport proteins that help nutrients, medications, and metabolites get back into the intestinal lumen. Only nanomolar amounts were available in the blood because of migration (117).

Many medicines that were transferred from *in vitro* to *in vivo* studies were rejected because their findings were insufficient. The chemicals were discovered to be unstable in the stomach and to have low bioavailability, which might have contributed to the clinical failure. Higher dosages were used to overcome the low absorption, which resulted in toxicity to numerous organs despite effectiveness (118). Adverse responses were also seen in some trials, including the SELECT (Selenium and Vitamin E Cancer Prevention Trial) in prostate cancer, which was terminated owing to a negligible rise in prostate cancer incidences. A follow-up analysis of the individuals revealed a substantial increase in prostate cancer incidence in the high vitamin E group years later, even though they had stopped using the supplements (119).

As a result, assessing the bioavailability of drugs purely based on their physicochemical characteristics becomes challenging. Molecular metabolism changes the bioavailability of the compound. Chemicals that prevent the metabolism of other chemicals can enhance their bioavailability. Piperine (derived from black pepper) inhibits the glucuronidation (metabolism) of some chemicals such as tea polyphenol, epigallocatechin-3-gallate, and curcumin increasing their bioavailability (120). Piperine has also been expected to enhance the length of the intestinal microvilli and the fluidity of the intestinal brush border membrane with an enlarged absorptive surface in the small intestine (121). Quercetin and myricetin can prevent resveratrol sulfation and glucuronidation, resulting in increased resveratrol bioavailability (122, 123).

DRUG DELIVERY SYSTEMS ENTRAPPING NATURAL BIOACTIVE COMPOUNDS FOR CANCER

Multiple novel drug delivery systems (NDDS) have been established during the last two decades, with the primary goal of improving medication bioavailability, preventing adverse impacts, and preventing drug degradation (124). A drug delivery system is based on the idea that pharmaceuticals should be given directly to the region of activity by the demand of the body, and another delivery system is routed *via* drug delivery into the site of action (125). Additional benefits of NDDS include greater solubility, improved bioavailability, less undesirable side effects, boosted therapeutic action, better stability, and better drug distribution. It also involves the regulation of pharmacokinetics, pharmacodynamics, and immunogenicity (126).

The benefit of NDDS is for more patient convenience in drug administration (126–128). Drugs are released from the drug delivery systems *via* two mechanisms, passive and active targeting. One instance of passive targeting is the preservation of chemotherapeutic drugs in solid tumors, which results in enhanced tumor vascular permeability. Active targeting which includes specific receptors on the surface of the cell and ligand-receptor interactions, is extremely specific for interaction (20, 129).

Through this review article, we tried to thoroughly evaluate recent statistics on the effectiveness of herbal medicines in cancer with nano-formulations. We have started searching through major databases

TABLE 1 | Herbal plants with anticancer properties.

Plant name	Part of plant	Family	Phytochemicals	Therapeutic anticancer action	Mechanism of action
Achillea wilhelmsii k. (Yarrow) (33)	Leaf essence	Asteraceae	Methanol, flavonoids, 1,8-cineole and α-piene	Breast, colon, and stomach cancer treatment	• Suppress reproduction of cancer cells through inducing apoptosis inhibition of
Aconitum napellus L. (Aconite) (29, 34)	Dried root	Ranunculaceae	Aconitine, hypaconitine, neopelline, napelli neoline	Treatment of rheumatism, inflammation, and melanoma	• Phosphatidylinositol 3-kinase (PI3K)/protein kinase B (AKT) signaling pathways • Mitogen-activated protein kinase (MAPK)/extracellular signal-regulated kinase (ERK)1/2 signaling pathways
Acronychia Baueri schott (Aspen) (29, 35)	Bark and leaf extract	Rutaceae	Triterpene lupeol and alkaloids-melicopine, acronycin, and normelicopidine.	Antitumor activity in adenocarcinoma and leukemia	• Cytotoxic-causes cell death
Allium sativum L. (Garlic) (29, 36–39)	Fresh garlic extract, aged garlic, garlic oil, and several organo sulfur compounds	Liliaceae	Methyl allyl trisulfide, diallyl trisulfide, allicin, s-allyl cysteine, s-allyl mercapto-L-cysteine	Anticancer activity in breast cancer cell lines	• Cell cycle arrest • Generating reactive oxygen species (ROS), • Activate stress kinases, • Stimulates the mitochondrial pathway for apoptosis • Cyclooxygenase 2 (COX-2) suppression, • Caspase-3 activation
Ammi majus L. (Bishop's weed, bullwort) (1, 40, 41)	White flower	Apiaceae	Psoralen	Anticancer effect on MCF7 and HeLa cell line	• Inhibit cytochrome p450 activity
Amomum tsaoko (Chinese black cardamom) (42, 43)	Essential oil, leaf, and seed extracts	Zingiberaceae	18-cineole, geraniol, geranial, α-terpineol, α-phellandrene, Neral, β-pinene, p-propyl benzaldehyde	Antiproliferative action in liver ovarian, and cervical cancer. For adenocarcinoma treatment.	• Suppression of signal transducer • Activator of transcription 3 (p-STAT3)/nuclear factor kappa-light-chain-enhancer of activated B cells (NF-kB)/interleukin 6 (IL-6) and vascular endothelial growth factor (VEGF) loop
Aniba rosaeodora ducke (Pau-rosa) (44)	Wood oil	Lauraceae	Essential oil, linalool	Cytotoxic activity in skin cancer	• Depolarization of the mitochondrial membrane • Caspase-dependent cell death characterized by phosphatidyl serine externalization
Artemisia absinthium L (Wormwood, absinthium) (30, 45)	Plant extract	Asteraceae	Quercetin, isorhamnetin, alphapinin, kamfrolinalol, limonene, myrcene, α-pinene, β-pinene, limonene, artemisinin, artesunate	Anticancer activity in leukemia, colon cancer, breast cancer, hepatic cancer, and melanoma	• Inhibiting cell's growth • Apoptosis • Preventing angiogenesis • Preventing cell migration, • Decreasing responses of core receptors
Artemisia capillaries thunb (Wormwood) (46, 47)	Unexpanded flower heads	Asteraceae	Essential oil, aantonin, artemisinin	Antioxidant, Anticancer effect in leukemia, prostate cancer, lung cancer, liver cancer, and breast cancer cell lines.	• Inhibiting cell growth and induction of apoptosis, • Reduction in expression of proliferating cell nuclear antigen (PCNA), • Inhibiting the PI3K/AKT pathway
Astragalus membranaceus Bunge (Milkvetch) (29, 48, 49)	The root	Fabaceae	Polysaccharides, Flavonoids, and Saponins	Antitumor, immuno modulating, antioxidant, and anti-inflammatory	• Direct antiproliferation or pro-apoptosis effect on tumor cells
*Astrodaucus Orientalis L (*1, 50, 51*).*	Extract of root and above-ground plant parts	Umbellate	α-Pinene, α-thujene, α-copaene, fenchyl-acetate, anisole, myrcene, and sabinene	Anti –proliferation effects on breast cancer cells (T47D)	• Inhibits cell cycle and also induction of apoptosis
Beta vulgaris L.(Beet) (52)	Root extract	Amaranthaceae	Betalains, betacyanins, and feruloylbetanin	Anticancer effect in breast cancer, and colorectal cancer	• Cytotoxic action
Boswellia sacra fluck (Arabian incense) (53, 54)	Resinous dried sap, and essential oil	Burseraceae	α-pinene, α-thujene, β-pinene, myrcene, boswellic acid, α-phellandrene	Antiproliferative, and anticancer action in breast and bladder carcinoma	• Inhibiting tumor growth • Induces apoptosis with severe damage to cells by activating caspases

(Continued)

TABLE 1 | Continued

Plant name	Part of plant	Family	Phytochemicals	Therapeutic anticancer action	Mechanism of action
Camellia sinensis (L.) kuntze (Green tea) (55, 56)	Prepared leaves and leaf buds	Theaceae	(+)-gallocatechin (–),-epicatechin (–),-epigallocatechin (–),-epicatechin gallate, epigallocatechin gallate	Antimutagenic, and antibacterial	• Inhibits 5-alfardoctase enzyme in prostate cancer
Camptotheca Acuminate decne (29, 57)	Bark seeds, and dried stem wood	Nyssaceae	Camptothecin, quinoline alkaloid (camptothecin, and 10- hydroxy camptothecin)	Antileukemia	• DNA–topoisomerase inhibitors
Casearia sylvestris Sw. (Wild sage) (58)	Shrub(wild)-leaf extract, essential oil, bark, seed oil, and macerated roots	Salicaceae	α-pinene, α-humulene, β-caryophyllene, bicyclogermacrene, spathulenol	Cytotoxic, and antitumor action	• Cell proliferation inhibition
Catharanthus roseus (L.).G.Don. (Vinca, periwinkle) (59)	Dried whole plant	Apocynaceae	Vinca alkaloids (Vincristine, vinblastine, leurosine, vindesine, and vinorelbine), ajmalicine, catharanthine, vindoline	Anticancer, and antineoplastic	• Cell cycle arrest by inhibition of spindle formation
Citrullus colocynthis(L.) Schrad (Bitter apple) (60, 61)	Yellow bitter fruit	Cucurbitaceae	Quercetin, β-sitosterol, and cucurbitales	Anticancer effect in liver cancer, breast cancer, and larynx cancer	• Inhibition of cell cycle and apoptosis induction
Commiphora gileadensis (L.)C.Chr (Balsam of Gilead) (62)	Gum, fruit, and essential oil	Burseraceae	Sabinene, germacrene-D, α-pinene, β-caryophyllene	Antiproliferative in skin cancer	• Increase in caspase 3 activity
Crocus sativus L. (Saffron) (63, 64)	Stigma	Iridaceae	Crocin, crocetin, picrocrocin, and safranal	Anticancer in cervical and breast cancer	• Inhibiting DNA synthesis
Curcuma longa L. (Turmeric) (65)	Dried as well as fresh rhizome	Zingiberaceae	Curcumin, and curcuminoids	Antitumor activity in cervical cancer, leukemia, and lymphoma	• Inhibition of telomerase activity
Curcuma zedoaria Salisb (White turmeric, zedoaria or gajutsu) (29, 66, 67)	Rhizome	Zingiberaceae	Isocurcumenol, α-curcumene	Antitumor activity in ovarian cancer, cervix cancer, and uterine cancer	• Inhibiting the proliferation of cancer cells without inducing significant toxicity to the normal cells. • Chromatin condensation, • DNA cleavage, nuclear fragmentation, and activation of caspases
Daucus carota L. (Wild carrot, birds nest, Queen Anne's lace, Devils Plague, Bee's nest Plant) (68)	Seed, root, leave, and flower	Apiaceae (Umbelliferae)	Epilaserine	Inhibitory effect on leukemia cells, breast cancer, and colon cancer	• Down-regulation of ERK
Ferula assa-foetida L. (Asafoe tida) (69)	Resin	Apiaceae	Coumarin compounds, β-sitosterol and oleic acid.	Antitumor activity in colon cancer, liver cancer, ovarian cancer, and lung cancer	• Impairing gene mutation, • Affecting enzyme function, • Preventing DNA degradation, • Influencing cell proliferation, and • Altering enzyme action in the cells.
Glycyrrhiza glabra L. (Licorice) (70)	Root and stolon	Leguminosae	Licochalcone, glycurrhizin, and glycyrrhizinic acid	Antitumor activity in gastric cancer	• Arrests cells in G2/M were accompanied by suppression of cyclin B1 and CDC2. • Phosphorylation of Rb inhibited • Expression of transcription factor E2F decreased along with the reduction of cyclin D1 • Down-regulation of cycline dependent kinase (CDK) 4 and 6 along with increased cyclin E expression
Hydrastis Canadensis L. (Golden seal) (71, 72)	Rhizome	Ranunculaceae	Hydrastine, berberine, berberastine, hydrastinine, tetrahydroberberastine, and canadine	Anticancer activity in liver, lung cancer, colon cancer, and oral cancer	• Inhibits serine/threonine-protein kinase (PAK) 4 activity and its signaling pathways

(Continued)

TABLE 1 | Continued

Plant name	Part of plant	Family	Phytochemicals	Therapeutic anticancer action	Mechanism of action
Inonotus obliquus (fungus) (Chaga mushroom) (73)	Leaves(wild)	Hymenochaetaceae	3β-hydroxy-lanosta-8, 24-dien-21-al, inotodiol and lanosterol	Anticancer-(lung carcinoma A-549 cells, stomach adenocarcinoma AGS cells, breast adenocarcinoma MCF-7 cells, and cervical adenocarcinoma HeLa cells)	• Stimulate the immune system, • Promote apoptosis, and inhibit angiogenesis
Lagenaria siceraria (molina) Standl (Bottle gourd) (74)	Aerial parts	Cucurbitaceae	Vitamin C, β-carotene, vitamin group B, saponins, and cucurbitacin	Breast cancer, and lung cancer treatment	• Cytotoxic to cells
Larrea divaricate Cav (Chaparral) (75)	Aqueous extract	Zygophyllaceae	Nordihydroguaiaretic acid, guaiaretic acid and its derivatives	Antiproliferative in breast cancer	• Cytotoxic effect in arresting cell viability
Lepidium sativum L. (Watercress, Rashad) (1, 76)	Seeds, and aerial part	Brassicaceae	Antioxidants-vitamins E, C, B, A, isotiosinat, and omega-3 fatty acids	Anticancer activity in leukemia, and bladder cancer	• Induction of apoptosis, and • Antioxidant action
Lippia alba (mill).N.E.Br (Bushy mat grass, bushy lippia, hierba Negra and pitiona) (77)	Essential oil	Verbenaceae	Geranial,neral,geraniol, trans-β-caryophyllene,6-methyl-5-hepten-2-one, limonene,linalool	Citral dependent toxicity	• Cytotoxicity resulting in cell cycle arrest and induction of apoptosis
Lycopersicum esculentum mill. (Tomato) (78)	Leaves	Solanaceae	Phenolics, lycopene, glycoalkaloids, anthocyanin, ascorbic acid, tomatine, and carotenoids	Anti-cancer activity in breast cancer, and prostate cancer	• Inhibition of PI3K/AKT signaling pathway
Medicago sativa L. (Alfalfa) (79, 80)	Plant extracts	Fabaceae	Phytoestrogens and trepans	Hormone-dependent cancer treatment	• Phytoestrogens-strong estrogenic activity of this plant is useful in treating hormone-dependent cancers.
Morus alba L. (White mulberry) (81)	Fruit, leaves, root, and bark	Moraceae	Kuwanon G, moracin M, steppogenin-4′-O-β-D-glucoside and mulberroside A.	Anticancer effect in lung cancer patients, and colorectal cancer	• Suppressing inducible nitric oxide synthase (iNOS), • Inhibit NF-κB activation, and cyclin D1 downregulation
Myrtus communis L. (Mort) (82)	Plant extracts	Myrtaceae	Polyphenols, myrtucommulone, and semi-myrtucommulone	Breast cancer treatment	• Cytotoxic effect on cell layer with cell apoptosis induction
Nigella sativa L. (Fennel flower) (83)	Black seed	Ranunculaceae	Kvyynvny compounds and dinitro-quinone	Anticancer activity in kidney cancer, colorectal cancer, and breast cancer	• Induction of apoptosis, and • Increased cell morphological changes
Olea Europe L. (Olive) (84)	Oil, and leaf	Oleaceae	Pinoresinol, oleuropein, maslinic acid and oleanolic acid	Anticancer activity in colon cancer, and breast cancer	• Inhibit cell proliferation and angiogenesis. • Breast cancer directly act on her-2 gene
Panax ginseng C.A.Mey (Ginseng) (85, 86)	Dried root	Araliaceae	Ginsenoside Rp1 panaxosides, chikusetsusaponin	Anticancer effect in breast cancer	• Natural killer (NK) cell activation
Pfaffia paniculata (martius) kuntze (Brazilian ginseng) (86)	Roots	Amaranthaceae	Butanolic extract	Anticancer effect in breast cancer	• Degeneration of cytoplasmic elements, • Significant morphological and nuclear modifications of cancer cells.
Platycodon grandiflorum (jacq.) A.DC. (Balloon flower, Chinese bellflower, or platy codon) (87)	Roots	Campanulaceae	Platycodin D (PD) and platycodin D3	Anticancer effect in lung cancer, and skin cancer patients	• Inducing apoptosis • Up-regulation of Fas/FasL, • Mitochondrial dysfunction, • Bcl-2 family protein modulation, • ROS generation, • Inhibition of inhibitors of apoptosis, • Mitotic arrest induction, • Activation of Mitogen-activated protein kinase (MAPK) pathway,

(Continued)

TABLE 1 | Continued

Plant name	Part of plant	Family	Phytochemicals	Therapeutic anticancer action	Mechanism of action
					• Telomerase activity activation and pro-survival pathways suppression -such as AKT, cell cycle arrest, autophagy, and inhibiting angiogenesis
Pelargonium peltatum L. (Mayapple, American mandrake, wild mandrake, and ground lemon) (29, 88)	Dried rhizomes and root of Podophyllum peltatum	Berberidaceae	Podophyllotoxin-resin, podophyllin	Lymphadenopathy, and treatment of certain tumors.	• Block cells in the late S to G2 of the cell cycle, • DNA synthesis inhibition, • Cell cycle arrest
Polygonum multiflorum Thunb. (He shouwu, Fo-ti) (89)	Root	Polygonaceae	Anthraquinones, physcion, emodin, and questin	Anti-cancer activity in colon cancer	• Inhibition of the enzymatic activity of Cdc25B phosphatase
Prunus armeniaca L.(Apricot) (90, 91)	Wood, kerne, seed	Rosaceae	Hydrogen cyanide, camphene, benzaldehyde, hexanol, γ-butyrolactone, γ-terpinene	Anticancer effect in lung cancer, and breast cancer patients	• Apoptosis induction, • Reduction in the expression level of Bax and c-FLIP genes
Ricinus communis L. (Castor seed) (92)	Seeds	Euphorbiaceae	Alkaloids, ricinoleic acid, stearic, linoleic, palmitic acid	Treatment of skin cancer	• Cytotoxic and apoptosis induction
Toxicodendron vernicifluaam (*Stokes) F.A.Barkley* (Chinese lacquer tree) (93–95)	Bark extract	Anacardiaceae	Gallic acid, fustin, fisetin, quercetin, butein, and sulfuretin	Anticancer effect in lung cancer, pancreatic cancer, breast cancer, colorectal cancer, and uterine cancer patients	• Modulation of 5' adenosine monophosphate-activated protein kinase (AMPK) pathway
Sanguinaria Canadensis L. (Bloodroot, Bloodwort, Coon Root) (96)	Rhizome	Papaveraceae	Sanguinarine, chelerythrine	Anticancer potential for prostate carcinoma	• Modulation of cyclin kinase inhibitor-cyclin-cyclin-dependent kinase machinery
Silybum marianum L. (Cardus marianus, M*ilk thistle*, Blessed milk thistle, Marian thistle) (1, 97)	Seeds	Asteraceae	Silymarin	Anticancer activity	• Cell cycle arrest and apoptosis
Solanum nigrum L. (Barley and wheat) (98, 99)	Juice of root, fruit	Solanaceae	Lunasin	Cancer-breast cancer treatment, chemopreventive, tonic, laxative, appetite stimulant, treating asthma, skin disease, whooping cough	• Increase in DNA fragmentation
Stephania tetrandra S.Moore (Agrimony) (100)	Root and aerial part	Menispermaceae	Tetrandrine, fangchinoline, cepharanthine, dehydrocrebanine, roemerine, *N*-methylcoclaurine	Anticancer activity in gastric cancer	• Inducing pro-death apoptosis and autophagy
*Handroanthus impetiginosus (Mart. ex DC.) Mattos (*Lapacho tree, Pink Tabebuia, Deep Pink Tahebuia) (29)	flowers, leaves, and roots	Bignoniaceae	β-lapachone, lapachol, napthoquinone	Chemopreventive for liver cancer	• DNA topoisomerase inhibition
Taxus Brevifolia Nutt (Western yew) (101)	Dried leaves, bark and root	Taxaceae	Taxane, taxol, cephalomannine, 10-diacetyl baccatin, docetaxel and paclitaxel	Lung carcinoma, gastric and cervical cancers and also carcinomas of head, breast, ovary, skin, neck, prostate and colon	• Preventing the de-polymerization of tubulins
Thymus fallax Fisch. et Mey (Thyme) (102)	Plant oil	Lamiaceae	Carvacrol,p-cymene, thymol, and γ-terpinene	Antioxidant, and antibacterial	• DNA repair modulation
Thymus vulgaris L. (Garden thyme) (103, 104)	Leaves	Lamiaceae	Thymol and carvacrol	Treatment of squamous cell carcinoma of the head and neck, breast and colorectal cancer treatment	• Cell proliferation inhibition
Tussilago farfara L. (Coltsfoot) (95, 105)	Flower bud, Leaves	Compositae	Senkirkin, kaempferol and quercetin glycosides,	Anticancer effect in lung cancer patients, colon cancer, and in brain cancer	• Cytotoxic effect

(Continued)

TABLE 1 | Continued

Plant name	Part of plant	Family	Phytochemicals	Therapeutic anticancer action	Mechanism of action
			saponins, ascorbic acid, sesquiterpenoid		
Uncaria tomentosa (Willd. ex Schult.) DC. (Cat's claw) (105)	Bark extract	Rubiaceae	Oxindole alkaloid	Treatment of breast cancer	• Cell decrease at the G_2/M phase
Urtica dioica L (106)	Aqueous and ethanolic root extract	Urticaceae	Phenolic compounds	Esophageal, and prostate cancer treatment	• Antiproliferative,antioxidant action
Viola Odorata L. (English violet) (107)	Dried aerial parts	Violaceae	Cycloviolacin O_2 Essential oil, alkaloid, saponins, glycoside of methyl salicylate.	Expectorant,anti-cancer diaphoretic, antibacterial, antipyretic	• Cell death by membrane permeabilization
Viscum album L. (European mistletoe) (108)	Plant extract	Santalaceae	Viscum album agglutinin-1	Treatment of murine tumors, Lewis lung carcinoma, colon adenocarcinoma 38 and C3H mammary adenocarcinoma 16/C	• Biological response modifying agent • Cytotoxic action
Vitis vinifera L. (Grapeseed) (109)	Leaves, and fruits	Vitaceae	Proanthocyanidins, Resveratrol (Trans-3,4',5-Trihydroxy-stilbene)	Antitumor,and antioxidant	• Simultaneous effects on signaling pathways related to extracellular growth factors and receptor tyrosine kinases; • Formation of multiprotein complexes and effect on cell metabolism
Zingiber officinale Roscoe (Ginger) (29, 110)	Rhizomes	Zingiberaceae	Volatile oil, fat, fiber, starch, inorganic material, residual moisture and acrid resinous matter.	Anti-cancer and anti-inflammatory agents.	• Inactivating NF-κB through the suppression of the pro-inflammatory tumor necrosis factor (TNF)-alpha

such as Web of Science, PubMed, Scopus, Elsevier, Springer, and Google Scholar with keywords like "herbs for cancer' "Nanoherbal formulations for cancer", "Anticancer Phytochemicals" and then we started with a specific search. From the identified components, first, we have omitted the components for which no strong literature support is available. From the remaining components, we have considered the compounds based on the *in vivo* data evaluation and searched for specific research around anticancer phytochemicals. Later on, from the highly researched components against anticancer phytochemicals, a clinical trial database is evaluated. We have incorporated clinical trial outcomes for the majority of the components if not then in certain cases a cogent discussion on *in vivo* studies is incorporated. Very recent published data is considered for the review of anticancer herbal nanoformulations. NDDS of various sorts are made up of various ingredients, and these drug delivery systems are used for drug administration in the body as well as with certain additional pharmacokinetics and pharmacodynamics properties. **Table 2** illustrates the various drug delivery systems for herbal anti-cancer substances while **Figure 2** summarizes the various nanotechnology-based drug delivery platforms for the delivery of anticancer phytochemicals.

The drug delivery systems listed in **Table 2** are extensively and separately discussed in the following section of this review.

Biopolymer-Based Nanocarrier (BBN)

Biopolymers are macromolecules that are divided into three classes: polysaccharides (chitosan, dextran, cyclodextrins, pectin, hyaluronan, guar gum, sodium alginate, cellulose, and starch), proteins (gelatin, albumin, and milk proteins), and nucleic acids (161). To use BBN as a drug delivery vehicle, it is critical to control particle size, the charge on the particle, and specific surface area (161, 162). BBN can provide the high possibility of transporting bioactive compounds to the site of action, which has attracted more attention from chemists, biologists, and pharmaceutical scientists (163). The primary goal of BBN is to elevate the drug's water solubility, stability, reduce destruction, improve bioavailability, bioactivity, biodegradability, lower toxicity, and flexibility of gel formation (164). Spray drying, electrospray, high–pressure homogenization, supercritical fluid, electrospinning, emulsion–diffusion, reverse micelle, and emulsion – droplet coalescence are just a few of the fabrication methods to engineer BBN (165).

Biopolymer-based biomaterials were studied for use in accelerated diabetic wound healing. Cashew gum (CG) based bio nanocomposite was used as a platform for trials. Crude samples of cashew gum exudate were collected from *Anacardium occidentale L.* for the trial, cashew gum-coated prussian blue nanoparticles (PBNPs) were prepared *in situ* and characterized. CG coating decreased the size of the spherical PBNPs from 50 to 5 nm and the crystallinity of PBNP's core was increased. The use of CG polysaccharides was found to be an excellent and effective strategy for covering and controlling the size, shape, and crystallinity of prussian blue *via* an *in-situ* synthesis (166). Sebak et al. created noscapine-loaded nanoparticles (NPs) with human serum albumin (HSA) for targeted administration and tested them on SK-BR-3 breast cancer cells using the pH coacervation technique. The results showed that noscapine NPs were substantially more effective than free noscapine in

TABLE 2 | Types of novel drugs delivery systems for herbal anti-cancer compounds.

Novel Drug Delivery Systems (NDDS)	Phytochemicals	Formulation Components	Remarks	References
Biopolymer-based nanocarrier (BBN)	Curcumin, Quercetin, Resveratrol, etc.	Gelatin, albumin, milk protein, chitosan, pectin, cellulose, guar gum, sodium alginate, starch	• Less toxicity, • More solubility, • More stability, • Lower degradation, • High biocompatibility	(124, 130)
Liposomes	Carotenoids, epigallocatechin gallate, Curcumin, Quercetin, Resveratrol, etc.	Phospholipids, steroids	• High biodistribution, and bioavailability, • Increase solubility, • Low toxicity	(130–134)
Dendrimers	Curcumin, Paclitaxel, Quercetin, Resveratrol, Ursolic and oleanolic acids, etc.	Polyamidoamine dendrimers (PAMAM), Polypropylene imine dendrimers (PPI), Folate-conjugated polypropylene imine dendrimers (FA-PPI)	• Enhanced solubility, • Increase drug efflux transporters, • Increase bioavailability, • Enhanced cell uptake, • Low cytotoxicity	(135–137)
Niosomes	Thymoquinone, Curcumin, Quercetin, Resveratrol, etc.	Polyoxyethylene alkyl ethers, Sorbitan monoesters (span 20,40,60 *and* 80), Polyoxyethylene sorbitan monoesters (tween 20, 60, 61 *and* 80)	• Lower toxicity, • Increase anticancer activity • Inhibit P-glycoprotein (P-gp) • Better targeted drug delivery	(138, 139)
Polymeric Micelles	Curcumin	Poly(ethylene oxide)(PEO), Poly(ethylene glycol)(PEG), Poly(N-vinyl pyrrolidone)(PVP), Poly(N-isopropyl acrylamide)(pNIPAAm)	• Enhanced permeability and retention effect, • High stability, • Enhanced nutrient and O_2 demand, • Inhibition of efflux pumps to improve the drug accumulation • Increase bioavailability of poorly water-soluble drugs • Release of the drug in a controlled manner at target sites	(140–142)
Magnetic Nanospheres	Opium alkaloids	Protein, silica, hydroxylapatite, magnetite(Fe_3O_4), magnetite (gamma Fe_2O_3)	• Increase patient compliance, • High bioavailability, • Reduction of an adverse effect of the drug, • Reduces the frequency of dose	(127, 143, 144)
Nanoemulsion	Paclitaxal, rutin, genistein, brucea javanica oil, and coixenolide, etc.	Oil, water, amphiphile, phospholipid, alkyl polyglycosides, PEGylated fatty acid ester, fatty alcohol	• Enhanced antigenicity, • More potency, • Increases humoral response, • Enhanced permeability, • Improved dispersion of active hydrophobic components and enhanced absorption, • Less pain or allergic reaction	(145–149)
Lipid-based Nanoparticles	Curcumin, Quercetin, Resveratrol, etc.	Phospholipids, polyethylene glycol (PEG) PEGylated surfactants	• Reduced tumor size, • Increase bioavailability to the central nervous system • Enhanced Permeability and Retention (EPR) Effect • Active drug targeting • Stimuli-Responsive and Triggered Release Systems	(127, 150, 151)

(Continued)

TABLE 2 | Continued

Novel Drug Delivery Systems (NDDS)	Phytochemicals	Formulation Components	Remarks	References
Carbon-based Nanoparticles	Tulsi extract, Polyphenols, etc.	Fullerenes, Carbon nanotubes (CNTs), Single-walled carbon nanotubes (SWCNTs), Graphene oxide (GO)	• High antimicrobial activity, • Inhibition of energy metabolism, • Increase of O_2 uptake, • Inhibition of bacterial growth	(152, 153)
Polymeric nanoparticles	Curcumin, Quercetin, Resveratrol, etc.	Chitosan, collagen, Poly(lactic acid) (PLA), Poly(lactic-co-glycolic acid) (PLGA)	• Increase accumulation in tumor cells, • Stability, • Increase therapeutic efficacy • Enhanced Permeability and Retention (EPR) Effect • Active drug targeting • Stimuli-Responsive and Triggered Release Systems	(124, 154)
Nanocrystals	Curcumin, Quercetin, Resveratrol, etc.	Sodium cholate, sodium lauryl sulfate, celluloses, polyvinyl alcohol, hydroxypropylene methylcellulose (HPMC), chitosan, benzalkonium chloride (BAC), hyaluronic acid, polyethylene glycol (PEG), poloxamer	• Increase bioavailability, • Enhanced transdermal efficacy of poorly soluble drugs, • Increases the dissolution rate of drugs, • Higher solubility and less tissue irritation • Ease of scaling-up	(155, 156)
Nanosphere	Curcumin, Quercetin, Resveratrol, etc.	Polylactic acid(PLA), Polyglycolic acid(PGA), Co-polymer of polylactide-coglycolide (PLGA)	• Drug release is delayed, • High stability, • Increases bioavailability, • Increases entrapment of the drug, • High antitumor efficiency • Optimal dug deposition at the target site	(124, 156)
Nanocapsule	Curcumin, Quercetin, Resveratrol, etc.	Biocompatible hydrophobic polymeric kernel with phospholipid monolayer, and an outer PEG layer	• High drug efficiency, • Improving poor aqueous solubility, • Stabilizing drugs by protecting the molecule from the environment, • Providing the desired pharmacokinetic profile, • Allowing controlled release, as well as facilitating oral administration	(124, 157)
Metal Nanoparticles	*Tribulus terrestris L.* extract	Gold, silver, iron oxide, copper, zinc oxide, titanium oxide, platinum, selenium, gadolinium, palladium, cerium dioxide	• Increase therapeutic action, • Enhanced the cellular uptake, • Easily combined with drugs, • Good biocompatibility, • Lower cytotoxicity of drugs, • Enhance the sensitivity, • Increase in potency, • Display antimicrobial activity • Radiotherapy enhancement	(158–160)

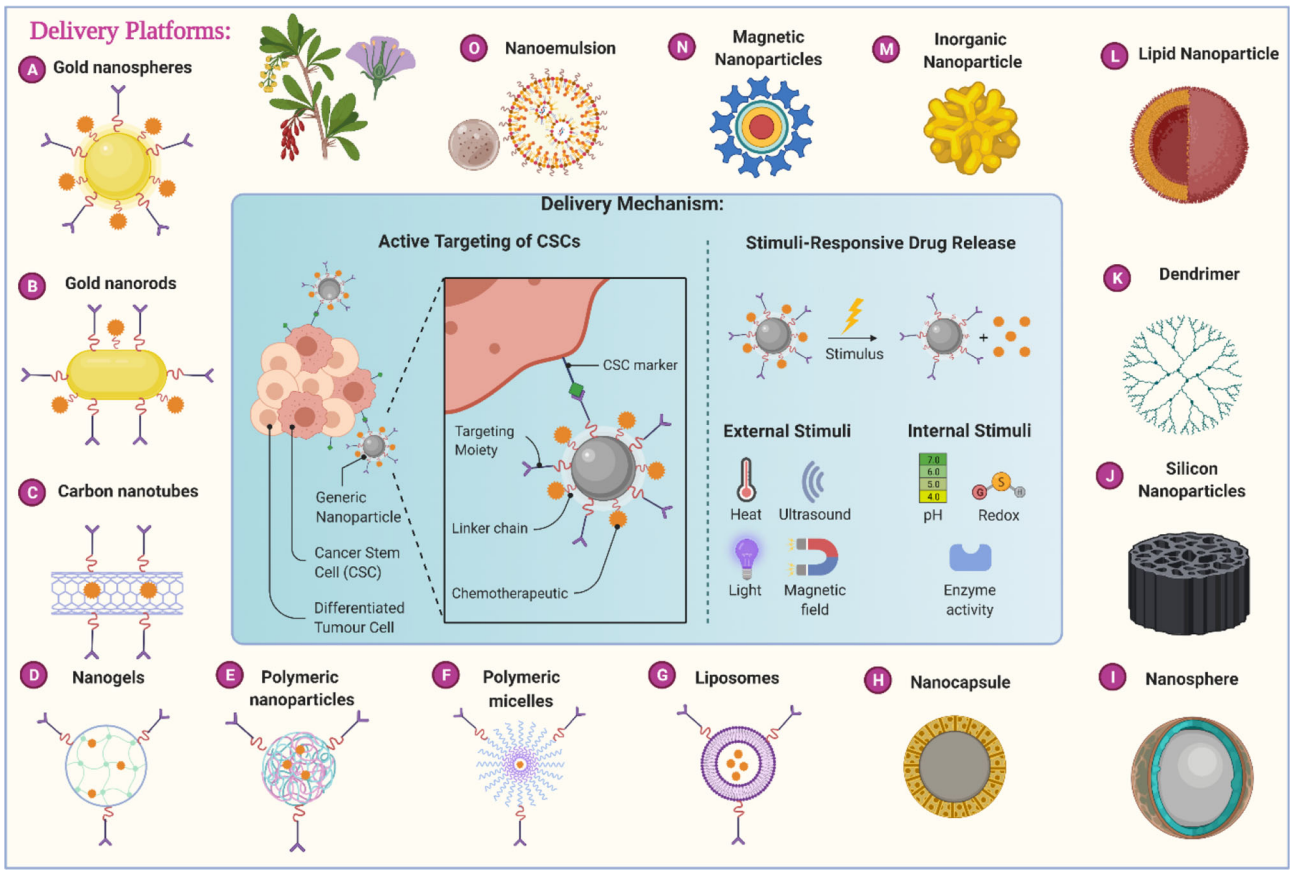

FIGURE 2 | Different nanotechnology-based carrier platforms for the efficient delivery of anticancer phytochemicals and different delivery mechanisms.

lowering SK-BR-3 cell viability (167). Cationic chitosan (CS)- and anionic sodium alginate (Alg)-coated PLGA NPs loaded with revasterol have been developed by the nanoprecipitation technique (168). For six months, the nanoparticles can inhibit trans isoform breakdown and revasterol escape from the carrier.

Liposomes

Liposomes are formed from combining cholesterol with phospholipids (128). They shield the enclosed medication from enzyme and other inhibitor activity. They can transport any medication *via* endocytosis and are hence commonly employed for compounds that cannot pass biological membranes. Their disadvantages involve instability, identification by the immune system, and phagocytosis. Conjugation with polyethylene glycol (PEGylation) can shield them from phagocytosis, making them particularly efficient in carrying anticancer medicines (169). Using a thin-film hydration and extrusion method, Lu et al. prepared folic acid conjugated PEGylated liposomes of vincristine for multidrug-resistant cancer therapy and evaluated their cytotoxicity on KBv200 carcinoma cell line and also performed *in vivo* antitumor efficacy studies (tumor growth inhibition and apoptosis assessment studies by TUNEL) (170). The IC50 of the PEGylated folic acid-linked vincristine liposomes was 23.99 nM, compared to 1.10 nM for free vincristine and 363.08 nM for PEG-LS/vincristine. *In vivo* tests revealed that folic acid conjugation greatly improved the antitumor activity of the PEGylated liposomes of vincristine, as well as a higher apoptotic index was captured in the TUNEL assay (24.1 *vs.* 14.4). In another research study, Liposomal ursolic acid showed improved anticancer activity for breast cancer and prostate cancer cell lines than free ursolic acid (171). Recently, a cationic liposome encapsulating hydroxycamptothecin and 5-aminolevulinic acid was administered along with chemo-sonodynamic therapy against metastatic lung cancer that has demonstrated a better apoptotic behavior (172). Moreover, a phase-1 study with 96 non-randomized participants was carried out to assess the effect of liposomal topotecan intravenous injection for the treatment of advanced solid lung tumors. Topotecan is the semi-synthetic derivative of the naturally obtained topoisomerase inhibitor, camptothecin, and the results are yet to be disclosed but the trial is reported to enter phase-2 study by the beginning of the year 2023 (NCT04047251). Inhalable liposomes are being developed and their preparation is studied for use in pulmonary diseases (173). Daunorubicin and cytarabine (vyxeos®) were encapsulated in liposomes (Vyxeos®, CPX-351) for the treatment of adults with newly diagnosed, therapy-related acute

myeloid leukemia or acute myeloid leukemia with myelodysplasia related changes (NCT01696084). Vyxeos® is an orphan drug and its clinical trial proved to be remarkable. A clinical study CLTR0310-301 (also referred to as Study 301) was a phase III, multicenter, open-label, randomized, trial of vyxeos® (daunorubicin-cytarabine) liposomal injection versus standard 3 + 7 daunorubicin and cytarabine in patients aged 60–75 years with untreated high-risk (secondary) (173, 174). A recent clinical trial is investigating the efficacy and safety of paclitaxel liposome as first-line therapy in patients with advanced pancreatic cancer. The patients were given paclitaxel liposome 175 mg/m^2 intravenously every 3 weeks for 3 weeks until the disease recurrence. All five parameters, including overall response rate, overall survival, disease control rate, quality of life, and adverse events are examined (NCT04217096). Moreover, an open-label, phase-1 study on the use of liposomal irinotecan injection was carried out on 136 participants to study its effects on advanced breast cancer and evaluate its efficacy and safety (NCT04728035). Transfersomes are phosphatidylcholine-containing liposomes with an edge activator (175). Because of greater penetration, celecoxib loaded into transfersomes containing soy phosphatidylcholine combined with sodium deoxycholate was found to be a therapeutically efficient drug-delivery approach for the treatment of rheumatoid arthritis (176).

Niosomes

Niosomes are obtained through combining an alkyl or dialkyl polyglycerol-based nonionic surfactant and subsequent hydration in an aqueous environment. Because of their comparable construction, they are frequently employed as a replacement for liposomes (132). They are not toxic and restrict the action of drugs to specific locations. Niosomes have also been shown to be manipulable as a part of advanced drug delivery strategies and can deliver drugs *via* intravenous, transdermal, ocular, and pulmonary routes. Cancer therapy, gene therapy, and targeting medicine *via* the nasal route are some of the other uses for niosome based drug delivery. It is also used in immunological applications, such as a hemoglobin transporter, and for cosmetic reasons (177). Morusin-loaded niosomes have been produced for cancer therapy (178). Nanomorusin, unlike free morusin, was shown to be easily dispersible in aqueous environments. Morusin was shown to have an extraordinarily high drug entrapment efficiency (97%), regulated and prolonged release, and increased therapeutic effectiveness in cancer cell lines from four distinct lineages. A different research study evaluated the anticancer activity of niosomes containing both curcumin and methotrexate against colorectal cancer cell lines (179). The niosomal formulation showed more *in vitro* cell toxicity than their combination in free form. The anti-arthritic efficiency of luteolin (LT)-loaded niosomes made with different nonionic surfactants was tested *in vitro* and *in vivo*, with improved entrapment efficacy and higher transdermal flow across the rat skinned discharge. The cytotoxicity study showed a lesser IC50 value from LT-NVs than the pure LT (180). Thus, it can be concluded that LT-NVs are a natural alternative to synthetic drug in the treatment of lung cancer. The therapeutic purpose of niosomes is to deliver anticancer drugs, protein, peptide, and natural product delivery with improved bioavailability. Numerous experts are now intrigued by the delivery of natural compounds such as curcumin, which has low solubility and bioavailability (177). As a result, clinical trials with the combination of *Curcuma longa L.* and doxorubicin are underway (NCT04996004). Aside from curcumin, there are natural compounds called morusin that have powerful antibacterial, anti-inflammatory, and anticancer properties. *Rahman et al.* developed a formulation in which morusin is loaded with niosomes as a carrier, removing the barrier of low solubility and stability to target the specific cell (126). A study to evaluate the efficacy and safety of niosomal docetaxel lipid suspension compared to taxotere® in triple-negative breast cancer patients (after failure to previous chemotherapy) was conducted (NCT03671044). In this randomized, open-label clinical trial, females 18-65 years of age were eligible to apply. The niosomal docetaxel lipid suspension was administered intravenously at three-week intervals at a dose of 75 mg/m^2. Patients received drug doses until disease progression and unacceptable toxicity occurred. This procedure was repeated with a 100 mg/m^2 dose of niosomal docetaxel lipid suspension. The trial's primary goal is to compare the proportion of patients with the best overall response rate in niosomal docetaxel lipid suspension and taxotere® (NCT03671044).

Polymeric Micelles

Micelles are lipid molecules that organize themselves in a spherical shape in aqueous solutions. They fluctuate in size from 10 to 100 nm and are generally quite narrow in terms of the size distribution (181). They can improve drug absorption and retention by shielding the drug from inactivation by its micellar environment. This system is made up of a core-shell structure with a lipophilic core and a shell made up of hydrophilic polymer blocks (182). The physicochemical properties of the drug and their position in the micelle influence their release. Certain physical stimuli, such as pH, temperature, ultrasound, and light can also promote drug release from the micelles in the targeted location (183). Micelles also provide an increased drug accumulation at the tumor site. Recently, doxorubicin delivery through covalent attachment with the hydrophobic portions of an amphiphilic block copolymer resulted in pH-regulated drug release (184). Paclitaxel, doxorubicin, 5-fluorouracil, 9-nitrocamptothecin, cisplatin, triptorelin, dexamethasone, and xanthone were all microencapsulated in poly lactic-co-glycolic acid (PLGA), polymerized lactic acid (PLA), and polycaprolactone (PCL) nanostructures with a micellar backbone (185). The medications are released to the target. Paclitaxel, for example, is encapsulated in polymeric micelles, which improves the systemic pyruvate kinase (PK) profile and interferes with drug-producing adverse effects such as neurotoxicity. It is USFDA approved and the formulation is marketed as Genexol® PM (183). As a solution to breast cancer and better intracellular delivery of docetaxel, novel pH-triggered biocompatible polymeric micelles have been developed based on heparin–α-tocopherol conjugate. For this, the amphiphilic copolymer was synthesized by grafting α-tocopherol onto the heparin backbone by a pH-cleavable bond (186). The paclitaxel and cisplatin-

loaded polymeric micelles in advance non-small cell lung cancer were evaluated as a comparative phase 2 study with 276 participants. The primary endpoint of this study is a response rate of up to 6 cycles to ensure that the overall anticancer response is achieved. The secondary outcome measure is overall survival over three years (NCT01023347). The safety results are satisfactory (data not available in the public domain) and they have started phase 3 studies (NCT02667743).

Magnetic Microspheres

Magnetic microspheres are made up of microscopic supramolecular particles that are surrounded by capillaries. The primary goal of magnetic microspheres is to deliver drugs to the specific site of action that ultimately reduces the adverse effects. Magnetic microspheres are composed of tiny particles such as protein, silica, hydroxylapatite, magnetite (Fe_3O_4), maghemite (gamma Fe_2O_3), and synthetic polymers (143). The drug delivery is divided into two parts: spatial placement and temporal delivery of the drug (143). Magnetic microspheres cause pharmaceuticals to be released in a sustained manner rather than having a high bioavailability. Examples of magnetic microspheres-containing products are lupron depot® and nutropin depot® (187). Solvent evaporation, multiple emulsion techniques, phase separation emulsion polymerization, emulsion solvent extraction method, hot melt microencapsulation, and dispersion copolymerization are some methods for producing magnetic microspheres (183). It is used for the treatment of alveolar echinococcosis, a human helminthic disease caused by the larvae of *Echinococcus multilocularis* tapeworms. Treatment of this disease uses iron oxide magnetic particles. Spray-drying was used to create magnetic microspheres, which were then studied for their physicochemical features and dissolution profile. They were also tested for therapeutic effectiveness in both *in vitro* and *in vivo* systems. *In vitro* experiments in B16 melanoma cells found that using 30 M or 50 M sulforaphane with iron oxide in the polymeric carrier inhibited cell survival by around 13% -16%. *In vivo* data from C57BL/6 mice demonstrated that magnetic microspheres (located to the tumor site with the assistance of a powerful magnet) prevented 18% more tumor development than sulforaphane in solution (188). The magnetic microsphere of curcumin and doxorubicin demonstrated potential *in vitro* anticancer activity in cell viability and MTT cytotoxicity studies (189).

Nanoemulsion

Nanoemulsions (NE) is a colloidal dispersion system, and one of their most essential functions is to act as a tool for increasing the bioavailability of poorly water-soluble medications (147, 148). They are composed of oil, water, amphiphile, phospholipid, alkyl polyglycosides, PEGylated fatty acid ester, and fatty alcohol. They are having mean droplet sizes less than 100 nm. The NE system has prolonged drug release, high solubility, higher skin permeability, more drug absorption, extremely low viscosity, less allergic response, and less drug degradation (190). Oral administration of the medication enhances bioavailability. The hydrophilic substances have higher permeability when administered subcutaneously or intramuscularly, and they are condensed into the lymphatic system (145). Over the last few years, NE has created novel systems such as Transcuto® P, alkyl polyglycosides, etc. Natural herbal medications like rutin, genistein, brucea javanica oil, and coixenolide have been grated into NE for some applications. The antioxidant properties of *Syagrus romanzoffiana (Cham.)Glassman*, fruit O/W (oil in water) NE are assessed using the phase inversion technique (190). Paclitaxel nanoemulsion containing tocopherol as oil phase has been developed and evaluated for targeted cancer therapy that reached phase 3 clinical trials (NCT01620190) (191). The effects of eugenol nanoemulsion on pain were studied *via* a randomized double-blinded controlled cross-over trial (158). For the phonophoretic application of glucosamine and chondroitin in the treatment of knee chondropathies, nanoemulsion (nano CG) has been made and evaluated. Nano CG was previously applied in randomized and controlled clinical trials (192). In this experiment, patients in arm 1 receive nanoemulsion curcumin orally twice daily for up to 3 months. In arm 2, a placebo was administered orally twice daily for three months. This trial's result was measured using the functional evaluation of cancer therapy (endocrine system inhibitor) to detect changes in aromatase inhibitor. This experiment is currently ongoing, however, it is not currently recruiting participants (NCT03865992). Plumbagin improves the efficacy of androgen deprivation therapy (ADT) in prostate cancer and it is now being evaluated in phase I clinical trial (193). A recent study found that plumbagin decreased PTEN-P2 driven tumor development only in castrated mice but not in intact animals, indicating that dihydrotestosterone (DHT) was generated in the testes and was primarily responsible for inhibiting prostate cell death (194). An oleic-acid-based nanoemulsion of plumbagin increases its antitumor efficacy (193). Nanoemulsion formulation of piplartine resulted in enhanced solubility, oral bioavailability, and anti-tumor efficacy of piplartine (195).

Nanoparticles (NPs)

NPs are constructed of a range of materials, some of which are poisonous. Biodegradable materials are less harmful. NP systems are being investigated for a wide range of biological applications. NP protects the drug from enzymatic breakdown and allows for regulated drug release (196). Through adhesion to the capillary wall, NPs may improve the oral bioavailability of poorly soluble medicines and tissue absorption following parenteral administration. They may also improve drug transport across membranes. They are vulnerable to phagocytosis and endocytosis because of their hydrophobic surface, which is quickly covered with plasma proteins and taken up through the mononuclear phagocytic system (MPS) present in organs like the liver, spleen, and bone marrow (169).

Applying the ionic gelation process, berberine-loaded NPs were synthesized for anticancer potential (197). The rotary evaporated film ultrasonication process was used to create glycyrrhizic acid-loaded NPs (198). For testing therapeutic synergy in the ulcerative colitis (UC) model, pH-sensitive NPs of the curcumin-celecoxib combination were optimized. Its effectiveness was later validated in a UC model in rats, as per the tests (199). Gold NPs (AuNP) were created using a greener

method that included digested *Acorus calamus L.* rhizome as a reductant and chloroauric acid as a starting material. The existence of a surface plasmon resonance (SPR) peak in the ultraviolet (UV)–visible spectral analysis revealed the formation of AuNP (200). Hexagonal antibacterial $Zn_{0.95}Ag_{0.05}O$ (ZnAgO) NPs have been made using rosemary leaf extracts as a green chemistry method whose formation was confirmed by X-Ray Diffraction (XRD), Fourier transform infrared spectroscopy (FTIR), and UV–visible spectra (201). Clinical trials on magnetic fluid hyperthermia based on magnetic NPs were conducted and studied (NCT01411904). Nanoparticle role in photodynamic therapy for solid tumors has been studied *via* a clinical trial. The aim of the use of nanotechnology-based approaches as delivery tools for photosensitizer (PS) is to study the improvement in their cancer cellular uptake and their toxic properties, as well as the photodynamic therapy's therapeutic impact (202). Potential anticancer activity is reported for apigenin-loaded PLGA nanoparticles against skin tumor in mice models (203). These nanoparticles showed ameliorative potentials in combating skin cancer and therefore have a greater prospect of use in the therapeutic management of skin cancer. Similarly, significant anticancer activity was reported against osteosarcoma cancer cells (MG63 and Saos-2 osteosarcoma cell lines) by formulating PLGA nanoparticles of etoposide and paclitaxel (204). The results of quercetin-loaded PLGA nanoparticle administration showed potential action against C6 glioma cells (205). It has demonstrated antioxidant properties and cellular oxidative resistance. The results showed that the improved batch (Qu1NPs) exhibited better cellular absorption at a lower IC50 value (29.9 gmL^{-1}) after 48 hours of incubation. The NPs may lessen resistance in brain cancers by lowering oxidative stress. A nano-phytocomposite consisting of phytochemical extract (BRM270) has cytotoxic potential against HepG2 human hepatoma cancer cells (206). A randomized, double-blind, placebo-controlled phase 2/3 study is now underway to assess the effectiveness of berberine hydrochloride against the development of new colorectal adenomas in 1,000 people who have a history of colorectal cancer (NCT03281096). A phase-2 trial is investigating the adverse effects of paclitaxel albumin-stabilized nanoparticle formulation for treating diseases such as fallopian tube cancer, primary peritoneal carcinoma, and recurrent ovarian carcinoma. The major goal of the experiment is to assess tumor response after each cycle for the first six months, as well as the frequency and severity of side effects seen. This research is open to people of all ages, however, only women are permitted (NCT00499252).

Lipid-Based Nanoparticles (Solid Lipid Nanoparticles - SLN)

PEGylated surfactants are used in the production of lipid-based NPs. Lipids act as penetration enhancers of drugs. It also enhances drug solubility and diffusion from the lymphatic to the circulatory system. One of its applications is to improve central nervous system (CNS) bioavailability. They may be manufactured *via* quick, solvent-free, and scalable procedures. Some methods of preparation include nanoprecipitation, emulsification–solvent evaporation (ESE), or high-pressure homogenization (207). The microemulsion technology was used to create curcuminoid solid lipid NPs with the active component being curcuminoids. It has antioxidant and anticancer effects (199). Exocytosis of NPs is the step that details the cytosolic administration of therapeutic agents *via* NP carriers (208). Silymarin-loaded nanostructured lipid carrier (NLC) is the best example that has been used clinically to overcome low solubility, permeability, and bioavailability issues in hepatic diseases (126). Cardamom essential oil (CEO)-loaded NLCs have successfully been synthesized using food-grade lipids which include cocoa butter and olive oil. This modification led to a small size (90%), improved loading capacity (>25%), and provided good physical and chemical stability (126). Paclitaxel-loaded solid lipid nanoparticles showed better anticancer action in the murine breast cancer mice model (209). Several solid lipid nanoparticles have been created for the administration of cytotoxic medications such as doxorubicin, idarubicin, paclitaxel, camptothecan, 7-ethyl-10-hydroxy-20(S)-CPT, etoposide, flurodooxyuridine, and retinoic acid, as well as cholesterylbutyrate (210). The *Ferula assafoetida* seed oil (FSEO) -SLN nanoparticles inhibited the development of the human NT-2 cancer stem cell line significantly (211). They caused apoptosis by increasing the expression of TNF-, P21, and Cas3 genes. The FSEO-SLN inhibited angiogenesis in CAM tissue by reducing the length and quantity of blood vessels. As a result, it has the potential to be investigated as an effective anti-cancer agent. Similarly, Epigallocatechin-3-gallate (EGCG) SLN can improve EGCG bioavailability and stability and can be employed as an alternate approach for EGCG oral delivery (212). In the rat model, SLN-EGCG had neither acute or sub-chronic toxicity when compared to free EGCG.

Carbon-Based Nanoparticles

Fullerenes, carbon nanotubes (CNTs), single-walled CNTs (SWCNTs), and graphene oxide (GO) are used in the production of carbon-based NPs. They have great antibacterial action and are utilized to limit energy metabolism, reduce or enhance O_2 absorption, and inhibit bacterial growth (152). They are 3–10 nm in diameter. Their interior structure is made up of graphite sheets that have been glued together to form a quasi-spherical nanoparticle. They are also utilized to make biosensors.

CNTs have been extensively investigated for their potential to deliver anticancer herbal compounds with better therapeutic effectiveness and safety (213). CNTs have been used in both therapeutic and environmental settings. *Ocimum tenuiflorum L.* (tulsi extract) containing photosynthesized silver nanoparticles (AgNP) loaded into emulsified multiwalled carbon nanotube (MWCNT) was developed for fertility analysis targeted to the intracellular part of the sperm cell. It was characterized by a spherical shape, 5–40 nm in size, and surface plasmon resonance imaging (SPR) at 430 nm (126). The total polyphenols content and antioxidant activity of *Echinacea purpurea (L.)Moench.* extracts were determined using glassy carbon electrodes modified with CNTs and chitosan (214). In a recent research study, carbon quantum dots of *Echinops persicus* extract demonstrated efficient antiradical activity (215). The biosynthesized silver nanoparticles of the leaf extract of

Teucrium polium exhibited significant anticancer activity against the MNK45 human gastric cancer cell line (216).

Polymeric Nanoparticle and Dendrimers

Polymeric nanoparticles (PNs) are colloidal solid particles that are made up of various polymers such as chitosan, collagen, polylactic acid (PLA), PLGA, or other biodegradable polymers (146). PN enhances the bioavailability of the poorly soluble drugs by allowing the oral administration of the drug and increasing accumulation of the drugs at the site of action since the smaller size of the particle allows penetration into the capillaries and the cells (155). Methods of preparation of polymeric NPs include complex coacervation method, coprecipitation, salting out method, solvent displacement method, and solvent emulsification-diffusion method (185). Solvent evaporation, emulsification/solvent diffusion, nanoprecipitation, emulsification/reverse, and salting-out methods are all used to create nanospheres while nanoprecipitation is used to create nanocapsules. An organic phase is initially generated in the solvent evaporation process, which comprises a polar organic solvent in which the polymer is dissolved and the active component has incorporated either by dissolving or dispersion. Now PNs are approved by FDA for clinical use in the treatment of breast and pancreatic cancer and also some clinical trials are performed in many of the compounds such as ABI-008, ABI-009, and ABI-011(NCT04229004). The free radical process was used to create *A. absinthium* extract-loaded polymeric NPs (NVA-AA), which were efficient against breast cancer cell lines; MCF-7 and MDA MB-231 (217). *Uncaria tomentosa* (Willd. ex Schult.) DC. (UT) extracts have been shown to have promising antitumor activity for the enhancement and delivery, in which PCL and PLGA were employed for the generation of NPs loaded with UT extract by a single emulsion solvent evaporation method (218).

Dendritic packaging of bioactive agents allows for the separation of the active site, which has a structure similar to active sites in biomaterials (137). In addition, unlike most polymers, water-soluble dendrimers may be created by functionalizing their outer shell with charged species or other hydrophilic groups. Capsaicin-loaded dendrimers showed significant cytotoxicity on VERO cell line with an IC50 of 1.25 µg/mL and MCF-7 and HEp2 cell lines with an IC50 of 0.62 µg/mL (219). Polyamidoamine (PAMAM) dendrimers as oral drug delivery carriers for quercetin were evaluated. It was discovered to be in the nanometer range (100 nm) with a low polydispersity index. An *in vitro* investigation indicated a biphasic release pattern of quercetin, with an initial rapid release phase followed by a sustained release phase, and a pharmacodynamic analysis offered early proof of concept for the potential of quercetin-PAMAM complexes (220). Poly (propylene imine) dendrimer is also evaluated for different anticancer phytochemicals (221).

Nanosphere (NS)

NSs are amorphous colloidal aqueous solutions with sizes ranging from 10 to 200 nm. Because they are tiny in size, they may be easily delivered orally, locally, and systemically, resulting in better bioavailability. They are made up of synthetic polymers such as PLA, polyglycolic acid (PGA), PLGA, and others (222). The main functions of the system include extending drug action due to delayed drug release, boosting bioavailability, enhancing drug entrapment, and boosting drug stability. It can also act against chemical degradation and minimize drug toxicity. Albumin NS, modified NS, starch NS, gelatin NS, polypropylene dextran NS, and polylactic acid NS are all examples of biodegradable NSs (223). Presently, two novel forms of NS have emerged: immune NS and magnetic NS. Both of these NSs are joined to form the immunomagnetic NS, and they considerably enhance drug targeting (222, 224). The targeting ability of the NS is currently being investigated in HeLa cells. Researchers have discovered that the C-phycocyanin (C-pc) NS is employed as a fluorescent producer. The intensity of fluorescence is higher in C-pc, indicating that it was directed at HeLa cells. Studies have revealed that the CD55 specific ligand peptide (CD55sp) is a potent anti-cancer factor. CD55sp is injected into the body of a mouse to assess the distribution of NSs, which are collected in the spleen, liver, and tumor. The liver and spleen metabolize the medication and start phagocytosis against malignancies (225). The pre-clinical trial such as oridonin (ORI)-loaded poly (D, L – lactic acid) (PLA) and polymer (RGD – Gly – Asp peptides) for the better antitumor actions (126). Another study created a near-infrared-responsive pharmacological system based on Au nanocages with Biotin–PEG–SH modification for the combination of doxorubicin and quercetin. The resulting nanocomplex have substantially more effective effects on MCF-7/ADR cell growth suppression under near-infrared irradiation. Furthermore, co-administration of doxorubicin and quercetin might significantly boost doxorubicin intracellular accumulation and dispersion in nuclei (226).

Nanocapsule

Nanocapsule (NC) is a colloidal dispersion system with a conventional core-shell structure, and the medicine is captured into the cavity of the central regions of the shell, which is surrounded by various polymer components such as polystyrene, titanium oxide (TIO_2), and silver (Ag). The NC platform has high drug encapsulation efficiency, low polymer content, and a core-shell that protects the medication from degradation elements such as pH and light (227). Nanoprecipitation, arc discharge method, emulsion–diffusion, double emulsification, interfacial polymerization, emulsion–coacervation, polymer coating, and layer–by–layer coating are some of the methods used to create nanocapsules. The layer–by–layer approach is used to improve the hydrophilicity of crystals, such as artemisinin (ART, *Artemisia annua L*) crystals, having good anticancer action. Herbal compounds have been encapsulated with polyelectrolytes for pharmacological self-release (150). There is one other method of preparation known as interfacial polymerization that yields a dispersion of aqueous core nanocapsules (228). Biogenic synthesis of PEG-enhanced *Moringa oleifera Lam* Ag nanocapsules was performed and its antibacterial activity was tested. The Ag nanocapsule (AgNs) formed had a single-phase cubic structure as seen under X-ray

spectroscopy (229). Chitosan nanocapsules of tarragon essential oil were made, and had low cytotoxicity and long-lasting activity as a green nano-larvicide. Its cytotoxicity was checked on human skin lines (230). This system is already a clinical trial is completed such as an anti – HER2 mAb with paclitaxel *and* a mAb with doxorubicin (Doxo®) (231). Mardani et al. discovered that curcumin nanomicelles might suppress lung metastasis and melanoma cell growth (B16 F10). The time and concentration of incubation are critical elements in imparting the potential activity of nanomicelle. Curcumin nanomicelles cause apoptosis even at low concentrations of 20 M. Curcumin also reduces angiogenesis and controls T Cell activation (232).

Metallic Nanoparticle

Metallic NPs (MNPs) are comprised of a metal core made of inorganic metal or metal oxide, which is generally surrounded by a shell also made of organic or inorganic material or metal oxide. Gold, silver, iron oxide, copper, zinc oxide, TiO_2, platinum, selenium, gadolinium, palladium, and cerium dioxide are some of the metals and metal oxides that are employed. Because NPs are poisonous to live cells, their manufacturing and usage in powder form are deemed risky. To address this issue, highly reactive MNPs can be encapsulated (233). Aqueous plant extracts were mixed with metal salt solutions to create MNPs. Secondary plant metabolites are continually involved in the redox process that produces environmentally favorable NPs. The initial indication for MNP production is detected as a color shift. UV visible spectroscopy can be used to track the development of the reaction. Because of the drawbacks of the other approaches, the biological synthesis of NPs is the ideal way for producing these MNPs (234). It is a one-step bio-reduction approach that requires less energy to synthesize eco-friendly NPs. The biochemical reaction of $AgNO_3$ reacting with plant broth results in the synthesis of AgNPs, according to the bio-reduction technique. *Tribulus terrestris L* extract was combined with various molar concentrations of silver nitrate solution to create eco-friendly AgNPs with distinct morphological properties. The methanolic extract of the *Callicarpa maingayi Kjng and Gamble* stem is employed in the manufacture of AgNPs and the formation of [Ag (*Callicarpa maingayi*)] + complex. The aldehyde group contained in the extract is mainly involved in the reduction of silver ions into metallic AgNPs (235). *Piper nigrum L.*, leaves were stated to contain an important bioactive compound, involved in the NP synthesis by an eco-friendly method. *Artemisia nilagirica(C.B.Clarke) Pamp.*, leaves were also used for the synthesis of NPs (224). These NPs are used because of their various properties. AgNPs are used as an antibacterial agent, wound dressing material, bone and tooth cement, and for water purification. MNPs are being used in a variety of fields, not simply in medicine and agriculture. MNPs are also employed in the manufacture of several bacteria, including *Klebsiella pneumonia* and *Pseudomonas aeruginosa*. It is also employed in the production of bioactive compounds and phytochemical constituents (236). In now a day the clinical trial is performed in some inorganic nanomaterials such as gold nanoparticles and silica nanoparticles (237). Folic acid surface modification improves the targetability of curcumin magnetic nanoparticles. Curcumin-loaded folate-grafted magnetic nanoparticles inhibit KB nasopharyngeal cancer cells and MCF-7 breast cancer cells significantly. The nanoparticles demonstrated targeted thermo-chemotherapy leading to apoptosis by a selective interaction with folate receptors, which are abundantly expressed in cancer cells, based on magnetic effect (238). The eupatorium-containing mPEG-b-PLGA-coated iron oxide nanoparticles were investigated towards prostate cancer cell lines (DU-145 and LNcaP). Furthermore, it exhibits increased apoptosis and reduced necrosis in the sub G1 phase, as well as enhanced cell populations, rendering it a suitable option for drug-resistant cancer treatment (239). The MTT experiment revealed that eupatorin-loaded Fe3O4@mPEG-b-PLGA nanoparticles significantly slowed the development of DU-145 and LNcaP cells, with IC50 values of 100 M and 75 M, respectively.

Inorganic Nanoparticle

Inorganic nanoparticles are composed of silver, gold, iron oxide, silica, platinum, and gadolinium hydroxide ($Gd(OH)_3$). Magnetic (superparamagnetic iron oxide particles), nanoshell (dielectric silica core in thin gold metal shell), metallic, and ceramic (porous biocompatible substance) nanoparticles are its additional subclassifications based on the material used (240). They have good biocompatibility, can reduce cytotoxicity of medicines, increase the formation of reactive oxygen species (ROS), and have antibacterial action. In comparison to organic materials, these NPs are nontoxic, hydrophilic, biocompatible, and very stable. Inorganic nano-drug delivery methods such as mesoporous silica NPs, CNTs, layered double hydroxides, superparamagnetic iron oxide NPs, and calcium phosphate NPs have been developed as therapeutic uses in a variety of disorders, including neurodegenerative diseases. Magnetic NPs (MN) are employed in magnetic resonance imaging (MRI). Using zirconium oxide NPs, the antifungal activity of neem and aloe vera formulations was sustained and increased (241). In recent years, inorganic NPs have been synthesized and conjugated with tiny drugs for a variety of therapies. Inorganic NPs, which are mostly based on selenium, metallic chalcogenide, silicon, and carbon, are employed in oncotherapy (242). A pre-clinical trial of Anti-EGFR antibody cetuximab (C255) approved by FDA for the treatment of EGFR – positive colorectal cancer and palladium compound (TOOKAD) is a clinical trial by photo-dynamic therapy for the treatment of prostate cancer (65).

RECENT PATENTS

Experts are currently working to modify particles by combining many newer sorts of compounds. The plant bioactive molecule has been found to provide considerable benefits in cancer therapy; however, administering this component is not easy (243). Consequently, a recent patent provides evidence of a unique herbal ingredient-delivery technique. Although there are still challenges to be resolved, this will become a significant delivery method soon. It has already achieved notable progress in the fields of NP separation, purification, and creation (145).

Table 3 shows several recently issued patents for nanoparticle formulations comprising natural anti-cancer molecules.

CHALLENGES

Medicinal plants may have a large number of active ingredients, some of which may be beneficial in therapy while others may be harmful (261). There is a lack of standard protocols and meta-analytic evidence for the use of herbal medications. The predominant role of herbal medication in cancer is to treat symptoms of neoplasm and strengthen the immune system (262). Herbal medicines are used as adjuvant therapy to treat side effects associated with chemotherapy but they have not been used alone to cure or prevent cancer. *In vitro* studies have been successfully performed for the treatment of cancer but in clinical trials, herbal medicine did not succeed much (32). Herbal medicines can be useful in the case of primary cancer but they cannot be useful to treat severe cases of cancer until yet (32). Satisfactory evidence regarding the administration of herbal medication through the parenteral route and proper guidance for the route of administration is not available. A target-based specific treatment for the cancerous cell is not commercially available in herbal therapy. The database of specific interactions of these medications along with other prescription drugs is deficient (263). Several compounds show structural similarity but verification of their structural relationship and function are not well defined (264). In a patient taking cancer treatment, herbal medicine may interfere and alter pharmacokinetic properties. Along with the above challenges, one more challenge is the clarity of the mechanism behind its pharmacological action. While conventional medicine has a proper monitoring system, Ayurvedic treatments do not have a sufficient monitoring system, data analysis, objective level, measuring of the drug, and tools of standardization (265). When herbal medication is used along with other chemotherapeutic agents, it can reduce the bioavailability of chemotherapeutic agents (169).

Some of the herbal medications do not just act on target cells, but also a wide range of normal cells. The limitation of herbal medication is that it can have numerous targets. In some instances, herbal extracts may produce adverse effects. Resistance is common in herbal treatments such as camptothecin (266). Vincristine, a component of the vinca alkaloid, may cause swelling because of fluid accumulation in tissue. If a person consumes vinca, it may cause heart and blood vessel problems. Coma, drowsiness, nerve discomfort, motor dysfunction, and other neurological problems might occur because of vinca ingestion. Vinca alkaloids cause skin responses, as well as baldness and rapid hair loss. Indigestion, vomiting, and cramping are some of the gastrointestinal complications associated with this therapy (267). Decreased bone marrow activity and pain due to nerve damage are consequences associated with taxols (e.g., paclitaxel) (268). Chaga mushroom powder, which is used to treat cancer, has been linked to calcium oxalate buildup, which can lead to tubular damage in the lumin of tubules, and oxalate crystals may be observed (269). Treatment with glycyrrhiza may result in tumor-bearing pressure, lack of appetite, and a reduction in potassium levels in the blood. It also causes hypokalemic conditions when other hypokalemic drugs are co-administered with it (270, 271). Patients who choose herbal medication as a cancer treatment may have various safety problems, such as a reduction of cancer drug concentration in the blood. Mephitic symptoms have been observed in cancer patients who are receiving herbal medicines. Herbal medications, in addition to their benefits, have certain disadvantages, such as changes in metabolism caused by drug interactions and changes in absorption. The maidenhair tree increases the harmful effects of paclitaxel by blocking its metabolism (272). Menorrhagia and dementia can occur when herbal medications are taken in conjunction with pregnancy-preventive medications (273).

FUTURE PROSPECTS

Currently, people are focusing on herbal medication, which is cheaper and is commonly available so, advancements in their formulation and proper drug delivery system should be introduced. Drug regulatory standards related to safety, quality, and efficacy should be developed and managed. Interaction of other anticancer drugs with herbal medications should be studied and data should be collected for proper buildup and usage of herbal drugs. A wide variety of compounds will be available because many types of research are ongoing for herbal medications. Advancement can be made by modification of constituents to produce semisynthetic medicines. Many genetically modified natural products can be established by the use of the latest biotechnological methods. Complementary and alternative medicine (CAM) formulations play an important role and have achieved significant results in anticancer treatment. Production, sale, marketing, and use of these medicines should be properly controlled by the government and specific norms should be introduced for their use. It has a high potential for treating cancer patients in the future. Some herbal drugs are administered *via* NPs-based formulations, which can cause toxicity, and some of their interactions should not be overlooked. As a result, a herbal bioactive chemical is loaded with a naturally produced NP, such as exosomes, which can create a high reaction while being low in toxicity. Many drugs are difficult to isolate at times, and the amount of substance available is sometimes limited. To solve this challenge, one must first obtain that specific gene implanted in a host and then provide the right environmental conditions for proper development and culture.

Theranostics is a concept that combines the phrases therapeutics and diagnostics, and it refers to the use of medications for cancer diagnosis and therapy using the concept of theranostic and for overcoming chemoresistance in breast cancer, the co-delivery system for doxorubicin (DOX) and *curcumin* (CUR) was designed, in a sustained pH-dependent manner, which acted as a chemosensitizer. The surface of magnetic NC was decorated by hydroxyapatite that was cross-linked with β-cyclodextrin leading to the improvement in *curcumin* bioavailability. The therapeutic efficiency was established by the reduction in tumor size (274, 275). In another research, nano curcumin was combined with rare-earth-doped upconversion nanoparticles (UCNPs). Poly (lactic-co-glycolic acid) (PLGA) was used to promote sustained drug delivery and drug release, targeting, minimizing the non-specific consumption by undesirable tissues, and enhancing its aqueous solubility (276). *Curcumin*-incorporated PLGA nanoparticles have exhibited

TABLE 3 | Summary of recently published patents related to nanoparticle formulation with the natural anti-cancer molecule.

Patent number/year	Title	Description of patent	Compound/herbal plant	Treatment of cancer	Reference
IN202241000705 (2022)	Lung cancer treatment using astragalus, cisplatin *and* vinorelbine	It describes the novel drug formulations of astragalus, cisplatin *and* vinorelbine for treating lung cancer	Astragalus, cisplatin *and* vinorelbine	Lung cancer *and* non -small cell carcinoma [NSCLC]	(244)
IN202111049427 (2021)	A novel herbal composition for anticancer activity	This invention relates to the herbal composition for cancer treatment where *cinnamon zeylanticum J.presl.*, is utilized	*Cinnamomum zeylanicum J.presl.*	Used in different cancer treatments	(245)
IN202141046188 (2021)	Enhanced anticancer activity of quercetin-loaded TPGS (Tocopherol polyethylene glycol succinate) nanosuspension for drug imperious MCF-7(Michigan cancer foundation -7) human breast cancer cells	This study provides a novel insight into the mechanism of action of quercetin-induced apoptosis in human breast cancer cells	Quercetin	Human breast cancer	(246)
IN202021048696 (2020)	Cytotoxic herbal silver nanoparticles as a remedy for mammary carcinoma	The present invention is herbal extract mediated silver nanoparticles acting as a cytotoxic agent to mammary carcinomatous cells by showing G2/M-phase cycle arrest	*Brassica oleracea L.*	Mammary carcinoma, cervical cancer, hepatocarcinoma cell	(247)
IN202041023550 (2020)	The non-invasive, novel polyherbal synergistic nanoformulation for the effective prevention and arrangement of human lung cancer	This formulation possesses anticancer, cytotoxic and wound healing properties for effectiveness in lung cancer	Tridax procumben L.,*curcuma longa L.*, and *trachyspermum amm(L.)Sprague.*	Lung cancer	(248)
IN202041025649 (2020)	The non-invasive novel polyherbal formulation for the prevention and management of gastric cancer, its preparation and uses thereof	The polyherbal formulation having nine ingredients has given very positive leads and evidence regarding its efficacy in the effective prevention and management of gastric cancer and also with extended scope of teat colon cancer also	*Plumbago zeylanica L., Zingiber officials Roscoe., Terminalia chebula Retz., Indigofera tinctoria L., Syzygium aromaticum (L)Merr.andL.M.perry., Tamarindus indica L., Piper nigrum L., Cissus quandragularis L., Trachyspermum ammi(L) Sprague.*	Gastric cancer *and* colon cancer.	(249)
US20170258929 (2017)	The method uses and combination composition in cancer treatment	The conjugate of GnRH and curcumin give along or in combination with 2',2'-difluoro-2'-deoxycytidine in pancreatic cancer treatment	Curcumin and its analog	Pancreatic cancer	(250)
EP3144006 (2017)	The combination of chemotherapeutic agent and curcumin analog used in the treatment of glioblastoma	Liposomes containing curcumin eliminate the QT- prolongation to treat glioblastoma	Curcumin	Glioblastoma	(251)
US20170035701 (2017)	Preparation method and uses of stabilized high drug load of nanocarrier	Formation of the micellar core of active compound by encapsulating the active compound by nanocarrier of lipid shell	Curcumin, reservatrol, honokiol, and magnolol	Brain cancer, liver cancer, and skin cancer	(252)
US20170189343 (2017)	Drug carrier for tumor-specific drug delivery and uses of it	It provides a nano drug carrier for tumor treating drugs to depolymerize -polymerize the human ferritin	Various anticancer bioactive compounds	Various hematological Cancer	(253)
US20170224636 (2017)	Curcumin-sophorolipid complex.	The present invention relates to a curcumin acidic sophorolipid complex is enhances the bioavailability of curcumin and nano- encapsulated in acidic sophorolipid	Curcumin	Specifically for breast cancer	(254)
US20160287533 (2016)	Bioavailability enhancing curcumin composition, method, and uses	The formulation which increasing the curcumin properties and treats the uncontrolled cellular growth in the human cell	It included at least one curcumin, resveratrol, catching derivative	Cervical cancer and precancerous cervical lesion	(255)
US20160287706 (2016)	Left helical 3D cage-like structure of DNA drug carrier nanocage	L-DNA (left helical structure of DNA) nanocage (3D cage) has high efficiency of cellular delivery so it is very suitable to deliver an active herbal drug into the cell	Genistein	Various cancer	(256)

(Continued)

TABLE 3 | Continued

Patent number/year	Title	Description of patent	Compound/herbal plant	Treatment of cancer	Reference
US20140369938 (2016)	Curcumin-coated magnetic nanoparticles for biomedical application	Curcumin and its derivatives are coated with ultra-small superparamagnetic nanoparticles of iron oxide directly without losing the therapeutic properties of curcumin	Curcumin	Breast cancer, lung cancer, pancreatic cancer	(257)
US20160263221 (2016)	Information of pharmaceutical formulation of controlled drug targeted delivery system	It provides a container having at least one herbal drug and adapted to release herbal compounds inside the cancer cell	Curcumin	Lung, breast, prostate, and colon cancer	(258)
W02016014337 (2016)	Nanoemulsion based drug delivery system	Drug delivery system forming a nanoemulsion for an anticancer agent	Curcumin	Colorectal cancer	(259)
US20150314006 (2015)	Particulate drug delivery methods.	It provides preparation of drug-polymer or oligomer conjugate which is useful in *in-vivo* drug delivery for therapeutic application	Genistein-like species which having one hydroxyl group and a thiol group	Prostate cancer	(260)

increased cellular uptake, induction of apoptosis, suppression of tumor cell proliferation, and improvement in bioavailability. The advantage of combining UCNP and nano *curcumin* lies in the upconversion of visible light leading to the excitement of photosensitizer and favoring the fluorescence resonance energy transfer (FRET) which can be used in the examination of *in vivo* interaction between bimolecular entities (276).

Berberine with etoposide *via* albumin nanoparticle was used in the Nano-in Nano approach. Co-encapsulation of BER was hypothesized to reduce the therapeutic dose of ETP, which would minimize its toxicity and overcome the problem of developing resistance and enhance its antitumor efficacy (275). When given in lung cancer-bearing mice, it leads to a decrease in vascular endothelial growth factor (VEGF) expression level, triggered caspase activation with tumor cell apoptosis, and enhanced antiangiogenic effect that might refer to synergistic topoisomerase II inhibition and reduction of multidrug resistance (MDR) effect in A549 cells (232, 275, 277). Thus, various plants possessing anticancer properties can be formulated with modifications to make them suitable for use as a theranostic leading to a substantial increase in the potency of anticancer drugs in the future.

CONCLUSION

Conventional cancer therapies are sometimes restricted due to their low specificity, which can result in significant side effects and toxicity, as well as the likely creation of MDR phenotype. As a corollary, the necessity to precisely destroy cancer cells, overcome MDR, and boost the specificity of a medication using spatial, temporal, and dosage regulation of its release is driving the hunt for more effective anti-cancer therapy. Natural products are a key source for the development of innovative anti-cancer medicines that may be used both preventively and therapeutically. Phytochemicals at lower doses initiate adaptive response but as one increases the dose it produces acute autophagic response and apoptosis. There are several types of drug carriers available today, each with distinct and varied qualities that make them suitable for the treatment of cancers. After appropriate studies, it is now possible to create multipurpose nanocarriers that permit the slow and selective release of various drugs at specific tumor locations. *In vitro* and preclinical research have shown that NPs transporting and delivering both chemotherapeutic drugs and natural ingredients are extremely efficient for both curative and chemosensitizing reasons. Allopathic drugs have some challenges with them, thus diverse research is ongoing for herbal medication to improve their effectiveness and for acknowledgment of their side effects. Plant extracts appear to be less effective and efficient than refined extracted herbal components. The inclusion of mixed elements may lead to antagonistic activity or undesirable side effects, as well as a reduction in the therapeutic potency of the main substance. The herbal component's anticancer activity should be recognized based on IC50 for cancer cell survival. Herbal medications with high IC50 values have little anti-cancer potency and so are not good options. Drug-drug interactions among herbal ingredients and other traditional FDA-approved drugs should be extensively explored to find the most effective additive mixtures. The importance of herbal medicines may increase in the future *via* such a nano-drug delivery system. Further research is requisite to address the safety issues related to these systems.

AUTHOR CONTRIBUTIONS

VC has prepared the backbone of the manuscript. VC and AP wrote the original draft of the manuscript with KM and SS. Z-SC, ZW, KH, AP, and VC refined the first draft. Z-SC and VC critically revise the manuscript for intellectually correct content. KH supports the project. All authors contributed to the article and approved the submitted version.

ACKNOWLEDGMENTS

VC wants to dedicate this article to L M College of Pharmacy, Ahmedabad (India) on the 75th Year celebration of the college. VC would like to thank Vishal Vaghasiya, Vishwa Modi, and Shivangi D. Bagadia for their support in this manuscript preparation. The figures are created with BioRender.com.

REFERENCES

1. Kooti W, Servatyari K, Behzadifar M, Asadi-Samani M, Sadeghi F, Nouri B, et al. Effective Medicinal Plant in Cancer Treatment, Part 2: Review Study. *J Evid Based Complement Altern Med* (2017) 22(4):982–95. doi: 10.1177/2156587217696927
2. Chavda VP, Ertas YN, Walhekar V, Modh D, Doshi A, Shah N, et al. Advanced Computational Methodologies Used in the Discovery of New Natural Anticancer Compounds. *Front Pharmacol* (2021) 12:702611. doi: 10.3389/fphar.2021.702611
3. Arruebo M, Vilaboa N, Sáez-Gutierrez B, Lambea J, Tres A, Valladares M, et al. Assessment of the Evolution of Cancer Treatment Therapies. *Cancers (Basel)* (2011) 3(3):3279–330. doi: 10.3390/cancers3033279
4. Mansoori B, Mohammadi A, Davudian S, Shirjang S, Baradaran B. The Different Mechanisms of Cancer Drug Resistance: A Brief Review. *Adv Pharm Bull* (2017) 7(3):339–48. doi: 10.15171/apb.2017.041
5. Jardim DL, Goodman A, de Melo Gagliato D, Kurzrock R. The Challenges of Tumor Mutational Burden as an Immunotherapy Biomarker. *Cancer Cell* (2021) 39(2):154–73. doi: 10.1016/j.ccell.2020.10.001
6. Ulbright TM. Germ Cell Tumors of the Gonads: A Selective Review Emphasizing Problems in Differential Diagnosis, Newly Appreciated, and Controversial Issues. *Mod Pathol* (2005) 18(2):S61–79. doi: 10.1038/modpathol.3800310
7. Zeeshan R, Mutahir Z. Cancer Metastasis - Tricks of the Trade. *Bosn J Basic Med Sci* (2017) 17(3):172–82. doi: 10.17305/bjbms.2017.1908
8. Hecker E. Definitions and Terminology in Cancer (Tumour) Etiology. *Bull World Health Organ* (1976) 54(1):1–10.
9. Weisburger JH. Antimutagens, Anticarcinogens, and Effective Worldwide Cancer Prevention. *J Environ Pathol* (1999) 18(2):85–93.
10. de Martel C, Georges D, Bray F, Ferlay J, Clifford GM. Global Burden of Cancer Attributable to Infections in 2018: A Worldwide Incidence Analysis. *Lancet Glob Heal* (2020) 8(2):e180–90. doi: 10.1016/S2214-109X(19)30488-7
11. Ferlay J, Colombet M, Soerjomataram I, Mathers C, Parkin DM, Piñeros M, et al. Estimating the Global Cancer Incidence and Mortality in 2018: GLOBOCAN Sources and Methods. *Int J Cancer* (2019) 144(8):1941–53. doi: 10.1002/ijc.31937
12. Martin MC. Radiation Oncology—External-Beam Radiation Therapy. *Health Phys* (2019) 116(2):184–8. doi: 10.1097/HP.0000000000001034
13. Dawood S, Leyland-Jones B. Pharmacology and Pharmacogenetics of Chemotherapeutic Agents. *Cancer Invest* (2009) 27(5):482–8. doi: 10.1080/07357900802574660
14. Frei E. Curative Cancer Chemotherapy. *Cancer Res* (1985) 45(12):6523–37.
15. Wyszomirska A. Iodine-131 for Therapy of Thyroid Diseases. Physical and Biological Basis. *Nucl Med Rev Cent East Eur* (2012) 15(2):120–3.
16. Cragg GM, Pezzuto JM. Natural Products as a Vital Source for the Discovery of Cancer Chemotherapeutic and Chemopreventive Agents. *Med Princ Pract* (2016) 25(2):41–59. doi: 10.1159/000443404
17. Aggarwal BB, Prasad S, Reuter S, Kannappan R, Yadev VR, Park B, et al. Identification of Novel Anti-Inflammatory Agents From Ayurvedic Medicine for Prevention of Chronic Diseases: "Reverse Pharmacology" and "Bedside to Bench" Approach. *Curr Drug Targets* (2011) 12(11):1595–653. doi: 10.2174/138945011798109464
18. Baliga MS, Meera S, Vaishnav LK, Rao S, Palatty PL. Rasayana Drugs From the Ayurvedic System of Medicine as Possible Radioprotective Agents in Cancer Treatment. *Integr Cancer Ther* (2013) 12(6):455–63. doi: 10.1177/1534735413490233
19. Pilmeijer A. Cancer & Ayurveda as a Complementary Treatment. *Int J Complement Altern Med* (2017) 6(5):00202. doi: 10.15406/ijcam.2017.06.00202
20. Smit HF, Woerdenbag HJ, Singh RH, Meulenbeld GJ, Labadie RP, Zwaving JH. Ayurvedic Herbal Drugs With Possible Cytostatic Activity. *J Ethnopharmacol* (1995) 47(2):75–84. doi: 10.1016/0378-8741(95)01255-C
21. Chauhan A, Semwal DK, Mishra SP, Semwal RB. Ayurvedic Research and Methodology: Present Status and Future Strategies. *Ayu* (2015) 36(4):364–9. doi: 10.4103/0974-8520.190699
22. Balachandran P, Govindarajan R. Cancer–An Ayurvedic Perspective. *Pharmacol Res* (2005) 51(1):19–30. doi: 10.1016/j.phrs.2004.04.010
23. Singh RH. An Assessment of the Ayurvedic Concept of Cancer and a New Paradigm of Anticancer Treatment in Ayurveda. *J Altern Complement Med* (2002) 8(5):609–14. doi: 10.1089/107555302320825129
24. Trawick M. An Ayurvedic Theory of Cancer. *Med Anthropol* (1991) 13(1–2):121–36. doi: 10.1080/01459740.1991.9966044
25. Cragg GM, Newman DJ. Plants as a Source of Anti-Cancer Agents. *J Ethnopharmacol* (2005) 100(1–2):72–9. doi: 10.1016/j.jep.2005.05.011
26. Jain R, Kosta S, Tiwari A. Ayurveda and Cancer. *Pharmacognosy Res* (2010) 2(6):393–4. doi: 10.4103/0974-8490.75463
27. Sumantran VN, Tillu G. Cancer, Inflammation, and Insights From Ayurveda. *Evid-Based Complement Altern Med* (2012) 2012:306346. doi: 10.1155/2012/306346
28. Kamboj VP. Herbal Medicine. *Curr Sci* (2000) 78(1):35–9. doi: 10.1186/CVM-1-1-035
29. Agarwal N, Majee C, Chakraborthy GS. Natural Herbs as Anticancer Drugs. *Int J PharmTech Res* (2012) 4(3):1142–53. doi: 10.1201/9781315366753-15
30. Bisht D, Kumar D, Kumar D, Dua K, Chellappan DK. Phytochemistry and Pharmacological Activity of the Genus Artemisia. *Arch Pharm Res* (2021) 44(5):439–74. doi: 10.1007/s12272-021-01328-4
31. Pan S-Y, Litscher G, Gao S-H, Zhou S-F, Yu Z-L, Chen H-Q, et al. Historical Perspective of Traditional Indigenous Medical Practices: The Current Renaissance and Conservation of Herbal Resources. *Evid-Based Complement Altern Med* (2014) 2014:525340. doi: 10.1155/2014/525340
32. Choudhari AS, Mandave PC, Deshpande M, Ranjekar P, Prakash O. Phytochemicals in Cancer Treatment: From Preclinical Studies to Clinical Practice. *Front Pharmacol* (2020) 10:1614. doi: 10.3389/fphar.2019.01614
33. Akter R, Uddin SJ, Grice ID, Tiralongo E. Cytotoxic Activity Screening of Bangladeshi Medicinal Plant Extracts. *J Nat Med* (2014) 68(1):246–52. doi: 10.1007/s11418-013-0789-5
34. Du J, Lu X, Long Z, Zhang Z, Zhu X, Yang Y, et al. *In Vitro* and *In Vivo* Anticancer Activity of Aconitine on Melanoma Cell Line B16. *Molecules* (2013) 18(1):757–67. doi: 10.3390/molecules18010757
35. Svoboda GH, Poore GA, Simpson PJ, Boder GB. Alkaloids of Acronychia Baueri Schott I: Isolation of the Alkaloids and a Study of the Antitumor and Other Biological Properties of Acronycine. *J Pharm Sci* (1966) 55(8):758–68. doi: 10.1002/jps.2600550803
36. Martha Thomson MA. Garlic [Allium Sativum]: A Review of its Potential Use as an Anti-Cancer Agent. *Curr Cancer Drug Targets* (2003) 3(1):67–81. doi: 10.2174/1568009033333736
37. Milner JA. A Historical Perspective on Garlic and Cancer. *J Nutr* (2001) 131(3):1027S–31S. doi: 10.1093/jn/131.3.1027S
38. Bianchini F, Vainio H. Allium Vegetables and Organosulfur Compounds: Do They Help Prevent Cancer? *Environ Health Perspect* (2001) 109(9):893–902. doi: 10.1289/ehp.01109893
39. Nakagawa H, Tsuta K, Kiuchi K, Senzaki H, Tanaka K, Hioki K, et al. Growth Inhibitory Effects of Diallyl Disulfide on Human Breast Cancer Cell Lines. *Carcinogenesis* (2001) 22(6):891–7. doi: 10.1093/carcin/22.6.891
40. Khalil N, Bishr M, Desouky S, Salama O. Ammi Visnaga L., a Potential Medicinal Plant: A Review. *Molecules* (2020) 25(2):301. doi: 10.3390/molecules25020301
41. Asadi-Samani M, Kooti W, Aslani E, Shirzad H. A Systematic Review of Iran's Medicinal Plants With Anticancer Effects. *J Evid-Based Complement Altern Med* (2016) 21(2):143–53. doi: 10.1177/2156587215600873
42. Yang Y, Yue Y, Runwei Y, Guolin Z. Cytotoxic, Apoptotic and Antioxidant Activity of the Essential Oil of Amomum Tsao-Ko. *Bioresour Technol* (2010) 101(11):4205–11. doi: 10.1016/j.biortech.2009.12.131
43. Chen C, You F, Wu F, Luo Y, Zheng G, Xu H, et al. Antiangiogenesis Efficacy of Ethanol Extract From Amomum Tsaoko in Ovarian Cancer Through Inducing ER Stress to Suppress P-STAT3/NF-Kb/IL-6 and VEGF Loop. *Evid-Based Complement Altern Med* (2020) 2020:2390125. doi: 10.1155/2020/2390125
44. Sœur J, Marrot L, Perez P, Iraqui I, Kienda G, Dardalhon M, et al. Selective Cytotoxicity of Aniba Rosaeodora Essential Oil Towards Epidermoid Cancer Cells Through Induction of Apoptosis. *Mutat Res - Genet Toxicol Environ Mutagen* (2011) 718(1–2):24–32. doi: 10.1016/j.mrgentox.2010.10.009
45. Zhou HJ, Wang WQ, Wu GD, Lee J, Li A. Artesunate Inhibits Angiogenesis and Downregulates Vascular Endothelial Growth Factor Expression in

Chronic Myeloid Leukemia K562 Cells. *Vascul Pharmacol* (2007) 47(2–3):131–8. doi: 10.1016/j.vph.2007.05.002
46. Kim J, Jung KH, Yan HH, Cheon MJ, Kang S, Jin X, et al. Artemisia Capillaris Leaves Inhibit Cell Proliferation and Induce Apoptosis in Hepatocellular Carcinoma. *BMC Complement Altern Med* (2018) 18(1):1–10. doi: 10.1186/s12906-018-2217-6
47. Jung KH, Rumman M, Yan H, Cheon MJ, Choi JG, Jin X, et al. An Ethyl Acetate Fraction of Artemisia Capillaris (ACE-63) Induced Apoptosis and Anti-Angiogenesis *via* Inhibition of PI3K/AKT Signaling in Hepatocellular Carcinoma. *Phyther Res* (2018) 32(10):2034–46. doi: 10.1002/ptr.6135
48. Cho WCS, Leung KN. *In Vitro* and *In Vivo* Anti-Tumor Effects of Astragalus Membranaceus. *Cancer Lett* (2007) 252(1):43–54. doi: 10.1016/j.canlet.2006.12.001
49. Li S, Sun Y, Huang J, Wang B, Gong Y, Fang Y, et al. Anti-Tumor Effects and Mechanisms of Astragalus Membranaceus (AM) and Its Specific Immunopotentiation: Status and Prospect. *J Ethnopharmacol* (2020) 258:112797. doi: 10.1016/j.jep.2020.112797
50. Abdolmohammadi MH, Fouladdel S, Shafiee A, Amin G, Ghaffari SM, Azizi E. Antiproliferative and Apoptotic Effect of Astrodaucus Orientalis (L.) Drude on T47D Human Breast Cancer Cell Line: Potential Mechanisms of Action. *Afr J Biotechnol* (2009) 8(17):4265–76. doi: 10.5897/AJB09.323
51. Nazemiyeh HSciences TU of M, , Razavi SM, Ardabili U of M, , Delazar A and Sciences TU of M, et al. Distribution Profile of Volatile Constituents in Different Parts of Astrodaucus Orientalis (L.) Drude. *Rec Nat Prod* (2009) 3 (3):126–30. Available at: https://acgpubs.org/article/records-of-natural-products/2009/3-july-september/distribution-profile-of-volatile-constituents-in-different-parts-of-astrodaucus-orientalis-l-drude.
52. Kapadia GJ, Azuine MA, Rao GS, Arai T, Iida A, Tokuda H. Cytotoxic Effect of the Red Beetroot (Beta Vulgaris L.) Extract Compared to Doxorubicin (Adriamycin) in the Human Prostate (PC-3) and Breast (MCF-7) Cancer Cell Lines. *Anticancer Agents Med Chem* (2011) 11(3):280–4. doi: 10.2174/187152011795347504
53. Suhail MM, Wu W, Cao A, Mondalek FG, Fung K-M, Shih P-T, et al. Boswellia Sacra Essential Oil Induces Tumor Cell-Specific Apoptosis and Suppresses Tumor Aggressiveness in Cultured Human Breast Cancer Cells. *BMC Complement Altern Med* (2011) 11:129. doi: 10.1186/1472-6882-11-129
54. Becer E, Kabadayı H, Başer KHC, Vatansever HS. Boswellia Sacra Essential Oil Manages Colon Cancer Stem Cells Proliferation and Apoptosis: A New Perspective for Cure. *J Essent Oil Res* (2021) 33(1):53–62. doi: 10.1080/10412905.2020.1839586
55. Filippini T, Malavolti M, Borrelli F, Izzo AA, Fairweather-Tait SJ, Horneber M, et al. Green Tea (Camellia Sinensis) for the Prevention of Cancer. *Cochrane Database Syst Rev* (2020) (3):CD005004. doi: 10.1002/14651858.CD005004.pub3
56. Rafieian-Kopaei M, Movahedi M. Breast Cancer Chemopreventive and Chemotherapeutic Effects of Camellia Sinensis (Green Tea): An Updated Review. *Electron Phys* (2017) 9(2):3838–44. doi: 10.19082/3838
57. Lorence A, Medina-Bolivar F, Nessler CL. Camptothecin and 10-Hydroxycamptothecin From Camptotheca Acuminata Hairy Roots. *Plant Cell Rep* (2004) 22(6):437–41. doi: 10.1007/s00299-003-0708-4
58. Felipe KB, Kviecinski MR, da Silva FO, Bücker NF, Farias MS, Castro LSEPW, et al. Inhibition of Tumor Proliferation Associated With Cell Cycle Arrest Caused by Extract and Fraction From Casearia Sylvestris (Salicaceae). *J Ethnopharmacol* (2014) 155(3):1492–9. doi: 10.1016/j.jep.2014.07.040
59. Ahmad NH, Rahim RA, Mat I. Catharanthus Roseus Aqueous Extract Is Cytotoxic to Jurkat Leukaemic T-Cells But Induces the Proliferation of Normal Peripheral Blood Mononuclear Cells. *Trop Life Sci Res* (2010) 21 (2):101–13.
60. Nayab D, Ali D, Arshad N, Malik A, Choudhary MI, Ahmed Z. Cucurbitacin Glucosides From Citrullus Colocynthis. *Nat Prod Res* (2006) 20(5):409–13. doi: 10.1080/14786410500044997
61. Wasfi IA. Some Pharmacological Studies on Citrullus Colocynthis. *J Herbs Spices Med Plants* (2010) 2(2):49–74. doi: 10.1300/J044v02n02_08
62. Wineman E, Douglas I, Wineman V, Sharova K, Jaspars M, Meshner S, et al. Commiphora Gileadensis Sap Extract Induces Cell Cycle-Dependent Death in Immortalized Keratinocytes and Human Dermoid Carcinoma Cells. *J Herb Med* (2015) 5(4):199–206. doi: 10.1016/j.hermed.2015.08.001
63. Zhang Z, Wang CZ, Wen XD, Shoyama Y, Yuan CS. Role of Saffron and Its Constituents on Cancer Chemoprevention. *Pharm Biol* (2013) 51(7):920–4. doi: 10.3109/13880209.2013.771190
64. Chryssanthi DG, Lamari FN, Iatrou G, Pylara A, Karamanos NK, Cordopatis P. Inhibition of Breast Cancer Cell Proliferation by Style Constituents of Different Crocus Species. *Anticancer Res* (2007) 27(1 A):357–62.
65. Tomeh MA, Hadianamrei R, Zhao X. A Review of Curcumin and Its Derivatives as Anticancer Agents. *Int J Mol Sci* (2019) 20(5):1033. doi: 10.3390/ijms20051033
66. Lakshmi S, Padmaja G, Remani P. Antitumour Effects of Isocurcumenol Isolated From Curcuma Zedoaria Rhizomes on Human and Murine Cancer Cells. *Int J Med Chem* (2011) 2011:1–13. doi: 10.1155/2011/253962
67. Shin Y, Lee Y. Cytotoxic Activity From Curcuma Zedoaria Through Mitochondrial Activation on Ovarian Cancer Cells. *Toxicol Res* (2013) 29 (4):257–61. doi: 10.5487/TR.2013.29.4.257
68. Shebaby WN, Mroueh M, Bodman-Smith K, Mansour A, Taleb RI, Daher CF, et al. Daucus Carota Pentane-Based Fractions Arrest the Cell Cycle and Increase Apoptosis in MDA-MB-231 Breast Cancer Cells. *BMC Complement Altern Med* (2014) 14:387. doi: 10.1186/1472-6882-14-387
69. Bagheri SM, Abdian-Asl A, Moghadam MT, Yadegari M, Mirjalili A, Zare-Mohazabieh F, et al. Antitumor Effect of Ferula Assa Foetida Oleo Gum Resin Against Breast Cancer Induced by 4T1 Cells in BALB/c Mice. *J Ayurveda Integr Med* (2017) 8(3):152–8. doi: 10.1016/j.jaim.2017.02.013
70. Gioti K, Papachristodoulou A, Benaki D, Beloukas A, Vontzalidou A, Aligiannis N, et al. Glycyrrhiza Glabra-Enhanced Extract and Adriamycin Antiproliferative Effect on PC-3 Prostate Cancer Cells. *Nutr Cancer* (2020) 72(2):320–32. doi: 10.1080/01635581.2019.1632357
71. Karmakar SR, Biswas SJ. ARK-B. Anti-Carcinogenic Potentials of a Plant Extract (Hydrastis Canadensis): I. Evidence From *In Vivo* Studies in Mice (Mus Musculus). *Asian Pac J Cancer Prev* (2010) 11(2):545–51.
72. Guo B, Li X, Song S, Chen M, Cheng M, Zhao D, et al. Hydrastine Suppresses the Proliferation and Invasion of Human Lung Adenocarcinoma Cells by Inhibiting PAK4 Kinase Activity. *Oncol Rep* (2016) 35(4):2246–56. doi: 10.3892/or.2016.4594
73. Arata S, Watanabe J, Maeda M, Yamamoto M, Matsuhashi H, Mochizuki M, et al. Continuous Intake of the Chaga Mushroom (Inonotus Obliquus) Aqueous Extract Suppresses Cancer Progression and Maintains Body Temperature in Mice. *Heliyon* (2016) 2(5):e00111–1. doi: 10.1016/j.heliyon.2016.e00111
74. Prajapati RP, Kalariya M, Parmar SK, Sheth NR. Phytochemical and Pharmacological Review of Lagenaria Sicereria. *J Ayurveda Integr Med* (2010) 1(4):266–72. doi: 10.4103/0975-9476.74431
75. Bongiovanni G, Cantero J, Eynard A, Goleniowski M. Organic Extracts of Larrea Divaricata Cav. Induced Apoptosis on Tumoral MCF7 Cells With an Higher Cytotoxicity Than Nordihydroguaiaretic Acid or Paclitaxel. *J Exp Ther Oncol* (2008) 7(1):1–7.
76. Al-Fatimi M, Friedrich U, Jenett-Siems K. Cytotoxicity of Plants Used in Traditional Medicine in Yemen. *Fitoterapia* (2005) 76(3–4):355–8. doi: 10.1016/j.fitote.2005.02.009
77. Montero-Villegas S, Crespo R, Rodenak-Kladniew B, Castro MA, Galle M, Cicció JF, et al. Cytotoxic Effects of Essential Oils From Four Lippia Alba Chemotypes in Human Liver and Lung Cancer Cell Lines. *J Essent Oil Res* (2018) 30(3):167–81. doi: 10.1080/10412905.2018.1431966
78. Mekuria AN, Tura AK, Hagos B, Sisay M, Abdela J, Mishore KM, et al. Anti-Cancer Effects of Lycopene in Animal Models of Hepatocellular Carcinoma: A Systematic Review and Meta-Analysis. *Front Pharmacol* (2020) 11:1306. doi: 10.3389/fphar.2020.01306
79. Gatouillat G, Magid AA, Bertin E, Okiemy-Akeli M-G, Morjani H, Lavaud C, et al. Cytotoxicity and Apoptosis Induced by Alfalfa (Medicago Sativa) Leaf Extracts in Sensitive and Multidrug-Resistant Tumor Cells. *Nutr Cancer* (2014) 66(3):483–91. doi: 10.1080/01635581.2014.884228
80. Rosenthal GA, Nkomo P. The Natural Abundance of L-Canavanine, an Active Anticancer Agent, in Alfalfa, Medicago Sativa (L.). *Pharm Biol* (2000) 38(1):1–6. doi: 10.1076/1388-0209(200001)3811-BFT001
81. Eo HJ, Park JH, Park GH, Lee MH, Lee JR, Koo JS, et al. Anti-Inflammatory and Anti-Cancer Activity of Mulberry (Morus Alba L.) Root Bark. *BMC Complement Altern Med* (2014) 14:1–9. doi: 10.1186/1472-6882-14-200

82. Alipour G, Dashti S, Hosseinzadeh H. Review of Pharmacological Effects of Myrtus Communis L. And its Active Constituents. *Phyther Res* (2014) 28 (8):1125–36. doi: 10.1002/ptr.5122
83. Majdalawieh AF, Fayyad MW. Recent Advances on the Anti-Cancer Properties of Nigella Sativa, a Widely Used Food Additive. *J Ayurveda Integr Med* (2016) 7(3):173–80. doi: 10.1016/j.jaim.2016.07.004
84. O'Hanlon FJ, Fragkos KC, Fini L, Patel PS, Mehta SJ, Rahman F, et al. Home Parenteral Nutrition in Patients With Advanced Cancer: A Systematic Review and Meta-Analysis. *Nutr Cancer* (2021) 73(6):943–55. doi: 10.1080/01635581.2020.1784441
85. Hong H, Baatar D, Hwang SG. Anticancer Activities of Ginsenosides, the Main Active Components of Ginseng. *Evid Based Complement Alternat Med* (2021) 2021:8858006. doi: 10.1155/2021/8858006
86. AL Shabanah OA, Alotaibi M, Al Rejaie SS, Alhoshani AR, Almutairi MM, Alshammari MA, et al. Inhibitory Effect of Ginseng on Breast Cancer Cell Line Growth *Via* Up-Regulation of Cyclin Dependent Kinase Inhibitor, P21 and P53. *Asian Pac J Cancer Prev* (2016) 17(11):4965–71. doi: 10.22034/APJCP.2016.17.11.4965
87. Deng Y, Ye X, Chen Y, Ren H, Xia L, Liu Y, et al. Chemical Characteristics of Platycodon Grandiflorum and Its Mechanism in Lung Cancer Treatment. *Front Pharmacol* (2021) 11:609825. doi: 10.3389/fphar.2020.609825
88. Shultz B, University W, Wilkes-Barre P. Medical Attributes of Podophyllum Peltatum - Mayapple. *Molecules* (2021) 26(17):5179.
89. Wu X, Li Q, Feng Y, Ji Q. Antitumor Research of the Active Ingredients From Traditional Chinese Medical Plant Polygonum Cuspidatum. *Evid Based Complement Alternat Med* (2018) 2018:2313021. doi: 10.1155/2018/2313021
90. Mahmoudi E, Abolfathi M, Hassanzadeh N, Milasi YE, Dehghani-Samani M, Khaledi M, et al. Prunus Armeniaca Effects on Expression of Genes Related to Apoptosis in Human Breast Cancer Cells. *Transl Med Commun* (2019) 4(1):4–9. doi: 10.1186/s41231-019-0036-5
91. Jeong SJ, Koh W, Kim B, Kim SH. Are There New Therapeutic Options for Treating Lung Cancer Based on Herbal Medicines and Their Metabolites? *J Ethnopharmacol* (2011) 138(3):652–61. doi: 10.1016/j.jep.2011.10.018
92. Majumder M, Debnath S, Gajbhiye RL, Saikia R, Gogoi B, Samanta SK, et al. Ricinus Communis L. Fruit Extract Inhibits Migration/Invasion, Induces Apoptosis in Breast Cancer Cells and Arrests Tumor Progression *In Vivo*. *Sci Rep* (2019) 9(1):14493. doi: 10.1038/s41598-019-50769-x
93. Choi W, Jung H, Kim K, Lee S, Yoon S, Park J, et al. Rhus Verniciflua Stokes Against Advanced Cancer: A Perspective From the Korean Integrative Cancer Center. *J BioMed Biotechnol* (2012) 2012:874276. doi: 10.1155/2012/874276
94. Lee JO, Moon JW, Lee SK, Kim SM, Kim N, Ko SG, et al. Rhus Verniciflua Extract Modulates Survival of MCF-7 Breast Cancer Cells Through the Modulation of AMPK-Pathway. *Biol Pharm Bull* (2014) 37(5):794–801. doi: 10.1248/bpb.b13-00893
95. Köhne CH, Bruce C, Folprecht G, Audisio R. Role of New Agents in the Treatment of Colorectal Cancer. *Surg Oncol* (2004) 13(2-3):75–81. doi: 10.1016/j.suronc.2004.09.004
96. Leaver CA, Yuan H, Wallen GR. Apoptotic Activities of Sanguinaria Canadensis: Primary Human Keratinocytes, C-33A, and Human Papillomavirus HeLa Cervical Cancer Lines. *Integr Med (Encinitas)* (2018) 17(1):32–7.
97. Gazak R, Walterova D, Kren V. Silybin and Silymarin - New and Emerging Applications in Medicine. *Curr Med Chem* (2007) 14(3):315–38. doi: 10.2174/092986707779941159
98. Jin BJ, Hyung JJ, Jae HP, Sun HL, Jeong RL, Hee KL, et al. Cancer-Preventive Peptide Lunasin From Solanum Nigrum L. Inhibits Acetylation of Core Histones H3 and H4 and Phosphorylation of Retinoblastoma Protein (Rb). *J Agric Food Chem* (2007) 55(26):10707–13. doi: 10.1021/jf072363p
99. Son YO, Kim J, Lim JC, Chung Y, Chung GH, Lee JC. Ripe Fruits of Solanum Nigrum L. Inhibits Cell Growth and Induces Apoptosis in MCF-7 Cells. *Food Chem Toxicol* (2003) 41(10):1421–8. doi: 10.1016/S0278-6915(03)00161-3
100. Bhagya N, Chandrashekar KR. Tetrandrine and Cancer – An Overview on the Molecular Approach. *BioMed Pharmacother* (2018) 97:624–32. doi: 10.1016/j.biopha.2017.10.116
101. Kingston DG. Taxol, an Exciting Anticancer Drug From Taxus Brevifolia. *Hum Med Agents Plants* (1993) 534(10):138–48. doi: 10.1021/bk-1993-0534.ch010
102. Gautam N, Mantha AK, Mittal S. Essential Oils and Their Constituents as Anticancer Agents: A Mechanistic View. *BioMed Res Int* (2014) 2014:154106. doi: 10.1155/2014/154106
103. Keefover-Ring K, Thompson JD. YBL. Beyond Six Scents: Defining a Seventh Thymus Vulgaris Chemotype New to Southern France by Ethanol Extraction. *Flavours Fragr J* (2009) 24(3):117–22. doi: 10.1002/ffj.1921
104. Abaza MSI, Orabi KY, Al-Quattan E, Al-Attiyah RJ. Growth Inhibitory and Chemo-Sensitization Effects of Naringenin, a Natural Flavanone Purified From Thymus Vulgaris, on Human Breast and Colorectal Cancer. *Cancer Cell Int* (2015) 15(1):1–19. doi: 10.1186/s12935-015-0194-0
105. Lee YJ, Song K, Cha SH, Cho S, Kim YS, Park Y. Sesquiterpenoids From Tussilago Farfara Flower Bud Extract for the Eco-Friendly Synthesis of Silver and Gold Nanoparticles Possessing Antibacterial and Anticancer Activities. *Nanomaterials* (2019) 9(6):819. doi: 10.3390/nano9060819
106. Esposito S, Bianco A, Russo R, Di Maro A, Isernia C, Pedone PV. Therapeutic Perspectives of Molecules From Urtica Dioica Extracts for Cancer Treatment. *Molecules* (2019) 24(15):2753. doi: 10.3390/molecules24152753
107. Yousefnia S, Naseri D, Seyed Forootan F, Tabatabaeian M, Moattar F, Ghafghazi T, et al. Suppressive Role of Viola Odorata Extract on Malignant Characters of Mammosphere-Derived Breast Cancer Stem Cells. *Clin Transl Oncol* (2020) 22(9):1619–34. doi: 10.1007/s12094-020-02307-9
108. Kienle GS, Glockmann A, Schink M, Kiene H. Viscum Album L. Extracts in Breast and Gynaecological Cancers: A Systematic Review of Clinical and Preclinical Research. *J Exp Clin Cancer Res* (2009) 28(1):79. doi: 10.1186/1756-9966-28-79
109. Balea ŞS, Pârvu AE, Pârvu M, Vlase L, Dehelean CA, Pop TI. Antioxidant, Anti-Inflammatory and Antiproliferative Effects of the Vitis Vinifera L. Var. Feteasc㠠Neagr㠠and Pinot Noir Pomace Extracts. *Front Pharmacol* (2020) 11:990. doi: 10.3389/fphar.2020.00990
110. Habib SHM, Makpol S, Hamid NAA, Das S, Ngah WZW, Yusof YAM. Ginger Extract (Zingiber Officinale) has Anti-Cancer and Anti-Inflammatory Effects on Ethionine-Induced Hepatoma Rats. *Clinics* (2008) 63(6):807–13. doi: 10.1590/S1807-59322008000600017
111. Rowland I, Gibson G, Heinken A, Scott K, Swann J, Thiele I, et al. Gut Microbiota Functions: Metabolism of Nutrients and Other Food Components. *Eur J Nutr* (2018) 57(1):1–24. doi: 10.1007/s00394-017-1445-8
112. Zhang X, Han Y, Huang W, Jin M, Gao Z. The Influence of the Gut Microbiota on the Bioavailability of Oral Drugs. *Acta Pharm Sin B* (2021) 11 (7):1789–812. doi: 10.1016/j.apsb.2020.09.013
113. Martínez-Ballesta Mc, Gil-Izquierdo Á, García-Viguera C, Domínguez-Perles R. Nanoparticles and Controlled Delivery for Bioactive Compounds: Outlining Challenges for New "Smart-Foods" for Health. *Foods (Basel Switzerland)* (2018) 7(5):72. doi: 10.3390/foods7050072
114. Weaver CM, Miller JW. Challenges in Conducting Clinical Nutrition Research. *Nutr Rev* (2017) 75(7):491–9. doi: 10.1093/nutrit/nux026
115. Benet LZ, Hosey CM, Ursu O, Oprea TI. BDDCS, the Rule of 5 and Drugability. *Adv Drug Deliv Rev* (2016) 101:89–98. doi: 10.1016/j.addr.2016.05.007
116. Karlsson JE, Heddle C, Rozkov A, Rotticci-Mulder J, Tuvesson O, Hilgendorf C, et al. High-Activity P-Glycoprotein, Multidrug Resistance Protein 2, and Breast Cancer Resistance Protein Membrane Vesicles Prepared From Transiently Transfected Human Embryonic Kidney 293-Epstein-Barr Virus Nuclear Antigen Cells. *Drug Metab Dispos* (2010) 38(4):705–14. doi: 10.1124/dmd.109.028886
117. Vasiliou V, Vasiliou K, Nebert DW. Human ATP-Binding Cassette (ABC) Transporter Family. *Hum Genomics* (2009) 3(3):281–90. doi: 10.1186/1479-7364-3-3-281
118. Wen H, Jung H, Li X. Drug Delivery Approaches in Addressing Clinical Pharmacology-Related Issues: Opportunities and Challenges. *AAPS J* (2015) 17(6):1327–40. doi: 10.1208/s12248-015-9814-9
119. Lippman SM, Klein EA, Goodman PJ, Lucia MS, Thompson IM, Ford LG, et al. Effect of Selenium and Vitamin E on Risk of Prostate Cancer and Other Cancers: The Selenium and Vitamin E Cancer Prevention Trial (SELECT). *JAMA* (2009) 301(1):39–51. doi: 10.1001/jama.2008.864

120. Kesarwani K, Gupta R, Mukerjee A. Bioavailability Enhancers of Herbal Origin: An Overview. *Asian Pac J Trop Biomed* (2013) 3(4):253–66. doi: 10.1016/S2221-1691(13)60060-X
121. De Santi C, Pietrabissa A, Spisni R, Mosca F, Pacifici GM. Sulphation of Resveratrol, a Natural Product Present in Grapes and Wine, in the Human Liver and Duodenum. *Xenobiotica* (2000) 30(6):609–17. doi: 10.1080/004982500406435
122. Lee J-A, Ha SK, Cho E, Choi I. Resveratrol as a Bioenhancer to Improve Anti-Inflammatory Activities of Apigenin. *Nutrients* (2015) 7(11):9650–61. doi: 10.3390/nu7115485
123. Li Y, Yao J, Han C, Yang J, Chaudhry MT, Wang S, et al. Quercetin, Inflammation and Immunity. *Nutrients* (2016) 8(3):167. doi: 10.3390/nu8030167
124. Rajalakshmi S, Vyawahare N, Pawar A, Mahaparale P, Chellampillai B. Current Development in Novel Drug Delivery Systems of Bioactive Molecule Plumbagin. *Artif Cells Nanomed Biotechnol* (2018) 46(sup1):209–18. doi: 10.1080/21691401.2017.1417865
125. Yun YH, Lee BK, Park K. Controlled Drug Delivery: Historical Perspective for the Next Generation. *J Control Release* (2015) 219:2–7. doi: 10.1016/j.jconrel.2015.10.005
126. Rahman HS, Othman HH, Hammadi NI, Yeap SK, Amin KM, Abdul Samad N, et al. Novel Drug Delivery Systems for Loading of Natural Plant Extracts and Their Biomedical Applications. *Int J Nanomed* (2020) 15:2439–83. doi: 10.2147/IJN.S227805
127. Chavda VP. Nanotherapeutics and Nanobiotechnology. In: *Applications of Targeted Nano Drugs and Delivery Systems*. Cambridge, MA: Elsevier (2019). p. 1–13. doi: 10.1016/B978-0-12-814029-1.00001-6
128. Chavda VP, Thomas SBT-A of TND and DS. Chapter 4 - Nanobased Nano Drug Delivery: A Comprehensive Review. In: SS Mohapatra, S Ranjan, N Dasgupta and RK Mishra, editors. *Micro and Nano Technologies*. Cambridge, MA: Elsevier (2019). p. 69–92. doi: 10.1016/B978-0-12-814029-1.00004-1
129. Yoo J, Park C, Yi G, Lee D, Koo H. Active Targeting Strategies Using Biological Ligands for Nanoparticle Drug Delivery Systems. *Cancers (Basel)* (2019) 11(5):640. doi: 10.3390/cancers11050640
130. Goktas Z, Zu Y, Abbasi M, Galyean S, Wu D, Fan Z, et al. Recent Advances in Nanoencapsulation of Phytochemicals to Combat Obesity and Its Comorbidities. *J Agric Food Chem* (2020) 68(31):8119–31. doi: 10.1021/acs.jafc.0c00131
131. Bozzuto G, Molinari A. Liposomes as Nanomedical Devices. *Int J Nanomed* (2015) 10:975–99. doi: 10.2147/IJN.S68861
132. Akbarzadeh A, Rezaei-Sadabady R, Davaran S, Joo SW, Zarghami N, Hanifehpour Y, et al. Liposome: Classification, Preparation, and Applications. *Nanoscale Res Lett* (2013) 8(1):102. doi: 10.1186/1556-276X-8-102
133. Bardania H, Shojaosadati SA, Kobarfard F, Morshedi D, Aliakbari F, Tahoori MT, et al. RGD-Modified Nano-Liposomes Encapsulated Eptifibatide With Proper Hemocompatibility and Cytotoxicity Effect. *Iran J Biotechnol* (2019) 17(2):e2008–8. doi: 10.21859/ijb.2008
134. Panahi Y, Farshbaf M, Mohammadhosseini M, Mirahadi M, Khalilov R, Saghfi S, et al. Recent Advances on Liposomal Nanoparticles: Synthesis, Characterization and Biomedical Applications. *Artif Cells Nanomed Biotechnol* (2017) 45(4):788–99. doi: 10.1080/21691401.2017.1282496
135. Noriega-Luna B, Godínez LA, Rodríguez FJ, Rodríguez A, Zaldívar-Lelo De Larrea G, Sosa-Ferreyra CF, et al. Applications of Dendrimers in Drug Delivery Agents, Diagnosis, Therapy, and Detection. *J Nanomater* (2014) 2014:1–35. doi: 10.1155/2014/507273
136. Kaur A, Jain K, Mehra NK, Jain NK. Development and Characterization of Surface Engineered PPI Dendrimers for Targeted Drug Delivery. *Artif Cells Nanomed Biotechnol* (2017) 45(3):414–25. doi: 10.3109/21691401.2016.1160912
137. Yousefi M, Narmani A, Jafari SM. Dendrimers as Efficient Nanocarriers for the Protection and Delivery of Bioactive Phytochemicals. *Adv Colloid Interf Sci* (2020) 278:102125. doi: 10.1016/j.cis.2020.102125
138. Chavda VP. Niosome: A Vesicular Weapon for Targeted and Controlled Drug Delivery. *Indian J Nov Drug Deliv* (2016) 8(3):133–56. doi: 10.22270/jddt.v11i1.4479
139. Barani M, Mirzaei M, Torkzadeh-Mahani M, Adeli-sardou M. Evaluation of Carum-Loaded Niosomes on Breast Cancer Cells: Physicochemical Properties, *In Vitro* Cytotoxicity, Flow Cytometric, DNA Fragmentation and Cell Migration Assay. *Sci Rep* (2019) 9(1):7139. doi: 10.1038/s41598-019-43755-w
140. Jhaveri AM, Torchilin VP. Multifunctional Polymeric Micelles for Delivery of Drugs and siRNA. *Front Pharmacol* (2014) 5:77. doi: 10.3389/fphar.2014.00077
141. Majumder N, Das N G, Das SK. Polymeric Micelles for Anticancer Drug Delivery. *Ther Deliv* (2020) 11(10):613–35. doi: 10.4155/tde-2020-0008
142. Abedanzadeh M, Salmanpour M, Farjadian F, Mohammadi S, Tamaddon AM. Curcumin Loaded Polymeric Micelles of Variable Hydrophobic Lengths by RAFT Polymerization: Preparation and *in-Vitro* Characterization. *J Drug Deliv Sci Technol* (2020) 58:101793. doi: 10.1016/j.jddst.2020.101793
143. Hamad Farah F. Magnetic Microspheres: A Novel Drug Delivery System. *J Anal Pharm Res* (2016) 3(4):14–12. doi: 10.15406/japlr.2016.03.00067
144. Taherkhani A, Fazli H, Taherkhani F. Application of Janus Magnetic Nanoparticle Fe3O4@SiN Functionalized With Beta-Cyclodextrin in Thymol Drug Delivery Procedure: An *In Vitro* Study. *Appl Organomet Chem* (2021) 35(11):e6399. doi: 10.1002/aoc.6399
145. Kotta S, Khan AW, Pramod K, Ansari SH, Sharma RK, Ali J. Exploring Oral Nanoemulsions for Bioavailability Enhancement of Poorly Water-Soluble Drugs. *Expert Opin Drug Deliv* (2012) 9(5):585–98. doi: 10.1517/17425247.2012.668523
146. Wang J, Hu X, Xiang D. Nanoparticle Drug Delivery Systems: An Excellent Carrier for Tumor Peptide Vaccines. *Drug Deliv* (2018) 25(1):1319–27. doi: 10.1080/10717544.2018.1477857
147. Jamali SN, Assadpour E, Jafari SM. Formulation and Application of Nanoemulsions for Nutraceuticals and Phytochemicals. *Curr Med Chem* (2020) 27(18):3079–95. doi: 10.2174/0929867326666190620102820
148. Chavda VP, Shah DB. A Review on Novel Emulsification Technique: A Nanoemulsion. *Res Rev J Pharmacol Toxicol Stud* (2017) 5(1):29–38.
149. Chavda VP, Shah DB, Domadiya K. Microemulsion: Novel Carrier for Drug Delivery. *Trends Drug Deliv* (2016) 3(1):1–18.
150. Moura RP, Pacheco C, Pêgo AP, des Rieux A, Sarmento B. Lipid Nanocapsules to Enhance Drug Bioavailability to the Central Nervous System. *J Control Rel* (2020) 322:390–400. doi: 10.1016/j.jconrel.2020.03.042
151. Chavda VP. Chapter 4 Nanobased Nano Drug Delivery A Comprehensive Review. In: *Micro and Nano Technologies*. United States: Elsevier (2021). p. 69–92. doi: 10.1016/B978-0-12-814029-1.00004-1
152. Maleki Dizaj S, Mennati A, Jafari S, Khezri K, Adibkia K. Antimicrobial Activity of Carbon-Based Nanoparticles. *Adv Pharm Bull* (2015) 5(1):19–23. doi: 10.5681/apb.2015.003"10.5681/apb.2015.003
153. Maiti D, Tong X, Mou X, Yang K. Carbon-Based Nanomaterials for Biomedical Applications: A Recent Study. *Front Pharmacol* (2019) 9. doi: 10.3389/fphar.2018.01401
154. Begines B, Ortiz T, Pérez-Aranda M, Martínez G, Merinero M, Argüelles-Arias F, et al. Polymeric Nanoparticles for Drug Delivery: Recent Developments and Future Prospects. *Nanomater (Basel Switzerland)* (2020) 10(7):1403. doi: 10.3390/nano10071403
155. Pan J, Rostamizadeh K, Filipczak N, Torchilin VP. Polymeric Co-Delivery Systems in Cancer Treatment: An Overview on Component Drugs' Dosage Ratio Effect. *Molecules* (2019) 24(6):1035. doi: 10.3390/molecules24061035
156. Gigliobianco MR, Casadidio C, Censi R, Di Martino P. Nanocrystals of Poorly Soluble Drugs: Drug Bioavailability and Physicochemical Stability. *Pharmaceutics* (2018) 10(3):134. doi: 10.3390/pharmaceutics10030134
157. Sivadasan D, Sultan MH, Madkhali O, Almoshari Y, Thangavel N. Polymeric Lipid Hybrid Nanoparticles (PLNs) as Emerging Drug Delivery Platform—A Comprehensive Review of Their Properties, Preparation Methods, and Therapeutic Applications. *Pharmaceutics* (2021) 13(8):1291. doi: 10.3390/pharmaceutics13081291
158. de Souza A, Marins DSS, Mathias SL, Monteiro LM, Yukuyama MN, Scarim CB, et al. Promising Nanotherapy in Treating Leishmaniasis. *Int J Pharm* (2018) 547(1–2):421–31. doi: 10.1016/j.ijpharm.2018.06.018
159. Bhattacharyya S, Kudgus RA, Bhattacharya R, Mukherjee P. Inorganic Nanoparticles in Cancer Therapy. *Pharm Res* (2011) 28(2):237–59. doi: 10.1007/s11095-010-0318-0
160. Yaqoob AA, Ahmad H, Parveen T, Ahmad A, Oves M, Ismail IMI, et al. Recent Advances in Metal Decorated Nanomaterials and Their Various

Biological Applications: A Review. *Front Chem* (2020) 8:341. doi: 10.3389/fchem.2020.00341
161. Vasile C, Pamfil D, Stoleru E, Baican M. New Developments in Medical Applications of Hybrid Hydrogels Containing Natural Polymers. *Molecules* (2020) 25(7):1539. doi: 10.3390/molecules25071539
162. Ulldemolins A, Seras-Franzoso J, Andrade F, Rafael D, Abasolo I, Gener P, et al. Perspectives of Nano-Carrier Drug Delivery Systems to Overcome Cancer Drug Resistance in the Clinics. *Cancer Drug Resist* (2021) 4(1):44–68. doi: 10.20517/cdr.2020.59
163. Duong TT, Isomäki A, Paaver U, Laidmäe I, Tõnisoo A, Yen TTH, et al. Nanoformulation and Evaluation of Oral Berberine-Loaded Liposomes. *Molecules* (2021) 26(9):2591. doi: 10.3390/molecules26092591
164. Macchione MA, Aristizabal Bedoya D, Figueroa FN, Muñoz-Fernández MÁ, Strumia MC. Nanosystems Applied to HIV Infection: Prevention and Treatments. *Int J Mol Sci* (2020) 21(22):8647. doi: 10.3390/ijms21228647
165. Nitta SK, Numata K. Biopolymer-Based Nanoparticles for Drug/Gene Delivery and Tissue Engineering. *Int J Mol Sci* (2013) 14(1):1629–54. doi: 10.3390/ijms14011629
166. Shah SA, Sohail M, Khan S, Minhas MU, de Matas M, Sikstone V, et al. Biopolymer-Based Biomaterials for Accelerated Diabetic Wound Healing: A Critical Review. *Int J Biol Macromol* (2019) 139:975–93. doi: 10.1016/j.ijbiomac.2019.08.007
167. Sebak S, Mirzaei M, Malhotra M, Kulamarva A, Prakash S. Human Serum Albumin Nanoparticles as an Efficient Noscapine Drug Delivery System for Potential Use in Breast Cancer: Preparation and *In Vitro* Analysis. *Int J Nanomed* (2010) :5:525–32. doi: 10.2147/IJN.S10443
168. Sanna V, Roggio AM, Siliani S, Piccinini M, Marceddu S, Mariani A, et al. Development of Novel Cationic Chitosan-and Anionic Alginate-Coated Poly (D,L-Lactide-Co-Glycolide) Nanoparticles for Controlled Release and Light Protection of Resveratrol. *Int J Nanomed* (2012) 7:5501–16. doi: 10.2147/IJN.S36684
169. Aqil F, Munagala R, Jeyabalan J, Vadhanam MV. Bioavailability of Phytochemicals and its Enhancement by Drug Delivery Systems. *Cancer Lett* (2013) 334(1):133–41. doi: 10.1016/j.canlet.2013.02.032
170. Wang C, Feng L, Yang X, Wang F, Lu W. Folic Acid-Conjugated Liposomal Vincristine for Multidrug Resistant Cancer Therapy. *Asian J Pharm Sci* (2013) 8(2):118–27. doi: 10.1016/j.ajps.2013.07.015
171. Caldeira de Araújo Lopes S, Vinícius Melo Novais M, Salviano Teixeira C, Honorato-Sampaio K, Tadeu Pereira M, Ferreira LAM, et al. Preparation, Physicochemical Characterization, and Cell Viability Evaluation of Long-Circulating and pH-Sensitive Liposomes Containing Ursolic Acid. Surguchov A, Editor. *BioMed Res Int* (2013) 2013:467147. doi: 10.1155/2013/467147
172. Xiao Z, Zhuang B, Zhang G, Li M, Jin Y. Pulmonary Delivery of Cationic Liposomal Hydroxycamptothecin and 5-Aminolevulinic Acid for Chemo-Sonodynamic Therapy of Metastatic Lung Cancer. *Int J Pharm* (2021) 601:120572. doi: 10.1016/j.ijpharm.2021.120572
173. Mehta PP, Ghoshal D, Pawar AP, Kadam SS, Dhapte-Pawar VS. Recent Advances in Inhalable Liposomes for Treatment of Pulmonary Diseases: Concept to Clinical Stance. *J Drug Deliv Sci Technol* (2020) 56:101509. doi: 10.1016/j.jddst.2020.101509
174. Tzogani K, Penttilä K, Lapveteläinen T, Hemmings R, Koenig J, Freire J, et al. EMA Review of Daunorubicin and Cytarabine Encapsulated in Liposomes (Vyxeos, CPX-351) for the Treatment of Adults With Newly Diagnosed, Therapy-Related Acute Myeloid Leukemia or Acute Myeloid Leukemia With Myelodysplasia-Related Changes. *Oncologist* (2020) 25(9):e1414–20. doi: 10.1634/theoncologist.2019-0785
175. Chen R-P, Chavda VP, Patel AB, Chen Z-S. Phytochemical Delivery Through Transferosome (Phytosome): An Advanced Transdermal Drug Delivery for Complementary Medicines. *Front Pharmacol* (2022) 13:850862. doi: 10.3389/fphar.2022.850862
176. Opatha SAT, Titapiwatanakun V, Chutoprapat R. Transfersomes: A Promising Nanoencapsulation Technique for Transdermal Drug Delivery. *Pharmaceutics* (2020) 12(9):855. doi: 10.3390/pharmaceutics12090855
177. Raafat KM, El-Zahaby SA. Niosomes of Active Fumaria Officinalis Phytochemicals: Antidiabetic, Antineuropathic, Anti-Inflammatory, and Possible Mechanisms of Action. *Chin Med (United Kingdom)* (2020) 15 (1):1–22. doi: 10.1186/s13020-020-00321-1
178. Agarwal S, Mohamed MS, Raveendran S, Rochani AK, Maekawa T, Kumar DS. Formulation, Characterization and Evaluation of Morusin Loaded Niosomes for Potentiation of Anticancer Therapy. *RSC Adv* (2018) 8 (57):32621–36. doi: 10.1039/C8RA06362A
179. Mousazadeh N, Gharbavi M, Rashidzadeh H, Nosrati H, Danafar H, Johari B. Anticancer Evaluation of Methotrexate and Curcumin-Coencapsulated Niosomes Against Colorectal Cancer Cell Lines. *Nanomedicine* (2022) 17 (4):201–17. doi: 10.2217/nnm-2021-0334
180. Imam SS, Alshehri S, Altamimi MA, Hussain A, Alyahya KH, Mahdi WA, et al. Formulation and Evaluation of Luteolin-Loaded Nanovesicles: *In Vitro* Physicochemical Characterization and Viability Assessment. *ACS Omega* (2022) 7(1):1048–56. doi: 10.1021/acsomega.1c05628
181. Hanafy NAN, El-Kemary M, Leporatti S. Micelles Structure Development as a Strategy to Improve Smart Cancer Therapy. *Cancers (Basel)* (2018) 10 (7):238. doi: 10.3390/cancers10070238
182. Modi G, Pillay V, Choonara YE, Ndesendo VMK, du Toit LC, Naidoo D. Nanotechnological Applications for the Treatment of Neurodegenerative Disorders. *Prog Neurobiol* (2009) 88(4):272–85. doi: 10.1016/j.pneurobio.2009.05.002
183. Li Z, Zhang G, Luo Y, Gao Q, Wang J, Chen C, et al. *In Vivo* Effect of Magnetic Microspheres Loaded With E2-A in the Treatment of Alveolar Echinococcosis. *Sci Rep* (2020) 10(1):12589. doi: 10.1038/s41598-020-69484-z
184. Xiao Y, Hong H, Javadi A, Jonathan W Engle WX, Yang Y, Zhang Y, et al. Multifunctional Unimolecular Micelles for Cancer-Targeted Drug Delivery and Positron Emission Tomography Imaging. *Biomaterials* (2012) 33 (11):3071–82. doi: 10.1016/j.biomaterials.2011.12.030
185. Kumari A, Yadav SK, Yadav SC. Biodegradable Polymeric Nanoparticles Based Drug Delivery Systems. *Colloids Surf B Biointerf* (2010) 75(1):1–18. doi: 10.1016/j.colsurfb.2009.09.001
186. Emami J, Kazemi M, Hasanzadeh F, Minaiyan M, Mirian M, Lavasanifar A. Novel pH-Triggered Biocompatible Polymeric Micelles Based on Heparin–α-Tocopherol Conjugate for Intracellular Delivery of Docetaxel in Breast Cancer. *Pharm Dev Technol* (2020) 25(4):492–509. doi: 10.1080/10837450.2019.1711395
187. Anselmo AC, Mitragotri S. An Overview of Clinical and Commercial Impact of Drug Delivery Systems. *J Control Rel* (2014) :190:15–28. doi: 10.1016/j.jconrel.2014.03.053
188. Enriquez GG, Rizvi SAA, D'Souza MJ, Do DP. Formulation and Evaluation of Drug-Loaded Targeted Magnetic Microspheres for Cancer Therapy. *Int J Nanomed* (2013) 8:1393–402. doi: 10.2147/IJN.S43479
189. Wang X, Jing X, Zhang X, Liu Q, Liu J, Song D, et al. A Versatile Platform of Magnetic Microspheres Loaded With Dual-Anticancer Drugs for Drug Release. *Mater Chem Phys* (2016) 177:213–9. doi: 10.1016/j.matchemphys.2016.04.021
190. Gugleva V, Ivanova N, Sotirova Y, Andonova V. Dermal Drug Delivery of Phytochemicals With Phenolic Structure *via* Lipid-Based Nanotechnologies. *Pharmaceuticals* (2021) 14(9):837. doi: 10.3390/ph14090837
191. Shakhwar S, Darwish R, Kamal MM, Nazzal S, Pallerla S, Abu Fayyad A. Development and Evaluation of Paclitaxel Nanoemulsion for Cancer Therapy. *Pharm Dev Technol* (2020) 25(4):510–6. doi: 10.1080/10837450.2019.1706564
192. Leite CBS, Coelho JM, Ferreira-Nunes R, Gelfuso GM, Durigan JLQ, Azevedo RB, et al. Phonophoretic Application of a Glucosamine and Chondroitin Nanoemulsion for Treatment of Knee Chondropathies. *Nanomedicine* (2020) 15(7):647–59. doi: 10.2217/nnm-2019-0317
193. Chrastina A, Baron VT, Abedinpour P, Rondeau G, Welsh J, Borgström P. Plumbagin-Loaded Nanoemulsion Drug Delivery Formulation and Evaluation of Antiproliferative Effect on Prostate Cancer Cells. *BioMed Res Int* (2018) 2018:9035452. doi: 10.1155/2018/9035452
194. Rondeau G, Abedinpour P, Chrastina A, Pelayo J, Borgstrom P, Welsh J. Differential Gene Expression Induced by Anti-Cancer Agent Plumbagin Is Mediated by Androgen Receptor in Prostate Cancer Cells. *Sci Rep* (2018) 8 (1):2694. doi: 10.1038/s41598-018-20451-9
195. Fofaria NM, Qhattal HSS, Liu X, Srivastava SK. Nanoemulsion Formulations for Anti-Cancer Agent Piplartine–Characterization, Toxicological, Pharmacokinetics and Efficacy Studies. *Int J Pharm* 498(1–2):12–22. doi: 10.1016/j.ijpharm.2015.11.045
196. Kamaly N, Yameen B, Wu J, Farokhzad OC. Degradable Controlled-Release Polymers and Polymeric Nanoparticles: Mechanisms of Controlling Drug

Release. *Chem Rev* (2016) 116(4):2602–63. doi: 10.1021/acs.chemrev.5b00346
197. Javed Iqbal M, Quispe C, Javed Z, Sadia H, Qadri QR, Raza S, et al. Nanotechnology-Based Strategies for Berberine Delivery System in Cancer Treatment: Pulling Strings to Keep Berberine in Power. *Front Mol Biosci* (2021) 7:624494. doi: 10.3389/fmolb.2020.624494
198. Ansari SH, Islam F, Sameem M. Influence of Nanotechnology on Herbal Drugs: A Review. *J Adv Pharm Technol Res* (2012) 3(3):142–6. doi: 10.4103/2231-4040.101006
199. Gugulothu D, Kulkarni A, Patravale V, Dandekar P. PH-Sensitive Nanoparticles of Curcumin-Celecoxib Combination: Evaluating Drug Synergy in Ulcerative Colitis Model. *J Pharm Sci* (2014) 103(2):687–96. doi: 10.1002/jps.23828
200. Ganesan RM, Gurumallesh Prabu H. Synthesis of Gold Nanoparticles Using Herbal Acorus Calamus Rhizome Extract and Coating on Cotton Fabric for Antibacterial and UV Blocking Applications. *Arab J Chem* (2019) 12 (8):2166–74. doi: 10.1016/j.arabjc.2014.12.017
201. Hojjati-Najafabadi A, Davar F, Enteshari Z, Hosseini-Koupaei M. Antibacterial and Photocatalytic Behaviour of Green Synthesis of Zn0.95Ag0.05O Nanoparticles Using Herbal Medicine Extract. *Ceram Int* (2021) 47(22):31617–24. doi: 10.1016/j.ceramint.2021.08.042
202. Alsaab HO, Alghamdi MS, Alotaibi AS, Alzhrani R, Alwuthaynani F, Althobaiti YS, et al. Progress in Clinical Trials of Photodynamic Therapy for Solid Tumors and the Role of Nanomedicine. *Cancers (Basel)* (2020) 12 (10):1–26. doi: 10.3390/cancers12102793
203. Das S, Das J, Samadder A, Paul A, Khuda-Bukhsh AR. Efficacy of PLGA-Loaded Apigenin Nanoparticles in Benzo[a]pyrene and Ultraviolet-B Induced Skin Cancer of Mice: Mitochondria Mediated Apoptotic Signalling Cascades. *Food Chem Toxicol* (2013) 62:670–80. doi: 10.1016/j.fct.2013.09.037
204. Chen Y, Zheng X-L, Fang D-L, Yang Y, Zhang J-K, Li H-L, et al. Dual Agent Loaded PLGA Nanoparticles Enhanced Antitumor Activity in a Multidrug-Resistant Breast Tumor Eenograft Model. *Int J Mol Sci* (2014) 15(2):2761–72. doi: 10.3390/ijms15022761
205. Ersoz M, Erdemir A, Derman S, Arasoglu T, Mansuroglu B. Quercetin-Loaded Nanoparticles Enhance Cytotoxicity and Antioxidant Activity on C6 Glioma Cells. *Pharm Dev Technol* (2020) 25(6):757–66. doi: 10.1080/10837450.2020.1740933
206. Gera M, Kim N, Ghosh M, Sharma N, Huynh DL, Chandimali N, et al. Synthesis and Evaluation of the Antiproliferative Efficacy of BRM270 Phytocomposite Nanoparticles Against Human Hepatoma Cancer Cell Lines. *Mater Sci Eng C Mater Biol Appl* (2019) 97:166–76. doi: 10.1016/j.msec.2018.11.055
207. Mukherjee A, Waters AK, Kalyan P, Achrol AS, Kesari S, Yenugonda VM. Lipid-Polymer Hybrid Nanoparticles as a Nextgeneration Drug Delivery Platform: State of the Art, Emerging Technologies, and Perspectives. *Int J Nanomed* (2019) 14:1937–52. doi: 10.2147/IJN.S198353
208. Kumar Sarwa K, Rudrapal M, Mazumder B. Topical Ethosomal Capsaicin Attenuates Edema and Nociception in Arthritic Rats. *Drug Deliv* (2015) 22 (8):1043–52. doi: 10.3109/10717544.2013.861041
209. Ma P, Mumper RJ. Paclitaxel Nano-Delivery Systems: A Comprehensive Review. *J Nanomed Nanotechnol* (2013) 4(2):1000164. doi: 10.4172/2157-7439.1000164
210. Wei T, Chen C, Liu J, Liu C, Posocco P, Liu X, et al. Anticancer Drug Nanomicelles Formed by Self-Assembling Amphiphilic Dendrimer to Combat Cancer Drug Resistance. *Proc Natl Acad Sci* (2015) 112(10):2978 LP–2983. doi: 10.1073/pnas.1418494112
211. Sadat Khadem F, Es-Haghi A, Homayouni Tabrizi M, Shabestarian H. The Loaded Ferula Assa-Foetida Seed Essential Oil in Solid Lipid Nanoparticles (FSEO-SLN) as the Strong Apoptosis Inducer Agents in Human NTERA-2 Embryocarcinoma Cells. *Mater Technol* (2021) 36(7):1–9. doi: 10.1080/10667857.2021.1924436
212. Ramesh N, Mandal AKA. Pharmacokinetic, Toxicokinetic, and Bioavailability Studies of Epigallocatechin-3-Gallate Loaded Solid Lipid Nanoparticle in Rat Model. *Drug Dev Ind Pharm* (2019) 45(9):1506–14. doi: 10.1080/03639045.2019.1634091
213. Jogi H, Maheshwari R, Raval N, Kuche K, Tambe V, Mak KK, et al. Carbon Nanotubes in the Delivery of Anticancer Herbal Drugs. *Nanomedicine* (2018) 13(10):1187–220. doi: 10.2217/nnm-2017-0397
214. Banica F, Bungau S, Tit DM, Behl T, Otrisal P, Nechifor AC, et al. Determination of the Total Polyphenols Content and Antioxidant Activity of Echinacea Purpurea Extracts Using Newly Manufactured Glassy Carbon Electrodes Modified With Carbon Nanotubes. *Processes* (2020) 8(7):833. doi: 10.3390/pr8070833
215. Nasseri MA, Keshtkar H, Kazemnejadi M, Allahresani A. Phytochemical Properties and Antioxidant Activity of Echinops Persicus Plant Extract: Green Synthesis of Carbon Quantum Dots From the Plant Extract. *SN Appl Sci* (2020) 2(4):670. doi: 10.1007/s42452-020-2466-0
216. Hashemi SF, Tasharrofi N, Saber MM. Green Synthesis of Silver Nanoparticles Using Teucrium Polium Leaf Extract and Assessment of Their Antitumor Effects Against MNK45 Human Gastric Cancer Cell Line. *J Mol Struct* (2020) 1208:127889. doi: 10.1016/j.molstruc.2020.127889
217. Mughees M, Wajid S, Samim M. Cytotoxic Potential of Artemisia Absinthium Extract Loaded Polymeric Nanoparticles Against Breast Cancer Cells: Insight Into the Protein Targets. *Int J Pharm* (2020) 586 (June):119583. doi: 10.1016/j.ijpharm.2020.119583
218. Ribeiro AF, Santos JF, Mattos RR, Barros EGO, Nasciutti LE, Cabral LM, et al. Characterization and *In Vitro* Antitumor Activity of Polymeric Nanoparticles Loaded With Uncaria Tomentosa Extract. *Acad Bras Cienc* (2020) 92(1):e20190336. doi: 10.1590/0001-3765202020190336
219. Khan T, Gurav P. PhytoNanotechnology: Enhancing Delivery of Plant Based Anti-Cancer Drugs. *Front Pharmacol* (2018) 8:1002. doi: 10.3389/fphar.2017.01002
220. Madaan K, Lather V, Pandita D. Evaluation of Polyamidoamine Dendrimers as Potential Carriers for Quercetin, a Versatile Flavonoid. *Drug Deliv* (2016) 23(1):254–62. doi: 10.3109/10717544.2014.910564
221. Singh V, Sahebkar A, Kesharwani P. Poly (Propylene Imine) Dendrimer as an Emerging Polymeric Nanocarrier for Anticancer Drug and Gene Delivery. *Eur Polym J* (2021) 158:110683. doi: 10.1016/j.eurpolymj.2021.110683
222. Singh A, Garg G, Sharma PK. Nanospheres: A Novel Approach for Targeted Drug Delivery System. *Int J Pharm Sci Rev Res* (2010) 5(3):84–8.
223. Hubenthal F. 1.13 - Noble Metal Nanoparticles: Synthesis and Optical Properties. In: DL Andrews, GD Scholes and T Wiederrecht GPBT-CN and, editors. *Comprehensive Nanoscience and Nanotechnology*. Amsterdam: Academic Press (2011). p. 375–435. doi: 10.1016/B978-0-12-374396-1.00034-9
224. Kuppusamy P, Yusoff MM, Maniam GP, Govindan N. Biosynthesis of Metallic Nanoparticles Using Plant Derivatives and Their New Avenues in Pharmacological Applications – An Updated Report. *Saudi Pharm J* (2016) 24(4):473–84. doi: 10.1016/j.jsps.2014.11.013
225. Liu G, Xu X, Jiang L, Ji H, Zhu F, Jin B, et al. Targeted Antitumor Mechanism of C-PC/CMC-CD55sp Nanospheres in HeLa Cervical Cancer Cells. *Front Pharmacol* (2020) 11(June):1–13. doi: 10.3389/fphar.2020.00906
226. Wei Q-Y, He K-M, Chen J-L, Xu Y-M, Lau ATY. Phytofabrication of Nanoparticles as Novel Drugs for Anticancer Applications. *Molecules* (2019) 24(23):4246. doi: 10.3390/molecules24234246
227. Burger KNJ, Staffhorst RWHM, de Vijlder HC, Velinova MJ, Bomans PH, Frederik PM, et al. Nanocapsules: Lipid-Coated Aggregates of Cisplatin With High Cytotoxicity. *Nat Med* (2002) 8(1):81–4. doi: 10.1038/nm0102-81
228. Kothamasu P, Kanumur H, Ravur N, Maddu C, Parasuramrajam R, Thangavel S. Nanocapsules: The Weapons for Novel Drug Delivery Systems. *BioImpacts* (2012) 2(2):71–81. doi: 10.5681/bi.2012.011
229. Aisida SO, Ugwoke E, Uwais A, Iroegbu C, Botha S, Ahmad I, et al. Incubation Period Induced Biogenic Synthesis of PEG Enhanced Moringa Oleifera Silver Nanocapsules and its Antibacterial Activity. *J Polym Res* (2019) 26(9):225. doi: 10.1007/s10965-019-1897-z
230. Osanloo M, Sedaghat MM, Sereshti H, Rahmani M, Landi FS, Amani A. Chitosan Nanocapsules of Tarragon Essential Oil With Low Cytotoxicity and Long-Lasting Activity as a Green Nano-Larvicide. *J Nanostructures* (2019) 9 (4):723–35. doi: 10.22052/JNS.2019.04.014
231. Thi TTH, Suys EJA, Lee JS, Nguyen DH, Park KD, Truong NP. Lipid-Based Nanoparticles in the Clinic and Clinical Trials: From Cancer Nanomedicine to COVID-19 Vaccines. *Vaccines* (2021) 9(4):359. doi: 10.3390/vaccines9040359
232. Mardani R, Hamblin MR, Taghizadeh M, Banafshe HR, Nejati M, Mokhtari M, et al. Nanomicellar-Curcumin Exerts its Therapeutic Effects *via* Affecting Angiogenesis, Apoptosis, and T Cells in a Mouse Model of Melanoma Lung

Metastasis. *Pathol Res Pract* (2020) 216(9):153082. doi: 10.1016/j.prp.2020.153082
233. Jeevanandam J, Barhoum A, Chan YS, Dufresne A, Danquah MK. Review on Nanoparticles and Nanostructured Materials: History, Sources, Toxicity and Regulations. *Beilstein J Nanotechnol* (2018) 9:1050–74. doi: 10.3762/bjnano.9.98
234. Gopinath V, MubarakAli D, Priyadarshini S, Priyadharsshini NM, Thajuddin N, Velusamy P. Biosynthesis of Silver Nanoparticles From Tribulus Terrestris and its Antimicrobial Activity: A Novel Biological Approach. *Colloids Surf B Biointerf* (2012) 96:69–74. doi: 10.1016/j.colsurfb.2012.03.023
235. Shameli K, Ahmad MB, Jaffar Al-Mulla EA, Ibrahim NA, Shabanzadeh P, Rustaiyan A, et al. Green Biosynthesis of Silver Nanoparticles Using Callicarpa Maingayi Stem Bark Extraction. *Molecules* (2012) 17(7):8506–17. doi: 10.3390/molecules17078506
236. Aboyewa JA, Sibuyi NRS, Meyer M, Oguntibeju OO. Green Synthesis of Metallic Nanoparticles Using Some Selected Medicinal Plants From Southern Africa and Their Biological Applications. *Plants* (2021) 10 (9):1929. doi: 10.3390/plants10091929
237. Tremi I, Spyratou E, Souli M, Efstathopoulos EP, Makropoulou M, Georgakilas AG, et al. Requirements for Designing an Effective Metallic Nanoparticle (NP)-Boosted Radiation Therapy (RT). *Cancers (Basel)* (2021) 13(13):3185. doi: 10.3390/cancers13133185
238. Montazerabadi A, Beik J, Irajirad R, Attaran N, Khaledi S, Ghaznavi H, et al. Folate-Modified and Curcumin-Loaded Dendritic Magnetite Nanocarriers for the Targeted Thermo-Chemotherapy of Cancer Cells. *Artif Cells nanomedicine Biotechnol* (2019) 47(1):330–40. doi: 10.1080/21691401.2018.1557670
239. Tousi MS, Sepehri H, Khoee S, Farimani MM, Delphi L, Mansourizadeh F. Evaluation of Apoptotic Effects of mPEG-B-PLGA Coated Iron Oxide Nanoparticles as a Eupatorin Carrier on DU-145 and LNCaP Human Prostate Cancer Cell Lines. *J Pharm Anal* (2021) 11(1):108–21. doi: 10.1016/j.jpha.2020.04.002
240. Mamillapalli V, Atmakuri AM, Khantamneni P. Nanoparticles for Herbal Extracts. *Asian J Pharm* (2016) 10(2):S54–60. doi: 10.22377/ajp.v10i2.623
241. Muthuvinothini A, Stella S. Green Synthesis of Metal Oxide Nanoparticles and Their Catalytic Activity for the Reduction of Aldehydes. *Process Biochem* (2019) 77:48–56. doi: 10.1016/j.procbio.2018.12.001
242. Sun M, Wang T, Li L, Li X, Zhai Y, Zhang J, et al. The Application of Inorganic Nanoparticles in Molecular Targeted Cancer Therapy: EGFR Targeting. *Front Pharmacol* (2021) 12(July):1–15. doi: 10.3389/fphar.2021.702445
243. Chauhan P, Tyagi BK. Herbal Novel Drug Delivery Systems and Transfersomes. *J Drug Deliv Ther* (2018) 8(3):162–8. doi: 10.22270/jddt.v8i3.1772
244. Karthigeyan P, Biswa BK, Sanjaya KP, Das D, Tapas KP, et al. Lung Cancer Treatment Using Astragalus, Cisplatin and Vinorelbine-IN202241000705. (2022) (15-02-02022). Available at: https://patentscope.wipo.int/search/en/detail.jsf?docId=IN348662046&_cid=P10-L0JOBD-96201-1.
245. Khan MA. - A Novel Herbal Composition for Anticancer Activity-IN202111049427. (2021) (18-02-2022). Available at: https://patentscope.wipo.int/search/en/detail.jsf?docId=IN342290833&_cid=P10-L0JOJ9-00214-1.
246. Sumathi DR, Tamizharasi DS, Punitha S, Sivakumar DT. Enhanced Anticancer Activity of Quercetin-Loaded Tags Nanosuspension for Drug Impervious Mcf-7 Human Breast Cancer Cells-IN202141046188. (2021) (11-02-2022). Available at: https://patentscope.wipo.int/search/en/detail.jsf?docId=IN346038271&_cid=P10-L0JPH5-16373-1.
247. Sonali BD, Ziyaurrahman A, Kiran SB. Cytotoxic Herbal Silver Nanoparticles as a Remedy for Mammary Carcinoma-IN202021048696. (2020) (19-02-2022). Available at: https://patentscope.wipo.int/search/en/detail.jsf?docId=IN312323714&_cid=P10-L0JPNY-19493-1.
248. Walter MT. Non Invasive, Novel Poly Herbal Synergistic Formulation for the Effective Prevention and Management of Human Lung Cancer-IN202041023550. (2020) (19-02-2022). Available at: https://patentscope.wipo.int/search/en/detail.jsf?docId=IN296580467&_cid=P10-L0JPT2-21531-1.
249. Walter MT. Non Invasive, Novel Poly Herbal Synergistic Formulation for the Prevention and Management of Gastric Cancer-IN202041025649. (2020) (09-02-2022). Available at: https://patentscope.wipo.int/search/en/detail.jsf?docId=IN298658813&_cid=P11-L0JQ0O-79635-1.
250. Cardelli J, Ana-Maria D. Cancer Treatment Combination Composition Methods and Uses-US20170258929. (2017) (19-02-2022). Available at: https://patentscope.wipo.int/search/en/detail.jsf?docId=US203767547&_cid=P11-L0JQ5J-81563-1.
251. Laura AS, Peter PS, Lawrence H. Use of a Combination of a Curcuminoid and a Chemotherapeutic Agent for Use in Treatment of Glioblastoma-EP3144006. (2017) (17-02-2022). Available at: https://patentscope.wipo.int/search/en/detail.jsf?docId=EP193434896&_cid=P11-L0JQ9K-83371-1
252. Ming TS, Ho HO, Shing CH, Yuan SH, Jun-jen L. Stabilized High Drug Load Nanocarriers Methods for their Preparation and Use there of-US20170035701. (2017) (14-02-2022). https://patentscope.wipo.int/search/en/detail.jsf?docId=US192184121&_cid=P11-L0JQEY-85764-1
253. Xiyun Y, Kelong F, Minmin L, Wang F, Demin D, Zhang D, et al. Drug Carrier for Tumor-Specific Targeted Drug Delivery and Use Thereof-US20170189343. (2017) (21-02-2022). Available at: https://patentscope.wipo.int/search/en/detail.jsf?docId=US200469162&_cid=P11-L0JQKR-87893-1.
254. Pradeep KS, Armitage AP, Satishchandra BO. Curcumin Sophorolipid Complex-US20170224636. (2017) (24-02-2022). Available at: https://patentscope.wipo.int/search/en/detail.jsf?docId=US202131929&_cid=P11-L0JQOG-89324-1
255. Banerjee P, Mario RC, Priya RD, Szerszen A, Jimmie EF, et al. Activity Enhancing Curcumin Composition and Method of Use-US20160287533. (2016) (15-02-2022). Available at: https://patentscope.wipo.int/search/en/detail.jsf?docId=US178074760&_cid=P11-L0JQS0-90576-1.
256. Dae RA. Drug Carrier Having L-DNA Nanocage Structure-US20160287706. (2016) (17-02-2022). Available at: https://patentscope.wipo.int/search/en/detail.jsf?docId=US178074933&_cid=P11-L0JQV4-91752-1.
257. Alias JP, Kunmoth NJ. Curcumin Coated Magnetize Nanoparticles for Biomedical Application-US20140369938. (2014) (20-02-2022). Available at: https://patentscope.wipo.int/search/en/detail.jsf?docId=US128464340&_cid=P11-L0JQXJ-92835-1.
258. George K, Elena E. Multi-Responsive Targeting Drug Delivery Systems for Controlled-Release Pharmaceutical Formulation-US20160263221. (2016) (25-02-2022). Available at: https://patentscope.wipo.int/search/en/detail.jsf?docId=US177607376&_cid=P11-L0JR0S-93959-1.
259. Ganta S, Coleman T. Drug Delivery Nanoemulsion Systems-WO2016014337. (2016) (27-02-2022). Available at: https://patentscope.wipo.int/search/en/detail.jsf?docId=WO2016014337&_cid=P10-KSU8AB-96626-1
260. Cheng J, Tong R. Particulate Drug Delivery Method-US20150314006. (2015) (17-02-2022). Available at: https://patentscope.wipo.int/search/en/detail.jsf?docId=US152963728&_cid=P21-L0JR7Q-96854-1.
261. Ekor M. The Growing Use of Herbal Medicines: Issues Relating to Adverse Reactions and Challenges in Monitoring Safety. *Front Pharmacol* (2014) 4:177. doi: 10.3389/fphar.2013.00177
262. Yin S-Y, Wei W-C, Jian F-Y, Yang N-S. Therapeutic Applications of Herbal Medicines for Cancer Patients. Motoo Y, Editor. *Evid-Based Complement Altern Med* (2013) 2013:302426. doi: 10.1155/2013/302426
263. Yang N-S, Shyur L-F, Chen C-H, Wang S-Y, Tzeng C-M. Medicinal Herb Extract and a Single-Compound Drug Confer Similar Complex Pharmacogenomic Activities in Mcf-7 Cells. *J BioMed Sci* (2004) 11 (3):418–22. doi: 10.1007/BF02254447
264. You L, An R, Liang K, Wang X. Anti-Breast Cancer Agents From Chinese Herbal Medicines. *Mini Rev Med Chem* (2013) 13(1):101–5. doi: 10.2174/138955713804484785
265. Yang S-YYN-S, Agricultural Biotechnology Research Center, Academia Sinica T, Taiwan RO. *Immuno-Modulatory Effects of Phytomedicines Evaluated Using Omics Approaches*. USA: IntechOpen (2011). p. 28.
266. Martino E, Della Volpe S, Terribile E, Benetti E, Sakaj M, Centamore A, et al. The Long Story of Camptothecin: From Traditional Medicine to Drugs. *Bioorg Med Chem Lett* (2017) 27(4):701–7. doi: 10.1016/j.bmcl.2016.12.085
267. Seneca. *CHAPTER 2 - Alkaloid Chemistry. In: Aniszewski TBT-A-S of L, Editor. Alkaloids - Secrets of Life*. Amsterdam: Elsevier (2007) p. 61–139. doi: 10.1016/B978-044452736-3/50004-0
268. Marupudi NI, Han JE, Li KW, Renard VM, Tyler BM, Brem H. Paclitaxel: A Review of Adverse Toxicities and Novel Delivery Strategies. *Expert Opin Drug Saf* (2007) 6(5):609–21. doi: 10.1517/14740338.6.5.609

269. Lee S, Lee HY, Park Y, Ko EJ, Ban TH, Chung BH, et al. Development of End Stage Renal Disease After Long-Term Ingestion of Chaga Mushroom: Case Report and Review of Literature. *J Korean Med Sci* (2020) 35(19):e122–2. doi: 10.3346/jkms.2020.35.e122
270. Nazari S, Maryam Rameshrad HH. Toxicological Effects of Glycyrrhiza Glabra (Licorice). *Phytother Res* (2017) 31(11):1635–50. doi: 10.1002/ptr.5893
271. Isbrucker RA, Burdock GA. Risk and Safety Assessment on the Consumption of Licorice Root (Glycyrrhiza Sp.), its Extract and Powder as a Food Ingredient, With Emphasis on the Pharmacology and Toxicology of Glycyrrhizin. *Regul Toxicol Pharmacol* (2006) 46(3):167–92. doi: 10.1016/j.yrtph.2006.06.002
272. Ben-Arye E, Samuels N, Goldstein LH, Mutafoglu K, Omran S, Schiff E, et al. Potential Risks Associated With Traditional Herbal Medicine Use in Cancer Care: A Study of Middle Eastern Oncology Health Care Professionals. *Cancer* (2016) 122(4):598–610. doi: 10.1002/cncr.29796
273. Izzo AA, Ernst E. Interactions Between Herbal Medicines and Prescribed Drugs. *Drugs* (2001) 61(15):2163–75. doi: 10.2165/00003495-200161150-00002
274. Rastegar R, Akbari Javar H, Khoobi M, Dehghan Kelishadi P, Hossein Yousefi G, Doosti M, et al. Evaluation of a Novel Biocompatible Magnetic Nanomedicine Based on Beta-Cyclodextrin, Loaded Doxorubicin-Curcumin for Overcoming Chemoresistance in Breast Cancer. *Artif Cells Nanomedicine Biotechnol* (2018) 46(sup2):207–16. doi: 10.1080/21691401.2018.1453829
275. Anwar DM, El-Sayed M, Reda A, Fang JY, Khattab SN, Elzoghby AO. Recent Advances in Herbal Combination Nanomedicine for Cancer: Delivery Technology and Therapeutic Outcomes. *Expert Opin Drug Deliv* (2021) 18(11):1609–25. doi: 10.1080/17425247.2021.1955853
276. Lakshmanan A, Akasov RA, Sholina NV, Demina PA, Generalova AN, Gangadharan A, et al. Nanocurcumin-Loaded UCNPs for Cancer Theranostics: Physicochemical Properties, *In Vitro* Toxicity, and *In Vivo* Imaging Studies. *Nanomaterials* (2021) 11(9):2234. doi: 10.3390/nano11092234
277. Elgohary MM, Helmy MW, Mortada SM, Elzoghby AO. Dual-Targeted Nano-in-Nano Albumin Carriers Enhance the Efficacy of Combined Chemo/Herbal Therapy of Lung Cancer. *Nanomed (Lond)* (2018) 13(17):2221–4. doi: 10.2217/nnm-2018-0097

Conflict of Interest: The authors declare that the research was conducted in the absence of any commercial or financial relationships that could be construed as a potential conflict of interest.

Publisher's Note: All claims expressed in this article are solely those of the authors and do not necessarily represent those of their affiliated organizations, or those of the publisher, the editors and the reviewers. Any product that may be evaluated in this article, or claim that may be made by its manufacturer, is not guaranteed or endorsed by the publisher.

Citation: *Chavda VP, Patel AB, Mistry KJ, Suthar SF, Wu Z-X, Chen Z-S and Hou K (2022) Nano-Drug Delivery Systems Entrapping Natural Bioactive Compounds for Cancer: Recent Progress and Future Challenges. Front. Oncol. 12:867655. doi: 10.3389/fonc.2022.867655*

frontiers | Frontiers in Oncology

TYPE Original Research
PUBLISHED 02 August 2022
DOI 10.3389/fonc.2022.890299

OPEN ACCESS

EDITED BY
Matiullah Khan,
AIMST University, Malaysia

REVIEWED BY
Junmin Zhang,
Lanzhou University, China
Feng Liu-Smith,
University of Tennessee Health Science Center (UTHSC), United States
Dong Zhou,
Northwest A&F University, China
Nana Yang,
Weifang Medical University, China
Pádraig D'Arcy,
Linköping University, Sweden

*CORRESPONDENCE
Sheikh Abdullah Tasduq
stabdullah@iiim.res.in/tasduq11@gmail.com

SPECIALTY SECTION
This article was submitted to Cancer Molecular Targets and Therapeutics, a section of the journal Frontiers in Oncology

RECEIVED 05 March 2022
ACCEPTED 01 July 2022
PUBLISHED 02 August 2022

CITATION
Nazir LA, Shahid NH, Amit K, Umar SA, Rajni S, Bharate S, Sangwan PL and Tasduq SA (2022) Synthesis and anti-melanoma effect of 3-O-prenyl glycyrrhetinic acid against B16F10 cells *via* induction of endoplasmic reticulum stress-mediated autophagy through ERK/AKT signaling pathway. *Front. Oncol.* 12:890299. doi: 10.3389/fonc.2022.890299

Synthesis and anti-melanoma effect of 3-O-prenyl glycyrrhetinic acid against B16F10 cells *via* induction of endoplasmic reticulum stress-mediated autophagy through ERK/AKT signaling pathway

Lone A. Nazir[1,2], Naikoo H. Shahid[1,2], Kumar Amit[3], Sheikh A. Umar[1,2], Sharma Rajni[3], Sandip Bharate[2,3], Pyare L. Sangwan[2,3] and Sheikh Abdullah Tasduq[1,2*]

[1]Pharmacokinetics-Pharmacodynamics and Toxicology Division, Council Of scientific and Industrial Research-Indian Institute of Integrative Medicine, Jammu, India, [2]Academy of Scientific and Innovative Research (AcSIR), Ghaziabad, India, [3]Natural Product and Medicinal Chemistry Division, CSIR-Indian Institute of Integrative Medicine, Jammu Tawi, India

Melanoma is an aggressive form of cancer with poor prognosis and survival rates and limited therapeutic options. Here, we report the anti-melanoma effect of 3-O-prenyl glycyrrhetinic acid (NPC-402), a derivative of glycyrrhtinic acid, from a reputed medicinal plant *Glycyrrhiza glabra* against B16F10 cells. We studied the cytotoxic effect of NPC-402 on melanoma cells and investigated the role of mitogen-activated protein (MAP) kinase, AKT axis, and endoplasmic reticulum (ER) stress/unfolded protein response (UPR)-mediated autophagy as the involved signaling cascade by studying specific marker proteins. In this study, 4-phenylbutyric acid (4PBA, a chemical chaperone) and small interference RNA (siRNA) knockdown of C/EBP Homologous Protein (CHOP)/growth arrest- and DNA damage-inducible gene 153(GAD153) blocked NPC-402-mediated autophagy induction, thus confirming the role of ER stress and autophagy in melanoma cell death. NPC-402 induced oxidative stress and apoptosis in melanoma cells, which were effectively mitigated by treatment with N-acetylcysteine (NAC). *In vivo* studies showed that intraperitoneal (i.p.) injection of NPC-402 at 10 mg/kg (5 days in 1 week) significantly retarded angiogenesis in the Matrigel plug assay and reduced the tumor size and tumor weight without causing any significant toxic manifestation in C57BL/6J mice. We conclude that NPC-402 has a high potential to be developed as a chemotherapeutic drug against melanoma.

KEYWORDS

melanoma, ER stress, autophagy, apoptosis, 3-O-prenyl glycyrrhetinic acid

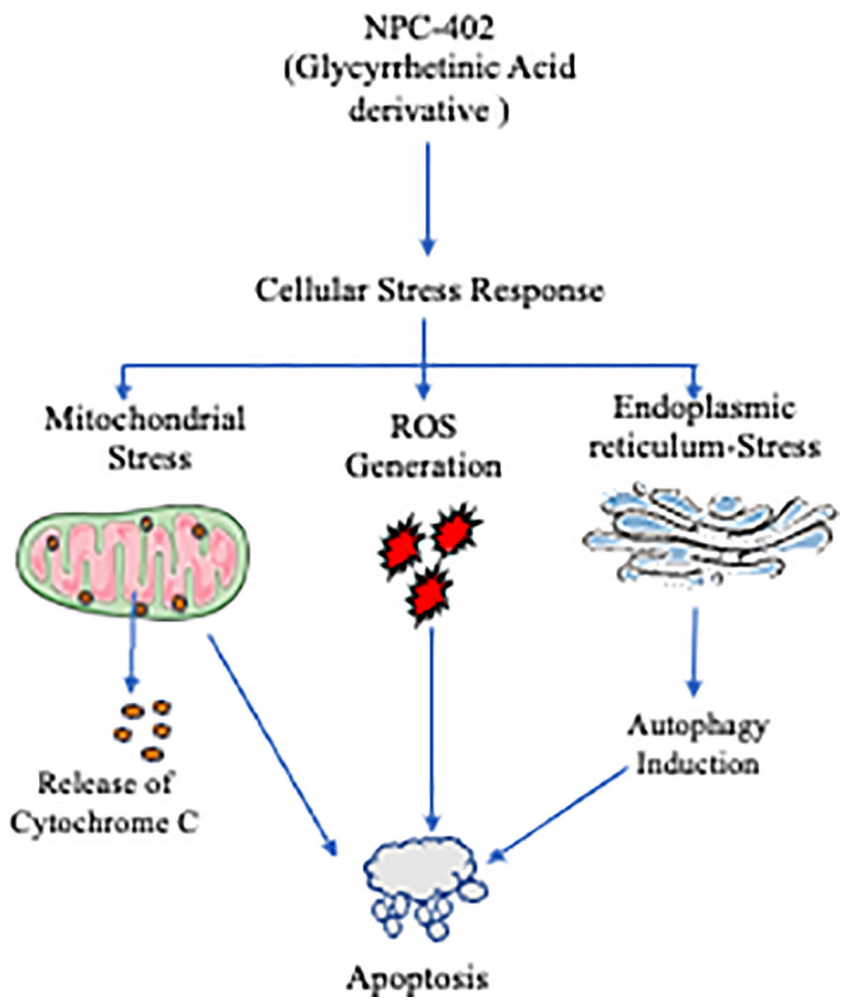

GRAPHICAL ABSTRACT
Graphical summary of NCP-402 effect on endoplamis reticulum and autophagy. NPC-102 induces ER, stress lading to UPR via elF 2a signaling, resulting in activabos of CHIOP and Causes aulophagy induction mediated cell death. NPC-402 causes generation of reactive axygen species that leads to MMP depolarization resulting in pro-apoptolic environment within the cells, NPC-d02 alo cause's felease of cylochrone C nio eytosol that in turn actrales irininsic apoptotic puthway. Application of chemical chaperone 4 Phenyl butyric acid (APBA) interferes will NPC-402 -induced ER-ares and its downward effects, N acetyl eysteine alio preveat NCP,A03 indaced cell death 5) relieving oxidative stres.

Abbreviations: NPC-402, 3-O-prenyl glycyrrhetinic acid;MAP kinase, mitogen-activated protein kinase; AKT, protein kinase B; JNK, c-Jun N-terminal kinase; ER, endoplasmic reticulum; UPR, unfolded protein response; 4PBA, 4-phenylbutyric Acid; siRNA, small interfering RNA; CHOP/GAD153, C/EBP homologous protein; NAC, N-acetylcysteine; GRP78/Bip, glucose-regulated protein 78; IRE1α, inositol-requiring transmembrane kinase/endoribonuclease 1α; PERK, protein kinase R-like endoplasmic reticulum kinase; ATF6, activating transcription factor 6; Bcl-2, B-cell lymphoma 2; Bim, Bcl-2 homology 3-only protein; Bax, BCL2-associated X; ATF4, activating transcription factor 4; MEK, mitogen-activated protein kinase kinase; ERK1/2, extracellular signal-regulated kinase 1/2; Nrf-2, nuclear factor erythroid 2-related factor 2; Cu/Zn SOD, copper/zinc superoxide dismutase; P62, ubiquitin-binding protein; GAPDH, glyceraldehyde 3-phosphate dehydrogenase

Introduction

Melanoma is the deadliest cancer among all skin cancers, with high metastasis, poor prognosis, and resistance to present treatment strategies (1). It represents less than 5% of skin malignancies but accounts for 80% of related mortalities (2). Due to its extraordinary opposition to conventional chemotherapeutic strategies, there is urgency for the development of novel and targetable therapeutic strategies to control this deadly disease (3). A high load of oxidative stress in melanoma tumors increases the aggressiveness of therapeutic agents imparting a high Reactive Oxygen Species (ROS) stress threshold in cancer cells and has shown promising potential to selectively target melanoma (4, 5). phosphoinositide 3-

kinase(PI3K)-AKT has been shown to increase in part the proliferative and anchorage-independent growth nature in melanoma cells (6, 7). Moreover, mitogen-activated protein kinase (MAPK) signaling has been found to be critical and constitutively activated by various mechanisms, making it a target for melanoma (8).

Endoplasmic reticulum (ER) is a membrane-bound cytosolic organelle with a high calcium (Ca^{2+}) storage and neutral pH and plays a pivotal role in protein folding due to the presence of chaperone proteins such as glucose-related protein (GRP)78/Bip collectively controlling cellular homeostasis. A hostile cellular environment causes misfolded proteins to accumulate, leading to imbalances in ER homeostasis and finally culminates into ER stress/unfolded protein response (UPR). The signaling pathways overseeing the ER stress response are inositol-requiring transmembrane kinase/endoribonuclease 1α (IRE1α), protein kinase R-like endoplasmic reticulum kinase (PERK), and activating transcription factor (ATF)6. UPR results in the induction of the expression of proteins called chaperones that are involved in the recovery process. However, in case of excessive stress or sustained insult, the function of the ER is compromised, triggering apoptosis, thereby removing the affected cell. Recent findings in this regard have well established that ER stress is a potent inducer of autophagy, a cellular self-degradative process having an adaptive function (9), and modulation of UPR by agents that actively induce ER stress may be effective as anti-melanoma agents (10, 11). These pieces of evidence are highly suggestive of ER stress-mediated autophagy as a therapeutic target against melanoma.

During physiological conditions, autophagy plays a housekeeping role in removing the misfolded proteins and in clearing damaged organelles from cells (12, 13). Previous studies have suggested that autophagy performs context-dependent roles in cell survival and death mechanisms (14). In cancer morbidity conditions, autophagy deficiency acts as a tumor suppressor or supports tumor progression by limiting stress (15). Induction of autophagy on stimulation can either be protective or promote apoptosis in cancer cells. Therefore, anticancer drugs acting through autophagy in tumors leads to autophagy-mediated cell death (16), and strategies targeting autophagy as a drug target are worth it in melanoma cancer therapy. In melanoma, c-Jun N-terminal kinase (JNK) signaling pathway has a major role to play in autophagy-mediated apoptotic cell death (17, 18). Therefore, it has been clearly inferred that autophagy and MAPK/JNK along with AKT signaling axis can also be targeted to induce autophagy-mediated cell death response in melanoma cells (19).

Nature-based agents have been the backbone of drug discovery in the area of cancer treatment strategies. Different derivatives of 18β-glycyrrhetinic acid, a secondary metabolite from a reputed plant used in most traditional medicine practices of the world, *Glycyrrhiza glabra*, are in various phases of clinical trials against various cancers (20, 21). In the present study, we synthesized and analyzed the anti-melanoma effect and the mechanistic basis of 3-(3-methyl-but-2-enyloxy)-11-oxo-olean-12-ene-29-oic acid (NPC-402), a pentacyclic triterpenoid ether derivative of glycyrrhetinic acid (GA), against several cellular models of melanoma and in C57BL/6J mice. The present study was designed to demystify the mechanistic basis and interrelationship of ER stress and autophagy in cell death by examining and looking for the changes in the PERK–ATF4–C/EBP Homologous Protein (CHOP) and MAPK and PI3K/AKT signaling pathway axes regulating cellular proliferation and death processes and evaluating their role as therapeutic targets for NPC-402 treatment to achieve an anti-melanoma effect. In addition, a reduction in tumor size/volume in C57BL/6J mice in the Matrigel plug assay was performed to assess the efficacy and potency of our study molecule (NPC-402) as an anti-melanoma agent.

Materials and methods

Chemicals and reagents

All of the chemicals/reagents were purchased from different authorized companies. Most of the cell culture-based chemicals and reagents were purchased from Sigma-Aldrich, and the cultureware was purchased from the Nunclon Thermo-Scientific-India. The Western blot apparatus, tools, and reagents were purchased from Bio-Rad Technologies, USA. Dulbecco's modified Eagle's medium (DMEM), penicillin–streptomycin, propidium iodide (PI), 2,7-H_2DCF-DA, proteinase K, ribonuclease-A, agarose, dimethyl sulfoxide (DMSO), Dulbecco's phosphate buffer saline (DPBS), fetal bovine serum (FBS), LC3I/II, and anti-β-actin antibodies were purchased from Sigma-Aldrich Chemicals (St. Louis, MO, USA). Antibodies against caspase-3/caspase-8, B-cell lymphoma 2 (Bcl-2), Bcl-2 homology 3-only protein (Bim), BCL2-associated X (Bax), ATF4, phospho-mitogen-activated protein kinase kinase (MEK), phospho-extracellular signal-regulated kinase (ERK), total ERK, total MEK, phospho-p38, p-38, phospho-JNK, JNK, phospho-AKT, nuclear factor erythroid 2-related factor 2 (Nrf-2), catalase, copper/zinc superoxide dismutase (Cu/Zn SOD), AKT, Beclin1, P62, and glyceraldehyde 3-phosphate dehydrogenase (GAPDH) were purchased from Santa Cruz Biotechnology, Inc. Glycyrrhizin was purchased from Sigma-Aldrich.

Synthesis and characterization of 3-(3-Methyl-But-2-Enyloxy)-11-Oxo-Olean-12-Ene-29-Oic Acid (NPC-402)

Hydrolysis of glycyrrhizin

GA was prepared by hydrolyzing glycyrrhizin in 5% aq. HCl and purified over a silica column in ethanol:hexane (25:75) and further characterized by comparison of melting point and spectral data with

values in literature. The modifications were done at the C-3 position for the synthesis of *O*-alkylated/benzylated GA derivatives.

General method for the preparation of *O*-Alkylated/Benzylated Glycyrrhetinic acid

K_2CO_3 (1.2 mmol) was added to the solution of 3β-hydroxy-11-oxo-olean-12-en-30-olic acid (100 mg, 1 mmol) in dry acetone (5 ml) followed by addition of different alkyl and benzyl halides (1 mmol). Stirring was done at room temperature for 8 h under inert atmosphere and concentrated under reduced pressure conditions. The resultant mixture was chloroform diluted and water was added, leading to the formation of a white precipitate in the aqueous layer. The organic layer was decanted, and the remaining residual solid material was washed 5–6 times with chloroform. Under reduced pressure, the combined chloroform layer was evaporated and the residue was purified by silica gel (#100-200) column chromatography using hexane-ethyl acetate as an eluent to yield the different alkylated products (Figures S1A, B).

Cell culture and animal experiments

Murine melanoma cell line B16F10, human immortalized fibroblast cell line from foreskin Hs68, and cell line A375 (human melanoma) were purchased from the American Type Culture Collection (Rockville, MD, USA). Human immortalized keratinocyte cell line HaCaT was purchased from CSL-Eppelheim Germany. The cell culture method was followed as described previously (22). Briefly, cells were seeded in DMEM supplemented with L-glutamine, glucose (3.5 g/L), and (4-(2-hydroxyethyl)-1-piperazineethanesulfonic acid) (HEPES) (15 mM). Additionally, penicillin G (120 mg/L), streptomycin (270 mg/L), amphotericin B (250 mg/L), sodium bicarbonate 1.2 g/L, sodium pyruvate 220 mg/L, and FBS (10% v/v) were added. The culture conditions for all cell culture experiments were 37°C and 5% CO_2 and kept for incubation in a water jacketed humidified incubator (Thermo-Scientific Model No. 3121). Cells were observed daily under light microscope (Olympus-Japan). Cells with passage nos. from 10 to 20 were used in most of the experiments.

Four-week-old male mice C57BL/6J (16–18 g weight) were procured from an institutional animal care facility and acclimated for 1 week. The study was duly approved by the institutional animal ethics committee (IAEC). Mice were divided into three groups (n = 7). Group 1: Control group was given 1 million B16F10 melanoma cells subcutaneously into the ventral area in Matrigel and Vascular endothelial growth factor (VEGF), Group 2: B16F10 cells + NPC-402 treatment, Group 3: B16F10 cells + dacarbazine treatment. NPC-402 was administered intraperitoneally (i.p.) at 10 mg/kg for 5 days in a week by preparing as a suspension in transketolase, while the dacarbazine standard group was administered Dacarbazine at 60 mg/kg as a suspension in transketolase at alternate intervals thrice a week. The study was scheduled for a week. All of the mice were separately caged at 24°C ± 2°C, having free access to food with 12-h light/dark cycle. Weekly weight patterns were monitored, and mice were sacrificed by CO_2 euthanasia. Blood was collected by cardiac puncture and subjected to centrifugation, and serum was stored at -80°C in the Matrigel plug assay.

Cell viability assay

Enzymatic reduction of 3-[4,5-dimethylthiazole-2-yl]-2,5-diphenyltetrazolium bromide (MTT) by metabolic active cells to MTT–formazan by mitochondrial enzyme succinate dehydrogenase was used for the evaluation of cell viability as described earlier (23, 24). Briefly, after cell culture and followed by treatment with the test compound, the cells were further incubated for 24 h. The absorbance was recorded by a Multiskan plate reader (Thermo Electron Corporation) at 570 nm.

Colony formation assay

B16F10 cells were seeded in six-well plates (250–300 cells/well). After 24 h, cells were subjected to treatment with different concentrations of NPC-402 for 24 h and further cultured for 5–7 days. Cells were fixed with 70% methanol and stained with crystal violet 0.1%. Stained colonies were captured by EVOS-FL Cell Imaging System (Thermo Fisher).

Scratch assay (cell migration)

The scratch assay was performed as described previously (25). Briefly, cell proliferation was inactivated by mitomycin-C, and then cells were wounded by a microtip and washed with PBS. Cells were treated with the required concentrations of NPC-402 and further supplemented with fresh medium with or without VEGF (20 ng/ml).

Annexin V/propidium iodide staining

Apoptosis was investigated using FITC Annexin-V/Dead Cell Apoptosis Kit (Molecular Probes-Life Technologies, OR, USA) as per protocol provided by the manufacturer. Stained samples were analyzed using BD FACS Calibur Aria flow cytometry.

DNA fragmentation assay

Analysis of DNA fragmentation was performed as described previously (26). Briefly, after the treatment schedule, B16F10 cells

were collected and washed with ice-cold 0.1 M Ethylenediamine tetra acetic acid (EDTA)-DPBS buffer and lysed in DNA lysis buffer and further incubated at 37°C for 1.5 h in a shaker water bath. After centrifugation, the supernatant was treated with proteinase K (250 µg/ml) at 50°C for an additional 60 min. DNA was extracted in phenol-chloroform and precipitated with ethanol and analyzed electrophoretically.

Reactive oxygen species measurement *via* fluorescence microscopy/flow cytometry

Dichlorofluorescin diacetate (H_2DCFDA) was used for the measurement of ROS generation as described previously (27). After completion of the treatment schedule, the dishes were incubated with H_2DCFDA (5 µM, Sigma-Aldrich) for 15 min then followed by DPBS washing, and images were captured on fluorescent microscope on GPF-filter at ×20 resolution. Camptothecin (5 µM) was used as a positive control for the indicated time points (Figures 4A, B). Fluorescence of the images was quantified by using ImageJ software as reported earlier (28). We have also evaluated the ROS generation by flow cytometry (BD FACS Calibur Aria) by looking for the change in fluorescence due to the production of 2', 7'-dichlorofluorescein (DCF). H_2O_2 (100 µM) was used as a positive control. B16F10 cells were exposed to H_2O_2 (100 µM) for 15 min prior to analysis.

Lipid peroxidation assay

Lipid peroxidation was measured by quantifying malondialdehyde (MDA-Thiobarbituric acid (TBA) adducts) by a commercially available colorimetric assay (Sigma-Aldrich) as per the manufacturer's protocol. Briefly, after termination of the experiment, cells were collected in 1.5-ml centrifuge tubes and homogenized on ice in MDA lysis buffer containing butylated hydroxytoluene (BHT) and then centrifuged at 13,000 g for 10 min to remove the insoluble material. The TBA solution was added to each Sample & Standard tube and incubated at 95°C for 60 min in a water bath and allowed to cool on an ice bath for 10 min. Finally, absorbance was documented at 532 nm by a spectrometer (Multiskan Spectrum plate reader, Thermo Electron Corporation).

Study of mitochondrial membrane potential using fluorescence microscopy

Mitochondrial membrane potential ($\Delta\Psi m$) was analyzed by JC-9 staining as described previously (28). Briefly, cells were grown on coverslips, and after attaining confluency of 60%–70%, the cells were treated with the indicated concentrations of NPC-402. After completion of treatment, JC-9 (5 µg/ml) dye in DPBS was given to cells and incubated for 25 min in culture conditions. After slide preparation, imaging was performed using EVOS-FL Microscope (Thermo Fisher) using red and green filters, and the images were quantified using the ImageJ software (28).

Immunocytochemistry assay

Immunocytochemistry (ICC) experiments were carried out as reported previously (22, 28). Briefly, cells were incubated on coverslips in 35-mm culture dishes. After the completion of the treatment schedule, fixation of cells was carried out with 4% paraformaldehyde for 10 min at Room Temperature (RT). Cells were further permeabilized with 0.1% Triton X-100 for 10 min at RT. After blocking in 1% bovine serum albumin (BSA), cells were incubated with primary antibody overnight at 4°C. After proper washing with DPBS-T (Tween 20 0.1%), appropriate secondary antibodies were added to cells and incubated in the dark for 2 h at RT. Cells were mounted with ProLong Gold antifade reagent (4′,6-diamidino-2-phenylindole) (DAPI), and images were taken on EVOS-FL Cell Imaging System at ×20.

Small interference RNA-mediated knockdown assay

Validated CHOP small interference RNA (siRNA) was procured from Santa Cruz Biotechnology, USA. Lipofectamine (Invitrogen, Life Technologies) and CHOP siRNA were diluted into opti-MEM 1 reduced serum medium (Gibco, Life Technologies) as per manufacturer's instruction. B16F10 cells were incubated with a transfection mixture for 16 h at a final siRNA concentration of 50 pmol and supplemented with fresh medium. The cells were further subjected to treatment of NPC-402 as per experimental design.

Cytochrome C release from mitochondrial membrane imaging assay

Cells were grown in coverslips overnight. Later, the cells were treated with/without NPC-402 for 12 h and then incubated with MitoTracker-DND-red (250 nM) for 30 min. The cells were washed thrice with warm DPBS followed by other steps in the ICC protocol by looking for the localization of cytochrome C as described.

Preparation of cell lysates for western blotting

Cell lysates for protein expression studies were prepared as per our previous reports (29, 30). Briefly, after cell harvesting, cells were lysed with Radioimmunoprecipitation assay buffer (RIPA buffer) and protein quantification of the samples was measured by the Bradford colorimetric assay (Sigma-Aldrich) using BSA as standard. Equal amounts of protein (40 µg) were

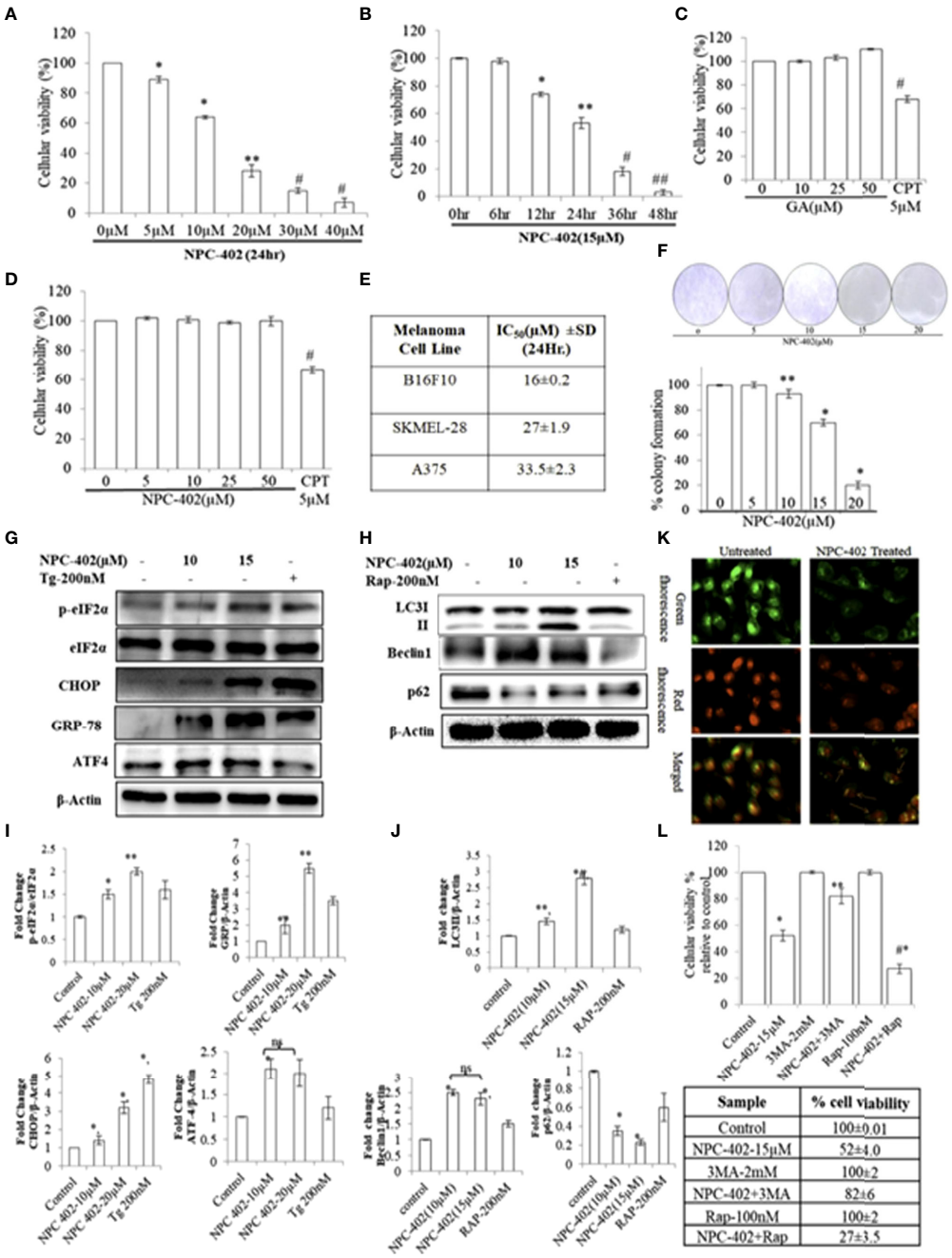

FIGURE 1
Continued

FIGURE 1 (Continued)
NPC-402 Shows Potent Growth Inhibition and ER stress-mediated autophagy induction in B16F10 melanoma cells. **(A)** Bar graph represents the cell viability analysis of B16F10 cells treated with/without NPC-402 for 24 h using the MTT assay (*represents $p < 0.001$, **$p < 0.01$, $^{\#}p < 0.05$, control vs. NPC-402 treatment). **(B)** Bar graph represents the cell viability analysis of B16F10 cells treated with 15 μM of NPC-402 for different time intervals using the MTT assay (*represents $p < 0.001$, **$p < 0.01$, $^{\#}p < 0.05$, control vs. NPC-402 treatment). **(C)** Bar graph represents the cell viability analysis of B16F10 cells treated with/without glycyrrhetinic acid (GA) for 24 h using the MTT assay. Camptothecin (CPT) serves as a positive control ($^{\#}p < 0.05$, control vs. CPT treatment). **(D)** Bar graph represents the cell viability analysis of HaCaT cells treated with/without NPC-402 for 24 h using the MTT assay. Camptothecin (CPT) serves as a positive control ($^{\#}p < 0.001$, control vs. CPT treatment). **(E)** Represents the IC50 of NPC-402 treatment in penal of melanoma cells. **(F)** The diagram represents the colony formation in NPC-402-treated B16F10 cells, and the bar graph represents the percentage colony formation in B16F10 cells treated with/without NPC-402 (*$p < 0.00$, **$p < 0.01$, control vs. NPC-402 treatment). Results are representative of three similar experiments. **(G)** Western blot represents the protein expression of p-elf2α, elf2α, CHOP, GRP-78, and ATF4 using beta-actin as a loading control in B16F10 cells treated with NPC-402. **(I)** Bar graph represents the densitometry analysis of protein in fold change p-elf2α/elf2α, CHOP, GRP-78, and ATF4 using beta- actin as a loading control in B16F10 cells treated with NPC-402 using Image Lab™ Software Version 3.0 (Bio-Rad). **(H)** Western blot represents the protein expression of LC3II, Beclin1, and P62 using beta-actin as a loading control in B16F10 cells treated with NPC-402. **(J)** Bar graph represents the densitometry analysis of protein in fold change of LC3II, Beclin1, and P62 using beta-actin as a loading control in B16F10 cells treated with NPC-402 using Image Lab™ Software Version 3.0 (Bio-Rad). **(K)** Microscopic images represent the detection of autolysosomes thru acridine orange staining in NPC-402-treated B16F10 cells. **(L)** The bar graph and table represent the cell viability analysis of B16F10 cells treated with/without NPC-402, 3MA, or Rap or in combinations for 24 h using the MTT assay (*represents $p < 0.001$ control vs. NPC-402, #$p < 0.001$ control vs. NPC-402+3MA) (*$p < 0.001$, **$p < 0.01$, control vs. NPC-402 treatment). ns, non-significant.

loaded to polyacrylamide gel, and the proteins were resolved in 8%–15% gel using Miniprotein Tetra System (Bio-Rad). The gel was transferred to Polyvinylidene fluoride (PVDF) membranes and immunoblotted using specific antibodies against various proteins. Secondary antibodies (Horseradish peroxidase (HRP)-conjugated) at a dilution of 1:2,000 (Santa Cruz/CST-USA) and directed against primary antibodies were used, and the blots were developed with Immobilon Western Chemiluminescent HRP Substrate. Signal intensities of bands were detected and quantified by ChemiDoc Imaging System (Bio-Rad).

Matrigel plug assay

The assay was performed as described previously (31). Briefly, 0.5 ml of Matrigel and VEGF (100 ng) with or without B16F10 melanoma cells (1 million cells/animal) were injected subcutaneously into the ventral area of C57BL/6J mice. Animals of group 2 were dosed daily with NPC-402 (10 mg/kg/body weight; i.p./oral) and animals of group 3 were dosed with standard drug dacarbazine at alternate intervals (60 mg/kg/body weight; i.p./oral) for 1 week. On day 7, animals were sacrificed, and intact Matrigel plugs were removed and photographed showing the extent of vascularization. Matrigel plugs were analyzed and quantified for neovascularization by measuring their size and hemoglobin (Hb) content using the Drabkin reagent.

Statistical analysis

Data are expressed as the mean ± standard deviation (SD). INSTANT statistical software was used to perform statistical analysis. Data are presented as mean ± SD from three independent experiments. Comparison between two groups was performed by Student's t-test and that among groups was carried out by one-way ANOVA for statistical significance. $p \leq 0.05$ was considered statistically significant.

Results

Screening of *O*-Alkylated/Benzylated Glycyrrhetinic acid analogs against melanoma

Eighteen different analogs were synthesized from glycyrrhizin through GA at the C3 position (Figure S1A). After the cell-based screening assay among the different analogs (Figure S1B), 3-(3-methyl-but-2-enyloxy)-11-oxo-olean-12-ene-29-oic acid (NPC-402) was found most potent against B16F10 melanoma cells with an IC_{50} of 16 μM. The yield percentage of NPC-402 obtained was 90% with a purity of 98.7% analyzed from HPLC-chromatogram $t_R = 48.4$ min (98% purity); yield: 90%; IR ($CHCl_3$): ν_{max} 3,441, 2,927, 2,867, 1,724, 1,658, 1,658, 1,619, 1,454, 1,385, 1,327, 1,310, 1,257, 1,210, 1,152, 1,084, and 1,046 cm^{-1} (Figure S1D). Figure S1C describes the ^1H NMR (400 MHz, $CDCl_3$): δ (ppm) 5.63 (s, 1H, CH-12), 5.34 (t, 1H, CH-2′), 4.62 (m, 2H, CH_2-1′), 3.23 (dd, 1H, CH-2), 2.81 (tt, 1H, CH-18), 2.34 (s, 1H, CH-9), 1.77 (s, 3H, CH-3′), 1.72 (s, 3H, CH-4′), 1.36 (s, 3H, Me-27), 1.26 (s, 3H, Me-25), 1.14 (s, 3H, Me-29), 1.13 (s, 3H, Me-26), 1.01 (s, 3H, Me-23), 0.81 (s, 3H, Me-24), 0.80 (s, 3H, Me-28), 0.71 (d, 1H, CH-5); HR-ESIMS: *m/z* 539.4106 $[M+H]^+$ calculated for $C_{35}H_{54}O_4 + H^+$ (539.4094).

NPC-402 shows potent growth inhibition in melanoma cells

The cytotoxic effect of NPC-402 was first investigated at various concentrations on different melanoma cell lines

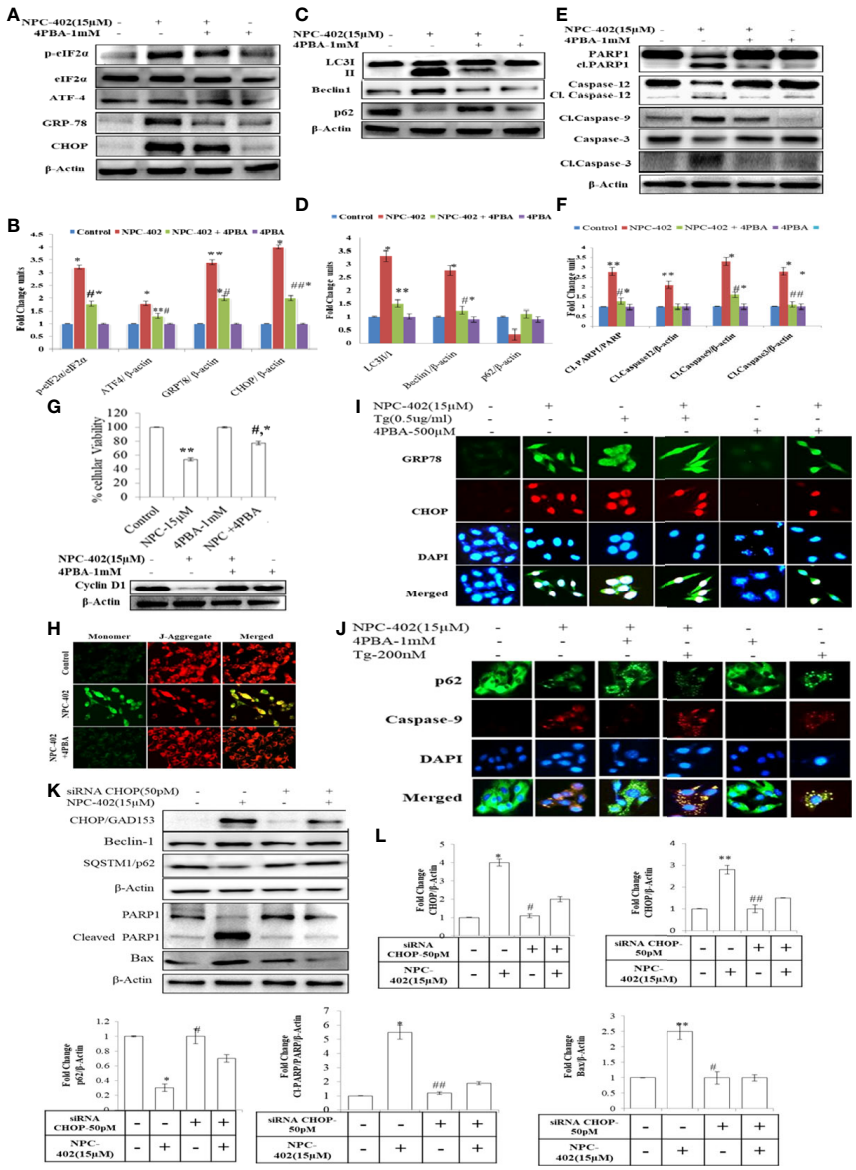

FIGURE 2
4PBA interferes with NPC-402-induced ER stress response and autophagy in B16F10 cells. **(A)** Represents the Western blot of protein expression of p-elf2α, elf2α, CHOP, GRP-78, and ATF4 using beta-actin as a loading control in B16F10 cells treated with NPC-402 along with/without 4PBA. **(B)** Bar graph represents the densitometry analysis of ER stress proteins in fold change in comparison to beta-actin in B16F10 cells treated with NPC-402 along with/without 4PBA using Image Lab™ Software Version 3.0 (Bio-Rad). **(C)** Represents the Western blot of protein expression of LC3I/II, Beclin1, and p62 using beta-actin as a loading control in B16F10 cells treated with NPC-402 along with/without 4PBA. **(D)** Bar graph represents the densitometry analysis of autophagy proteins in fold change in comparison to beta-actin in B16F10 cells treated with NPC-402 along with/without 4PBA using Image Lab™ Software Version 3.0 (Bio-Rad). **(E)** Represents the Western blot of protein expression of PARP1, caspase-12, caspase-9, and caspase-3 using beta-actin as a loading control in B16F10 cells treated with NPC-402 along with/without 4PBA. **(F)** Bar graph represents the densitometry analysis of apoptosis proteins in fold change in comparison to beta-actin in B16F10 cells treated with NPC-402 along with/without 4PBA using Image Lab™ Software Version 3.0 (Bio-Rad). **(G)** Bar graph represents cell viability percentage of B16F10 cells treated with NPC-402 along with/without 4PBA. Western blot represents the protein expression of cyclin D1 in B16F10 cells treated with NPC-402 along with/without 4PBA. **(H)** Microscopic images represent the JC-9 staining for the detection of $\Delta\Psi m$ in B16F10 cells treated with/without NPC-402 along with/without 4PBA. **(I)** ICC images of GRP-78 (green), CHOP (red), costained with DAPI (blue) on B16F10 treated with NPC-402 along with/without 4PBA. The images were taken at ×40 under microscope (EVOS). **(J)** ICC images of p62-78 (green) cleaved caspase-9 (red) costained with DAPI (blue), on B16F10 treated with NPC-402 along with/without 4PBA. The images were taken at ×40 under microscope (EVOS). **(K)** Represents the Western blot of protein expression of CHOP, Beclin1, p62, caspase-12, caspase-9, and caspase-3 using beta-actin as a loading control in B16F10 cells treated with NPC-402 along with/without 4PBA. **(L)** The bar graphs represents the fold change expression of proteins evaluated by densitometry method using Image Lab™ Software Version 3.0 (Bio-Rad) (*$p < 0.01$, **$p < 0.05$ for control vs. NPC-402 and $^{\#}p < 0.01$, $^{\#\#}p < 00.05$ for NCP-402 vs. NPC-402+4PBA).

(B16F10, A375, and SKMEL-28) and normal cell lines (human immortalized keratinocyte HaCaT). Upon treatment of B16F10 cells with NPC-402, cellular viability decreases significantly and dose-dependently (Figure 1A). We calculated the IC_{50} of NPC-402 treatment of melanoma cells at 24 h and found it to be 16 ± 0.2 μM for B16F10, 27 ± 1.9 μM for A375, and 33.5 ± 2.3 μM for SKMEL-28 (Figure 1E). B16F10 cells were treated with 15-μM concentration of NPC-402 at different time intervals, and NPC-402 induces a significant cell death effect in a time-dependent manner, and we achieved 96% ± 2% cell death 48 h posttreatment (Figure 1B). We have also checked the effect of parent compound GA on B16F10 cells and found that it did not alter cell growth. Camptothecin 5 μM was used as a standard positive cytotoxic control (Figure 1C). In contrast, NPC-402 shows no significant cytotoxic effect on human immortalized keratinocyte cell line HaCaT up to a concentration >50 μM (Figure 1D), indicating the specificity of NPC-402 for melanoma cells over normal cells. Furthermore, we performed colony formation assay and found that NPC-402 significantly decreases cell colony formation at higher concentrations (Figure 1F). The percentage of colony formation clearly reveals that NPC-402 at lower concentrations was cytostatic whereas NPC-402 at higher concentrations was cytotoxic (Figure 1F).

These results cite that the effectiveness of NPC-402 in inducing toxicity is cell type-specific and indicate that NPC-402 is capable of eliciting different cellular responses that need comprehensive characterization to fully understand how it can be taken forward as a potential anti-melanoma candidate drug.

NPC-402 leads to endoplasmic reticulum stress-mediated autophagy induction that culminates into apoptosis in B16F10 melanoma cells

To investigate the effect of NPC-402 on ER stress response, we evaluated the expression levels of key proteins related to ER stress: p-eIF2α, GRP78, CHOP, and ATF4. We found that NPC-402 at 12 h posttreatment significantly upregulates the expression of ER stress response proteins (Figures 1G, I), indicating that NPC-402 leads to the induction of ER stress. Thapsigargin (Tg; 200 nM) was used as an ER stress positive control. The exact role of autophagy in melanoma is not yet known, but research reports suggest that ER stress triggers autophagy induction. We investigated whether NPC-402 has any effect on cellular autophagy response by looking for the expression profile of autophagy-related proteins LC3I/II, Beclin1, and p62. We observed an elevated expression level of LC3-II by calculating the conversion ratio of LC3-I to LC3-II after NPC-402 treatment of cells (Figures 1H, J). The expression level of Beclin1 is upregulated significantly compared to that of control (Figures 1H, J). In addition, we observed downregulation of p62 in NPC-402-treated cells, being an essential protein in the autophagy process (Figures 1H, J). Furthermore, we looked for autolysosomes in NPC-402-treated B16F10 cells, and acridine orange staining revealed an increase in the volume of acidic vesicular organelles (AVOs) that indicates the autophagy response (Figure 1K). All of these findings indicate the induction of autophagy by NPC-402 treatment in B16F10 cells. To confirm the cell death role of autophagy in NPC-402-treated B16F10 cells, cell viability analysis was performed and autophagy inducer rapamycin (Rap) and autophagy inhibitor 3-methyladenine (3MA) were used as respective controls. We found that NPC-402 (at 15 μM) alone induces 48% cell death compared to control, whereas NPC-402+3MA (2 mM) induce 18% cell death compared to control and NPC-402+Rap (100 nM) significantly induce 73% cell death compared to control (Figure 1L). From the above results, we conclude that inhibition of autophagy by 3MA blocks NPC-402-induced cell death and activation of autophagy by Rap enhances NPC-402-induced cell death and confirm that the nature of autophagy induced by exposure to NPC-402 of B16F10 cells has a cytotoxic effect.

Chemical chaperone 4-phenylbutyric acid interferes with NPC-402-induced apoptosis *via* relieving endoplasmic reticulum stress-mediated autophagy induction in B16F10 melanoma cells

To investigate whether NPC-402 exposure of melanoma B16F10 cells leads to ER stress-mediated autophagy induction and apoptosis, we employed chemical chaperone 4-phenylbutyric acid (4PBA) and evaluated its cytoprotective nature upon treatment of B16F10 cells with NPC-402 as it rescues cells from ER stress effects. 4PBA is a well-known attenuator of ER stress/UPR used in different models of mammalian cell cultures and has great clinical potential in restoring ER stress-disturbed homeostasis (32). 4PBA treatment was given 2 h prior to NPC-402 in B16F10 cells. We found significant downregulation in ER stress-related proteins p-eIF2α, CHOP/GAD153, and GRP78 after cotreatment of B16F10 cells with NPC-402 and 4PBA compared to NPC-402 only treatment (Figures 2A, B), indicating that 4PBA attenuates NPC-402-induced ER stress response. We also found that attenuation of ER stress by 4PBA leads to inhibition of NPC-402-induced autophagy by observing significant downregulation of Beclin1 and accumulation of p62 after cotreatment of B16F10 cells with 4PBA+NPC-402 compared to NPC-402 only treatment (Figures 2C, D). This confirms that NPC-402 exposure of melanoma cells induces an ER stress response that leads to the induction of autophagy. We also tested whether 4PBA interferes with NPC-402-induced apoptosis and found a significant decrease in cell death rate after cotreatment of B16F10 cells with 4PBA+NPC-402

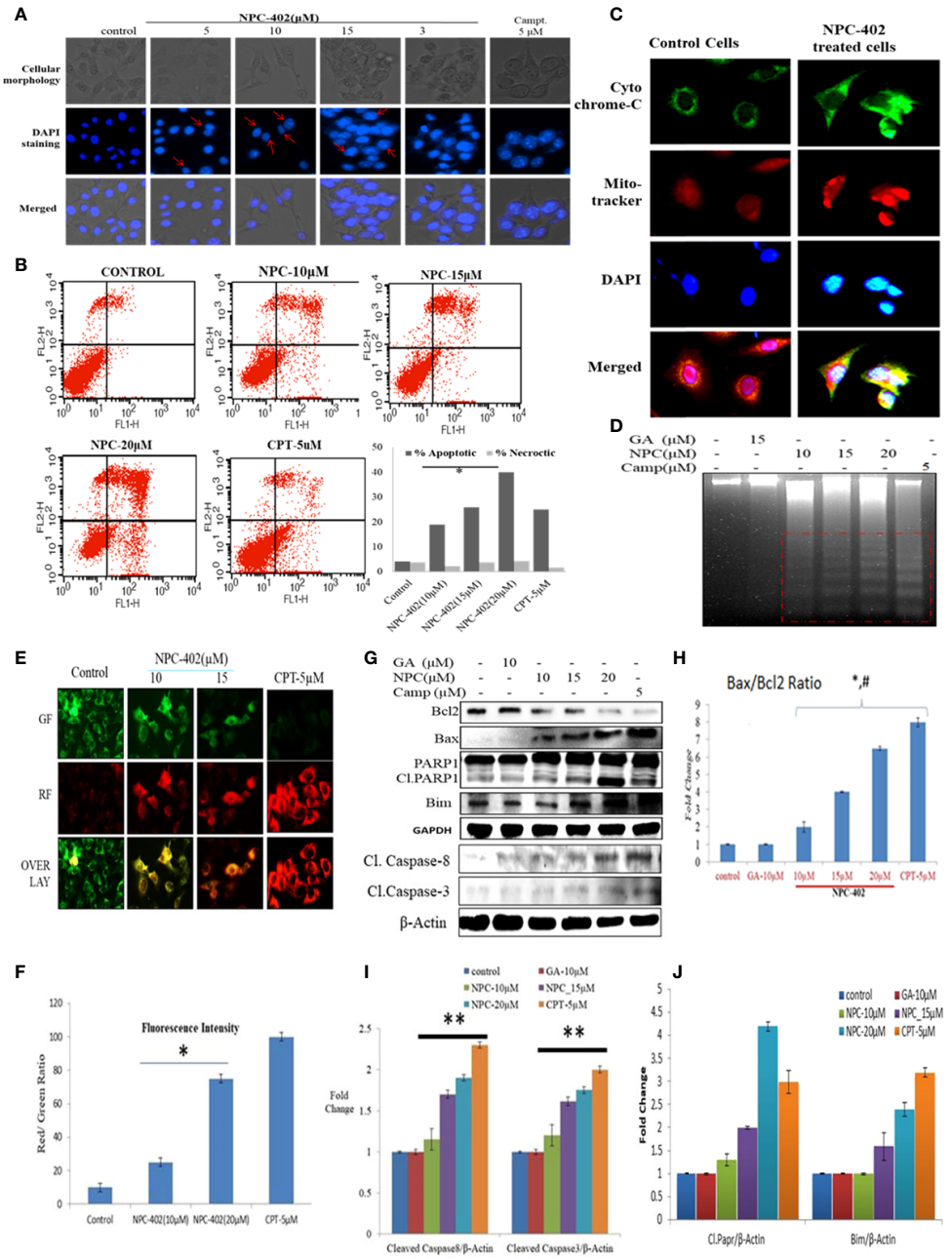

FIGURE 3
NPC-402 induces mitochondrial dysfunction and modulates the expression level of proapoptotic and antiapoptotic markers. **(A)** Staining of B16F10 cells with DAPI on treatment with NPC-402. Cellular morphology and nuclear fragmentation, indicated by red arrows, were seen in melanoma cell line post 24 h treatment, and camptothecin was used as a positive control. **(B)** Annexin V/PI FITC staining of B16F10 cells was done to find the apoptosis induction in B16F10 cells post 12 h treatment of NPC-402 and found increasing percentages of Annexin-V-bound cells. **(C)** Represents the confocal imaging for the detection of cytochrome C translation into cytosol upon exposure of B16F10 cells to NPC-402 treatment for 12 h compared with untreated cells. **(D)** Gel diagram represents DNA fragmentation in B16F10 cells treated with/without NPC-402 for 24 h, camptothecin as a positive control, and GA as a parent molecule of NPC-402. **(E)** Microscopic images represent the JC-9 staining for the detection of $\Delta\Psi m$ in B16F10 cells treated with/without NPC-402; CPT acts as a positive control. **(F)** Red/green fluorescences of panel **(B)** were quantified by using ImageJ software (*$p < 0.001$; control vs. NPC-402 treatment). **(G)** Represents the Western blots of Bcl2, Bax, Parp1, Bim, caspase-8, and caspase-3 in B16F10 cells treated with NPC-402 for 24 h. β-Actin was used as a loading control. **(H)** Bar graphs represent the densitometry analysis of Bax/Bcl_2 ratio in B16F10 cells treated with NPC-402 for 24 h using Image Lab^{TM} Software Version 3.0 (Bio-Rad). **(I)** Bar graphs represent the densitometry analysis of cleaved caspase-8 and cleaved caspase-3 in B16F10 cells treated with NPC-402 for 24 h using Image Lab^{TM} Software Version 3.0 (Bio-Rad). (**J**) Bar graphs represent the densitometry analysis of cleaved PARP1 and Bim in B16F10 cells treated with NPC-402 for 24 h (*$p < 0.001$, control vs. NPC-402 treatment; **$p < 0.01$, control vs. NPC-402 treatment; $p<0.05$ GA treated vs. NPC-402).

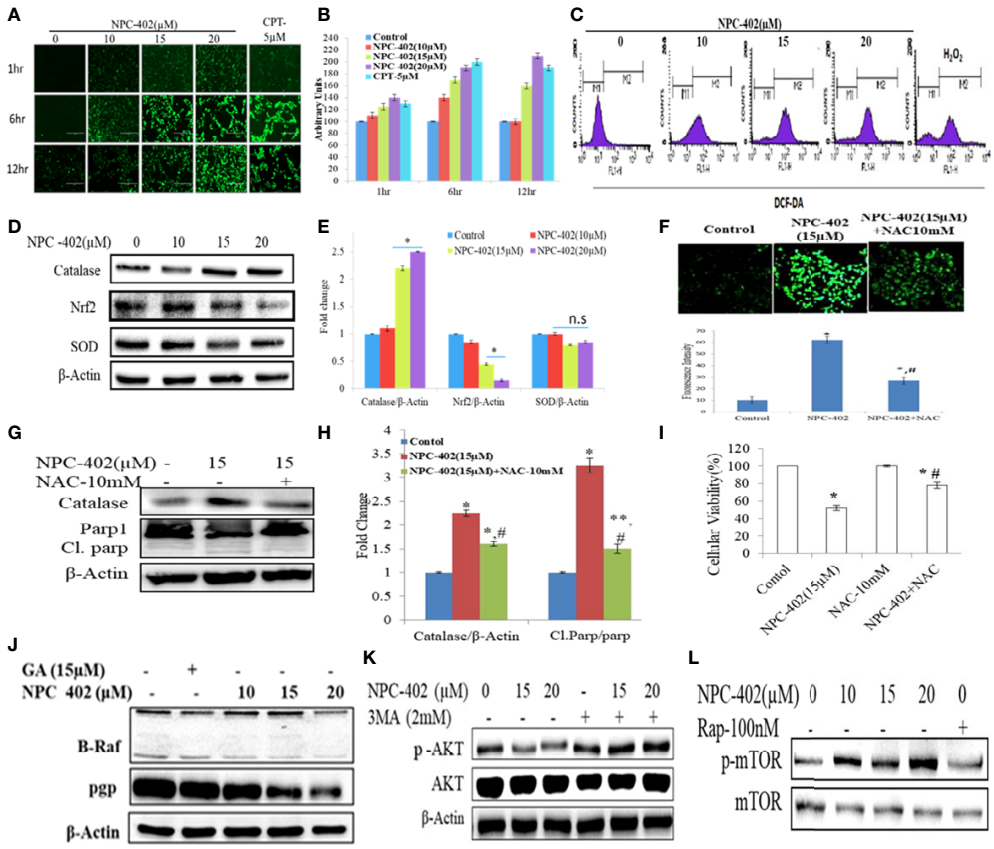

FIGURE 4
Induction of oxidative stress leads to apoptosis and inhibition of MAP kinase/AKT pathways in NPC-402-treated B16F10 cells. **(A)** Microscopic images represent time-dependent ROS fluorescence in B16F10 cells treated with/without NPC-402 by using H_2DFDA dye. **(B)**. Bar graphs represent fluorescence intensity time- and dose-dependently in NPC-402-treated/without treatment B16F10 cells using ImageJ software. **(C)** Represents flow cytometric analysis of ROS generation dose-dependently in NPC-402-exposed B16F10 cells, and H_2O_2 was used as an experimental control. **(D)** Represents Western blots of protein SOD, catalase, and Nrf2 in B16F10 cells treated with NPC-402. **(E)** Bar graph represents the densitometry analysis of catalase, Nrf2, and SOD using Image Lab™ Software Version 3.0 (Bio-Rad). **(F)** Microscopic images represent the ROS fluorescence by H_2DFCA staining in B16F10 cells treated with NPC-402 or NAC or both, and the bar graphs represent ROS quantification thru ImageJ software. **(G)** Immunoblots of catalase, Parp1 in B16F10 cells treated with NPC-402/NAC or both. β-Actin was used as a loading control. **(H)** Bar graph represents the densitometry analysis of catalase, Parp1 in B16F10 cells treated with NPC-402/NAC or both using Image Lab™ Software Version 3.0 (Bio-Rad). **(I)** Bar graph represents the cell viability analysis of B16F10 cells treated with/without NPC-402 or NAC for 24 h using the MTT assay (*p < 0.001 control vs. NPC-402, $^{\#}p$ < 0.001, NPC-402 vs. NPC-402+NAC) (*p < 0.001, control vs. NPC-402 treatment, **p < 0.01, control vs. NPC-402 treatment, $^{\#}p$ < 0.001, control vs. NAC treatment). **(J)** Immunoblot represents the protein expression of B-RAF and PGP using β-actin as a loading control in B16F10 cells treated with NPC-402. **(K)** Immunoblot represents the protein expression of p-AKT/AKT using β-actin as a loading control in B16F10 cells treated with NPC-402 and 3MA. **(L)** Immunoblots represent the protein expression of p-mTOR/mTOR using β-actin as a loading control in B16F10 cells treated with NPC-402. Rapamycin serves as a positive control (*p < 0.001, **p <0.01, control vs. NCP402 treatment).

compared to NPC-402 only treatment, demonstrating that relieving ER stress by 4PBA attenuates the apoptotic effect of NPC-402 (Figure 2G). We also observed significant downregulation in the expression level of caspase-12, cleaved caspase-3, and caspase-9 in these cells cotreated with 4PBA +NPC-402 (Figures 2E, F). NPC-402 also leads to inhibition of cyclin D1 in B16F10 cells, depicting cell cycle arrest at G1-stage that promotes apoptosis, and restoration of cyclin D1 in cotreated (4PBA+NPC-402) conditions releases cells from G1-stage and promotes cell proliferation (Figure 2G). These results suggest an indispensable role of NPC-402-mediated ER stress response in regulating caspase-dependent apoptosis signaling *via* autophagy in B16F10 cells. We further investigated the molecular mechanism of NPC-402-induced cell death effect *via* ER stress and autophagy. We knocked down the expression of CHOP, as it is known to regulate autophagy by increasing the expression of autophagy-related proteins by using 50 pM concentration of CHOP siRNA and analyzed apoptosis. We found that Beclin1 is significantly decreased and the expression of SQSTM/p62 is increased in siRNA-transfected cells treated with NPC-402 compared to

NPC-402 only treatment (Figures 2K, L). Blockage of NPC-402-induced ER stress by silencing CHOP prevents cell death in B16F10 cells as is clear from the expression of cleaved Parp1 and Bax (Figures 4K, 4K.d, 4K.e). ICC of CHOP and GRP78 confirms our finding (Figure 2I), and the results of p62 and cleaved caspase-9 were also confirmed by ICC (Figure 2J). We have also verified that 4PBA treatment of B16F10 cells alleviates the loss of ΔΨm analyzed *via* rhodamine-123 staining (Figure 2H). ER stress results in accumulation of ROS causing oxidative stress and also upregulates CHOP that plays a great role in potentiating the oxidative stress-mediated cell death response (33).

NPC-402 induces apoptosis in B16F10 cells

NPC-402 exposure of B16F10 cells in 24-h treatment induces morphological changes compared to control cells. These changes include surface detachment, cell shrinkage, and multinucleation, and increasing the concentration of NPC-402 causes disruptive changes in the nuclei of cells. Chromatin condensation was observed with significant nuclear shrinkage and fragmentation in treated cells compared to control (Figure 3A). We further evaluated the induction of apoptosis in B16F10 cells upon NPC-402 treatment through Annexin V-FITC staining by looking for inner membrane-bound phosphatidylserine (PS). NPC-402-treated B16F10 cells after 24 h significantly increased Annexin V-positive cells. Camptothecin was used as an experimental control (Figure 3B). Mitochondrial cytochrome C plays an important role in apoptosis *via* the apoptotic protease-activating factor (Apaf) and the release of cytochrome C from mitochondria to cytosol, leading to the cascade of events that leads to the activation of caspases that in turn leads to nuclear DNA fragmentation (34). Translocation of cytochrome C to cytosol (Figure 3C) in NPC-402-treated B16F10 cells was confirmed through confocal microscopy by using MitoTracker as shown in Figure 3C. We have also found that NPC-402 induces DNA fragmentation in B16F10 cells compared to untreated and GA-treated cells (Figure 3D). Rhodamine-123 was used to analyze the effect of NPC-402 on Δψm, and we found that NPC-402 leads to a significant loss of Δψm in a dose-dependent nature compared to untreated cells (Figures 3E, F). Loss of green fluorescence clearly indicates mitochondrial depolarization due to NPC-402 treatment of B16F10 cells. The activation of caspases, Bcl-2/Bax ratio, and other proteins associated with apoptosis were examined by Western blotting. Bax/Bcl-2 ratio acts as a rheostat that determines cellular susceptibility to apoptosis, and elevated levels of this ratio indicate apoptosis (35) and NPC-402 significantly increases the ratio of Bax/Bcl-2 dose-dependently compared to untreated cells (Figures 3G, H). Apoptosis induction by NPC-402 is also clear from increased levels of initiator cleaved caspase-8 and executor caspase-3 in a dose-dependent nature (Figures 3G, I). Cleaved Poly [ADP-ribose] polymerase 1 (PARP-1) is also significantly increased in NPC-402-treated cells compared to untreated cells (Figures 3G, H). Taken together, these results suggest that NPC-402 causes stable induction of apoptosis and decreases the expression level of proapoptotic proteins.

NPC-402 induces oxidative stress in B16F10 cells

To investigate the effect of NPC-402 on ROS generation, DCFH-DA-based flow cytometry and fluorescent imaging analysis were performed to study oxidative stress response. We detected a significant elevation of intracellular ROS in NPC-402-treated B16F10 cells time- and dose-dependently compared to untreated cells (Figures 4A, B), and the same results were obtained in cytometry analysis, as NPC-402-treated samples show increased area under the curve of FL-2 peak (Figure 4C). Furthermore, we analyzed the potential of NPC-402 to induce oxidative stress by measuring the MDA levels in NPC-402-treated B16F10 cells, and we observed that NPC-402 dose-dependently increased the lipid peroxidation levels as compared to that of control (Figure S3). To confirm our microscopy findings, we additionally performed Western blotting analysis of key oxidative stress-related proteins catalase, Nrf2, and SOD and found that NPC-402 increases the expression of catalase and decreases the expression of Nrf2 in a dose-dependent manner (Figures 4D, E). This disturbance related to the change in the expression of oxidative marker proteins leads to the induction of apoptosis in B16F10 melanoma cells. N-acetylcysteine (NAC) is a potent quencher of ROS, and here, NAC 10 mM was used to quench the NPC-402-induced ROS in B16F10 cells. We found that NAC significantly alleviates ROS generation, restores catalase expression, and blocks activation of cleaved PARP-1 in cotreated (NAC+NPC-402) B16F10 cells compared to NPC-402 only treatment (Figures 4F–I).

NPC- 402 attenuates MAPK/AKT signaling pathway in B16F10 melanoma cells

The MAPK pathway is activated in all melanomas, regulating cell survival, proliferation, and metastasis (36). We studied the effect of NPC-402 on MAPK signaling in B16F10 melanoma cells by Western blotting and found that NPC-402 treatment decreases the expression of phospho-MEK, phospho-ERK (Figure 4J, Figure S2A), and P-AKT (Figure 4K, Figure S2B) significantly in a dose-dependent nature. The effect of NPC-402 on stress kinases was explored, and it was found that NPC-402 downregulates the

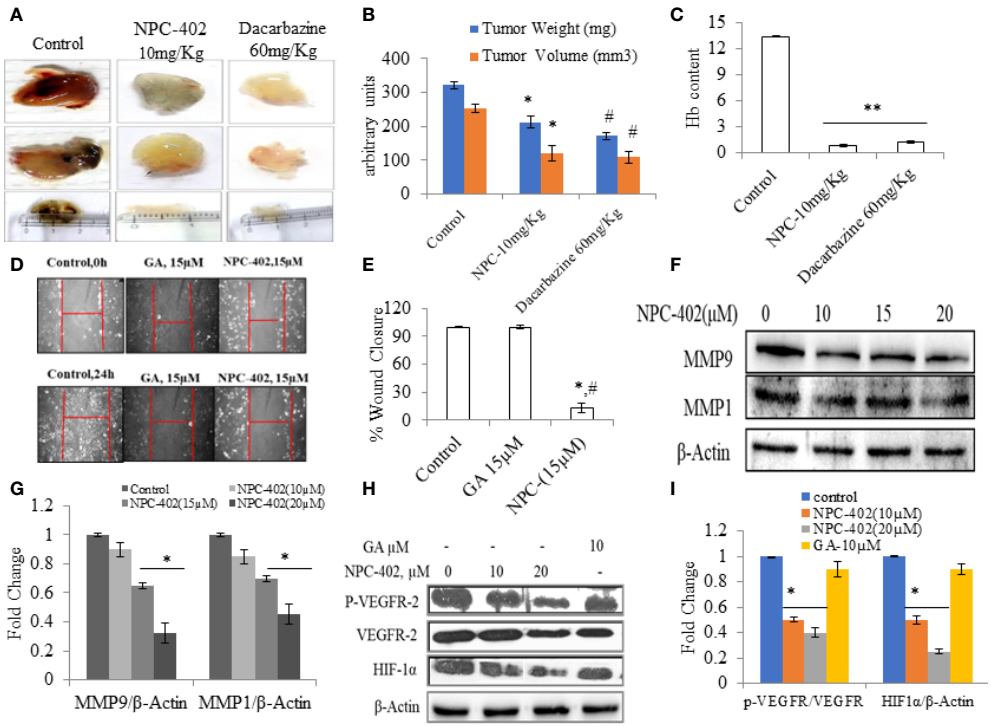

FIGURE 5
NPC-402 inhibits VEGF-mediated tumor angiogenesis in Matrigel assay. **(A)** Represents *in vivo* angiogenesis *via* Matrigel assay in C57BL/6J mice treated with/without NPC-402, and dacarbazine was used as a standard drug against melanoma. **(B)** Bar graph represents the tumor weight and volume of C57BL/6J mice treated with/without NPC-402 (*$p < 0.001$ control vs. NPC-402 group, $^{\#}p < 0.001$ control vs. dacarbazine group). **(C)** Bar graph represents Hb content of tumors, C57BL/6J mice treated with/without NPC-402 (*$p < 0.001$ control vs. NPC-402 group, $^{\#}p < 0.001$ control vs. dacarbazine group). **(D)** Images represent the cell migration assay (*in vitro*) in B16F10 cells treated with NPC-402. **(E)** Bar graphs describes the percentage wound closure in B16F10 cells treated with/without NPC or GA (*$p < 0.001$ control vs. NPC-402, $^{\#}p < 0.001$ GA vs. NPC-402). **(F)** Represents the Western blots of MMP1 and MMP9 in B16F10 cells treated with NPC-402 for 24-h. β-Actin was used as a loading control. **(G)** Bar graphs represent the densitometry analysis of MMP9 and MMP1 in B16F10 cells treated with NPC-402 for 24 h using Image Lab™ Software Version 3.0 (Bio-Rad). **(H)** Represents the Western blots of p-VEGFR2, VEGFR2, and HIF1α in B16F10 cells treated with NPC-402 for 24 h. β-Actin was used as a loading control. **(I)** Bar graphs represent the densitometry analysis of p-VEGFR2, VEGFR2, and HIF1α in B16F10 cells treated with NPC-402 for 24 h using Image Lab™ Software Version 3.0 (Bio-Rad) (*$p < 0.001$, control vs. NPC-402 treatment; **$p < 0.01$, control vs. NPC-402 treatment).

expression of phospho-P38 dose-dependently. However, NPC-402 significantly increases the expression in phosphorylation of p-JNK (Figures S2D–S2I). It has been reported that p-JNK induces cell death *via* c-Jun/cyclin D1 axis and plays a key role in ER stress-mediated autophagy induction. In 60% of melanoma cases, the primary cause is BRAF mutation, thus we analyzed the effect of NPC-402 on BRAF expression and observed that BRAF is significantly downregulated by 3-fold at higher concentrations (Figure 4J, Figure S2A). In addition, we also checked the PGP protein that is related to drug efflux in case of cancer cells and is normally active to efflux out the drugs taken in by cells in defense response. NPC-402 was found to reduce PGP levels (Figure 4J, Figure S2A), suggesting that the drug effusion property of B16F10 cells is reduced drastically, inducing apoptosis-related events. We further checked for the expression of p-mTOR and p-AKT through Western blotting analysis and found that NPC-402 treatment induces the expression of p-mTOR but downregulates p-AKT (Figures 4K, L), suggesting that the cell death potential of NPC-402 is independent of mTOR but is executed through involvement of AKT. Overall, these results suggest that NPC-402 treatment inhibits MAPK family proteins toward potentiating ER stress-mediated apoptosis.

NPC-402 inhibits VEGF-induced tumor angiogenesis in the Matrigel plug assay

Angiogenesis is the key stride in tumor metastasis (37). We analyzed the effects of NPC-402 on VEGF-induced angiogenesis *in vivo*. C57BL/6J mice were dosed i.p. with NPC-402 (10 mg/kg/body weight) after implantation of Matrigel with or without B16F10 cells. The Matrigel plug of the control group revealed a

marked increase in vascularization and tumor size as is evident from deep red appearance and high Hb content (Figures 5A, C). Matrigel plugs of animals dosed with NPC-402 (10 mg/kg/body weight) and dacarbazine (60 mg/kg/body weight) show significant alleviation in vascularization, tumor volume, and weight and appear white with negligible Hb content (Figures 5A, B), indicating that NPC-402 significantly inhibited angiogenesis. Furthermore, we also investigated Vascular endothelial growth factor receptor 2 (VEGFR2) and Hypoxia-inducible factor 1-alpha (HIF1α) protein expression that activates genes involved in migration, angiogenesis, and survival, such as VEGFs that are found to be overexpressed in tumor cells, suggesting that these proteins also have involvement in tumor progression (38). We found that NPC-402 reduces the expression of these proteins (Figures 5H, I), suggesting that NPC-402 alters the signaling response of melanoma cells that is associated with growth, development, and migration of the tumor. In addition, we performed a wound healing assay and found that NPC-402 significantly reduces the wound-healing ability of B16F10 cells as compared to that of control (Figures 5D, E). In melanoma, upregulation of matrix metalloproteinases (MMPs) is associated with migration of the tumor, and upon treatment of B16F10 cells with NPC-402, it dose-dependently downregulates the expression of MMP1 and MMP9 compared to untreated (Figures 5F, G). Similar results were obtained in dacarbazine-treated mice that was used as a positive control and is a standard anticancer drug used against melanoma treatment.

Discussion

Cancer is generally defined as a malignant process of autonomous uncontrolled cell proliferation with the ability to metastasize and resistant to a normal cell death program. Cancer is the second leading cause of death in the world—only surpassed by cardiovascular diseases. Natural products have been widely used for their chemopreventive potential by interfering with cancer morbidities, but lately, drug resistance has become a challenge in cancer chemoprevention, so there is a need for discovering new chemical entities (NCEs) to overcome the burden of cancer pathologies. Among biologically beneficial organic compounds synthesized by plants, pentacyclic triterpenoids have been extensively explored for their appealing pharmacological properties. However, due to poor biological effects of pentacyclic triterpenoids on their molecular targets, these natural products have been used as important templates for the preparation of more active derivatives.

The 18β-glycyrrhetinic acid, a pharmacologically active secondary metabolite from a medicinally reputed plant *G. glabra*, shows significant cytotoxic and antitumor properties. The molecular mechanisms and proapoptotic targets of 18β-glycyrrhetinic acid have been exhaustively explored over the last decade. With the advantage of being an easily available and inexpensive triterpene, a large number of analogs have been synthesized on the basis of 18β-glycyrrhetinic acid scaffold with IC_{50} <30 μM.

In the present study, we have explored the therapeutic efficacy and molecular mechanism of the anti-melanoma effect of NPC-402 [3-(3-methyl-but-2-enyloxy)-11-oxo-olean-12-ene-29-oic acid], a triterpenoid ether derivative of GA (Figures S1A–S1D) on melanoma cells (B16F10) with only marginal toxicity on normal cells. In a cancer therapeutic perspective, it is indispensable for chemotherapeutics to kill cancerous lesions with minimum toxic manifestations on normal tissues (39). Therefore, human keratinocytes (HaCaT cells) were used as a reference model of normal or non-tumorigenic skin cells. We found that NPC-402 is non-toxic up to a concentration of 50 μM in HaCaT cells in 24-h treatment (Figure 1D) compared to B16F10 cells with an IC_{50} at 16 μM (Figure 1A). Moreover, NPC-402 was found to induce cell death in a time-dependent manner (Figure 1B). GA, the parent molecule of NCP-402, was found to be devoid of toxic effects on B16F10 cells (Figure 1C). We tested the toxicity of NPC-402 on various melanoma cell line models and evaluated the IC_{50} as shown in Figure 1E and performed colony formation assay and found that NPC-402 acts as a cytostatic agent at lower concentrations and caused cytotoxicity at higher concentrations (Figure 1F).

We evaluated the effect of NPC-402 on ER stress. ER is a cytoplasm-based dynamic membrane-bound organelle that is responsible for protein folding and also involved in posttranslational modification, calcium storage, and lipid metabolism (10). Inimical conditions such as calcium depletion, truncated or misfolded proteins, and oxidative stress in the cell lead to a condition known as ER stress that leads to UPR *via* activating associated signaling pathways (10). Targeting ER stress is considered as the therapeutic future in melanoma treatment (40). In line with this, we observed that NPC-402 treatment induces ER stress response in cells as was evident by the increased expression of GRP78 that evokes the UPR and also halts protein translation *via* GRP78-eIF2α-CHOP signal transduction pathway (Figures 1G, I). Severe and prolonged ER stress deteriorates cellular physiology and switches cell fate toward apoptosis. Numerous studies have suggested that ER stress and autophagy are systematically interconnected, wherein the UPR and ER stress pathway stimulates the induction of basal autophagy that potentiates cell death. Induction of autophagy was observed upon NPC-402 treatment of melanoma cells corroborated by increased acidic vacuole formation (Figure 1K), LC3I/II lipidation, upregulation of Beclin1, and downregulation of cargo cum adapter protein SQSTM1/P62 (Figures 1H, J). In order to validate the role of autophagy in NPC-402-mediated cell death, the cell viability assay was performed in the presence of an autophagy activator, Rap, and

an autophagy inhibitor, 3MA. The results clearly indicate that Rap potentiated, whereas 3MA mitigated, the cell death effects of NPC-402 (Figure 1L).

Chemical chaperone 4PBA is a noticeable molecule that mitigates the ER stress induced by hostile conditions that has been confirmed in our previous studies (41). We analyzed whether 4PBA interferes with NPC-402-induced apoptosis *via* relieving ER stress-mediated autophagy induction in B16F10 melanoma cells. We observed that 4PBA mitigates ER stress induced by NPC-402 evident from the expression of GRP78/Bip that in turn prevented downstream activation of eIF2α-CHOP and finally culminated into alleviation of autophagy response in cells (Figures 2A–D) and thereby prevented NPC-402 apoptosis as analyzed by Western blotting (Figures 2E, F) and immunostaining assay (Figures 2I, J). Cell viability analysis also supports that 4PBA retards NPC-402-induced cell death in B16F10 cells (Figure 2G), and cyclin D1 expression clearly explains the prevention of cell cycle arrest caused by exposure of B16F10 cells to NPC-402 (Figure 2G). Transcriptional factor CHOP also plays a highly significant role in ER stress-mediated apoptosis, as the sustained activation of UPR causes upregulation of CHOP *via* GRP78/ATF4 signaling pathway (42). Sustained CHOP upregulation increases the induction of autophagy that leads cells toward apoptosis. We silenced CHOP by using specific siRNA transfection in B16F10 cells and observed that knockdown of CHOP prevented the induction of autophagy that blocked cell death in NPC-402-treated, CHOP siRNA-transfected B16F10 cells compared to NPC-402 only-treated cells (Figures 2K, L).

ROS generation and ER stress along with UPR lead to oxidative and mitochondrial damage and induce cell death in cancer cells when treated with anticancer drugs (43, 44). Here, we observed that NPC-402 markedly increases ROS in B16F10 cells as analyzed by microscopy (Figures 4A, B) and flow cytometry assay (Figure 4C). It was found that NPC-402 reduced the Nrf-2 expression and modulated downstream redox signaling proteins SOD and catalase probably due to DNA damage and elevation of the oxidative stress response in B16F10 cells (Figures 4D, E). We also observed that antioxidant NAC diminished the effect of NPC-402 on oxidative stress (Figures 4F–H) and prevented NPC-402-induced cell death (Figure 4I).

Finally, we evaluated the effect of NPC-402 on cell death signaling. In melanoma therapy, target-specific cell death is very important for melanoma tumors (45). NPC-402 was found to be a potential cell death-inducing agent in melanoma cells through dysregulation of survival signaling pathways and activation of apoptotic signaling and prevented the proliferation and transformation of cancer cells into tumors. The proapoptotic effects of NPC-402 in B16F10 cells can be attributed to a change in $\Delta\Psi m$ (Figures 3E, F), PARP-1 cleavage, activation of caspases (Figures 3G–J), DNA damage (3D), and nuclear fragmentation (Figure 3A). We have also confirmed the release of cytochrome C from the mitochondrial inner membrane space that conveys that, upon treatment, NPC-402 induced a cascade of apoptotic events in B16F10 cells (Figure 3C). Taken together, these events constitute diverse mechanisms behind the anti-melanoma activity of NPC-402 in B16F10 cells through intrinsic and extrinsic apoptotic pathways.

Anticancer drugs are known to alter/hinder multiple intracellular signaling pathways in melanoma (46). Classically, MAPK signaling pathway plays a protective and pivotal role in response to varied external stimuli (47). Based on the findings of the present study, it was evident that NPC-402 decreased the activity of MAPK signaling axis in favor of increased apoptosis (Figures S2D–S2G). Furthermore, NPC-402 downregulated AKT survival signaling pathway (Figures 4K, L) albeit upregulated the expression of p-mTOR (Figure 4L), corroborating with growth inhibitory effects of NPC-402 in B16F10 melanoma cells. Moreover, NPC-402 is pharmacologically active through the i.p. route of drug administration. NPC-402 administration effectively inhibits B16F10 cell growth in the Matrigel plug assay. NPC-402 was equally effective as a standard clinical drug, dacarbazine, in retarding angiogenesis as was found through estimation of Hb through the Drabkin test (Figures 5A–I). These results suggest that NPC-402 inhibits VEGF-mediated angiogenesis, with relatively fewer toxic manifestations on normal cells.

Conclusion

Overall, the present study supports the use of NPC-402 against melanoma cells as a potential therapeutic lead that may have relevance clinically. Furthermore, more mechanism-based and preclinical studies are required to confirm the therapeutic safety, efficacy, and potency of NPC-402 in its use as a promising melanoma drug.

Author's note

We dedicate this work to the memory of Dr P.L. Sangwan, the Co-author of this article, who left for heavenly abode on 6th of August 2021. We will miss him for his uncanny knowledge of Natural Products Chemistry, for being a great human being, a great friend and a great collaborator.

Data availability statement

The original contributions presented in the study are included in the article/Supplementary Material. Further inquiries can be directed to the corresponding author.

Ethics statement

The animal study was reviewed and approved by Institutional Animal Ethics Committee, IAEC-IIIM, Jammu.

Author contributions

LN, NS, US performed the experiments. KA, SR, SB and PS performed the synthesis of NPC402. ST made hypothesis, coordinated and procured the funding for the study. ST and LN wrote the MS.

Acknowledgments

Senior Research Fellowship to LN by University Grants commission, New Delhi, India under NET-JRF scheme and Senior Research Fellowship to US by Department of science and technology vide no. IF-160982, New Delhi, India is acknowledged. This work was supported by council of scientific research and industrial research (CSIR), New Delhi, India vide project No GAP 2166. The manuscript has been passed through the research committee of the Institute CSIR-IIIM vide publication no: IIIM/IPR/00150.

Conflict of interest

The authors declare that the research was conducted in the absence of any commercial or financial relationships that could be construed as a potential conflict of interest.

Publisher's note

Supplementary material

The Supplementary Material for this article can be found online at: https://www.frontiersin.org/articles/10.3389/fonc.2022.890299/full#supplementary-material

References

1. Bhatia S, Tykodi SS, Thompson JA. Treatment of metastatic melanoma: an overview. *Oncology* (2009) 23(6):488.

2. Narayanan DL, Saladi RN, Fox JL. Ultraviolet radiation and skin cancer. *Int J Dermatol* (2010) 49(9):978–86. doi: 10.1111/j.1365-4632.2010.04474.x

3. Winder M, Virós A. Mechanisms of drug resistance in melanoma. *Mech Drug Resist Cancer Ther* (2017) 249:91–108. doi: 10.1007/164_2017_17

4. Wondrak GT. Redox-directed cancer therapeutics: molecular mechanisms and opportunities. *Antioxid Redox Signaling* (2009) 11(12):3013–69. doi: 10.1089/ars.2009.2541

5. Obrador E, Liu-Smith F, Dellinger RW, Salvador R, Meyskens FL, Estrela JM. Oxidative stress and antioxidants in the pathophysiology of malignant melanoma. *Biol Chem* (2019) 400(5):589–612. doi: 10.1515/hsz-2018-0327

6. Leung AM, Hari DM, Morton DL. Surgery for distant melanoma metastasis. *Cancer J (Sudbury Mass)* (2012) 18(2):176. doi: 10.1097/PPO.0b013e31824bc981

7. Mosca PJ, Teicher E, Nair SP, Pockaj BA. Can surgeons improve survival in stage IV melanoma? *J Surg Oncol* (2008) 97(5):462–8. doi: 10.1002/jso.20950

8. Downward J. Targeting RAS signalling pathways in cancer therapy. *Nat Rev Cancer* (2003) 3(1):11. doi: 10.1038/nrc969

9. Lee W-S, Yoo W-H, Chae H-J. ER stress and autophagy. *Curr Mol Med* (2015) 15(8):735–45. doi: 10.2174/1566524015666150921105453

10. Rafiq RA, Bhagat M, Singh SK. Oncogenic BRAF, endoplasmic reticulum stress, and autophagy: Crosstalk and therapeutic targets in cutaneous melanoma. *Mutat Res/Rev Mutat Res* (2020) 785:108321. doi: 10.1016/j.mrrev.2020.108321

11. Hill DS, Lovat PE, Haass NK. Induction of endoplasmic reticulum stress as a strategy for melanoma therapy: is there a future? *Melanoma Manage* (2014) 1 (2):127–37. doi: 10.2217/mmt.14.16

12. Mizushima N. Autophagy: process and function. *Genes Dev* (2007) 21 (22):2861–73. doi: 10.1101/gad.1599207

13. Glick D, Barth S, Macleod KF. Autophagy: cellular and molecular mechanisms. *J Pathol* (2010) 221(1):3–12. doi: 10.1002/path.2697

14. Boya P, Reggiori F, Codogno P. Emerging regulation and functions of autophagy. *Nat Cell Biol* (2013) 15(7):713–20. doi: 10.1038/ncb2788

15. Baehrecke EH. Autophagy: dual roles in life and death? *Nat Rev Mol Cell Biol* (2005) 6(6):505–10. doi: 10.1038/nrm1666

16. Debnath J, Baehrecke EH, Kroemer G. Does autophagy contribute to cell death? *Autophagy* (2005) 1(2):66–74. doi: 10.4161/auto.1.2.1738

17. Wong CH, Iskandar KB, Yadav SK, Hirpara JL., Loh T, Pervaiz S. Simultaneous induction of non-canonical autophagy and apoptosis in cancer cells by ROS-dependent ERK and JNK activation. *PLoS One* (2010) 5(4):e9996. doi: 10.1371/journal.pone.0009996

18. Lopez-Bergami P, Habelhah H, Bhoumik A, Zhang W, Wang LH, Ronai ZE. Rewired ERK-JNK signaling pathways in melanoma. *Cancer Cell* (2007) 11(5):447–60. doi: 10.1016/j.ccr.2007.03.009

19. Puissant A, Robert G, Fenouille N, Luciano F, Cassuto JP, Raynaud S, et al. Resveratrol promotes autophagic cell death in chronic myelogenous leukemia cells via JNK-mediated p62/SQSTM1 expression and AMPK activation. *Cancer Res* (2010) p:0008–5472. doi: 10.1158/0008-5472.CAN-09-3537

20. Shanmugam MK, Dai X, Kumar AP, Tan BK, Sethi G, Bishayee A. Ursolic acid in cancer prevention and treatment: molecular targets, pharmacokinetics and clinical studies. *Biochemical Pharmacology* (Elsevier) (2013) 85(11):1579–87. doi: 10.1016/j.bcp.2013.03.006

21. Hussain H, Green IR, Shamraiz U, Saleem M, Badshah A, Abbas G, et al. Therapeutic potential of glycyrrhetinic acids: a patent review (2010-2017). *Expert Opin Ther Patents* (2018) 28(5):383–98. doi: 10.1080/13543776.2018.1455828

22. Naikoo S, Tasduq SA. Trigonelline, a naturally occurring alkaloidal agent protects ultraviolet-b (UV-b) irradiation induced apoptotic cell death in human skin fibroblasts via attenuation of oxidative stress, restoration of cellular calcium

homeostasis and prevention of endoplasmic reticulum (ER) stress. *J Photochem Photobiol B: Biol* (2020) 202:111720. doi: 10.1016/j.jphotobiol.2019.111720

23. Adil MD, Kaiser P, Satti NK, Zargar AM, Vishwakarma RA, Tasduq SA. Effect of emblica officinalis (fruit) against UVB-induced photo-aging in human skin fibroblasts. *J Ethnopharmacol* (2010) 132(1):109–14. doi: 10.1016/j.jep.2010.07.047

24. Präbst K, Engelhardt H, Ringgeler S, Hübner H. Basic colorimetric proliferation assays: MTT, WST, and resazurin. *Cell Viability Assays* (2017) 1601:1–17. doi: 10.1007/978-1-4939-6960-9_1

25. Song Y, Dai F, Zhai D, Dong Y, Zhang J, Lu B, et al. Usnic acid inhibits breast tumor angiogenesis and growth by suppressing VEGFR2-mediated AKT and ERK1/2 signaling pathways. *Angiogenesis* (2012) 15(3):421–32. doi: 10.1007/s10456-012-9270-4

26. Fishman D, Irena B, Kellman-Pressman S, Karas M, Segal S. The role of MHC class I glycoproteins in the regulation of induction of cell death in immunocytes by malignant melanoma cells. *Proc Natl Acad Sci* (2001) 98 (4):1740–4. doi: 10.1073/pnas.98.4.1740

27. Umar SA, Tanveer MA, Nazir LA, Divya G, Vishwakarma RA, Tasduq SA. Glycyrrhizic acid prevents oxidative stress mediated DNA damage response through modulation of autophagy in ultraviolet-B-Irradiated human primary dermal fibroblasts. *Cell Physiol Biochem* (2019) 53:242–57. doi: 10.33594/000000133

28. Sharma L, Lone NA, Knott RM, Hassan A, Abdullah T. Trigonelline prevents high cholesterol and high fat diet induced hepatic lipid accumulation and lipo-toxicity in C57BL/6J mice, via restoration of hepatic autophagy. *Food Chem Toxicol* (2018) 121:283–96. doi: 10.1016/j.fct.2018.09.011

29. Afnan Q, Adil MD, Nissar-Ul A, Rafiq AR, Amir HF, Kaiser P, et al. Glycyrrhizic acid (GA), a triterpenoid saponin glycoside alleviates ultraviolet-b irradiation-induced photoaging in human dermal fibroblasts. *Phytomedicine* (2012) 19(7):658–64. doi: 10.1016/j.phymed.2012.03.007

30. Rafiq RA, Quadri A, Nazir LA, Peerzada K, Ganai BA, Tasduq SA. A potent inhibitor of phosphoinositide 3-kinase (PI3K) and mitogen activated protein (MAP) kinase signalling, quercetin (3, 3', 4', 5, 7-pentahydroxyflavone) promotes cell death in ultraviolet (UV)-b-irradiated B16F10 melanoma cells. *PLoS One* (2015) 10(7):e0131253. doi: 10.1371/journal.pone.0131253

31. Pyun B-J, Choi S, Lee Y, Kim TW, Min JK, Kim Y, et al. Capsiate, a nonpungent capsaicin-like compound, inhibits angiogenesis and vascular permeability via a direct inhibition of src kinase activity. *Cancer Res* (2008) 68 (1):227–35. doi: 10.1158/0008-5472.CAN-07-2799

32. Kolb PS, Ayaub EA, Zhou W, Yum V, Dickhout JG, Ask K. The therapeutic effects of 4-phenylbutyric acid in maintaining proteostasis. *Int J Biochem Cell Biol* (2015) 61:45–52. doi: 10.1016/j.biocel.2015.01.015

33. Cao SS, Kaufman RJ. Endoplasmic reticulum stress and oxidative stress in cell fate decision and human disease. *Antioxid Redox Signaling* (2014) 21(3):396–413. doi: 10.1089/ars.2014.5851

34. Cai J, Yang J, Jones D. Mitochondrial control of apoptosis: the role of cytochrome c. *Biochim Biophys Acta (BBA)-Bioenerg* (1998) 1366(1-2):139–49. doi: 10.1016/S0005-2728(98)00109-1

35. Raisova M, Hossini AM, Eberle J, Riebeling C, Wieder T, Sturm I, et al. The Bax/Bcl-2 ratio determines the susceptibility of human melanoma cells to CD95/Fas-mediated apoptosis. *J Invest Dermatol* (2001) 117(2):333–40. doi: 10.1046/j.0022-202x.2001.01409.x

36. Yamada E, Singh R. Mapping autophagy on to your metabolic radar. *Diabetes* (2012) 61(2):272–80. doi: 10.2337/db11-1199

37. Tozer GM, Kanthou C, Baguley BC. Disrupting tumour blood vessels. *Nat Rev Cancer* (2005) 5(6):423. doi: 10.1038/nrc1628

38. Panka DJ, Atkins MB, Mier JW. Targeting the mitogen-activated protein kinase pathway in the treatment of malignant melanoma. *Clin Cancer Res* (2006) 12(7):2371s–5s. doi: 10.1158/1078-0432.CCR-05-2539

39. Liu B, Ezeogu L, Zellmer L, Yu B, Xu N, Joshua Liao D. Protecting the normal in order to better kill the cancer. *Cancer Med* (2015) 4(9):1394–403. doi: 10.1002/cam4.488

40. Hassan M, Selimovic D, Hannig M, Haikel Y, Brodell RT, Megahed M. Endoplasmic reticulum stress-mediated pathways to both apoptosis and autophagy: significance for melanoma treatment. *World J Exp Med* (2015) 5 (4):206. doi: 10.5493/wjem.v5.i4.206

41. Nissar AU, Sharma L, Mudasir MA, Nazir LA, Umar SA, Sharma PR, et al. Chemical chaperone 4-phenyl butyric acid (4-PBA) reduces hepatocellular lipid accumulation and lipotoxicity through induction of autophagy. *J Lipid Res* (2017) 58(9):1855–68. doi: 10.1194/jlr.M077537

42. Hu H, Tian M, Ding C, Yu S. The C/EBP homologous protein (CHOP) transcription factor functions in endoplasmic reticulum stress-induced apoptosis and microbial infection. *Front Immunol* (2019) 9:3083. doi: 10.3389/fimmu.2018.03083

43. Rafiq RA, Ganai BA, Tasduq SA. Piperine promotes ultraviolet (UV)-b-induced cell death in B16F10 mouse melanoma cells through modulation of major regulators of cell survival. *RSC Adv* (2015) 5(16):11884–94. doi: 10.1039/C4RA12860E

44. Banerjee A, Banerjee V, Czinn S, Blanchard T. Increased reactive oxygen species levels cause ER stress and cytotoxicity in andrographolide treated colon cancer cells. *Oncotarget* (2017) 8(16):26142. doi: 10.18632/oncotarget.15393

45. Grossman D, Altieri DC. Drug resistance in melanoma: mechanisms, apoptosis, and new potential therapeutic targets. *Cancer Metastasis Rev* (2001) 20(1-2):3–11. doi: 10.1023/A:1013123532723

46. Heck DE, Gerecke DR, Vetrano AM, Laskin JD. Solar ultraviolet radiation as a trigger of cell signal transduction. *Toxicol Appl Pharmacol* (2004) 195(3):288–97. doi: 10.1016/j.taap.2003.09.028

47. Kitagawa D, Tanemura S, Ohata S, Shimizu N, Seo J, Nishitai G, et al. Activation of extracellular signal-regulated kinase by ultraviolet is mediated through src-dependent epidermal growth factor receptor phosphorylation ITS IMPLICATION IN AN ANTI-APOPTOTIC FUNCTION. *J Biol Chem* (2002) 277 (1):366–71. doi: 10.1074/jbc.M107110200

frontiers | Frontiers in Oncology

TYPE Original Research
PUBLISHED 14 September 2022
DOI 10.3389/fonc.2022.932156

OPEN ACCESS

EDITED BY
Chen Ling,
Fudan University, China

REVIEWED BY
Youssef Naguib,
Minia University, Egypt
Nidhi Gupta,
Inspiration Innovation Synergy University, India
Binbin Cheng,
Second Military Medical University, China

*CORRESPONDENCE
Jia Wu
wujia20210327@163.com

SPECIALTY SECTION
This article was submitted to Pharmacology of Anti-Cancer Drugs, a section of the journal Frontiers in Oncology

RECEIVED 29 April 2022
ACCEPTED 22 August 2022
PUBLISHED 14 September 2022

CITATION
Xie M-H, Fu Z-L, Hua A-L, Zhou J-F, Chen Q, Li J-B, Yao S, Cai X-J, Ge M, Zhou L and Wu J (2022) A new core–shell-type nanoparticle loaded with paclitaxel/norcantharidin and modified with APRPG enhances anti-tumor effects in hepatocellular carcinoma. *Front. Oncol.* 12:932156. doi: 10.3389/fonc.2022.932156

A new core–shell-type nanoparticle loaded with paclitaxel/norcantharidin and modified with APRPG enhances anti-tumor effects in hepatocellular carcinoma

Ming-Hua Xie[1], Zai-Lin Fu[1], Ai-Lian Hua[1], Ji-Fang Zhou[1], Qian Chen[1], Jian-Bo Li[1], Shen Yao[1], Xin-Jun Cai[2], Min Ge[1], Li Zhou[3] and Jia Wu[1]*

[1]Department of Pharmacy, First People's Hospital of Linping District, Hangzhou, China, [2]Department of Pharmacy, Zhejiang Integrated Traditional Chinese and Western Medicine Hospital, Hangzhou, China, [3]Department of Oncology, First People's Hospital of Linping District, Hangzhou, China

Nanoparticle delivery systems have been shown to improve the therapeutic efficacy of anti-cancer drugs, including a variety of drugs for the treatment of hepatocellular carcinoma (HCC). However, the current systems show some limitations, and the delivery of more effective nanoparticle systems for anti-HCC drugs with better targeting ability are needed. Here, we created paclitaxel (PTX)/norcantharidin (NCTD)-loaded core–shell lipid nanoparticles modified with a tumor neovasculature-targeted peptide (Ala-Pro-Arg-Pro-Gly, APRPG) and investigated their anti-tumor effects in HCC. Core–shell-type lipid nanoparticles (PTX/NCTD-APRPG-NPs) were established by combining poly(lactic-co-glycolic acid) (PLGA)-wrapped PTX with phospholipid-wrapped NCTD, followed by modification with APRPG. For comparison, PTX-loaded PLGA nanoparticles (PTX-NPs) and PTX/NCTD-loaded core–shell-type nanoparticles without APRPG (PTX/NCTD-NPs) were prepared. The *in vitro* and *in vivo* anti-tumor effects were examined in HepG2 cells and tumor-bearing mice, respectively. Morphological and release characterization showed that PTX/NCTD-APRPG-NPs were prepared successfully and achieved up to 90% release of PTX in a sustained manner. Compared with PTX/NCTD-NPs, PTX/NCTD-APRPG-NPs significantly enhanced the uptake of PTX. Notably, the inhibition of proliferation and migration of hepatoma cells was significantly higher in the PTX/NCTD-APRPG-NP group than those in the PTX-NP and PTX/NCTD-NP groups, which reflected significantly greater anti-tumor properties as well. Furthermore, key molecules in cell proliferation and apoptosis signaling pathways were altered most in the PTX/NCTD-APRPG-NP group, compared with the PTX-NP and PTX/NCTD-NP groups. Collectively, PTX/NCTD-loaded core–shell lipid nanoparticles modified with APRPG enhance the effectiveness of anti-HCC drugs and may be an effective system for the delivery of anti-HCC drugs.

KEYWORDS
hepatocellular carcinoma, paclitaxel, norcantharidin, core–shell lipid nanoparticles, APRPG

Introduction

Hepatocellular carcinoma (HCC) is the most common malignancy of the liver and a leading cause of cancer-related death worldwide (1). The majority of HCC cases occur in Asian countries and account for approximately 50% of all the new HCC cases globally (2, 3). Paclitaxel (PTX) is a naturally occurring anti-tumor agent that is isolated from the bark of *Taxus brevifolia*. PTX has been approved as a chemotherapeutic drug and is widely used as first-line treatment of a broad spectrum of cancers, including HCC, breast cancer, metastatic ovarian cancer, and malignant melanoma (4–7). PTX exerts its therapeutic effects through multiple effects, including inducing cell growth arrest at the G2/M phase, apoptosis, and autophagy, and proapoptotic death receptor (DR) 4 and DR5 have been shown to play a role in its mechanisms of action (6, 7). However, a number of limitations for PTX have been reported, such as its poor aqueous solubility, and PTX is usually formulated with solubilizing agents [Cremophor EL (CrEL) and ethanol] for clinical usage to avoid these limitations. However, CrEL in the PTX formulation has been reported to result in toxic effects, such as severe anaphylaxis, a potentially life-threatening allergy (8, 9). Therefore, research efforts have been made to develop novel formulations using agents other than CrEL, such as nanospheres (10), liposomes (11), nano-emulsions (12), and solid lipid nanoparticles (13), to prolong the *in vivo* half-life and residence time, and reduce the dosage and dosing frequency.

Nanoparticles have shown promising application in the delivery of anti-cancer drugs, including anti-HCC drugs (14, 15). Rapid progress has been made in the development of various nanoparticles, such as polymer, lipid, and metal nanoparticles, for the treatment of HCC (15). The use of nanoparticles has been shown to improve the targeting and therapeutic efficacy of anti-HCC drugs (14, 15). Nanoparticle drug delivery systems have advantages over traditional drug delivery methods, including a prolonged *in vivo* half-life and reduced systemic toxicity. Currently, liposome-based, polymer-based, and micelle-like nanoparticles are commonly used nanoparticle delivery systems for the treatment of malignant tumors (16, 17). However, these conventional nanoparticle-based delivery systems are clinically unsatisfactory (18–20).

Core–shell lipid nanoparticles have recently emerged as a new type of nanoparticle for drug delivery and show several beneficial characteristics, such as core–shell structure and programmable drug release (20). In the core–shell lipid nanoparticle delivery system, nanoparticles loaded with a drug in the core can be co-loaded with another drug in the phospholipid shell to form a more stable delivery system. Considering the advantages, such as controlled drug release, modifiable surface structure, and excellent biocompatibility, the core–shell lipid nanoparticle delivery system has become a research hotspot in the field of pharmaceutics (21). Notably, the loading of one drug in the core and the co-loading of another drug in the shell in the core–shell lipid nanoparticle delivery system enhances the therapeutic efficacy of the drugs compared with the conventional nanoparticle delivery systems. To date, anti-tumor drugs delivered using core–shell lipid nanoparticle delivery systems have not been explored for the treatment of HCC.

Norcantharidin (NCTD) is a demethylated derivative of cantharidin, an anti-cancer active ingredient of traditional Chinese medicine (22). Although NCTD has been shown as a promising anti-tumor oral agent for the treatment of various malignancies, the exact mechanism of action of NCTD remains unknown (22). However, the narrow therapeutic window and high renal toxicity have largely limited its clinical application (23). Therefore, it is urgent to develop novel formulations to improve the therapeutic effects and reduce the renal distribution of NCTD. Ala-Pro-Arg-Pro-Gly (APRPG) is a synthetic peptide that specifically targets tumor angiogenesis and was recently applied as a targeting peptide loaded in liposomes (24, 25).

In the present study, we prepared novel core–shell lipid nanoparticles loaded with PTX in the core as well as NCTD in the shell and modified with APRPG and investigated their anti-tumor effects in HCC.

Materials and methods

Preparation of PTX/NCTD-loaded core–shell lipid nanoparticles modified with APRPG (PTX/NCTD-APRPG-NPs)

PTX/NCTD-loaded core–shell lipid nanoparticles modified with APRPG (PTX/NCTD-APRPG-NPs) were prepared as described (20, 21). Briefly, we determined the optimal concentration of phospholipid as follows. We mixed 100 mg of cholesterol, 10 mg of mannose glycolipid, 10 mg of APRPG-PEG2000-DSPE, and 30

mg of NCTD in a flask and different concentrations of phospholipid (10 mg/ml, 20 mg/ml, and 30 mg/ml) were added. The phospholipid used in the formulation was lecithin (Shanghai Yuanye Bio-Technology Co., Ltd, Shanghai, China). The mixture was placed in a round-bottom flask in a rotary evaporator, 20 ml of chloroform was added, and the flask was placed in a 37°C water bath until the mixture was completely dissolved. After drying the remaining chloroform, the samples were dissolved in 10 ml of hexyl hydride. The sample was subjected to centrifugation; the supernatant was collected and the organic solvents were dried. The remaining mixture was dissolved in chloroform and a film was formed using a rotary evaporator. An appropriate volume of the PTX-PLGA nanoparticle suspension was added to the film, followed by hydration for 12 h. Finally, PTX/NCTD-APRPG-NPs were obtained. The particle size and uniformity of the film were measured to determine the optimal concentration of phospholipid. The minimal particle size and uniform film formation were observed in the 10 mg/ml phospholipid group. Therefore, a concentration of 10 mg/ml was used as the optimal phospholipid concentration in subsequent experiments.

The optimal ratio of phospholipid to cholesterol was determined from screening different ratios (1:1, 1:2, 2:1, 4:3, and 3:4) using the optimal phospholipid concentration of 10 mg/ml. The minimal particle size and uniform film formation were found in the 4:3 ratio group, and this was considered the optimal ratio of phospholipid to cholesterol.

After the optimal conditions were determined, we prepared PTX/NCTD-APRPG-NPs by dissolving 200 mg of phospholipid, 150 mg of cholesterol, 30 mg of NCTD, 10 mg of mannose glycolipid, and 10 mg of APRPG-PEG2000-DSPE in 20 ml of chloroform following the procedures described above.

For a comparative study, we also prepared core–shell lipid nanoparticles loaded with PTX/NCTD without 10 mg of APRPG-PEG2000-DSPE (PTX/NCTD-NPs) using similar procedures as described above. In addition, conventional PTX-loaded poly(lactic-co-glycolic acid) (PLGA) nanoparticles (PTX-NPs) with a core but without a shell structure were prepared as described previously (26).

The particle size was measured using the Beckman particle size analyzer (Beckman, CA, USA). The micromorphology of the APRPG-NPs and nanoparticles was observed by transmission electron microscopy. The encapsulation efficiency (EE) of the APRPG-NPs and nanoparticles was calculated after determining the PTX concentration in the APRPG-NPs and nanoparticles using high-performance liquid chromatography (HPLC). The APRPG-NPs and nanoparticles were placed under 4°C, 37°C, and 25°C for 24 h, and changes in the particle size were observed using the Beckman particle size analyzer (Beckman).

In vitro release determination of PTX/NCTD-APRPG-NPs

Phosphate-buffered saline (PBS) containing 1% Tween 80 at pH 7.4 was used as the release medium. A 2-ml suspension of PTX/NCTD-APRPG-NPs was carefully transferred into a dialysis bag and placed into 20 ml of the release medium. The *in vitro* release assay was performed at 37°C with 100 shocks per minute. Three milliliters of media was collected at certain time points with supplementation of fresh media. The collected media was dried and the dried samples were dissolved in 1 ml of methyl alcohol, followed by filtration using a 0.22-μm Millipore filter. HPLC was used to detect the concentration of PTX and mass spectrometry (MS) was used to determine the concentration of NCTD in the samples to calculate the cumulative release percentage and generate the release curve as reported previously (27).

Cell culture and cellular uptake assay

HepG2 cells were purchased from the American Type Culture Collection (ATCC) (Manassas, VA, USA) and cultured in Dulbecco's Modified Eagle Medium (DMEM) supplemented with 10% fetal bovine serum (FBS) at 37°C and 5% CO_2.

A cellular uptake assay was performed with HepG2 cells. The water-insoluble fluorescent dye coumarin 6 (COU6) used in the cellular uptake assay was purchased from Sigma-Aldrich (St Louis, MO, USA). Briefly, cells were incubated with COU6 (10 mg/ml) alone, COU6 (10 mg/ml) in combination with nanoparticles (COU6-nano), or COU6 (10 mg/ml) combined with PTX/NCTD-APRPG-NPs. After incubation for 2 h and washing three times with PBS buffer, the cells were visualized under an inverted fluorescence microscope (Olympus, Tokyo, Japan) at 37°C. The cellular uptake mechanism was investigated with a blocking experiment using free APRPG (10 mg/ml) and a low temperature test was conducted at 4°C.

Cell proliferation assay

The 3-[4,5-dimethylthiazol-2-yl]-2,5 diphenyl tetrazolium bromide (MTT) assay was conducted to assess cell proliferation. In brief, HepG2 cells were seeded in 96-well plates at a density of 5×10^3 cells/well in 200 μl of DMEM supplemented with 10% FBS and incubated with 200 μl of MTT solution (1 mg/ml) for 4 h. After removing the supernatant, 150 μl of dimethyl sulfoxide (DMSO) was added to solubilize the MTT-formazan crystals. Following incubation for 15 min, the absorbance at 570 nm was read on a Microplate Reader (PerkinElmer, MA, USA).

Transwell assay

Transwell assays were performed using a Transwell kit (BD Bioscience, CA, USA). Briefly, HepG2 cells (8×10^4 cells) were

suspended in 300 µl of serum-free DMEM medium and placed in the upper chamber of the insert; complete medium was added into the lower chamber. After incubation for 36 h, the cells were fixed with methanol and stained with Giemsa; the cells on the top surface of the membrane were wiped off and the cells on the lower surface were analyzed under a microscope (Olympus DP72, Olympus, Tokyo, Japan). The average number of migrated cells was determined to measure the migration capacity.

Animals

Female BALB/c nude mice (4–6 weeks of age, 16–20 g) were purchased from Shanghai Slac Laboratory Animal Co. Ltd. (Shanghai, China) [animal certificate: SCXK (Shanghai) 2007-0005]. Experimental mice were housed in a specific-pathogen-free (SPF) animal facility at the Animal Experimental Center, Zhejiang University (Hangzhou, Zhejiang, China) and maintained under controlled conditions: room temperature (22°C), SPF conditions, and a 12/12-h light/dark cycle with free access to normal chow and water. The protocols involving the use of experimental animals were approved by the Laboratory Animal Care and the Department of Laboratory Animal Research of Zhejiang University.

Tumor model and tissue distribution assay

A total of 27 BALB/c nude mice were used to generate a tumor-bearing model for an *in vivo* tissue distribution assay. BALB/c nude mice were injected subcutaneously with 5×10^6 HepG2 cells to establish a tumor-bearing mouse model.

After 7 days of implantation, when the tumor volume reached approximately 500 mm^3, the mice were injected through the tail vein with PTX-NPs, PTX/NCTD-NPs, and PTX/NCTD-APRPG-NPs [in normal saline (NC)] at a dose of 10 mg/kg (PTX). The mice were euthanized at 0.5, 2, and 6 h post-injection (n = 9 for each time point). Heart, lung, spleen, stomach, kidney, and tumor were collected and washed with NC, followed by homogenization. The concentration of PTX and NCTD in the tissues was measured using HPLC coupled with electrospray ionization MS (LC-MS) (Supplementary Figures 1, 2). The conditions for HPLC were as follows: Agilent ZORBAX HPLC analytic column-C18 (3.0×100 mm, 1.7 µm particle diameter); column temperature, 40°C; mobile phase composition (mobile phase A, pure water; mobile phase B, acetonitrile solution); wavelength (210 nm, 227 nm) for HPLC UV detector; flow rate, 0.4 ml/min; and an injection volume of 10 µl (28, 29). The conditions for MS were as follows: mass spectrometer (Xevo G2-XS QTOF, Waters, USA); ion generation, electrospray ionization (ESI); quantification, multiple reaction monitoring (MRM) mode; scan mode, negative ion mode; capillary voltage, 2 kV; cone voltage, 40 V; scan time, 0.2 s; data acquisition mode, MSE.

In vivo imaging for assessment of tissue distribution

The distribution of PTX was visualized with a Bruker Small Animal Optical Imaging System (*In Vivo* Xtreme II, MA, USA). The PTX/NCTD-NPs and PTX/NCTD-APRPG-NPs were prepared with fluorescein isothiocyanate (FITC)-PTX (Sigma, New York, NY, USA) according to the manufacturer's instructions. BALB/c nude mice were injected subcutaneously with 5×10^6 HepG2 cells. After 7 days, when the tumor volume reached 500 mm^3, the mice were injected through the tail vein with FITC-PTX-NPs, FITC-PTX/NCTD-NPs (prepared with FITC-PTX), and PTX/NCTD-APRPG-NPs (prepared with FITC-PTX). The tissue distributions of PTX were visualized and imaged on the Bruker Small Animal Optical Imaging System (*In-Vivo* Xtreme II; MA, USA) at 2 h post-injection.

Examination of anti-tumor effects in mice

To examine the *in vivo* anti-tumor effects of the NPs, 27 BALB/c nude mice were injected subcutaneously with 5×10^6 HepG2 cells. After the tumor volume reached approximately 200 mm^3, the mice were injected through the tail vein with NC (as the control), PTX-NPs, PTX/NCTD-NPs, or PTX/NCTD-APRPG-NPs at a dosage of 6 mg/kg (PTX) on days 1, 4, 7, 10, 13, and 16. Tumor volume and body weights were measured on days 1, 4, 7, 10, 13, and 16. Upon completion of the experiments, the mice were euthanized and the tumors were collected and weighted. The inhibitory rate was calculated in each group.

Flow cytometry

Flow cytometry was performed to examine the effects of PTX-NPs, PTX/NCTD-NPs, and PTX/NCTD-APRPG-NPs on apoptosis and the cell cycle distribution in HepG2 cells. Apoptotic cells were determined using an FITC Annexin V Apoptosis Detection Kit I (BD Pharmingen, CA, USA) according to the manufacturer's instructions. Briefly, 5 µl of propidium iodide (PI) and 5 µl of Annexin V were added to HepG2 cells (1×10^6 cells) and cells were incubated at room temperature for 30 min. For cell cycle analysis, cellular DNA content was examined following cell staining with PI. The percentages of cell populations in different phases of the cell cycle (G0/G1, S, and G2/M) were assayed on the BD flow cytometer (BD Pharmingen, CA, USA) following the manufacturer's protocol.

Western blot analysis

Total proteins were isolated from treated HeG2 cells using radioimmunoprecipitation assay (RIPA) Lysis Buffer (Beyotime, Shanghai, China) and protein concentrations were quantified with a BCA kit (Beyotime). Protein samples were separated by 12% sodium dodecyl sulfate polyacrylamide gel electrophoresis (SDS-PAGE) and transferred to polyvinylidene difluoride (PVDF) membranes. After blocking with 5% bovine serum albumin (BSA), the membrane was incubated with primary antibodies against phosphorylated protein kinase B (p-AKT; 1:1,000, CST, Boston, MA, USA), AKT (1:1,000, CST), phosphorylated extracellular signal-regulated protein kinase (p-ERK1/2; 1:1,000, CST), ERK1/2 (1:1,000, CST), phosphorylated mitogen-activated protein kinase kinase (p-MEK; 1:1,000, CST), MEK (1:1,000, CST), caspase-3 (1:1,000, CST), cleaved caspase-3 (1:1,000, CST), B-cell lymphoma 2 (Bcl-2; 1:1,000, CST), and glyceraldehyde 3-phosphate dehydrogenase (GAPDH; 1:1,000, CST) at 4°C overnight. The membranes were then incubated with secondary antibody at room temperature for 1.5 h. Protein bands were visualized using ECL solution (Beyotime, Shanghai, China) on the Tanon 5200-multi (Tanon, Shanghai, China). Quantification was performed using ImageJ software to determine the relative expression level of the target proteins.

Statistical analysis

Data are expressed as the means ± standard deviation (SD) of at least three independent experiments. The unpaired Student's *t*-test was used to compare quantitative data between two study groups when the groups were not matched. One-way analysis of variance (ANOVA) followed by Tukey's test for *post-hoc* analysis was used to determine statistical differences between the mean values for multiple groups. *p*-values lower than 0.05 were considered to be statistically significant.

Results

Preparation and characterization of PTX-NPs, PTX/NCTD-NPs, and PTX/NCTD-APRPG-NPs

We prepared PTX-loaded PLGA nanoparticles (PTX-NPs), PTX/NCTD-loaded core–shell-type nanoparticles (PTX/NCTD-NPs), and PTX/NCTD-loaded core–shell-type nanoparticles modified with APRPG (PTX/NCTD-APRPG-NPs). The structure and composition of PTX-NPs, PTX/NCTD-NPs, and PTX/NCTD-APRPG-NPs are schematically illustrated in Figures 1A–C. Their morphological and release characteristics are shown in Figures 1D, E. The PTX-NPs were morphologically spherical and uniform in shape and size (~100 nm). Similarly, the PTX/NCTD-APRPG-NPs presented a spherical shape and size of around 100 nm (Figures 1F, G). We evaluated the *in vitro* release characteristics of the PTX/NCTD-APRPG-NPs, and the findings are presented in Figure 1H. Notably, up to 85% of PTX/NCTD was released into the cell culture medium within 18–20 h in a sustained manner.

PTX/NCTD-APRPG-NPs enhanced the inhibitory effects of PTX on the proliferation and migration of hepatoma cells

Before determining the anti-tumor effects of the PTX/NCTD-APRPG-NPs, we first examined the uptake of APRPG-modified nanoparticles in HepG2 cells. As shown in Figure 2A and Supplementary Figure 3, using an incubation temperature of 4°C as the negative control, the fluorescence intensity at 37°C in the APRPG-COU6-nano group was significantly higher than that in the COU6 only and COU6-nano groups ($p < 0.05$). Moreover, when cells were incubated with APRPG (10 mg/ml) before the COU6 formulations, the intracellular fluorescence intensity of APRPG-COU6-nano was substantially reduced, whereas the fluorescence intensity in the COU6 and COU6-nano groups remained unchanged (Figure 1D and Supplementary Figure 3). The difference may be attributed to the specific binding of APRPG in HepG2 cells. Free APRPG peptide competitively combined with the ligands instead of APRPG-COU6-nano.

We further investigated the effects of PTX/NCTD-APRPG-NPs on the proliferation of human hepatocytes (L0 cells) and hepatoma cells (HepG2, Huh-7, and Hep3B cells). As shown in Figure 2B, PTX/NCTD-APRPG-NPs exhibited significantly greater inhibitory effects than PTX/NCTD-NPs, with half-maximal inhibitory concentration (IC_{50}) values of 4.173 ng/ml versus 7.976 ng/ml against HepG2 cells, 4.973 ng/ml versus 9.264 ng/ml against Huh-7 cells, and 6.933 ng/ml versus 13.06 ng/ml against Hep3B cells (all $p < 0.05$). In addition, analysis of hepatoma cell migration capabilities showed that the number of migrated cells was significantly suppressed in the PTX-NP, PTX-NCTD-NP, and PTX/NCTD-APRPG-NP groups compared with the number in the control groups (Figure 2C). The PTX/NCTD-APRPG-NP group had the lowest number of migrated cells ($p < 0.05$ vs. control, $p < 0.05$ vs. PTX-NPs, $p < 0.01$ vs. PTX/NCTD-NPs). These data indicated that the PTX/NCTD-APRPG-NPs enhanced the inhibitory effects of the drugs on the proliferation and migration of hepatoma cells compared with the PTX-NPs and PTX/NCTD-NPs.

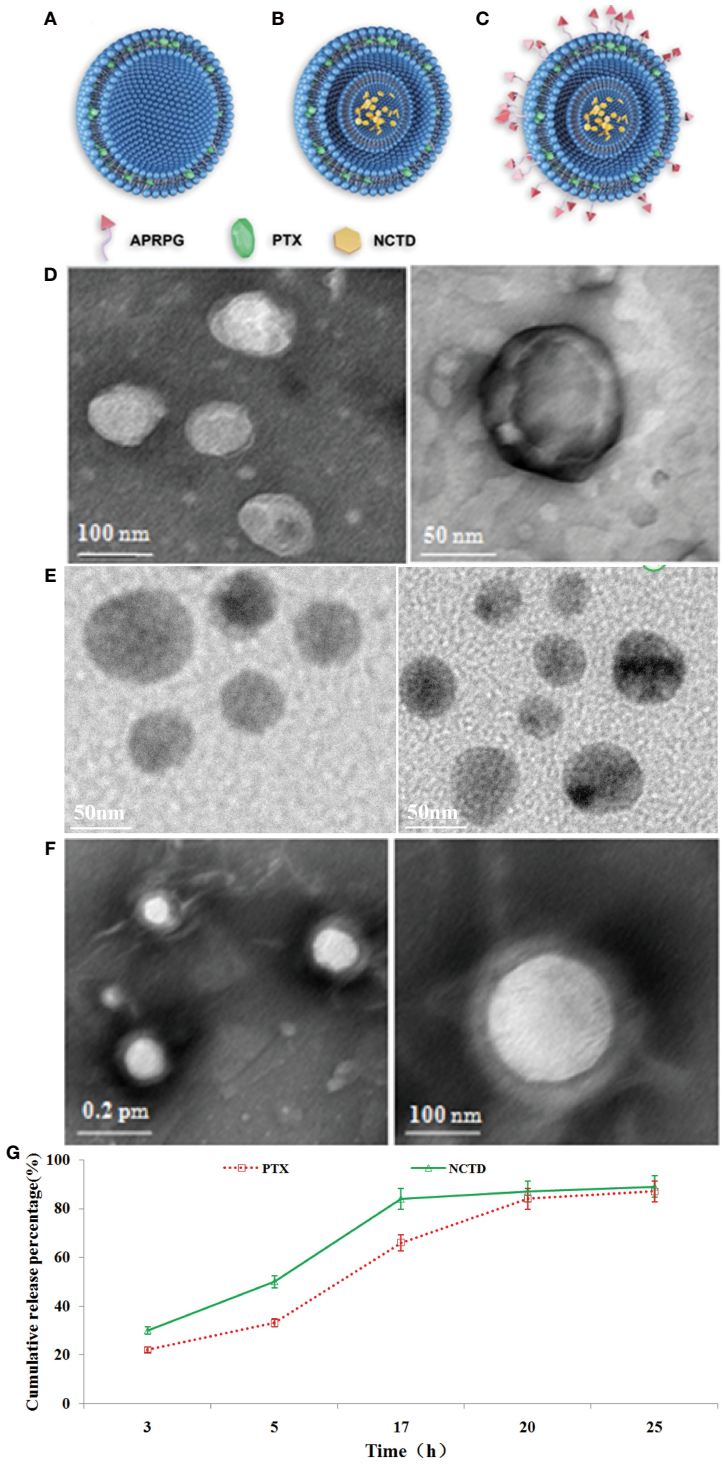

FIGURE 1
The structural, morphological, and release characteristics of PTX-NPs and PTX/NCTD-APRPG-NPs. Schematic illustration of the structure and composition of nanoparticles used in this study, including **(A)** PTX-loaded PLGA nanoparticles (PTX-NPs); **(B)** PTX/NCTD-loaded core–shell-type nanoparticles (PTX/NCTD-NPs); and **(C)** PTX/NCTD-loaded core–shell lipid nanoparticles modified with APRPG (PTX/NCTD-APRPG-NPs). The morphological characteristics of PTX-NPs and PTX/NCTD-APRPG-NPs, including the shape and size, were examined with transmission electron microscopy (TEM) and the Zetasizer instrument, respectively. **(D)** The shape of the PTX-NPs; **(E)** The shape of the PTX/NCTD-NPs; **(F)** The shape of the PTX/NCTD-APRPG-NPs; **(G)** *in vitro* release characteristic of PTX/NCTD-APRPG-NPs. PTX, paclitaxel; PLGA, poly(lactic-co-glycolic acid); NPs, nanoparticles; NCTD, norcantharidin; APRPG, tumor neovasculature-targeted peptide (Ala-Pro-Arg-Pro-Gly).

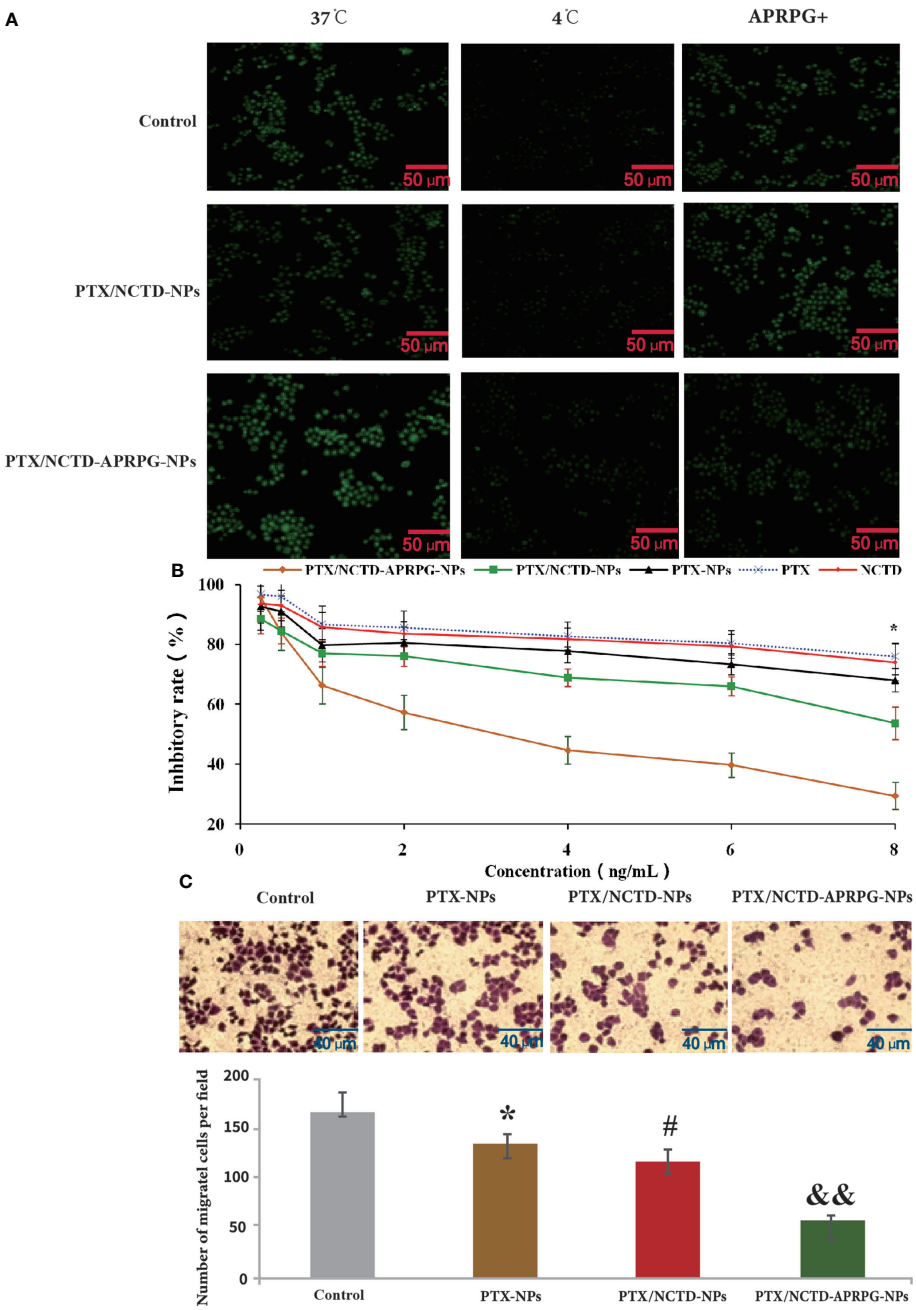

FIGURE 2
In vitro uptake and anti-tumor effects of PTX-NPs, PTX/NCTD-NPs, and PTX/NCTD-APRPG-NPs. HepG2 cells were treated with PTX-NPs, PTX/NCTD-NPs, or PTX/NCTD-APRPG-NPs, and the proliferation and migration abilities were assayed using MTT and Transwell assays, respectively. A fluorescence assay was performed to examine the uptake of PTX. **(A)** Fluorescence microscopic images showing nanoparticle uptake in HepG2 cells. HepG2 cells were incubated with COU6 (10 mg/ml) alone, COU6 (10 mg/ml) in combination with nanoparticles (COU6-nano), or COU6-nano modified with APRPG (APRPG-COU6-nano). After incubation for 2 h and washing three times with PBS buffer, cells were visualized under a fluorescence microscope. **(B)** Comparison of the effects of PTX/NCTD-NPs and PTX/NCTD-APRPG-NPs on the proliferation of HepG2 cells. HepG2 cells were treated with PTX/NCTD-APRPG-NPs, PTX/NCTD-NPs, PTX-NPs, PTX, or NCTD, and proliferation was assayed using MTT; *$p < 0.001$. **(C)** Effects of PTX-NPs, PTX/NCTD-NPs, and PTX/NCTD-APRPG-NPs on the migration ability of HepG2 cells. HepG2 cells were treated with PTX-NPs, PTX/NCTD-NPs, or PTX/NCTD-APRPG-NPs, and migration ability was examined using Transwell assays. *$p < 0.05$ vs. control; #$p < 0.05$ vs. PTX; &&$p < 0.01$ vs. nanoparticles.

PTX/NCTD-APRPG-NPs exerted significant anti-tumor effects in mice

Based on the *in vitro* studies, we further investigated the anti-tumor effects of PTX/NCTD-APRPG-NPs in tumor-bearing nude mice. The tissue distribution and anti-tumor effects of PTX-NPs, PTX/NCTD-NPs, and PTX/NCTD-APRPG-NPs are illustrated in Figure 3. At the three examined time points, the concentration of PTX in the tumor tissues was in the following order: PTX/NCTD-APRPG-NPs > PTX/NCTD-NPs > PTX-NPs, indicating that the PTX/NCTD-APRPG-NPs had a better targeting effect than the PTX/NCTD-NPs and PTX-NPs. The tissue distribution of the injected PTX/NCTD-APRPG-NPs and PTX/NCTD-NPs was further confirmed by *in vivo* imaging. As shown in Figure 3D, higher fluorescence intensity was observed in the tumor tissues and lower fluorescence intensity was detected in the liver tissues of PTX/NCTD-APRPG-NP-treated animals compared with the PTX/NCTD-NP group, indicating that PTX/NCTD-APRPG-NPs had potential lower toxicity and higher tumor-targeting characteristics.

The anti-tumor effects and toxicity are shown in Figure 4 and Supplementary Figure 4. The tumor volume was suppressed to the greatest extent by PTX/NCTD-APRPG-NPs, followed by PTX/NCTD-NPs and PTX-NPs ($p < 0.05$ vs. control, $p < 0.01$ vs. control, $p < 0.05$ vs. PTX-NPs, $p < 0.01$ vs. PTX-NPs, $p < 0.05$ vs. PTX/NCTD-NPs, $p < 0.01$ vs. PTX/NCTD-NPs) (Figure 4A). As shown in Figure 4B, the body weights were slightly lower in the PTX/NCTD-APRPG-NP group, followed by the PTX/NCTD-NP and PTX-NP groups ($p < 0.05$ vs. control, $p < 0.01$ vs. control). The tumor weight was significantly lower in the PTX-NP group compared with controls and was dramatically further inhibited in the PTX/NCTD-NP group (Figure 4C). A pronounced decrease in the tumor weight was observed in the PTX/NCTD-APRPG-NP group compared with the PTX/NCTD-NP group ($p < 0.01$ vs. control, $p < 0.01$ vs. PTX-NPs, $p < 0.01$ vs. PTX/NCTD-NPs). As shown in Figures 4D, E, the PTX/NCTD-APRPG-NPs exhibited the greatest anti-tumor effects, with the smallest tumor size in the PTX/NCTD-APRPG-NP group (Figure 4D) and highest inhibitory rate of 78.67%. The inhibitory rate was 62.98% in the PTX/NCTD-NP group and 35.01% in the PTX-NP group ($p < 0.01$ vs. PTX-NPs, $p < 0.01$ vs. PTX/NCTD-NPs). Histological examinations of tumor tissues further revealed the greatest anti-tumor effect of PTX/NCTD-APRPG-NPs compared with the other treatments (Supplementary Figure 4).

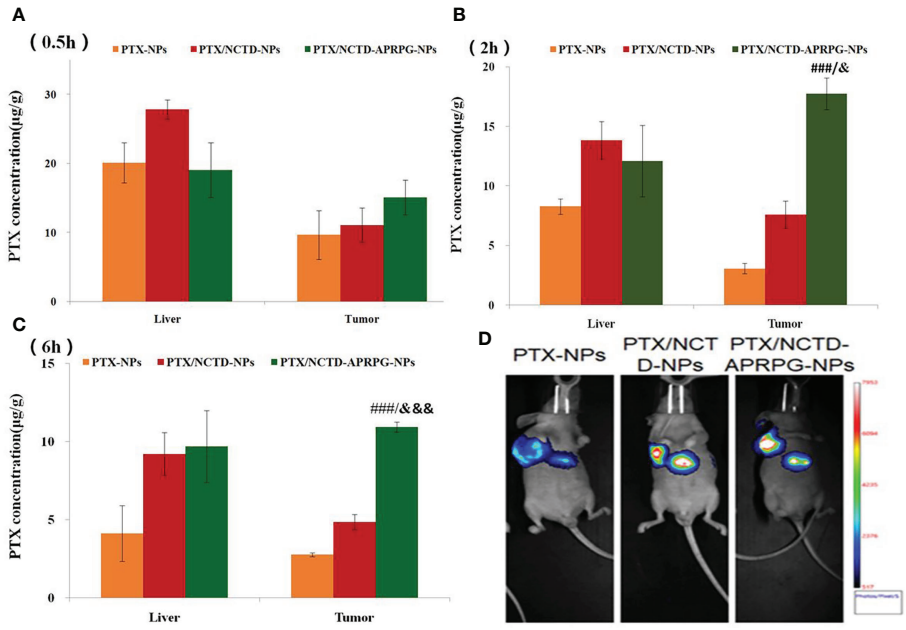

FIGURE 3
In vivo distribution of PTX in tumor-bearing mice treated with PTX-NPs, PTX/NCTD-NPs, and PTX/NCTD-APRPG-NPs. The experimental mice were randomly divided into three groups (PTX-NP, PTX/NCTD-NP, and PTX/NCTD-APRPG-NP groups) and injected with PTX-NPs, PTX/NCTD-NPs, or PTX/NCTD-APRPG-NPs at the dosage of 10 mg/kg. The tissue distribution of PTX was detected at 0.5, 2, and 6 h following injection. Bar graphs show PTX concentrations in various organs (heart, liver, spleen, lung, kidney, and stomach) and tumor tissues at **(A)** 0.5 h, **(B)** 2 h, and **(C)** 6 h after injection; ###$p < 0.001$ vs. PTX-NPs; &$p < 0.05$, &&&$p < 0.001$ vs. PTX/NCTD-NPs. **(D)** *In vivo* imaging assay to visualize the distribution of PTX in tumor-bearing mice treated with PTX-NPs, PTX/NCTD-NPs, and PTX/NCTD-APRPG-NPs. At 2 h after injection, the tissue distributions of PTX in the three experimental groups were imaged on the Bruker Small Animal Optical Imaging System.

10.3389/fonc.2022.932156

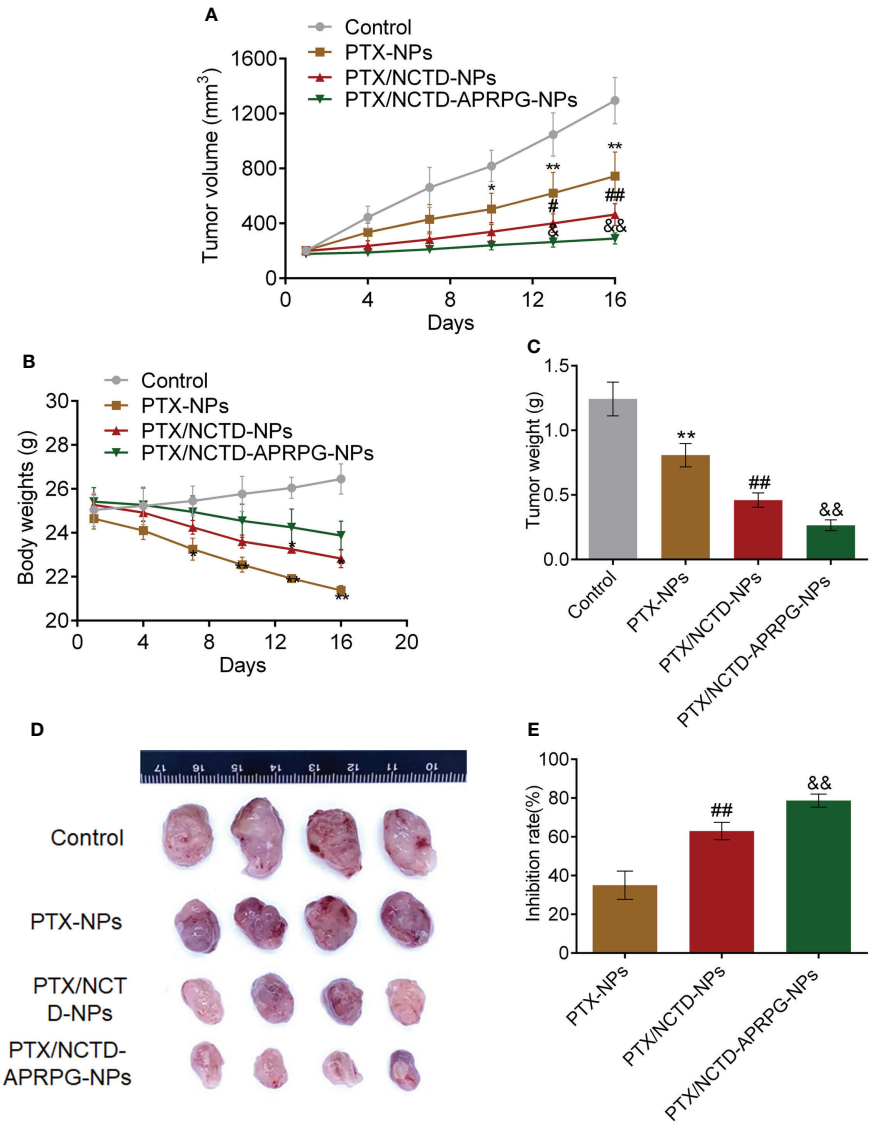

FIGURE 4
In vivo anti-tumor effects of PTX-NPs, PTX/NCTD-NPs, and PTX/NCTD-APRPG-NPs in the HepG2 xenograft mouse model. **(A)** Effects of PTX-NPs, PTX/NCTD-NPs, and PTX/NCTD-APRPG-NPs on the tumor volume at different time points (days 1, 4, 7, 10, 13, and 16 after the first administration); **(B)** effects of PTX-NPs, PTX/NCTD-NPs, and PTX/NCTD-APRPG-NPs on the body weights at different time points (days 1, 4, 7, 10, 13, and 16 after the first administration); **(C)** effects of PTX-NPs, PTX/NCTD-NPs, and PTX/NCTD-APRPG-NPs on the tumor weight on day 16 after the first administration; **(D)** effects of PTX-NPs, PTX/NCTD-NPs, and PTX/NCTD-APRPG-NPs on the tumor size; and **(E)** effects of PTX-NPs, PTX/NCTD-NPs, and PTX/NCTD-APRPG-NPs on tumor growth in the HepG2 xenograft animal model. *$p < 0.05$ vs. control, **$p < 0.01$ vs. control, #$p < 0.05$ vs. PTX-NPs, ##$p < 0.01$ vs. PTX-NPs, &$p < 0.05$ vs. PTX/NCTD-NPs, &&$p < 0.01$ vs. PTX/NCTD-NPs.

PTX/NCTD-APRPG-NPs induced apoptosis through the AKT and ERK pathways

To investigate whether the PTX/NCTD-APRPG-NPs exerted the anti-tumor effects through targeting apoptosis, we compared apoptotic rates between groups and examined key molecules related to apoptosis in HepG2 cells. As shown in Figure 5, the apoptotic rate was 24.13% in the PTX/NCTD/APRPG-NP group, which was significantly higher than 14.74% in the PTX/NCTD-NP group, 11.13% in the PTX-NP group, and 8.08% in the control group ($p < 0.05$ vs. control, $p < 0.05$ vs. PTX-NPs, and $p < 0.01$ vs. PTX/NCTD-NPs). In addition, the proportion of cells arrested at the G0/G1 phase was 70.28% in the PTX-NP group, which was significantly greater than 50.5% in the control group ($p < 0.05$ vs. control). Notably, the proportion of cells arrested at the G0/G1 phase in the PTX/NCTD-APRPG-NP group was 83.69%, which was significantly

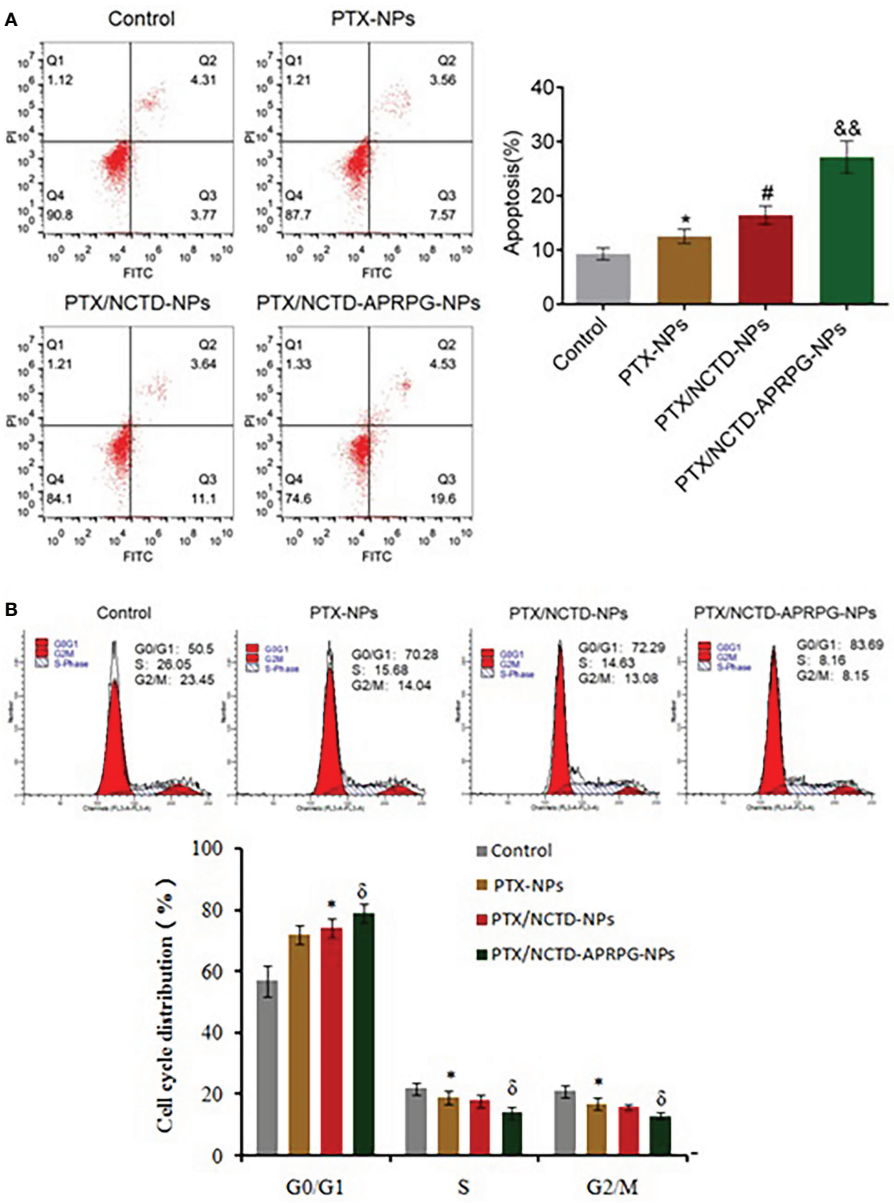

FIGURE 5
Apoptosis and cell cycle arrest were induced by PTX/NCTD-APRPG-NPs. Flow cytometry was conducted to determine the number of apoptotic cells and cell cycle distribution in HepG2 cells treated with PTX-NPs, PTX/NCTD-NPs, and PTX/NCTD-APRPG-NPs. **(A)** Effects of PTX-NPs, PTX/NCTD-NPs, and PTX/NCTD-APRPG-NPs on apoptotic rates in HepG2 cells; **(B)** effects of PTX-NPs, PTX/NCTD-NPs, and PTX/NCTD-APRPG-NPs on the cell cycle distribution in HepG2 cells. *$p < 0.05$ vs. control, #$p < 0.05$ vs. PTX-NPs, &$p < 0.05$ vs. PTX/NCTD-NPs, &&$p < 0.01$ vs. PTX/NCTD-NPs.

greater than 72.29% in the PTX/NCTD-NP group ($p < 0.05$ vs. PTX/NCTD-NPs). These data indicated that apoptosis and cell cycle arrest at the G0/G1 phase were induced to a significantly greater extent by the PTX/NCTD-APRPG-NPs than by the PTX/NCTD-NPs or PTX-NPs.

We further performed Western blot analysis to determine whether the AKT and ERK signaling pathways were involved in the PTX/NCTD-APRPG-NP-induced apoptosis. As shown in Figure 6, p-AKT, p-MEK, p-ERK1/2, and Bcl-2 protein expression was significantly suppressed by the introduction of PTX-NPs compared with the control group and was further inhibited by treatment with the PTX/NCTD-NPs. p-AKT, p-MEK, p-ERK1/2, and Bcl-2 protein expressions were markedly decreased by treatment with PTX/NCTD-APRPG-NPs ($p < 0.05$ vs. control, $p < 0.01$ vs. control, $p < 0.05$ vs. PTX-NPs, $p < 0.01$ vs. PTX-NPs, $p < 0.05$ vs. PTX/NCTD-NPs, and $p < 0.01$ vs. PTX/

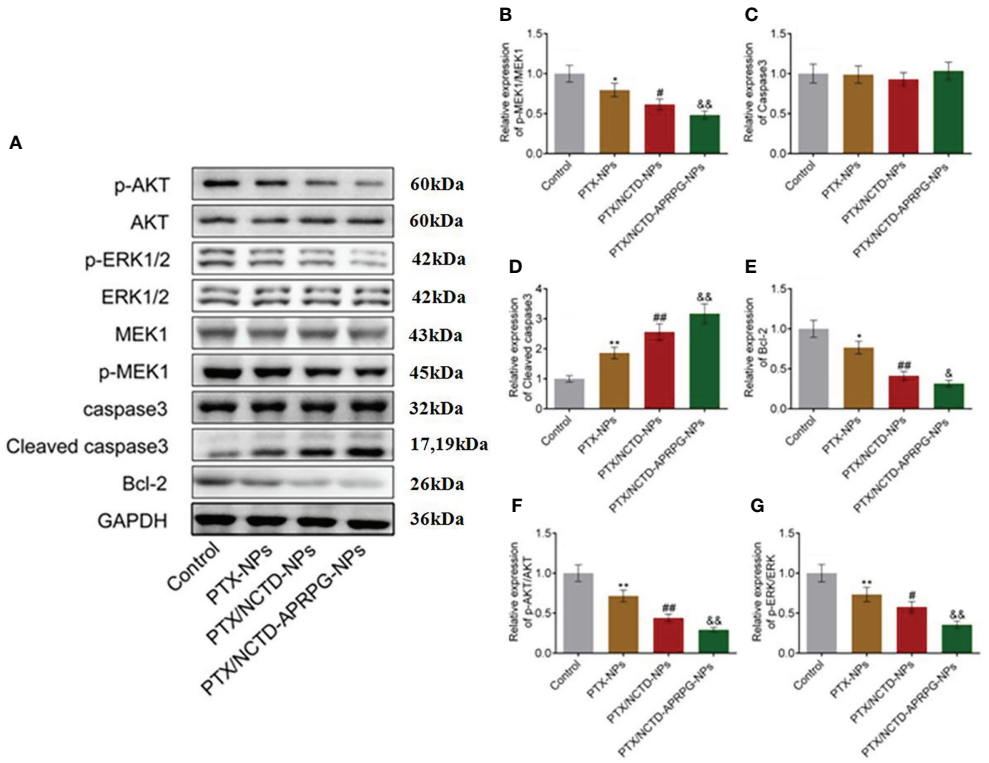

FIGURE 6
Effects of PTX-NPs, PTX/NCTD-NPs, and PTX/NCTD-APRPG-NPs on the AKT and ERK signal pathways in HepG2 cells. Western blot analysis was performed on AKT and ERK pathway protein expression in HepG2 cells treated with PTX-NPs, PTX/NCTD-NPs, and PTX/NCTD-APRPG-NPs. **(A)** Western blot images; **(B)** quantitative analysis of relative expression of p-MEK1/MEK1; **(C)** relative expression of caspase-3; **(D)** relative expression of cleaved caspase-3; **(E)** relative expression of Bcl-2; **(F)** relative expression of pAKT/AKT; and **(G)** relative expression of p-ERK/ERK. *$p < 0.05$ vs. control, **$p < 0.01$ vs. control, #$p < 0.05$ vs. PTX-NPs, ##$p < 0.01$ vs. PTX-NPs, &$p < 0.05$ vs. PTX/NCTD-NPs, &&$p < 0.01$ vs. PTX/NCTD-NPs.

NCTD-NPs). In addition, PTX-NP-induced cleaved caspase-3 protein expression was significantly promoted by treatment with PTX/NCTD-NPs and further enhanced by PTX/NCTD-APRPG-NPs ($p < 0.01$ vs. control, $p < 0.01$ vs. PTX-NPs, $p < 0.01$ vs. PTX/NCTD-NPs). These findings, together with those of others, suggested that the AKT and ERK signal pathways were involved in apoptosis induced by PTX/NCTD-APRPG-NPs (30–32).

Discussion

In this study, we developed new core–shell-type nanoparticles loaded with chemically distinct drugs PTX/NCTD and modified with APRPG and assessed the anti-tumor effects in hepatoma cells (HepG2, Huh-7, and Hep3B) and tumor-bearing nude mice. The novel findings of our study are summarized as follows (1): PTX/NCTD-APRPG-NPs with a core–shell structure were prepared successfully and achieved up to 90% release of PTX in a sustained manner; (2) PTX/NCTD-APRPG-NPs led to significantly greater anti-tumor effects in comparison with PTX-NPs and PTX/NCTD-NPs in both *in vitro* and *in vivo* studies; and (3) mechanistic studies revealed that PTX/NCTD-APRPG-NPs markedly induced apoptosis through the AKT and ERK signal pathways, and the effects of these nanoparticles were the greatest among the groups evaluated. These findings demonstrated that the PTX/NCTD-APRPG-NPs enhanced the effectiveness of anti-HCC drugs.

Core–shell lipid nanoparticles are a novel group of lipid/polymer particle assemblies composed of lipid shells and nanoparticle cores that possess the physical characteristics of both lipid vesicles and nanoparticles (33, 34). Recently, core–shell lipid nanoparticles have been applied in multiple biomedical fields, such as drug delivery and genetic transmission (35). Based on differences in the materials, especially those used in the core, core–shell lipid nanoparticles can be classified into four groups, of which silica (36), nanogel (37), polysaccharide (38), and polymer nanoparticles were used as the nanoparticle core (39). In the present study, PLGA was used as the nanoparticle core to load PTX. PLGA is derived from

the polymerization between lactic acid and glycolic acid [poly(D, L-lactic-co-glycolic acid)]. PLGA has various advantages, including beneficial characteristics such as biocompatibility and degradation, which make PLGA the most widely used polymer in the design of nanoparticles (40). In the present study, the concentration of emulsifier, PLGA, PTX, and phospholipid; the shear velocity; and the ratio of phospholipid versus cholesterol were screened to obtain a minimal particle size and uniform film formation. According to the previous findings (41), we observed uniform spherical morphology, 100-nm particle size, and sustained release with the core–shell lipid nanoparticles prepared in this study.

Combination drug therapy using two or more drugs is an important application for core–shell lipid nanoparticles. Sengupta first reported the application of core–shell lipid nanoparticles in anti-tumor combination drug therapy (42). With combretastatin wrapped in the phospholipid shell and adriamycin wrapped in the nanoparticles, core–shell lipid nanoparticles were prepared with both promising anti-angiogenesis and cytotoxic properties, leading to more significant effects than the mixture of combretastatin and adriamycin. Wong (43) reported that core–shell lipid nanoparticles loaded with both the inhibitor of P-gp protein and adriamycin showed significant inhibitory effects on adriamycin-resistant breast cancer cell lines. In the present study, we prepared core–shell lipid nanoparticles loaded with PTX in the core and NCTD in the shell and compared the anti-tumor effects with those of PTX-NPs and PTX/NCTD-NPs. Notably, PTX/NCTD-APRPG-NPs showed more significant inhibitory effects on the proliferation and migration of hepatoma cells, as well as higher inhibitory rates on tumor growth in the HepG2 xenograft animal model in mice. These results demonstrate that the anti-tumor property of PTX was markedly enhanced by the combination of PTX and NCTD using core–shell lipid nanoparticles.

Notably, our results showed that PTX/NCTD-APRPG-NPs exhibited the greatest anti-tumor activity among the tested nanoparticles. APRPG is a short peptide that targets neovascularization and specifically targets the vascular endothelial growth factor receptor 1 (VEGFR-1), which is highly expressed in neovascularization tissues (44). Recent studies have reported the application of nanoliposomes modified with APRPG for targeting angiogenesis (45, 46). In the present study, APRPG was used to modify the core–shell lipid nanoparticles to enhance the tumor-targeting property. Compared with PTX/NCTD-NPs without APRPG, PTX/NCTD-APRPG-NPs showed more significant inhibitory effects on the proliferation and migration of hepatoma cells, as well as greater inhibitory effects on tumor growth in the HepG2 xenograft animal model in mice. These *in vitro* and *in vivo* findings indicated that the anti-tumor property of PTX/NCTD-NPs was dramatically elevated by the addition of APRPG in PTX/NCTD-APRPG-NPs. In addition, *in vitro* uptake assays and *in vivo* imaging revealed that the tumor targeting property of PTX/NCTD-NPs was significantly promoted by the modification with APRPG.

Previous reports have shown that PTX alone induces cell growth arrest at the G2/M phase (1–3). In the present study, we found that PTX-NPs, PTX/NCTD-NPs, and PTX/NCTD-APRPG-NPs markedly induced cell cycle arrest at the G0/G1 phase, which was different from the induction of cell cycle arrest at the G2/M phase by PTX alone. In addition, cell cycle arrest at the G0/G1 phase was significantly induced to a greater extent by the PTX/NCTD-APRPG-NPs than by the PTX/NCTD-NPs or PTX-NPs. Further mechanistic studies confirmed that the AKT and ERK signal pathways were involved in the PTX/NCTD-APRPG-NP-induced cell cycle arrest at the G0/G1 phase. This may be related to MEPK pathway, in which MEK and ERK pathways are all important branch pathways. Previous studies have found that MEK inhibitor can truly induce G1 cell cycle arrest in tumor cells. The ERK pathway is constitutively activated, which indicated that the ERK pathway might be a potential therapeutic target (47, 48). Moreover, there is an interesting observation that cell cycle arrest was induced at the G2/M phase by PTX alone and at the G0/G1 phase by PTX/NPs as well. Further in-depth mechanistic studies are needed to gain insight into the mechanism of action. In addition, further investigations, including *in vitro* angiogenesis assays (e.g., chick embryo chorioallantoic membrane assay, tube formation assay), are necessary to confirm the enhanced neovascularization targeting property of PTX/NCTD-APRPG-NPs and are underway in our laboratory.

Taken together, our study has demonstrated that APRPG-modified PTX/NCTD-loaded core–shell lipid nanoparticles markedly improved the anti-tumor effectiveness of anti-HCC drugs. Therefore, the newly developed PTX/NCTD-APRPG-NPs hold promise as a potent nanoparticle delivery system in the treatment of HCC.

Data availability statement

The raw data supporting the conclusions of this article will be made available by the authors, without undue reservation.

Ethics statement

The animal study was reviewed and approved by the Animal Laboratory Committee of Zhejiang University (Hangzhou, Zhejiang, China).

Author contributions

M-HX: Experimental design, literature inquiry, prescription design and optimization, animal experiment, and data processing. Z-LF and A-LH: Literature inquiry and preparation of the drug delivery system. QC and J-BL: Animal experiment. J-FZ, SY, and LZ: Cell experiment. X-JC and MG: Preparation of the drug delivery system. JW: Experimental guidance. All authors contributed to manuscript revision, read, and approved the submitted version.

Funding

This work was financially supported by the Science and Technology Project of Hangzhou City (Agriculture and Social Development, No. 2016007), the Science and Technology Project of Yuhang District, Hangzhou City (No. 2017002), the Project of Hangzhou City (Agriculture and Social Development, No. 20201231Y131), the Science and Technology Project of Yuhang District, Hangzhou City (2014003), the Science and Technology Project of Hangzhou City (Social Development) (20140633B57), and the Health Science and Technology Project of Hangzhou City (2015B32).

Conflict of interest

The authors declare that the research was conducted in the absence of any commercial or financial relationships that could be construed as a potential conflict of interest.

Publisher's note

All claims expressed in this article are solely those of the authors and do not necessarily represent those of their affiliated organizations, or those of the publisher, the editors and the reviewers. Any product that may be evaluated in this article, or claim that may be made by its manufacturer, is not guaranteed or endorsed by the publisher.

Supplementary material

The Supplementary Material for this article can be found online at: https://www.frontiersin.org/articles/10.3389/fonc.2022.932156/full#supplementary-material

References

1. Torre LA, Bray F, Siegel RL, Ferlay J, Lortet-Tieulent J, Jemal A. Global cancer statistics, 2012. *CA Cancer J Clin* (2015) 65(2):87–108. doi: 10.3322/caac.21262

2. Chen W, Zheng R, Baade PD, Zhang S, Zeng H, Bray F, et al. Cancer statistics in China, 2015. *CA Cancer J Clin* (2016) 66(2):115–32. doi: 10.3322/caac.21338

3. Balogh J, Victor D3rd, Asham EH, Burroughs SG, Boktour M, Saharia A, et al. Hepatocellular carcinoma: a review. *J Hepatocell Carcinoma* (2016) 3:41–53. doi: 10.2147/jhc.s61146

4. Srivastava V, Negi AS, Kumar JK, Gupta MM, Khanuja SP. Plant-based anticancer molecules: a chemical and biological profile of some important leads. *Bioorg Med Chem* (2005) 13(21):5892–908. doi: 10.1016/j.bmc.2005.05.066

5. Rowinsky EK, Cazenave LA, Donehower RC. Taxol: a novel investigational antimicrotubule agent. *J Natl Cancer Inst* (1990) 82(15):1247–59. doi: 10.1093/jnci/82.15.1247

6. Elomaa L, Joensuu H, Kulmala J, Klemi P, Grenman R. Squamous cell carcinoma is highly sensitive to taxol, a possible new radiation sensitizer. *Acta Otolaryngol* (1995) 115(2):340–4. doi: 10.3109/00016489509139325

7. Huang S, Zhang Y, Wang L, Liu W, Xiao L, Lin Q, et al. Improved melanoma suppression with target-delivered TRAIL and paclitaxel by a multifunctional nanocarrier. *J Control Release* (2020) 325:10–24. doi: 10.1016/j.jconrel.2020.03.049

8. Wall ME, Wani MC. Camptothecin and taxol: from discovery to clinic. *J Ethnopharmacol* (1996) 51(1-3):239–53. doi: 10.1016/0378-8741(95)01367-9

9. Szebeni J, Muggia FM, Alving CR. Complement activation by cremophor EL as a possible contributor to hypersensitivity to paclitaxel: an *in vitro* study. *J Natl Cancer Inst* (1998) 90(4):300–6. doi: 10.1093/jnci/90.4.300

10. Crosasso P, Ceruti M, Brusa P, Arpicco S, Dosio F, Cattel L. Preparation, characterization and properties of sterically stabilized paclitaxel-containing liposomes. *J Control Release* (2000) 63(1-2):19–30. doi: 10.1016/s0168-3659(99)00166-2

11. Patil YP, Jadhav S. Novel methods for liposome preparation. *Chem Phys Lipids* (2014) 177:8–18. doi: 10.1016/j.chemphyslip.2013.10.011

12. Sy PM, Anton N, Idoux-Gillet Y, Dieng SM, Messaddeq N, Ennahar S, et al. Pickering Nano-emulsion as a nanocarrier for pH-triggered drug release. *Int J Pharm* (2018) 549(1-2):299–305. doi: 10.1016/j.ijpharm.2018.07.066

13. Rajpoot K. Solid lipid nanoparticles: A promising nanomaterial in drug delivery. *Curr Pharm Des* (2019) 25(37):3943–59. doi: 10.2174/1381612825666190903155321

14. Chen M, Zhou X, Chen R, Wang J, Ye RD, Wang Y, et al. Nano-carriers for delivery and targeting of active ingredients of Chinese medicine for hepatocellular carcinoma therapy. *Materials Today* (2019) 25:66–87. doi: 10.1016/j.mattod.2018.10.040

15. Kong FH, Ye QF, Miao XY, Liu X, Huang SQ, Xiong L, et al. Current status of sorafenib nanoparticle delivery systems in the treatment of hepatocellular carcinoma. *Theranostics* (2021) 11(11):5464–90. doi: 10.7150/thno.54822

16. Shieh MJ, Hsu CY, Huang LY, Chen HY, Huang FH, Lai PS. Reversal of doxorubicin-resistance by multifunctional nanoparticles in MCF-7/ADR cells. *J Control Release* (2011) 152(3):418–25. doi: 10.1016/j.jconrel.2011.03.017

17. Jun YJ, Park MK, Jadhav VB, Song JH, Chae SW, Lee HJ, et al. Tripodal amphiphiles tunable for self-assembly to polymersomes. *J Control Release* (2010) 142(1):132–7. doi: 10.1016/j.jconrel.2009.10.004

18. Chen G, Wang Y, Xie R, Gong S. A review on core-shell structured unimolecular nanoparticles for biomedical applications. *Advanced Drug delivery Rev* (2018) 130:58–72. doi: 10.1016/j.addr.2018.07.008

19. Sharma N, Bietar K, Stochaj U. Targeting nanoparticles to malignant tumors. *Biochim Biophys Acta Rev Cancer* (2022) 1877(3):188703. doi: 10.1016/j.bbcan.2022.188703

20. Kopecka J, Campia I, Olivero P, Pescarmona G, Ghigo D, Bosia A, et al. A LDL-masked liposomal-doxorubicin reverses drug resistance in human cancer cells. *J Control Release* (2011) 149(2):196–205. doi: 10.1016/j.jconrel.2010.10.003

21. Galindo-Rodriguez SA, Allemann E, Fessi H, Doelker E. Polymeric nanoparticles for oral delivery of drugs and vaccines: a critical evaluation of *in vivo* studies. *Crit Rev Ther Drug Carrier Syst* (2005) 22(5):419–64. doi: 10.1615/critrevtherdrugcarriersyst.v22.i5.10

22. Zhang Z, Yang L, Hou J, Xia X, Wang J, Ning Q, et al. Promising positive liver targeting delivery system based on arabinogalactan-anchored polymeric micelles of norcantharidin. *Artif Cells Nanomed Biotechnol* (2018) 46(sup3): S630–S40. doi: 10.1080/21691401.2018.1505742

23. Ye K, Wei Q, Gong Z, Huang Y, Liu H, Li Y, et al. Effect of norcantharidin on the proliferation, apoptosis, and cell cycle of human mesangial cells. *Ren Fail* (2017) 39(1):458–64. doi: 10.1080/0886022X.2017.1308257

24. Cai XJ, Fei WD, Xu YY, Xu H, Yang GY, Cao JW, et al. Liposome-encapsulated zoledronate favors tumor vascular normalization and enhances anticancer efficacy of cisplatin. *AAPS PharmSciTech* (2020) 21(2):57. doi: 10.1208/s12249-019-1614-6

25. Lai K, Li Y, Gong Y, Li L, Huang C, Xu F, et al. Triptolide-nanoliposome-APRPG, a novel sustained-release drug delivery system targeting vascular endothelial cells, enhances the inhibitory effects of triptolide on laser-induced choroidal neovascularization. *BioMed Pharmacother* (2020) 131:110737. doi: 10.1016/j.biopha.2020.110737

26. Jiménez-López J, El-Hammadi MM, Ortiz R, Cayero-Otero MD, Cabeza L, Perazzoli G, et al. A novel nanoformulation of PLGA with high non-ionic surfactant content improves *in vitro* and *in vivo* PTX activity against lung cancer. *Pharmacol Res* (2019) 141:451–65. doi: 10.1016/j.phrs.2019.01.013

27. Zhou R, Teng L, Zhu Y, Zhang C, Yang Y, Chen Y. Preparation of amomum longiligulare polysaccharides 1- PLGA nanoparticle and its immune enhancement ability on RAW264.7 cells. *Int Immunopharmacol* (2021) 99:108053. doi: 10.1016/j.intimp.2021.108053

28. Xiang Y, Xiao M, Han S, Xu S, Cao Y, Lv Z, et al. Preparation and investigation of high solid content PTX-loaded nanoparticles dispersion *via* nanoprecipitation method. *J Biomater Sci Polym Ed* (2014) 25(11):1144–58. doi: 10.1080/09205063.2014.923365

29. Zhu J, Zhang W, Wang D, Li S, Wu. W. Preparation and characterization of norcantharidin liposomes modified with stearyl glycyrrhetinate. *Exp Ther Med* (2018) 16(3):1639–46. doi: 10.3892/etm.2018.6416

30. Zheng X, Wang C, Xing Y, Chen S, Meng T, You H, et al. SB-T-121205, a next-generation taxane, enhances apoptosis and inhibits migration/invasion in MCF-7/PTX cells. *Int J Oncol* (2017) 50(3):893–902. doi: 10.3892/ijo.2017.3871

31. Kilbas PO, Sonmez O, Uysal-Onganer P, Gurkan C, Yerlikaya PO, Arisan ED. Specific c-jun n-terminal kinase inhibitor, JNK-IN-8 suppresses mesenchymal profile of PTX-resistant MCF-7 cells through modulating PI3K/Akt, MAPK and wnt signaling pathways. *Biol (Basel)* (2020) 9(10):320. doi: 10.3390/biology9100320

32. Zhang S, Yang Y, Hua Y, Hu C, Zhong Y. NCTD elicits proapoptotic and antiglycolytic effects on colorectal cancer cells *via* modulation of Fam46c expression and inhibition of ERK1/2 signaling. *Mol Med Rep* (2020) 22(2):774–82. doi: 10.3892/mmr.2020.11151

33. Troutier AL, Ladaviere C. An overview of lipid membrane supported by colloidal particles. *Adv Colloid Interface Sci* (2007) 133(1):1–21. doi: 10.1016/j.cis.2007.02.003

34. Haidar ZS, Hamdy RC, Tabrizian M. Protein release kinetics for core-shell hybrid nanoparticles based on the layer-by-layer assembly of alginate and chitosan on liposomes. *Biomaterials* (2008) 29(9):1207–15. doi: 10.1016/j.biomaterials.2007.11.012

35. Fletcher JI, Haber M, Henderson MJ, Norris MD. ABC Transporters in cancer: more than just drug efflux pumps. *Nat Rev Cancer* (2010) 10(2):147–56. doi: 10.1038/nrc2789

36. Ren F, Chen R, Wang Y, Sun Y, Jiang Y, Li G. Paclitaxel-loaded poly(n-butylcyanoacrylate) nanoparticle delivery system to overcome multidrug resistance in ovarian cancer. *Pharm Res* (2011) 28(4):897–906. doi: 10.1007/s11095-010-0346-9

37. von Hoegen P. Synthetic biomimetic supra molecular biovector (SMBV) particles for nasal vaccine delivery. *Adv Drug Delivery Rev* (2001) 51(1-3):113–25. doi: 10.1016/s0169-409x(01)00175-2

38. Patel NR, Rathi A, Mongayt D, Torchilin VP. Reversal of multidrug resistance by co-delivery of tariquidar (XR9576) and paclitaxel using long-circulating liposomes. *Int J Pharm* (2011) 416(1):296–9. doi: 10.1016/j.ijpharm.2011.05.082

39. Kievit FM, Wang FY, Fang C, Mok H, Wang K, Silber JR, et al. Doxorubicin loaded iron oxide nanoparticles overcome multidrug resistance in cancer. *vitro J Control Release* (2011) 152(1):76–83. doi: 10.1016/j.jconrel.2011.01.024

40. Harada A, Tsutsuki H, Zhang T, Lee R, Yahiro K, Sawa T, et al. Preparation of biodegradable PLGA-nanoparticles used for pH-sensitive intracellular delivery of an anti-inflammatory bacterial toxin to macrophages. *Chem Pharm Bull (Tokyo)* (2020) 68(4):363–68. doi: 10.1248/cpb.c19-00917

41. Li B, Xu H, Li Z, Yao M, Xie M, Shen H, et al. Bypassing multidrug resistance in human breast cancer cells with lipid/polymer particle assemblies. *Int J Nanomedicine* (2012) 7:187–97. doi: 10.2147/IJN.S27864

42. Messerschmidt SK, Musyanovych A, Altvater M, Scheurich P, Pfizenmaier K, Landfester K, et al. Targeted lipid-coated nanoparticles: delivery of tumor necrosis factor-functionalized particles to tumor cells. *J Control Release* (2009) 137 (1):69–77. doi: 10.1016/j.jconrel.2009.03.010

43. Troutier AL, Veron L, Delair T, Pichot C, Ladaviere C. New insights into self-organization of a model lipid mixture and quantification of its adsorption on spherical polymer particles. *Langmuir* (2005) 21(22):9901–10. doi: 10.1021/la050796l

44. Koide H, Asai T, Furuya K, Tsuzuku T, Kato H, Dewa T, et al. Inhibition of akt (ser473) phosphorylation and rapamycin-resistant cell growth by knockdown of mammalian target of rapamycin with small interfering RNA in vascular endothelial growth factor receptor-1-targeting vector. *Biol Pharm Bull* (2011) 34 (5):602–8. doi: 10.1248/bpb.34.602

45. Okamoto A, Asai T, Ryu S, Ando H, Maeda N, Dewa T, et al. Enhanced efficacy of doxorubicin by microRNA-499-Mediated improvement of tumor blood flow. *J Clin Med* (2016) 5(1):10. doi: 10.3390/jcm5010010

46. Wang Y, Liu P, Duan Y, Yin X, Wang Q, Liu X, et al. Specific cell targeting with APRPG conjugated PEG-PLGA nanoparticles for treating ovarian cancer. *Biomaterials* (2014) 35(3):983–92. doi: 10.1016/j.biomaterials.2013.09.062

47. Mekkawy AI, Naguib YW, Alhaj-Suliman SO, Wafa EI, Ebeid K, Acri T, et al. Paclitaxel anticancer activity is enhanced by the MEK 1/2 inhibitor PD98059 *in vitro* and by PD98059-loaded nanoparticles in BRAF V600E melanoma-bearing mice. *Int J Pharm* (2021) 606:120876. doi: 10.1016/j.ijpharm.2021.120876

48. Hoshino R, Tanimura S, Watanabe K, Kataoka T. M kohno. blockade of the extracellular signal-regulated kinase pathway induces marked G1 cell cycle arrest and apoptosis in tumor cells in which the pathway is constitutively activated: up-regulation of p27(Kip1). *J Biol Chem* (2001) 276(4):2686–92. doi: 10.1074/jbc.M006132200

Glossary

APRPG	Ala-Pro-Arg-Pro-Gly
ATCC	American Type Culture Collection
COU6	coumarin 6
DMEM	Dulbecco's Modified Eagle Medium
DMSO	dimethyl sulfoxide
EE	encapsulation efficiency
FBS	fetal bovine serum
FITC	fluorescein isothiocyanate
HCC	hepatocellular carcinoma
HPLC	high-performance liquid chromatography
MTT	3-[4,5-dimethylthiazol-2-yl]-2, 5 diphenyl tetrazolium bromide
NC	normal saline
NCTD	norcantharidin
PBS	Phosphate-buffered saline
PLGA	poly (lactic-co-glycolic acid)
PTX	paclitaxel
PTX/NCTD-APRPG-NPs	PTX/NCTD-loaded core–shell lipid nanoparticles modified with APRPG
PTX/NCTD-NPs	PTX/NCTD-loaded core–shell-type nanoparticles
PTX-NPs	PTX-loaded PLGA nanoparticles
PVDF	polyvinylidene difluoride
RIPA	radioimmunoprecipitation assay
SD	standard deviation
SDS-PAGE	sodium dodecyl sulfate polyacrylamide gel electrophoresis
WB	Western blot

frontiers | Frontiers in Oncology

TYPE Original Research
PUBLISHED 27 October 2022
DOI 10.3389/fonc.2022.933750

OPEN ACCESS

EDITED BY
Zhenhua Chen,
Jinzhou Medical University, China

REVIEWED BY
Xianyi Cai,
Huazhong University of Science and Technology, China
Hamed Barabadi,
Shahid Beheshti University of Medical Sciences, Iran
Fang-Fang Cheng,
Nanjing University of Chinese Medicine, China

*CORRESPONDENCE
Amr Hassan
Amrhassan.nanotechnology@gmail.com

SPECIALTY SECTION
This article was submitted to Pharmacology of Anti-Cancer Drugs, a section of the journal Frontiers in Oncology

RECEIVED 01 May 2022
ACCEPTED 12 September 2022
PUBLISHED 27 October 2022

CITATION
Hassan A, Al-Salmi FA, Abuamara TMM, Matar ER, Amer ME, Fayed EMM, Hablas MGA, Mohammed TS, Ali HE, Abd EL-fattah FM, Abd Elhay WM, Zoair MA, Mohamed AF, Sharaf EM, Dessoky ES, Alharthi F, Althagafi HAE and Abd El Maksoud AI (2022) Ultrastructural analysis of zinc oxide nanospheres enhances anti-tumor efficacy against Hepatoma. *Front. Oncol.* 12:933750. doi: 10.3389/fonc.2022.933750

Ultrastructural analysis of zinc oxide nanospheres enhances anti-tumor efficacy against Hepatoma

Amr Hassan[1]*, Fawziah A. Al-Salmi[2], Tamer M. M. Abuamara[3], Emadeldin R. Matar[4], Mohamed E. Amer[3], Ebrahim M. M. Fayed[3], Mohamed G. A. Hablas[3], Tahseen S. Mohammed[5], Haytham E. Ali[3], Fayez M. Abd EL-fattah[6], Wagih M. Abd Elhay[3], Mohammad A. Zoair[7], Aly F. Mohamed[8], Eman M. Sharaf[9], Eldessoky S. Dessoky[2], Fahad Alharthi[2], Hussam Awwadh E. Althagafi[10] and Ahmed I. Abd El Maksoud[11]

[1]Department of Bioinformatics, Genetic Engineering and Biotechnology Research Institute (GEBRI), University of Sadat City, Sadat, Egypt, [2]Biology Department, College of Sciences, Taif University, Taif, Saudi Arabia, [3]Department of Histology, Faculty of Medicine, Al-Azhar University, Cairo, Egypt, [4]Departments of Pathology, Faculty of Medicine, Al-Azhar University, Cairo, Egypt, [5]Department of Public Health and Community Medicine, Faculty of Medicine, Al-Azhar University, Cairo, Egypt, [6]Department of Anatomy and Embryology, Faculty of Medicine, Al-Azhar University, Cairo, Egypt, [7]Department of Physiology, Faculty of Medicine, Al-Azhar University, Cairo, Egypt, [8]Research and development department, Egyptian Organization for Biological Products and Vaccines [Holding Company for Vaccine and Sera Production (VACSERA)], Giza, Egypt, [9]Department of Bacteriology, Immunology, and Mycology, Animal Health Research Institute (AHRI), Shebin El Kom, Egypt, [10]Biology Department, Faculty of Science and Arts, Al-Baha University, Al-Mikhwah, Saudi Arabia, [11]Department of Industrial Biotechnology, Genetic Engineering and Biotechnology Research Institute (GEBRI), University of Sadat City, Sadat, Egypt

Zinc oxide nanomaterial is a potential material in the field of cancer therapy. In this study, zinc oxide nanospheres (ZnO-NS) were synthesized by Sol-gel method using yeast extract as a non-toxic bio-template and investigated their physicochemical properties through various techniques such as FTIR, XR, DLS, and TEM. Furthermore, free zinc ions released from the zinc oxide nanosphere suspended medium were evaluated by using the ICP-AS technique. Therefore, the cytotoxicity of ZnO nanospheres and released Zn ions on both HuH7 and Vero cells was studied using the MTT assay. The data demonstrated that the effectiveness of ZnO nanospheres on HuH7 was better than free Zn ions. Similarly, ZnO-Ns were significantly more toxic to HuH7 cell lines than Vero cells in a concentration-dependent manner. The cell cycle of ZnO-Ns against Huh7 and Vero cell lines was arrested at G_2/M. Also, the apoptosis assay using Annexin-V/PI showed that apoptosis of HuH7 and Vero cell lines by ZnO nanospheres was concentration and time-dependent. Caspase 3 assay results showed that the apoptosis mechanism may be intrinsic and extrinsic pathways. The mechanism of apoptosis was

10.3389/fonc.2022.933750

determined by applying the RT-PCR technique. The results revealed significantly up-regulated Bax, P53, and Cytochrome C, while the Bcl_2 results displayed significant down-regulation and the western blot data confirmed the RT-PCR data. There is oxidative stress of the ZnO nanospheres and free Zn^{+2} ions. Results indicated that the ZnO nanospheres and free Zn^{+2} ions induced oxidative stress through increasing reactive oxygen species (ROS) and lipid peroxidation. The morphology of the HuH7 cell line after exposure to ZnO nanospheres at different time intervals revealed the presence of the chromatin condensation of the nuclear periphery fragmentation. Interestingly, the appearance of canonical ultrastructure features of apoptotic morphology of Huh7, Furthermore, many vacuoles existed in the cytoplasm, the majority of which were lipid droplets, which were like foamy cells. Also, there are vesicles intact with membranes that are recognized as swollen mitochondria.

KEYWORDS

zinc oxide nanosphere, reactive oxygen species, Zn+2 ion, G2/M transition, apoptotic morphology, P53, Bax

Introduction

Hepatocellular carcinoma is an aggressive malignancy and is ranked as the third most common cause of cancer-related death globally (1). Annually, more than 600,000 people die due to liver cancer (2). Generally, hepatocellular carcinoma (HCC) is diagnosed at end-stage after metastasizing (3). Hepatocellular carcinoma (HCC) is defined as the progressive development of pre-neoplastic and neoplastic lesions and the acquisition of multiple genetic and epigenetic events contributing to the biochemical and molecular heterogeneity of the disease (4, 5). Hepatic cancer is widely spread in Asian countries because of the increasing number of patients suffering from chronic viral hepatitis. HuH7 is a hepatocyte cell line established in 1982 from a 57-year-old Japanese male with well-differentiated hepatocellular carcinoma (6). It's available in the Japan Health Science Research Resources Bank (catalog number JCRB0403) (7). Currently, there are many strategies for HCC therapy, like surgery, radiotherapy, or chemotherapy. Unfortunately, HCC is more resistant to chemotherapy (8–11). Sorafenib is the only drug that is effective against HCC (12). Recently, there has been progress in the treatment of HCC. Only 14% of hepatic cancer patients survived after treatment (13). Chemotherapy is inactive in clinical trials against hepatic cancer due to its adverse effects (14). Therefore, modern therapeutic agents advance with better efficiency against HCC such as Atezolizumab and Beacizumab (15). Scientists are now working on allowing malignant cells to undergo apoptosis after identifying biochemical and morphological markers of apoptotic cells (16, 17). P53 is a tumor suppressor protein that has a powerful caretaker to protect cells from malignant transformation by transcriptional up-regulation of pro-apoptotic DNA repair and cell cycle arrest-related proteins (18). Therefore, nanobiotechnology is considered the preferable approach to identify a novel, sophisticated therapy (19). In the last decade, nanomaterials have played a central role in medical applications such as tumor diagnosis and therapy. It can be classified as a noble metal or a metal oxide material. Also, it is classified into one dimension and two dimensions (19). Nanomedicine is a novel field have utilize the path for novel targeted cancer therapies by allowing therapeutic compounds to be encapsulated in nanoparticulate materials and delivered selectively to tumors *via* passive permeation and active internalization mechanisms. Employing nanoparticles for therapeutic purposes has also been found to minimize resistance, addressing one of the most significant obstacles to conventional therapy (20). Metal oxide nanoparticle such as ZnO NPs and Fe_3O_4 NPs have shown a promising anticancer behaviour besides its therapeutic activity against other diseases such as diabetes (20), microbial infections (21), inflammations (22), and wound healing (17) and environmental (23). ZnO-NPs have received considerable attention in various fields due to their excellent physicochemical properties, safety, biodegradability (24), and their fast delivery to different tissues and organs in addition to various biological purposes including drug delivery and immune-modulatory agent (Kalpana et al., 2018 (25, 26);). Zinc oxide nanoparticles have been applied in biomedical and preclinical research especially in cellular imaging and drug

delivery. Fujihara and colleagues reported that intravenous administration of ZnO nanoparticles can be accumulate in several tissues, particularly lung tissues, and elicit ROS-related phenomena using healthy mice (27, 28). In addition, ZnO-NPs can also be approved to have a potential molecular effect including a reduction in cellular viability, loss of membrane integrity, and activation of the programmed cell death (apoptosis) (29). Also, zinc oxide is approved by the US Food and Drug Administration (FDA) for its properties like stability, safety, and the intrinsic potential to neutralize UV radiation. Based upon the unique properties of zinc oxide nanoparticles, here, zinc oxide nanospheres were synthesized by a green chemistry technology using yeast as a bio-template. Then, the cytotoxicity, apoptotic mechanisms, and antioxidant biomarkers of zinc oxide nanospheres were determined against Hepatoma HuH7 and green kidney monkey cell lines (Vero). Furthermore, the ultrastructure analysis of HuH7 cells was carried out to observe apoptosis stages in the human hepatotome.

Materials and methods

Preparation of ZnO nanosphere

Zinc oxide nanospheres were synthesized by using a modified sol-gel method (30). Briefly, three grams of yeast extract were nurtured in 100 mL of ultrapure water and left for one hour. Then, 25 mM of zinc acetate solution were added and mixed it with 50 ml of yeast extract solution under vigorous stirring at 1400 rpm for one hour, followed by thermal treatment at 500 °C for two hour. The resulting white precipitate has been dried and powdered and is ready to be characterized.

Characterization of ZnO nanosphere

ZnO nanospheres spectra were assayed by ultraviolet-visible (UV-VIS) spectrometry (JASCO V-630 spectrophotometer, Japan). A Fourier transformed infrared (FT-IR) spectrum of the ZnO nanospheres was characterized *via* the Nicolet 6700 apparatus (Thermo Scientific Inc., USA). The crystalline nature and grain size were analyzed by X-ray powder diffraction (XRD) at a temperature of 25–28 °C using a D8 Advance X-ray diffractometer (Bruker, Germany) with a nickel (Ni) filter and CuKα (λ= 1.54184 A^0) radiation as an X-ray source. The average size of ZnO nanospheres in cell culture medium was determined by dynamic light scattering (DLS) (Nano-ZetaSizer-HT, Malvern Instruments, Malvern, UK) (30). The morphology of zinc nanospheres was examined by Field Emission Transmission Electron Microscopy (FETEM) (JSM 2100F, Joel Inc., Tokyo, Japan) at 15 and 200 kV accelerator voltages, respectively.

Measurement of Zn (II) released from ZnO nanospheres

Following quantification of the final concentration of released zinc ions from suspended ZnO-NS, the following products occurred: Firstly, dilution the stock suspension of a concentration of 100 µg/ml ZnO nanospheres by Dulbecco's Modified Eagle's Medium (DMEM) to a final volume of 15 ml. Then, incubate all samples at 37 C in a humidified atmosphere (with 5% CO_2) at different times (0, 3, 6, 18, and 24 h). followed by centrifugation for 20 min at 10,000 x g, and then transferring the supernatant (10 ml) into a test tube containing 0.5 ml of Conc HNO_3. The solution was filled with up to 50 ml of water and the Zn^{+2} ions were quantified with inductively coupled plasma atomic emission spectroscopy (ICP-AES) (Perkin-Elmer, USA) (31).

Cell lines

Human hepatocellular carcinoma (HuH7) cells (catalog number JCRB0403) were obtained from the Japan Health Science-Research Resources Bank. The Green Kidney Monkey (Vero cells) was purchased from ATCC (American Type Culture Collection) (Clone CCL-81). The cells were maintained in a 95% air and 5% CO_2 humidified atmosphere at 37°C. DMEM and MEM-E medium supplemented with 10% FBS and 1% PS were used for routine sub-culturing and all experiments.

Cell viability assays

The viability of HuH7 and Vero cell lines was assessed by the MTT assay as described by Mossman (32) with some modifications. Briefly, 1×10^4 cells/well were seeded in 96-well plates and exposed to Zinc Oxide Nanosphere and $ZnCl_2$ at the concentrations of 100µg/ml, 50µg/mL, 25µg/mL, 12.5µg/mL and 6.25 µg/mL for 24 hour. At the end of exposure, culture medium was removed from each well to avoid interference of ZnO NPs and $ZnCl_2$, then replaced with new medium containing MTT solution (0.5 mg/mL) in an amount equal to 10% of the culture volume and incubated for 4 hour at 37°C until a purple-colored formazan product developed. The resulting formazan product was dissolved in acidified isopropanol. Further, the 96-well plate was centrifuged at 2300 × g for 5 minutes to settle the remaining ZnO NPs and $ZnCl_2$. Then, a 100 µL supernatant was transferred to the other fresh wells of a 96-well plate, and absorbance was measured at 570 nm by a microplate reader (ELX-800 n, Biotek, USA).

DNA content analysis

HuH7 cells (1×10^6) were seeded in T25 flasks and at 70–80% con-fluence the cells were treated with suspended ZnO nanospheres at different concentrations. After 24 h, media was aspirated and cells were harvested with 0.25% trypsin and fixed in70% ice cold ethanol at −20°C for 30 min. Cell pellets were washed with PBS and re-suspended in 500 µl PBS containing 20 µl RNAse (5 mg/ml) and stained with 10 µl PI (1 mg/ml) for 30 min at 37°C. Data acquisition was performed with a fluorescence-activated cell sorter (FACS Canto, Becton-Dickinson, Franklin Lakes, NJ). For each sample, 10,000 events were acquired and the analysis was carried out using BD FACS Diva software (Becton-Dickinson, Franklin Lakes,NJ-USA) (33).

Apoptosis assay with Annexin V-FITC/PI staining

Huh7 and Vero cells ($1x10^4$/well) were seeded in T25 flasks and treated different concentrations of ZnO nanospheres at different times. Cells were then harvested and washed twice with PBS, resuspended in 0.5 ml binding buffer containing FITC-Annexin V and PI and kept at room temperature in the dark for 30 min. The fluorescence of the cells was then analyzed by flow cytometer (Becton-Dickinson, Franklin Lakes, NJ -USA). For each sample, 10,000 events were acquired and the analysis was carried out using BD FACS Diva software (Becton-Dickinson, Franklin Lakes, NJ-USA) (33).

Cell apoptotic mechanisms for RNA extraction and quantitative RT-PCR

The HuH7 cells were cultured in six-well plates and exposed to ZnO nanospheres (100 µg/ml) for 24 hour. At the end of the exposure process, according to the manufacturer's protocol, total RNA was extracted by RNeasy mini Kit (Qiagen,Valencia, CA, USA) according to the manufacturer's instructions. Concentration of the extracted RNA was determined using Nanodrop 8000 spectrophotometer (Thermo-Scientific, Wilmington, DE), and the integrity of RNA was visualized on a 1% agarose gel using a gel documentation system (Universal Hood II, BioRad, Hercules, CA). The first strand of cDNA was synthesized from 1 µg of total RNA by reverse transcriptase using M-MLV (Promega, Madison, WI) and oligo (dT) primers (Promega) according to the manufacturer's protocol. Quantitative real-time PCR was performed by QuantiTect SYBR Green PCR kit (Qiagen) using an ABI PRISM 7900HT Sequence Detection System (Applied Biosystems, Foster City, CA). Two microliters of template cDNA were added to the final volume of 20 µL of reaction mixture. Real-time PCR cycle parameters included 10 minutes at 95°C followed by 40 cycles involving denaturation at 95°C for 15 seconds, annealing at 60°C for 20 seconds, and elongation at 72°C for 20 seconds. The sequences of the specific sets of primer for p53, bax, bcl-2, cytochrome C, and β-actin. Expressions of selected genes were normalized to the β-actin gene, which was used as an internal housekeeping control. All the real-time PCR experiments were performed in triplicate, and data were expressed as the mean of at least three independent experiments (34–36).

Gene expression by flow cytometry

All flow cytometric analyses were performed on a FACS Calibur flow cytometer (BD, Biosciences, CA, USA). The instrument was aligned and calibrated daily with the use of a 4-color mixture of CaliBRITE beads (BD, Biosciences) and FACS Comp Software (BD, Biosciences), according to the manufacturer's instructions (35). The flow cytometry technique evaluated the Bcl_2, Bax, P53, and Cytochrome C oncoproteins. After HuH7 cells were treated with ZnO nanospheres (100 µg/ml) for 24 h. Cells were collected by cold centrifugation at approximately 5000 x g for 10 min, then washed twice and re-suspended in 500 µl of cold (+4 °C) 1X PBS buffer containing Triton X-100 (permeabilization step). After centrifugation as previously described, the supernatant was removed, and the pellet was re-suspended again in PBS containing 1% BSA and diluted primary antibody rabbit monoclonal antibody (1:100) (Oncogene, Cambridge, MA, USA) for P53, Bax, Bcl_2, and cytochrome C, followed by incubation at room temperature for 1 hr. After centrifugation, the pellet was washed three times using PBS, and the cells were incubated with secondary antibodies, anti-rabbit (all from Santa Cruz Biotechnology, USA) in a dilution of 1:100, followed by incubation in the dark for 30 min at RT. Finally, the cells were centrifuged, and the supernatant was removed. The cells had been washed as previously described. The pellet was finally re-suspended in 500 µl PBS. The cells were immediately analyzed by flow cytometry (BD FASC Calibur-USA) (37).

Western analysis

After treatment with various concentrations of ZnO-NPs, cells were collected by centrifuging at 100 x g and washed twice with ice-cold PBS (pH 7.4) and lysed in 1 ml lysis buffer (2 mM Tris-HCl, pH 8.0, 1% Nonident P-40, 13.7 mM NaCl, 10%

glycerol, 1 mM sodium orthovanadate (NaVO3), 1 mM phenylmethyl-sulfonyl fluoride and 10 µg/ml Aprotinin) for 20 min on ice. Lysates were centrifuged at19 000 x g for 15 min at 4°C, and aliquots of the supernatants were used to determine protein concentration using the BCA assay (Pierce, Rockford, USA). Aliquots containing equal amounts of proteins (20 - 30 µg) were boiled in 2 x sodium dodecyl sulfate (SDS) sample loading buffer (125 mM Tris-HCl, 4% (w/v) SDS, 20% (v/v) glycerol, 10% (v/v) 2-mercaptoethanol, pH 6.8) before being resolved on a 12% sodium dodecyl sulfate-polyacrylamide gel (SDS-PAGE). Proteins on the gels were then electro-blotted onto Immobilon-P transfer membrane (Millipore Corporation, Bedford, USA) using a blotting buffer (10% methanol, 10 mM CAPS, pH 11.0) at 200 mA for 2 h at 4°C. Following electro-blotting, the membranes were blocked with 0.05% TBS-Tween (20 mM Tris-HCl, 200 mM NaCl, pH 7.4) containing 5% non-fat dry milk for 1 h at room temperature. After blocking, the membranes were washed three times for 10 min each with wash buffer (0.05% TBS-Tween without milk), and then incubated with specific primary goat anti mouse Bcl-2 antibody (1: 1000), goat anti-mouse Bax antibody (1: 500), goat anti-mouse p53 antibody (1: 1000) and goat anti-mouse anti- cytochrome c (1:2000) for overnight at 4°C. After washing three times with washing buffer for 10 min each, membranes were further incubated for 1 h in the presence of a peroxidase (HRP)-conjugated secondary antibody (1: 10 000) diluted with blocking buffer. The membranes were washed again as described above and immunoreactive proteins were then detected using the Western blotting luminol reagent (Santa-Cruz Biotechnology Inc., Santa-Cruz, CA, USA) following the manufacturer's protocol (38).

Caspase-3 assay

The Activity of caspase-3 enzyme was determined by the standard fluorometric microplate assay (33). Briefly, HuH7 cells (1×10^4 cells/well) were cultured in a 96-well plate and exposed to ZnO nanospheres at concentrations of 50, 100, 150, and 200 µg/mL for 24 hour. After the exposure was completed, the cells were harvested in ice-cold phosphate buffer saline for preparing the cell lysate. Further, a reaction mixture containing 30 µL of cell lysate, 20 µL of (Ac-DEVD-pNA) (caspase-3 substrate), and 150 µL of protease reaction buffer (50 mM Hepes, 1 mM EDTA, and 1 mM DTT) (pH 7.2) was incubated for 15 min. Fluorescence of the reaction mixture was measured at 5-minute intervals for 15 minutes at excitation and emission wavelengths of 430/535 nm using an ELISA reader apparatus (ELX-800n, Biotek, USA). A 7-amido-4-tri-fluoromethyl coumarin (AFC) standard ranging from 5m to 15 µM was prepared, and its fluorescence was recorded to calculate caspase-3 activity in terms of pmol AFC released/minute/mg protein.

Oxidative stress biomarkers

ROS measurement

ROS was measured using 2, 7-dichlorofluorescein diacetate (DCFH-DA). The DCFHDA passively enters the cell, where it reacts with ROS to form the highly fluorescent compound dichlorofluorescein (DCF). In brief, 10 mM DCFH-DA stock solution (in methanol) was diluted in culture medium without serum or another additive to yield a 100 µM working solution. HuH7 cells were treated with ZnO NPs at a concentration of 100 µg/mL for 24 hour. At the end of exposure, cells were washed twice with HBSS and then incubated in 1 mL of working solution of DCFH-DA at 37°C for 30 minutes. Cells were lysed in an alkaline solution and centrifuged at 2300 × g for 10 minutes. A 200 µL supernatant was transferred to a 96-well plate, and fluorescence was measured at 485 nm excitation and 520 nm emissions using a microplate reader (ELX-800n, Biotek, USA). The values were expressed as a percent of fluorescence intensity relative to control wells (33).

Lipid peroxidation measurement

HuH7 cells were exposed to different ZnO nanospheres and free Zn^{+2} ions (released from 100 µg/ml ZnO-nanospheres) for 24 h. After the exposure, the cells were washed and harvested in cold PBS at 4°C. The harvested cell pellets were lysed using a cell lysis buffer (20 mM Tris-HCl [pH 7.5], 150 mM NaCl, 1 mM Na_2EDTA, 1% Triton X 100, and 2.5-mM sodium pyrophosphate). After cold centrifugation at 15,000 g for 10 min, the supernatant (cell extract) was maintained on ice until assayed for oxidative-stress biomarkers. The extent of membrane lipid peroxidation (LPO) was estimated by quantifying malondialdehyde (MDA) (39). MDA is one of the final products of membrane LPO. In brief, 0.1 ml of cell extract was mixed with 1.9 ml of 0.1 M sodium phosphate buffer (pH 7.4) and incubated at a temperature of 37°C for 1 hour. After precipitation with trichloroacetic acid (TCA) (5% v/v), the incubated mixture was centrifuged (2500 g for 15 min at room temperature). The supernatant was collected and to which 1 ml of TBA (1% v/v) was added and placed in boiling water for 15 min. After cooling to room temperature, the absorbance of the mixture was taken at a wavelength of 532 nm and converted to nmol/mg protein using the molar extinction coefficient of 1.56×10^5 M^{-1} Cm^{-1} (40).

Antioxidant biomarkers

Assay for reduced glutathione (GSH)

The level of the reduced glutathione (GSH) was estimated using Ellman's reagent (41). Based on the development of yellow color when DTNB (5, 5' dithiobis-(2-nitrobenzoic acid) is added to compounds containing sulfhydryl groups. In brief, mixed with

100 µg of ZnO nanospheres and Zn^{+2} ions (released from 100 µg of ZnO nanospheres) after treatment with Huh7 cell line for 24 hr. was added to 0.3 ml of 0.25% sulfosalycylic acid, and then tubes were centrifuged at 2500 ×g for 15 min. Supernatant (0.5 ml) was mixed with 0.025ml of 0.01 M DTNB and 1 ml phosphate buffer (0.1 M, pH = 7.4). The absorbance at 412 nm was recorded. Finally, total GSH content was expressed as nmol GSH/mg protein.

Assay for nitric oxide (NO)

Nitric oxide (NO) radical scavenging assay was carried out oxide radical scavenging activity was carried out as per the method of Green et al. (1982) (42). NO radicals were generated from sodium nitroprusside solution. 0.6 mL of 10 mM sodium nitroprusside was mixed with 100 µg of ZnO nanospheres and Zn^{+2} ions (released from 100 µg of ZnO nanospheres) after exposure to Huh7 cell line for 24 hr. The mixture was incubated at 25°C for 150 min, followed by mixing with 1.0 mL of pre-prepared Griess reagent (1% sulfanilamide, 0.1% naphthyl ethylenediamine dichloride, and 2% phosphoric acid). Ascorbic acid and trolox were used as standards. The absorbance was measured at 546 nm. The inhibition was calculated by the following equation:

$$\%\ \ Inhibition\ \ of\ \ NO\ \ radical = [A_0 - A_1]/A_0 \times 100$$

Where, A_0 is the absorbance before the reaction and A_1 is the absorbance after the reaction has taken place with Griess reagent. The decreasing absorbance indicates a high NO scavenging activity.

Assay for superoxide dismutase (SOD)

Superoxide dismutase (SOD) assay is a mixture containing sodium pyrophosphate buffer, nitro blue tetrazolium (NBT), phenazine methosulphate (PMS), reduced nicotinamide adenine dinucleotide (NADH), and the required volume of cell extract. Superoxide dismutase enzyme activity is defined as the amount of enzyme required to inhibit chromogen production (optical density at 560 nm) by 50% in 1 minute under assay conditions and is expressed as specific activity in units/mg protein (33).

Ultrastructure of HuH7 using a transmission electron microscope

HuH7 cells were remedied with ZnO nanospheres at a concentration of 100 µg/ml at different time intervals. After the exposure, cells were collected and washed with PBS, then fixed in ice-cold glutaraldehyde (2.5%) for one hour. The cells were washed with PBS three times for 15 min and post-fixed in OsO_4 (1%) for one hour, then stained with uranyl acetate (2%) for 30 min at room temperature. The cells were dehydrated by serial dilutions of ethanol (50, 70, and 90%) for 15 minutes each, followed by 20 minutes in ethanol (100%) and 20 minutes in acetone (100%), respectively. Consequently, the cells were embedded in Epon812. Ultrathin sections (120 nm) were obtained and stained with uranyl acetate (2%) for 20 min, and lead citrate for 5 min, then examined using Field Emission Transmission Electron Microscopy (FETEM) (JSM 2100F, Joel Inc., Tokyo, Japan) at accelerating voltages of 15 kV and 200 kV, respectively (43).

Statistical analysis

Statistical analysis was expressed as the mean ± standard deviation of triplicate (independent) experiments. Two sample comparisons of means were carried out using Student's t-test analysis. All analyses were conducted using SPSS 17.0 software (SPSS Inc., Chicago, IL, USA). P <0.05 was considered a statistically significant difference.

Result and discussion

Characterization of ZnO nanospheres

As shown in Figure 1A, the FT-IR spectra of the ZnO nanospheres, there is a band at 3,429 cm^{-1} corresponding to the hydroxyl group of a water molecule on the surface of ZnO nanospheres that occurred because of the ZnO-nanosphere's thermal treatment at 500°C. The band at 1,628 cm^{-1} is related to the OH bend in ZnO. Also, a strong band at 418 cm-1 was attributed to ZnO. As illustrated in Figure 1B, the XRD patterns of ZnO nanospheres showed that the peaks at 2 θ = 31.746°, 34.395°, 47.526°, 56.549°, 62.832°, 67.893° and 69.028° were assigned to (100), (002), (101), (110), (103), (200), (112), and (201) of ZnO nanospheres. All peaks are consistent with a polycrystalline Wurtzite structure (Zincite, JCPDS no. 89-1397). There are no characteristic peaks of any impurities, and this indicates a high ZnO nanospheres quality. Scherer's equation estimated the average crystallite size (d) of ZnO nanospheres to be approximately 20 nm. DLS determined the average hydrodynamic size of the ZnO nanospheres in cell culture media, and it was about 20 nm, as revealed in Figure 1C.

$$d = k\lambda\beta\ \ Cos\ \ \theta$$

As Figure 1D showed, TEM images confirmed that the morphological shape of the nanosphere with approximately size of 20 nm. Also, it was like the data obtained by XRD.

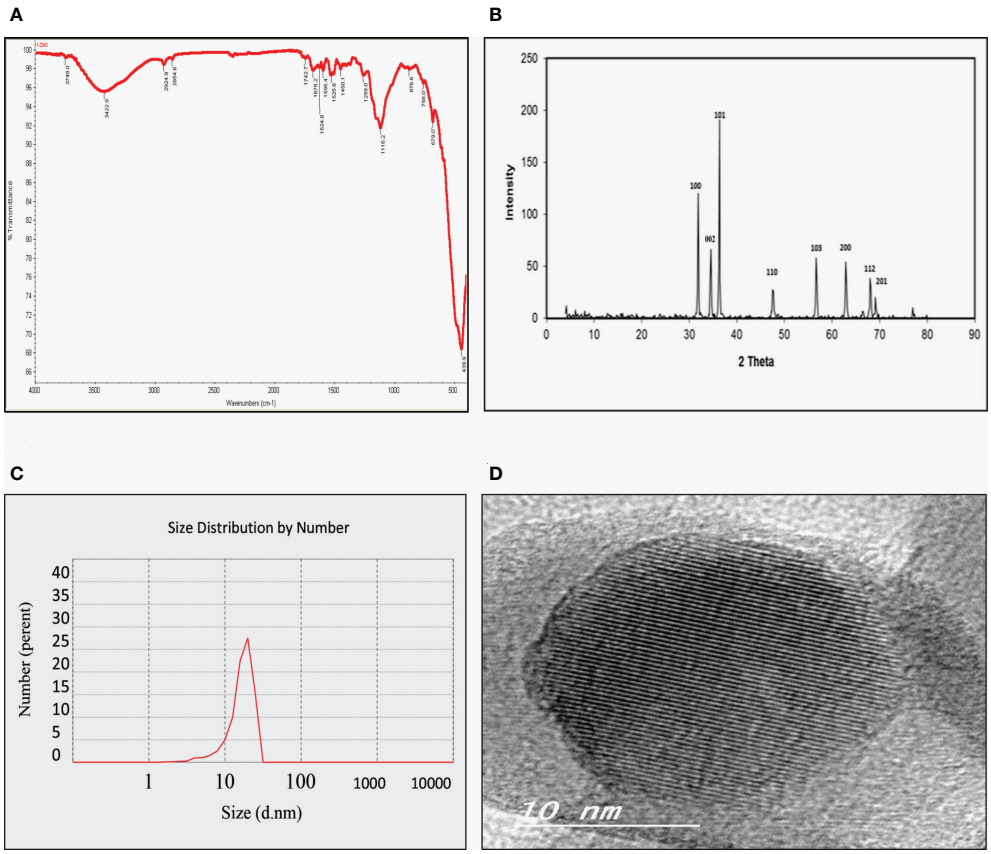

FIGURE 1
Physicochemical characterization of Zinc Oxide nanospheres. **(A)** FT-IR spectra **(B)** XRD patterns of ZnO nanospheres **(C)** DLS of ZnO nanospheres **(D)** HR-TEM of ZnO nanospheres.

Measurement of Zn (II) released from ZnO nanospheres

ICP-AES measured the quantity of the Zn (II) ions released in the supernatant of the dispersed ZnO nanospheres (100 µg/ml). As presented in Figure 2, the total amount of ZnO nanospheres varied within different intervals of time. Free Zn^{+2} ions were 20ppm after 24 h, 15 ppm after 18 h, 10 ppm after 12 hr, 6.5 ppm after 6 h, 3.5 ppm after 3 h, and 1.0 ppm after 1 hr.

Cell viability by MTT assay

MTT assay is the best technique to measure the cytotoxicity of ZnO nanospheres and $ZnCl_2$ against human hepatocellular carcinoma (HuH7) and green kidney monkey cell lines (Vero). As shown in Figure 3A, the viability of HuH7 cells was reduced from 100% at 0.5 µg to less than 10% and 15% (for ZnO–Ns and ZnCl2, respectively) after being treated with 100 µg (ZnO nanospheres and $ZnCl_2$) for 24 hour. Similarly, as shown in Figure 3B, the viability of HuH7 cells after 48 hour of treatment was reduced from 100% to 20% and 15% for ZnO–Ns and $ZnCl_2$, respectively.

The viability of Vero cells was less affected than that of HuH7. As Figure 3C displays, after treatment of Vero cells by ZnO nanospheres and $ZnCl_2$, for 24 hour, the viability of Vero cells decreased from 100 percent at 0.25 µg to less than 15 and 10 percent at 250 µg of ZnO nanospheres and $ZnCl_2$, respectively. Similarly, the viability of Vero cells after 48 hour of exposure to ZnO-Ns and $ZnCl_2$ was reduced from 100 percent to 20 and 15 percent. As Figure 3D shows, the results changed gradually after exposure of Vero cells to ZnO nanospheres and $ZnCl_2$ for 48 hour.

DNA content analysis

Due to extensive ROS generation and DNA damage, cells may arrest at different phases of the cell cycle. After 24 h

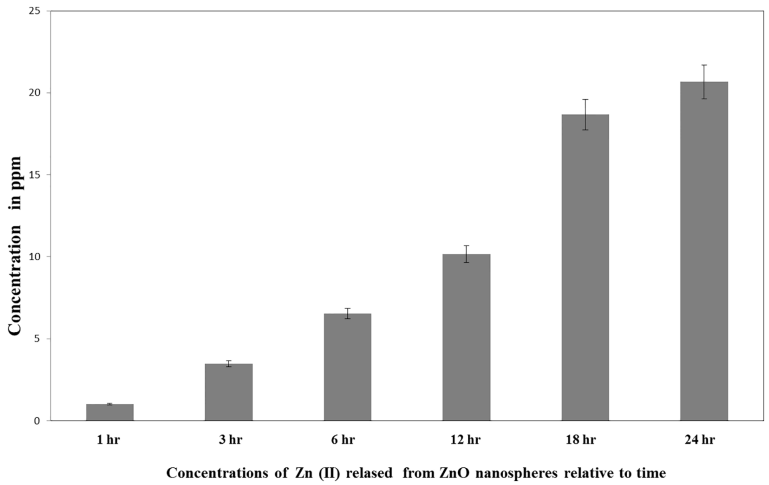

FIGURE 2
Released Zn^{+2} ions from ZnO nanospheres by ICP-AES.

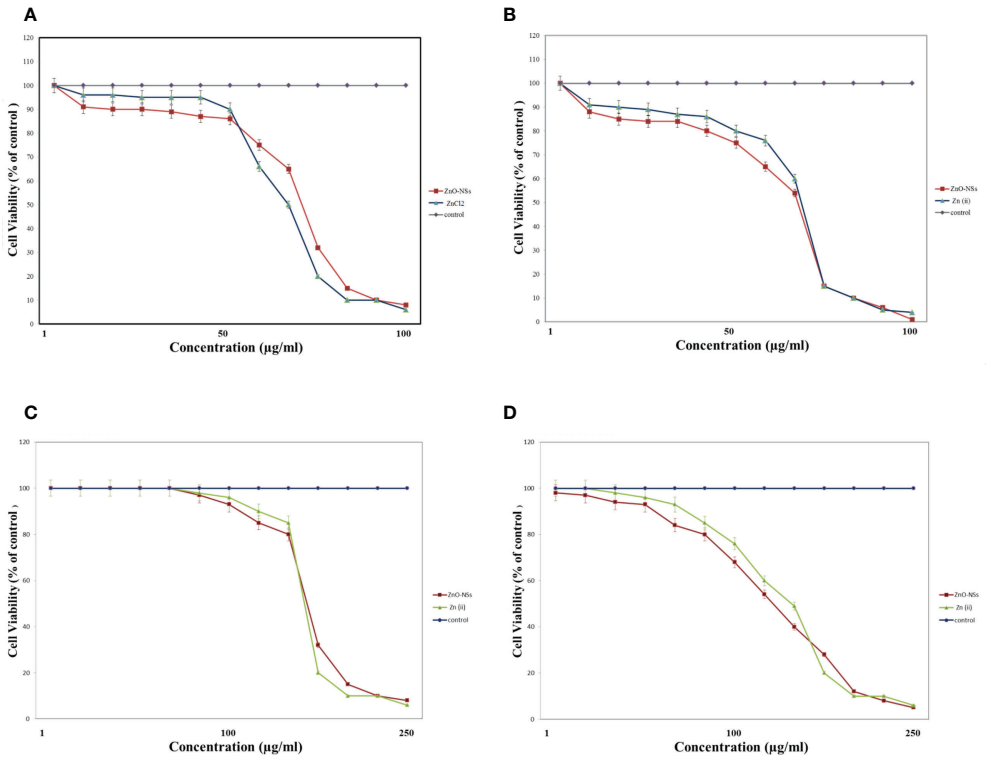

FIGURE 3
Cytotoxicity effect of ZnO nanospheres and released Zn ion different concentrations on HuH7 cell line with concentrations using MTT assay. **(A)** Cytotoxicity effect of ZnO nanospheres and released Zn ion different concentrations on HuH7 cell lines with concentrations using MTT assay after 24 hour. **(B)** Cytotoxicity effect of ZnO nanospheres and released Zn ion different concentrations on HuH7 cell line with concentrations using MTT assay after 48 hour. **(C)** Cytotoxicity effect of ZnO nanospheres and released Zn ion different concentrations on Vero cell line with concentrations using MTT assay after 24 hour. **(D)** Cytotoxicity effect of ZnO nanospheres and released Zn ion different concentrations on Vero cell line with concentrations using MTT assay after 48 hour.

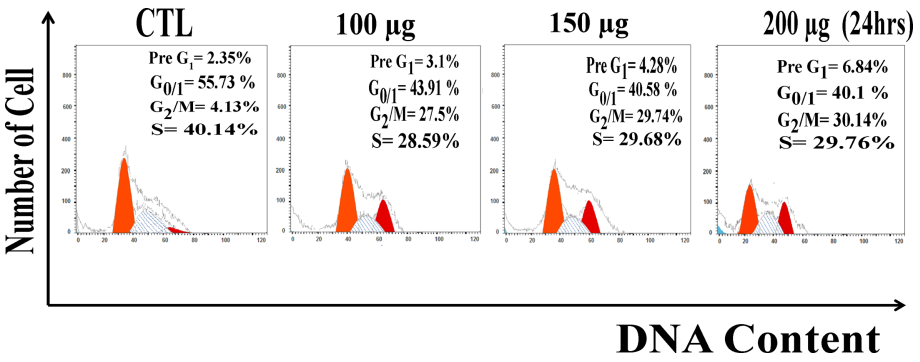

FIGURE 4
DNA content analysis HuH7 cell line treated with of ZnO nanospheres.

treatment Huh7 were analyzed for the distribution of cell cycle phases. Measurement of the cell cycle phase ratio using flow cytometry with propidium iodide (PI) staining to investigate the anti-proliferative effect of zinc oxide nanospheres was triggered by cell cycle arrest. As shown in Figure 4, ZnO nanospheres treatment enhanced the accumulation of the HuH7 cells at the G_2/M phase significantly ($P<0.05$) compared with the control. The percentage of the cells at G_2/M increased significantly ($P<0.05$) with increasing ZnO nanospheres concentration. The growth of the HuH7 treated with 200 µg/ml ZnO nanospheres was about 55.73, 4.13, and 40.14% at G_0/1, G_2/M, and S, respectively, compared to the non-treated cells, in which the growth was about 40.1, 30.4, and 29.6% at G_0/1, G_2/M, and S, respectively, which indicated that the cell cycle arrest at G_2/m phase is activated by Cyclin-A (CDK1).

Huh7 cells are induced to apoptosis by zinc oxide nanospheres

As a result, Figure 5 revealed a flow cytometric analysis of zinc oxide nanospheres-induced apoptosis in Huh7 cells using Annexin V-FITC/PI staining. The percentage of the apoptotic cells (including early and late apoptotic cells) increased with the

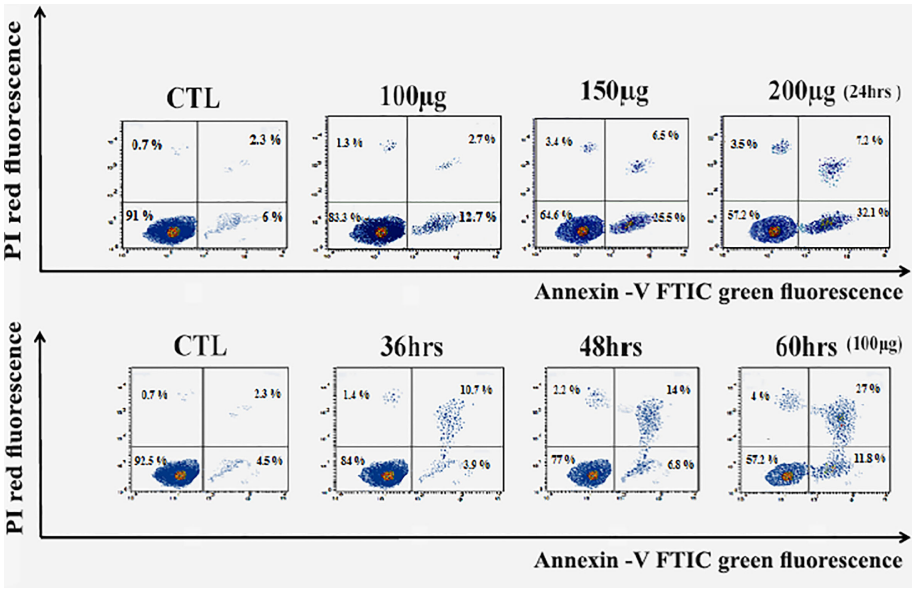

FIGURE 5
Apoptosis Assay with Annexin V-FITC/PI staining of HuH7 cell line. LL, Viable cells (Annexin V −/PI −), LR, early apoptotic cells (Annexin V +/PI −), UL, late necrotic cells (Annexin V −/PI +) and UR, late apoptotic/necrotic cells (Annexin V +/PI +).

increasing concentration of ZnO nanospheres from 8.3 to 39.3%, respectively. Also, as the time of treatment increased, the apoptotic percentage increased from 6.8 to 38.8%.

Also, zinc oxide nanosphere has less effect on Vero cells than on HuH7. As Figure 6 displayed, the percentage of apoptotic cells (including early and late apoptotic cells) increased with the increasing concentration of ZnO nanospheres from 1.02 to 13.25%, respectively. Also, as the time of exposure increased, the apoptotic percentage increased with time from 3 to 15%, respectively. Our data indicated the zinc oxide nanospheres are safer for normal cells.

Quantitative RT-PCR

The levels of apoptotic genes (p53, Bax, Bcl_2, and cytochrome C) in the HuH7 cell were studied by treating the cell with ZnO nanospheres at a concentration 100 µg/ml for 24 h. The result revealed that ZnO nanospheres altered the expression of genes in HuH7 cells. The mRNA expression levels of tumor suppressor gene p53 (Figure 7A), pro-apoptotic gene Bax (Figures 7B, D) were significantly unregulated, while the expression of antiapoptotic gene BCL-2 (Figure 7C) was significantly down-regulated in ZnO NSs-treated cells as compared with the untreated control cells (P, 0.05 for each). Bax/Bcl_2 ratio displayed the activity of ZnO-NSs show a good anticancer activity against HuH7 cell as S1 Figure displayed.

Gene expression by flow cytometry

The relative expression of P53, Bax, and Bcl_2 has been detected in all treated cells. Treatment of the HuH7 cells with ZnO nanospheres enhanced the relative expression of P53 significantly ($P<0.05$) by 85% (Figure 8B). Similarly, it increased the relative expression of Bax and Bcl_2 to 65 and 10%, respectively (Figure 8C). Also, the relative expression of cytochrome C increased in the HuH7 cells treated with ZnO nanospheres by 55% (Figure 8D) compared to control cells treated with DMSO (Figure 8A). These findings indicated that ZnO nanospheres regulated cell cycles *via* stimulating the

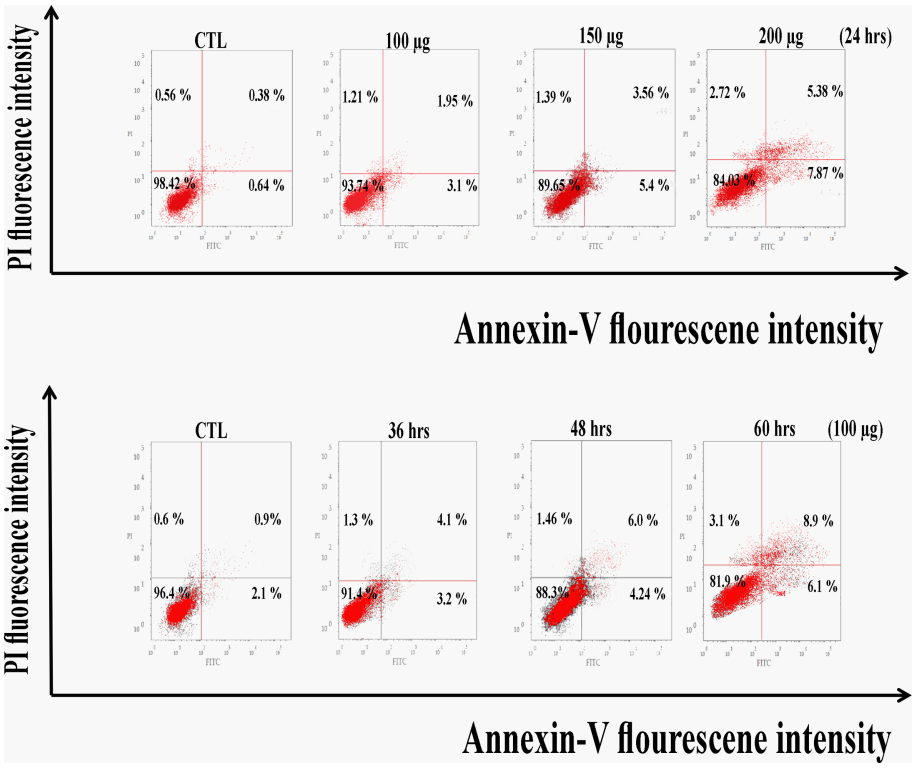

FIGURE 6
Apoptosis Assay with Annexin V-FITC/PI staining of Vero cell line.

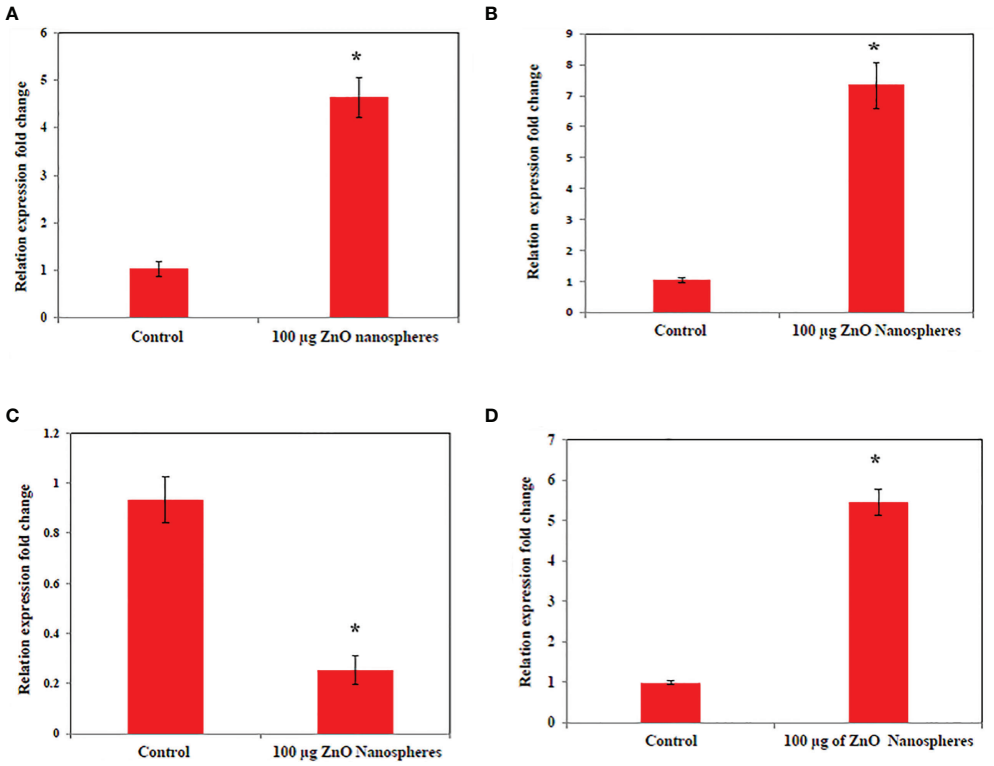

FIGURE 7
Quantitative real-time PCR measure mRNA levels of HuH7 exposed to 100 µg/ml of ZnO nanospheres (ZnO-NS) for 24 hour. *Statistically significant difference as compared with the controls (*P*, 0.05 for each). **(A)** P53 **(B)** Bax **(C)** Bcl2 **(D)** Cytochrome C.

expression of P53 and Bax genes. Bcl2 was less detected than P53 and Bax.

Western analysis

As shown in Figure 9, the western blot of the expressed protein demonstrated that P53, Bax, and cytochrome C were up-regulated as compared with control. While Bcl_2 was down-regulated as compared with control, Zinc oxide nanosphere induces caspase-dependent apoptosis.

Caspase-3 assay

Caspase-3 is one of the executioner caspase members. As Figure 10 displayed, as the concentration of zinc oxide increased, the caspase 3 enzyme activity increased from 0.75 at a concentration of 50 µg to 2 at a concentration of 200 µg/ml. The data confirmed that zinc oxide nanospheres activated caspase-3 cleavage in a concentration-dependent manner.

Oxidative stress and antioxidant biomarkers

The primary pathway required to trigger apoptosis mechanistically in a cancerous cell was to induce oxidant generation and antioxidant depletion. Therefore, the oxidants (ROS, LPO, and NO) and antioxidants (GSH and SOD) were studied in the HuH7 cells treated with 100 µg of ZnO nanospheres and Zn^{+2} ions (released from 100 µg of ZnO nanospheres) after exposure to 24 hr. The results illustrated in Figures 11A, B showed that markers of oxidative stress (ROS and LPO) levels were significantly ($P<0.05$) higher in the HuH7 cells treated with ZnO nanospheres. As Figures 12A-C revealed, all the antioxidant indicators were increased due to the exposure to ZnO nanospheres and released Zn^{+2} ions. Nevertheless, the released Zn^{+2} ions were less than ZnO nanospheres.

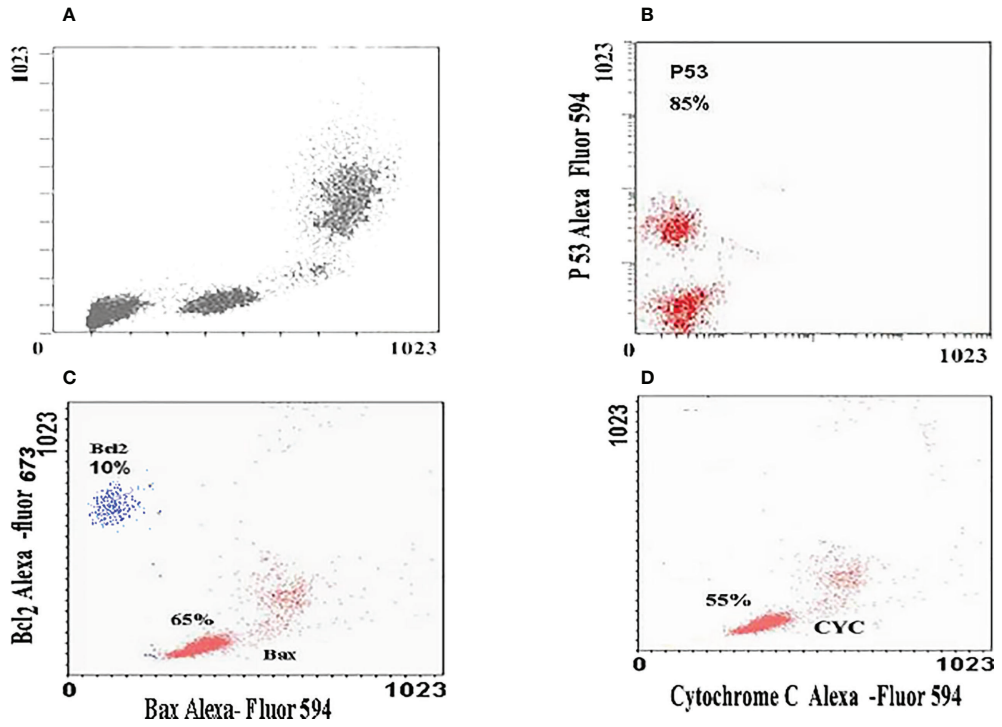

FIGURE 8
Immunoflorescent images of HuH7 exposed to 100 µg/ml of ZnO nanospheres (ZnO-NS) for 24 hour for up-regulation of P53, Bax, Bcl_2 and Cytochrome C. **(A)** The immunoflorescent of huh7 remedied with DMSO **(B)** The immunoflorescent of P53 **(C)** The immunoflorescent of Bax and BcL_2 **(D)** The immunoflorescent of Cytochrome C.

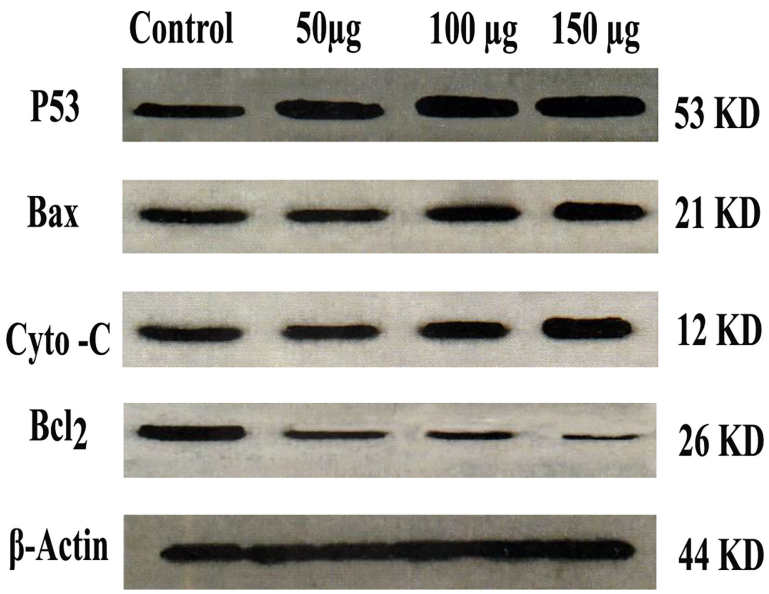

FIGURE 9
Western blot of P53, Bax, Cytochrome C and BcL_2.

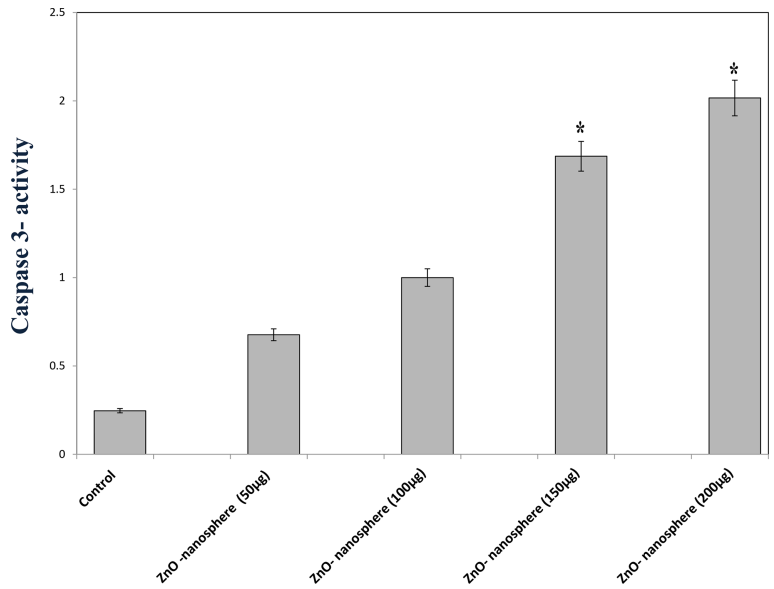

FIGURE 10
Caspase-3 measurement of ZnO nanospheres. *Statistically significant difference as compared with the controls (P> 0.05 for each).

Ultrastructure of HuH7 using a transmission electron microscope

TEM analysis of Huh7 cells remedied with zinc oxide nanospheres at different times demonstrated the typical features of apoptotic cell stages: To begin with, as shown in Figure 13B, the cells rounded up with the disappearance of cytoplasmic Secondly, as time increased, there were many changes in appearance because of chromatin condensation at the nuclear periphery, as Figures 13C, D revealed. Finally, as shown in Figures 13E, there is nuclear fragmentation (a vescicle budded from the nucleus) as compared with the control cell. As in Figure 13A. The control cell (untreated cell) displayed the morphology of regular cells with hyperchromatic nuclei and nuclear pleomorphism. As Figure 13A displayed, at high magnification, the cytoplasmic vacuoles were droplets. Similarly, other vacuoles with a double membrane existed, as Figure 13E showed. Consequently, chromatin condensation, as Figure 13E displays, Also, during the apoptosis process, mitochondria tend to be conserved till secondary necrosis is carried out during treatment of a Hepatoma cell model treated with zinc oxide nanosphere. The number of swollen mitochondria transfers to an apoptotic nuclear morphology within an intact plasma membrane.

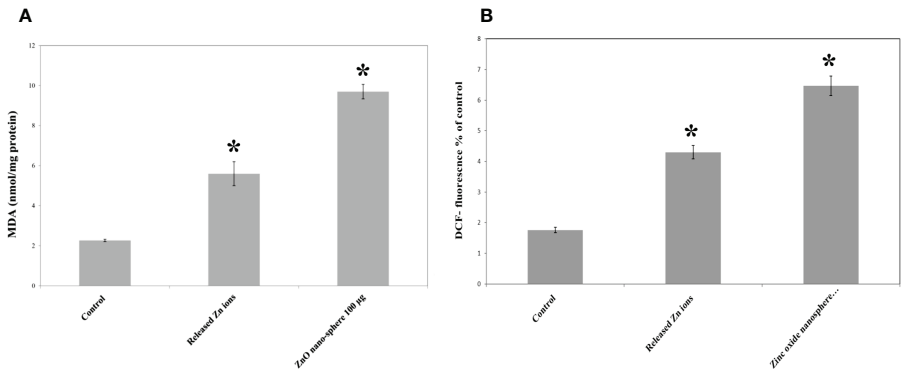

FIGURE 11
Oxidative stress and of human Hepatoma (HuH7) cells after treated with 100 µg/mL ZnO NPs and released Zn ion for 24 hour. *Statistically significant difference as compared with the controls (P > 0.05 for each). **(A)** ROS **(B)** MDA.

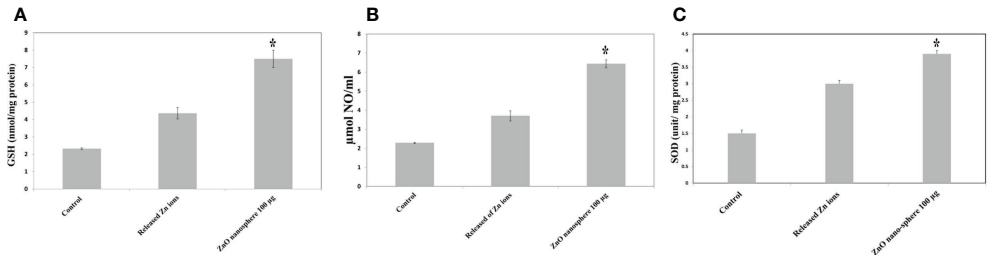

FIGURE 12
Antioxidant assay of human Hepatoma (HuH7) cells after treated with 100 µg/mL ZnO NSs and released Zn ion for 24 hour. *Statistically significant difference as compared with the controls (P > 0.05 for each). **(A)** Glutathione (GSH) **(B)** Superoxide dismutase (SOD) **(C)** Nitric oxide (NO).

Discussion

Cancer therapy concerns the challenging aim of creating selective, effective, and safe therapy (44). MTX is the best antitumor chemotherapeutic drug (antineoplastic or cytotoxic) when used at high doses. However, those doses cause an adverse effect. Hence, scientists are working to find a novel drug with high performance and safety (45). Sorafenib is categorized as the most successful anticancer drug against hepatocellular carcinoma. Sorafenib, an oral multiple kinase inhibitor, significantly induces apoptosis in cancer model processes as well as inhibits tumor angiogenesis and cell proliferation to exert

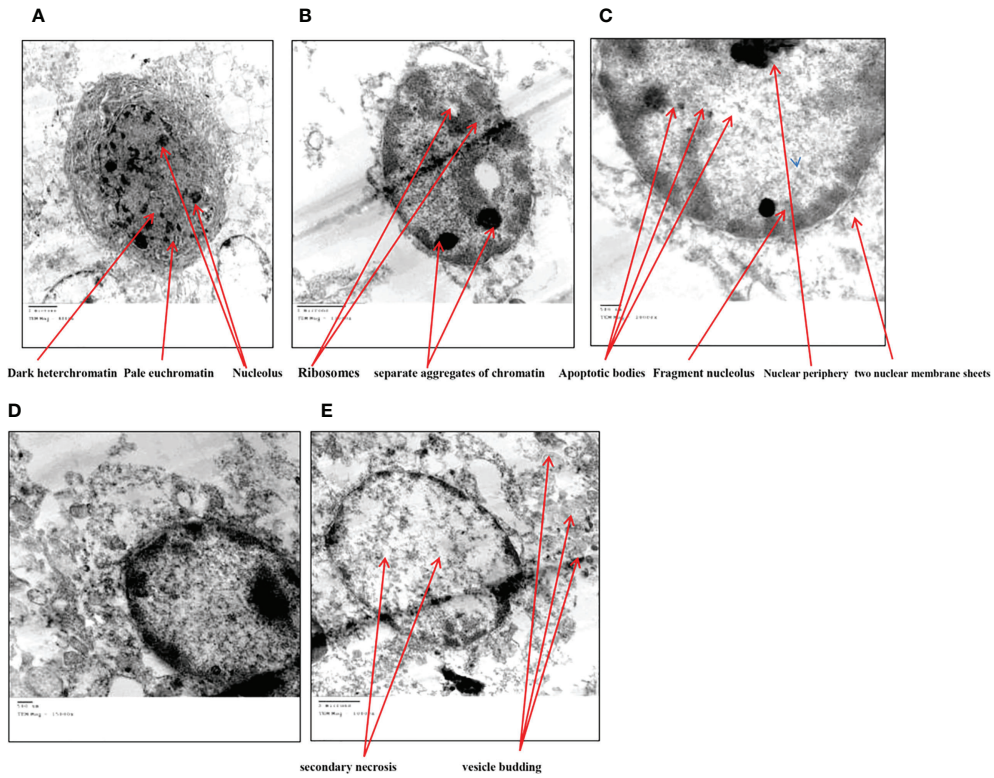

FIGURE 13
Transmission electron microscope of HuH7 exposed to 100 µg/ml of ZnO nanospheres (ZnO-NS) for 24 hour. **(A)** Control cell **(B)** Treated cell with to 100 µg/ml of ZnO nanospheres (ZnO-NS) for 3 hour. **(C)** Treated cell with to 100 µg/ml of ZnO nanospheres (ZnO-NS) for 6 hour. **(D)** Treated cell with to 100 µg/ml of ZnO nanospheres (ZnO-NS) for 12 hour. **(E)** Treated cell with to 100 µg/ml of ZnO nanospheres (ZnO-NS) for 24 hour.

its anticancer activity, but it has severe cytotoxicity and may lead to adverse events (46). Previous research suggested that zinc oxide nanoparticles could be used as an anticancer drug agent by targeting cancerous cells and increasing cytotoxicity and cell death (47). Due to their less toxic nature toward normal cells, zinc oxide nanoparticles haven't had any adverse effects on liver and renal tissues. Basically, the positive charge of a nanoparticle has more affinity to be engulfed by cells than neutral or negative nanoparticles. It is supposedly due to favorable electrostatic interactions with the negatively charged cell membrane (48). The surface of zinc oxide nanoparticles has a neutral hydroxyl group, which plays a central role in nanoparticle charging behavior (49). In an acidic medium, the proton more likely to bind to the surface of a nanoparticle may cause a positively charged surface ($ZnOH^{2+}$). However, in an alkaline medium, protons moved away from the metal surface, inducing a negatively charged surface partly bonded oxygen atom (ZnO^{-}). Under physiological conditions (acidic medium of tumor cells), the isoelectric point value ranges from 9 to 10, indicating that zinc oxide nanoparticles have a strongly positive-charged surface (50). Cancer cell outer layer membranes are characterized by the presence of a large number of anionic phospholipids (48). As a result, ZnO-NPs may be attracted electrostatically to tumor tissues, increasing nanoparticle cellular uptake (51). In contrast, normal healthy cells are either charge-neutral or slightly positive, which shows insignificant binding to the NPs (52). Also, the circulation of nanoparticles with a size less than 100 nm takes a longer time with the ability to avoid clearance by the reticuloendothelial system, also increasing intratumor concentrations (53, 54).

Mechanism of preparation of zinc oxide nanosphere

The preparation of zinc oxide nanospheres meets the concept of green chemistry. Green synthesis of nanomaterials is an interesting topic of material science research (55). This study was focused on the construction of zinc oxide nanospheres based on the accumulation of zinc ions on yeast extract, which was used as a bio-template (29). The plausible mechanism to explain the formation of zinc oxide nanospheres is that the dissolution of zinc acetate in distilled water released zinc ions that accumulated on the outer surface of yeast extract. Then, zinc ions formed on a spherical yeast extract. Afterwards, gradual thermal treatment leads to the formation of zinc oxide nanospheres and the removal of any yeast extract residuals. The physicochemical techniques such as FTIR, XR, DLS, and TEM emphasized the formation of ZnO nanoparticles in a spherical shape of 20 nm. ICP-AS is the routine method to evaluate the amount of zinc ions released from suspended ZnO nanospheres.

Cytotoxicity and apoptosis of zinc oxide nanospheres against HuH7 and Vero cells

The antiproliferative effect of ZnO-NS and Zn^{+2} ions was determined using the MTT assay, which links directly to the mitochondrial enzymes (25). Our results showed a significant reduction in HuH7 viability in the treated groups compared with the nontreated group. Therefore, the ZnO nanospheres are more selective for cancerous cells than normal cells. The cell cycle is controlled by numerous mechanisms that ensure correct cell division. It is a transition between various phases mediated by different cellular proteins. It divides the cell into two consecutive processes, the majority of which are characterized by DNA replication and the segregation of replication chromosomes into two separate cells. Our findings show that ZnO nanospheres induced cell cycle arrest at the G2/M phase and aided in the inhibition of HuH7 cell proliferation. The cells can be able to initialize a cell cycle arrest in the presence or absence of P53. Interestingly, maintenance of CDK1 in its inhibitory phosphorylation state prevents cell cycle entry into mitosis. Also, P53 may play a central role in the regulation of the G2/M checkpoint and DNA damage-dependent increases in p53 (53). The Annexin V-FITC/PI double-staining assay indicates the occurrence of apoptosis. Treatment of HuH7 and Vero cells with different concentrations as well as different times confirmed that the ZnO nanospheres have a less adverse effect on normal cells. Importantly, the apoptosis process depends on the activation of caspase, which is considered a hallmark of apoptosis (56). Indeed, caspase results emphasized that caspase induces the apoptotic mechanism.

Molecular mechanism of zinc oxide nanospheres against HuH7 and Vero cells

Generally, zinc oxide nanoparticles may promote micropinocytosis. Hence, ROS toxicity after ZnO NPs uptake led to ZnO genotoxicity *in vitro* and *in vivo*. In particular, lacking normal TP53, which is the typical feature of small-cell lung cancer, should be taken into account for the use of ZnO treatment for small-cell lung cancer (27). Setyawati and colleagues reported that DLD1 and SW480 cells that have mutant TP53 produce more ROS by ZnO nanoparticles, and those cells were more susceptible to the cytotoxicity than

NCM460 and HCT116 cells that have functional TP53 (57). Lee and colleagues reported that the ATM protein reacts to ROS and is necessary to phosphorylate TP53 (Ser 15) under ROS-induced oxidative stress. The loss of normal ATM protein results in deficiencies in mitochondrial function, autophagy, and intracellular protein aggregation (58). In addition, damaged mitochondria also produce intracellular ROS (27). RT-PCR, flowcytometry, and immunoblotting are common techniques to study the molecular mechanisms of apoptosis like P53, Bax, Bcl_2, and cytochrome C. As Figure 14 shows, there are a couple of mechanisms that meet the concept of apoptosis. The first one is the extrinsic pathway, which depends on ligation of the death receptor family, followed by the formation of the death-inducing signaling complex that leads to the activation of caspase (55). The second mechanism is the intrinsic pathway that depends on the pro and anti-apoptotic pathways of Bcl-2 family proteins. Furthermore, the mitochondrial cytochrome C release facilitates the formation of the apoptosome complex that cleaves and activates the effector caspase (56, 59). Also, there is another approach to inducing apoptosis by activating P53 to engage the mitochondria and release cytochrome C. Caspase 3 assay displayed that the mechanism of zinc oxide nanosphere is an extrinsic pathway that depends on ligation of the death receptor family, followed by the formation of the death-inducing signaling complex that leads to the activation of caspase (59).

Oxidative stress of zinc oxide nanospheres

Oxidative stress, including H_2O_2, $^{\cdot}OH$, and. O^{2-}, may react with nucleophilic centers, leading to DNA fragmentation and apoptosis upregulation, ultimately leading to carcinoma cell death (25). Our findings agree with Bai et al. (60) who reported a significant increase in the DNA damage in the ZnO-NP-treated group compared with the nontreated SEC group. Treatment of HuH7 cells with ZnO nanospheres caused an increase in pro-oxidants (ROS and LPO). According to Finucane et al. (1999), ZnO nanoparticles generate reactive oxygen species that activate the peroxidation reactions (55). Also, as Figure 14 shows, the elevated ROS level can inflict direct damage to lipids (61, 62). Because of its reaction with thiobarbituric acid (TBA), MDA is regarded as a useful biomarker for the peroxidation of omega-3 and omega-6 fatty acids. Similarly, excessive Zn^{2+} ions trigger harmful oxidative stress. According to Lee et al. (2018), zinc deficiency or excess can cause cellular oxidative stress (63, 64). Hence, liberated zinc ions released from suspended zinc oxide nanospheres medium indirectly contributed to stimulating the oxidative stress on HuH7 cells. Moreover, GSH, SOD, and NO attenuated the deleterious effect of ROS. GSH was an important ROS scavenger. An enzyme catalyses the transformation of the

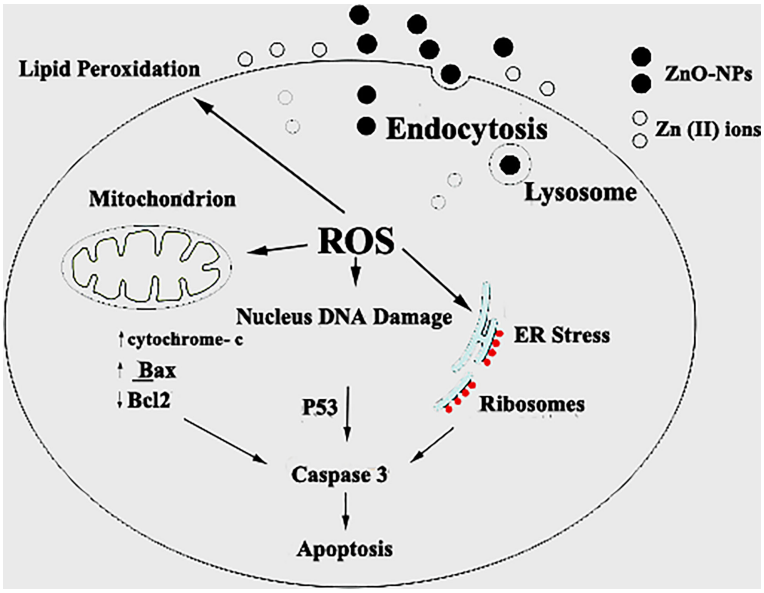

FIGURE 14
Schematic diagram of the probable mechanism of synergy of ZnO-NS. ZnO-NS are involved in reactive oxygen species (ROS) generation and increased cell wall lipid peroxidation (LPO) leading to cytotoxic and genotoxic effects.

highly reactive O^{-2} to H_2O_2. Also, NO is a special scavenger against ROS (61). Our findings support the findings of Xia et al. (65), who found that ZnO-NPs increase cancer cytotoxicity and cell death. Other studies have shown that increased ROS levels cause oxidative damage to cellular structures and decrease antioxidant enzymes SOD and CAT activity in tumor tissue compared to the SEC group, as SOD catalyzes the dismutation of superoxide anion (O_2) to H_2O_2 and O_2, and the CAT enzyme reduces H_2O_2 to H_2O. Interestingly, treatment with ZnO-NPs revealed a marked increase in MDA levels, which indicates lipid peroxidation and depletion of GSH in ESC tissues (25). Also, some studies have reported that both solid ZnO-NPs as well as dissolved Zn ions are responsible for the toxic responses of exposed cells (62). Heim et al. (66) found higher values of Zn^{2+} in the nucleus compared to the cytoplasm, indicating the enrichment of dissolved Zn^{2+}. However, contrary to this observation, Sharma et al. (67) also addressed the Zn^{2+} contribution towards the ZnO-NPs toxicity These authors observed that toxic responses from exposure to ZnO-NPs are due to the NPs per se rather than the Zn^{2+} released from them.

Ultrastructural analysis of zinc oxide nanospheres against hepatoma

The transmission electron microscope (TEM) has become a standard method for describing and analyzing the ultrastructure of inner cells and organelles in physiological and pathological conditions (68). TEM is the most powerful morphological method to describe apoptosis and necrosis. Its images are qualitative and static. As a result, the best method for studying apoptotic and necrotic phenomena should be carried out at different times, beginning with their early-stage appearance (69). Apoptosis is a regulated process that controls many morphological and physiological pathways in an active manner. It's characterized by various biochemical processes with cascades that respond to the change in the morphology of the cell that may lead to the death of the cell. Multi-factors control the type of cell termination. The main role of apoptosis is caspase activation, which influences the level of intracellular ATP. As a result, mitochondria are concerned with this type of cell death. During the apoptosis process, the cell size shrinks and loses connectivity with adjacent cells. The cells miss their surface elements such as microvilli and cell-to-cell linkage. Because of the liberation of the cell fluid, the cytoplasm will condensate, leading to a change in the cell volume. Therefore, the convolution of the nuclear and cellular outlines Initially, condensed chromatin tends toward the formation of cup-shaped masses beneath the nuclear envelope to fill thymocyte cells that occupy most of the nuclear volume (56). Finally, the apoptosis process will undergo progressive fragmentation, leading to the formation of several plasma membrane-bound apoptotic bodies, including nuclear and/or cytoplasmic elements (70). On the other hand, necrosis is another form of cell deletion. In the necrosis process, the plasma membrane will be permeable rapidly. Generally, cell hydration and swelling, as well as organelle disruption, appear. Inflammation is caused by the release of cytosolic components into the extracellular space (71–74). In contrast to the apoptosis process, the nucleus shape appears well in the early stages. Transmission electron microscopy analysis of HuH7 cells exposed to zinc oxide nanospheres demonstrated the stages of apoptosis. However, vacuolization was also demonstrated. Some of these vacuoles were double membrane bound vesicles, as shown in Figure 14. These vacuoles include residual cristae structure and may be due to mitochondrial swelling. As Harris and Ralph (1985) (75) reported, the apoptotic condition can induce a cell to differentiate. That can transfer the cell to a partial differentiation state (75–80).

Conclusion

We conclude empirical evidence of the genotoxic anticancer effects of ZnO in hepatic cancer cells, which may be executed safer and more effective antitumor activity, leading to SEC growth reduction as shown in Figure 14, with a low cytotoxic effect on normal cells. Therefore, new therapeutic strategies for cancer treatment, including ZnO-NS, could be developed. Moreover, long-term toxicity studies are required to rule out any long-term side effects. Overall, the data showed that ZnO nanospheres might have a good choice as a potential candidate as an anti-tumor agent.

Data availability statement

The original contributions presented in the study are included in the article/Supplementary Material. Further inquiries can be directed to the corresponding author.

Author contributions

Conceptualization: AH and AM; formal analysis: AH; funding acquisition: AH, FA-S, ED, FA, and HAA; investigation: AH, AM, and AE; investigation: MH, Wagih M. Adelhay, TM, FAE-F, and EF; methodology: AH, TA, and EM; project administration: AH and AE; Resource: AE; supervision: AH; Validation: AH, AE, and AM; visualization: AE, ES, MZ, HEA, MA, and AH; writing original draft: AH and AM; writing -review edition; AH and AM. All author approved the final version of the manuscript.

Funding

This work was fully supported by Taif University Researchers supporting project number (TURSP-2020/113), Taif University, Saudi Arabia.

Acknowledgments

The authors would like to thank the Deanship of Scientific Research at Taif University for funding this work through Taif University Researchers Supporting Project number (TURSP - 2020/113), Taif University, Taif, Saudi Arabia.

Conflict of interest

The authors declare that the research was conducted in the absence of any commercial or financial relationships that could be construed as a potential conflict of interest.

Publisher's note

Supplementary material

The Supplementary Material for this article can be found online at: https://www.frontiersin.org/articles/10.3389/fonc.2022.933750/full#supplementary-material

SUPPLEMENTAL IMAGE S1
Bax/bcl2 ratio.

References

1. Bruix J, Raoul JL, Sherman M, Mazzaferro V, Bolondi L, Craxi A, et al. Efficacy and safety of sorafenib in patients with advanced hepatocellular carcinoma: subanalyses of a phase III trial. *J Hepatol* (2012) 57(4):821–9. doi: 10.1016/j.jhep.2012.06.014

2. Jemal A, Bray F, Center MM, Ferlay J, Ward E, Forman D. Global cancer statistics. *CA: Cancer J Clin* (2011) 61(2):69–90. doi: 10.3322/caac.20107

3. Sawada Y, Yoshikawa T, Nobuoka D, Shirakawa H, Kuronuma T, Motomura Y, et al. Phase I trial of a glypican-3–derived peptide vaccine for advanced hepatocellular carcinoma: immunologic evidence and potential for improving overall survival. *Clin Cancer Res* (2012) 18(13):3686–3696. doi: 10.1158/1078-0432.CCR-11-3044

4. Feo F, Simile MM, Pascale RM. Focal loss of long non-coding RNA-PRAL, as determinant of cell function and phenotype of hepatocellular carcinoma. *Ann Trans Med* (2016) 4(9):183. doi: 10.21037/atm.2016.03.47

5. Ries LA, Harkins D, Krapcho M, Mariotto A, Miller BA, Feuer EJ, et al. *SEER cancer statistics review, 1975–2005*. Bethesda, MD: National Cancer Institute (2008), 2999. http://seer.cancer.gov/csr/1975_2005.

6. Nakabayashi H, Taketa K, Miyano K, Yamane T, Sato J. Growth of human hepatoma cell lines with differentiated functions in chemically defined medium. *Cancer Res* (1982) 42(9):3858–63.

7. Goldring CE, Kitteringham NR, Jenkins R, Lovatt CA, Randle LE, Abdullah A, et al. Development of a transactivator in hepatoma cells that allows expression of phase I, phase II, and chemical defense genes. *Am J Physiology-Cell Physiol* (2006) 290(1):C104–15. doi: 10.1152/ajpcell.00133.2005

8. Yoon HI, Seong J. Multimodality treatment involving radiotherapy for advanced liver-confined hepatocellular carcinoma. *Oncology* (2014) 87 (Suppl.1):90–8. doi: 10.1159/000368151

9. Yeo W, Mok TS, Zee B, Leung TW, Lai PB, Lau WY, et al. A randomized phase III study of doxorubicin versus cisplatin/interferon α-2b/doxorubicin/fluorouracil (PIAF) combination chemotherapy for unresectable hepatocellular carcinoma. *J Natl Cancer Institute* (2005) 97(20):1532–8. doi: 10.1093/jnci/dji315

10. Gish RG, Porta C, Lazar L, Ruff P, Feld R, Croitoru A, et al. Phase III randomized controlled trial comparing the survival of patients with unresectable hepatocellular carcinoma treated with nolatrexed or doxorubicin. *J Clin Oncol* (2007) 25(21):3069–75. doi: 10.1200/JCO.2006.08.4046

11. Wang XQ, Ongkeko WM, Chen L, Yang ZF, Lu P, Chen KK, et al. Octamer 4 (Oct4) mediates chemotherapeutic drug resistance in liver cancer cells through a potential Oct4–AKT–ATP-binding cassette G2 pathway. *Hepatology* (2010) 52 (2):528–39. doi: 10.1002/hep.23692

12. Ohta K, Hoshino H, Hata K, Wang J, Huang S, Menon V, et al. MicroRNA mir-93 activates oncogenic c-Met/PI3K/Akt pathway targeting PTEN in hepatocellular carcinoma. *Cancer Res* (2014) 74(19_Supplement):4686–86. doi: 10.1158/1538-7445.AM2014-4686

13. Siegel R, Ward E, Brawley O, Jemal A. The impact of eliminating socioeconomic and racial disparities on premature cancer deaths. *Ca-a Cancer J Clin* (2011) 61(4):212–36. doi: 10.3322/caac.20121

14. Iwamoto H, Torimura T, Nakamura T, Hashimoto O, Inoue K, Kurogi J, et al. Metronomic s-1 chemotherapy and vandetanib: an efficacious and nontoxic treatment for hepatocellular carcinoma. *Neoplasia* (2011) 13(3):187–97. doi: 10.1593/neo.101186

15. Peck-Radosavljevic M. Drug therapy for advanced-stage liver cancer. *Liver Cancer* (2014) 3(2):125–31. doi: 10.1159/000343868

16. Schwarz M, Andrade-Navarro MA, Gross A. Mitochondrial carriers and pores: key regulators of the mitochondrial apoptotic program? *Apoptosis* (2007) 12 (5):869–76. doi: 10.1007/s10495-007-0748-2

17. Hassan A, Elebeedy D, Matar ER, Fahmy Mohamed Elsayed A, Abd El Maksoud AI. Investigation of angiogenesis and wound healing potential mechanisms of zinc oxide nanorods. *Front Pharmacol* (2021) 12:661217. doi: 10.3389/fphar.2021.661217

18. An WG, Kanekal M, Simon MC, Maltepe E, Blagosklonny MV, Neckers LM. Stabilization of wild-type p53 by hypoxia-inducible factor 1α. *Nature* (1998) 392 (6674):405–8. doi: 10.1038/32925

19. Fakruddin M, Hossain Z, Afroz H. Prospects and applications of nanobiotechnology: a medical perspective. *J nanobiotechnology* (2012) 10(1):1–8. doi: 10.1186/1477-3155-10-31

20. Siddiqui SA, Or Rashid M, Uddin M, Robel FN, Hossain MS, Haque M, et al. Biological efficacy of zinc oxide nanoparticles against diabetes: a preliminary study conducted in mice. *Bioscience Rep* (2020) 40(4):BSR20193972. doi: 10.1042/BSR20193972

21. Sharaf EM, Hassan A, AL-Salmi FA, Albalwe FM, Albalaw HMR, Darwish DB, et al. Synergistic antibacterial activity of compact silver/magnetite core-shell nanoparticles core shell against gram-negative foodborne pathogens. *Front Microbiol* (2022) 13:929491. doi: 10.3389/fmicb.2022.929491

22. Nagajyothi PC, Cha SJ, Yang IJ, Sreekanth TVM, Kim KJ, Shin HM. Antioxidant and anti-inflammatory activities of zinc oxide nanoparticles synthesized using polygala tenuifolia root extract. *J Photochem Photobiol B: Biol* (2015) 146:10–7. doi: 10.1016/j.jphotobiol.2015.02.008

23. Hassan A, Sorour NM, El-Baz A, Shetaia Y. Simple synthesis of bacterial cellulose/ magnetite nanoparticles composite for the removal of antimony from

aqueous solution. *Internati onal J Environ Sci Technol* (2019) 16:1433–48. doi: 10.1007/s13762-018-1737-4

24. Anjum S, Hashim M, Malik SA, Khan M, Lorenzo JM, Abbasi BH, et al. Recent advances in zinc oxide nanoparticles (ZnO NPs) for cancer diagnosis, target drug delivery, and treatment. *Cancers* (2021) 13:4570. doi: 10.3390/cancers13184570

25. Nabil A, Elshemy MM, Asem M, Abdel-Motaal M, Gomaa HF, Zahran F, et al. Zinc oxide nanoparticle synergizes sorafenib anticancer efficacy with minimizing its cytotoxicity. oxidative medicine and cellular longevity, 2020.S.-e. jin and h. e. jin, "Synthesis, characterization, and threedimensional structure generation of zinc oxide-based nanomedicine for biomedical applications,". *Pharmaceutics* (2020) 11(11):575. doi: 10.1155/2020/1362104

26. Kielbik J, Kaszewski, Dominiak B, Damentko M, Serafińska I, Rosowska J, et al. Preliminary studies on biodegradable zinc oxide nanoparticles doped with fe as a potential form of iron delivery to the living organism. *Nanoscale Res Lett* (2019) 14(1):373. doi: 10.1186/s11671-019-3217-2

27. Tanino R, Amano Y, Tong X, Sun R, Tsubata Y, Harada M, et al. Anticancer activity of ZnO nanoparticles against human small-cell lung cancer in an orthotopic mouse ModelZnO nanoparticles inhibit growth of small-cell lung cancer. *Mol Cancer Ther* (2020) 19(2):502–12. doi: 10.1158/1535-7163.MCT-19-0018

28. Fujihara J, Tongu M, Hashimoto H, Yamada T, Kimura-kataoka K, Yasuda T, et al. Distribution and toxicity evaluation of ZnO dispersion nanoparticles in single intravenously exposed mice. *J Med Invest* (2015) 62:45–50. doi: 10.2152/jmi.62.45

29. Wang J, Deng X, Zhang F, Chen D, Ding W. ZnO nanoparticle-induced oxidative stress triggers apoptosis by activating JNK signaling pathway in cultured primary astrocytes. *Nanoscale Res Lett* (2014) 9(1):1–12. doi: 10.1186/1556-276X-9-117

30. Bao SJ, Lei C, Xu MW, Cai CJ, Jia DZ. Environment-friendly biomimetic synthesis of TiO2 nanomaterials for photocatalytic application. *Nanotechnology* (2012) 23(20):205601. doi: 10.1088/0957-4484/23/20/205601

31. Tada-Oikawa S, Ichihara G, Suzuki Y, Izuoka K, Wu W, Yamada Y, et al. Zn (II) released from zinc oxide nano/micro particles suppresses vasculogenesis in human endothelial colony-forming cells. *Toxicol Rep* (2015) 2:692–701. doi: 10.1016/j.toxrep.2015.04.003

32. Mosmann T. Rapid colorimetric assay for cellular growth and survival: application to proliferation and cytotoxicity assays. *J Immunol Methods* (1983) 65 (1-2):55–63. doi: 10.1016/0022-1759(83)90303-4

33. Pal A, Alam S, Mittal S, Arjaria N, Shankar J, Kumar M, et al. UVB irradiation-enhanced zinc oxide nanoparticles-induced DNA damage and cell death in mouse skin. *Mutat Research/Genetic Toxicol Environ Mutagenesis* (2016) 807:15–24. doi: 10.1016/j.mrgentox.2016.06.005

34. Hamouda RA, Abd El Maksoud AI, Wageed M, Alotaibi AS, Elebeedy D, Khalil H, et al. Characterization and anticancer activity of biosynthesized Au/Cellulose nanocomposite from chlorella vulgaris. *Polymers* (2021) 13:3340. doi: 10.3390/polym13193340

35. Khella KF, Abd El Maksoud AI, Hassan A, Abdel-Ghany SE, Elsanhoty RM, Aladhadh MA, et al. Carnosic acid encapsulated in albumin nanoparticles induces apoptosis in breast and colorectal cancer cells. *Molecules* (2022) 27(13):4102. doi: 10.3390/molecules27134102

36. Taher RF, Al-Karmalawy AA, Abd El Maksoud AI, Khalil H, Hassan A, El-Khrisy EDA, et al. Two new flavonoids and anticancer activity of hymenosporum flavum: *in vitro* and molecular docking studies. *J Herbmed Pharmacol* (2021) 10 (4):443–58. doi: 10.34172/jhp.2021.52

37. Akhtar MJ, Ahamed M, Kumar S, Khan MM, Ahmad J, Alrokayan SA. Zinc oxide nanoparticles selectively induce apoptosis in human cancer cells through reactive oxygen species. *Int J nanomedicine* (2012) 7:845. doi: 10.2147/IJN.S29129

38. Del Principe MI, Dal Bo M, Bittolo T, Buccisano F, Rossi FM, Zucchetto A, et al. Clinical significance of bax/bcl-2 ratio in chronic lymphocytic leukemia. *haematologica* (2016) 101(1):77. doi: 10.3324/haematol.2015.131854

39. Ohkawa H, Ohishi N, Yagi K. Assay for lipid peroxides in animal tissues by thiobarbituric acid reaction. *Analytical Biochem* (1979) 95(2):351–8. doi: 10.1016/0003-2697(79)90738-3

40. Mbazima VG, Mokgotho MP, February F, Rees DJG, Mampuru LJM. Alteration of bax-to-Bcl-2 ratio modulates the anticancer activity of methanolic extract of commelina benghalensis (Commelinaceae) in jurkat T cells. *Afr J Biotechnol* (2008) 7(20).

41. Ellman GL. Tissue sulfhydryl groups. *Arch Biochem biophysics* (1959) 82 (1):70–7. doi: 10.1016/0003-9861(59)90090-6

42. Green LC, Wagner DA, Glogowski J, Skipper PL, Wishnok JS, Tannenbaum SR. Analysis of nitrate, nitrite, and [15N] nitrate in biological fluids. *Analytical Biochem* (1982) 126(1):131–8. doi: 10.1016/0003-2697(82)90118-X

43. Bozzola JJ, Russell LD. *Electron microscopy: principles and techniques for biologists*. Jones & Bartlett Learning (1999).

44. Astolfi L, Ghiselli S, Guaran V, Chicca M, Simoni E, Olivetto E, et al. Correlation of adverse effects of cisplatin administration in patients affected by solid tumours: a retrospective evaluation. *Oncol Rep* (2013) 29(4):1285–92. doi: 10.3892/or.2013.2279

45. Nabil A, Elshemy MM, Asem M, Abdel-Motaal M, Gomaa HF, Zahran F, et al. Zinc oxide nanoparticle synergizes sorafenib anticancer efficacy with minimizing its cytotoxicity. *Oxid Med Cell Longevity* (2020) 2020:11. doi: 10.1155/2020/1362104

46. Ekenel M, Iwamoto FM, Ben-Porat LS, Panageas KS, Yahalom J, DeAngelis LM, et al. Primary central nervous system lymphoma: the role of consolidation treatment after a complete response to high-dose methotrexate based chemotherapy. *Cancer Res* (2008) 113(5):1025–31. doi: 10.1002/cncr.23670

47. Liu C-Y, Tseng LM, Su JC, Chang KC, Tai WT, Shiau CW, et al. Novel sorafenib analogues induce apoptosis through SHP-1 dependent STAT3 inactivation in human breast cancer cells. *Breast Cancer Res* (2013) 15(4):3254. doi: 10.1186/bcr3457

48. Rasmussen JW, Martinez E, Louka P, Wingett DG. Zinc oxide nanoparticles for s elective destruction of tumor cells and potential for drug delivery applications. *Expert Opin Drug Delivery* (2010) 7(9):1063–77. doi: 10.1517/17425247.2010.502560

49. Kundu M, Sadhukhan P, Ghosh N, Chatterjee S, Manna P, Das J, et al. pH-responsive and targeted delivery of curcumin via phenylboronic acid-functionalized ZnO nanoparticles for breast cancer therapy. *J Advanced Res* (2019) 18:161–72. doi: 10.1016/j.jare.2019.02.036

50. Forest V, Pourchez J. Preferential binding of positive nanoparticles on cell membranes is due to electrostatic interactions: a too simplistic explanation that does not take into account the nanoparticle protein corona. *Materials Sci Eng* (2017) 70:889–96. doi: 10.1016/j.msec.2016.09.016

51. Qu F, Morais PC. The pH dependence of the surface charge density in oxide-based semiconductor nanoparticles immersed in aqueous solution. *IEEE Trans Magnetics* (2001) 37:2654–6. doi: 10.1109/20.951264

52. Degen A, Kosec M. Effect of pH and impurities on the surface charge of zinc oxide in aqueous solution. *J Eur Ceramic Soc* (2000) 20(6):667–73. doi: 10.1016/S0955-2219(99)00203-4

53. Peetla C, Vijayaraghavalu S, Labhasetwar V. Biophysics of cell membrane lipids in cancer drug resistance: implications for drug transport and drug delivery with nanoparticles. *Advanced Drug Delivery Rev* (2013) 65(13-14):1686–1698. doi: 10.1016/j.addr.2013.09.004

54. Le W, Chen B, Cui Z, Liu Z, Shi D. Detection of cancer cells based on glycolytic-regulated surface electrical charges. *Biophysics Rep* (2019) 5(1):10–8. doi: 10.1007/s41048-018-0080-0

55. Brannon-Peppas L, Blanchette JO. Nanoparticle and targeted systems for cancer therapy. *Advanced Drug Delivery Rev* (2004) 56(11):1649–59. doi: 10.1016/j.addr.2004.02.014

56. Qu Y, Kang M, Cheng X, Zhao J. Chitosan-coated titanium dioxide-embedded paclitaxel nanoparticles enhance anti-tumor efficacy against osteosarcoma. *Front Oncol* (2020) 10:1837. doi: 10.3389/fonc.2020.577280

57. Setyawati MI, Tay CY, Leong DT. Effect of zinc oxide nanomaterials-induced oxidative stress on the p53 pathway. *Biomaterials* (2013) 34:10133–42.41. doi: 10.1016/j.biomaterials.2013.09.024

58. Lee JH, Mand MR, Kao CH, Zhou Y, Ryu SW, Richards AL, et al. ATM Directs DNA damage responses and proteostasis via genetically separable pathways. *Sci Signal* (2018) 11:eaan5598. doi: 10.1126/scisignal.aan5598

59. Vermeulen K, Van Bockstaele DR, Berneman ZN. The cell cycle: a review of regulation, deregulation and therapeutic targets in cancer. *Cell proliferation* (2003) 36(3):131–49. doi: 10.1046/j.1365-2184.2003.00266.x

60. Bai D-P, Zhang XF, Zhang GL, Huang YF, Gurunathan S. Zinc oxide nanoparticles induce apoptosis and autophagy in human ovarian cancer cells. *Int J Nanomedicine* (2017) 12:6521–35. doi: 10.2147/IJN.S140071

61. Zhuo Z, Hu J, Yang X, Chen M, Lei X, Deng L, et al. Ailanthone inhibits Huh7 cancer cell growth *via* cell cycle arrest and apoptosis *in vitro* and *in vivo*. *Sci Rep* (2015) 5(1):1–15. doi: 10.1038/srep16185

62. Luo X, Budihardjo I, Zou H, Slaughter C, Wang X. Bid, a Bcl2 interacting protein, mediates cytochrome c release from mitochondria in response to activation of cell surface death receptors. *Cell* (1998) 94(4):481–90. doi: 10.1016/S0092-8674(00)81589-5

63. Li H, Zhu H, Xu CJ, Yuan J. Cleavage of BID by caspase 8 mediates the mitochondrial damage in the fas pathway of apoptosis. *Cell* (1998) 94(4):491–501. doi: 10.1016/S0092-8674(00)81590-1

64. Julia H, Eva F, Nawaz MT, Anke K, Ulf RH, Christoph B, et al. Genotoxic effects of zinc oxide nanoparticles. *Nanoscale* (2015) 7:8931–8. doi: 10.1039/C5NR01167A

65. Xia T, Kovochich M, Brant J, Hotze M, Sempf J, Oberley T, et al. Comparison of the abilities of ambient and manufactured nanoparticles to induce cellular toxicity according to an oxidative stress paradigm. *Nano Lett* (2006) 6(8):1794–807. doi: 10.1021/nl061025k

66. Song W, Zhang J, Guo J, Ding F, Li L, Sun Z. Role of the dissolved zinc ion and reactive oxygen species in cytotoxicity of ZnO nanoparticles. *Toxicol Lett* (2009) 199(3):389–97. doi: 10.1016/j.toxlet.2010.10.003

67. Sharma V, Anderson D, Dhawan A. Zinc oxide nanoparticles induce oxidative DNA damage and ROS-triggered mitochondria mediated apoptosis in human liver cells (HepG2). *Apoptosis* (2012) 17:852–70. doi: 10.1007/s10495-012-0705-6

68. Gross A, Yin XM, Wang K, Wei MC, Jockel J, Milliman C, et al. Caspase cleaved BID targets mitochondria and is required for cytochrome c release, while BCL-XL prevents this release but not tumor necrosis factor-R1/Fas death. *J Biol Chem* (1999) 274(2):1156–63. doi: 10.1074/jbc.274.2.1156

69. Finucane DM, Bossy-Wetzel E, Waterhouse NJ, Cotter TG, Green DR. Bax-induced caspase activation and apoptosis *via* cytochromec release from mitochondria is inhibitable by bcl-xL. *J Biol Chem* (1999) 274(4):2225–33. doi: 10.1074/jbc.274.4.2225

70. Moldovan L, Moldovan NI. Oxygen free radicals and redox biology of organelles. *Histochem Cell Biol* (2004) 122(4):395–412. doi: 10.1007/s00418-004-0676-y

71. Schneider C, Boeglin WE, Yin H, Porter NA, Brash AR. Intermolecular peroxyl radical reactions during autoxidation of hydroxy and hydroperoxy arachidonic acids generate a novel series of epoxidized products. *Chem Res Toxicol* (2008) 21(4):895–903. doi: 10.1021/tx700357u

72. Lee SR. Critical role of zinc as either an antioxidant or a prooxidant in cellular systems. *Oxid Med Cell Longevity* (2018) 2018:11. doi: 10.1155/2018/9156285

73. Bai W, Zhang Z, Tian W, He X, Ma Y, Zhao Y, et al. Toxicity of zinc oxide nanoparticles to zebrafish embryo: a physicochemical study of toxicity mechanism. *J Nanoparticle Res* (2010) 12(5):1645–54. doi: 10.1007/s11051-009-9740-9

74. Burattini S, Ferri P, Battistelli M, Curci R, Luchetti F, Falcieri E. C2C12 murine myoblasts as a model of skeletal muscle development: morpho-functional characterization. *Eur J Histochem* (2004) 48(3), 223–34. doi: 10.4081/891

75. Harris P, Ralph P. Human leukemic models of myelomonocytic development: a review of the HL-60 and U937 cell lines. *J leukocyte Biol* (1985) 37(4):407–22. doi: 10.1002/jlb.37.4.407

76. Di Baldassarre A, Secchiero P, Grilli A, Celeghini C, Falcieri E, Zauli G. Morphological features of apoptosis in hematopoietic cells belonging to the T-lymphoid and myeloid lineages. *Cell Mol Biol* (2000) 46(1):153–61.

77. Falcieri E, Luchetti F, Burattini S, Canonico B, Santi S, Papa S. Lineage-related sensitivity to apoptosis in human tumor cells undergoing hyperthermia. *Histochem Cell Biol* (2000) 113(2):135–44. doi: 10.1007/s004180050016

78. Golstein P, Kroemer G. Cell death by necrosis: towards a molecular definition. *Trends Biochem Sci* (2007) 32(1):37–43. doi: 10.1016/j.tibs.2006.11.001

79. Klöditz K, Fadeel B. Three cell deaths and a funeral: macrophage clearance of cells undergoing distinct modes of cell death. *Cell Death Discovery* (2019) 5 (1):65. doi: 10.1038/s41420-019-0146-x

80. Llovet JM, Hernandez-Gea V. Hepatocellular carcinoma: reasons for phase III failure and novel perspectives on trial design. *Clin Cancer Res* (2014) 20 (8):2072–9. doi: 10.1158/1078-0432.CCR-13-0547

frontiers | Frontiers in Oncology

TYPE Review
PUBLISHED 14 February 2023
DOI 10.3389/fonc.2023.1116532

OPEN ACCESS

EDITED BY
Yanmin Zhang,
Xi'an Jiaotong University, China

REVIEWED BY
Ke Shi,
Beijing Ditan Hospital, Capital Medical University, China
Emil Bulatov,
Kazan Federal University, Russia

*CORRESPONDENCE
Jinyao Li
ljyxju@xju.edu.cn
Lijie Xia
xlj@xju.edu.cn

SPECIALTY SECTION
This article was submitted to Pharmacology of Anti-Cancer Drugs, a section of the journal Frontiers in Oncology

RECEIVED 05 December 2022
ACCEPTED 31 January 2023
PUBLISHED 14 February 2023

CITATION
Wang Y, Li J and Xia L (2023) Plant-derived natural products and combination therapy in liver cancer.
Front. Oncol. 13:1116532.
doi: 10.3389/fonc.2023.1116532

Plant-derived natural products and combination therapy in liver cancer

Yuqin Wang, Jinyao Li* and Lijie Xia*

Xinjiang Key Laboratory of Biological Resources and Genetic Engineering, College of Life Science and Technology, Xinjiang University, Urumqi, China

Liver cancer is one of the malignant cancers globally and seriously endangers human health because of its high morbidity and mortality. Plant-derived natural products have been evaluated as potential anticancer drugs due to low side effects and high anti-tumor efficacy. However, plant-derived natural products also have defects of poor solubility and cumbersome extraction process. In recent years, a growing numbers of plant derived natural products have been used in combination therapy of liver cancer with conventional chemotherapeutic agents, which has improved clinical efficacy through multiple mechanisms, including inhibition of tumor growth, induction of apoptosis, suppression of angiogenesis, enhancement of immunity, reversal of multiple drug resistance and reduction of side effects. The therapeutic effects and mechanisms of plant-derived natural products and combination therapy on liver cancer are reviewed to provide references for developing anti-liver-cancer strategies with high efficacy and low side effects.

KEYWORDS

plant-derived natural products, immunotherapy, combination therapy, liver cancer, molecular mechanisms

Introduction

Liver cancer is one of the most common malignant cancers with more than 906,000 new cases and 830,000 deaths annually worldwide (1). Liver cancer has brought significant threats and challenges to human's physical and mental health as well as social and economic development (2). Currently, the main treatments for liver cancer include surgical resection (3), radiotherapy (4), chemotherapy (5), local ablation therapy (6) and liver transplantation (7). Although traditional therapies are effective for liver cancer at early stage, they have limited efficacy for advanced liver cancer due to severe side effect, drug resistance, multiple recurrences and metastases (8, 9). For the past few years, plant-derived natural products have been evaluated as potential anticancer drugs that preferentially kill tumor cells with low toxic effect on normal cells. A variety of plant-derived natural products with antitumor activities have been identified, such as alkaloids, terpenoids, phenols, flavonoids, which can inhibit tumor-cell invasion and migration (10), induce apoptosis (11), suppress angiogenesis (12) and proliferation (13). Although these plant-derived natural products have many advantages, such as abundant resources, low toxic effect and diversity in targets and molecular

mechanisms, they have limited efficacy for clinical application due to low solubility and poor bioavailability (14). Therefore, there is an urgent need to develop new therapy with high efficacy and low side effects to prevent and treat liver cancer.

Numerous studies have shown that combined therapy has great potential value in treating of liver cancer. The combination of chemotherapy with natural compounds is likely to increase the efficacy of drug treatment as well as reduce the adverse responses (15). Some natural products may sensitize to conventional cytotoxic therapy, reinforce the drug effective concentration, reverse drug resistance, intensify the combined effect of both administered therapeutics or exert cytotoxic effects specifically on tumor cells (16). Moreover, natural products combined with immunotherapy, can reduce the development of cancer and enhance the immune function by targeting multiple signaling pathways (17). The desired effect could be to diminish burden on the patient's organ by replacing part of the dose of a conventional chemotherapeutic with a natural substance with a defined effect. Many natural compounds are well tolerated by the patients and do not cause toxic effects even at high doses. Interaction of conventional chemotherapeutics with natural compounds introduces a new aspect in the research and therapy of cancer. It could be a complementing approach to potentially achieve improvements, while minimizing side effects associated with conventional chemotherapy. In this paper, we review the recent studies on the functions and mechanisms of plant-derived natural products and combination therapy in the treatment of liver cancer.

Search strategy

This review followed the PRISMA guidelines. The primary search for article screening used in this review was conducted using PubMed (387), CNKI (277), Web of science (236), X-MOL (193) and the Wanfang database (178), and the medical subject headings (natural product, liver cancer, combination). After completing the initial search, therefore to avoid duplication, we removed 550 articles from the literature, and selected 721 articles. After screening for eligibility of the articles, 128 articles were included in the study. PRISMA flow chart indicates only the identification and screening processes of the anti-liver-cancer activity of plant-derived plant products and combination therapy (Figure 1).

Plant-derived natural products in the treatment of liver cancer

Alkaloids

Alkaloid is a kind of basic organic compounds containing nitrogen in plants. The representative anti-tumor compounds include matrine, berberine, evodiamine, camptothecin, vincristine and caffeine. Matrine exists in dried roots of *Sophora flavescent* and induces HepG2 cell apoptosis through increasing Bax/Bcl-2 ratio and inhibiting the ERK1/2 signaling pathway (18). Dai et al. reported that matrine inhibits BEL-7402 cell and SMMC-7721 cell invasion and metastasis by upregulating the expression of microRNA-199a-5p (miR-199a-5p) and reduces the levels of hypoxia-inducible factor-1α (HIF-1α) (19). Moreover, matrine also inhibits liver cancer migration and induces apoptosis through increasing the expression of microRNA-345-5p (miR-345-5p) and reduces the levels of circular RNA_0027345 (circ_0027345) and homeobox-containingD3 (HOXD3) (20). In addition, Zhang et al. researched that matrine at non-toxic dose could significantly suppress PLC/PRF/5 and MHCC97L cells migration and invasion. And, it also significantly decreased lung metastasis in orthotopic HCC mouse models (21). Berberine, an isoquinoline alkaloid, has been extracted from the rhizome of *Coptis* and *Phellodendri* and considered as anticancer drug in China because of its wide range of pharmacological effects. Berberine induced autophagy of HepG2 and MHCC97-L cells through activating Beclin-1 *via* enhancing p38 mitogen-activated protein kinase (MAPK) signaling pathway and inhibiting protein kinase B (Akt) activity (22). Hou et al. researched that berberine decreased the expression of CD147, thereby induced apoptosis of HepG2 and SMMC7721 cells in a dose-and time-dependent manner (23). In addition, berberine inhibits transforming growth factor-β/Smad (TGF-β/Smad) signaling pathway and interferes epithelial-mesenchymal transition (EMT), thereby inhibiting migration and invasion of HepG2 cells (24). A study showed that evodiamine induced apoptosis of HepG2 and PLHC-1 cells in a dose-dependent manner by inactivating phosphatidylinositol 3-kinase (PI3K) signaling pathway, downregulating B-cell lymphoma 2 (Bcl-2) expression and upregulating Bcl-2-associated X protein (Bax) (25). Evodiamine can also inhibit the proliferation of hepatocellular carcinoma cells by activating Hippo-Yes-associated protein signaling pathway *in vitro* and *in vivo* (26). Camptothecin has been used clinically to treat liver cancer, stomach and colorectal cancer for a long time, which can inhibit Huh7 and H22 cell proliferation,

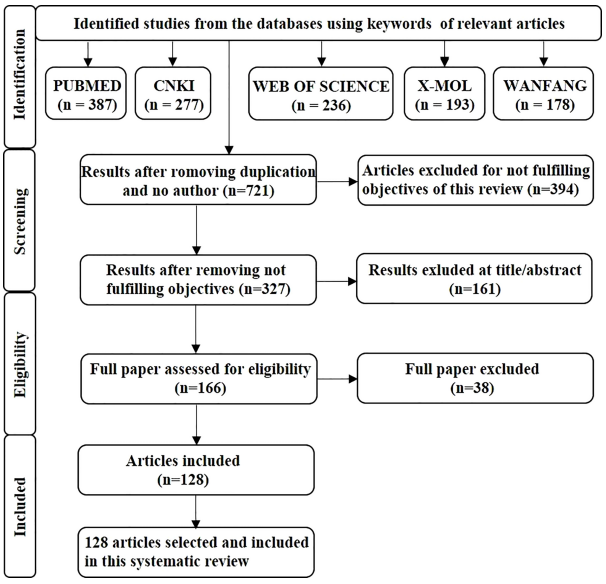

FIGURE 1
The flowchart provides an overview of the study search and selection process. A search of the databases PubMed, CNKI, Web of Science, X-MOL, and the Wanfang database was undertaken, and then duplicate articles and any which did not meet the criteria of our study were removed before the relevant articles were selected for further study.

metastasis and angiogenesis by upregulating of reactive oxygen species (ROS) and nuclear factor E2-related factor 2 (Nrf2) expression, reducing the expression of N-cadherin, matrix metalloproteinase 9 (MMP9), Snail and Twist, and increasing E-cadherin (27). Notably, 10-hydroxycamptothecin (0.5 mg/L) inhibited the proliferation of BEL-7402 cells through induction of apoptosis, and showed synergistic effect with human cytokine-induced killer cells (optimal target ratio of 20:1) (28). According to reports, vincristine could decrease the expression of Ki-67, MMP2 and MMP9, and increase the expression of cleaved caspase 3, thereby inhibiting proliferation and reducing metastasis by PI3K/Akt signaling pathway in Hep3B cells (29). Caffeine is an alkaloids compound extracted from tea, cocoa bean and coffee fruit. Caffeine and X-ray irradiation have synergistic effect on the inhibition of cell proliferation and induction of apoptosis, and cell cycle arrest at G2/M phase (30). Cinchonine is a natural compound present in Cinchona bark. It exerts multidrug resistance reversal activity and synergistic apoptotic effect with paclitaxel in uterine sarcoma cells. Jin et al. demonstrated that cinchonine inhibited liver cancer cell proliferation and promoted apoptosis in a dose-dependent manner. It can activate caspase-3 and PARP1 cleavage, increased the expression of GRP78 and PERK, and suppressed HepG2 xenograft tumor growth in mice (31). As a transcription factor, the tumor suppressor p53 can participate in many important biological processes, such as cell cycle arrest and apoptosis. It can activate the expression of antioxidant proteins such as catalase, glutathione peroxidase 1 (GPX 1), manganese superoxide dismutase (MnSOD), which leads to the imbalance of ROS, and finally leads to apoptotic (32). Moreover, Sanguinarine significantly inhibited liver cancer cell proliferation in a p53-dependent manner by inducing cell cycle arrest and ROS-associated apoptosis. Importantly, it dramatically suppressed tumor growth in an HCC xenograft model, with little cytotoxicity (33).

Terpenoids

Terpenoids are hydrocarbons and oxygenic derivatives in natural plants, which contain isoprene structure. It has been found that terpenoids have antitumor activities, such as saikosaponin D, triptolide, ginsenoside, artemisinin, celastrol and norcantharidin. Saikosaponin D is the most important active component of the Chinese medicinal herb *Bupleurum*, which can selectively up-regulate the protein expression of light chain 3II (LC3II) and Beclin 1, down-regulate the protein expression of P-S6K1, and induce autophagy by negatively regulating the mammalian target of rapamycin complex (mTORC) signaling pathway to reduce liver cancer cell growth (34). Moreover, it can increase radiation-induced apoptosis of liver cells *via* inhibiting mTOR phosphorylation to provide a possible potential therapeutic method for radio sensitization of liver cancer (35). In addition, Wu et al. discovered that saikosaponin D inhibited HepG2 cell proliferation by induction of apoptosis, improved the survival rate and suppressed the growth of liver tumors (36). Triptolide, a natural diterpenoid compound, is the main active ingredient of *Tripterygium wilfordii*, which inhibits the proliferation of HepG2 cells through induction of autophagy and apoptosis *via* up-regulating the expression of microRNA-194 (miR-194), LC3 and Beclin-1, and Bax/Bcl-2 ratio (37). Another study showed that it induced HepG2 cell apoptosis by inhibiting the expression of Ras (38). Gan et al. demonstrated that triptolide significantly suppressed the proliferation of H22 cells with IC_{50} value of 266.8 ng/mL at 24 h and induced apoptosis in H22 cells through decreasing the expression of cycloxygenase-2 (COX-2) (39). Ginsenoside-Rg3 inhibited cell proliferation and invasion of SMMC-7721 cells through PI3K/AKT pathway, which effectively decreased the levels of phosphorylated (p)-AKT, p-PI3K, MMP2, MMP9 and long non-coding RNA HOX antisense intergenic (lncRNA HOTAIR) (40). Recently, Zhang et al. showed that artemisinin enhanced the effect of anti-programmed cell death-ligand 1 (anti-PD-L1) immunotherapy by blocking the accumulation and function of myeloid-derived suppressor cells (MDSCs) *via* regulating PI3K/AKT/mTOR and MAPK signaling pathways and polarizing M2-like pro-tumor phenotype to M1-like anti-tumor phenotype (41). Dihydroartemisinine inhibits proliferation and induces apoptosis of HepG2 cells through regulating Bcl-2/Bax/caspase-3 apoptosis signal pathway (42). It can also induce liver cancer ferroptosis by promoting the formation of phosphatidylethanolamine-binding protein 1/15-Lipoxygenases (PEBP1/15-LO) and lipid peroxidation in cell membrane (43). Celastrol is a quinone methyl triterpene monomer compound of *T. wilfordii Hook. f.* and inhibits HepG2 cell proliferation by activating AMPK signaling pathway to suppress lipid metabolism and proliferation signal (44). Moreover, it can reduce the expression of nuclear factor kappa-B (NF-κB) and tumor necrosis factor alpha (TNF-α) in HepG2 and SMMC-7721 cells in a dose- and time-dependent manner (45). Recent studies have found that p53 can downregulate the expression of asparagine synthetase (ASNS) at the transcriptional level, thereby inhibiting asparagine synthesis and disrupting aspartate homeostasis, which can suppress the growth of lymphoma and colon tumors *in vivo* and *in vitro*. And depleting the levels of asparagine in cancer cells could release liver kinase B1 (LKB 1), and activated monophosphate-activated protein kinase (AMPK) -p53 signaling, triggered p21-dependent cell cycle arrest and promoted survival of cancer cells in asparagine-deficient conditions (46). Norcantharidin inhibits Huh7 cell proliferation and induces apoptosis in a time-and dose-dependent manner by activating p53 and p21 proteins and arresting cell cycle at G2/M phase (47). Tan et al. reported that genipin suppressed orthotopic HCC tumour growth through inhibiting IRE1a-mediated infiltration and priming of tumour associated macrophages (TAMs). It could reduce infiltration of inflammatory monocytes into liver and tumour, and inhibited the TAMs migration (48). Natural compound andrographolide (Andro), isolated from medicinal herb *Andrographis paniculata*, was reported to inhibit hepatoma tumor growth. It can inhibit the hepatoma tumor growth and alters the expression of miRNAs profile and downstream signals (49).

Ployphenols

Polyphenol is a compound with multiple phenolic groups and includes curcumin, resveratrol, 6-gingerol, epigallocatechin gallate, and tannic acid. Curcumin is a spice and food coloring extracted from

the rhizome of the perennial herb *turmeric* in Zingiberaceae. *In vitro* and *in vivo* results showed that curcumin downregulated the expression of Bcl2-associated transcription factor (BCLAF1), inhibited the activation of PI3K/AKT/glycogen synthase kinase-3β (GSK-3β) pathway, and triggered mitochondria-mediated apoptosis in liver cancer (50). Sun et al. reported that curcumin inhibited SMMC-7721 cell proliferation by induction of apoptosis *via* activating C/EBP homologous protein (CHOP) signaling pathway, reducing the expression of Bcl-2 and increasing cleaved caspase-3 and suppressed SMMC-7721 cell growth in xenograft tumor nude mice by activating endoplasmic reticulum (ER) stress pathway (51). Curcumin can induce liver cancer cell death by induction of apoptosis and pyroptosis. In addition, curcumin activates the gasdermin E (GSDME)-related scorch death and mitochondria-dependent apoptosis signaling pathways (52). Resveratrol is a phytoestrogen derived from grapes and berries and has several potential biological effects, including antioxidant, anti-inflammatory, cardioprotective and anticancer properties (53). Resveratrol inhibited the wound healing and invasion of HepG2 and Huh7 cells, increased the expression of E-cadherin, and decreased the expression of vimentin and Twist1. It inhibited metastasis and EMT through up-regulating the expression of microRNA-186-5p (miR-186-5p) (54). Furthermore, resveratrol can decrease the expression of membrane-associated RING-CH protein 1 (MARCH1) and p-Akt, increase the expression of phosphatase and tensin homolog deleted on chromosome 10 (PTEN) dose-dependently, hence inducing apoptosis and inhibiting the proliferation and invasion of HepG2 and Hep3B cells (55). 6-gingerol is an active polyphenolic compound extracted from ginger and can regulate the AKT/extracellular signal-regulated kinases 1/2 (ERK1/2) signaling pathway, increase P27/Kip1 and p21/Cip1 expression and inhibit cyclins D1, c-myc and cyclin-dependent kinase 4 (CDK4) protein expression, thereby arresting cell cycle at G2/M phase in Huh7 cells (56). Notably, a study showed that epigallocatechin gallate (EGCG) and EGCG derivative Y6 could significantly inhibit tumor growth and angiogenesis through MAPK/ERK1/2 and PI3K/AKT/HIF-1α/vascular endothelial factor (VEGF) pathways (57). Guo et al. demonstrated that EGCG combined with paclitaxel effectively inhibited the proliferation of HepG2 cells and the tumor growth in bearing cancer nude mice (58). In addition, it combined with adriamycin to exert synergistic anti-liver cancer effect, which induced apoptosis of BEL-7404/ADR cells and arrested cells in S/G2 phase of the cell cycle in a dose-dependent manner (59). Tannic acid is a natural polyphenol compound primarily found in fruits and nuts. Tannic acid can induce apoptosis by DNA disruption *via* caspase-dependent and caspase-independent mechanisms. It can also induce oxidative stress to promote liver cancer cell death (60). The combination of tannic acid with cisplatin induced HepG2 cell apoptosis through enhancing the activation of ER stress ATF6-CHOP pathway (61). Magnolol, a natural compound extracted from herbal plant *Magnolia officinalis*, has been recognized as a liver protection and antitumor drugs. It can significantly suppress tumor size and tumor growth rate, decreased the expression of p-ERK, NF-κB p65 (Ser536), MMP-9, VEGF, X-linked inhibitor of apoptosis protein (XIAP), and cyclinD1, and increased the expression of caspase-8 and caspase-9, which in turn induced apoptosis *in vivo* (62). Rosmarinic acid is a natural polyphenolic compound that exists in many medicinal species of Boraginaceae and Lamiaceae. Rosmarinic acid can regulated immune response and induced apoptosis of H22 cells. It could effectively inhibit the tumor growth through decreasing the expressions of IL-6, IL-10 and signal transducer and activator of transcription 3, up-regulating Bax, caspase-3 and down-regulating Bcl-2 (63).

Flavonoids

Flavonoids are phenolic phytochemicals and are commonly found in fruits, vegetables and plant-based beverages (e.g., green tea and wine), which have a polyphenolic structure and are usually composed of a 15-carbon skeleton (including two benzene rings) and a heterocyclic nucleus containing an oxygen atom. Many studies have reported that flavonoids have a significant role in tumor treatment, such as kaempferol, silymarin, quercetin, chrysin and diosmetin. Kaempferol is a natural flavonol and widely distributes in many vegetables and fruits. Kaempferol remarkably decreased the expression of miR-21 and increased the expression of PTEN, thereby inhibiting HepG2 cell proliferation and metastasis through inactivating PI3K/AKT/mTOR signaling pathway (64). Moreover, it can promote apoptosis of HepG2 cells in a dose-dependent manner through decreasing the expression of CDK1 and increasing the expression of Bax and JUN (65). Another study showed that kaempferol was able to increase the protein expression of Bax, glucose-regulated protein of 78 kDa (GRP78), GRP94, PERK, cleaved ATF6, IRE1α, CHOP, caspase-3 and caspase-4, thereby inducing HepG2 cell apoptosis by mitochondrial pathway and ER stress pathway (66). Silymarin is a lipid compound extracted from the fruit of *Silybum marianum* and inhibits MHCC97 cell invasion and metastasis through reducing Akt phosphorylation and integrin β1, VEGF and MMP-9 expression. Moreover, it can restore the cell adhesion ability by upregulating E-cadherin, thereby inhibiting invasion and metastasis of liver cancer cells (67). Silibinin is another bioactive polyphenolic flavonoid isolated from the fruits and seeds of *S. marianum* (68), which can achieve anti-liver-cancer effects through multiple mechanisms, including induction of apoptosis, suppression of angiogenesis and block of cell cycle (69, 70). Quercetin is a dietary polyphenolic compound with wide distribution in onions, grapes, berries, apples, broccoli and cereals (71), and has the capability to reduce the expression of markers in cancer stem cells and myofibroblasts, as well as the expression of ABCC3 to reduce the acquisition of drug resistance in the early liver cancer stages (72). Quercetin inhibited the growth of HepG2 cells in a dose- and time-dependent manner, with IC_{50} values of 110.50, 63.73 and 46.38 μmol/L at 24 h, 48 h and 72 h, respectively, and suppressed the growth of subcutaneous xenografts in BALB/c mice (73). Another study showed that quercetin inhibited HepG2 cell proliferation by NF-κB pathway and activator protein-1 (AP-1)/c-Jun N-terminal kinase (JNK) pathway, which increased the expression of p-JNK, p-AKT, p-p38, caspase-3 and decreased the expression of Bcl-xL, p-ERK and NF-κB (74). Chrysin, also known as aspicin, is a natural flavonoid compound extracted from *Pterophylla globulina*, with extensive pharmacological activities (75). Chrysin significantly inhibited SMMC-7721 cell proliferation and induced apoptosis by activating

MAPK signaling pathway (76). Moreover, chrysin could effectively inhibit the progression of tumor and promote the antitumor immunity of mice concomitant with increased $CD4^+$ and $CD8^+$ T cell proportions in tumor tissues of H22 xenograft mice model. Additionally, chrysin reduced the expression of PD-L1 through blocking of STAT3 and NF-κB pathways *in vitro* and *in vivo* (77). Diosmetin is an effective component of medicinal plants in southern China. Liu et al. found that diosmetin inhibited liver cancer cell metastasis, invasion and adhesion by regulating the PKCδ/MAPK/MMP pathway (78). It also can significantly downregulate the levels of Bcl-2, CDC2 and cyclinB1, and upregulate the levels of Bax, cleaved-caspase-3, cleaved-caspase-8, cleaved-PARP, Bak, p53 and p21, thereby inhibiting HepG2 cell proliferation and inducing cell apoptosis and arresting cell cycle at G2/M phase (79). Similarly, another study showed that diosmetin reduced the expression of Bcl-2, CDK1 and CCND1 in a dose-dependent manner *in vitro* and the expression of Ki67 *in vivo*, thereby inhibiting the proliferation and migration and arresting cell cycle at G1 phase of liver cells (80). Tan et al. observed that oral administration of baicalin completely blocked orthotopic growth of implanted HCC. And it induced repolarisation of TAM and M2-like macrophages, which is associated with elevated autophagy, and transcriptional activation of RelB/p52 pathway (81).

Others

Emodin is an anthraquinone compound extracted from *Palmar rhubarb* and *Amomum amomatum* and inhibits liver cancer cell proliferation and metastasis by regulating VEGFR2-AKT-ERK1/2 signaling pathway and miR-34a signaling pathway (82). Aloin is a natural anthracycline compound, which can inhibit MHCC97H cell proliferation, migration and invasion and induce apoptosis through regulating Bcl-2/Bax ratio (83). Tanshinone is a phenoquinone derivative extracted from *Salvia miltiorrhiza* and inhibits HepG2 and Huh7 cell proliferation by blocking G0/G1 phase cell cycle *via* decreasing the expression of cyclin D1 and increasing p21, as well as inhibiting p53/damage-regulated autophagy and inducing apoptosis (84). As the most frequently mutated gene in human tumors, p53 can induce apoptosis, cell cycle arrest and cell senescence. And it plays an important role in suppressing proliferation of tumor, and is a major target for developing new drugs to reactivate its tumor suppressing activity for anticancer therapies. Taking p53 mutant Y220C as the core, Joseph et al. studied the structure-guided development of high-affinity small molecules stabilizing p53-Y220C *in vitro* and the synthetic route developed in the process. They found two new chemical probes with submicromolar binding affinity *in vitro*, which represents an important step toward the novel and effective Y220C ligand in the clinical evaluation of tumors (85). Cryptotanshinone significantly inhibited the cell viability of HepG2 cells with an IC_{50} of 93.73 μmol/L and induced ferroptosis by ROS accumulation *via* reducing glutathione (GSH) level and the expression of cystine/glutamate antiporter system light chain (xCT) and glutathione peroxidase 4 (GPX4) (86).

Natural polysaccharides are rich dietary components with significant roles in tumor prevention and treatment. Astragalus polysaccharides are the active component of the dried root of *Radix astragali* and can inhibit HepG2 cell proliferation (87), reverse the drug resistance of 5-fluorouracil (88), suppress EMT (89) and induce apoptosis (90). Astragalus polysaccharides can inhibit the growth of HepG2.215 cells by blocking HepG2.215 cells from entering the G2/M phase and inducing apoptosis (91). *Poria cocos* polysaccharides induced HepG2 cell apoptosis by inhibiting the expression of NOD-like receptor thermal protein domain associated protein 3 (NLRP3)/caspase-1/gasdermin D (GSDMD) in the classical pyroptosis pathway (92). Another study showed that *Lycium barbarum* polysaccharides inhibited SMMC-7721 cell proliferation and metastasis and induced apoptosis by reducing the expression of MMP-2, MMP-9 and VEGF (93). Saponins can significantly inhibit tumor cell proliferation. Astragaloside IV, also known as astragalus saponins, was able to upregulate the expression of caspase-3 and downregulate the expression of interleukin (IL)-6 by inhibiting the STAT3 signaling pathway, thereby inducing the apoptosis of liver cancer cells (94). Astragaloside IV also inhibits HepG2 cell proliferation and induces apoptosis by regulating oxidative stress and NF-κB signaling pathway (95). In addition, astragalus saponins promoted the secretion of IL-2 to enhance the proliferation and transformation of lymphocytes, thereby improving the immune function of rats and inhibiting liver cancer cells growth (96).

Compounds

Zhu et al. investigated the influence of Huangqi Sijunzi decoction on 80 patients undergoing primary liver cancer operation. They found that Huangqi Sijunzi decoction can promote postoperative recovery of the liver function and immunologic function of the patients undergoing primary liver cancer operation, alleviate clinical symptoms and facilitate postoperative recovery of the patients (97). Yiqi Huoxue Fuzheng Jiedu detoxification is a compound with many kinds of traditional Chinese medicine, Jiang et al. explored the clinical effect of supplementing qi and activating blood circulation to assist the treatment of patients with advanced liver cancer. It is an effective method in adjuvant treatment of patients with advanced liver cancer, and it may be helpful to improve its clinical symptoms and liver function (98). Moreover, Zheng et al. researched that in the treatment of severe cancer pain due to primary liver cancer, external application of compound Gleditsiae Spina ointment has a marked analgesic effect, and can reduce the dose of opioid painkillers and the number of times of breakthrough pain and improve patients' quality of life (99). Jing et al. observed the clinical effect of the therapy of Xingqi Sanjie Huayu prescription combined with reduced glutathione on 80 patients who had undergone surgery for primary liver cancer. It can effectively improve the clinical symptoms, reduce the levels of serum tumor markers, enhance the immune function and liver function, and reduce the incidence of adverse reactions (100). To investigate the clinical effect of Thymalfasin injection combined with Kanglaite injection and Chinese medicine Zhenggan prescription in the prevention of postoperative recurrence of primary liver cancer, chen et al. selected sixty patients with primary liver cancer. The triple therapy of Thymalfasin injection combined with Kanglaite injection and Chinese medicine Zhenggan prescription can significantly improve patients' clinical syndrome and quality of life,

promote the improvement of liver function, regulate immune function, reduce AFP level, has the advantages of low recurrence rate, has significant curative effect, and is worthy of further promotion and application (101). Furthermore, Zhao et al. founded that the therapy of Fuzheng Huayu Jiedu prescription can effectively improve the clinical effect on advanced liver cancer with less adverse reactions and high safety, and its mechanism may be related to its remarkable reduction of levels of inflammatory factors, inhibition of inflammatory responses, improvement of immune function and enhancement of resistance (102). Hedyotis diffusa injection is a Chinese patent medicine, which has the effect of clearing heat and detoxifying, benefiting dampness and swelling. Hedyotis diffusa injection combined with transarterial chemoembolization in the treatment of the patients with primary liver cancer can improve the disease control rate and improve the levels of T cell subsets. Moreover, it is superior to single transarterial chemoembolization (103).

Supplementary Table 1 summarized the effects and mechanisms of plant-derived natural products on liver cancer. Although many plant-derived natural products are effective, they have limited efficacy for clinical application. Conventional mono-therapeutic methods target rapidly proliferating cells and destroy their growth, which it does not differentiate between healthy and cancerous cells. Chemotherapy can be toxic to the patient with multiple side effects and risks, such as nausea and vomiting and tumor metastasis (104). And it can also strongly reduce their immune system by affecting peripheral blood lymphocyte subsets and increasing susceptibility to host diseases (105). Although combination therapy can be toxic if one of the technologies is chemotherapeutic, the toxicity is remarkably less because a lower therapeutic dosage of each individual drug is demanded (106). It may be able to prevent the toxic effects on normal cells while concurrently producing cytotoxic effects on cancer cells. Further, monotherapy treatment is more develop drug resistance because continuous treatment with a single compound induces cancer cells to create alternative salvage approach (107). The most common mechanism of multidrug resistance is the elimination of drugs from the cell by ATP-dependent efflux pumps, thereby reducing intracellular drug concentrations and giving rise to resistance. As an example, cells in adenocarcinoma, when treated with adriamycin, upregulate the expression of ATP-binding cassette (ABC) transporter family, P-glycoprotein, to eliminate the drug, leading to a state of drug resistance (108). However, combination therapy also produced a more effective treatment response which target different pathways, and therefore this treatment modality reverses the drug resistance (109). Generally, conventional chemotherapy only targets non-stem cell tumor cells, resulting in an increasing proportion of stem cells in tumors after chemotherapy. And it is also a key mechanism for induction of drug resistance, regulation of metastasis and recurrence of malignant (110). However, combination therapy (for example quercetin in combination with chemotherapy drug doxorubicin) could reduce drug resistance and attenuated the likelihood of relapse (111). Therefore, combination therapy of plant-derived natural products with chemotherapeutics or immunotherapy is drawing researcher's attention on liver cancer to induce apoptosis and inhibit cell proliferation and angiogenesis. It has the potential to develop therapeutic or adjuvant agents for human liver cancers.

Anti-liver cancer mechanism by combination of plant-derived natural product ingredients

Mutations and epigenetic changes allow cancer cells to grow and replicate uncontrollably and invade normal tissues. This uncontrolled growth and proliferation arise due to loss of function mutations in tumour organelles such as lysosome (112), mitochondria (113), as well as endoplasmic reticulum (114). The limited efficiency and serious side effects associated with the use of conventional anticancer therapies encouraged scientists to focus on the discovery and development of new anticancer agents derived from natural products. For much of history, people have used plants and plant extracts to treat their ailments. Although the established natural plants as monotherapy of cancer had many advantages, they had limited efficacy for clinical application. If they are used in combination with other natural products, their anti-cancer effect is more effective. Secondary metabolites from plant sources like flavonoids, alkaloids, terpenoids, saponins, and others had been reported as important sources for potent anticancer agents. It was demonstrated that combination treatment acts by reducing the concentration of the compound required for drug efficacy through enhancing the effect on the same target or mechanism of action. The anticancer effect of these natural products in combination with others is mediated by different mechanisms, including inhibiting proliferation, blocking cell cycle and reversing multidrug resistance.

Inhibit liver cancer cells proliferation

Proliferation and invasion of liver cancer cells were inhibited through decreasing the expression of the tumor suppressor gene deleted in liver cancer 1 (DLC1), translationally controlled tumor protein (TCTP) and Cdc42 (115). Resveratrol in combination with dihydroartemisinine acts by regulating DLC1/TCTP protein expression and inhibiting migration-related signaling pathways in HepG2 and MDA-AB231 cells through inducing Cdc42 regulation of JNK/NF-κB and N-WASP signaling pathways (116). PI3K-AKT signaling pathway is closely related to the proliferation of liver cancer cells (117). The combination of natural products acts by inducing anti-tumor effect through inhibiting the invasion and proliferation of tumor cells. Sodium arsenite and astrageoside IV inhibit HepG2 cell proliferation, block cell cycle, promote apoptosis, and suppress tumor growth. It can reduce the expression of PI3K, AKT, mTOR through PI3K/AKT/mTOR signaling effect, and the synergistic effect is more significant (118). Apoptosis an active and ordered multistep cell death process that controlled by genes, and involves two major pathways, including intrinsic and extrinsic apoptosis pathways in human cancer cells. The intrinsic pathway of apoptosis is mediated mainly by mitochondria within the cell, and this pathway is regulated by pro-apoptosis Bcl-2 family proteins (119). Natural products principally induced liver cancer cells apoptosis and inhibited proliferation through caspase cascade reaction and NF-κB signaling pathway.

Wen et al. developed citrus net skin black tea (CRPBT) by combining citrus reticulate peel and black tea. CRPBT can significantly down-regulate the phosphorylation of PI3K and AKT in liver cancer cells, up-regulate the Bax/Bcl-2 ratio, and inhibit the expression of MMP2/3, N-cadherin and Vimetin proteins. It can inhibit invasion, proliferation and induce apoptosis of liver cancer cells (120). A combination of curcuma zedoary and kelp could inhibit liver cancer cell proliferation and metastasis by inhibiting endogenous H2S production and down-regulating the transcription activator 3 (STAT3)/BCL-2 and VEGF pathway *in vitro* and *in vivo* (121). Bufalin (BFL) and cinobufagin (CBF) have a synergistic effect. Metabolic pathways, including methionine metabolism, energy metabolism, lipid metabolism, and amino acid metabolism, were modulated and subsequently led to apoptosis and cell cycle arrest of HepG2 cells. Zhang et al. researched that the cotreatment group can significantly decrease mitochondrial membrane potential (MMP) and oxygen consumption rate (OCR), which associated with maximal respiration (122). Triptolide and sodium cantharidinate exert a synergistic toxic effect on hepatoma cell line 7721, which is related to increasing capase-3 activity and suppression of NF-κB (123). Quercetin and rosmarinic acid had a more significant synergistic effect on inhibiting HepG2 cells proliferation and migration in a dose-dependent manner by up-regulating the expression of E-cadherin and down-regulating N-cadherin gene expression (124). Manikandan et al. showed that curcumin in combination with catechin which is polyphenolic compound have a synergistic effect on inhibiting the proliferation and inducing cell apoptosis. It treated HepG2 cells showed small morphological changes which significantly destruction of monolayer, and change the DNA fragmentation (125). Wang et al. evaluated the effects of co-treatment of vincristine and berberine on hepatic carcinoma cell lines. They find that combinational usage of these two drugs can significantly induce cell growth inhibition and apoptosis even under a concentration of vincristine barely showing cytotoxicity in the same cells when used alone (126). The combination of arsenic trioxide and tanshinone have synergistic effect, attenuation and antihepatocarcinoma effect. Tanshinone can reduce the blood routine changes and liver and kidney function damage caused by arsenic trioxide (127). Cryptotanshinone induced liver cancer cells apoptosis and enhanced the effect of Arsenic trioxide by downregulating phosphorylated STAT3, Bcl-2 *in vitro* and *in vivo* (128).

Block liver cancer cells cycle

The cell cycle system plays a critical role in regulating activities such as cancer cell proliferation and apoptosis. The pathogenesis of neoplasms because of lost control in cycle progression is common. Uncontrol cell division is an essential factor in the development of cancer. The cell cycle consists of G1, the S-phase, G2, and the M (mitotic) phase (129). Cells are preparing for DNA synthesis during G1 and they perform surveillance to establish the integrity of newly synthesized DNA during G2 before initiating mitosis. Chromosomal DNA is replicated during the S-phase. If this phase arrest, the cells will undergo variation or abnormal division, which will then terminate the proliferative (130). In the G2 phase, after the nucleic acid is amplified, the other cellular components are partitioned between two daughter cells during the M-phase. If the stagnation occurs, the normal growth and gathering of the cells is hindered, which inhibit proliferation (131). Cyclins and their cognate cyclin-dependent protein kinases (CDKs) are necessary components required for traversing the cell division cycle, with controlling balance of all stages in cell cycle (132). CDK2/4/6, Cyclin D1, and Cyclin E are the major regulatory proteins in the G1 phase; and the reduction of Cyclin B1 and CDK1/2 activity is a key marker of cycle arrest in the G2/M phase (133, 134).

Zhang Di demonstrated that chrysin in combination with diosmetin or triptolide acted by the induction of apoptosis through inhibiting HepG2 cells migration as well as arresting the cell cycle in G1 and G2 phases *in vitro*. Moreover, it had a stronger inhibitory effect on H22 solid tumors than single drug application (135). Xiao et al. revealed that a combination of biochanin A with BRAF inhibitor SB590885 synergistically inhibiting proliferation by disrupting of the ERK MAPK and the PI3K/AKT pathways *in vitro*, and promoting cell cycle arrest and apoptosis (136). Quercetin in combination with maleic anhydride derivatives acts by inducing apoptosis of liver cancer cells through arresting cells in S-phase by oxidative stress response, causing DNA damageactivating the intrinsic apoptosis pathway (137). Curcumin (20 μmol/L) combined with vincristine (1 pg/L) inhibits proliferation and clone formation of HepG2 cells, reduces mitochondrial membrane potential and MDR1 and LRP protein expression, increases P21 expression, thereby blocking G2/M phase cell cycle and inducing apoptosis (138). Curcumin (5 pg/L) and glycyrrhetinic acid (10 pg/L) obviously inhibited HepG2 cells proliferation in a concentration- and time-dependent manner, arrested the G2 phase, and the synergistic effect is more remarkably (139). The combination of Curcumin (40 μmol/L) and artemisinin (80 μmol/L) could effectively inhibit HepG2 cells proliferation and arrest cell cycle and promote apoptosis. In addition, it can inhibit telomerase activity in liver cancer cells (140). Tanshinone IIA block subG1 phase cell cycle, while resveratrol arrest S phase and G2/M phase of HepG2 cells. The combination of them induce cell apoptosis and arrest subG1 cell cycle. Moreover, it exerted synergistic cytotoxicity and robustly induces apoptosis, and DNA fragmentation (141). Berberine (15 μmol/L) combined with tarpinine derivative HMQ1611 (15 μmol/L) inhibits cyclin D1, cyclin E, CDK1 expression and arrests the cell cycle at G1 phase through PI3K/AKT/mTOR signaling pathways to induce apoptosis of HepG2 cells. Furthermore, the combination therapy had strong suppressive effect on proliferation by inhibiting the phosphorylation of LDL receptor-associated protein, which was related to Wnt/β-catenin signaling pathway (142). Liu et al. showed that different concentrations of norcantraridin (12.5-200 μmol/L) and evodiamine (2.5-40 μmol/L) inhibited HepG2 cells growth and arrested G2/M phase cell cycle and induced apoptosis. Moreover, it has obvious synergistic inhibitory effect on anti-proliferation and pro-apoptosis through increasing the expression of Bax and decreasing the expression of Bcl-2 (143). Triptolide (0.01-5 pg/L), glycyrrhetinic acid (1-10 pg/L), rhein (1-10 pg/L) and paclitaxel (1-20 pg/L) inhibit HepG2 cell proliferation in a dose-dependent manner through blocking G2/M phase cell cycle. In addition, glycyrrhetinic acid, paclitaxel and rhein can enhance the inhibitory effect of low concentration of tripterine on HepG2 cell proliferation (144).

Reverse liver cancer cells multidrug resistance

Liver cancer cells will be exposed to a certain chemotherapy drug for a long time under chemotherapy. And it can develop multidrug resistance (MDR) to this drug and cross-resistance to other chemotherapy drugs with different functional structures, leading to chemotherapy failure (145). This mechanism of multidrug resistance arises due to activity of the superfamily members of adenosine triphosphate binding cassette (ABC) such as P-glycoprotein (P-gP), multidrug resistance associated protein (MRP) and breast tumor resistance protein (BCRP) (146). Plant-derived natural products act by enhancing the tumor killing effect of chemotherapeutic drugs and inducing their anti-tumor activity through reversing the multidrug resistance of liver cancer cells.

Sun et al. demonstrated that curcumin reversed the multi-drug resistance caused by cucurbitacin B through inhibiting the expression of P-gP, thereby inducing liver cancer cell apoptosis (147). Shen et al. researched that coumarin derivatives, as an inhibitor of microtubule affinity-regulating kinase 4 (MARK4), induce apoptosis of liver cancer cell by increasing microtubule dynamics and the sensitivity of paclitaxel (148). The curcumin antiproliferative effect was confirmed by Nan et al., who reported marked induction apoptosis of liver cancer cells, reversed the drug resistance of paclitaxel through inhibiting NF-κB pathway stimulated Lin28B expression (149). Xu et al. prepared folate-PEG-mesoporous silica nanoparticles loaded with paclitaxel, which had a good targeting effect on liver cancer cells and enhanced the anti-tumor effect of paclitaxel (150). A combination of esculetin with paclitaxel acted by induce apoptosis of liver cancer cells through up-regulating Bax/Bcl, inducing the activation of caspase-8 and caspase-3, as well as ERK signal pathway (151). Jiang et al. identified the antitumor effects of resveratrol on HepG2 cell, in addition to up-regulate p53, Bax and other proteins, and reverse drug resistance of paclitaxel (152). The combination of emodin (10 mg/L) and curcumin (10 mg/L) enhances sensitivity of BEL-7402 hepatoma cells and reduces the dosage of emodin and induces apoptosis (153). Curcumin (5-20 μmol/L) and paclitaxel (0.05-0.2 μmol/L) have synergistic anti-proliferation and pro-apoptosis effects on Hep3B cells. It can decrease paclitaxel-induced NF-κB activation, mediate Lin28 level, thereby enhancing sensitivity of liver cancer cells to paclitaxel (154). Matrine also reverses resistance of K562/ADM cells to doxorubicin and vincristine by arresting cell cycle and inducing autophagy (155). Table 1 summarizes their effects and mechanisms on liver cancer.

The synergistic effect of plant-derived natural products in combination with chemotherapy

Clinical chemotherapy drugs mainly include cisplatin which is platinum compounds, and doxorubicin which is antibiotics, and hormones. Cisplatin and adriamycin mainly affect cell division and induce apoptosis by interfering with DNA replication (156). However, chemotherapeutic drugs significantly reduce the immune function of the body, and induce multiple organ damage (157, 158). Radiation and chemotherapeutic agents as the backbone for cancer are not very effective and toxic not only to tumor cells but also to normal cells, and are not affordable for most. Therefore, plant-derived natural products in combination with chemotherapeutic drugs are generally free of deleterious side effects and usually inexpensive, which have played a significant role in the development of anticancer drugs over the years. It remains to mention that extraction from natural plants is also contributed to the synergistic effects with other anticancer drugs such as cisplatin, doxorubicin, and hormones. Plant-derived natural products in combination with chemotherapeutic agents act as an anticancer agent by inhibition of tumor cell angiogenesis, invasion and migration, induction of autophagy.

Suppress liver cancer cells angiogenesis

Liver cancer is a kind of tumor rich in blood vessels. And blood vessels providing essential nutrients and oxygen for the occurrence and development of liver cancer cells, and are closely related to the growth and metastasis of liver cancer cells (159). Vascular endothelial growth factor (VEGF) is the most important type of angiogenesis regulatory factor, which promotes the division and proliferation of vascular endothelial cells through paracrine and promoting formation of blood vessels (160). Angiopoietin (Ang)/Tie2 pathway regulates vascular and lymphatic development, vascular permeability, angiogenesis remodeling, and tumor vascularization (161, 162). Tumor cells act by up-regulating VEGF through inducing miR-21 targeting AKT and ERK signaling pathways, thereby promoting tumor angiogenesis (163). The mTOR pathway can also promote tumor angiogenesis through inducing the transformation of tumor-associated macrophages (TAM) into M2-type. Therefore, it can reduce proliferation and metastasis of liver cancer cells through preventing the formation of new blood vessels (164, 165).

Ao et al. found that the main component of kanglite injections is the extract from coix seed in traditional Chinese medicine, this active compound in combination with thalidomide can significantly inhibit human liver cancer blood vessels through inhibiting VEGF and B-FGF, thereby inducing angiogenesis. At the same time, it can regulate cellular immunity of the body, which has synergistic effect with chemotherapy (166). Compared with cisplatin group, the alcohol extracts of *Liuwei rehmannium* (mainly composed of polysaccharide, paeonol, flavonoids, trace elements, etc.) in combination with cisplatin, can significantly induce apoptosis of BEL-7402 cells, and inhibit angiogenesis by down-regulating the expression of VEGF and ANG-2 proteins, up regulating the expression of TSP and TIMP-2 (167). Lin et al. reported that compared to model group, a combination of astragalus polysaccharide with cisplatin and adriamycin could significantly reduce the expressions of Ki-67, HIF-1α and VEGF, and had a significant synergistic and toxic effect on inhibition of tumor growth (168). Zang et al. confirmed that radix astragali or curcuma in combination with cisplatin acted by inhibiting angiogenesis and metastasis of liver cancer through down-regulating the expression of CD147 and iNOS (169). Luo et al. showed that a combination of cisplatin with astragaloside IV or curcumin which is flavonoid compound have a significant inhibition the formation of new blood vessels in liver cancer by down-regulating the expression of

TABLE 1 Effect and mechanism by combination of plant-derived natural product ingredients on liver cancer.

Combination Therapy	Concentration	Cell Line/ Model	Mechanism	Reference
Dihydroartemisinine/ Resveratrol	dihydroartemisinine: 25 μmol/L resveratrol: 50 μmol/L	HepG2 MDA-AB-231	Regulated DLC1/TCTP protein expression and induced Cdc42 regulation of JNK/NF-κB and N-WASP signaling pathways	(116)
Sodium arsenite/ Astrageoside IV	sodium arsenite: 0.5 μg/mL astrageoside IV: 0.8 μg/mL	HepG2	Reduced the expression of PI3K, AKT, mTOR through PI3K/AKT/mTOR signaling effect	(118)
Citrus reticulate peel/ Black tea	CRPBT: 0-1 mg/mL	HepG2 Bel 7402	Down-regulated the phosphorylation of PI3K and AKT, up-regulated the Bax/Bcl-2 ratio, and inhibited the expression of MMP2/3, N-cadherin and Vimetin proteins	(120)
Curcuma zedoary/ Kelp	curcuma zedoary: 4000 mg/kg kelp: 4000 mg/kg	H22	Inhibited endogenous H2S production and down-regulated the pSTAT3/BCL-2 and VEGF pathway *in vitro* and *in vivo*	(121)
Bufalin/ Cinobufagin	bufalin: 8 nmol/L cinobufagin: 50 nmol/L	HepG2	Decreased mitochondrial membrane potential (MMP) and oxygen consumption rate (OCR), which associated with maximal respiration	(122)
Triptolide/ Sodium cantharidinate	triptolide: 9-36 μg/mL sodium cantharidinate: 12-50 μg/mL	SMMC7721	Increased capase-3 activity and suppression of NF- κB	(123)
Quercetin/ rosmarinic acid	quercetin: 12.5-100 μmol/L rosmarinic acid:12.5-100μmol/L	HepG2	Up-regulated the expression of E-cadherin and down-regulated N-cadherin gene expression	(124)
Curcumin/ Catechin	curcumin: 50 μmol/L catechin: 25 μmol/L	HepG2	Inhibited the proliferation and induce cell apoptosis	(125)
Vincristine/ Berberine	vincristine: 0-4 nmol/L berberine: 0-40 nmol/L	HepG2 SMMC7721	Regulated the signals related to mitochondrial function, apoptotic pathway and endoplasmic reticulum stress	(126)
Arsenic trioxide/ Tanshinone	arsenic trioxide: 2.5 mg/kg tanshinone: 500 mg/kg	Bel-7404 nude mice	Reduced the blood routine changes and liver and kidney function damage caused by As2O3	(127)
Cryptotanshinone/ Arsenic trioxide	cryptotanshinone: 10,20 μmol/L arsenic trioxide: 1, 2 μmol/L	Bel-7404	Induced liver cancer cells apoptosis and enhanced the effect of Arsenic trioxide by downregulating phosphorylated STAT3, Bcl-2 *in vitro* and *in vivo*	(128)
Chrysin/ Diosmetin/ Triptolide	chrysin: 1.25-20 μmol/L diosmetin: 3.125-50 μmol/L triptolide: 0.78-12.5 nmol/L	HepG2 H22	Induced apoptosis and inhibited cell migration as well as arrested the cell cycle in G1 and G2 phases	(135)
Biochanin A/ SB590885	biochanin A: 75 μmol/L SB590885: 12 μmol/L	Bel-7402 SK-Hep-1	Inhibited proliferation by disrupting of the ERK MAPK and the PI3K/AKT pathways *in vitro*, and promoted cell cycle arrest and apoptosis	(136)
Quercetin/ Maleic anhydride derivatives	quercetin: 50 mmol/L maleic anhydride derivatives: 0.01 mmol/L	HuH7 HepG2	Induced apoptosisand arresting S-phase cell cycle by oxidative stress response, causing DNA damageactivating the intrinsic apoptosis pathway	(137)
Curcumin/ Vincristine	curcumin: 20 μmol/L vincristine: 1 pg/L	HepG2	Reduced mitochondrial membrane potential and MDR1 and LRP protein expression, increased P21 expression	(138)
Curcumin/ Glycyrrhetinic acid	curcumin: 5 pg/L glycyrrhetinic acid: 10 pg/L	HepG2	Inhibited the proliferation, promoted apoptosis and arrested the G2 phase in a concentration- and time-dependent manner	(139)
Curcumin/ Artemisinin	curcumin: 40 μmol/L artemisinin: 80 μmol/L	HepG2	Inhibited proliferation and telomerase activity and arrested cell cycle and promoted apoptosis	(140)
Tanshinone IIA/ Resveratrol	tanshinone IIA: 5 μg/mL resveratrol: 5 μg/mL	HepG2	Induced cell apoptosis and arrested subG1 cell cycle and DNA fragmentation	(141)
Berberine/ HMQ1611	berberine: 15 μmol/L HMQ1611: 15 μmol/L	HepG2 Bel-7402 SMMC-7721	Inhibited the phosphorylation of LDL receptor-associated protein, which is related to Wnt/β-catenin signaling pathway	(142)

(Continued)

TABLE 1 Continued

Combination Therapy	Concentration	Cell Line/ Model	Mechanism	Reference
Norcantraridin/ Evodiamine	norcantraridin: 12.5-200 μmol/L evodiamine: 2.5-40 μmol/L	HepG2	Increased the expression of Bax and decreased the expression of Bcl-2	(143)
Triptolide/ Glycyrrhetinic acid/ Rhein/ Paclitaxel	triptolide: 0.01-5 pg/L glycyrrhetinic acid: 1-10 pg/L rhein: 1-10 pg/L Paclitaxel: 1-20 pg/L	HepG2	Inhibited proliferation through block G2/M phase cell cycle	(144)
cucurbitacin B/ Curcumin	cucurbitacin B: 143.2 μmol/L curcumin: 108.6 μmol/L	BEL7402/5-Fu	Reversed the multi-drug resistance caused by terpenoid cysurin B through inhibiting the expression of P-gP, thereby inducing liver cancer cell apoptosis	(147)
Coumarinderivatives/ Paclitaxel	coumarinderivatives: 2.5 μmol/L paclitaxel: 2.5 μmol/L	HepG2 SMMC-7721	Induced apoptosis by increasing microtubule dynamics and the sensitivity of paclitaxel	(148)
Curcumin/ Paclitaxel	curcumin: 5-20 μmol/L paclitaxel: 1 μmol/L	Hep3B HepG2	Induced apoptosis, and reversed the drug resistance of paclitaxel through inhibiting NF-κB pathway stimulated Lin28B expression	(149)
Folate/ Paclitaxel	FA-PEG-MSNs-PTX: 100 μg/mL	SMMC-7721	Had a good targeting effect on SMMC-7721 cells and enhanced the anti-tumor effect of paclitaxel	(150)
Esculetin/ Paclitaxe	esculetin: 50-100 μmol/L paclitaxe: 0.5 μmol/L	HepG2	Induced apoptosis through up-regulating Bax/Bcl, inducing the activation of caspase-8 and caspase-3, as well as ERK signal pathway	(151)
Resveratrol/ Paclitaxel	resveratrol: 10 μg/mL paclitaxel: 5, 10 μg/mL	HepG2	Up-regulated P53, Bax and other proteins, and reversed drug resistance of paclitaxel	(152)
Emodin/ Curcumin	emodin: 10 mg/L curcumin: 10 mg/L	BEL-7402	Enhanced sensitivity and reduce the dosage of emodin and induce apoptosis	(153)
Curcumin/ Paclitaxel	curcumin: 5-20 μmol/L paclitaxel: 0.05-0.2 μmol/L	Hep3B	Decreased paclitaxel-induced NF-κB activation, mediated Lin28 level, thereby enhancing sensitivity of liver cancer cells to paclitaxel	(154)

HIF-1α and VEGF (170). Chen et al. researched that combining epigallocatechin gallate (EGCG) derivative Y6 with dunorubicin which is anthracycline antitumor drug, acts by inhibiting of angiogenesis and toxic effects *in vivo* through inhibiting of MAPK/ERK and PI3K/AKT signaling pathways to down-regulate the expression of HIF-1α, Carbonyl Reductase1 (CBR1) and VEGF (171). Zhao et al. developed doxorubicin (DOX) and curcumin (Cur) co-delivery lipid nanoparticles (DOX/Cur-NPs) and examined its inhibitory effect on diethylnitrosamine (DEN)-induced liver cancer in mice. The mRNA levels of MDR1, Bcl-2 and HIF-1α, and protein levels of P-gP, Bcl-2 and HIF-1α were decreased in DOX/Cur-NPs than those in DOX-NPs, indicating that Cur might reverse multidrug resistance (MDR) through these pathways (172).

Inhibit invasion and migration of liver cancer cells

A critical event during tumorigenesis is the transformation from a static primary tumor to an aggressive and invasive oner. During the processes, tumor cells show an increased capacity to migrate, and multitudinous intracellular molecules participate in migration. Metastasis is significantly pathological characterized by malignant tumors, while the invasion and migration of liver cancer cells lead to poor prognosis of liver cancer patients, prone to recurrence and short median survival (173). The invasion and migration of tumor cells is a complex process controlled by multiple factors (174). It mainly included EMT, inhibition of matrix metalloproteinases (MMPs) hydrolysis and cell adhesion to basement membrane and extracellular matrix (175). And it is affected by the regulation of tumor metastasis genes and tumor metastasis suppressor genes (176). Combining natural products with chemotherapy drugs can prevent and cure cancer metastasis safely and effectively.

Shan et al. confirmed that mannose and cisplatin had a synergistic effect, which inhibited proliferation and migration of HepG2 cells, furthermore, it can change morphology with separation, shedding and aggregation (177). A combination of emodin with cisplatin can up-regulate the expression of E-cadherin, acts by inhibiting proliferation, invasion and migration of HepG2 cells through inhibiting EMT (178). Yang et al. showed that kaempferol and doxorubicin synergistically inhibited the proliferation, migration and invasion of liver cancer cells by inhibiting PI3K/mTOR/MMP protein pathway in a dose-and time-dependent manner (179). The sinosinine thiocyanate extracted from the herbaceous plants of The Cross family, could target the multidrug-resistant related proteins ABCB1 and ABCG2, enhance the sensitivity of HepG2 cells to gemcitabine, and inhibit the invasion and migration (180). Wang et al. conducted an investigation about the potential anti-tumor mechanism of alkaloid caffeine in combination with 5-fluorouracil. It can exhibit a synergistic anti-liver cancer effect by increasing the expression of cleaved PARP, p-JNK, p-p38, and decreasing the expression of Bcl-2, Bcl-xL, CDK2/4/6, p-ERK, p38, *via* inducing

generation of ROS and influencing MAPK signaling pathway, thereby inhibiting the proliferation and metastasis and inducing apoptosis of SMMC-7721 and Hep3B cells (181). Data from a study *in vitro* revealed that combined metformin (10 mmol/L) and curcumin (5 and 10 μmol/L) could induce apoptosis and inhibit metastasis in HepG2 and PLC/PRF/5 cells. The anticancer effects could be attributed to inhibition of VEGF, MMP2/9, and VEGFR-2 protein expression (182).

Induce liver cancer cells autophagy

Autophagy is a genetically controlled and evolutionarily conserved form of cell death, which is also related to occurrence and development of tumor, thereby has becoming a new tumor therapy method. Several cellular classical signaling pathways of natural plants target intracellular autophagy including Beclin-1, phosphoinositide 3-kinase/Akt/mechanistic target of rapamycin pathway (PI3K/AKT/mTOR) and p53, have been known to control cell proliferation and apoptosis (183, 184). Beclin-1 and LC3 are two key markers of autophagy. Beclin-1 can enhance autophagy and induce apoptosis of tumor cells (185). p53 can induce autophagy by activating cathepsin D (CTSD), and further enhance the p53-mediated tumor suppression effect (186). In addition, p53 can activate the expression of transglutaminase 2 (TGM 2) to promote autophagy and tumor suppression functions, and TGM 2 contributes to the development of p53-induced autophagy program and the function of tumor suppressor (187). Moreover, autophagy is also regulated by p53 in the elimination of aberrant mitochondria. In radiation-resistant cancer cells, p53 induces mitophagy by increasing the levels of BCL 2 interacting protein 3 (BNIP 3) to remove abnormal mitochondria to maintain mitochondrial oxidative phosphorylation (OXPHOS) and inhibit the glycolytic pathway (188). Importantly, PI3K-AkT-mTOR signaling pathway is a well-characterized anti-apoptotic cascade in human cancers, since its activation leads to cell proliferation and cell survival. The inducing cell survival of this pathway was mediated by activating anti-apoptotic factors and inhibiting pro-apoptotic factors. AKT can induce anti-apoptotic effect through phosphorylating target proteins by a variety of pathways, such as prevent the apoptosis cascade through inhibiting caspase-9 activity (189). Natural products act by inducing autophagy and apoptosis of cells through down-regulating the expression of mTOR, AKT, PI3K and other proteins (190).

Hu et al. suggested that a combination of matrine with cisplatin promoted apoptosis through activating the caspase apoptosis pathway and inhibiting expression of survivin-related caspase-9 protein (191). A combination of tannic acid with cisplatin acts by inducing apoptosis through activating caspase-3 signaling cascade (192). Xu et al. revealed that saikosaponin D in combination with doxorubibin significantly induced autophagy and apoptosis of HepG2 cells. It suppressed cell proliferation and invasion through up-regulating of ROS, Oatp1b1 as well as TGF-β1 (193). Wang et al. showed that ginsenosides in combination with anti-cancer drugs regorafenib acted by inhibiting growth of HepG2 cells through regulating the expression of Survivin and Caspase-3 genes (194). Ginkgol C17:1 inhibited cisplatin-induced autophagy *via* AMP-activated protein kinase/ULK1signaling and increased cisplatin-induced apoptosis in HepG2 cells *via* the PI3K/AKT/mTOR signaling pathway (195). Astragaloside IV effectively protected against cisplatin-induced injury by inducing autophagy and limiting the expression of NLRP3 (196). Aloin in combination with metformin synergistically inhibited HepG2 and Bel-7402 cell proliferation and invasion and induced apoptosis and autophagy through activating PI3K/AKT/mTOR pathway *in vitro*. In addition, it has a synergistic effect by inhibiting growth and promoting apoptosis and autophagy in HepG2 xenograft mice model (197). Sinapic acid combined with cisplatin inhibits proliferation and migration of HepG2 and SMMC-7221 cells. At the same time, this combination therapy induces autophagy by upregulating the protein expressions of LC3II, Beclin-1 and Atg5, and downregulating the expression of p62 (198). The combination of 6-shogaol and 5-FU inhibit AKT/mTOR/MRP1 signaling pathway and induce liver cancer cell apoptosis by decreasing the expression of AKT, mTOR, MRP1 and cyclin-related proteins (199).

With the development of nanotechnology, nano-drug delivery system can improve drug solubility improve drug stability, increase drug targeting, reduce drug toxicity and side effects. Ceria Nanoparticles can kill cancer cells through induce cancer cells to produce ROS, reduce the expression level of various antioxidant enzymes, cause mitochondrial damage and apoptosis (200). Xu et al. synthesized a composite material DCQ which dextran-coated cerium oxide nanoparticlesloaded quercetin, and discovered that the composite material was more toxic to HepG2 cells, and had no obvious toxic effect on normal cells, human umbilical vein endothelial cells (HUVEC). The composite material can induce the production of ROS, inhibit the fusion of autophagosomes and lysosomes in HepG2 cells and cause the accumulation of autophagosomes, block autophagy and promote apoptosis of HepG2 cells (201). Dong et al. synthesized a nano-layered double hydroxide (NLDH) co-loaded fluorouracil (Fu) and curcumin (Cur) mixed dosage form (LDH-Fu-Cur, LFC). Compared with pure fluorouracil, fluorouracil plus curcumin, and LDH-Fu, LDH-Fu-Cur more efficiently inhibited the growth and promoted the apoptosis of 7721, LM3 and Hep G2 cell lines. It also could significantly down-regulate the Bcl-2 gene expression of 7721 cells and induce cell apoptosis by activating caspase 3 and caspase 9 (202). Moreover, han explored a unique amphiphilic PCL-AuNC/Fe (OH)3-PAA Janus nanoparticle (JNP) to simultaneously preserve the hydrophilic drug (doxorubicin) and hydrophobic drug (docetaxel) in their distinct domains. It realized the optional sequential drug release by a single inorganic JNP for the first time, and the simultaneous release of the two drugs can improve efficacy and reduce toxic side effects. Furthermore, the mice treated with dual drug loaded PCL-AuNC/Fe (OH)3-PAA JNPs under near infrared (NIR) laser irradiation showed better tumor inhibition than solo drug, cocktail and dual drug treated groups, induced aopotosis and blocked the cell cycle of HepG2, and inhibited the growth of tumor *in vivo*, indicated the effectivity and significance of combined cancer therapy (203). To improve the utilization of curcumin (CUR) and 5-fluorouracil (5-FU) chemotherapeutic drugs in the treatment of liver tumors, increase the accumulation of drugs in tumor sites and reduce the side effects of drugs on the systemic system, Ni Wenfeng constructed a novel targeting nanocarrier to transport the drug to the liver tumor site. In their study, an amphiphilic triblock PEG-PLGA-PEG copolymer was coupled with two targeting ligands (BIO and LAC) to prepare

dual-targeted nanoparticles (BLPPNPs), which encapsulated curcumin (CUR) and 5-FU. And the mechanism of synergistic anti-hepatocarcinogenesis of the two drugs may be that CUR down-regulates the expression of DPYP protein by up-regulating the expression of p53 protein, increasing the cytotoxicity of 5-FU and enhancing the anti-tumor effect. At the same time, CUR may decrease the expression of Bcl-2 protein, increase the release of cyt c, and promote the apoptosis of hepatoma cells (204). Zhang successfully prepared a kind of multifunctional nanoparticles: Janus-magnetic mesoporous silica nanoparticles (Fe_3O_4-MSNs), with the surface modified by hyaluronic acid (HA) and nano fluorescent probe quantum dots (QD), and chemotherapy drug doxorubicin and berberine (ber), Fe_3O_4-MSN/Dox+Ber@HA-QD. The *in vitro* experiments showed that the nanoparticles could selectively enter HepG2 cells through the CD44 receptor mediated endocytosis pathway and release dox and rer rapidly, which had better cytotoxic effects at low concentrations. The *in vivo* results also suggested that the nanoparticles have a significantly lower recurrence of the hepatocellular carcinoma induced by dox and significantly reduced the toxic and side effect of doxorubicin while having a better antitumor effect than other groups. In addition, the nanoparticles can also achieve MRI and fluorescence imaging of the tumor site, providing the possibility of drug delivery and therapeutic effects (205). Table 2 summarizes their effects and mechanisms on liver cancer.

Anti-liver cancer mechanism of plant-derived natural products in combination with immunotherapy

The immune system of the body can recognize and eliminate foreign invading antigens, mutated cells and senescent cells of the body, and maintain the stability of the internal environment. However, tumor cells have the ability to escape immune surveillance, immune identification, and eradication, and immune system dysfunction lead to the development of malignant cells with clinical manifestationsb (206). According to the immune escape mechanism of tumor cells, who established a variety of immunotherapies of cancer (207). This kind of breakthrough therapy is defined that regulates immunological response through activating the organism's immune defense system or action of biological compounds to suppress and prevent tumor growth. At present, the commonly immunotherapy methods include immune checkpoint blockade therapy (208), antibody therapy (209), tumor vaccine therapy (210). Cancer immunotherapy has become an irreversible trend herald in the field of cancer therapy and is regarded as the fourth type of anti-tumor treatment after surgery, radiotherapy, and chemotherapy due to the obvious efficacy and low side effects. Although immunotherapy has made significant progress in the treatment of liver cancer, it needed to be further improved the clinical efficacy, find more specific immune targets, while avoid unnecessary targeting and off-target toxicity (211). Therefore, a combination of natural products and tumor immunotherapy can learn from each other and coordinate with each other to improve the effective rate of treatment.

Regulate immune function

It has been known that immune function of body is closely related to the occurrence and development of tumors. As host immune function is low or suppressed, the incidence of tumor will be increased. And in the progressive growth of tumor, the immune function will also be inhibited by the tumor. These two factors are mutual causation and the fluctuation directly affects the occurrence and development of tumor. Tumor microenvironment is an extremely complex system that involves several kinds of multifunctional immunizing cells and molecules, as well as tumor cells. It is a dynamic system composed of cancer cells, cytokines, extracellular matrix and immune cell subsets (212). Formation of Individual tumor is likely to develop because the tumor-associated microenvironment promotes tumor cell growth and protects tumor cells from elimination of systemic effector cells (213). Natural products in combination with immunotherapy act by inducing antitumor effects through restoring immune recognition and immune elimination by regulating the immune function.

Hu et al. revealed that *Lycium barbarum* polysaccharide in combination with cytokine CXCL10 acts by improving immune function against liver cancer. It also promotes secretion of Th1 cytokines and restores balance of Thl/Th2, improving number and function of dendritic cells (DC) and intervening immune suppression state of tumor-bearing bodies (214). Chen et al. demonstrated that a combination of anti-PD-L1 antibody and high concentration of vitamin C acts by promoting the expression of PD-L1 *in vivo* and *in vitro* and enhance the efficacy of anti- PD-L1 antibody. It can promote liver tumor blood vessels normalization and eventually increase T cell infiltration through activating cyclic GMP-AMP synthase (cGAS) and promoting the secretion of its product cGAMP, and then activating the STING pathway of vascular endothelial cells (215). Song et al. proved that a combination of 10-hydroxycamptotenin and DC hepa-6 fusion vaccine acts by inducing improving immune function and significantly inducing CTL cytotoxicity, and resisted against the rechallenge of Hepal-6 cells (216). Yang et al. reported that Chinese herb medicine combine with targeted therapy of TCM immune for patients with end-stage liver cancer, after treatment, improved symptoms of abdominal distension and jaundice, nutritional status and quality, alleviated the pain, and prolonged overall survival time (217). Yu et al. suggested that sorafenib combined with Poria Lingsini decoction can significantly improve immune function and the survival outcome of patients with advanced primary liver cancer (218).

Induce liver cancer cell apoptosis

Endoplasmic reticulum (ER) stress results from the accumulation of unfolded or misfolded proteins in the ER, is involved in regulating apoptotic process in tumor cells (219). It will trigger endogenous and exogenous apoptotic signals as ER dysfunction persists in eukaryotic cells, in addition, the heavy and continuing endoplasmic reticulum stress can lead to cell dysfunction and even cell death. When endoplasmic reticulum stress (ERS) occurs in cells, the expression

TABLE 2 Effect and mechanism of plant-derived natural products combination Chemotherapy drugs.

Combination Therapy	Concentration	Cell Line/ Model	Mechanism	Reference
Kanglite injection/ Thalidomide	kanglite injections: 200 mL/d thalidomide: 100 mg/d	76 patients of primary liver cancer	Inhibited blood vessels through inhibiting VEGF and B-FGF induced angiogenesis, and regulate cellular immunity of the body	(166)
Liuwei Dihuang/ Cisplatin	liuwei dihuang: 100 mg/mL cisplatin: 1 mg/mL	BEL-7402	Downregulated the expressions of VEGF and Ang-2, upregulated the expression of TSP and TIMP-2	(167)
Astragalus polysaccharide/ Cisplatin/ Doxorubicin	astragalus polysaccharide: 50-200 mg/kg cisplatin: 2 mg/kg doxorubicin: 6 mg/kg	HepG2 tumor-bearing mice	Reduced the expressions of Ki-67, HIF-1α and VEGF	(168)
Radix astragali/ Curcuma/ Cisplatin	radix astragali: 3-12 g/kg/d curcuma: 3-12 g/kg/d cisplatin: 2 mg/kg	HepG2 tumor-bearing mice	Down-regulated the expression of CD147 and In-OS	(169)
Astragaloside IV/ Curcumin/ Cisplatin	astragaloside IV: 12 g/kg/d curcumin: 10 g/kg cisplatin: 2 mg/kg	HepG2 tumor-bearing mice	Inhibited the formation of new blood vessels in liver cancer by down-regulating the expression of HIF-1α and VEGF	(170)
Epigallocatechin gallate/Derivative Y6/ Daunrrubicin	EGCG: 40 mg/kg Y6: 27.5-110 mg/kg daunrrubicin:2 mg/kg	HepG2 tumor-bearing mice	Inhibited MAPK/ERK and PI3K/AKT signaling pathways and down-regulated the expression of HIF-1 α, CBR1 and VEGF	(171)
Curcumin/ Doxorubicin	DOX/Cur-NPs: 2 mg/kg	Liver cancer mice	Decreased the mRNA levels of MDR1, Bcl-2 and HIF-1α, and protein levels of P-gP, Bcl-2 and HIF-1α	(172)
Mannose/ Cisplatin	mannose: 25 mmol/L cisplatin: 10 μmol/L	HepG2	Inhibited proliferation and migration and changed morphology with separation, shedding and aggregation	(177)
Emodin/ Cisplatin	emodin: 6.25-50 μg/mL cisplatin: 2.5 μg/mL	HepG2	Up-regulated the expression of e-cadherin, and inhibited EMT	(178)
Kaempferol/ Doxorubicin	kaempferol: 0-40 mmol/L doxorubicin: 300-1200 nmol/L	Huh-7, Huh-1, HepG2 HepG2.2.15 SK-Hep-1 PLC/PRF/5 HLE, HLF, Hep3B	Inhibited PI3K/mTOR/MMP protein pathway in a dose-and time-dependent manner153	(179)
Sinosinine thiocyanate/ Gemcitabine	sinosinine thiocyanate: 50 μmol/L gemcitabine: 0-20 μmol/L	HepG2	Inhibited the expression of multidrug-resistant related proteins ABCB1 and ABCG2,155 enhance the sensitivity to gemcitabine	(180)
Caffeine/ 5-fluorouracil	caffeine: 0.5-1 mmol/L 5-fluorouracil: 0-50 μmol/L	SMMC-7221 HepG3B	Increased the e156xpression of cleaved PARP, p-JNK, p-p38, and decreased the expression of Bcl-2, Bcl-xL, CDK2/4/6, p-ERK, p38, *via* inducing generation of ROS and influencing MAPK signaling pathway,	(181)
Curcumin/ Metformin	curcumin: 5-10 μmol/L metformin: 10 mmol/L	HepG2 PLC/PRF/5	Inhibted the expression of VEGF, MMP2/9, and VEGFR-2	(182)

(Continued)

TABLE 2 Continued

Combination Therapy	Concentration	Cell Line/ Model	Mechanism	Reference
Matrine/ Cisplatin	matrine: 100 mg/kg cisplatin: 2 mg/kg	HepG2 nude mice	Activated the caspase apoptosis pathway and inhibiting expression of Survivin-related caspase-9 protein	(188)
Tannic acid/ Cisplatin	tannic acid: 90-540 μmol/L cisplatin: 0.6-3.6 μg/L	HepG2	Induced apoptosis through activating caspase-3 signaling cascade	(192)
Saikosaponin D/ Doxorubibin	saikosaponin D: 2-16 μg/mL doxorubibin: 0.5-16 μg/mL	H22 mice model	Suppressed cell proliferation and invasion through up-regulating of ROS, Oatp1b1 as well as TGF-β1	(193)
Ginsenoside/ Regorafenib	ginsenoside: 10 mg/L regorafenib: 1 mg/L	HepG2	Regulated the expression of Survivin and Caspase-3 genes	(194)
Ginkgol C17:1/ Cisplatin	ginkgol C17:1: 0-80 μg/mL cisplatin: 2 μg/mL	HepG2	Induced AMP-activated protein kinase/ULK1signaling and the phosphoinositide 3-kinase/Akt/ mechanistic target of rapamycin pathway	(195)
Astragaloside IV/ Cisplatin	astragaloside IV:40-80 mg/kg cisplatin:15 mg/kg	Liver cancer SD rats	Induced autophagy and limiting the expression of NLRP3	(196)
Aloin/ Metformin	aloin: 50 μmol/L metformin: 400 μmol/L	HepG2 Bel-7402	Activated PI3K/AKT/mTOR pathway	(197)
Sinapic acid/ Cisplatin	sinapic acid: 0-2,000 μmol/L cisplatin: 5 μmol/L	HepG2 SMMC-7721	Upregulated the protein expressions of LC3II, Beclin-1 and Atg5, and downregulated the expression of P62	(198)
6-shogaol/ 5-fluorouracil	6-Shogaol: 10 μmol/L 5-fluorouracil: 10 μmol/L	HepG2 Li-7	Inhibited AKT/mTOR/MRP1 signaling pathway and decreased the expression of AKT, mTOR, MRP1 and cyclin-related proteins	(199)
Quercetin/ Ceria nanoparticles	DCQ: 33-165 μmol/L	HepG2	Induced the production of ROS, inhibited the fusion of autophagosomes and lysosomes in HepG2 cells and caused the accumulation of autophagosomes, blocked autophagy and promoted apoptosis of HepG2 cells	(201)
Curcumin/ Fluorouracil	LFC: 15-35 μg/mL	LM3 Hep G2 7721	Down-regulated the Bcl-2 gene expression of 7721 cells and induced cell apoptosis by activating caspase 3 and caspase 9	(202)
Docetaxel/ Doxorubicin	PCL-AuNC/Fe $(OH)_3$-PAA JNPs: 1.56-100 μg/mL	HepG2/H22 BALB/c tumor-bearing mice	Induced apoptosis and blocked the cell cycle of HepG2, and inhibited the growth of tumor *in vivo*	(203)
Curcumin/ 5-fluorouracil	combined feeding ratio: 1:2.5 (5-FU: CUR)	HepG2 HL7702 HepG2 tumor-bearing nude mice	Down-regulated the expression of DPYP protein by up-regulating the expression of p53 protein, increasing the cytotoxicity of 5-FU and enhancing the anti-tumor effect, decreased the expression of Bcl-2 protein, increased the release of cyt c, and promoted the apoptosis of hepatoma cells	(204)
Berberine/ Doxorubicin	Fe_3O_4-MSN/Dox +Ber@HA-QD: 4 mg/kg	HepG2 H22 ICR tumor-bearing mice	Reduced the toxic and side effect of doxorubicin while having a better antitumor effect than other groups	(205)

of anti-apoptotic molecule BiP (immunoglobulin binding protein) and pro-apoptotic molecules, such as CHOP and caspase-12, is regulated to determine whether the cells will undergo apoptosis or survive to adapt to the environment (220). Plant-derived natural products in combination with immunotherapy can induce apoptosis of tumor cells.

Jin et al. prepared paclitaxel-loaded nanoparticles decorated with anti-CD133 antibody, which could effectively target liver cancer stem

cells and induce apoptosis of liver cancer cells (221). Wang et al. demonstrated that paclitaxel in combination with anti-human stathmin1 antibody inhibits proliferation and induces apoptosis of liver cancer cells (222). Lin et al. found that the combination of taxol and immunosuppressant cyclosporin A increases the expression of caspase-9 and caspase-3, induces apoptosis of liver cancer cells through PI3K-mTOR pathway, and effectively reverses drug resistance of paclitaxel (223). Huang et al. confirmed that a combination of gambogic acid and proteasome inhibitors induces liver cancer cell apoptosis and inhibits growth through inducing cytotoxicity and enhancing proteasome inhibition and ER stress (224). A combination of n-glycosylation inhibitor tunicamycin and camptothecin acts by inducing resistance through up-regulating GRP78 and blocking G1 phase cell cycle (225). Nicotinamide and STAT3 inhibitor significantly induced apoptosis and inhibited proliferation by reducing phosphorylation of STAT3 Y705 in HepG2 cells, down-regulating the expression of SNAIL1, VEGFA and ZEB1, EMT-related gene and glucose metabolism. Moreover, the synergistic effect is more significant (226).

Photodynamic therapy (PDT), with its unique advantages of minimally invasive, good selectivity, high safety and unique efficacy, has been used as a new therapeutic method for liver tumor treatment. As a natural product, hypocrellin B (HB) can be used as a photosensitive agent for PDT treatment of many diseases, especially for tumor treatment. In order to improve poor water solubility, fast metabolism *in vivo* and no specific tissue distribution of HB, zhang collected liver cell membrane (CCCM) and modified tumor-targeting ligand (transferrin, TF) into homologous liver cancer cell membrane (TF-CCCM), and prepared ethylene nanoparticles (HB NPs) by double emulsion method. Then TF-CCCM-HB NPs was prepared by extrusion method by mixing the two in a certain proportion. TF-CCCM-HB NPs has strong targeting ability and phagocytosis in homologous liver cells, and suppress the proliferation of tumor cells in a dose-dependent manner. Moreover, it has a synergistic effect with PDT, which can promote the production of ROS and reduce mitochondrial membrane potential. At the same time, TF-CCCM-HB NPs combined with PDT can inhibit the growth of tumor in mice model with liver cancer, prolong the survival time of tumor-bearing mice, and inhibit tumor metastasis and recurrence, which has good biosafety (227). Bai prepared a form drug/gene co-loaded nanoparticles (sCDP/DOX/miR-122), which a nanosystem based on β-cyclodextrin-cored star polymer (sCDP) and co-deliver antitumor drug doxorubicin (DOX) and miRNA-122. s CDP/DOX/miR-122 nanoparticles can remarkably inhibit HepG2 cell proliferation, promote cell apoptosis and increase the expression of p53 and cleaved caspase 3; it also can downregulate the expression of Bcl-w and CCNG1 leading to irreversible cell apoptosis, decrease the expression of MDR1, MRP and P-gp, and improve the sensitivity to DOX of HepG2 cells, thus realizing the synergistic antitumor effect *in vitro*. sCDP/DOX/miR-122 nanoparticles can slow down the weight loss of nude mice bearing tumor and significantly inhibit tumor growing, thus realizing a synergistic anti-tumor effect *in vivo* (228). Yuan synthesis iron oxide nanoparticles loaded polydopamine (PDA) and doxorubicin (Dox). Rats were treated with hepatic artery *via* interventional methods, and it was verified that Fe_2O_3-PDA-Dox nanoparticles can simultaneously have the ecceft of Transcatheter arterial chemoembolization (TACE) and photothermal ablation (PTA). It also confirmed that combretastatin A-4 phosphate disodium (CA4P) can increase the uptake of Fe_2O_3-PDA-Dox nanoparticles by rat hepatocellular carcinoma, which can enhance the combined treatment of transcatheter arterial chemoembolization and photothermal ablation without additional increase in liver and kidney toxicity (229).

Reduce liver cancer cells metastasis

Plant-derived natural products in combination with immunotherapy act by inhibiting tumor cell proliferation and metastasis through inhibiting angiogenesis and arresting cell cycle. Lai Chunhui prepared nanoparticles which mannose (M)/CpG oligodeoxynucleotide (CpG-ODN)-conjugated liposomes lipo loaded with tumor-associated antigens. It specifically induced the activation and maturation of DCs *in vivo* and the activated DCs stimulated effector cells to kill tumor cells in mice, thereby achieving the effect of anti-tumor immunotherapy (230). Zhong et al. revealed that tubacin, an inhibitor of histone deacetylase 6 (HDAC6), in combination with docetaxel, could arrest the cell cycle, inhibit metastasis and proliferation, as well as induce apoptosis of liver cancer cells (231). Shen et al. found that evocorine in combination with autophagy inhibitor chloroquine (CQ) acts by inhibiting angiogenesis of HepG2 cells through inducing autophagy. It can decrease the expression of VEGFA and inhibit invasion (232). Lai et al. demonstrated that evodiamine or paclitaxel in combination with CDK1 inhibitors acts by inducing the apoptosis of hepatocarcinoma cells through arresting G2/M phase cell cycle. Evodiamine in combination with R03306 have a synergistic effect on upregulating the expression of cyclin E and decreasing the expression of cyclin B1. Moreover, paclitaxel combined with R03306 can decrease the expression of Bcl-2 and cyclin B1, increase the expression of Bax, thereby inducing apoptosis in HepG2 cells (233). Compound kushen injection significantly enhanced the anticancer activity of sorafenib at a subclinical dose without obvious side effects, and prevented the postsurgical recurrence and rechallenged tumor growth. It activated proinflammatory responses and relieved immunosuppression of tumor-associated macrophages in the liver cancer cell microenvironment by triggering tumor necrosis factor receptor superfamily member 1 (TNFR1)-mediated NF-κB and p38 MAPK signaling cascades, which subsequently resulted in apoptosis of liver cancer cells (234). Table 3 summarizes their effects and mechanisms on liver cancer.

Conclusion

The high mortality and morbidity of liver cancer remain a primary challenge for scientific research. Although traditional therapies, such as surgical resection, radiotherapy and chemotherapy, are effective for liver cancer at early stage, the five-year survival rate of liver cancer patients is meager and often ends in

TABLE 3 Effect and mechanism of plant-derived natural products in combination with immunotherapy.

Combination Therapy	Concentration	Cell Line/ Model	Mechanism	Reference
Lycium barbarum polysaccharide/ CXCL10	lycium barbarum polysaccharide: 100 mg/kg CXCL10: 15 μg/kg	H22 mice model	Improved immune function and promoted secretion of Th1 cytokines and restore balance of Thl/Th2, improved number and function of DC cells and intervened immune suppression state of tumor-bearing bodies	(214)
Vitamin C/ Anti-PD-L1 antibody	vitamin C: 4 g/kg Anti-PD-L1 antibody: 75 μg/3day	Hepa1-6 cancer mice	Activated cyclic GMP-AMP synthase (cGAS) and promoted the secretion of its product cGAMP, and then activated the STING pathway of vascular endothelial cells	(215)
10-hydroxycamptothecinc/ DC hepa1-6fusion vaccine	10-hydroxycamptothecinc: 50-100 μg/mL	Hepa1-6 cancer mice	Induced improving immune function and inducing significantly CTL cytotoxicity	(216)
Chinese herb medicine/ Camrelizumab/ Lenvatinib	camrelizumab: 200 mg/ 3weeks lenvatinib: 8 mg/day	Advanced liver cancer patient	Improved symptoms of abdominal distension and jaundice, nutritional status and quality, alleviated the pain, and prolonged overall survival time	(217)
Fuling sini decoction/ Sorafenib	sorafenib: 800 mg/day	Liver cancer patient	Improved the survival outcome of patients with advanced primary liver cancer, improve immune function	(218)
Paclitaxel/ Anti-CD133 antibody	nanoparticles: 7.51-56.92 ng/mL	Huh-7 HepG2	Targeted liver cancer stem cells and induced apoptosis	(221)
Paclitaxel/ Anti-human stathmin1antibody	paclitaxel: 0.1-1.6 μg/ mL anti-human stathmin 1 antibody: 10-160 μg/mL	HepG2	Inhibited proliferation and induced apoptosis	(222)
Taxol/ Cyclosporin A	taxol: 0.1 μmol/L cyclosporin A: 0-10 μmol/L	Hep3B HepG2 HA22T VGH Hepa 1-6	Increased the expression of caspase-9 and caspase-3, induced apoptosis of liver cancer cells through PI3K-mTOR pathway, and effectively reversed drug resistance of paclitaxel	(223)
Gambogic acid/ Bortezomib	gambogic acid: 0.4-0.6 μmol/L bortezomib: 40-60 nmol/L	HepG2 H22	Induced cytotoxicity and enhanced proteasome inhibition and ER stress	(224)
Camptothecin/ Etoposide/ Tunicamycin	camptothecin:3 μmol/L etoposide: 5 μmol/L tunicamycin: 1 μg/mL	Hep3B	Induced resistance through up-regulating GRP78 and block G1 phase cell cycle	(225)
Nicotinamide/ STAT3 inhibitor	nicotinamide: 5 mmol/ L S3I-201:100 μmol/L stattic: 1.5 μmol/L	HepG2	Reduced phosphorylation of STAT3 Y705, down-regulated the expression of SNAIL1, VEGFA and ZEB1, and decreased epithelial-mesenchymal transition and glucose metabolism	(226)
Hypocrellin B/ Transferrin/ Membrane	TF-CCCM-HB-NPs: 0-100 μg/mL	HepG2 LO2 HepG2 tumor-bearing mice model	Promoted the production of ROS and reduced MMP, inhibited the growth of tumor in mice model with liver cancer, prolonged the survival time of tumor-bearing mice	(227)
Doxorubicin/ miRNA-122	sCDP/DOX/miR-122: 2.1 μg/mL	Hep G2 Liver nude mice bearing tumor	Increased the expression of p53 and cleaved caspase-3, downregulated the expression of Bcl-w and CCNG1 leading to irreversible cell apoptosis, decreased the expression of MDR1, MRP and P-gp, and improved the sensitivity to DOX of HepG2 cells	(228)
Doxorubicin/ Combretastatin A-4 phosphate disodium	Fe_2O_3-PDA-Dox: 0.4 mg/mL CA4P: 0.1 mg/mL	Liver tumor rats model	Enhanced the combined treatment of transcatheter arterial chemoembolization and photothermal ablation without additional increase in liver and kidney toxicity	(229)

(Continued)

TABLE 3 Continued

Combination Therapy	Concentration	Cell Line/ Model	Mechanism	Reference
Mannose/ Tumor-assoclated antigens	M/CpG-ODN-H22-Lipo: 100 μL/mice	H22 bearing mice model	Induced the activation and maturation of DCs *in vivo* and the activated DCs stimulated effector cells to kill tumor cells in mice	(230)
Docetaxel/ Tubacin	docetaxel: 0-32 μmol/L tubacin: 10 μmol/L	SNU449 SNU387	Arrested the cell cycle, inhibit metastasis and proliferation, as well as induce apoptosis of liver cancer cells	(231)
Evodiamine/ Chloroquine	evodiamine: 10 μmol/L chloroquine: 25 μmol/L	HepG2	Inhibited angiogenesis through inducing autophagy, and decreased the expression of VEGFA and inhibited invasion	(232)
Evodiamine/ Paclitaxel/ CDK1 inhibitors	evodiamine:1-4 μmol/L paclitaxel: 0.2 μmol/L R0306: 2 μmol/L	HepG2	Decreased the expression of Bcl-2 and cyclin B1, increased the expression of Bax and cyclin E	(233)
Compound kushen injection/ Sorafenib	compound kushen injection: 0.43-1.32 mg/mL sorafenib: 10, 30 mg/kg	Hepa1-6 tumor nude mice	Activated proinflammatory responses and relieved immunosuppression of tumor-associated macrophages in the liver cancer cell microenvironment by triggering tumor necrosis factor receptor superfamily member 1 (TNFR1)-mediated NF-κB and p38 MAPK signaling cascades	(234)

failure. In recent years, plant derived natural products and their secondary metabolites possess characteristics of abundant products, low toxicity and side effects, diverse biologic activities, and high content of active ingredients. It has been considered as the most promising candidates for oncology therapies. However, due to poor water solubility, difficult extraction, and easy to develop drug resistance, a single treatment may not be able to achieve satisfactory efficacy. Therapies that combine natural products with chemotherapy drugs or immunotherapy have been developed to target a variety of cancer pathways. The dose requirement of each agent in combination therapy can be reduced, which reduces the side-effects compared to monotherapy. Targeting various pathways *via* multiple drug combinations can control disease preferably and decrease the chance of cancer cells becoming increasingly malignant and incurable. It can also target the heterogeneity of the tumor by two or more pathways to toxicity of cancer cells and disruption of their homeostasis (235). This review mainly focused on the mechanisms of plant-derived natural products and combination therapy against liver cancer. We have listed the mainly compounds and combination therapy and individually summarized their antitumour effects and mechanisms (Figure 2). Like many other cancers, liver cancer arises as a result of accumulation of multiple genetic mutations that cause

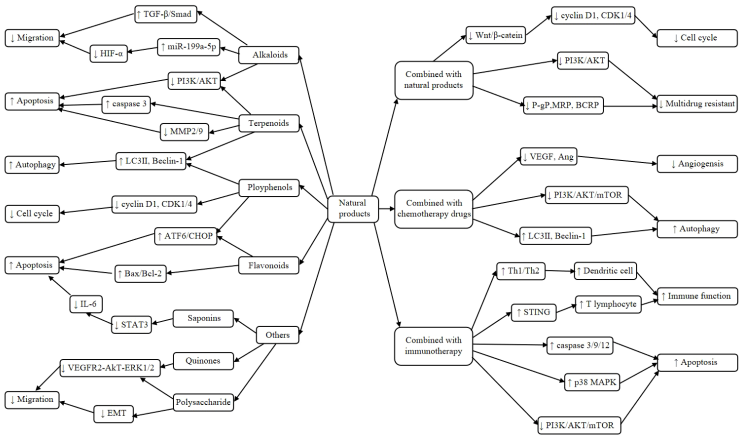

FIGURE 2
Mechanisms of natural products and combination therapy against liver cancer. Alkaloids could inhibits migration through up-regulating TGF-β/Smad and miR-199a-5p, and down-regulating HIF-α expression. Terpeniods promotes apoptosis by inhibiting the PI3K/AKT pathway and the expression of caspase3. It also induces autophagy through up-regulating the expression of LC3II and Beclin-1. Ployphenols inhibits Cyclin D1 and CDK1/4 expression, which in turn block the cell cycle. It also induces apoptosis by activating ATF6/CHOP signaling pathway. Flavonoids induces apoptosis through activation of the ATF6/CHOP pathway and upregulation the ratio of Bax/Bcl-2. Moreover, other natural products inhibit migration through down-regulating VEGFR2-AKT-ERK1/2 signaling pathway and suppressing EMT. Combination of Natural product ingredients inhibits Cyclin D1 and CDK1/4 expression through downregulation of the Wnt/β-catenin pathway, which in turn inhibits cell proliferation. It also reverses multidrug resistant by decreasing the expression of P-gP, MRP and BCRP. Natural product in combination with chemotherapy suppress angiogensis through down-regulating VEGF and Ang expression. It also induces autophagy by upregulating expression of LC3ii and Beclin-1. Natural product in combination with immunotherapy act by inducing antitumor effects through restoring immune recognition and immune elimination by regulating the immune function. It also induces apoptosis by inhibiting the PI3K/AKT and p38MAPK pathway, which in turn induces apoptosis.

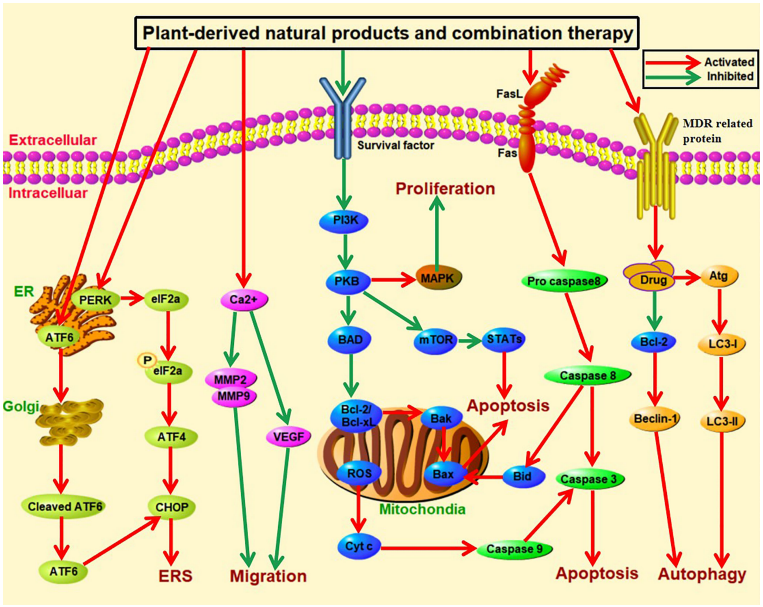

FIGURE 3
Overview of signaling pathways against liver cancer. Plant-derived natural products and different combination therapy can achieve practical anti-liver-cancer effects through multiple mechanisms, including activation of continuing endoplasmic reticulum stress, suppression of migration, inhibition of cell proliferation, induction of apoptosis and autophagy. For example, it could promote apoptosis through the heavy and continuing endoplasmic reticulum stress; and it coula promote the expression of ATF6, PERK, eIF2α, p-eIF2α, ATF4, CHOP. It also could suppress migration through increasing the concentration of intracellular calciumions, reduce transcriptional activities of MMP-2 and MMP9 and VEGF to inhibit metastasis. Besides, it could increase the expression of Bcl-x; downregulating the expression of Bcl-xL and Bcl-2; suppressing the PI3K/AKT/mTOR signaling pathway and caspase cascade reaction. In the next place, combination therapy could reduce cancer cell proliferation by binding PI3K and subsequently suppressing PKB function and regulating MAPK signaling pathway. It also coula induce apoptosis through activation of STAT3 *via* inhibiting the phosphorylation of mTOR. Moreover, it could promote aopotosis through caspase cascade reactor and. In addition, autophagy is also related to occurrence and development of tumor, natural plants target intracellular autophagy including Beclin-1, PI3K/AKT/mTOR, have been known to control cell proliferation and apoptosis.

abnormal cellular proliferation. Our study reviewed natural products and different combination therapy that have antitumor effects on liver cancer, which showed possible benefits in treating patients with liver cancer through mechanisms, such as activation of continuing endoplasmic reticulum stress, suppression of migration, inhibition of cell proliferation, induction of apoptosis and autophagy (Figure 3). Therefore, it could provide effectively alternative or adjuvant treatment strategies for cancer patients.

However, it is important to note that the study also revealed some disadvantages of combination therapy for cancer. Multiple drug combinations can synergistically increase efficacy, but may also produce unnecessary side effects (236). The target molecular mechanisms of most natural products have not been fully elucidated, especially those related to combinations. Researchers need to further systematically and comprehensively study the immunity or molecular pathology of liver cancer to clarify the relevant mechanisms. Meanwhile, there is still a considerable long way in developing the antitumor strategy of combining natural products with other methods.

Author contributions

YW: Conceptualization, Data curation, Formal analysis, Investigation, Writing-original draft, Visualization. JL: Writing-review & editing, Supervision. LX: Writing-review & editing, Supervision. All authors contributed to the article and approved the submitted version.

Funding

The work was financially supported by the National Natural Science Foundation of China, China (NSFC) (Grant No: 31860258, and 32060229).

Conflict of interest

The authors declare that the research was conducted in the absence of any commercial or financial relationships that could be construed as a potential conflict of interest.

Publisher's note

Supplementary material

The Supplementary Material for this article can be found online at: https://www.frontiersin.org/articles/10.3389/fonc.2023.1116532/full#supplementary-material

References

1. Sung H, Ferlay J, Siegel RL, Laversanne M, Soerjomataram I, Jemal A, et al. Global cancer statistics 2020: GLOBOCAN estimates of incidence and mortality worldwide for 36 cancers in 185 countries. *CA Cancer J Clin* (2021) 71(3):209–49. doi: 10.3322/caac.21660

2. Su TS, Lu HZ, Cheng T, Zhou Y, Huang Y, Gao YC, et al. Long-term survival analysis in combined transarterial embolization and stereotactic body radiation therapy versus stereotactic body radiation monotherapy for unresectable hepatocellular carcinoma >5 cm. *BMC Cancer* (2016) 16(1):834. doi: 10.1186/s12885-016-2894-9

3. Tang A, Hallouch O, Chernyak V, Kamaya A, Sirlin CB. Epidemiology of hepatocellular carcinoma: Target population for surveillance and diagnosis. *Abdom Radiol (NY)* (2018) 43(1):13–25. doi: 10.1007/s00261-017-1209-1

4. Zaheer J, Kim H, Lee YJ, Kim JS, Lim SM. Combination radioimmunotherapy strategies for solid tumors. *Int J Mol Sci* (2019) 20(22):5579. doi: 10.3390/ijms20225579

5. Hindson J. Combined TACE and sorafenib for HCC treatment. *Nat Rev Gastroenterol Hepatol* (2020) 17(2):66. doi: 10.1038/s41575-020-0265-0

6. Izzo F, Granata V, Grassi R, Fusco R, Palaia R, Delrio P, et al. Radiofrequency ablation and microwave ablation in liver tumors: An update. *Oncologist* (2019) 24(10): e990–e1005. doi: 10.1634/theoncologist.2018-0337

7. Kardashian A, Florman SS, Haydel B, Ruiz RM, Klintmalm GB, Lee DD, et al. Liver transplantation outcomes in a U.S. multicenter cohort of 789 patients with hepatocellular carcinoma presenting beyond Milan criteria. *Hepatology* (2020) 72(6):2014–28. doi: 10.1002/hep.31210

8. Xia F, Wu LL, Lau WY, Huan HB, Wen XD, Ma KS, et al. Adjuvant sorafenib after heptectomy for Barcelona clinic liver cancer-stage c hepatocellular carcinoma patients. *World J Gastroenterol* (2016) 22(23):5384–92. doi: 10.3748/wjg.v22.i23.5384

9. Chuma M, Terashita K, Sakamoto N. New molecularly targeted therapies against advanced hepatocellular carcinoma: From molecular pathogenesis to clinical trials and future directions. *Hepatol Res* (2015) 45(10):E1–E11. doi: 10.1111/hepr.12459

10. Yang MD, Sun Y, Zhou WJ, Xie XZ, Zhou QM, Lu YY, et al. Resveratrol enhances inhibition effects of cisplatin on cell migration and invasion and tumor growth in breast cancer MDA-MB-231 cell models. *In Vivo In Vitro Molecules* (2021) 26(8):2204. doi: 10.3390/molecules26082204

11. Xin M, Wang Y, Ren Q, Guo Y. Formononetin and metformin act synergistically to inhibit growth of MCF-7 breast cancer cells *in vitro*. *BioMed Pharmacother* (2019) 109:2084–9. doi: 10.1016/j.biopha.2018.09.033

12. Piao XM, Gao F, Zhu JX, Wang LJ, Zhao X, Li X, et al. Cucurbitacin b inhibits tumor angiogenesis by triggering the mitochondrial signaling pathway in endothelial cells. *Int J Mol Med* (2018) 42(2):1018–25. doi: 10.3892/ijmm.2018.3647

13. Wei T, Xiaojun X, Peilong C. Magnoflorine improves sensitivity to doxorubicin (DOX) of breast cancer cells *via* inducing apoptosis and autophagy through AKT/mTOR and p38 signaling pathways. *BioMed Pharmacother* (2020) 121:109139. doi: 10.1016/j.biopha.2019.109139

14. Bayat Mokhtari R, Homayouni TS, Baluch N, Morgatskaya E, Kumar S, Das B, et al. Combination therapy in combating cancer. *Oncotarget* (2017) 8(23):38022–43. doi: 10.18632/oncotarget.16723

15. Pons-Fuster López E, Gómez García F, López Jornet P. Combination of 5-florouracil and polyphenol EGCG exerts suppressive effects on oral cancer cells exposed to radiation. *Arch Oral Biol* (2019) 101:8–12. doi: 10.1016/j.archoralbio.2019.02.018

16. Panji M, Behmard V, Zare Z, Malekpour M, Nejadbiglari H, Yavari S, et al. Synergistic effects of green tea extract and paclitaxel in the induction of mitochondrial apoptosis in ovarian cancer cell lines. *Gene* (2021) 787:145638. doi: 10.1016/j.gene.2021.145638

17. Kamat AM, Tharakan ST, Sung B, Aggarwal BB. Curcumin potentiates the antitumor effects of bacillus calmette-guerin against bladder cancer through the downregulation of NF-kappaB and upregulation of TRAIL receptors. *Cancer Res* (2009) 69(23):8958–66. doi: 10.1158/0008-5472.CAN-09-2045

18. He YL, Yang W, Wang P, Li B, Zheng Y, Lu LX, et al. Experimental study on matrine promoting hepatoma cells apoptosis through ERK1/2 signaling pathway. *Chin J Gastroenterol Hepatol* (2022) 31(09):1045–9.

19. Dai M, Chen N, Li J, Tan L, Li X, Wen J, et al. *In vitro* and *in vivo* anti-metastatic effect of the alkaliod matrine from sophora flavecens on hepatocellular carcinoma and its mechanisms. *Phytomedicine* (2021) 87:153580. doi: 10.1016/j.phymed.2021.153580

20. Lin S, Zhuang J, Zhu L, Jiang Z. Matrine inhibits cell growth, migration, invasion and promotes autophagy in hepatocellular carcinoma by regulation of circ_0027345/miR-345-5p/HOXD3 axis. *Cancer Cell Int* (2020) 20:246. doi: 10.1186/s12935-020-01293-w

21. Zhang J, Gao Y, Han H, Zou C, Feng Y, Zhang H. Matrine suppresses lung metastasis of human hepatocellular carcinoma by directly targeting matrix metalloproteinase-9. *Biochem Biophys Res Commun* (2019) 515(1):57–63. doi: 10.1016/j.bbrc.2019.04.063

22. Wang N, Feng Y, Zhu M, Tsang CM, Man K, Tong Y, et al. Berberine induces autophagic cell death and mitochondrial apoptosis in liver cancer cells: The cellular mechanism. *J Cell Biochem* (2010) 111(6):1426–36. doi: 10.1002/jcb.22869

23. Hou Q, Tang X, Liu H, Tang J, Yang Y, Jing X, et al. Berberine induces cell death in human hepatoma cells *in vitro* by downregulating CD147. *Cancer Sci* (2011) 102(7):1287–92. doi: 10.1111/j.1349-7006.2011.01933.x

24. Chen CM, Zhang GZ, Liu PP, Huo YF, Li TL. Berberine inhibits TGF-β1-induced epithelial-mesenchymal transition in human liver cancer HepG2 cells *via* TGF-β/Smad pathway. *Chin Pharmacol Bull* (2020) 36(02):261–7.

25. Jia J, Kang X, Liu Y, Zhang J. Inhibition of human liver cancer cell growth by evodiamine involves apoptosis and deactivation of PI3K/AKT pathway. *Appl Biol Chem* (2020) 63(1):1–8. doi: 10.1186/s13765-020-00551-9

26. Zhao S, Xu K, Jiang R, Li DY, Guo XX, Zhou P, et al. Evodiamine inhibits proliferation and promotes apoptosis of hepatocellular carcinoma cells *via* the hippo-Yes-Associated protein signaling pathway. *Life Sci* (2020) 251:117424. doi: 10.1016/j.lfs.2020.117424

27. Liu Q, Zhao S, Meng F, Wang H, Sun L, Li G, et al. Nrf2 down-regulation by camptothecin favors inhibiting invasion, metastasis and angiogenesis in hepatocellular carcinoma. *Front Oncol* (2021) 11:661157. doi: 10.3389/fonc.2021.661157

28. Ma QQ. The inhibitory effect of hydroxycamptothecin combined with human cytokine-induced killer cells on the proliferation of hepatoma cells. *Jilin Med J* (2020) 41 (04):773–6.

29. Diao YH, Liu L, Sha JP, Xue M. Vincristine regulates PI3K/Akt signaling pathway to inhibit the proliferation, migration, invasion of hepatocellular carcinoma cell line Hep3B and promote apoptosis. *Chin J Int Tradit Wes Med Liver Dis* (2019) 31(08):726–30.

30. Yu L, Wang ZC, Wang TJ. Inhibitory effect of caffeine combined with ionizing radiation on proliferation of hepatocellular carcinoma stem cells silenced by chk-1 and its apoptosis-induced effect. *J Jilin Univ (Med Edition)* (2018) 44(01):52–7. doi: 10.13481/j.1671-587x.20180110

31. Jin ZL, Yan W, Qu M, Ge CZ, Chen X, Zhang SF. Cinchonine activates endoplasmic reticulum stress-induced apoptosis in human liver cancer cells. *Exp Ther Med* (2018) 15(6):5046–50. doi: 10.3892/etm.2018.6005

32. Hussain SP, Amstad P, He P, Robles A, Lupold S, Kaneko I, et al. p53-induced up-regulation of MnSOD and GPx but not catalase increases oxidative stress and apoptosis. *Cancer Res* (2004) 64(7):2350–6. doi: 10.1158/0008-5472.can-2287-2

33. Zhang B, Wang X, Deng J, Zheng H, Liu W, Chen S, et al. p53-dependent upregulation of miR-16-2 by sanguinarine induces cell cycle arrest and apoptosis in hepatocellular carcinoma. *Cancer Lett* (2019) 459:50–8. doi: 10.1016/j.canlet.2019.05.042

34. Wang ZM, Wang M, Xiao HZ. Effect of mechanism of saikosaponin d on autophagy by regulating mTORC signaling pathway in human hepatocellular carcinoma cells. *Chin Pharmaceut J* (2018) 53(19):1652–7.

35. Wang B, Min W, Lin S, Song L, Yang P, Ma Q, et al. Saikosaponin-d increases radiation-induced apoptosis of hepatoma cells by promoting autophagy *via* inhibiting mTOR phosphorylation. *Int J Med Sci* (2021) 18(6):1465–73. doi: 10.7150/ijms.53024

36. Wu QX, Li HC, Qiao ZQ, Jia TY. Inhibitory of saikosaponin d on cell proliferation of HepG2 cells and tumor growth if liver cancer. *Chin J Immunol* (2018) 34(11):1664–8.

37. Li CY, Yang H. Triptolide induces apoptosis and autophagy in HepG2 cells by regulating the expression of miR-194. *Jilin Med J* (2022) 43(01):7–11.

38. Zhang N, Liu T, Chen D, Zeng CJ, Zeng J. Influence and the mechanisms of triptolide on growth of hepatocellular carcinoma cells. *Contemp Med* (2020) 26(24):103–5.

39. Gan CL, Zou YL, Huang XW, Xu JH. Effects of triptolide on proliferation, apoptosis and cycloxygenase-2 expression in hepatic cancer cell line H22. *J Fujian Med Univ* (2017) 51(03):146–149+165.

40. Pu Z, Ge F, Wang Y, Jiang Z, Zhu S, Qin S, et al. Ginsenoside-Rg3 inhibits the proliferation and invasion of hepatoma carcinoma cells *via* regulating long non-coding RNA HOX antisense intergenic. *Bioengineered* (2021) 12(1):2398–409. doi: 10.1080/21655979.2021.1932211

41. Zhang M, Wang L, Liu W, Wang T, De Sanctis F, Zhu L, et al. Targeting inhibition of accumulation and function of myeloid-derived suppressor cells by artemisinin *via* PI3K/AKT, mTOR, and MAPK pathways enhances anti-PD-L1 immunotherapy in melanoma and liver tumors. *J Immunol Res* (2022) 2022:2253436. doi: 10.1155/2022/2253436

42. Peng XY, Li RC, Rao Q, Gao QH, Duan YJ, Zhao G. Dihydroartemisinin inhibits proliferation and induces apoptosis of hepatocellular carcinoma HepG2 cells and its mechanism. *Lishizhen Med Materia Med Res* (2022) 33(09):2139–42.

43. Su Y, Zhao D, Jin C, Li Z, Sun S, Xia S, et al. Dihydroartemisinin induces ferroptosis in HCC by promoting the formation of PEBP1/15-LO. *Oxid Med Cell Longev* (2021) 2021:3456725. doi: 10.1155/2021/3456725

44. Sun Y, Song YY, Zhang C, Lu YZ, Zheng GH, Tian XX, et al. Effect and mechanism of celastrol on the proliferation of hepatocellular carcinoma HepG2 cells by activating AMPK signaling pathway. *China Pharmacist* (2021) 24(11):1961–1966+1982. doi: 10.19962/j.cnki.issn1008-049X.2021.11.001

45. Sheng L, Li X, Rao H, Zheng GH, Wang GH, Hu JJ. Celastrol delays hepatocellular carcinoma *via* downregulating NF-κB signaling pathway. *Modernizat Tradit Chin Med Materia Medica-World Sci Technol* (2021) 23(07):2372–9.

46. Deng L, Yao P, Li L, Ji F, Zhao S, Xu C, et al. p53-mediated control of aspartate-asparagine homeostasis dictates LKB1 activity and modulates cell survival. *Nat Commun* (2020) 11(1):1755. doi: 10.1038/s41467-020-15573-6

47. Dong X, Gao H. Mechanisms of norcantharidin induced apoptosis and cycle arrest in human hepatocellular carcinoma Huh7 cells. *Global Tradit Chin Med* (2021) 14 (08):1366–70.

48. Tan HY, Wang N, Tsao SW, Che CM, Yuen MF, Feng Y. IRE1α inhibition by natural compound genipin on tumour associated macrophages reduces growth of hepatocellular carcinoma. *Oncotarget* (2016) 7(28):43792–804. doi: 10.18632/oncotarget.9696

49. Lu B, Sheng Y, Zhang J, Zheng Z, Ji L. The altered microRNA profile in andrographolide-induced inhibition of hepatoma tumor growth. *Gene* (2016) 588 (2):124–33. doi: 10.1016/j.gene.2016.05.012

50. Bai C, Zhao J, Su J, Chen J, Cui X, Sun M, et al. Curcumin induces mitochondrial apoptosis in human hepatoma cells through BCLAF1-mediated modulation of PI3K/AKT/GSK-3β signaling. *Life Sci* (2022) 306(1):120804. doi: 10.1016/j.lfs.2022.120804

51. Sun J, Xu W, Lu RZ, Zhu XR, Xu XM, Jiang YQ, et al. Inhibitory effect of curcumin on human carcinoma SMMC-7721 cells xenografted in nude mice and its mechanism. *J Jiangsu Univ (Med Sci)* (2022) 32(03):219–225+230. doi: 10.13312/j.issn.1671-7783.y210066

52. Tian S, Liao L, Zhou Q, Huang X, Zheng P, Guo Y, et al. Curcumin inhibits the growth of liver cancer by impairing myeloid-derived suppressor cells in murine tumor tissues. *Oncol Lett* (2021) 21(4):286. doi: 10.3892/ol.2021.12547

53. Ko JH, Sethi G, Um JY, Shanmugam MK, Arfuso F, Kumar AP, et al. The role of resveratrol in cancer therapy. *Int J Mol Sci* (2017) 18(12):2589. doi: 10.3390/ijms18122589

54. Song F, Zhang Y, Pan Z, Zhang Q, Lu X, Huang P. Resveratrol inhibits the migration, invasion and epithelial-mesenchymal transition in liver cancer cells through up- miR-186-5p expression. *Zhejiang Da Xue Xue Bao Yi Xue Ban* (2021) 50(5):582–90. doi: 10.3724/zdxbyxb-2021-0197

55. Dai H, Li M, Yang W, Sun X, Wang P, Wang X, et al. Resveratrol inhibits the malignant progression of hepatocellular carcinoma *via* MARCH1-induced regulation of PTEN/AKT signaling. *Aging (Albany NY)* (2020) 12(12):11717–31. doi: 10.18632/aging.103338

56. El-Melegy MG, Eltaher HM, Gaballah A, El-Kamel AH. Enhanced oral permeability of trans-resveratrol using nanocochleates for boosting anticancer efficacy; *in-vitro* and ex-vivo appraisal. *Eur J Pharm Biopharm* (2021) 168:166–83. doi: 10.1016/j.ejpb.2021.08.020

57. Liao ZH, Zhu HQ, Chen YY, Chen RL, Fu LX, Li L, et al. The epigallocatechin gallate derivative Y6 inhibits human hepatocellular carcinoma by inhibiting angiogenesis in MAPK/ERK1/2 and PI3K/AKT/ HIF-1α/VEGF dependent pathways. *J Ethnopharmacol* (2020) 259:112852. doi: 10.1016/j.jep.2020.112852

58. Guo HL, Bai Y. Inhibitory effect of paclitaxel combined with epigallo catechin galate on hepatocellular carcinoma cell multiplication and tumor growth in bearing cancer nude mice. *J Xinxiang Med Univ* (2015) 32(03):216–9.

59. Ou BB, Lin XZ, Liang G, Sun YW. The-epigallocatechin gallate and adriamycin apoptosis of BEL-7404/ADR *in vivo*. *Lishizhen Med Materia Med Res* (2012) 23(08):1854–5.

60. Mhlanga P, Perumal PO, Somboro AM, Amoako DG, Khumalo HM, Khan RB. Mechanistic insights into oxidative stress and apoptosis mediated by tannic acid in human liver hepatocellular carcinoma cells. *Int J Mol Sci* (2019) 20(24):6145. doi: 10.3390/ijms20246145

61. Geng NN, Wu MS, Zheng X, Yang L, Wang HY, Li XY. Tannic acid enhances cisplatin-induced apoptosis of hepatocellular carcinoma HepG2 cells by activating ATF6-CHOP pathway. *J Pract Med* (2018) 34(01):12–5.

62. Tsai JJ, Chen JH, Chen CH, Chung JG, Hsu FT. Apoptosis induction and ERK/NF-κB inactivation are associated with magnolol-inhibited tumor progression in hepatocellular carcinoma *in vivo*. *Environ Toxicol* (2020) 35(2):167–75. doi: 10.1002/tox.22853

63. Cao W, Mo K, Wei S, Lan X, Zhang W, Jiang W. Effects of rosmarinic acid on immunoregulatory activity and hepatocellular carcinoma cell apoptosis in H22 tumor-bearing mice. *Korean J Physiol Pharmacol* (2019) 23(6):501–8. doi: 10.4196/kjpp.2019.23.6.501

64. Zhu G, Liu X, Li H, Yan Y, Hong X, Lin Z. Kaempferol inhibits proliferation, migration, and invasion of liver cancer HepG2 cells by down-regulation of microRNA-21. *Int J Immunopathol Pharmacol* (2018) 32:2058738418814341. doi: 10.1177/2058738418814341

65. Zhang Q. *Study on the effect of kaempferol on the proliferation and apoptosis of human hepatoma cells HepG2 and its mechanism*. Hebei Med University (2022).

66. Guo HQ, Liu YL, Ren F. Zahng J.Research on the effect of kaempferol on HepG2 apoptosis and its mechanism. *Beijing Med J* (2021) 43(09):899–904. doi: 10.15932/j.0253-9713.2021.09.015

67. Zhang J, Ma H, Yang L. Silymarin inhibits invasion and migration of hepatoma cell line MHCC97. *Basic Clin Med* (2019) 39(12):1741–5. doi: 10.16352/j.issn.1001-6325.2019.12.019

68. Shi WY, Li HQ, Wang DQ, Yang YJ, Pan KJ, Xu J. Study on extraction and purification of silhistbinin in tistle. *China Food Addit* (2022) 33(10):99–105. doi: 10.19804/j.issn1006-2513.2022.10.013

69. Liu ZG, Li XL, Weng LD, Liu Q, Zhu HX, Huang ZG. Research progress in pharmacological effects of silymarin. *J Liaoning Univ Tradit Chin Med* (2012) 14(10):91–3. doi: 10.13194/j.jlunivtcm.2012.10.93.liuzhg.066

70. Zhao YF, Wan J, Dai Y. Silibinin inhibits the proliferation and migration of HepG2 hepatic cancer cells. *Chin J Histochem Cytochem* (2017) 26(02):142–6. doi: 10.16705/j.cnki.1004-1850.2017.02.008

71. Granado-Serrano AB, Martín MA, Bravo L, Goya L, Ramos S. Quercetin modulates NF-kappa b and AP-1/JNK pathways to induce cell death in human hepatoma cells. *Nutr Cancer* (2010) 62(3):390–401. doi: 10.1080/01635580903441196

72. Reyes-Avendaño I, Reyes-Jiménez E, González-García K, Pérez-Figueroa DC, Baltiérrez-Hoyos R, Tapia-Pastrana G, et al. Quercetin regulates key components of the cellular microenvironment during early hepatocarcinogenesis. *Antioxidants (Basel)* (2022) 11(2):358. doi: 10.3390/antiox11020358

73. Zhou M, Liao XM, Wang S, Gong ZP, Zhang RH. *In vivo* and *in vitro* anticancer activity of quercetin against human liver cancer HepG2 cells. *Anhui Med Pharmaceut J* (2019) 23(11):2136–41.

74. Liao CY, Lee CC, Tsai CC, Hsueh CW, Wang CC, Chen IH, et al. Novel investigations of flavonoids as chemopreventive agents for hepatocellular carcinoma. *BioMed Res Int* (2015) 2015:840542. doi: 10.1155/2015/840542

75. Wu SH, Luo ZY, Zhang JS. Study on the antitumor effect of chrysin and its mechanism. *J Hunan Normal University(Med Sci)* (2006) 2006(04):78–81.

76. Wei XT, Peng WR, Jiang Q, Li Q, Feng ZY, Qi ZL, et al. Chrysin promotes SMMC-7721 cells apoptosis by regulating MAPKs signaling pathway. *J South Med Univ* (2018) 38 (10):1187–94.

77. Rong W, Wan N, Zheng X, Shi G, Jiang C, Pan K, et al. Chrysin inhibits hepatocellular carcinoma progression through suppressing programmed death ligand 1 expression. *Phytomedicine* (2022) 95:153867. doi: 10.1016/j.phymed.2021.153867

78. Liu J, Wen X, Liu B, Zhang Q, Zhang J, Miao H, et al. Diosmetin inhibits the metastasis of hepatocellular carcinoma cells by downregulating the expression levels of MMP-2 and MMP-9. *Mol Med Rep* (2016) 13(3):2401–8. doi: 10.3892/mmr.2016.4872

79. Yang Y, Lin MZ, Huang YW, Chen M. Promoting effect of diosmetin on the cell cycle arrest and cell apoptosis in HepG2 cell and its mechanism. *Hainan Med J* (2016) 27 (3):354–7.

80. Pan L, Feng F, Wu J, Li L, Xu H, Yang L, et al. Diosmetin inhibits cell growth and proliferation by regulating the cell cycle and lipid metabolism pathway in hepatocellular carcinoma. *Food Funct* (2021) 12(23):12036–46. doi: 10.1039/d1fo02111g

81. Tan HY, Wang N, Man K, Tsao SW, Che CM, Feng Y. Autophagy-induced RelB/p52 activation mediates tumour-associated macrophage repolarisation and suppression of hepatocellular carcinoma by natural compound baicalin. *Cell Death Dis* (2015) 6(10): e1942. doi: 10.1038/cddis.2015.271

82. Bai J, Wu J, Tang R, Sun C, Ji J, Yin Z, et al. Emodin, a natural anthraquinone, suppresses liver cancer *in vitro* and *in vivo* by regulating VEGFR2 and miR-34a. *Invest New Drugs* (2020) 38(2):229–45. doi: 10.1007/s10637-019-00777-5

83. Du YC, Zheng TX, Shi H, Qian BL, Chen H, Zhang H, et al. Effect of aloin on proliferation, migration and invasion of hepatocellular carcinoma MHCC97H cells. *Chin J Clin Pharmacol* (2020) 36(12):1669–71. doi: 10.13699/j.cnki.1001-6821.2020.12.018

84. Liu X, Liu J. Tanshinone I induces cell apoptosis by reactive oxygen species-mediated endoplasmic reticulum stress and by suppressing p53/DRAM-mediated autophagy in human hepatocellular carcinoma. *Artif Cells Nanomed Biotechnol* (2020) 48(1):488–97. doi: 10.1080/21691401.2019.1709862

85. Stephenson Clarke JR, Douglas LR, Duriez PJ, Balourdas DI, Joerger AC, Khadiullina R, et al. Discovery of nanomolar-affinity pharmacological chaperones stabilizing the oncogenic p53 mutant Y220C. *ACS Pharmacol Transl Sci* (2022) 5 (11):1169–80. doi: 10.1021/acsptsci.2c00164

86. Liu JL, Tong L, Luo Y, Gao YJ. Cryptotanshinone may induce ferroptosis of human liver cancer HepG2 cells[J]. *Zhongguo yi xue ke xue yuan xue bao*. (2021) 43(3):366–70. Acta Academiae Medicinae Sinicae.

87. Liu L, Yuan CJ, Guo JJ, Yu T, Lv XW, Liu JP, et al. Inhibitory effect of astragalus polysaccharide on the proliferation of HepG2 cells and its potential mechanism. *Pract Prevent Med* (2018) 25(4):385–7.

88. Mei J, Wang XM, Xie L, Jin XW, Li YL. Astragalus polysaccharide inhibits proliferation of Bel-7402/5-FU drug-resistant cells and its effect on drug-resistance genes. *Chin J Integrat Tradit West Med Liver Dis* (2020) 30(04):326–9.

89. Li X, Li P, Chang Y, Xu Q, Wu Z, Ma Q, et al. The SDF-1/CXCR4 axis induces epithelial-mesenchymal transition in hepatocellular carcinoma. *Mol Cell Biochem* (2014) 392(1-2):77–84. doi: 10.1007/s11010-014-2020-8

90. Lu J, Zhu PF, Liu YM, Zeng QL, Yu ZJ. Astragalus polysaccharides downregulated apoptosis in HepG2 cell through wnt/β-catenin signaling pathway. *Chin Tradit Herbal Drugs* (2018) 49(21):5155–60.

91. Chan LJ, Yang SW, Yan YD, Wang WJ, Li R, Chen J. Et.al. study on the inhibitory effect of astragalus polysaccharides on HepG2.215 cells and its mechanism. *Infect Dis Informat* (2022) 35(02):130–4.

92. Yang Y, Song N, Guo JF, Yu N, Zhao Z, Gao H, et al. Inhibitory effect and its mechanism of pachymaran on HepG2 hepatoma cells by regulating NLRP3/pyrogen pathway. *Chin Arch Tradit Chin Med* (2022) 40(09):171–175+282-283. doi: 10.13193/j.issn.1673-7717.2022.09.038

93. Zhang DQ, Xin GJ. Lycium barbarum polysaccharide inhibits VEGF expression, migration and invasion iof SMMC-7721 hepatocellular carcinoma cells. *Chin J Histochem Cytochem* (2019) 28(01):26–31. doi: 10.16705/j.cnki.1004-1850.2019.01.005

94. Yan CL, Luo YL, An FY, Liu XS, Liu YQ, Wang YF, et al. Inhibitory effects of total astragalosides combined with cisplatin on STAT3-mediated inflammatory signaling pathway in H22 tumor-bearing mice. *Chin J Biochem Molr Biol* (2020) 36(11):1359–66. doi: 10.13865/j.cnki.cjbmb.2020.09.1200

95. An XC, Zhu RX, Lin SM, Shi L. Mechanism of astragaloside IV promoting proliferation and apoptosis of hepatoma cells by inhibiting ROSNF-κB signaling pathway. *Modern Digest Intervent* (2019) 24(12):1399–403.

96. An FY, Liu XS, Yan CL, Luo YL, Liu YQ, Shi XF, et al. Inhibitory effect of total astragalus saponins on tumor and its mechanism in H22 bearing mice. *Chin J Public Health* (2017) 33(4):596–8.

97. Zhu HY, Shen HJ, Wang Y. Analysis on influence of huangqi sijunzi decoction on postoperative recovery and immunologic function of patients undergoing primary liver cancer operation. *Liaoning J Tradit Chin Med* (2022), 1–9.

98. Jiang CM, Ding SZ, Zhang ZF. Effect of supplementing qi and activating blood circulation to help the patients with primary hepatocellular carcinoma to assist the treatment and improve the effect of digestive tract symptoms. *Pract J Cancer* (2018) 33 (09):1528–31.

99. Zheng WC, Li H, Gong WJ. Clinical effect of external application of compound gleditsiae spina ointment in treatment of severe cancer pain due to primary liver cancer: An analysis of 28 cases. *Hunan J Tradit Chin Med* (2022) 38(10):8–11. doi: 10.16808/j.cnki.issn1003-7705.2022.10.003

100. Jing T. Clinical study on xingqi sanjie huayu prescription combined with reduced glutathione for patients after surgery for primary liver cancer. *New Chin Med* (2022) 54 (17):187–91. doi: 10.13457/j.cnki.jncm.2022.17.040

101. Chen WL, Fan XX, Liang F, Lv JZ, Zhang YC, Ran Y, et al. Clinical observation on triple therapy in the prevention and treatment of recurrence of primary liver cancer after hepatectomy. *Guangming J Chin Med* (2022) 37(16):2949–2951+2994.

102. Zhao Y, Yu JJ, Li H. Clinical study on fuzheng huayu jiedu prescription for advanced liver cancer. *New Chin Med* (2022) 54(15):153–7. doi: 10.13457/j.cnki.jncm.2022.15.032

103. Yang HJ, Jing XH. Effects of hedyotis diffusa injection combined with transarterial chemoembolization in treatment of patients with primary liver cancer. *Med J Chin People's Health* (2022) 34(13):107–9.

104. Tokumoto H, Akita S, Nakamura R, Yamamoto N, Kubota Y, Mitsukawa N. Investigation of the association between breast cancer-related lymphedema and the side effects of taxane-based chemotherapy using indocyanine green lymphography. *Lymphat Res Biol* (2022) 20(6):612–7. doi: 10.1089/lrb.2021.0065

105. Liu K, AiKeM WFR, Wang RZ. Changes of peripheral blood lymphocyte subsets in patients with nasopharyngeal carcinoma before and after radiotherapy. *J Xinjiang Med Univ* (2015) 38(01):6–10+16.

106. Mokhtari RB, Kumar S, Islam SS, Yazdanpanah M, Adeli K, Cutz E, et al. Combination of carbonic anhydrase inhibitor, acetazolamide, and sulforaphane, reduces the viability and growth of bronchial carcinoid cell lines. *BMC Cancer* (2013) 13:378. doi: 10.1186/1471-2407-13-378

107. Elmeliegy M, Vourvahis M, Guo C, Wang DD. Effect of p-glycoprotein (P-gP) inducers on exposure of p-gP substrates: Review of clinical drug-drug interaction studies. *Clin Pharmacokinet* (2020) 59(6):699–714. doi: 10.1007/s40262-020-00867-1

108. Sun L, Chen W, Qu L, Wu J, Si J. Icaritin reverses multidrug resistance of HepG2/ADR human hepatoma cells *via* downregulation of MDR1 and pglycoprotein expression. *Mol Med Rep* (2013) 8(6):1883–7. doi: 10.3892/mmr.2013.1742

109. Chen XR, Zhou SH, Wang RC, Xu L. Effect and mechanism of β-elemene on SKOV3/DDP resistant ovarian cancer cells. *Pharmaceut Clin Res* (2021) 29(02):81–5.

110. Carnero A, Garcia-Mayea Y, Mir C, Lorente J, Rubio IT, LLeonart ME. The cancer stem-cell signaling network and resistance to therapy. *Cancer Treat Rev* (2016) 49:25–36. doi: 10.1016/j.ctrv.2016.07.001

111. Wang XY, Zhao Q, Wang B, Yuan S, Li K. Mechanism of quercetin reversing drug resistance of human breast cancer MCF-7 cells to doxorubicin. *Modern Prevent Med* (2018) 45(10):1844–1849+1859.

112. Li L. *Antcancer mechanism investigations of natural product derivatives targeting for subcellular organelles*. Shandong University (2018).

113. Neuzil J, Dong LF, Rohlena J, Truksa J, Ralph SJ. Classification of mitocans, anti-cancer drugs acting on mitochondria. *Mitochondrion* (2013) 13(3):199–208. doi: 10.1016/j.mito.2012.07.112

114. Ebrahimi N, Saremi J, Ghanaatian M, Yazdani E, Adelian S, Samsami S, et al. The role of endoplasmic reticulum stress in the regulation of long noncoding RNAs in cancer. *J Cell Physiol* (2022) 237(10):3752–67. doi: 10.1002/jcp.30846

115. Chai RF. *Resveratrol inhibits proliferation and migration through SIRT1 mediated post-translational modification of PI3K/AKT/DLC1 in hepatocellular carcinoma cells*. Shandong Normal University (2017).

116. Gao J, Ma F, Wang X, Li G. Combination of dihydroartemisinin and resveratrol effectively inhibits cancer cell migration *via* regulation of the DLC1/TCTP/Cdc42 pathway. *Food Funct* (2020) 11(11):9573–84. doi: 10.1039/d0fo00996b

117. Feng Y, Zu LL, Zhang L. MicroRNA-26b inhibits the tumor growth of human liver cancer through the PI3K/Akt and NF-κB/MMP-9/VEGF pathways. *Oncol Rep* (2018) 39(5):2288–96. doi: 10.3892/or.2018.6289

118. Guo Z, Xia Y, Hao G, Gao ZZ, Li R, Yang Y. *In vitro* analysis on inhibitory effect of sodium arsenite combined with astragaloside IV on HepG2 liver cancer cells. *Alexandria Engin J* (2021) 60(6):5749–64. doi: 10.1016/j.aej.2021.03.043

119. Opferman JT, Kothari A. Anti-apoptotic BCL-2 family members in development. *Cell Death Differ* (2018) 25(1):37–45. doi: 10.1038/cdd.2017.170

120. Wen S, Sun L, An R, Zhang W, Xiang L, Li Q, et al. A combination of citrus reticulata peel and black tea inhibits migration and invasion of liver cancer *via* PI3K/AKT and MMPs signaling pathway. *Mol Biol Rep* (2020) 47(1):507–19. doi: 10.1007/s11033-019-05157-z

121. Han H, Wang L, Liu Y, Shi X, Zhang X, Li M, et al. Combination of curcuma zedoary and kelp inhibits growth and metastasis of liver cancer *in vivo* and *in vitro via* reducing endogenous H2S levels. *Food Funct* (2019) 10(1):224–34. doi: 10.1039/c8fo01594e

122. Zhang J, Hong Y, Jiang L, Yi X, Chen Y, Liu L, et al. Global metabolomic and lipidomic analysis reveal the synergistic effect of bufalin in combination with cinobufagin against HepG2 cells. *J Proteome Res* (2020) 19(2):873–83. doi: 10.1021/acs.jproteome.9b00681

123. Zhou Y, Wang M, Pan X, Dong Z, Han L, Ju Y, et al. Combination of triptolide with sodium cantharidinate synergistically enhances apoptosis on hepatoma cell line 7721. *Zhong Nan Da Xue Xue Bao Yi Xue Ban* (2016) 41(9):911–7. doi: 10.11817/j.issn.1672-7347.2016.09.005

124. Liu QD, Bai TY, Wang YF, Yao Y. Effect of combined use of quercetin and rosmarinic acid on proliferation and apoptosis of HepG2 cells *in vitro*. *Anhui Med Pharmaceut J* (2020) 24(09):1705–7.

125. Manikandan R, Beulaja M, Arulvasu C, Sellamuthu S, Dinesh D, Prabhu D, et al. Synergistic anticancer activity of curcumin and catechin: An *in vitro* study using human cancer cell lines. *Microsc Res Tech* (2012) 75(2):112–6. doi: 10.1002/jemt.21032

126. Wang L, Wei D, Han X, Zhang W, Fan C, Zhang J, et al. The combinational effect of vincristine and berberine on growth inhibition and apoptosis induction in hepatoma cells. *J Cell Biochem* (2014) 115(4):721–30. doi: 10.1002/jcb.24715

127. Liao GH, Zhang GS, Lou ZH, Cheng RB, Zhang GJ. Study on the effeciency and attenuating mechanism of arsenic trioxide combined with tanshinone against liver cancer. *J Zhejiang Chin Med Univ* (2020) 44(01):15–23. doi: 10.16466/j.issn1005-5509.2020.01.003

128. Shen L, Zhang G, Lou Z, Xu G, Zhang G. Cryptotanshinone enhances the effect of arsenic trioxide in treating liver cancer cell by inducing apoptosis through downregulating phosphorylated- STAT3 *in vitro* and *in vivo*. *BMC Complement Altern Med* (2017) 17 (1):106. doi: 10.1186/s12906-016-1548-4

129. Roskoski RJr. Cyclin-dependent protein serine/threonine kinase inhibitors as anticancer drugs. *Pharmacol Res* (2019) 139:471–88. doi: 10.1016/j.phrs.2018.11.035

130. Cao YJ, Zhou YJ, He XZ, Zhou CX, Cui L, Zhuang QF, et al. Overexpression of β-arrestin2 induces G1-phase cell cycle arrest and suppresses tumorigenicity in renal cell carcinoma. *Eur Rev Med Pharmacol Sci* (2017) 21(8):1729–37.

131. Ye K, Wei Q, Gong Z, Huang Y, Liu H, Li Y, et al. Effect of norcantharidin on the proliferation, apoptosis, and cell cycle of human mesangial cells. *Ren Fail* (2017) 39 (1):458–64. doi: 10.1080/0886022X.2017.1308257

132. Roskoski RJr. Cyclin-dependent protein kinase inhibitors including palbociclib as anticancer drugs. *Pharmacol Res* (2016) 107:249–75. doi: 10.1016/j.phrs.2016.03.012

133. Song D, Liang H, Qu B, Li Y, Liu J, Chen C, et al. Moxidectin inhibits glioma cell viability by inducing G0/G1 cell cycle arrest and apoptosis. *Oncol Rep* (2018) 40(3):1348–58. doi: 10.3892/or.2018.6561

134. Lohberger B, Leithner A, Stuendl N, Kaltenegger H, Kullich W, Steinecker-Frohnwieser B. Diacerein retards cell growth of chondrosarcoma cells at the G2/M cell cycle checkpoint *via* cyclin B1/CDK1 and CDK2 downregulation. *BMC Cancer* (2015) 15:891. doi: 10.1186/s12885-015-1915-4

135. Zhang D. *Study on anti-hepatocellular carcinoma activity of chrysin combined with diosmetin or triptolide in vivo and in vitro*. Wuhan Polytechnic University (2020).

136. Xiao Y, Gong Q, Wang W, Liu F, Kong Q, Pan F, et al. The combination of biochanin a and SB590885 potentiates the inhibition of tumour progression in hepatocellular carcinoma. *Cancer Cell Int* (2020) 20:371. doi: 10.1186/s12935-020-01463-w

137. Carrasco-Torres G, Baltiérrez-Hoyos R, Andrade-Jorge E, Villa-Treviño S, Trujillo-Ferrara JG, Vásquez-Garzón VR. Cytotoxicity, oxidative stress, cell cycle arrest, and mitochondrial apoptosis after combined treatment of hepatocarcinoma cells with maleic anhydride derivatives and quercetin. *Oxid Med Cell Longev* (2017) 2017:2734976. doi: 10.1155/2017/2734976

138. Zhang W, Wang L, Xu PY, Xiao HY. Synergistic tumor suppression by curcumin and low-concentration vincristine in hepatoma cell lines. *Carcinog Teratog Mutag* (2012) 24(4):270–4.

139. Chang MX, Wu MM, Li HM. Inhibition on proliferation of hepatoma HepG2 cell treated with curcumin combined with glycyrrhetinic acid. *Drug Evaluat Res* (2017) 40 (01):42–7.

140. Li GZ. *Effects of combination of artesunate with curcumin of proliferation apoptosis and telomerase activity of human hepatoma cell line HepG2*. Guangxi Med University (2013).

141. Chang TW, Lin CY, Tzeng YJ, Lur HS. Synergistic combinations of tanshinone IIA and trans-resveratrol toward cisplatin-comparable cytotoxicity in HepG2 human hepatocellular carcinoma cells. *Anticancer Res* (2014) 34(10):5473–80.

142. Dai B, Ma Y, Yang T, Fan M, Yu R, Su Q, et al. Synergistic effect of berberine and HMQ1611 impairs cell proliferation and migration by regulating wnt signaling pathway in hepatocellular carcinoma. *Phytother Res* (2019) 33(3):745–55. doi: 10.1002/ptr.6267

143. Liu YM, Zhang JQ, You ZM, Liao H. Inhibitory effect of norcantharidin combined with evodiamine on the growth of human hepatic carcinoma cell line HepG2 *in vitro*. *Chin J Cell Mol Immunol* (2014) 8):824–8. doi: 10.13423/j.cnki.cjcmi.006975

144. Zhang X, Ouyang HZ, Xu W, Wang XY. Effect of celastrol combined medication on the inhibition of HepG2 cell proliferation. *J China Pharmaceut Univ* (2020) 51 (02):185–92.

145. Ling S, Li J, Shan Q, Dai H, Lu D, Wen X, et al. USP22 mediates the multidrug resistance of hepatocellular carcinoma *via* the SIRT1/AKT/MRP1 signaling pathway. *Mol Oncol* (2017) 11(6):682–95. doi: 10.1002/1878-0261.12067

146. He S, Liu F, Xie Z, Zu X, Xu W, Jiang Y. P-Glycoprotein/MDR1 regulates pokemon gene transcription through p53 expression in human breast cancer cells. *Int J Mol Sci* (2010) 11(9):3309–051. doi: 10.3390/ijms11093039

147. Sun Y, Zhang J, Zhou J, Huang Z, Hu H, Qiao M, et al. Synergistic effect of cucurbitacin b in combination with curcumin *via* enhancing apoptosis induction and reversing multidrug resistance in human hepatoma cells. *Eur J Pharmacol* (2015) 768:28–40. doi: 10.1016/j.ejphar.2015.10.003

148. Shen X, Liu X, Wan S, Fan X, He H, Wei R, et al. Discovery of coumarin as microtubule affinity-regulating kinase 4 inhibitor that sensitize hepatocellular carcinoma to paclitaxel. *Front Chem* (2019) 7:366. doi: 10.3389/fchem.2019.00366

149. Tian N, Shangguan W, Zhou Z, Yao Y, Fan C, Cai L. Lin28b is involved in curcumin-reversed paclitaxel chemoresistance and associated with poor prognosis in hepatocellular carcinoma. *J Cancer* (2019) 10(24):6074–87. doi: 10.7150/jca.33421

150. Xu X, Wu C, Bai A, Liu X, Lv H, Liu Y. Folate-functionalized mesoporous silica nanoparticles as a liver tumor-targeted drug delivery system to improve the antitumor effect of paclitaxel. *J Nanomater* (2017) 2017:1–13. doi: 10.1155/2017/2069685

151. Kuo HC, Lee HJ, Hu CC, Shun HI, Tseng TH. Enhancement of esculetin on taxol-induced apoptosis in human hepatoma HepG2 cells. *Toxicol Appl Pharmacol* (2006) 210 (1-2):55–62. doi: 10.1016/j.taap.2005.06.020

152. Jiang Q, Yang M, Qu Z, Zhou J, Zhang Q. Resveratrol enhances anticancer effects of paclitaxel in HepG2 human liver cancer cells. *BMC Complement Altern Med* (2017) 17 (1):477. doi: 10.1186/s12906-017-1956-0

153. Lei X, Li J, Chen KL. Inhibitory effect of emodin and curcumine on hepatoma BEL-7402 cell. *Chin J Hosp Pharm* (2009) 29(12):971–3.

154. Zhou M, Li Z, Han Z, Tian N. Paclitaxel-sensitization enhanced by curcumin involves down-regulation of nuclear factor-κB and Lin28 in Hep3B cells. *J Recept Signal Transduct Res* (2015) 35(6):618–25. doi: 10.3109/10799893.2015.1041644

155. Li Z, Wang N, Yue T, Liu L. Matrine reverses the drug resistance of K562/ADM cells to ADM and VCR *via* promoting autophagy. *Transl Cancer Res* (2020) 9(2):786–94. doi: 10.21037/tcr.2019.12.11

156. Wang YX, Liu XJ. Research progress of cisplatin target and resistance mechanism. *China Med Biotechnol* (2020) 15(03):316–9.

157. Kim IH, Kwon MJ, Jung JH, Nam TJ. Protein extracted from porphyra yezoensis prevents cisplatin-induced nephrotoxicity by downregulating the MAPK and NF-κB pathways. *Int J Mol Med* (2018) 41(1):511–20. doi: 10.3892/ijmm.2017.3214

158. Xue DF, Pan ST, Huang G, Qiu JX. ROS enhances the cytotoxicity of cisplatin by inducing apoptosis and autophagy in tongue squamous cell carcinoma cells. *Int J Biochem Cell Biol* (2020) 122:105732. doi: 10.1016/j.biocel.2020.105732

159. Yang ZF, Poon RT. Vascular changes in hepatocellular carcinoma. *Anat Rec (Hoboken)* (2008) 291(6):721–34. doi: 10.1002/ar.20668

160. Ferrara N, Houck K, Jakeman L, Leung DW. Molecular and biological properties of the vascular endothelial growth factor family of proteins. *Endocr Rev* (1992) 13(1):18–32. doi: 10.1210/edrv-13-1-18

161. Dalton AC, Shlamkovitch T, Papo N, Barton WA. Correction: Constitutive association of Tie1 and Tie2 with endothelial integrins is functionally modulated by angiopoietin-1 and fibronectin. *PLoS One* (2017) 12(5):e0179059. doi: 10.1371/journal.pone.0179059

162. Augustin HG, Koh GY, Thurston G, Alitalo K. Control of vascular morphogenesis and homeostasis through the angiopoietin-tie system. *Nat Rev Mol Cell Biol* (2009) 10(3):165–77. doi: 10.1038/nrm2639

163. Liu LZ, Li C, Chen Q, Jing Y, Carpenter R, Jiang Y, et al. MiR-21 induced angiogenesis through AKT and ERK activation and HIF-1α expression. *PLoS One* (2011) 6(4):e19139. doi: 10.1371/journal.pone.0019139

164. Fayette J, Soria JC, Armand JP. Use of angiogenesis inhibitors in tumour treatment. *Eur J Cancer* (2005) 41(8):1109–16. doi: 10.1016/j.ejca.2005.02.017

165. Zhuang PY, Shen J, Zhu XD, Lu L, Wang L, Tang ZY, et al. Prognostic roles of cross-talk between peritumoral hepatocytes and stromal cells in hepatocellular carcinoma involving peritumoral VEGF-c, VEGFR-1 and VEGFR-3. *PLoS One* (2013) 8(5):e64598. doi: 10.1371/journal.pone.0064598

166. Ao M, Xiao X, Ao YZ. Observation on effect and adverse reactions of thalidomide combined with kanglaite injection in treating primary liver cancer. *Doctor* (2017) 3(7):9–10+24. doi: 10.19604/j.cnki.dys.2017.07.005

167. Zhou MN, Liu J, Liu R, Shu P, Zou ZZ, Shi D. Effects of alcohol extract from luwei dihuang combined with cisplatin on apoptosis and tumor angiogenesis factors of hepatocellular carcinoma BEL-7402 cells. *Pharmacol Clin Chin Materia Med* (2020) 36 (03):61–6. doi: 10.13412/j.cnki.zyyl.2020.03.005

168. Lin XY, Song GC. Effects of astragalus polysaccharide injection on the expression of ki-67,HIF-1α and VEGF in HepG2 mice during chemotherapy. *J North Pharm* (2020) 17(08):77–8.

169. Zang WH, Hu JL, Tang DC, Yin G, Zhi L, Ding SC. Effects on expression of CD147, iNOS in nude mice of human hepatocarcinoma transplantation model by compatibility of radix astragali and curcuma and combination with cisplatin. *Lishizhen Med Materia Med Res* (2020) 31(04):785–8.

170. Luo S, Yin G, Tang DC. Effect of astragaloside IV and curcumin on angiogenesis of human hepatocellular carcinoma xenografts in nude mice. *Chin J Cancer Prevent Treat* (2016) 23(S1):12–3. doi: 10.16073/j.cnki.cjcpt.2016.s1.006

171. Chen YY. *Effect of EGCG derivative Y6 on anti-angiogenesis and synergistic attenuated daunorubicin anti-hepatocarcinoma and its mechanism in vivo*. Guangxi Med University (2018).

172. Zhao X, Chen Q, Li Y, Tang H, Liu W, Yang X. Doxorubicin and curcumin co-delivery by lipid nanoparticles for enhanced treatment of diethylnitrosamine-induced hepatocellular carcinoma in mice. *Eur J Pharm Biopharm* (2015) 93:27–36. doi: 10.1016/j.ejpb.2015.03.003

173. Yan Y, Zhang HY, Pan JH, Wang DY, Zhou XS, Yuan YF, et al. Effect of dopamine receptor 4 on proliferation and metastasis of hepatocellular carcinoma cells and its prognostic significance. *J Sun Yat-sen Univ (Med Sci)* (2020) 41(05):669–80. doi: 10.13471/j.cnki.j.sun.yat-sen.univ(med.sci).2020.0088

174. Neelakantan D, Zhou H, Oliphant MUJ, Zhang X, Simon LM, Henke DM, et al. EMT cells increase breast cancer metastasis *via* paracrine GLI activation in neighbouring tumour cells. *Nat Commun* (2017) 8:15773. doi: 10.1038/ncomms15773

175. Bae MJ, Karadeniz F, Oh JH, Yu GH, Jang MS, Nam KH, et al. MMP-inhibitory effects of flavonoid glycosides from edible medicinal halophyte limonium tetragonum. *Evid Based Complement Alternat Med* (2017) 2017:6750274. doi: 10.1155/2017/6750274

176. Sun B, Lin Y, Wang X, Lan F, Yu Y, Huang Q. Single nucleotide polymorphism of the enhancer of zeste homolog 2 gene rs2072408 is associated with lymph node metastasis and depth of primary tumor invasion in gastric cancer. *Clin Lab* (2016) 62(11):2099–105. doi: 10.7754/Clin.Lab.2016.160302

177. Shan TT. *The inhibitory effect of mannose on human hepatocellular carcinoma cell line HepG2*. Hunan University Chin Med (2020).

178. Wang HL. Experimental study on the effects of emodin and cisplatin on the invasion and migration og HepG2 cells. *Changchun Univ Chin Med* (2020).

179. Yang G, Xing J, Aikemu B, Sun J, Zheng M. Kaempferol exhibits a synergistic effect with doxorubicin to inhibit proliferation, migration, and invasion of liver cancer. *Oncol Rep* (2021) 45(4):32. doi: 10.3892/or.2021.7983

180. Sun YM, Zeng ZR, Wang JY, Peng MB, Lei S, Yang YS, et al. Effects of sinapine thiocyanate in promoting the sensitivity of HepG2 cells to gemcitabine. *Chin Tradit Patent Med* (2021) 43(4):901–7.

181. Wang ZL. *Mechanism research on caffeine synergistically promotes the anti-tumor effects of 5-fluorouracil in hepatocellular carcinoma*. Guangzhou Med University (2020).

182. Zhang HH, Zhang Y, Cheng YN, Gong FL, Cao ZQ, Yu LG, et al. Metformin incombination with curcumin inhibits the growth, metastasis, and angiogenesis of hepatocellular carcinoma *in vitro* and *in vivo*. *Mol Carcinog* (2018) 57(1):44–56. doi: 10.1002/mc.22718

183. Wu LH. *Correlation analysis of hepatitis b virus X gene mutation with autophagy-related proteins (Beclin-1, LC3B and P62) on hepatocellular carcinoma*. Guangxi Med University (2019).

184. Wang F, Mao Y, You Q, Hua D, Cai D. Piperlongumine induces apoptosis and autophagy in human lung cancer cells through inhibition of PI3K/Akt/mTOR pathway. *Int J Immunopathol Pharmacol* (2015) 28(3):362–73. doi: 10.1177/0394632015598849

185. Fernández ÁF, Sebti S, Wei Y, Zou Z, Shi M, McMillan KL, et al. Disruption of the beclin 1-BCL2 autophagy regulatory complex promotes longevity in mice. *Nature* (2018) 558(7708):136–40. doi: 10.1038/s41586-018-0162-7

186. Zheng W, Chen Q, Wang C, Yao D, Zhu L, Pan Y, et al. Inhibition of cathepsin d (CTSD) enhances radiosensitivity of glioblastoma cells by attenuating autophagy. *Mol Carcinog* (2020) 59(6):651–60. doi: 10.1002/mc.23194

187. Yeo SY, Itahana Y, Guo AK, Han R, Iwamoto K, Nguyen HT, et al. Transglutaminase 2 contributes to a TP53-induced autophagy program to prevent oncogenic transformation. *ELife* (2016) 5:e07101. doi: 10.7554/eLife.07101

188. Chang HW, Kim MR, Lee HJ, Lee HM, Kim GC, Lee YS, et al. p53/BNIP3-dependent mitophagy limits glycolytic shift in radioresistant cancer. *Oncogene* (2019) 38 (19):3729–42. doi: 10.1038/s41388-019-0697-6

189. Liu Z, Shi A, Song D, Han B, Zhang Z, Ma L, et al. Resistin confers resistance to doxorubicin-induced apoptosis in human breast cancer cells through autophagy induction. *Am J Cancer Res* (2017) 7(3):574–83.

190. Ciruelos Gil EM. Targeting the PI3K/AKT/mTOR pathway in estrogen receptor-positive breast cancer. *Cancer Treat Rev* (2014) 40(7):862–71. doi: 10.1016/j.ctrv.2014.03.004

191. Hu G, Cao C, Deng Z, Li J, Zhou X, Huang Z, et al. Effects of matrine in combination with cisplatin on liver cancer. *Oncol Lett* (2021) 21(1):66. doi: 10.3892/ol.2020.12327

192. Geng N, Zheng X, Wu M, Yang L, Li X, Chen J. Tannic acid synergistically enhances the anticancer efficacy of cisplatin on liver cancer cells through mitochondria-mediated apoptosis. *Oncol Rep* (2019) 42(5):2108–16. doi: 10.3892/or.2019.7281

193. Xu YW, Geng SN, Wang MQ, Du GJ. Effect of saposide d on hepatocellular carcinoma in mice treated with doxorubicin. *Chin Tradit Herbal Drugs* (2021) 52 (03):778–88.

194. Wang B, Wang F, Ding A, Zhao H, Bu X. Regorafenib and ginsenoside combination therapy: Inhibition of HepG2 cell growth through modulating survivin and caspase-3 gene expression. *Clin Transl Oncol* (2020) 22(9):1491–8. doi: 10.1007/s12094-019-02283-9

195. Liu J, Li Y, Yang X, Dong Y, Wu J, Chen M. Effects of ginkgol C17:1 on cisplatin-induced autophagy and apoptosis in HepG2 cells. *Oncol Lett* (2018) 15(1):1021–9. doi: 10.3892/ol.2017.7398

196. Qu X, Gao H, Tao L, Zhang Y, Zhai J, Sun J, et al. Astragaloside IV protects against cisplatin-induced liver and kidney injury *via* autophagy-mediated inhibition of NLRP3 in rats. *J Toxicol Sci* (2019) 44(3):167–75. doi: 10.2131/jts.44.167

197. Sun R, Zhai R, Ma C, Miao W. Combination of aloin and metformin enhances the antitumor effect by inhibiting the growth and invasion and inducing apoptosis and autophagy in hepatocellular carcinoma through PI3K/AKT/mTOR pathway. *Cancer Med* (2020) 9(3):1141–51. doi: 10.1002/cam4.2723

198. Zhao J, Li H, Li W, Wang Z, Dong Z, Lan H, et al. Effects of sinapic acid combined with cisplatin on the apoptosis and autophagy of the hepatoma cells HepG2 and SMMC-7721. *Evid Based Complement Alternat Med* (2021) 2021:6095963. doi: 10.1155/2021/6095963

199. Zhang Y, Qu Y, Chen YZ. Influence of 6-shogaol potentiated on 5-fluorouracil treatment of liver cancer by promoting apoptosis and cell cycle arrest by regulating AKT/mTOR/MRP1 signalling. *Chin J Nat Med* (2022) 20(5):352–63. doi: 10.1016/S1875-5364(22)60174-2

200. Kalashnikova I, Mazar J, Neal CJ, Rosado AL, Das S, Westmoreland TJ, et al. Nanoparticle delivery of curcumin induces cellular hypoxia and ROS-mediated apoptosis *via* modulation of bcl-2/Bax in human neuroblastoma. *Nanoscale* (2017) 9(29):10375–87. doi: 10.1039/c7nr02770b

201. Xu WD, Yang L, Chen C, Zhou W. Quercetin-loaded ceria nanoparticles induce autophagy blockage in hepatoma cells. *Chin J Biochem Molr Bio* (2022) 38(11):1538–46. doi: 10.13865/j.cnki.cjbmb.2022.08.1107

202. Dong W, Liu FC, Ni JS, Li PP, Guo XG, Liu H. Co-Delivery of fluorouracil and curcumin by nano-layered double hydroxide for inhibition of hepatocellular carcinoma cells *in vitro*. *China J Modern Med* (2016) 26(09):16–22.

203. Han QH. *Synthesis and application of dual drug Delivery/Controlled release nanotheranostic agent in liver cancer*. Jilin University (2019).

204. Ni WF. *Dual-targeted nanoparticles transporting curcumin and 5-fluorouracil for the treatment of hepatocarcinoma*. Tianjin Med University (2019). doi: 10.27366/d.cnki.gtyku.2019.000567

205. Zhang F. *Study on the treatment of hepatocellular carcinoma and recurrence by magnetic mesoporous nanoparticles with doxorubicin and berberine*. Jilin University (2018).

206. Xu J, Fang Y, Xu RZ, Li Y. Effect of Chinese medicine on immune regulation mechanism of lung cancer. *Acta Chin Med* (2021) 36(06):1210–6. doi: 10.16368/j.issn.1674-8999.2021.06.258

207. Xing XY, Wang XC, He W. Advances in research on tumor immunotherapy and its drug development. *J China Pharmaceut Univ* (2021) 52(01):10–9.

208. El-Khoueiry AB, Sangro B, Yau T, Crocenzi TS, Kudo M, Hsu C, et al. Nivolumab in patients with advanced hepatocellular carcinoma (CheckMate 040): An open-label, non-comparative, phase 1/2 dose escalation and expansion trial. *Lancet* (2017) 389(10088):2492–502. doi: 10.1016/S0140-6736(17)31046-2

209. Ishiguro T, Sano Y, Komatsu SI, Kamata-Sakurai M, Kaneko A, Kinoshita Y, et al. An anti-glypican 3/CD3 bispecific T cell-redirecting antibody for treatment of solid tumors. *Sci Transl Med* (2017) 9(410):eaal4291. doi: 10.1126/scitranslmed.aal4291

210. Sawada Y, Yoshikawa T, Ofuji K, Yoshimura M, Tsuchiya N, Takahashi M, et al. Phase II study of the GPC3-derived peptide vaccine as an adjuvant therapy for hepatocellular carcinoma patients. *Oncoimmunology* (2016) 5(5):e1129483. doi: 10.1080/2162402X.2015.1129483

211. Ning YM, Suzman D, Maher VE, Zhang L, Tang S, Ricks T, et al. FDA Approval summary: Atezolizumab for the treatment of patients with progressive advanced urothelial carcinoma after platinum-containing chemotherapy. *Oncologist* (2017) 22(6):743–9. doi: 10.1634/theoncologist.2017-0087

212. Chew V, Lai L, Pan L, Lim CJ, Li J, Ong R, et al. Delineation of an immunosuppressive gradient in hepatocellular carcinoma using high-dimensional proteomic and transcriptomic analyses. *Proc Natl Acad Sci U.S.A.* (2017) 114(29):E5900–9. doi: 10.1073/pnas.1706559114

213. Du NW, Bai RL, Cui JW. Mechanism of tumor immune escape and treatment strategy. *Chin J Cancer Biother* (2019) 26(04):454–62.

214. Hu N. *Immunological mechanisms of the antitumor effects of lycium barbarum polysaccharide alone or combined with CXCL10*. Guangzhou University Chin Med (2015).

215. Chen CA. *Study on effect and mechanism of high-dose vitamin c combined with immune checkpoint inhibitor in treating liver cancer*. PLA Naval Med University (2020). doi: 10.26998/d.cnki.gjuyu.2020.000166

216. Song WG, Xun QU, Li YL, Xu YP, Wu C, Qin QL. Anti-tumor effects of 10-hydroxycamptothecinc-treated DC-Hepa1-6 fusion vaccines. *Chin J Hepatol* (2004) 12(6):344–6.

217. Yang N, Xu JL, Lu LB, Sheng GG. Chinese Medicine combined with immunosuppressive agents and targeted drugs in the treatment of advanced liver cancer with multiple lung metastases: A case report. *Chin J Integrat Tradit West Med Liver Dis* (2022) 32(07):658–60.

218. Yu JF, Li ZP, Zhou XL, Li C, Liu Y, Zhang Y, et al. Effect of fuling sini decoction combined with sorafenib on advanced primary liver cancer. *Acta Chin Med Pharmacol* (2021) 49(06):76–80. doi: 10.19664/j.cnki.1002-2392.210143

219. Wang Y, Guo SH, Shang XJ, Yu LS, Zhu JW, Zhao A, et al. Triptolide induces sertoli cell apoptosis in mice *via* ROS/JNK-dependent activation of the mitochondrial pathway and inhibition of Nrf2-mediated antioxidant response. *Acta Pharmacol Sin* (2018) 39(2):311–27. doi: 10.1038/aps.2017.95

220. Ariyasu D, Yoshida H, Hasegawa Y. Endoplasmic reticulum (ER) stress and endocrine disorders. *Int J Mol Sci* (2017) 18(2):382. doi: 10.3390/ijms18020382

221. Jin C, Wang SQ, Bai L. Preparation of paclitaxel nanoparticles targeting hepatocellular carcinoma stem cells and its effect on hepatocellular carcinoma huh-7 and HepG2 cells. *Cancer Res Clin* (2021) 33(02):99–103.

222. Wang S, Liu X, Yuan S, Chen WJ, Wang SM, Xu N. Effects of monoclonal antibodies against human stathmin 1 combined paclitaxel on proliferation of human hepatocellular carcinoma cell lines. *Chin German J Clin Oncol* (2009) 8(10):603–6. doi: 10.1007/s10330-009-0138-z

223. Lin HL, Lui WY, Liu TY, Chi CW. Reversal of taxol resistance in hepatoma by cyclosporin a: involvement of the PI-3 kinase-AKT 1 pathway. *Br J Cancer* (2003) 88(6):973–80. doi: 10.1038/sj.bjc.6600788

224. Liu N, Huang H, Xu L, Hua X, Li X, Liu S, et al. The combination of proteasome inhibitors bortezomib and gambogic acid triggers synergistic cytotoxicity *in vitro* but not *in vivo*. *Toxicol Lett* (2014) 224(3):333–40. doi: 10.1016/j.toxlet.2013.11.021

225. Hsu JL, Chiang PC, Guh JH. Tunicamycin induces resistance to camptothecin and etoposide in human hepatocellular carcinoma cells: Role of cell-cycle arrest and GRP78. *Naunyn Schmiedebergs Arch Pharmacol* (2009) 380(5):373–82. doi: 10.1007/s00210-009-0453-5

226. Zhan WJ, Liang MJ, Liu Y, Huang YF, Wang WX. Effects and mechanism of STAT3 inhibitor and nicotinamide combination on the inhibiting proliferation of hepatocarcinoma HepG2 cells. *Tianjin Med J* (2022) 50(07):686–92.

227. Zhang ZQ. *Targeted inhibition of hepatocellular carcinoma by membrane loaded natural product hypocrellin b nanovesicles and its mechanism*. Nanjing University Chin Med (2021). doi: 10.27253/d.cnki.gnjzu.2021.000076

228. Bai Y. *Study on the co-delivery of doxorubicin and miR-122 with nanosystem for hepatocellular carcinoma therapy*. Tianjin Med University (2017).

229. Yuan HJ. *Experimental study of interventional photothermal ablation combinaed with Fe2O3-PDA-Dox nanocomposites and combretastatin a-4 phosphate disodium for hepatocellular carcinoma in the rats*. Chinese general hospital&medical school PLA (2019). doi: 10.27637/d.cnki.gjyjc.2019.000262

230. Lai CH. *Investigation of the anti-tumor effects of mannose/CPG oligodeoxynucleotide-conjugated liposome containing tumor-assoclated antigens via specific activation of dendritic cell*. Guangxi Med University (2014).

231. Zhong XR. *Study on the mechanism of HDAC6 inhibitor tubacin enhancing the sensitivity of docetaxel against liver cancer*. Jilin University (2020).

232. Shen XX, Shi L, Yao LY, Niu YZ, Liang T. Effect of evodiamine combined with chloroquine on hepatocarcinoma. *J Nanjing Univ Tradit Chin Med* (2021) 37(03):400–3. doi: 10.14148/j.issn.1672-0482.2021.0400

233. Lai XC. *Study on the mechanism of evodiamine joint CDK1 inhibitor on hepatoma cell lines*. Guangzhou University Chin Med (2012).

234. Yang Y, Sun M, Yao W, Wang F, Li X, Wang W, et al. Compound kushen injection relieves tumor-associated macrophage-mediated immunosuppression through TNFR1 and sensitizes hepatocellular carcinoma to sorafenib. *J Immunother Cancer* (2020) 8(1):e000317. doi: 10.1136/jitc-2019-000317

235. Parhi P, Mohanty C, Sahoo SK. Nanotechnology-based combinational drug delivery: an emerging approach for cancer therapy. *Drug Discovery Today* (2012) 17(17-18):1044–52. doi: 10.1016/j.drudis.2012.05.010

236. Delbaldo C, Michiels S, Syz N, Soria JC, Le Chevalier T, Pignon JP. Benefits of adding a drug to a single-agent or a 2-agent chemotherapy regimen in advanced non-small-cell lung cancer: a meta-analysis. *JAMA* (2004) 292(4):470–84. doi: 10.1001/jama.292.4.470

frontiers | Frontiers in Oncology

TYPE Review
PUBLISHED 05 May 2023
DOI 10.3389/fonc.2023.1150492

OPEN ACCESS

EDITED BY
Marco Cordani,
Faculty of Biology (UCM), Spain

REVIEWED BY
Ilaria Genovese,
CNLS_IIT (Istituto Italiano Tecnologia), Italy
Chandra Sekhar Bhol,
National Institute of Technology Rourkela, India
Md. Rizwanullah,
Jamia Hamdard University, India
Kokkarachedu Varaprasad,
San Sebastián University, Chile

*CORRESPONDENCE
Marveh Rahmati
m_rahmati@sina.tums.ac.ir

RECEIVED 24 January 2023
ACCEPTED 19 April 2023
PUBLISHED 05 May 2023

CITATION
Gharoonpour A, Simiyari D, Yousefzadeh A, Badragheh F and Rahmati M (2023) Autophagy modulation in breast cancer utilizing nanomaterials and nanoparticles. *Front. Oncol.* 13:1150492. doi: 10.3389/fonc.2023.1150492

Autophagy modulation in breast cancer utilizing nanomaterials and nanoparticles

Azar Gharoonpour, Dorsa Simiyari, Ali Yousefzadeh, Fatemeh Badragheh and Marveh Rahmati*

Cancer Biology Research Center, Cancer Institute, Tehran University of Medical Sciences, Tehran, Iran

Autophagy regenerates cellular nutrients, recycles metabolites, and maintains hemostasis through multistep signaling pathways, in conjunction with lysosomal degradation mechanisms. In tumor cells, autophagy has been shown to play a dual role as both tumor suppressor and tumor promoter, leading to the discovery of new therapeutic strategies for cancer. Therefore, regulation of autophagy is essential during cancer progression. In this regard, the use of nanoparticles (NPs) is a promising technique in the clinic to modulate autophagy pathways. Here, we summarized the importance of breast cancer worldwide, and we discussed its classification, current treatment strategies, and the strengths and weaknesses of available treatments. We have also described the application of NPs and nanocarriers (NCs) in breast cancer treatment and their capability to modulate autophagy. Then the advantages and disadvantaged of NPs in cancer therapy along with future applications will be disscussed. The purpose of this review is to provide up-to-date information on NPs used in breast cancer treatment and their impacts on autophagy pathways for researchers.

KEYWORDS

autophagy, breast cancer, drug resistance, nanomaterial, nanoparticles

1 Introduction

Despite the advances in breast cancer diagnosis and treatment, the incidence and mortality rates of breast cancer are still increasing especially in poorly developed regions of the world (1). The results of many studies represent the fact that a decline in infection-associated cancers is offset by the rising number of cancer cases being highly related to dietary, hormonal, and reproductive factors in countries with fast transitions in economic and communal issues. Hence, fundamental strategies for prevention, diagnosis in early stages, and novel targeted therapies can result in a decrease in expected cancer incidence (2). Most breast cancer survivors have encountered aggressive relapse. It is mainly explained by the fact that breast cancer tumors are highly heterogeneous and difficult to

target (3). In anticancer therapies, the primary objective is the specific inhibition of the malignant function of cancerous cells while unaffected cells remain healthy. Ordinary treatments for cancers are encountered with inevitable side effects and drug resistance, which are discussed in the body of this article (4). In this regard, an intracellular mechanism such as autophagy targeting may be a good approach for breast cancer-targeted therapy. Autophagy as a conserved intracellular mechanism prepares the primary materials for the synthesis of vital macromolecules such as proteins by removing the unwanted molecules or organelles. Furthermore, autophagy preserves normal cells from intrinsic and extrinsic stressors promoting DNA mutations and instability that mainly lead to pre-neoplastic changes and propagation (3). Deficiency in autophagy function has led to diseases such as different malignancies. In cancer cells, autophagy has a dual role in homeostasis maintenance as a tumor suppressor in early stages and a tumor promoter at advanced stages. This important function of autophagy in cancer has led to more investigations in the field of targeting autophagy, which both inhibits and induces it in different cancers with different characteristics being critical. Many investigations in mammary cancer models revealed that the inhibition of autophagy genes can weaken the initial growth in tumors while paradoxically can result in overt metastasis and outgrowth in cancerous cells. In breast cancer, the genetic inhibition of autophagy in both early and late stages leads to the spread of tumor cells, which offers differentiation in pro-metastatic basal epithelial cells (5). In cancer initiation of mammary glands, the autophagy-related genes confer a suppressive role; however, this function is lost throughout breast cancer development, and impaired autophagy results in cancer progression (3). Of note, autophagy is detected as one of the main causes of chemotherapy resistance in breast cancer patients in a way that the inhibition of autophagy dramatically enhances the sensitivity of cancer cells to anticancer medicines (6). However, autophagy inducers could be effective in such situations and push the cells to apoptosis. Generally, efficient and genuine progress in this treatable disorder is not achieved unless a persistent and interconnected effort toward innovative procedures in cancer treatment (1). Most of the autophagy modulators that are currently available have low specificity, as they do not preferentially target a single cell type. Nanoparticles (NPs) can improve the efficacy of drugs through their high power of permeability and reduce their toxicity due to nanosized properties. They lead to more effective targeting of tissue, cells, or organelles and enhance the pharmaceutical properties of drugs such as stability, solubility, plasma half-life, and tumor accumulation. The connection between NPs and their impact on autophagy has shown that they can impact autophagy through both its induction and inhibition (7). In this review article, we aim to describe the application of different NPs and nanocarriers (NCs) in breast cancer treatment and their capability to modulate autophagy. We then discuss the advantages and disadvantages of NPs in cancer therapy, along with their future applications. The purpose of this review is to provide researchers with up-to-date information on NPs used in breast cancer treatment and their impacts on autophagy pathways.

2 Breast cancer

Breast cancer is one of the main causes of death in most parts of the world, especially in low-income areas (1). The incidence of breast cancer has increased in Western countries from the 1980s to 1990s and then has been stable due to better detection and the use of modern treatment. In 2020, almost 2.3 million women were diagnosed with breast cancer worldwide, and approximately 700,000 individuals died (8). According to the World Health Organization (WHO) prediction, by 2040, newly diagnosed breast cancer cases are expected to rise by almost 40% every year. A dramatic increase in the trend of breast cancer will be observed especially in countries with a low human development index (HDI), where the number of new cases and the mortality rate is projected to be doubled by 2040 (9). In Iran, breast cancer was determined to have the highest incidence rate per 100,000 women and the second-highest mortality rate after colorectal cancer in 2020 (10).

The risk factors for breast cancer are categorized as reproductive and non-reproductive factors, based on economic issues. Major reproductive factors include age, age of menarche, age at first pregnancy, some indicators of ovarian activity, age at natural menopause, duration of breastfeeding, history of breast disease, genetic status, nulliparity, and familial history of breast cancer (11). However, non-reproductive risk factors comprise obesity, lifestyle, being overweight during a post-menopausal state, and drinking level (2, 12). In Iran, other factors such as hormone replacement therapy, passive smoking, advanced maternal age at pregnancy, abortion, high levels of sugar consumption, and the genotype of Arg/Arg could also increase the risk of breast cancer development, whereas late menarche, breastfeeding for at least 13–24 months, routine exercise, and having vegetables in diet reduce the risk of breast cancer. The relationship between the polymorphism in codon 72 of the p53 gene and the risk of breast cancer shows that although the genotype of Arg/Pro was not related to the development of breast cancer, the genotype of Arg/Arg raised the risk of breast cancer significantly (13).

2.1 Breast cancer staging

In the 1940s and 1950s, the first staging of breast cancer was reported by Pierre De-noix, which was mainly based on the anatomic shape of the breast (14, 15). Lately, an extensively detailed system of staging cancers has been developed by the American Joint Committee on Cancer (AJCC) and has been updated eight times. In the breast cancer chapter, levels of estrogen receptor (ER) and progesterone receptor (PR) expression, human epidermal growth factor receptor 2 (HER2) or erythroblastic oncogene B (ERBB2) expression, histologic grade, regional lymph node involvement, distant metastases, and prognostic biomarkers are included in order to confer precise prognosis and guide treatment decisions (14, 16). This system is named TNM staging, which shows the status of tumors (T), lymph node involvement (N), and the level of tumor metastasis (M).

The combination of immune histological data such as the tumor grade, the determination of hormone receptor status, and a multi-gene panel with anatomic information results in a more explicit prognosis. However, tumors with lower-graded ER– and PR– tend to be more common among populations; therefore, multi-gene panels should be performed for further information (17).

2.2 Biomarkers in breast cancer

The biomarkers can be extremely helpful in the determination of breast cancer, especially in the early stage, to achieve a better prescription. In general, they are classified into tissue, genetic, and serum markers. The tissue markers or hormone receptors, namely, ER and PR, are critical for identifying patients that should be treated with hormone therapy. ER and PR should be tested for all patients with a breast cancer diagnosis. Nevertheless, ER alone is a weak prognostic factor (18). HER2 measurement is essential for all patients with invasive breast cancer and is the indicator for the patients who may be treated with trastuzumab and who may benefit from anthracycline-based adjuvant chemotherapy (19).

The most important genetic markers of breast cancer are defined as breast cancer gene 1 (BRCA1) and breast cancer gene 2 (BRCA2) mutation genes, which are the most powerful predictive tools to identify patients suffering from breast and ovarian cancer with a 40%–80% risk of developing cancer (20). In primary tumors, DNA ploidy is found to be an independent prognostic tool for surgical cases. Aneuploidy implies genetic abnormalities like single-nucleotide point mutations and changes in chromosome structure. Diploid tumors have a slightly longer survival time than those diagnosed with aneuploid tumors (21). The use of circulating tumor DNA (ctDNA), as a representative of tumorous DNA in the plasma or other body fluids of patients with cancer, is also important in detecting tumor cells. Detecting ctDNA reduces the need for tumor biopsy and helps a physician to determine the effective treatment, and a decrease in the levels of ctDNA in the process of treatment indicates a successful therapy (22).

The serum biomarkers are of great significance in breast cancer management therapy protocol, as they may help determine early diagnosis, prognosis, and response to therapies. They consist of carcinoembryonic antigen (CEA), the MUC-1 family agents (CA15-3, BR 27.29, MCA, and CA549), the serum cytokeratins [e.g., tissue polypeptide antigen (TPA) and tissue polypeptide-specific antigen (TPS)], and the serum oncoproteins (e.g., HER2/c-erbB-2). The approved serum markers designed for breast cancer are CA15-3 and CEA. Increased levels of CA15-3 (e.g., to 150 U/ml) and/or CEA (e.g., to 120 ng/ml) in a patient indicate a non-metastatic tumor (23). The measurement of two parameters such as urokinase-type plasminogen activator (UPA) and plasminogen activator inhibitor (PAI-1) is mostly performed in lymph node-negative patients, for whom adjuvant chemotherapy would not be helpful. Low levels of both the UPA and PAI-1 factors in such patients show a low risk of disease relapse (24).

2.3 Breast cancer treatment

According to the classification of breast cancer into ER and PR expression and HER2/ERBB2 gene amplification, different treatment strategies are applied (25). For ER- or PR-positive breast cancers, the first choice is the use of endocrine agents to downregulate ER signaling. For those with HER2 or HER2/neu positive, ERBB2-targeted therapy is suggested, including anti-ERBB2 antibodies (e.g., trastuzumab and pertuzumab) and small-molecule tyrosine kinase inhibitors (such as lapatinib and neratinib) (26). The main purpose of therapy for non-metastatic breast cancers is the removal of all the tumors or axillary lymph nodes by surgery, followed by postoperative radiation. Systemic therapy can also be performed preoperatively (neoadjuvant), postoperatively (adjuvant), or both. For metastatic breast cancers, the same basic categories of systemic therapy are used as neoadjuvant/adjuvant approaches (27).

For patients undergoing refractory metastatic breast cancer with a diagnosed deletion in BRCA1/2 genes, treatment with poly adenosine diphosphate-ribose polymerase (PARP) inhibitors like olaparib and talazoparib is approved by the US Food and Drug Administration (FDA) (28). Conventional chemotherapy for breast cancer targets the cells non-selectively and inhibits the proliferation of both normal and cancerous cells. Therefore, gastrointestinal problems and hair loss are some of their important side effects. The other major problem is drug resistance (4), which is discussed in the following paragraph. Figure 1 illustrates the treatment protocol for different breast cancers.

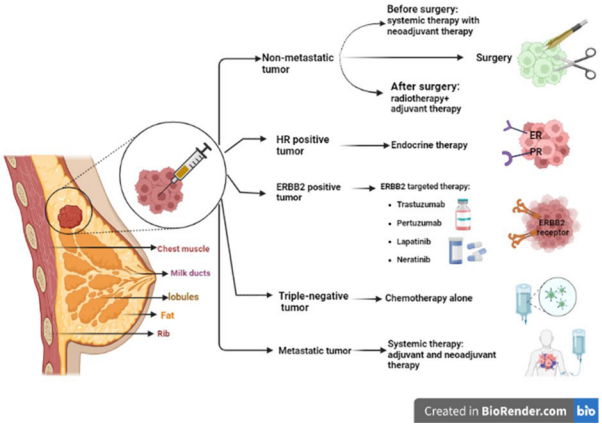

FIGURE 1
Different strategies to treat different types of breast cancer. ER/PR-positive breast cancers are much more likely to respond to hormone therapy. For HER2 or HER2/neu-positive patients, targeted therapy including anti-ERBB2 antibodies (trastuzumab and pertuzumab) and small-molecule tyrosine kinase inhibitors (such as lapatinib and neratinib) are used. For non-metastatic breast cancer, complete removal of the tumor or axillary lymph nodes by surgery and postoperative radiation is recommended. For metastatic breast cancer, systemic therapy is prescribed, such as neoadjuvant/adjuvant therapies. ER, estrogen receptor; PR, progesterone receptor; HER2, human epidermal growth factor receptor 2; ERBB2, erythroblastic oncogene B.

2.4 Breast cancer and drug resistance

Multidrug resistance (MDR) is the main reason for the relapse of breast cancer. The development of MDR is due to various molecular mechanisms, including increased expression of efflux transporters, epithelial-to-mesenchymal transition (EMT), and stem cell drug resistance (29). Cancer cells prevent the accumulation of chemical drugs inside the tumor and hinder their effectiveness *via* different mechanisms. Drug efflux transporters or efflux pumps are defensive mechanisms of cancer cells that direct anticancer drugs out of tumors. They are members of the ATP-binding cassette (ABC) superfamily involved in transporting substances into and out of cells with ATP hydrolysis (29).

Another mechanism is defined as EMT, a process by which epithelial cells lose their intercellular adhesion and apical-basal polarity properties and migrate into the mesenchyme. These cells gain new features that lead to increased drug efflux and resistance to apoptosis (30).

Breast cancer stem cells (BCSCs) are one of the major problems in drug resistance, metastasis, and cancer recurrence. Due to properties such as self-renewal, long lifespan, slow proliferation, high drug transport capacity, DNA repair mechanisms, and anti-apoptotic properties, BCSCs show intrinsic resistance to conventional therapies, and their removal is considered to increase drug susceptibility. One reasonable approach is targeting self-renewal pathways, and the other plan attacks the BCSC microenvironment. At present, some novel techniques are being discovered, including the use of cyclin-dependent kinase (CDK) inhibitors, factors that induce stem cell differentiation, and targeted immunotherapies (31).

Cancer stem cells (CSCs) also play a role in the induction of the mitochondrial-expressed genes involved in oxidative stress response, tumor survival, and drug resistance (32).

Under stressful conditions, such as reactive oxygen species (ROS) production or nutrient starvation, mitochondria undergo membrane potential depolarization and sequester into autophagosomes, under the process named mitophagy. During severe and prolonged stress, mitophagy is suppressed, and cell death pathways are activated (33). Indeed, mitophagy is a cytoprotective process during tumor progression and has a critical role in drug resistance and maintenance of stemness and self-renewal of CSCs. However, reports point to the role of mitophagy as a cellular tumor suppressor. Thus, both induction and inhibition of mitophagy contribute to the drug sensitivity of tumor cells (34). Another cause of MDR is intracellular mechanisms such as autophagy activation, discussed later in detail, which can potentially be modulated in cancer therapy.

3 Autophagy

Autophagy is defined as a "self-degradative" pathway that manages cellular homeostasis to provide precursors such as amino acids for the assembly of vital cellular components *via* catabolic pathways (35). In other words, autophagy helps the cells eliminate the malfunctioned organelles or macromolecules and then return the primary building materials to the manufacturing cycles of the cell, to reestablish cellular homeostasis. Autophagy is induced by various cellular stresses such as hypoxia, starvation, and infection (36). This phenomenon was indicated with studies in yeast in the 1990s by detecting autophagy-related genes (ATGs). Autophagy is classified into three types: microautophagy, macroautophagy, and chaperone-mediated autophagy (CMA) (37). Although all three types take the misfolded proteins to the lysosome, their mechanisms and morphologies are different. In microautophagy, cytoplasmic materials are directly absorbed into the lysosomal lumen through the invagination of the lysosomal membrane (38). In CMA, soluble proteins in the cytosol are selectively recognized by a 70-kDa heat shock protein (hsp70), unfolded, and translocated to lysosomes. These cytoplasmic proteins have special recognition motifs called pentapeptides. The CMA targeting motif is recognized as KFERQ and varies at different residues. For example, at "K" and "R" positions, up to two positively charged amino acids [e.g., arginine (R) or lysine (K)]; at position "F", two hydrophobic residues [e.g., isoleucine (I), leucine (L), phenylalanine (F), or valine (V)]; and at "E" position, single negatively charged [e.g., glutamate (E) or aspartate (D)] can be placed. The "Q" can be at the N- or C-terminus of the pentapeptide and is flexible for negatively or positively charged or hydrophobic amino acids. This variation of proteins exists in approximately one-third of all the soluble cytosolic proteins. This protein–chaperone complex binds to a receptor of the lysosome and lysosome-associated membrane protein type 2A (LAMP-2A), and the substrate is released. Then, the unwanted proteins are degraded by lysosomal enzymes and reused in the next protein synthesis process (39).

Macroautophagy initiates with special double-membrane vesicles, known as autophagosomes, that progressively isolate autophagic cargo and deliver them to lysosomes by membrane fusion. An organelle that results from the fusion of an autophagosome and a lysosome is often referred to as the autophagolysosome. The digestion of cargo prepares nutrients for cell survival. Macroautophagy is directly related to autophagy (40) and is mainly considered a non-selective or general process. Nevertheless, it is noteworthy that in many cases the selective autophagy pathway has been also observed, which turns out to be essential only for cellular health. Deficiency in autophagy function can lead to diseases such as susceptibility to infections and inflammation, metabolic disorders, cardiovascular and liver problems, cancer, neurodegeneration, and acute brain damage. In tumorigenicity, autophagy performs a two-faced role of tumor suppressor and pre-oncogene (5). Because of these dual roles, finding a new targeted therapy for both activating and inhibiting autophagy pathways is under investigation (38) and will be discussed in the following sections.

3.1 Autophagy machinery

Autophagy contains complex steps that lead to the generation of autophagosomes and their fusion into lysosomes. The process includes several phases, namely, initiation, elongation, lysosomal fusion, and degradation, which are mediated by ATGs (3).

3.1.1 Induction and initiation

In mammalian cells, the autophagy is induced by unc-51-like kinase family (ULK1/ULK2) complex (homolog of the Atg1 complex in yeast), ATG13, and RB1-inducible coiled-coil 1 (RB1CC1/FIP200). Then, C12orf44/ATG101 protein binds directly to ATG13, which occurs in mammals and not in yeast. ULK1 complex induces membrane formation in the phagophore assembly site (PAS). Accordingly, ATG2 transfers phospholipids from the endoplasmic reticulum, Golgi, and mitochondria membrane to PAS, and ATG9 transfers them to the luminal layer of the autophagosome membrane (41). As the phagophore expands, the membrane wraps around the substrate and forms a spherical autophagosome.

Autophagy is immensely regulated by two main kinases, including the mammalian target of rapamycin complex 1 (mTORC1) and AMP-activated protein kinase (AMPK), which affect ULK1 complex formation (42). mTORC1 associates with the ULK1/ULK2 complex in autophagosome under rich nutrients and inactivates the complex by its phosphorylation. However, under rapamycin treatment or starvation, mTORC1 dissociates from the complex and induces autophagy. In other words, in the abundance of amino acids and nutrients, mTORC1 inhibits autophagy through the phosphorylation of ULK1 and ATG13 (43). However, the AMPK (the autophagy inducer) can sense the AMP : ATP ratio caused by energy deprivation and be activated to start autophagy by phosphorylating several sites in the central intrinsically disordered region (IDR) in ULK1. Furthermore, the AMPK is an indirect inducer of autophagy by phosphorylation of the regulatory-associated protein of mTOR (RAP-TOR), which leads to mTOR inhibition (44).

3.1.2 Nucleation

In this step, ATG14-containing class III phosphatidylinositol 3-kinase (PtdIns3K) complex binds to the autophagosome. The PtdIns3K generates the PtdIns3P complex, which is involved in the nucleation of the phagophore and consists of PIK3C3/VPS34, PIK3R4/p150, and BECN1. Some reports suggest the association of this complex with ATG14 and UVRAG is necessary for autophagosome formation. Regulation of the PtdIns3K complex is mediated through the proteins that interact with BECN1 such as BCL2. As the BCL2 binds to BECN1, it inhibits the interaction of BECN1 with PIK3C3 and inactivates autophagy (45).

3.1.3 Elongation

Phagophore expands with the formation of the ATG5, ATG12, and ATG16L1 complex. As the phagophore is completed, it dissociates from the complex. The ATG8/LC3 system is also involved in the phagophore expansion. In mammals, there are several Atg8-like proteins that are the LC3 and GABARAP subfamilies. The LC3 forms LC3-1 by ATG4 and its phosphatidylethanolamine (PE)-conjugated or lipidation form, called LC3-II. The form of LC3-II is activated under starvation or other autophagy stressors. ATG9 is a transmembrane protein involved in phagophore expansion and membrane recruitment (46).

3.1.4 Autophagosome fusion with lysosome

The structure of autolysosome is formed by the fusion of the outer membrane of the mature autophagosome with the lysosome (47). There are three main machinery protein families playing a crucial role in the regulation of the fusion process, including membrane-tethering factors (such as HOPS and EPG5), soluble *N*-ethylmaleimide-sensitive factor attachment proteins (SNAREs), and Rab GTPases, which are situated on the membrane. They hire the tethering complex to bridge to the facing lipid bilayer; therefore, the tethering complex employs SNARE proteins and promotes them to move autophagosomes toward the lysosome and facilitate the fusion process (48). Recently, a growing number of studies have conferred the great role of ATG8 family members in driving autophagosomes near the lysosome. In addition, the role of these members has been suggested as probable hubs in the final fusion stages. In mammals, amphisomes emerge if the autophagosome fuses with the endosome before reaching the lysosome. Microtubules are also involved in driving the autophagosomes to the lysosomes (49). Being able to assist with the UVRAG PtdIns3K complex, the UVRAG activates GTPase RAB7, which promotes autophagosome–lysosome fusion (50). Recent studies have suggested other components of the SNARE machinery system that play role in the fusion process like VAM9 and VAM7 (51).

One of the mechanisms that macroautophagy uses to selectively identify cargo is ubiquitination. The ubiquitin-binding protein SQSTM1/p62 targets the ubiquitinated proteins and then interacts with LC3-II to clear these aggregate proteins from the cytosol and move them to the lysosome (52).

3.1.5 Degradation

Once the autophagosome formation is completed, its outer membrane merges with the lysosomal membrane; then, the inner layer and cargo will be degraded by hydrolases and subsequently with permeases to be competent for cell biosynthetic processes and the generation of energy (53). The product of autophagosome and the lysosome fusion is called “autophagolysosome” or “outolysosome”. The heterophagic (no-self) materials are needed in autolysosomes since approximately all lysosomes take constant flow made by endocytic pathway (54). All the autophagy steps are shown in Figure 2.

3.2 Autophagy and cancer

Autophagy has two completely different behaviors in cancer, depending on the severity of cellular stress and the state of the immune system. During tumor initiation, autophagy prevents carcinogenesis, and in the advanced stages of tumors, it aids cancer progression. In fact, autophagy acts as a tumor suppressor in the early stages of carcinogenesis by maintaining genomic stability and paradoxically promotes tumor progression in established cells by providing nutrients (36, 55). It is noteworthy that in cancer cells, autophagy suppresses the immune system by affecting T cells, cytokines, and other immune system cells. In fact, autophagy helps the immune system by removing damage-

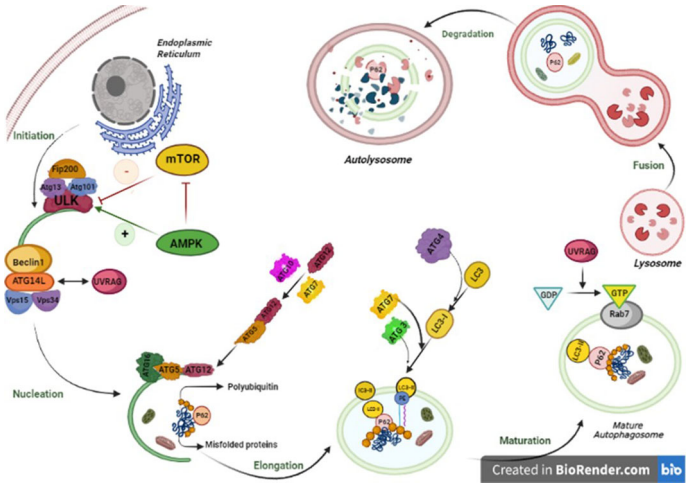

FIGURE 2
Autophagy pathway is performed in five steps from initiation to fusion with lysosome. In mammalian cells, the initiation phase of autophagy consists of autophagosome formation, which is significantly dependent on the stable complex known as ULK1-Atg13-FIP200-Atg101. The activation of the ULK1 kinase launches the activity of Beclin1 (BECN1)–VPS34 complex including BECN1, VPS34, and Beclin1 regulator 1 (AMBRA-1). In the elongation phase, the WIPI2B scaffold binds to PI3P. The mentioned complex is highly essential for employing two main proteins, ATG7 and ATG10, that can couple ATG5 to ATG12, which makes a complex with ATG16L. The Atg12–Atg5–Atg16 complex positions on the outer membrane due to ATG 5 available binding sites. The next step is the fusion of autophagosome–lysosome and includes two main phases. First, the autophagosome migration to lysosomes, which is implemented by the cytoskeleton in eukaryotic cells by Rab7 and guanosine triphosphate (GTP)-binding protein to microtubules, and second, the fusion of lysosomes, with a single bilayer membrane, and mature autophagosomes, with two lipid bilayer membranes. The last step is degradation of all components in the lysosome. The lysosomal enzymes degrade autophagic cargo.

associated molecular patterns (DAMPs) and pathogen-associated molecular patterns (PAMPs). Thus, the immune system is prevented from functioning properly in cancerous health conditions due to the increase in autophagy and removal of excessive DAMPs and PAMPs. In other words, the function of T cells, NK cells, cytokines, and other vital parts of the immune system is overshadowed by complicated processes of autophagy (56, 57).

In preclinical breast cancer models, autophagy has performed a strong role in the survival of quiescent disseminated cells (58). Compared to normal tissues, breast cancer cells hold a low level of Beclin1 proteins (59). Human *BECN1* monoallelic deletions are reported in up to 50% of breast cancers and 75% of ovarian cancers (60, 61). Numerous studies in the area of breast cancer survivors on the METABRIC (Molecular Taxonomy of Breast Cancer International Consortium) dataset demonstrated that a lower expression of *BECN1* is associated with a worse probability of survival (61).

The defective activity of any autophagic genes may affect carcinogenesis. It is detected that the mono-allelically deleted Beclin-1, as a haploid tumor suppressor, has an insufficient function in different cancers such as human hepatocellular carcinoma and breast, ovarian, and prostate cancers (62). Notably, many studies on ATG genes have demonstrated that ATG2B, ATG5, ATG9B, ATG12, and ATG16L1 are also oncologically linked to tumorigenesis. Furthermore, the somatic mutations in the ATG5 gene ruin the binding sites of ATG5 and Atg16L1, resulting in an impaired conjugation site for ATG12, and autophagy failure (63).

Evidence shows that in some situations, inhibition of autophagy and, in some cases, induction of autophagy has been beneficial for the treatment of cancers, depending on the tumor type or the stage of disease (64). Autophagy-dependent genes and proteins are valuable markers in tissue samples of patients for better diagnostics (65).

3.3 Autophagy and drug resistance

Several studies indicate that autophagy has a critical role in the survival of tumors and drug resistance. Obviously, autophagy is induced by chemotherapeutic drugs and then prepares the tumor cells for the nutrients by degradation of unwanted proteins or organelles. Accordingly, autophagy prevents DNA damage and enhances drug resistance in tumors (66). Although the exact mechanism of drug resistance with autophagy induction is not fully understood, some reports have suggested the role of autophagy in the induction of DNA damage response and the increase of drug efflux pumps in tumor cells (67). In this regard, autophagy may be involved in apoptosis inhibition by the inactivation of pro-apoptotic factors or the activation of anti-apoptotic agents. In this case, autophagy induction is used to overcome drug resistance. Prolonged autophagy promotes autophagic cell death (type II cell death), which is independent of apoptosis (type I cell death) or necrosis (type III cell death). In tumors, when the cells resist apoptosis, induction of autophagic cell death is an approach to trigger drug resistance. There are some drugs (like bortezomib, rapamycin, and butyrate) that induce autophagosome formation

(68). However, considering the dual role of autophagy in cancer, another approach to target tumor drug resistance is autophagy inhibition. The use of gene silencing of autophagy-related genes or chemical inhibitors such as bafilomycin A1, 3-methyladenine (3-MA), and chloroquine (CQ) is commonly used to inhibit autophagosome formation (69).

3.4 Autophagy modulation

Enhanced autophagy in tumors, as a survival mechanism and a cause of MDR, leads to the use of autophagy inhibitors to suppress tumor cell proliferation and induce cell death. The application of autophagy inhibitors in combination with antitumor drugs sensitizes the cancerous cells to chemotherapy (70). For example, treatment of HER-positive breast cancer cells with depletion of Atg5, Atg7, or beclin1 resulted in enhanced effectiveness of tamoxifen or the combination therapy of 3-MA, as an autophagy inhibitor, and trastuzumab, as a chemotherapeutic drug, increasing the effectiveness of chemotherapy in HER2-positive breast cancer cells as compared to monotherapy (71).

However, the use of anticancer drugs induces autophagy as a survival mechanism. However, therapies involving both excessive autophagy induction upon cytotoxic drug treatment or using autophagy inducers may also lead to autophagic cell death (72, 73). Accordingly, there are some autophagy inducers that have been used as anticancer treatments. For example, proteasome inhibitors (PIs) have also been shown to stimulate autophagy. Bortezomib, a PI used in the treatment of multiple myeloma and mantle cell lymphoma, has been shown to increase the early formation of autophagosomes and LC3-II, demonstrating its inducing effects on autophagy (74). A well-known class of autophagy inductors includes analogs of the mTOR inhibitor rapamycin, such as temsirolimus and everolimus. These compounds, which can be used alone or in combination with chemotherapy drugs, show an anti-proliferative effect in mantle cell lymphoma and acute lymphoblastic leukemia by overstimulating autophagy, which might cause tumor cell death. A large number of ongoing trials demonstrate that autophagy modulation in combinatory treatments could successfully overcome the resistance to existing anticancer drugs. For instance, RUBCN (Rubicon autophagy regulator), as a negative regulator of autophagosome biogenesis, leads to the inhibition of basal differentiation and attenuates metastatic growth *in vivo* (5, 73). There are many FDA-approved and unapproved autophagy modulatory drugs that are introduced for cancer treatment. For example, CQ and hydroxychloroquine (HCQ) are determined as autophagy inhibitors, rapamycin and metformin are used as autophagy inducers in various cancers, and CQ and metformin are mainly used in breast cancer. The mechanism of CQ is suppressing the fusion of autophagosome and lysosome, while metformin activates AMPK (74) through ROS production in the mitochondria and inhibition of the mitochondrial respiratory chain complex 1 (75).

3.5 Breast cancer treatment by autophagy modulation

Since autophagy has a significant role in the survival of cancer cells, its modulation is considered a hopeful strategy for cancer treatment. Previous studies have shown that autophagy is the main reason for resistance to chemotherapy in breast cancer and has resulted in decreased sensitivity to chemotherapy with doxorubicin (DOX). Experiments indicated that the use of autophagy inhibitors can reverse doxorubicin resistance and enhance its efficacy in triple-negative breast cancer MDA-MB-231 cells (76). In addition, the cotreatment of DOX and 3-MA resulted in a necroptotic form of cell death in breast cancer (76). Using CQ is another approach to return DOX sensitivity in breast cancer MCF-7 cells (77).

Overexpression and accumulation of LAMP2A were observed in breast cancer tissue samples, and its inhibition conferred sensitivity to DOX in MCF-7 and T47D breast cancer cells (78). A novel adipokine, resistin, is highly stimulated in patients with breast cancer and facilitates cell proliferation, metastasis, and breast cancer cell migration. Resistin can activate AMPK/mTOR/ULK1 and JNK signaling pathways. Interestingly, the blockage of the two mentioned pathways reduces the ratio of LC3-II/LC3-I, which grants increasing apoptosis in breast cancer cells induced by DOX (79). In addition, in DOX-resistant breast cancer cells, psammaplin A (a natural product isolated from marine sponges with anticancer effects) can stimulate overexpression of damage-regulated autophagy modulator (DRAM) that is induced by p53 protein (80). In estrogen receptor-positive breast cancer, attenuated autophagy sensitized resistant tumors to tamoxifen-induced cell death (81). The summary of some autophagy inhibitors and inducers that are used in breast cancer is listed in Tables 1, 2 respectively.

4 Autophagy modulations by nanoparticles and nanocarriers

Most of the autophagy modulators that are currently available have low specificity, as they do not preferentially target a single cell type. In addition, multiple autophagy mediators contribute to several cellular processes and are involved in autophagy-independent functions. For instance, rapamycin, as a well-known autophagy inducer, has an impact on the inhibition of T-cell proliferation, which results in strong immunosuppression (99). These challenges lead to limitations in the use of autophagy regulators in cancer treatment. In this regard, NPs have multiple advantages to overcome these issues. They can improve the efficacy of drugs by their high power of permeability and reduce their toxicity due to nanosized properties. They lead to more effective targeting of tissue, cells, or organelles and enhance the pharmaceutical properties of drugs such as stability, solubility, plasma half-life, and tumor accumulation (7). NPs can be used alone or in combination with drugs. However, NC is a nanomaterial

TABLE 1 The compounds with autophagy inhibition characteristics.

Compound	Mechanism of action	References
SB02024	The compound is a VPS34 inhibitor; it blocks autophagy and increases the sensitivity of breast cancer to sunitinib and erlotinib drugs	(6)
3-Methyladenine (3-MA) or bafilomycin A1	The combination of 3-MA and gefitinib (Ge) enhance the effect of treatment in triple-negative breast cancer *in vitro* and *in vivo*. An increased level of BAX/Bcl-2, cytochrome *C* and CASP3 has been observed	(82)
Tioconazole	An antifungal drug that inhibits ATG4B and autophagy; it induces sensitivity to chemotherapy	(83)
3-MA	3-MA is an autophagy inhibitor. However, its combination with anticancer drugs is autophagy-independent	(84)
(2*S*)-8-[(3*R*)-3-Methylmorpholin-4-yl]-1-(3-methyl-2-oxobutyl)-2-(trifluoromethyl)-3,4-dihydro-2*H*-pyrimido [1,2-*a*]pyrimidin-6-one	The compound is a VPS34 inhibitor and suppresses autophagy pathway	(85)
Mefloquine (MQ)	The drug inhibits autophagy through lysosomal function disruption; induces endoplasmic reticulum stress and apoptosis in both hormone receptor-positive or receptor-negative breast cancer cell lines	(86)
IITZ-01 and IITZ-02	They inhibit maturation of lysosomal enzymes and increase accumulation of autophagosomes, which leads to autophagy inhibition	(87)
GDC-0941	The compound is a PI3K inhibitor. The combination of GDC-0941 and an autophagy inhibitor enhances the sensitivity of estrogen receptor (ER)-positive breast cancer to treatment	(88)

that is used as a transport mediator for other substances, such as a drug. Generally, NCs are categorized as micelles, polymers, carbon-based materials, liposomes, and other materials and are used in drug delivery, especially in chemotherapy (100).

The connection between NPs and their impact on autophagy has shown that they can impact autophagy through both its induction and inhibition. The induction of autophagy is mainly mediated through oxidative stress activation. Under external stress, the phagocytosis of NPs or NCs is enhanced, and mitochondrial respiration is also increased. Hence, the accumulation of a large number of incompletely reduced oxygen atoms results in the generation of a large number of ROS, which leads to programmed cell death (101). Autophagy induction by NPs may be a defensive mechanism against external signals. The use of CQ and NPs enhances the effectiveness of chemotherapy by the accumulation of NPs in the tumor and decreases the immunological clearance of NPs. The NPs can directly reach the tumor cells; therefore, they can reduce the non-specific functions of autophagy regulators, enhance the accumulation of drugs at tumor sites, and consequently enhance the antitumor efficacy (89).

Although NPs have several advantages in biomedical applications, they have shown some cytotoxic effects on cancerous cells. For example, inflammation, ROS production, apoptosis, or

TABLE 2 The compounds with autophagy induction characteristics.

Compound	Mechanism of action	References
LYN-1604	The compound activates ULK1 and autophagy through apoptosis induction in triple-negative breast cancer.	(89)
Metformin	Metformin inhibits the mTOR effector, p70S6K1, and induces AMPK activity.	(90)
Tat-BECLIN1	The compound blocks the HER2/Beclin1 binding and enhances autophagy in HER2-positive breast cancer.	(91)
Paratocarpin E	The compound induces autophagy by increasing the ratio of LC3-II/LC3-I and Beclin-1 levels; it induces apoptosis *via* alteration of Bax and Bcl-2 expression; it activates caspase-8, caspase-9, and PARP cleavage.	(92)
Sarsaparilla (Smilax Glabra Rhizome) extract	The compound induces autophagy *via* ERK1/2 pathway and also inhibits cancer growth through apoptosis induction in breast cancer cell line.	(93)
Isoliquiritigenin (ISL)	The compound induces autophagy through miR-25 overexpression and ULK1 activation.	(94)
Gelomulide K	The compound increases the paclitaxel effects through reactive oxygen species (ROS) production, autophagy induction, and caspase-independent cell death.	(95)
Juglanin	The compound induces autophagy through the ROS/JNK signaling pathway and subsequent apoptosis activation.	(96)
CYT-Rx20	The compound induces autophagy through activation of Beclin-1, ATG5, and LC-3 proteins and also induces apoptosis.	(97)
Resveratrol	The compound induces autophagy through inhibition of the breast cancer stem cell and Wnt/β-catenin signaling pathway.	(98)

necrosis occurs following the toxicity of NPs, limiting their application. To overcome these barriers, some modifications are necessary in order to increase the efficacy of NPs. For example, changing the dose of treatment or modifying their shape or formulation could reduce the toxicity level. The dose of NPs used in treatment is important in their aggregation and distribution. Moreover, the direct administration of NPs on the skin is less toxic than intravenous injection. Consequently, conducting an accurate protocol for using NPs in biomedicine is critical (90).

The different effects of NPs on autophagy, induction, or inhibition, in different situations, lead to antitumor activity or an increase in cell death (89). In practice, the choice between inhibition and promotion of autophagy is controversial, as it may depend on the role of autophagy in tumor development. As long as autophagy exerts a positive effect on the treatment of certain cancers, strategies that promote autophagy remain desirable. However, when autophagy adversely affects cancer treatment, inhibition of autophagy is the appropriate strategy. Depending on the type of cancer, therapy should involve an appropriate treatment in combination with autophagy modulation (72). Figure 3 illustrates the role of autophagy in cancer, drug resistance, and the modulation of autophagy in breast cancer.

4.1 Nanocarriers

NCs, as a specific type of drug delivery system, can target tumor cells through passive and active targeting methods and accumulate more in cancerous tissue, compared to normal tissues. Passive targeting means the direct permeation of drugs into tumor tissue, which depends on the action of the enhanced retention system or enhanced permeation system (EPS) effect. As a tumor develops in size and shape, an increased demand for oxygen and nutrients leads to the requirement for new blood vessels. These vessels are often not properly developed and are, therefore, permeable to some particles of certain sizes, usually below 700 nm (90). To function properly, NCs should be less than 100 nm in diameter and have a naturally hydrophilic surface, indicatively to avoid macrophage clearance and adhesion to plasma proteins. Polyethylene glycol, polysaccharides, poloxamines, poloxamers, and amphiphilic copolymers are some NCs with passive targeting ability (102). In active targeting, NCs are coated with specific ligands that can recognize their targets on the surface of cancer cells (91). NCs can be transferred directly to the cancer cells mainly through the following mechanisms. First, they can be delivered directly to the cancer cells through carbohydrate targeting, as the tumor cells have more carbohydrates in their membranes than normal cells. The second approach to the delivery of NCs is through receptor targeting. Some of the NCs are equipped with ligands of specific tumor cell receptors to recognize the tumor cells. In this method, after connecting the NCs to the tumor receptors, the drug is dissociated from the carrier and transferred to the target sites (92).

There are structurally different types of NCs explored for the effective treatment of breast cancer, including polymeric micelles, dendrimers, nanoliposomes, carbon nanotubes, solid lipid NPs (SLNs), nanostructured lipid carriers (NLCs), nanoemulsions (NEs), gold-based NPs (AuNPs), protein nano cargoes, and aptamers (93). In Table 3, we discussed the structure and

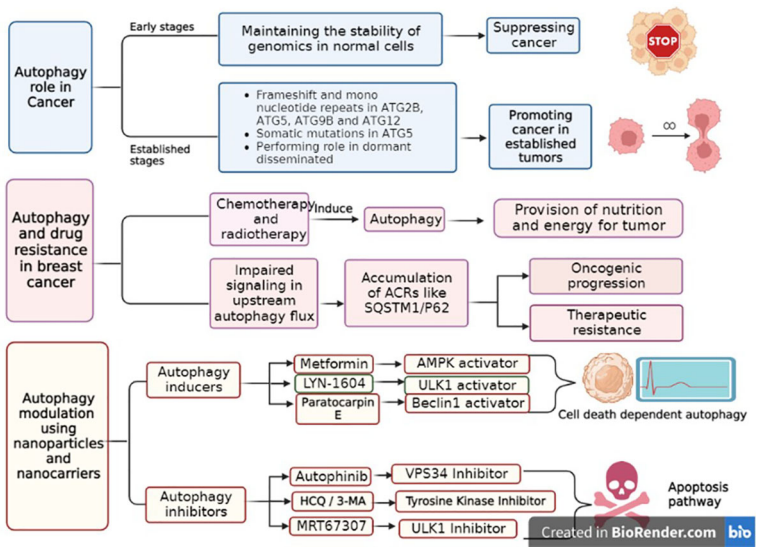

FIGURE 3
The role of autophagy in breast cancer, its drug resistance and the approaches of autophagy pathway modulation. Autophagy plays a dual role in cancers, according to the stage of tumors. In general, it acts as a tumor suppressor in early stages, while in established tumors, it promotes tumor progression. During chemotherapy or radiotherapy, autophagy is activated to provide nutrients for tumors and induce drug resistance. Autophagy inducers lead to autophagy activation, which finally promotes cell death in an autophagy-dependent manner. In contrast, autophagy inhibitors suppress the nutrient pathway for tumors, ultimately leading to apoptotic cell death.

TABLE 3 The application of different types of nanocarriers (NCs) with their structures and characteristics in breast cancer experimental models.

Systems	Structure	Characteristics	References
Polymeric micelles	Amphiphilic in nature; hydrophobic core and hydrophilic shell	Biocompatible and biodegradable; self-assembly and functional modification capability; active and passive targeting	(93)
Dendrimers	Synthetic, uniform structures, composed of core, branches, and surface regions	Equity in size, shape, and the length of branches; enhanced surface area, loading capacity, and targeting ability; improve pharmacokinetics and biodistribution of drugs	(95)
Liposomes	Lipid bilayer membrane forming self-assembled closed colloidal structures with an aqueous core	Biocompatible and biodegradable; providing improved pharmacokinetics altered biodistribution of the drug; sustained and slow release of the drug; can deliver hydrophilic, hydrophobic, and amphiphilic drugs	(96)
Carbon nanotubes	Cylindrical nanoshape structures made of allotropes of carbon a) single-walled carbon nanotubes (SWCNTs), with one layer of graphene sheet and b) multiwalled carbon nanotubes (MWCNTs), with multiple layers of SWCNTs coaxially arranged	Multiple functions; high entrapment efficacy; monodispersity, feasibility of synthesis and sterilization; chemical modification; water-soluble, biocompatible; ability to incorporate any functional groups; active or passive targeting; showing prolonged distribution and localized effects	(97)
Solid lipid nanoparticles (NPs) (SLNs)	A surfactant layer on the surface with a lipid matrix consistent with solid lipid (s)	Biocompatible and biodegradable; non-toxic; high stability and feasibility of scale-up; high drug loading; reduced toxicity, enhanced bioavailability of poorly water-soluble and bioactive agents; targeting; capable of loading hydrophobic and hydrophilic drugs	(98)
Nanostructured lipid carriers (NLCs)	Second generation of SLNs; composed of a surfactant outer layer and solid lipid matrix along with a liquid lipid	Higher drug encapsulation and loading compared to SLNs	(103)
Nanoemulsions (NEs)	Droplets of water and oil dispersed biphasically and stabilized by an amphiphilic surfactant	Higher solubility than micellar dispersions; long-term physical stability; passive targeting with enhanced permeability and retention (EPR) effect; they can carry very hydrophobic drugs, improving their bioavailability	(104)
Gold-based NCs (AuNCs)	Different structures, including nanocubes, nanospheres, nanorods, nanoshells, nanobranches, nanocages, and nanowires	The most stable NPs; capable of active and passive targeting; can be PEGylated easily; scattering and light absorption characteristics when exposed to near-infrared wavelength (NIR) and heat production, which can ablate tumor cells	(105)
Protein nanocages	Shell-like containers, with intrinsic homogeneous chambers circumscribed by protein walls; have three distinct surfaces: exterior and interior surfaces, the interfaces between subunits	Smaller particles can deliver targeted therapy; monodisperse, biocompatible, water-soluble, biodegradable; selective for cancer cells; extremely homogenous size distribution; can be efficiently produced by genetic engineering	(106)
Aptamers	Single-strand oligonucleotides	Feasibility of synthesis and modification; showing low immunogenicity and efficient delivery to different types of cells; modification with siRNAs, miRNAs, and anti-miRNAs can serve for gene delivery	(107)

properties of each nano-drug delivery system in the breast cancer experimental models (94).

4.2 Nanoparticles

NPs are commonly described as particulate subjects at least smaller than 100 nm in one dimension (108). NPs are structurally different from each other and include liposomal NPs composed of phospholipids (109); polymeric NPs synthesized from natural products like gelatin, albumin, or artificial polymers (e.g., polylactides); poly alkyl cyanoacrylates; inorganic NPs involving silica NPs; quantum dots; and metal NPs. In addition, other properties such as size, shape, surface charge, and inflexibility are important when choosing NPs as treatment tools. These properties impact the NPs' cellular uptake through reticuloendothelial systems, targeting the right cells and tissue distribution (110). In the following, the physiochemical properties of NPs are explained in detail (109).

4.2.1 Size of NPs

The size of NPs is a significant factor in drug delivery and activation of the immune system and also modulates the pharmacokinetic actions of therapeutic agents, such as cell uptake, biodistribution, and body fluid half-life (111, 112). For example, gold-based NPs with a size of 10 nm have a longer blood circulation time and a reduced accumulation in the liver and spleen, compared to a size of 20 nm. Large NPs with a diameter between 100 and 200 nm are needed to deliver enough medication to disease sites (111). NPs from 30 to 50 nm exhibit efficient cellular absorption due to increased specific surface area and membrane encapsulation process. Phagocytic activity is considered to be the main pathway by which larger NPs from 250 to 3000 nm in size are internalized into the cells. Glomerular capillary walls have

physiological pores between 4.5 and 5 nm; therefore, NPs smaller than 6 nm are effectively filtered, while those larger than 8 nm cannot be eliminated by glomerular filtration (113).

The 100–200-nm NPs, including microparticles, are useful for drug loading, considering their high capacity. However, these large particles undergo active opsonization, readily trigger immune responses, and accumulate rapidly in the liver and spleen, thereby exhibiting poor systemic circulation (114). Small NPs lower than 5 nm should be considered not only because of their low carrying capacity but also because of their fast rate of renal clearance. However, many studies have found that small NPs are advantageous in several respects compared to their larger counterparts, including minimal immunogenicity, long systemic circulation, and easy entry and aggregation in the tumor, as well as independence for caveolin-dependent cell pathways uptake (114). Because of their excellent absorption efficiency and significant tumor accumulation, NPs with a size of 30–200 nm have been widely used in numerous investigations (113).

4.2.2 Shape of NPs

NPs can be used in a variety of nanomaterials, including liposomes, micelles, dendrimers, and metal NPs. The ability of NPs to interact with cell membranes depends on their shape. For instance, non-spherical NPs might yield multivalent interactions with cell surface receptors, whereas spherical ones only interact with a small number of binding site receptors (115).

4.2.3 Surface charge

The plasma membranes of the cells show a moderate negative voltage difference, varying from −90 to −20 mV from cell to cell. The pharmacokinetics and blood circulation time of NPs are influenced by the electrostatic interactions between NPs and the proteins (115). For instance, cationic polymeric NPs encapsulating tetrandrine had superior anticancer activity in A549 cells and a higher cellular absorption efficiency than anionic NPs (116).

4.2.4 Elasticity

It has been thoroughly investigated whether the elasticity of NPs plays a significant physicochemical role in determining their pharmacokinetics and biodistribution. According to certain studies, the flexibility of NPs affects how they interact with tissues and immune cells (117). Additionally, the rigidity or softness of NPs is an important factor in their distribution. The uptake of the stiffer NPs is shown to disrupt the architecture of the cell, while soft NPs can enter the cells through micropinocytosis easily (118). The absorption process is thought to have changed from fusion, which has a low energy dependence, to endocytosis, which has a high energy dependence due to the differential uptake of soft and stiff NPs by cells (117). Soft NPs have a longer half-life in the bloodstream due to the lower absorption by macrophage cells, which is also reliant on their elasticity (117). Commonly, a significant factor that affects the pharmacokinetic behavior of NP therapies is their elastic modulus. It has been demonstrated that elastic modulus optimization affects the interactions of NPs with different cells and their circulating half-life, tumor targeting, and aggregation effectiveness (119).

4.3 NPs and autophagy modulation

Considering the aforementioned data, autophagy modulation may be a promising treatment, alone or in a combination with other therapeutic methods to combat resistance and ensure a successful treatment of breast cancer. However, most current autophagy regulators suffer from low specificity, poor targeting, and bioavailability, as they are insufficiently solubilized in aqueous media and cannot specifically target tumor tissues (120). Leveraging nano-drug delivery systems reduces toxicity and increases drug efficacy through more appropriate targeting (121). The NPs being studied for drug delivery can be divided into different categories considering the type of therapy in which they are implemented. Three major therapeutic NPs are chemotherapeutic, phototherapeutic (including photodynamic therapy, and photothermal therapy), and immuno-therapeutic NPs, along with other categories such as sonodynamic therapeutic NPs. Each of the categories induces cytotoxicity *via* different intracellular mechanisms such as inhibition or induction of autophagy (72, 121, 122). NPs are divided into three categories: metal, organic polymer, and inorganic non-metallic NPs (115). The NP-based drug delivery into the cell is schematically illustrated in Figure 4 and is discussed in detail in the following section.

4.3.1 Silver-based NPs

Silver-based NPs (AgNPs) have been shown to induce autophagy in breast cancer cells, ultimately leading to apoptosis. One experiment that used the AgNPs embedded in specific polysaccharides showed good entrance to the cells, generation of ROS, and induction of endoplasmic reticulum stress, leading to cell death through autophagy or apoptosis (123). The effect of AgNPs on cytotoxicity in breast cancer cells also confirmed that regardless of the shape and structure of the AgNPs, they are cytotoxic for triple-negative breast cancer (TNBC) *in vitro* and xenograft model but have no effect on non-malignant cells. Hence, the application and development of AgNPs in breast cancer treatment should be safe (124).

4.3.2 Gold-based NPs

The effect of gold-based NP (AuNP) cytotoxicity on cells has a different intracellular mechanism. AuNPs enter the cells by endocytosis, accumulate in the lysosome, and change the pH value. Impaired lysosome function has implications for the autophagy pathway. Indeed, AuNPs induce the accumulation of autophagy in cells; however, the formation of autophagy flux is blocked due to an impairment of lysosome degradation (125). Another research showed that induction of apoptosis in AuNP-treated breast cancer cells occurred through p53 and bax/bcl-2 activation (126).

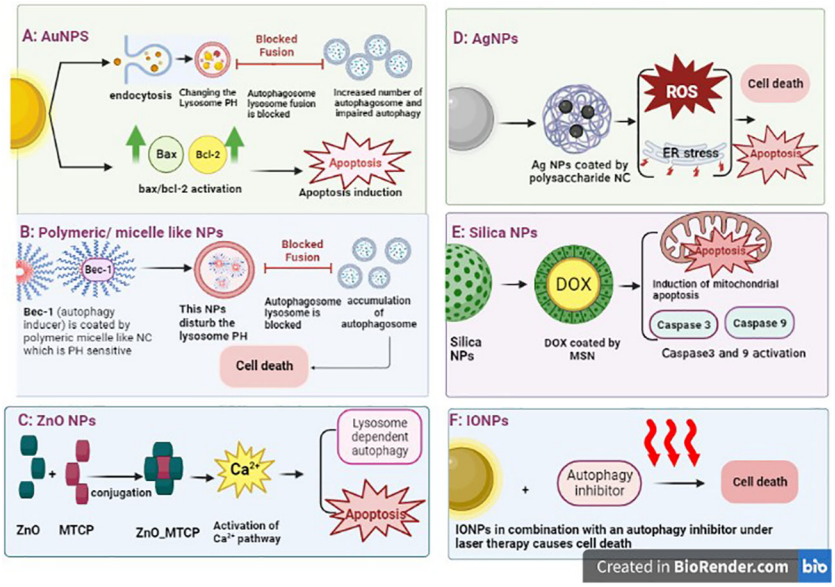

FIGURE 4
Different nanoparticle-mediated autophagy. **(A)** AuNP delivery system enters the cells, accumulates in the lysosome, and changes its pH. The impairment of lysosome function leads to accumulation of autophagosomes in cells without fusion with lysosomes. Then, apoptosis is induced. Another study has shown the effect of NPs on the Bax/Bcl2 activation that leads to apoptosis. **(B)** Polymeric/micelle-like NPs can encapsulate the autophagy inducer that disturbs the pH of lysosome leading to cell death. **(C)** ZnO can conjugate with drugs and impact calcium pathway, which ultimately leads to autophagy. **(D)** AgNPs induce autophagy through activation of Atg5 expression, which can result in cell death through autophagy or apoptosis induction. **(E)** Silica NPs can encapsulate chemotherapeutic drugs, such as doxorubicin, and induce intrinsic apoptosis through mitochondria. **(F)** The effect of photothermal therapy of IONPs in breast cancer cells has been observed through autophagy induction, independently of apoptosis. The use of autophagy inhibitors and IONPs under laser therapy causes cell death. AuNP, gold-based nanoparticles; AgNPs, silver-based nanoparticles; IONPs, iron oxide nanoparticles.

4.3.3 Zinc oxide NPs

The lethal toxicity of zinc oxide NPs (ZnO NPs) on cells could be modified by NP stabilization. An experiment with the conjugation of ZnNPs with porphyrin (MTCP) yielded a cytotoxic effect of NPs in breast cancer cell lines through the calcium signaling pathway, which regulates lysosomal-dependent autophagy and apoptotic cell death (127).

4.3.4 Iron oxide NPs

The effect of photothermal therapy of iron oxide NPs (IONPs) in breast cancer cells was observed by inducing autophagy but not leading to apoptosis. The use of autophagy inhibitors and IONPs under laser therapy causes cell death in both MCF-7 and xenograft breast cancer models (128).

4.3.5 Copper oxide NPs

The cytotoxicity of using copper oxide NPs (CuONPs) in MCF3 breast cancer cells was observed *via* oxidative stress and autophagy induction. In these cells, autophagy is activated in order to survive the tumor cells. Therefore, the cotreatment of autophagy inhibitors and CuONPs could be a potent treatment against breast cancer cells (129).

4.3.6 Silica-based NPs

The use of nano-drug delivery in cancer cells has been demonstrated to improve biodistribution and increase the sensitivity of the drugs. For instance, the use of DOX-loaded mesoporous silica nanoparticle (MSN) in breast cancer treatment has shown an increased level of apoptosis, in comparison with DOX treatment alone in both *in vitro* and *in vivo* experiments. The intracellular mechanisms also confirmed the induction of the pro-death autophagy signaling pathway through inhibition of the AKT-mTOR-p70S6K signaling pathway (130). Another study has shown the cytotoxic effects of silica-based NPs (SiNPs) in breast cancer cell lines through the mitochondrial apoptotic pathway. The NPs with 5–15 nm could induce caspase-9 and caspase-3 activities (131).

4.3.7 Polymeric NPs

Synthetic pH-sensitive polymeric NPs have been used to increase chemical stability and specific biodistribution. For instance, the Bec-1 peptide, as an autophagy inducer, was engineered into the pH-sensitive polymers and then self-assembled with polyethylene glycol to form micellar-like NPs. This structure of NPs alters the acidic status of lysosomes and prevents autophagosome–lysosome fusion. Accumulation of autophagosomes leads to cell death, not tumor survival (132). In Table 4, we have summarized several studies looking at the implementation of an autophagy modulator with a nano-drug delivery system, some of which were also combined with chemotherapeutic agents. In addition, it is shown that NCs are able to modulate autophagy, simultaneously targeting cancer cells and delivering therapeutic agents.

TABLE 4 The compounds with autophagy modulation properties in breast cancer.

Autophagy modulator	Combined chemo-therapeutic agent	Nano-delivery drug system	Details	References
Chloroquine (CQ) phosphate (inhibition)	Doxorubicin (DOX); docetaxel (DTXL)	Block copolymer PEG5K-*b*-PLA8K (PEG-PLA)	1. DOX or DTXL induce autophagy and lead to resistance in breast cancer stem cells (CSCs). Inhibition of autophagy promotes efficiency of chemotherapy 2. Cotreatment of CQ with wortmannin and 3-methyladenine (3-MA) showed enhanced effect 3. A nanoparticle delivery system increases drug accumulation in tumors and CSCs *in vitro* and *in vivo*	(133)
CQ		Gold-based NPs (AuNPs)	Drug release at acidic PH environment; autophagic death of MCF-7 cells	(134)
Hydroxychloroquine (HCQ) (inhibition)		CCM-HMTNPs	HMTNPs enable active targeting by being conjugated with cancer cell membrane (CCM) and are sensitive to ultrasound (sonodynamic therapy (SDT)); generate ROS when activated; HCQ blocks autophagy flux and eliminates resistance to SDT	(135)
SiRNAs (inhibition)	Paclitaxel	Polymeric micelles or NPs	SiRNAs target autophagic proteins and mRNAs	(136)
Bec1 (induction)		pH-sensitive poly(β-amino ester)s-PEG (micelle)	By covalently linking the nanocomposites with Beclin1, higher drug uptake efficiency and enhanced autophagy induction are achieved; P-Bec1 (polymer beclin1) displays enhanced cytotoxicity to breast cancer cells through induction of autophagy	(132)
Primaquine (PQ) (inhibition)		Nanocapsule HCG	HCP@PQ/ICG is a combination of PQ and ICG (a photothermal agent), which combats cytoprotective autophagy induced by phototherapy	(137)
Berberine (BB)		Au-Col	Au-Col consists of gold NPs fabricated with biocompatible collagen; Au-Col-BB shows enhanced cellular uptake and significant inhibition of cell migration, expression of apoptotic cascade proteins, and a remarkable decrease in tumor weight	(138)
Salinomycin (SAL) (induction)	DOX	Liposomes	SAL is an antibiotic with potency of autophagy and subsequent apoptosis induction; this combination is able to eliminate both CSCs and breast cancer, thus preventing recurrence of tumor and showing complete response	(139, 140)
Dihydroartemisinin (DHA) (induction)	Epirubicin	PEGylated liposomes	Increased anticancer effects in treatment of heterogeneous breast cancer	(141)
CQ	DOX	Liposomes	Higher efficacy with respect to liposomal DOX or free DOX	(142)
Thymoquinone (TQ) (induction or inhibition, according to cell type)	DTXL	Chitosan-grafted lipid nanocapsules; PEGylated liposomes	Implication in drug-resistant breast cancers, triple-negative breast cancers (TNBCs), and metastatic breast cancers; increased circulation time and enhanced cytotoxicity	(143)
CQ		PAMAM-DEACM	PAMAM is an NC with anticancer capability; it was modified with a photocleavable curamin (DEACM), loaded with CQ, and used to combat the cytoprotective autophagy induced by PAMAM	(144)
Ginsenosides (induction)		Polymeric NPs, liposomes, protein-based nanocarriers, etc.	Low bioavailability can be improved by NPs. It can be conjugated to liposomes to enhance stability and avoid adverse effects and can be used as a biological drug delivery system. View reference for detailed information	(145)
Rapamycin (Rap) (induction)	Epothilone B (EpoB)	Bioresorbable micelles functionalized with biotin (PLA-PEG-BIO)	Combination therapy with Rap with EpoB was very effective in reducing cell metabolic activity and survival. PLA–PEG-BIO enhanced the cytotoxic effects of these agents	(146)
TQ	DTXL	Borage oil-based nanoemulsion (B-NE)	Treatment with DTX, along with other therapeutic effects, promotes autophagic death in MCF-7. (DTX + TQ) B-NE can increase the autophagic cell death values significantly	(147)
Artemisinin (ART)	TF; paclitaxel; epirubicin; daunorubicin	Inorganic NPS; liposomes; micelles; polymer-based NPs; carbon-based NPs; niosomes	ART induces regulated cell death mechanisms, such as apoptosis, ferroptosis, autophagy, necroptosis, and pyroptosis. ART-related NC can resolve low solubility, low bioavailability, short plasma half-life, and chronic toxicity of ART. View reference for detailed information	(148)

(Continued)

TABLE 4 Continued

Autophagy modulator	Combined chemo-therapeutic agent	Nano-delivery drug system	Details	References
Bcl-2 and PKC-ι siRNAs (inhibition)		Aptamer-coupled QD-lipid nanocarriers (aptamo-QLs)	Simultaneous reduction of Bcl-2 and PKC-ι expression can synergistically inhibit TNBC cell proliferation and metastasis, and promote autophagic cell death	(107)
CQ		Triphenylphosphonim-functionalized dendrimer	A mitochondrial **tropictri** phenyl phosphonium-functionalized dendrimer manifested substantial cytotoxicity both alone and after encapsulation of chloroquine	(149)
CQ		Frizzled7 antibody-coated nanoshells (FZD7-NS)	Inhibition of Wnt signaling pathway with Frizzled7 antibody in TNBC can lead to upregulation of autophagy and cause therapeutic resistance. A combinational therapy of CQ with FZD7-NS led to inhibition of TNBC cell migration and self-renewal more effectively	(150)

5 The advantages and disadvantages of using nanomaterials in breast cancer treatment

NPs are an ideal drug delivery vehicle due to their nanosized structure, good biodistribution, and cost-saving properties (151), Furthermore, it is widely established that NCs aid in boosting the solubility, bioavailability, and stability of a variety of pharmacological drugs (152). Additionally, by improving cancer cell targeting, NPs could reduce the harmful effect of active cancer drugs. Finally, a safe and efficient agent for combination therapy involving autophagy regulation is one of the nano-drug delivery system advantages (153). Despite their small size, NPs can be easily and specifically delivered to the cells and absorbed by the tissue of interest. NPs may be used in conjugation with target drugs specific to cancer cells without disrupting normal cells' structure or function. They have specific qualities, including high encapsulation efficiency, biocompatibility, reduced toxicity, and ease of manufacture, making them useful for medications (153). Moreover, NP-based therapy is useful for personalized medicine and biomarker identification. NPs are easily engineered to be pH or temperature sensitive in different situations to transport and release the drug to their specific targets. Despite all these advantages of NPs, not all of them enter the clinical phase because there are some problems like biological and technological difficulties in manufacturing NPs (154). The biological issues, including the route of administration (e.g., oral, intravenous, or skin injected), biological barriers, the toxicity of NPs, and their degradation are essential factors in NP efficacy. To overcome these challenges, some modifications are necessary to improve the NP application. For example, the use of low concentrations, which may decrease the toxicity effects, or the production of NPs with more biocompatible materials, such as chitosan, are beneficial (155). Technological challenges including the scale-up synthesis of NPs and *in vitro* or *in vivo* experimental models are not enough to directly use NPs in the clinical study due to little supporting data. In this way, using computational models or organs-on-chip can be a good solution alongside the laboratory results (154).

6 The future of NPs in breast cancer

NPs have a high potential to be used in the future treatments of breast cancer. They overcome the challenges of current treatments and combat drug resistance. They help increase the sensitivity of drugs (65, 156). In addition to therapy, nanomedicine may assist patients in some other aspects, such as diagnostics in the early stages and tumor imaging. Nanotechnology offers potential solutions to the problems that have made breast cancer so challenging to treat. These problems include the diversity of cancer and the rapid evolutionary changes in patients, the multiple pathways driving disease progression simultaneously, the emergence of tolerance, creating therapeutic cocktails, distant breast cancer metastasis, and the severity of side effects of therapies and very poor biodistribution of the injected medications in the body (72, 157). However, nanomedicine has some important challenges and controversies that should be resolved. The major issue is the toxicity of nanomaterials. For instance, ROS production leads to DNA damage and protein denaturation. By standard protocols, deep toxicological studies prior to the application of NPs for human therapy are suggested.

Among many nanomaterials in biomedicine, only a few of them have reached clinical trials and obtained FDA approval. The process by which a new drug passes all the preclinical phases and clinical trials to obtain the license for use in humans is estimated to be approximately 10–15 years (158). The preclinical phases are usually cellular testing, animal studies, toxicology control, safety, efficacy, and dose ranges of the new drugs (159). The clinical trials involve three phases, named I (testing dose and toxicity), II (safety and testing in a larger group), and III (randomized multicenter testing), that should be passed before introducing the new drugs to the market (158). Nanomedicine needs phase IV of post-marketing to consider the limitation or benefits of the application. In this regard, many studies are under investigation to obtain a license in order to enter clinical trials (160). According to clinical trials (www.ClinicalTrials.gov), there are currently 39 studies available that use different shapes and structures of NPs in breast cancer treatment, confirming the importance of using NPs in cancer treatment. Here, we summarize the 10 top studies in Table 5.

TABLE 5 Clinical trial of nanoparticles (NP)-based treatment strategies in breast cancer (https://clinicaltrials.gov)

Number	Nanoparticle	Status	Conditions
1	Albumin-Bound (Nab) Paclitaxel/Cyclophosphamide	Completed, Phase II	Early stage of breast cancer
2	Nanoparticle-based Paclitaxel vs Solvent-based Paclitaxel as Part of Neoadjuvant Chemotherapy	Completed, phase III	➢Tubular Breast Cancer Stage II ➢Mucinous Breast Cancer Stage II ➢Breast Cancer Female NOS
3	Carbon NPs	Recruiting, phase not applicable	Lymph Nodes positive patients
4	Paclitaxel Albumin-Stabilized Nanoparticle	Completed, phase II	Metastatic breast cancer patients
5	Carboplatin, Paclitaxel, and Bevacizumab	Completed, phase II	Locally Recurrent or Metastatic Breast Cancer
6	Pertuzumab, Trastuzumab, and Paclitaxel Albumin-Stabilized Nanoparticle	Active but not recruiting, phase II	Patients With HER2-Positive Advanced Breast Cancer
7	Carboplatin and Paclitaxel Albumin-Stabilized Nanoparticle	Active but not recruiting, phase II	➢Inflammatory triple negative breast cancer ➢Stage IIA Breast Cancer ➢Stage IIIA Breast Cancer
8	Doxorubicin Hydrochloride, Cyclophosphamide, and Filgrastim Followed By Paclitaxel Albumin-Stabilized Nanoparticle Formulation With or Without Trastuzumab	Completed, phase II	➢Estrogen Receptor-positive Breast Cancer ➢HER2-positive Breast Cancer ➢Stage IA Breast Cancer
9	Nanoparticle Albumin Bound Paclitaxel, Doxorubicin and Cyclophosphamide (NAC)	Terminated, phase I	Stages II-III Breast Cancer (NAC)
10	Paclitaxel Albumin-Stabilized Nanoparticle Formulation	Active not recruiting, phase II	Treating Patients of Different Ages With Metastatic Breast Cancer

7 Conclusion

NPs are an ideal drug delivery vehicle due to their nanosized structure, good biodistribution, and cost-saving properties. Additionally, by improving cancer cell targeting, NPs could reduce the harmful effect of active cancer drugs. It is challenging to modulate autophagy in breast cancer treatment utilizing NPs due to the different behaviors of autophagy in tumorigenicity. To deal with this problem, a large number of studies are recommended. The different effects of NPs on autophagy, induction, or inhibition, in different situations, lead to antitumor activity or an increase in cell death. In practice, the choice between inhibition and promotion of autophagy is controversial, as it may depend on the role of autophagy in tumor development. As long as autophagy exerts a positive effect on the treatment of certain cancers, strategies that promote autophagy remain desirable. However, when autophagy adversely affects cancer treatment, inhibition of autophagy is the appropriate strategy. Depending on the type of cancer, therapy should involve an appropriate treatment in combination with autophagy modulation. However, NPs have some disadvantages and cannot be used directly in clinical trials. To improve their lethal properties in cancerous cells, more modifications on NPs are needed, or cotreatment with targeted drugs is proposed. Despite some difficulties in the usage of NPs in medicine, their future application is promising and could be a new path for cancer treatment.

Author contributions

AG has contributed as co-author for sections on breast cancer and autophagy mechanisms. She also designs the figures of the manuscript. DS has written the section on nanocarriers. AY has contributed and written the nanoparticles sections. FB has written the autophagy section and prepared the abbreviation section. MR has been invited by the editorial board of the Frontiers in Oncology, proposed the topic, and is a corresponding author of the manuscript. All authors contributed to the article and approved the submitted version.

Conflict of interest

The authors declare that the research was conducted in the absence of any commercial or financial relationships that could be construed as a potential conflict of interest.

Publisher's note

References

1. Wilkinson L, Gathani T. Understanding breast cancer as a global health concern. *Br J Radiol* (2022) 95:20211033. doi: 10.1259/bjr.20211033

2. Bray F, Jemal A, Grey N, Ferlay J, Forman D. Global cancer transitions according to the human development index (2008-2030): a population-based study. *Lancet Oncol* (2012) 13:790–801. doi: 10.1016/S1470-2045(12)70211-5

3. Niklaus NJ, Tokarchuk I, Zbinden M, Schläfli AM, Maycotte P, Tschan MP. The multifaceted functions of autophagy in breast cancer development and treatment. *Cells* (2021) 10(6):1447. doi: 10.3390/cells10061447

4. Gyanani V, Haley JC, Goswami R. Challenges of current anticancer treatment approaches with focus on liposomal drug delivery systems. *Pharmaceuticals* (2021) 14:835. doi: 10.3390/ph14090835

5. Marsh T, Debnath J. Autophagy suppresses breast cancer metastasis by degrading NBR1. *Autophagy* (2020) 16:1164–5. doi: 10.1080/15548627.2020.1753001

6. Dyczynski M, Yu Y, Otrocka M, Parpal S, Braga T, Henley AB, et al. Targeting autophagy by small molecule inhibitors of vacuolar protein sorting 34 (Vps34) improves the sensitivity of breast cancer cells to sunitinib. *Cancer Lett* (2018) 435:32–43. doi: 10.1016/j.canlet.2018.07.028

7. Shi J, Kantoff PW, Wooster R, Farokhzad OC. Cancer nanomedicine: progress, challenges and opportunities. *Nat Rev Cancer* (2017) 17:20–37. doi: 10.1038/nrc.2016.108

8. Cariolou M, Abar L, Aune D, Balducci K, Becerra-Tomás N, Greenwood DC, et al. Postdiagnosis recreational physical activity and breast cancer prognosis: global cancer update programme (CUP global) systematic literature review and meta-analysis. *Int J Cancer* (2023) 152:600–15. doi: 10.1002/ijc.34324

9. Arnold M, Morgan E, Rumgay H, Mafra A, Singh D, Laversanne M, et al. Current and future burden of breast cancer: global statistics for 2020 and 2040. *Breast* (2022) 66:15–23. doi: 10.1016/j.breast.2022.08.010

10. Zendehdel K. Cancer statistics in I.R. Iran in 2020. *Basic Clin Cancer Res* (2021) 12(4):159–65. doi: 10.18502/bccr.v12i4.7985

11. Macmahon B, Cole P, Brown J. Etiology of human breast cancer: a review. *JNCI J Natl Cancer Inst* (1973) 50:21–42. doi: 10.1093/jnci/50.1.21

12. Key T, Appleby P, Barnes I, Reeves GEndogenous Hormones and Breast Cancer Collaborative Group. Endogenous sex hormones and breast cancer in postmenopausal women: reanalysis of nine prospective studies. *J Natl Cancer Inst* (2002) 94:606–16. doi: 10.1093/jnci/94.8.606

13. Shamshirian A, Heydari K, Shams Z, Aref AR, Shamshirian D, Tamtaji OR, et al. Breast cancer risk factors in Iran: a systematic review & meta-analysis. *Horm Mol Biol Clin Investig* (2020) 41(4). doi: 10.1515/hmbci-2020-0021

14. Amin MB, Greene FL, Edge SB, Compton CC, Gershenwald JE, Brookland RK, et al. The eighth edition AJCC cancer staging manual: continuing to build a bridge from a population-based to a more "personalized" approach to cancer staging. *CA Cancer J Clin* (2017) 67(2):93–9. doi: 10.3322/caac.21388

15. Amin M. American Joint committee on cancer and American cancer society AJCC cancer staging manual. 8th Ed. *Am Jt. Commun Cancer* (2017)

16. Hortobagyi GN, Edge SB, Giuliano A. New and important changes in the TNM staging system for breast cancer. *Am Soc Clin Oncol Educ book Am Soc Clin Oncol Annu Meet* (2018) 38:457–67. doi: 10.1200/EDBK_201313

17. Giuliano AE, Connolly JL, Edge SB, Mittendorf EA, Rugo HS, Solin LJ, et al. Breast cancer-major changes in the American joint committee on cancer eighth edition cancer staging manual. *CA Cancer J Clin* (2017) 67:290–303. doi: 10.3322/caac.21393

18. Early Breast Cancer Trialists' Collaborative Group (EBCTCG). Effects of chemotherapy and hormonal therapy for early breast cancer on recurrence and 15-year survival: an overview of the randomised trials. *Lancet (London England)* (2005) 365:1687–717. doi: 10.1016/S0140-6736(05)66544-0

19. Bernardo G, Palumbo R, Bernardo A, Villani G, Melazzini M, Poggi G, et al. Final results of a phase II study of weekly trastuzumab and vinorelbine in chemonaive patients with HER2-overexpressing metastatic breast cance. *J Clin Oncol* (2004) 22:731–1. doi: 10.1200/jco.2004.22.90140.731

20. Donepudi MS, Kondapalli K, Amos SJ, Venkanteshan P. Breast cancer statistics and markers. *J Cancer Res Ther* (2014) 10:506–11. doi: 10.4103/0973-1482.137927

21. Cufer T, Lamovec J, Bracko M, Lindtner J, Us-Krasovec M. Prognostic value of DNA ploidy in breast cancer stage I-II. *Neoplasma* (1997) 44:127–32.

22. Tong Y-K, Lo YMD. Diagnostic developments involving cell-free (circulating) nucleic acids. *Clin Chim Acta* (2006) 363:187–96. doi: 10.1016/j.cccn.2005.05.048

23. Duffy MJ. Serum tumor markers in breast cancer: are they of clinical value? *Clin Chem* (2006) 52:345–51. doi: 10.1373/clinchem.2005.059832

24. Look MP, van Putten WLJ, Duffy MJ, Harbeck N, Christensen IJ, Thomssen C, et al. Pooled analysis of prognostic impact of urokinase-type plasminogen activator and its inhibitor PAI-1 in 8377 breast cancer patients. *J Natl Cancer Inst* (2002) 94:116–28. doi: 10.1093/jnci/94.2.116

25. Fentiman IS. Breast cancer treatment. *Br J Nurs* (1995) 4:431–9. doi: 10.12968/bjon.1995.4.8.431

26. Yin L, Duan J-J, Bian X-W, Yu S-C. Triple-negative breast cancer molecular subtyping and treatment progress. *Breast Cancer Res* (2020) 22:61. doi: 10.1186/s13058-020-01296-5

27. Pasha N, Turner NC. Understanding and overcoming tumor heterogeneity in metastatic breast cancer treatment. *Nat Cancer* (2021) 2:680–92. doi: 10.1038/s43018-021-00229-1

28. Cortes-Ciriano I, Lee S, Park W-Y, Kim T-M, Park PJ. A molecular portrait of microsatellite instability across multiple cancers. *Nat Commun* (2017) 8:15180. doi: 10.1038/ncomms15180

29. Gote V, Nookala AR, Bolla PK, Pal D. Drug resistance in metastatic breast cancer: tumor targeted nanomedicine to the rescue. *Int J Mol Sci* (2021) 22:4673. doi: 10.3390/ijms22094673

30. Du B, Shim J. Targeting epithelial–mesenchymal transition (EMT) to overcome drug resistance in cancer. *Molecules* (2016) 21:965. doi: 10.3390/molecules21070965

31. Zeng X, Liu C, Yao J, Wan H, Wan G, Li Y, et al. Breast cancer stem cells, heterogeneity, targeting therapies and therapeutic implications. *Pharmacol Res* (2021) 163:105320. doi: 10.1016/j.phrs.2020.105320

32. Genovese I, Vezzani B, Danese A, Modesti L, Vitto VAM, Corazzi V, et al. Mitochondria as the decision makers for cancer cell fate: from signaling pathways to therapeutic strategies. *Cell Calcium* (2020) 92:102308. doi: 10.1016/j.ceca.2020.102308

33. East DA, Campanella M. Ca 2+ in quality control. *Autophagy* (2013) 9:1710–9. doi: 10.4161/auto.25367

34. Yan C, Li TS. Dual role of mitophagy in cancer drug resistance. *Anticancer Res* (2018) 38(2):617–21. doi: 10.21873/anticanres.12266

35. Lin P-W, Chu M-L, Liu H-S. Autophagy and metabolism. *Kaohsiung J Med Sci* (2021) 37:12–9. doi: 10.1002/kjm2.12299

36. Huang F, Wang B-R, Wang Y-G. Role of autophagy in tumorigenesis, metastasis, targeted therapy and drug resistance of hepatocellular carcinoma. *World J Gastroenterol* (2018) 24:4643–51. doi: 10.3748/wjg.v24.i41.4643

37. Li X, He S, Ma B. Autophagy and autophagy-related proteins in cancer. *Mol Cancer* (2020) 19:12. doi: 10.1186/s12943-020-1138-4

38. Galluzzi L, Bravo-San Pedro JM, Levine B, Green DR, Kroemer G. Pharmacological modulation of autophagy: therapeutic potential and persisting obstacles. *Nat Rev Drug Discov* (2017) 16:487–511. doi: 10.1038/nrd.2017.22

39. Cuervo AM, Wong E. Chaperone-mediated autophagy: roles in disease and aging. *Cell Res* (2014) 24:92–104. doi: 10.1038/cr.2013.153

40. Feng Y, He D, Yao Z, Klionsky DJ. The machinery of macroautophagy. *Cell Res* (2014) 24:24–41. doi: 10.1038/cr.2013.168

41. Dooley HC, Razi M, Polson HEJ, Girardin SE, Wilson MI, Tooze SA. WIPI2 links LC3 conjugation with PI3P, autophagosome formation, and pathogen clearance by recruiting Atg12-5-16L1. *Mol Cell* (2014) 55:238–52. doi: 10.1016/j.molcel.2014.05.021

42. He C, Klionsky DJ. Regulation mechanisms and signaling pathways of autophagy. *Annu Rev Genet* (2009) 43:67–93. doi: 10.1146/annurev-genet-102808-114910

43. Kim J, Kundu M, Viollet B, Guan K-L. AMPK and mTOR regulate autophagy through direct phosphorylation of Ulk1. *Nat Cell Biol* (2011) 13:132–41. doi: 10.1038/ncb2152

44. Tamboli IY, Tien NT, Walter J. Sphingolipid storage impairs autophagic clearance of Alzheimer-associated proteins. *Autophagy* (2011) 7:645–6. doi: 10.4161/auto.7.6.15122

45. Parzych KR, Klionsky DJ. An overview of autophagy: morphology, mechanism, and regulation. *Antioxidants Redox Signal* (2014) 20:460–73. doi: 10.1089/ars.2013.5371

46. Young ARJ, Chan EYW, Hu XW, Köchl R, SG C, High S, et al. Starvation and ULK1-dependent cycling of mammalian Atg9 between the TGN and endosomes. *J Cell Sci* (2006) 119:3888–900. doi: 10.1242/jcs.03172

47. Ganley IG. Autophagosome maturation and lysosomal fusion. *Essays Biochem* (2013) 55:65–78. doi: 10.1042/bse0550065

48. Nakamura S, Yoshimori T. New insights into autophagosome–lysosome fusion. *J Cell Sci* (2017) 130(7):1209–16. doi: 10.1242/jcs.196352

49. Monastyrska I, Rieter E, Klionsky DJ, Reggiori F. Multiple roles of the cytoskeleton in autophagy. *Biol Rev* (2009) 84:431–48. doi: 10.1111/j.1469-185X.2009.00082.x

50. Jäger S, Bucci C, Tanida I, Ueno T, Kominami E, Saftig P, et al. Role for Rab7 in maturation of late autophagic vacuoles. *J Cell Sci* (2004) 117:4837–48. doi: 10.1242/jcs.01370

51. Itakura E, Kishi-Itakura C, Mizushima N. The hairpin-type tail-anchored SNARE syntaxin 17 targets to autophagosomes for fusion with Endosomes/Lysosomes. *Cell* (2012) 151:1256–69. doi: 10.1016/j.cell.2012.11.001

52. Bjørkøy G, Lamark T, Brech A, Outzen H, Perander M, Øvervatn A, et al. p62/SQSTM1 forms protein aggregates degraded by autophagy and has a protective effect on huntingtin-induced cell death. *J Cell Biol* (2005) 171:603–14. doi: 10.1083/jcb.200507002

53. Yorimitsu T, Klionsky DJ. Autophagy: molecular machinery for self-eating. *Cell Death Differ* (2005) 12:1542–52. doi: 10.1038/sj.cdd.4401765

54. Gordon PB, Seglen PO. Prelysosomal convergence of autophagic and endocytic pathways. *Biochem Biophys Res Commun* (1988) 151:40–7. doi: 10.1016/0006-291X(88)90556-6

55. Liu B, Wen X, Cheng Y. Survival or death: disequilibrating the oncogenic and tumor suppressive autophagy in cancer. *Cell Death Dis* (2013) 4:e892. doi: 10.1038/cddis.2013.422

56. Pan H, Chen L, Xu Y, Han W, Lou F, Fei W, et al. Autophagy-associated immune responses and cancer immunotherapy. *Oncotarget* (2016) 7:21235–46. doi: 10.18632/oncotarget.6908

57. Deretic V, Levine B. Autophagy balances inflammation in innate immunity. *Autophagy* (2018) 14:243–51. doi: 10.1080/15548627.2017.1402992

58. Vera-Ramirez L, Vodnala SK, Nini R, Hunter KW, Green JE. Autophagy promotes the survival of dormant breast cancer cells and metastatic tumour recurrence. *Nat Commun* (2018) 9:1944. doi: 10.1038/s41467-018-04070-6

59. Qu X, Yu J, Bhagat G, Furuya N, Hibshoosh H, Troxel A, et al. Promotion of tumorigenesis by heterozygous disruption of the beclin 1 autophagy gene. *J Clin Invest* (2003) 112:1809–20. doi: 10.1172/JCI20039

60. Cicchini M, Chakrabarti R, Kongara S, Price S, Nahar R, Lozy F, et al. Autophagy regulator BECN1 suppresses mammary tumorigenesis driven by WNT1 activation and following parity. *Autophagy* (2014) 10:2036–52. doi: 10.4161/auto.34398

61. Delaney JR, Patel CB, Bapat J, Jones CM, Ramos-Zapatero M, Ortell KK, et al. Autophagy gene haploinsufficiency drives chromosome instability, increases migration, and promotes early ovarian tumors. *PloS Genet* (2020) 16:e1008558. doi: 10.1371/journal.pgen.1008558

62. Liang XH, Jackson S, Seaman M, Brown K, Kempkes B, Hibshoosh H, et al. Induction of autophagy and inhibition of tumorigenesis by beclin 1. *Nature* (1999) 402:672–6. doi: 10.1038/45257

63. Kharaziha P, Panaretakis T. Dynamics of Atg5-Atg12-Atg16L1 aggregation and deaggregation. *Methods Enzymol* (2017) 587:247–55. doi: 10.1016/bs.mie.2016.09.059

64. Tanida I. Autophagosome formation and molecular mechanism of autophagy. *Antioxid Redox Signal* (2011) 14:2201–14. doi: 10.1089/ars.2010.3482

65. Adibzadeh R, Golhin MS, Sari S, Mohammadpour H, Kheirbakhsh R, Muhammadnejad A, et al. Combination therapy with TiO2 nanoparticles and cisplatin enhances chemotherapy response in murine melanoma models. *Clin Transl Oncol* (2021) 23:738–49. doi: 10.1007/s12094-020-02463-y

66. Yoon J-H, Ahn S-G, Lee B-H, Jung S-H, Oh S-H. Role of autophagy in chemoresistance: regulation of the ATM-mediated DNA-damage signaling pathway through activation of DNA–PKcs and PARP-1. *Biochem Pharmacol* (2012) 83:747–57. doi: 10.1016/j.bcp.2011.12.029

67. Zhang L, Yang A, Wang M, Liu W, Wang C, Xie X, et al. Enhanced autophagy reveals vulnerability of p-gp mediated epirubicin resistance in triple negative breast cancer cells. *Apoptosis* (2016) 21:473–88. doi: 10.1007/s10495-016-1214-9

68. Chang H, Zou Z. Targeting autophagy to overcome drug resistance: further developments. *J Hematol Oncol* (2020) 13:159. doi: 10.1186/s13045-020-01000-2

69. Chang Z, Shi G, Jin J, Guo H, Guo X, Luo F, et al. Dual PI3K/mTOR inhibitor NVP-BEZ235-induced apoptosis of hepatocellular carcinoma cell lines is enhanced by inhibitors of autophagy. *Int J Mol Med* (2013) 31:1449–56. doi: 10.3892/ijmm.2013.1351

70. Singh SS, Vats S, Chia AY, Tan TZ, Deng S, Ong MS, et al. Dual role of autophagy in hallmarks of cancer. *Oncogene* (2018) 37:1142–58. doi: 10.1038/s41388-017-0046-6

71. Jain K, Paranandi KS, Sridharan S, Basu A. Autophagy in breast cancer and its implications for therapy. *Am J Cancer Res* (2013) 3(3):251–65.

72. Cordani M, Somoza Á. Targeting autophagy using metallic nanoparticles: a promising strategy for cancer treatment. *Cell Mol Life Sci* (2019) 76:1215–42. doi: 10.1007/s00018-018-2973-y

73. Levy JMM, Towers CG, Thorburn A. Targeting autophagy in cancer. *Nat Rev Cancer* (2017) 17:528–42. doi: 10.1038/nrc.2017.53

74. Fauzi YR, Nakahata S, Chilmi S, Ichikawa T, Nueangphuet P, Yamaguchi R, et al. Antitumor effects of chloroquine/hydroxychloroquine mediated by inhibition of the NF-κB signaling pathway through abrogation of autophagic p47 degradation in adult T-cell leukemia/lymphoma cells. *PloS One* (2021) 16:e0256320. doi: 10.1371/journal.pone.0256320

75. Feng J, Wang X, Ye X, Ares I, Lopez-Torres B, Martínez M, et al. Mitochondria as an important target of metformin: the mechanism of action, toxic and side effects, and new therapeutic applications. *Pharmacol Res* (2022) 177:106114. doi: 10.1016/j.phrs.2022.106114

76. Aydinlik S, Erkisa M, Cevatemre B, Sarimahmut M, Dere E, Ari F, et al. Enhanced cytotoxic activity of doxorubicin through the inhibition of autophagy in triple negative breast cancer cell line. *Biochim Biophys Acta - Gen Subj* (2017) 1861:49–57. doi: 10.1016/j.bbagen.2016.11.013

77. Guo B, Tam A, Santi SA, Parissenti AM. Role of autophagy and lysosomal drug sequestration in acquired resistance to doxorubicin in MCF-7 cells. *BMC Cancer* (2016) 16:762. doi: 10.1186/s12885-016-2790-3

78. Saha T. LAMP2A overexpression in breast tumors promotes cancer cell survival *via* chaperone-mediated autophagy. *Autophagy* (2012) 8:1643–56. doi: 10.4161/auto.21654

79. Kang J-H, Yu B-Y, Youn D-S. Relationship of serum adiponectin and resistin levels with breast cancer risk. *J Korean Med Sci* (2007) 22:117. doi: 10.3346/jkms.2007.22.1.117

80. Kim TH, Kim HS, Kang YJ, Yoon S, Lee J, Choi WS, et al. Psammaplin a induces sirtuin 1-dependent autophagic cell death in doxorubicin-resistant MCF-7/adr human breast cancer cells and xenografts. *Biochim Biophys Acta* (2015) 1850:401–10. doi: 10.1016/j.bbagen.2014.11.007

81. Qadir MA, Kwok B, Dragowska WH, To KH, Le D, Bally MB, et al. Macroautophagy inhibition sensitizes tamoxifen-resistant breast cancer cells and enhances mitochondrial depolarization. *Breast Cancer Res Treat* (2008) 112:389–403. doi: 10.1007/s10549-007-9873-4

82. Liu Z, He K, Ma Q, Yu Q, Liu C, Ndege I, et al. Autophagy inhibitor facilitates gefitinib sensitivity *in vitro* and *in vivo* by activating mitochondrial apoptosis in triple negative breast cancer. *PloS One* (2017) 12:e0177694. doi: 10.1371/journal.pone.0177694

83. Liu PF, Tsai KL, Hsu CJ, Tsai WL, Cheng JS, Chang HW, et al. Drug repurposing screening identifies tioconazole as an ATG4 inhibitor that suppresses autophagy and sensitizes cancer cells to chemotherapy. *Theranostics* (2018) 8:830–45. doi: 10.7150/thno.22012

84. Sheng Y, Sun B, Guo W-T, Zhang Y-H, Liu X, Xing Y, et al. 3-methyladenine induces cell death and its interaction with chemotherapeutic drugs is independent of autophagy. *Biochem Biophys Res Commun* (2013) 432:5–9. doi: 10.1016/j.bbrc.2013.01.106

85. Pasquier B, El-Ahmad Y, Filoche-Rommé B, Dureuil C, Fassy F, Abecassis PY, et al. Discovery of (2S)-8-[(3R)-3-methylmorpholin-4-yl]-1-(3-methyl-2-oxobutyl)-2-(trifluoromethyl)-3,4-dihydro-2H-pyrimido[1,2-a]pyrimidin-6-one: a novel potent and selective inhibitor of Vps34 for the treatment of solid tumors. *J Med Chem* (2015) 58:376–400. doi: 10.1021/jm5013352

86. Sharma N, Thomas S, Golden EB, Hofman FM, Chen TC, Petasis NA, et al. Inhibition of autophagy and induction of breast cancer cell death by mefloquine, an antimalarial agent. *Cancer Lett* (2012) 326:143–54. doi: 10.1016/j.canlet.2012.07.029

87. Guntuku L, Gangasani JK, Thummuri D, Borkar RM, Manavathi B, Ragampeta S, et al. IITZ-01, a novel potent lysosomotropic autophagy inhibitor, has single-agent antitumor efficacy in triple-negative breast cancer *in vitro* and *in vivo*. *Oncogene* (2019) 38:581–95. doi: 10.1038/s41388-018-0446-2

88. Yang W, Hosford SR, Traphagen NA, Shee K, Demidenko E, Liu S, et al. Autophagy promotes escape from phosphatidylinositol 3-kinase inhibition in estrogen receptor-positive breast cancer. *FASEB J* (2018) 32:1222–35. doi: 10.1096/fj.201700477R

89. Pelt J, Busatto S, Ferrari M, Thompson EA, Mody K, Wolfram J. Chloroquine and nanoparticle drug delivery: a promising combination. *Pharmacol Ther* (2018) 191:43–9. doi: 10.1016/j.pharmthera.2018.06.007

90. Raj R, Mongia P, Kumar Sahu S, Ram A. Nanocarriers based anticancer drugs: current scenario and future perceptions. *Curr Drug Targets* (2016) 17:206–28. doi: 10.2174/1389450116666150722141607

91. Nogueira E, Gomes AC, Preto A, Cavaco-Paulo A. Design of liposomal formulations for cell targeting. *Colloids Surf B Biointerfaces* (2015) 136:514–26. doi: 10.1016/j.colsurfb.2015.09.034

92. Kirpotin DB, Drummond DC, Shao Y, Shalaby MR, Hong K, Nielsen UB, et al. Antibody targeting of long-circulating lipidic nanoparticles does not increase tumor localization but does increase internalization in animal models. *Cancer Res* (2006) 66:6732–40. doi: 10.1158/0008-5472.CAN-05-4199

93. Tanaka T, Decuzzi P, Cristofanilli M, Sakamoto JH, Tasciotti E, Robertson FM, et al. Nanotechnology for breast cancer therapy. *BioMed Microdevices* (2009) 11:49–63. doi: 10.1007/s10544-008-9209-0

94. Kumar L, Baldi A, Verma S, Utreja P. Exploring therapeutic potential of nanocarrier systems against breast cancer. *Pharm Nanotechnol* (2018) 6:94–110. doi: 10.2174/2211738506666180604101920

95. Jain NK, Gupta U. Application of dendrimer-drug complexation in the enhancement of drug solubility and bioavailability. *Expert Opin Drug Metab Toxicol* (2008) 4:1035–52. doi: 10.1517/17425255.4.8.1035

96. Condello M, Mancini G, Meschini S. The exploitation of liposomes in the inhibition of autophagy to defeat drug resistance. *Front Pharmacol* (2020) 66(13):6732–40. doi: 10.3389/fphar.2020.00787

97. Sahoo NG, Bao H, Pan Y, Pal M, Kakran M, Cheng HKF, et al. Functionalized carbon nanomaterials as nanocarriers for loading and delivery of a poorly water-soluble anticancer drug: a comparative study. *Chem Commun (Camb)* (2011) 47:5235–7. doi: 10.1039/c1cc00075f

98. Müller RH, Mäder K, Gohla S. Solid lipid nanoparticles (SLN) for controlled drug delivery - a review of the state of the art. *Eur J Pharm Biopharm* (2000) 50:161–77. doi: 10.1016/S0939-6411(00)00087-4

99. Calne RY, Lim S, Samaan A, Collier DSJ, Pollard SG, White DJG, et al. Rapamycin for immunosuppression in organ allografting. *Lancet* (1989) 334:227. doi: 10.1016/S0140-6736(89)90417-0

100. Wang S, Sun, Zhu, Du, Liu, Qian W-Y. pH-sensitive strontium carbonate nanoparticles as new anticancer vehicles for controlled etoposide release. *Int J Nanomedicine* (2012) 7:5781. doi: 10.2147/IJN.S34773

101. Dewaele M, Maes H, Agostinis P. ROS-mediated mechanisms of autophagy stimulation and their relevance in cancer therapy. *Autophagy* (2010) 6:838–54. doi: 10.4161/auto.6.7.12113

102. Moghimi SM, Hunter AC. Poloxamers and poloxamines in nanoparticle engineering and experimental medicine. *Trends Biotechnol* (2000) 18:412–20. doi: 10.1016/S0167-7799(00)01485-2

103. Zhang X-G, Miao J, Dai Y-Q, Du Y-Z, Yuan H, Hu F-Q. Reversal activity of nanostructured lipid carriers loading cytotoxic drug in multi-drug resistant cancer cells. *Int J Pharm* (2008) 361:239–44. doi: 10.1016/j.ijpharm.2008.06.002

104. Singh Y, Meher JG, Raval K, Khan FA, Chaurasia M, Jain NK, et al. Nanoemulsion: concepts, development and applications in drug delivery. *J Control Release* (2017) 252:28–49. doi: 10.1016/j.jconrel.2017.03.008

105. Huang X, Jain PK, El-Sayed IH, El-Sayed MA. Gold nanoparticles: interesting optical properties and recent applications in cancer diagnostics and therapy. *Nanomedicine (Lond)* (2007) 2:681–93. doi: 10.2217/17435889.2.5.681

106. Chen H, Tan X, Fu Y, Dai H, Wang H, Zhao G, et al. The development of natural and designed protein nanocages for encapsulation and delivery of active compounds. *Food Hydrocoll* (2021) 121:107004. doi: 10.1016/j.foodhyd.2021.107004

107. Kim MW, Jeong HY, Kang SJ, Jeong IH, Choi MJ, You YM, et al. Anti-EGF receptor aptamer-guided Co-delivery of anti-cancer siRNAs and quantum dots for theranostics of triple-negative breast cancer. *Theranostics* (2019) 9:837–52. doi: 10.7150/thno.30228

108. Khan I, Saeed K, Khan I. Nanoparticles: properties, applications and toxicities. *Arab J Chem* (2019) 12:908–31. doi: 10.1016/j.arabjc.2017.05.011

109. Han S-M, Na Y-G, Lee H-S, Son G-H, Jeon S-H, Bang K-H, et al. Improvement of cellular uptake of hydrophilic molecule, calcein, formulated by liposome. *J Pharm Investig* (2018) 48:595–601. doi: 10.1007/s40005-017-0358-0

110. Jo DH, Kim JH, Lee TG, Kim JH. Size, surface charge, and shape determine therapeutic effects of nanoparticles on brain and retinal diseases. *Nanomedicine Nanotechnology Biol Med* (2015) 11:1603–11. doi: 10.1016/j.nano.2015.04.015

111. Liu Y, Hardie J, Zhang X, Rotello VM. Effects of engineered nanoparticles on the innate immune system. *Semin Immunol* (2017) 34:25–32. doi: 10.1016/j.smim.2017.09.011

112. Rahmati M, Amanpour S, Mohammadpour H. The role of nanoparticles in cancer therapy through apoptosis induction. In: *Nanoparticle Drug Deliv. Syst. Cancer Treat*. London: Jenny Stanford Publishing, CorporateTaylor & Francis Group (2020). p. 45–74.

113. Choi HS, Liu W, Misra P, Tanaka E, Zimmer JP, Itty Ipe B, et al. Renal clearance of quantum dots. *Nat Biotechnol* (2007) 25:1165–70. doi: 10.1038/nbt1340

114. Su Y-L, Fang J-H, Liao C-Y, Lin C-T, Li Y-T, Hu S-H. Targeted mesoporous iron oxide nanoparticles-encapsulated perfluorohexane and a hydrophobic drug for deep tumor penetration and therapy. *Theranostics* (2015) 5:1233–48. doi: 10.7150/thno.12843

115. Kiio TM, Park S. Physical properties of nanoparticles do matter. *J Pharm Investig* (2021) 51:35–51. doi: 10.1007/s40005-020-00504-w

116. Meng R, Li K, Chen Z, Shi C. Multilayer coating of tetrandrine-loaded PLGA nanoparticles: effect of surface charges on cellular uptake rate and drug release profile. *J Huazhong Univ Sci Technolog Med Sci* (2016) 36:14–20. doi: 10.1007/s11596-016-1535-5

117. Anselmo AC, Zhang M, Kumar S, Vogus DR, Menegatti S, Helgeson ME, et al. Elasticity of nanoparticles influences their blood circulation, phagocytosis, endocytosis, and targeting. *ACS Nano* (2015) 9:3169–77. doi: 10.1021/acsnano.5b00147

118. Hartmann R, Weidenbach M, Neubauer M, Fery A, Parak WJ. Stiffness-dependent *in vitro* uptake and lysosomal acidification of colloidal particles. *Angew Chem Int Ed Engl* (2015) 54:1365–8. doi: 10.1002/anie.201409693

119. Guo P, Liu D, Subramanyam K, Wang B, Yang J, Huang J, et al. Nanoparticle elasticity directs tumor uptake. *Nat Commun* (2018) 9:130. doi: 10.1038/s41467-017-02588-9

120. Rahmati M, Ebrahim S, Hashemi S, Motamedi M, Moosavi MA. New insights on the role of autophagy in the pathogenesis and treatment of melanoma. *Mol Biol Rep* (2020) 47:9021–32. doi: 10.1007/s11033-020-05886-6

121. Mohammadinejad R, Moosavi MA, Tavakol S, Vardar DÖ, Hosseini A, Rahmati M, et al. Klionsky DJ %J a (2019) necrotic, apoptotic and autophagic cell fates triggered by nanoparticles. *Autophagy* 15(1):4–33. doi: 10.1080/15548627.2018.1509171

122. Azimee S, Rahmati M, Fahimi H, Moosavi MA. TiO2 nanoparticles enhance the chemotherapeutic effects of 5-fluorouracil in human AGS gastric cancer cells *via* autophagy blockade. *Life Sci* (2020) 248:117466. doi: 10.1016/j.lfs.2020.117466

123. Buttacavoli M, Albanese NN, Di Cara G, Alduina R, Faleri C, Gallo M, et al. Anticancer activity of biogenerated silver nanoparticles: an integrated proteomic investigation. *Oncotarget* (2018) 9:9685–705. doi: 10.18632/oncotarget.23859

124. Swanner J, Fahrenholtz CD, Tenvooren I, Bernish BW, Sears JJ, Hooker A, et al. Silver nanoparticles selectively treat triple-negative breast cancer cells without affecting non-malignant breast epithelial cells *in vitro* and *in vivo*. *FASEB BioAdvances* (2019) 1:639–60. doi: 10.1096/fba.2019-00021

125. Ma X, Wu Y, Jin S, Tian Y, Zhang X, Zhao Y, et al. Gold nanoparticles induce autophagosome accumulation through size-dependent nanoparticle uptake and lysosome impairment. *ACS Nano* (2011) 5:8629–39. doi: 10.1021/nn202155y

126. Selim ME, Hendi AA. Gold nanoparticles induce apoptosis in MCF-7 human breast cancer cells. *Asian Pacific J Cancer Prev* (2012) 13:1617–20. doi: 10.7314/APJCP.2012.13.4.1617

127. Mozdoori N, Safarian S, Sheibani N. Augmentation of the cytotoxic effects of zinc oxide nanoparticles by MTCP conjugation: non-canonical apoptosis and autophagy induction in human adenocarcinoma breast cancer cell lines. *Mater Sci Eng C Mater Biol Appl* (2017) 78:949–59. doi: 10.1016/j.msec.2017.03.300

128. Ren X, Chen Y, Peng H, Fang X, Zhang X, Chen Q, et al. Blocking autophagic flux enhances iron oxide nanoparticle photothermal therapeutic efficiency in cancer treatment. *ACS Appl Mater Interfaces* (2018) 10:27701–11. doi: 10.1021/acsami.8b10167

129. Laha D, Pramanik A, Maity J, Mukherjee A, Pramanik P, Laskar A, et al. Interplay between autophagy and apoptosis mediated by copper oxide nanoparticles in human breast cancer cells MCF7. *Biochim Biophys Acta - Gen Subj* (2014) 1840:1–9. doi: 10.1016/j.bbagen.2013.08.011

130. Duo Y, Li Y, Chen C, Liu B, Wang X, Zeng X, et al. DOX-loaded pH-sensitive mesoporous silica nanoparticles coated with PDA and PEG induce pro-death autophagy in breast cancer. *RSC Adv* (2017) 7:39641–50. doi: 10.1039/C7RA05135B

131. Krętowski R, Jabłońska-Trypuć A, Cechowska-Pasko M. The effect of silica nanoparticles (SiNPs) on cytotoxicity, induction of oxidative stress and apoptosis in breast cancer cell lines. *Int J Mol Sci* (2023) 24:2037. doi: 10.3390/ijms24032037

132. Wang Y, Lin Y-X, Qiao Z-Y, An H-W, Qiao S-L, Wang L, et al. Self-assembled autophagy-inducing polymeric nanoparticles for breast cancer interference in-vivo. *Adv Mater* (2015) 27:2627–34. doi: 10.1002/adma.201405926

133. Sun R, Shen S, Zhang Y-J, Xu C-F, Cao Z-T, Wen L-P, et al. Nanoparticle-facilitated autophagy inhibition promotes the efficacy of chemotherapeutics against breast cancer stem cells. *Biomaterials* (2016) 103:44–55. doi: 10.1016/j.biomaterials.2016.06.038

134. Joshi P, Chakraborti S, Ramirez-Vick JE, Ansari ZA, Shanker V, Chakrabarti P, et al. The anticancer activity of chloroquine-gold nanoparticles against MCF-7 breast cancer cells. *Colloids Surf B Biointerfaces* (2012) 95:195–200. doi: 10.1016/j.colsurfb.2012.02.039

135. Feng Q, Yang X, Hao Y, Wang N, Feng X, Hou L, et al. Cancer cell membrane-biomimetic nanoplatform for enhanced sonodynamic therapy on breast cancer *via* autophagy regulation strategy. *ACS Appl Mater Interfaces* (2019) 11:32729–38. doi: 10.1021/acsami.9b10948

136. Tang S, Yin Q, Su J, Sun H, Meng Q, Chen Y, et al. Inhibition of metastasis and growth of breast cancer by pH-sensitive poly (β-amino ester) nanoparticles co-delivering two siRNA and paclitaxel. *Biomaterials* (2015) 48:1–15. doi: 10.1016/j.biomaterials.2015.01.049

137. Wu X, Wu Y, Wang Z, Liu L, Sun C, Chen Y, et al. A cascade-targeting nanocapsule for enhanced photothermal tumor therapy with aid of autophagy inhibition. *Adv Healthc Mater* (2018) 7:1800121. doi: 10.1002/adhm.201800121

138. Chiu CF, Fu RH, Hsu S, Yu YA, Yang SF, Tsao TC, et al. Delivery capacity and anticancer ability of the berberine-loaded gold nanoparticles to promote the apoptosis effect in breast cancer. *Cancers (Basel)* (2021) 13:5317. doi: 10.3390/cancers13215317

139. He D, Wu B, Du J, Li L, Zhao J. Synergistic inhibition of the growth of MDA −MB−231 cells in triple−negative breast cancer by salinomycin combined with 17 −AAG and its mechanism. *Oncol Lett* (2022) 23:138. doi: 10.3892/ol.2022.13258

140. Markowska A, Kaysiewicz J, Markowska J, Huczyński A. Doxycycline, salinomycin, monensin and ivermectin repositioned as cancer drugs. *Bioorg Med Chem Lett* (2019) 29:1549–54. doi: 10.1016/j.bmcl.2019.04.045

141. Hu Y-J, Zhang J-Y, Luo Q, Xu J-R, Yan Y, Mu L-M, et al. Nanostructured dihydroartemisinin plus epirubicin liposomes enhance treatment efficacy of breast cancer by inducing autophagy and apoptosis. *Nanomaterials* (2018) 8:804. doi: 10.3390/nano8100804

142. Qiu L, Gao M, Xu Y. Enhanced combination therapy effect on paclitaxel-resistant carcinoma by chloroquine co-delivery *via* liposomes. *Int J Nanomedicine* (2015) 10:6615–32. doi: 10.2147/IJN.S91463

143. Zafar S, Akhter S, Ahmad I, Hafeez Z, Alam Rizvi MM, Jain GK, et al. Improved chemotherapeutic efficacy against resistant human breast cancer cells with co-delivery of docetaxel and thymoquinone by chitosan grafted lipid nanocapsules: formulation optimization, *in vitro* and *in vivo* studies. *Colloids Surf B Biointerfaces* (2020) 186:110603. doi: 10.1016/j.colsurfb.2019.110603

144. Jing M, Li Y, Wang M, Zhang H, Wei P, Zhou Y, et al. Photoresponsive PAMAM-assembled nanocarrier loaded with autophagy inhibitor for synergistic cancer therapy. *Small* (2021) 17:e2102295. doi: 10.1002/smll.202102295

145. Wang H, Zheng Y, Sun Q, Zhang Z, Zhao M, Peng C, et al. Ginsenosides emerging as both bifunctional drugs and nanocarriers for enhanced antitumor therapies. *J Nanobiotechnology* (2021) 19:322. doi: 10.1186/s12951-021-01062-5

146. Zajdel A, Wilczok A, Jelonek K, Kaps A, Musiał-Kulik M, Kasperczyk J. Cytotoxic effect of targeted biodegradable epothilone b and rapamycin co-loaded nanocarriers on breast cancer cells. *J BioMed Mater Res A* (2021) 109:1693–700. doi: 10.1002/jbm.a.37164

147. Alkhatib MH, Bawadud RS, Gashlan HM. Incorporation of docetaxel and thymoquinone in borage nanoemulsion potentiates their antineoplastic activity in breast cancer cells. *Sci Rep* (2020) 10:18124. doi: 10.1038/s41598-020-75017-5

148. Zhou X, Suo F, Haslinger K, Quax WJ. Artemisinin-type drugs in tumor cell death: mechanisms, combination treatment with biologics and nanoparticle delivery. *Pharmaceutics* (2022) 14:395. doi: 10.3390/pharmaceutics14020395

149. Stagni V, Kaminari A, Sideratou Z, Sakellis E, Vlahopoulos SA, Tsiourvas D. Targeting breast cancer stem-like cells using chloroquine encapsulated by a triphenylphosphonium-functionalized hyperbranched polymer. *Int J Pharm* (2020) 585:119465. doi: 10.1016/j.ijpharm.2020.119465

150. Wang J, Dang MN, Day ES. Inhibition of wnt signaling by Frizzled7 antibody-coated nanoshells sensitizes triple-negative breast cancer cells to the autophagy regulator chloroquine. *Nano Res* (2020) 13:1693–703. doi: 10.1007/s12274-020-2795-8

151. Nie S, Xing Y, Kim GJ, Simons JW. Nanotechnology applications in cancer. *Annu Rev BioMed Eng* (2007) 9:257–88. doi: 10.1146/annurev.bioeng.9.060906.152025

152. Kalota A, Shetzline SE, Gewirtz AM. Progress in the development of nucleic acid therapeutics for cancer. *Cancer Biol Ther* (2004) 3:4–12. doi: 10.4161/cbt.3.1.517

153. Jain V, Kumar H, Anod HV, Chand P, Gupta NV, Dey S, et al. A review of nanotechnology-based approaches for breast cancer and triple-negative breast cancer. *J Control Release* (2020) 326:628–47. doi: 10.1016/j.jconrel.2020.07.003

154. Gavas S, Quazi S, Karpiński TM. Nanoparticles for cancer therapy: current progress and challenges. *Nanoscale Res Lett* (2021) 16:173. doi: 10.1186/s11671-021-03628-6

155. Awasthi R, Pant I T, Kulkarni G, Satiko Kikuchi I, de Jesus Andreoli Pinto T, Dua K, et al. Opportunities and challenges in nano-structure mediated drug delivery: where do we stand? *Curr Nanomedicine* (2016) 6:78–104. doi: 10.2174/2468187306666160808160330

156. Avitabile E, Bedognetti D, Ciofani G, Bianco A, Delogu LG. How can nanotechnology help the fight against breast cancer? *Nanoscale* (2018) 10:11719–31. doi: 10.1039/C8NR02796J

157. Anselmo AC, Mitragotri S. Nanoparticles in the clinic: an update. *Bioeng Transl Med* (2019) 4(3):e10143. doi: 10.1002/btm2.10143

158. Bobo D, Robinson KJ, Islam J, Thurecht KJ, Corrie SR. Nanoparticle-based medicines: a review of FDA-approved materials and clinical trials to date. *Pharm Res* (2016) 33:2373–87. doi: 10.1007/s11095-016-1958-5

159. Dobrovolskaia MA. Pre-clinical immunotoxicity studies of nanotechnology-formulated drugs: challenges, considerations and strategy. *J Control Release* (2015) 220:571–83. doi: 10.1016/j.jconrel.2015.08.056

160. Huang Y, Fan C-Q, Dong H, Wang S-M, Yang X-C, Yang S-M. Current applications and future prospects of nanomaterials in tumor therapy. *Int J Nanomedicine Volume* (2017) 12:1815–25. doi: 10.2147/IJN.S127349

10.3389/fonc.2023.1150492

Glossary

3-MA	3-methyladenine
AgNPs	silver-based NPs
AMBRA-1	activating molecule in Beclin1-regulated autophagy
AMPK	AMP-activated protein kinase
ATG	autophagy-related genes
AuNPs	gold-based NPs
BCRP	breast cancer resistance protein
BCSCs	breast cancer stem cells
BECN1	Beclin1
CA15-3	cancer antigen 15-3
CEA	carcinoembryonic antigen
CMA	chaperon-mediated autophagy
CQ	chloroquine
DAMPs	damage-associated molecular patterns
DOX	doxorubicin
DRAM	damage-regulated autophagy modulator
DTXL	docetaxel
ER	estrogen receptor
ER-α	estrogen receptor α
ERK	extracellular signal-regulated kinase
FIP200	focal adhesion kinase interacting protein 200 kDa
GABARAPs	gamma aminobutyric acid receptor-associated proteins
GEMMs	genetically engineered mouse models
GSK3	glycogen synthase kinase 3
GTP	guanosine triphosphate
HCC	human hepatocellular carcinoma
HCQ	hydroxychloroquine
HER2	human epidermal growth factor receptor 2
HMGB1	high mobility group protein B1
IP3	inositol-3 triphosphate
JNK	c-Jun N-terminal kinase
Lamp2	lysosomal membrane-associated protein 2
LC3	microtubule-associated protein 1A/1B-light chain 3
MCF-7	Michigan Cancer Foundation-7 cell line
MDA-MB-231	highly aggressive, invasive and poorly differentiated triple-negative breast cancer (TNBC) cell line
MDR	multidrug resistance
MEK	mitogen-activated extracellular signal-regulated kinase
MQ	mefloquine
mTORC1	mechanistic target of rapamycin complex 1
NCs	nanocarriers
NLCs	nanostructured lipid carriers
NEs	nanoemulsions
NP	nanoparticles
PAI-1	plasminogen activator inhibitor
PAMPs	pathogen-associated molecular patterns
PARP	poly adenosine diphosphate-ribose polymerase
PAS	phagophore assembly site
PD-L1	programmed death-ligand 1
PE	phosphatidylethanolamine
PEG	polyethylene glycol
Pgp	P-glycoprotein
PI3K III (PI3KC3)	mammalian type III phosphatidylinositol-3 kinase
PI3P	phosphatidylinositol-3-phosphate
PKD	protein kinase D
PR	progesterone receptor
ROS	reactive oxygen species
SAL	salinomycin
SERCA	sarco-endoplasmic reticulum Ca^{2+}-ATPase
shRNA	short hairpin RNA
SiNPs	silica nanoparticles
SLNs	solid lipid NPs
SNARE	soluble *N*-ethylmaleimide-sensitive factor attachment protein receptor
SQSTM1	sequestosome 1
SWCNTs	single-walled carbon nanotubes
TNBC	triple-negative breast cancer
TQ	thymoquinone
ULK	Unc-51 like autophagy activating kinase (ULK1/2)
VPS	vacuolar protein sorting

frontiers | Frontiers in Pharmacology

TYPE Original Research
PUBLISHED 09 May 2023
DOI 10.3389/fphar.2023.1176232

OPEN ACCESS

EDITED BY
Raffaele Strippoli,
Sapienza University of Rome, Italy

REVIEWED BY
Miguel Pereira-Silva,
University of Coimbra, Portugal
Duoyi Zhao,
Fourth Affiliated Hospital of China Medical University, China

*CORRESPONDENCE
Shangyong Li,
lisy@qdu.edu.cn
Cheng Zhao,
zhaochengdr@163.com

RECEIVED 28 February 2023
ACCEPTED 25 April 2023
PUBLISHED 09 May 2023

CITATION
Zhang H, Xue Q, Zhou Z, He N, Li S and Zhao C (2023), Co-delivery of doxorubicin and hydroxychloroquine via chitosan/alginate nanoparticles for blocking autophagy and enhancing chemotherapy in breast cancer therapy. *Front. Pharmacol.* 14:1176232. doi: 10.3389/fphar.2023.1176232

Co-delivery of doxorubicin and hydroxychloroquine via chitosan/alginate nanoparticles for blocking autophagy and enhancing chemotherapy in breast cancer therapy

Hui Zhang[1], Qingwen Xue[1], Zihan Zhou[2], Ningning He[2,3], Shangyong Li[2]* and Cheng Zhao[1]*

[1]Department of Abdominal Ultrasound, The Affiliated Hospital of Qingdao University, Qingdao, Shandong, China, [2]School of Basic Medicine, Qingdao Medical College, Qingdao University, Qingdao, China, [3]Sino Genomics Technology Co., Ltd, Qingdao, China

Breast cancer (BC) is the most common malignancy in women worldwide, and the standard treatment is chemotherapy or radiotherapy after surgery. In order to reduce the side effects of chemotherapy, various nanoparticles (NPs) have been discovered and synthesized, which has become a promising treatment for BC. In this study, a co-delivery nanodelivery drug system (Co-NDDS) was designed and synthesized with 2,3-dimercaptosuccinic acid (DMSA) coated Fe_3O_4 NPs as core encapsulated into chitosan/alginate nanoparticles (CANPs) shell, doxorubicin (DOX) and hydroxychloroquine (HCQ) as loading drugs. Smaller NPs carrying DOX (FeAC-DOX NPs) were loaded into larger NPs containing HCQ (FeAC-DOX@PC-HCQ NPs) by ionic gelation and emulsifying solvent volatilization methods. The physicochemical properties of this Co-NDDS were characterised, followed by *in vitro* studies of the anticancer effects and mechanisms using two different BC cell lines, MCF-7 cells and MDA-MB-231 cells. The results indicated that the Co-NDDS showcases exemplary physicochemical qualities and encapsulation capacity, facilitating accurate intracellular release through pH-sensitive attributes. Importantly, NPs can significantly increase the *in vitro* cytotoxicity of co-administered drugs and effectively inhibit the autophagy level of tumour cells. The Co-NDDS constructed in this study provides a promising strategy for the treatment of BC.

KEYWORDS

co-delivery, combination chemotherapy, nanoparticles, breast cancer, autophagy

1 Introduction

Breast cancer (BC) is one of the most common malignancies in the world, and its increasing morbidity and mortality rates threaten the health and even the lives of millions of patients every year (Global Burden of Disease Cancer et al., 2018; Sun et al., 2018). At present, the treatment of BC is a multimodal strategy combining surgery, chemotherapy, radiotherapy and hormone therapy. The main clinical treatment is post-operative chemotherapy, where patients are given effective chemical anti-tumour cytotoxic drugs

to combat the tumour. Chemotherapy prevents the unrestricted growth of tumour cells and inhibits the metastatic spread of tumours to a certain extent (Yang et al., 2021; O'Grady and Morgan, 2021). Despite its efficiency, single chemotherapy is associated with a range of serious side effects, such as a compromised immune system, liver and kidney issues, a reduction in white blood cells, and even the possibility of tumour cells becoming resistant to chemotherapy drugs, making it a challenging treatment choice. In order to reduce the toxic side effects of the drugs on the whole body, enhance the sensitivity of tumour cells to the drugs and thus effectively avoid drug resistance, some combination chemotherapy regimens have emerged (Li et al., 2017a; Hu et al., 2018).

Recent studies (Aiello et al., 2021) have demonstrated a growing interest in the loading of anti-cancer drugs into nanodelivery drug systems (NDDSs) as a means of treatment. NDDS have made notable advances when used in combination with anti-cancer drugs, resulting in enhanced therapeutic efficacy and fewer toxic side effects (Farooq et al., 2019; Huang et al., 2019). As early as 1995, researchers announced the first liposome-based nanomedicine, Doxil®, for the treatment of tumours (Irvine and Dane, 2020). Based on the above background, co-delivery NDDS (Co-NDDS) were gradually developed, where at least two anticancer drugs with different physicochemical and pharmacological properties are loaded into a co-delivery system for clinical combination chemotherapy (Qi et al., 2017). Wang *et al.* loaded the anticancer drugs doxorubicin (DOX) and paclitaxel (PTX) onto co-delivered polyethylene glycol poly (lactic-co-glycolic acid) (PEG-PLGA) nanoparticles (NPs) which were co-delivered to increase the effectiveness of free DOX and PTX combination chemotherapy for non-small cell lung cancer (Wang et al., 2011). A similar synergistic effect was obtained by Xiao *et al.* in the evaluation of biodegradable polymers co-releasing DOX and oxaliplatin to enhance anticancer therapy (Xiao et al., 2012).

As a common chemotherapeutic agent for BC, DOX is an antibiotic with broad-spectrum anti-tumour activity (Molinaro et al., 2020). Its main mechanism of action is to block the synthesis of nucleic acids embedded in DNA, thereby inducing DNA damage and apoptosis in cancer cells, and has a strong cytotoxic effect (Bao et al., 2012; Tun et al., 2019). In recent years, due to the fact that DOX alone can lead to an increased autophagy level of tumour cells and their resistance to chemotherapeutic drugs, there has been a growing number of studies focusing on the combination of chemotherapeutic drugs and chemosensitizers. Chemosensitizers are compounds that are not cytotoxic to cancer cells, but when combined with chemotherapy drugs it can enhance their effects (Karagounis et al., 2016). Autophagy inhibitors are one of the common chemosensitizers (Wang et al., 2021; Wong, 2021). When exposed to chemotherapeutic drugs, tumour cells tend to increase the level of intracellular autophagy, allowing them to evade the chemotherapeutic stimulus and develop resistance to the drugs (Li et al., 2017b; Smith and Macleod, 2019). Thus, co-delivery of chemotherapeutic agents with autophagy inhibitors may be a beneficial strategy for treating BC. Recent research has shown that the antimalarial drug hydroxychloroquine (HCQ) has an inhibitory effect on cellular autophagy and is a lysosomal inhibitor (Vyas et al., 2022). Its mechanism of action is to affect the degradation of autophagosomes in the later stages of autophagy by inhibiting the fusion of autophagosomes with lysosomes, resulting in the accumulation of autophagosomes, and therefore has potential application in synergy with chemotherapeutic drugs (Piao et al., 2017; Onorati et al., 2018; Amaravadi et al., 2019). In summary, if DOX and HCQ are simultaneously encapsulated in a NDDS, it can not only successfully reduce the high autophagy level of tumour cells caused by chemotherapeutic drugs and enhance the sensitivity of tumour cells to the drugs, but also simultaneously avoid the adverse effects of both drugs on normal tissues.

For NDDSs, the biocompatibility of the delivery system, various physicochemical properties and the ability to release precisely within the cell depend on the choice of biomaterial. According to the survey, chitosan (CS) is a biocompatible and biodegradable polymer with mucosal adhesion and high solubility under acidic conditions (Muxika et al., 2017; Ryu et al., 2020). Alginate (ALG) is a natural polysaccharide consisting of D - mannuronic acid and L - guluronic acid with excellent properties of biodegradability and low toxicity (Natrajan et al., 2015; Rastogi and Kandasubramanian, 2019). The electrostatic binding between CS and ALG increases in an acidic environment, thus allowing the nanomaterial composed of both to protect the drug from excessive release in an acidic environment (Zhang et al., 2018). Poly (D, L-lactide-co-glycolide) (PLGA) is a widely used functional polymeric organic compound, also with remarkable biocompatibility, which is widely used in the preparation of nanodelivery vehicles (Dong and Feng, 2005).

In this study, we designed and prepared Co-NDDSs (FeAC-DOX@PC-HCQ NPs) that encapsulated two drugs simultaneously, where the chemotherapeutic drug DOX was encapsulated in the smaller nanoparticle FeAC-DOX NPs, and then the autophagy inhibitor HCQ was co-encapsulated with FeAC-DOX NPs in the larger NPs. In addition, we characterised their physical and chemical properties (e.g., particle size, zeta potential, transmission electron microscopy, Fourier transform infrared spectroscopy and encapsulation efficiency) and further investigated their anti-cancer ability *in vitro* and their effect in inhibiting autophagy.

2 Materials and methods

2.1 Materials

All reagents and solvents were obtained from commercial suppliers and were used without further purification. Doxorubicin and 2,3-dimercaptosuccinic acid (DMSA) coated Fe_3O_4 NPs were acquired from Solarbio (Beijing, China). Hydroxychloroquine sulfate was obtained from TCI (Tokyo, Japan). PLGA (lactide: glycolide = 50:50, ester terminated, Mw = 38,000–54,000) and Polyvinylal-cohol (PVA, 86.5%–89% hydrolyzed, viscosity 4.6–5.4 mPa·s were purchased from Aladdin (Shanghai, China). Chitosan (molecular weight, 50,000–190,000; viscosity, 20–30cP; and deacetylation 75%) and sodium alginate (low viscosity, 80,000–120,000; molecular weight, viscosity 2000cP) were obtained from Sigma-Aldrich (St. Louis, MO, UnitedStates).

All other materials are analytical grade. Distilled water is used throughout the process.

2.2 Synthesis of FITC labeled CS

The synthesis of chitosan labelled by FITC is based on the reaction between the isothiocyanate group of FITC and the primary amino group of chitosan (Moussa et al., 2013). CS was dissolved in 0.1 M acetic acid solution to give 20 mL of 1% (w/v) chitosan solution. 20 mL of FITC solution (20 mg dissolved in 20 mL of dehydrated methanol) was added to the above solution. The reaction was stirred in the dark for 4 h. The pH was adjusted to 10 with 0.5 M sodium hydroxide solution to precipitate the labelled product (FITC-CS). Centrifuge and wash with distilled water until the supernatant is free of fluorescence. The labelled product was redissolved in 20 mL of 0.1 M acetic acid solution and dialyzed in 4 L of distilled water in the dark for 3 days, with daily water changes.

2.3 Preparation of NPs

2.3.1 Preparation of drug-loaded NPs

Based on the existing literature, DOX was wrapped around the DMSA coated Fe_3O_4@DMSA NPs (Oh et al., 2017). Briefly, about 0.1mLFe_3O_4@DMSA (~4mg/mLFe_3O_4) were incubated with 0.5mL of DOX solution (500mg DOX) at 4°C for 12 h to obtain DOX coupled Fe_3O_4@DMSA-DOX NPs, which were washed several times with water to remove the unattached free DOX molecules. Then, add 3 mL of ALG solution under gentle stirring, ultrasonic for 10 min, centrifuge at 11,000 g for 20 min and washed off the residual ALG with water. Finally, a total of 3 mL of CS solution (1% w/v acetic acid dissolved in water) was dropped at a rate of 2 drops/s, stirred for 1 h and washed off the residual CS with water. Specifically, centrifuge three times and discard the waste liquid and re-add single distilled water after each centrifugation. The above NPs were collected and freeze-dried for later use, resulting in the smaller NPs in this study, which were named FeAC-DOX NPs.

Larger NPs were prepared by the water-in-oil-in-water (W/O/W) double-emulsion solvent diffusion-volatilization method (Jin et al., 2021). FeAC-DOX NP and 4 mg of HCQ were mixed and added to 10 mL of 2% (w/v) PVA solution as the water phase, and the water phase was added dropwise to PLGA solution (80 mg/3 mL acetone) and sonicated for 1 min to form an O/W emulsion. The emulsion was poured into 100 mL of distilled water and stirred for 3 h to evaporate the organic solvent to form PLGA NPs. A total of 20mL of CS solution (1% w/v acetic acid dissolved in water) was added dropwise at a rate of 2 drops/s, stirred for 1 h and the residual CS was washed away with water. The above NPs were collected and freeze-dried for further study, resulting in the larger NPs in this study, which were named FeAC-DOX@PC-HCQ NPs.

2.3.2 Preparation of tracing NPs

FITC-labelled NPs (FeAC-DOX@PC-FITC-HCQ) were prepared on the basis of the NPs prepared above. The FITC-loaded CS were used as the outer chitosan layer and were prepared in the same way as described above.

2.4 Physical and chemical characterization

FeAC-DOX@PC-HCQ was observed using a transmission electron microscope (TEM, H7650; Hitachi, Tokyo, Japan) at an accelerating voltage of 100 kV. The deionised water-diluted sample suspension was placed on a copper grid coated with carbon film. After drying, the samples were observed by TEM. The size distribution of NPs and zeta potential were determined by dynamic light scattering (DLS) and electrophoretic light scattering (ELS) using Zetasizer Nano ZS (Malvern Instruments, UK). All samples were resuspended in deionised water and three measurements were required, with results expressed as mean ± standard deviation (SD). The raw material, empty NPs and drug-loaded NPs were measured by Fourier transform infrared spectroscopy (FT-IR, Alpha type, Bruker, Billerica, MA, UnitedStates) in the transmittance range of 4,000-400 cm^{-1} and the chemical structure of each sample was analysed.

2.5 Pharmaceutical characterization

2.5.1 Encapsulation efficiency (EE) and drug loading capacity (LC)

Standard curves were obtained for the concentrations of DOX and HCQ in the aqueous phase using a UV-Vis spectrophotometer (Thermo Fisher Scientific, Wilmington, DE, UnitedStates) at 480 nm and 343 nm. The amount of DOX in FeAC-DOX NPs was determined indirectly by measuring the amount of free drug in the supernatant after three washes of FeAC-DOX NPs. After the supernatant was collected, the absorbance of the solution was measured at 343 nm by UV spectrophotometry and the amount of free drug was calculated from the standard curve.

For HCQ, the amount of free drug in the supernatant of FeAC-DOX@PC-HCQ NPs after 3 washes was determined by the same method, and the amount of HCQ in FeAC-DOX@PC-HCQ NPs was determined indirectly. The EE and LC formulas are as follows:

$$\text{EE\%} = \frac{\text{Total DOX or HCQ weight} - \text{Free DOX or HCQ weight}}{\text{Total DOX or HCQ weight}} \times 100\%$$

$$\text{LC\%} = \frac{\text{Total DOX or HCQ weight} - \text{Free DOX or HCQ weight}}{\text{Total NPs weight}} \times 100\%$$

2.5.2 *In Vitro* drug release

The *in vitro* release characteristics of FeAC-DOX@PC-HCQ NPs and FeAC-DOX NPs were studied by the classical dialysis bag method for *in vitro* release studies. For FeAC-DOX@PC-HCQ NPs, approximately 5 mg of FeAC-DOX@PC-HCQ NPs were suspended in 5 mL of buffer solution at different pH values (5.8 and 7.4) to simulate the cytoplasmic (pH 5.8) and physiological (pH 7.4) environments of cancer cells. The suspension was then transferred to a dialysis bag (molecular weight 7 K, Solarbio, Beijing, China), placed in 200 mL of the same pH PBS and incubated at 37°C at 70 rpm. 2 mL of HCQ release solution was removed at predetermined time intervals and the HCQ

concentration was measured at 343 nm using a UV spectrophotometer while an equal amount of fresh buffer was added.

For FeAC-DOX NPs, NPs were suspended in 5 mL of buffer solution at different pH values (5.0, 5.8 and 7.4) to simulate lysosomes (pH 5.0), the cytoplasmic environment of cancer cells (pH 5.8) and the nucleus (pH 7.4). DOX concentrations were measured at 480 nm by the above method. The cumulative drug release formula is as follows:

$$\text{The cumulative drug release\%} = \frac{\text{HCQ or DOX released amount}}{\text{total amount of HCQ or DOX in NPs}} \times 100\%$$

2.6 *In Vitro* biological effect experiment

2.6.1 Cell culture

MCF-7 and MDA-MB-231 human BC cells were cultured at 37°C in a humid atmosphere containing 5% CO_2 (Thermo Fisher Scientific), and the cells were cultured in DMEM medium. Penicillin (100 U/mL), streptomycin (100 U/mL) and heat-inactivated fetal bovine serum (10%, Atlanta Biologics; Flowery Branch, GA, UnitedStates) were added to the medium.

2.6.2 *In Vitro* cytotoxicity of empty NPs and drug-loaded NPs

In the cytotoxicity assay with material and drug-loaded NPs, cell concentrations were first determined by hemocytometry, cells were inoculated in 96-well plates at a density of 5×10^3 cells per well and incubated at 37°C in a 5% CO_2 atmosphere for 24 h. The original medium was removed and MCF-7 and MDA-MB-231cells were treated with 100 μL of medium containing DOX at concentrations ranging from 0 to 10.0 μg/L (actual DOX content was calculated based on the loading of NP) in different concentrations of empty NP, free DOX, free DOX + HCQ, FeAC-DOX NPs and FeAC-DOX@PC-HCQ NPs, and set blank and control groups. The concentration of HCQ in this co-administration system was a fixed value and 10 μg/mL low cytotoxicity was chosen for the experiment. At the fixation time (24 h), the medium containing the material and drug-loaded NPs was removed and the cells were washed twice with PBS. Then 10 μL of CCK-8 reagent was added and the plates were placed in an incubator for 1.5 h. Finally, absorbance was measured at 450 nm using a microplate reader. A treatment concentration of 50% inhibition (IC 50) was used for further studies. Each set of experiments was repeated three times. The formula for cell viability was as follows:

$$\text{The cell viability} = \frac{\text{OD treat} - \text{OD blank}}{\text{OD control} - \text{OD blank}} \times 100$$

2.6.3 *In Vitro* migration assay

The effect of different drugs on the migration of BC cells was also assessed by a wound healing assay. MCF-7 and MDA-MB-231 cells were pre-inoculated in 6-well plates and cell monolayers were carefully scratched with the tip of a 10 μL sterile pipette when the cells had grown to a 90% concentration. Cell debris was washed with PBS and photographed under a microscope as a control at 0 h. After incubation with different drugs for 48h, photographs were taken for comparison with the 0 h control and the relative migration area of the cells was calculated using ImageJ.

2.6.4 Cellular uptake

Experiments were performed using FITC-labelled NPs (FeAC-DOX@PC-FITC-HCQ NPs) and cellular uptake of NPs was analysed by fluorescence microscopy imaging. Briefly, MCF-7 and MDA-MB-231 cells were inoculated in 24-well plates and incubated in a 5% CO_2 incubator at 37°C for wall attachment. Drug-containing medium was then added and the cells were incubated together for 0 h, 6 h, 12 h and 24 h. The medium was aspirated and excess NPs was removed using PBS. The cells were then fixed with 4% paraformaldehyde for 20 min and DAPI was added for staining for 5 min. The images were viewed with an Olympus fluorescence microscope, and the images were acquired using the RBITC channel, DAPI channel and DOX intrinsic red fluorescence.

2.7 Autophagy analysis

2.7.1 Western blot assay

The expression of autophagy-associated marker protein (LC3) was detected by immunoblotting. MCF-7 and MDA-MB-231 cells from different groups were collected after 24 h incubation with drugs, and approximately 100 mL of lysate was added to each group separately to ensure that all proteins were solubilized. The proteins extracted from each group of cells were collected and they were diluted to the same concentration. Each group of proteins was electrophoresed with equal micrograms of SDS-PAGE and then transferred onto polyvinylidene fluoride membranes (PVDF). After blocking for 60 min, the monoclonal antibodies LC3 (1:1000, Affinity) and β-actin (1:100,000, Abclonal) were incubated overnight at 4°C respectively. After incubation, protein expression is observed after incubation with goat anti-rabbit HRP antibody (1: 8,000, Abclonal) for 60 min at room temperature. The assay was repeated at least three times. Bands were quantified using ImageJ.

2.7.2 Monodansylcadaverine (MDC) staining assay

MDC staining was performed to detect autophagic vesicles in MCF-7 and MDA-MB-231 cells after different drug treatments to reflect the level of autophagy. After 24 h of treatment of cells with different drugs, cells were collected and incubated with MDC (Solarbio, Beijing, China) for 20 min at 37°C in the dark. Cells were centrifuged at 800 *g* for 5 min, washed with 1× WASH buffer and then resuspended. Cell suspensions were dropped onto slides and sealed, and staining results were observed using a fluorescent microscope (Ti2-A, Nikon, Japan).

3 Results

3.1 Preparation of NPs

Firstly, smaller NPs loaded with DOX (FeAC-DOX) were prepared using the ionic gelation method by exploiting the

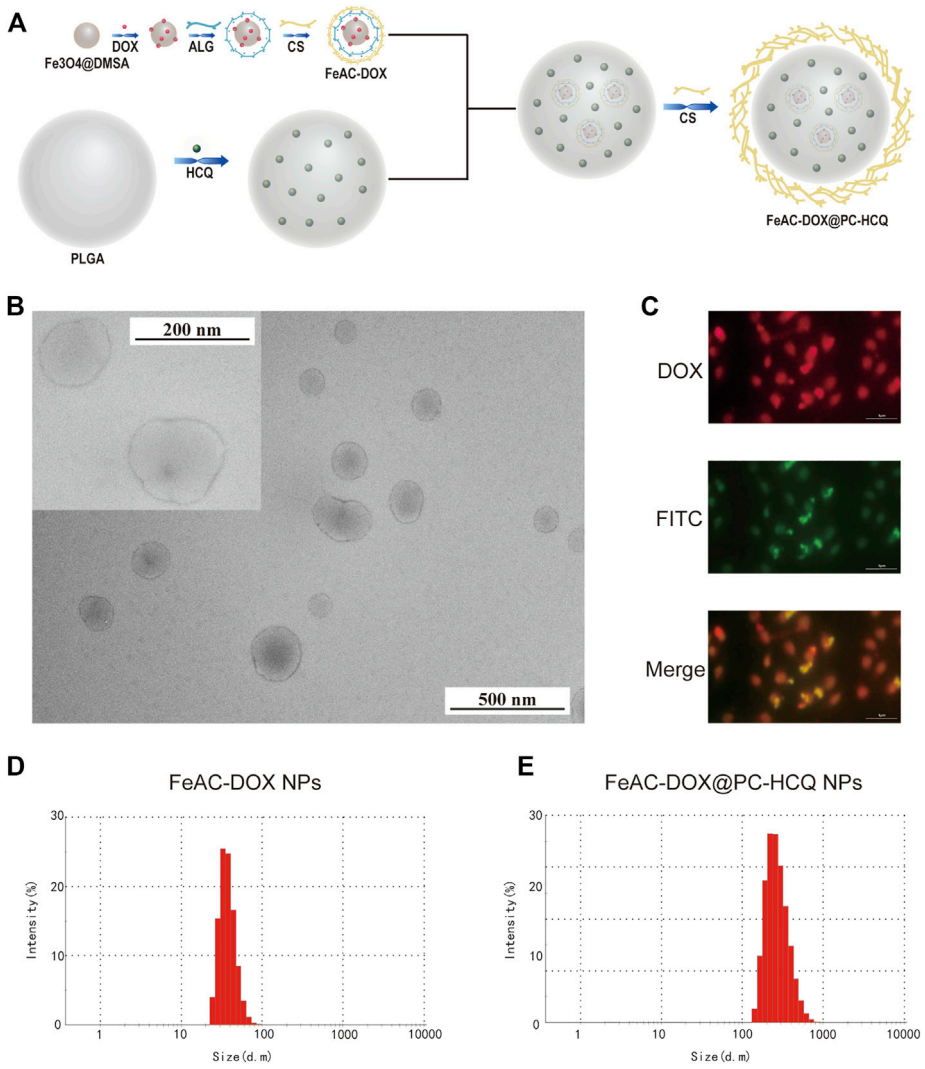

FIGURE 1
Preparation and characterization of co-delivery NPs. **(A)** Preparation scheme of co-delivery NPs. **(B)** TEM images of co-delivery NPs under 200 nm field of view and 500 nm field of view. **(C)** The fluorescence images of FeAC-DOX@PC-FITC-HCQ NPs. The average particle size of FeAC-DOX NPs **(D)** and FeAC-DOX@PC-HCQ NPs **(E)** detected by Zetasizer Nano ZS.

electrostatic interactions between the self-carboxyl groups of Fe_3O_4@DMSO nanomaterials and the amino groups of DOX, and between the negatively charged carboxyl groups in ALG and the positively charged amino groups in CS. Next, FeAC-DOX NPs and HCQ were used as the aqueous phase and PVA was used as the emulsifier to encapsulate them in PLGA using the O/W emulsion technology, and CS was added to the outermost layer to make the NPs more stable as a whole. This procedure resulted in the preparation of larger NPs loaded with both DOX and HCQ (FeAC-DOX@PC-HCQ NPs), as shown in Figure 1A.

3.2 Physical and chemical characterization

Observation of FeAC-DOX@PC-HCQ NPs under transmission electron microscopy shows that FeAC-DOX@PC-HCQ NPs loaded with both FeAC-DOX NPs and HCQ are approximately spherical and have a smooth surface with a diameter of about 200 nm. Figure 1B shows the field of view of FeAC-DOX@PC-HCQ NPs at 200 nm and 500 nm.

The fluorescence tracking technique was used to verify that the smaller NPs FeAC-DOX NPs is co-wrapped with HCQ in the larger NPs FeAC-DOX@PC-HCQ NPs (Figure 1C). Since HCQ does not have fluorescent properties while DOX is self-fluorescent in red, FITC-labelled NPs (FeAC-DOX@PC-FITC-HCQ NPs) were prepared to trap HCQ by using the FI-TC-loaded CS as the outermost layer of the NPs. In the fluorescence images, the outer CS and DOX exhibited green and red fluorescence, respectively. The results show that the yellow fluorescence appears in the centre of the NPs, indicating the superposition of red (DOX) and green (HCQ) fluorescence, which indicates that FeAC-DOX NPs are co-encapsulated with HCQ in FeAC-DOX@PC-HCQ NPs.

The specific size distribution of the above NPs as well as the potential were measured by dynamic light scattering. FeAC-DOX

TABLE 1 Mean diameter and zeta potential of nanoparticles.

Nanoparticles	Size (nm)	PDI	Zate potential (mV)
FeAC-DOX NPs	59.3 ± 7.1	0.337 ± 0.101	+13.6 ± 2.1
FeAC-DOX@PC-HCQ NPs	255.7 ± 18.45	0.224 ± 0.083	+22.3 ± 0.8

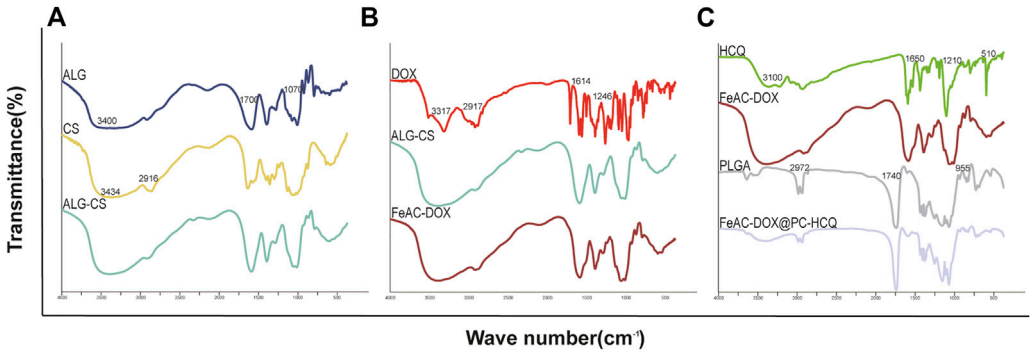

FIGURE 2
The chemical structure of the raw materials, empty NPs, and drug-loaded NPs are analyzed by FT-IR. **(A)** ALG, CS, ALG-CS NPs; **(B)** DOX, ALG-CS NPs, FeAC-DOX NPs; **(C)** HCQ, FeAC-DOX NPs, PLGA, FeAC-DOX@PC-HCQ NPs.

NPs is classified as 59.3 ± 7.1 nm (Figure 1D) and FeAC-DOX@PC-HCQ NPs as 255.7 ± 18.45 nm (Figure 1E) with PDI values of 0.337 ± 0.101 and 0.224 ± 0.083 respectively (Table 1), similar to those observed under transmission electron microscopy, with suitable dimensions and good dispersion. Among the many parameters, the size of the NPs played an important role in the EPR effect, with a cut-off size of approximately 400 nm for penetration into the tumour, with particles less than 200 nm in diameter being the most effective (Sun et al., 2014). The Zeta potential of FeAC-DOX@PC-HCQ NPs was +22.3 ± 0.8 mV and that of FeAC-DOX NPs. The uptake of the negatively charged nanodrugs by tumour cells was increased, and the ability to escape from lysosomes after cell entry was also improved, resulting in enhanced anticancer efficacy (Du et al., 2011).

DOX, HCQ, ALG, CS, PLGA, ALG-CS NPs, FeAC-DOX NPs and FeAC-DOX@PC-HCQ NPs were chemically characterised by FT-IR spectroscopy, and Figure 2 shows the potential interactions between them. The basic characteristic peaks for ALG appear at 3400 cm^{-1} (O-H stretching and N-H stretching, overlapping), 1700 cm^{-1} (C=O stretching), 1070 cm^{-1} (C-O-C stretching) and 955 cm^{-1} (O-H stretching). The IR spectrum of CS shows characteristic peaks at 3434 cm^{-1} (O-H stretching and N-H stretching, overlapping), 1596 cm^{-1} (N-H stretching), 1465 cm^{-1} (C-H stretching) and 1150 cm^{-1} (C-O-C stretching). The infrared spectra of CS-ALG NPs demonstrate a stretching vibration shift of -OH and -NH_2 at 3434 cm^{-1} to 3424 cm^{-1} and a stretching shift of the -COO- group to 1579 cm^{-1}. The results demonstrate that the amino group of CS reacts with the carboxyl group of ALG to form an amide group and these changes are chemically bound.

The basic characteristic peaks of DOX appear at 3317 cm^{-1} (O-H stretching), 2917 cm^{-1} (C-H stretching), 1729 cm^{-1} (C=O stretching), 1614 cm^{-1} (C=C in the benzene ring) and 1246 cm^{-1} (C-O stretching). The disappearance of the characteristic absorption peaks of DOX in FeAC-DOX NPs may indicate that DOX has been successfully encapsulated in FeAC-DOX NPs.

In addition, the HCQ results show characteristic peaks for N-H at 3319 cm^{-1} and 3100 cm^{-1} and three peaks at 1650 cm^{-1}, 1571 cm^{-1} and 1501 cm^{-1} suggesting the presence of an aromatic ring structure. C-H in PLGA has a broadband at 2972 cm^{-1}, C=O has an absorption peak at 1740 cm^{-1}, C-H produces absorption peaks at 1470 cm^{-1} and 1380 cm^{-1} stretching, and O-H produces an absorption peak at 955 cm^{-1} from carboxyl vibrations. After the formation of FeAC-DOX@PC-HCQ NPs, some of the absorption peaks weaken or disappear in intensity and the wave number shifts. For example, the IR spectrum of the final NPs shows a weakening of the broad absorption peak at 2972 cm^{-1} and the appearance of the broad absorption peak at 1650 cm^{-1}. These changes suggest that the formation of FeAC-DOX@PC-HCQ NPs is not a physical combination of the various materials and drugs, but a chemical reaction between them, meaning that both DOX and HCQ drugs are successfully encapsulated in the final NPs.

The drug EE and LE of FeAC-DOX NPs and FeAC-DOX@PC-HCQ NPs were 81.7% and 67.2% and 6.71% and 8.94%, respectively (Table 2). These results suggest that the co-delivery NPs are ideal NDDSs.

3.3 *In Vitro* drug release

The ability of the synthesised larger NPs FeAC-DOX@PC-HCQ NPs to release the drug in buffers of different pH was examined by a classical cumulative drug release method to simulate a neutral blood environment or an acidic tumour cell environment. Figure 3A shows the cumulative release of HCQ

TABLE 2 Encapsulation efficiency (EE) and loading efficiency (LE) of nanoparticles.

Nanoparticles	EE of DOX (%)	LC of DOX (%)	EE of HCQ (%)	LC of HCQ (%)
FeAC-DOX NPs	81.7	6.71	-	-
FeAC-DOX@PC-HCQ NPs	-	-	67.2	8.94

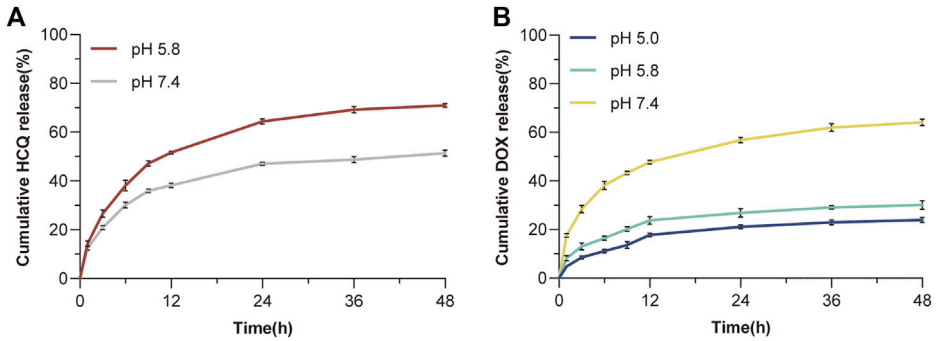

FIGURE 3
In vitro drug release. **(A)** The release curve of HCQ from FeAC-DOX@PC-HCQ NPs in PBS (pH 5.8 and pH 7.4). **(B)** The release curve of DOX from FeAC-DOX NPs in PBS (pH 5.0, pH 5.8, and pH 7.4).

from larger NPs (FeAC-DOX@PC-HCQ NPs) at pH values of cancer cell cytoplasm (pH 5.8) and blood or normal organs (pH 7.4). The cumulative release of FeAC-DOX@PC-HCQ NPs at pH 5.8 was 71.1% at 48 h and the cumulative release of HCQ at pH 7.4 was 51.3% at 48 h, respectively, indicating that the drug release from the NPs in the simulated blood or normal organ environment was less than that in the simulated cancer cell cytoplasm. For the smaller nanoparticle FeAC-DOX NPs, their ability to release DOX was assayed by the same method (Figure 3B), including simulated lysosomal environment (pH 5.0), cancer cell cytoplasmic environment (pH 5.8) and cytosolic environment (pH 7.4). The results showed that the cumulative DOX release from FeAC-DOX NPs at pH 7.4 was 64.1% for 48 h, while at pH 5.8 and pH 5.0, the cumulative DOX release for 48 h was 30.1% and 24.0%, respectively.

The above results indicate that FeAC-DOX@PC-HCQ NPs is pH sensitive and that the encapsulated drug is released sequentially. From the release characteristics of the larger NPs, it can be concluded that the release of HCQ in the simulated blood environment is much smaller than that in the simulated cancer cell cytoplasm. This is due to the fact that the outer chitosan layer keeps the larger NPs relatively stable in a neutral blood environment (Li et al., 2018), whereas in the acidic environment of cancer cell cytoplasm the CS dissolves due to the weakened inter-chain interactions caused by the protonation of amino groups in the CS, resulting in the release of the drug from the NPs (Rizeq et al., 2019). For smaller NPs, FeAC-DOX NPs is more stable and less likely to release drugs in an acidic cytoplasmic environment and lysosomal environment than in a neutral environment at pH 7.4 (which can also as the pH of the nucleus). This is due to the enhanced binding of electrostatic interactions between CS and ALG in the acidic environment (Biswas et al., 2015), which slows drug release.

It is clear that FeAC-DOX@PC-HCQ NPs protect the drug encapsulated in them well during blood transport, while HCQ and smaller NPs are better released when transported into the acidic tumour cell environment, where the released HCQ will act on its pharmacological target to inhibit autophagy and protect FeAC-DOX NPs from being removed by autophagy. After lysosomal escape, the FeAC-DOX NPs protected DOX in an acidic environment (cytoplasm and lysosomes), while entering the nucleus, they release DOX at pH 7.4 and thus have a cytotoxic effect on DNA.

3.4 *In Vitro* biological effect

3.4.1 Cell viability of empty NPs

Biocompatibility is a major factor in the evaluation of drug delivery systems targeting tumours. Different concentrations of blank NPs were applied to MCF-7 and MDA-MB-231 BC cells and cytotoxicity tests were performed using the CCK-8 kit to obtain cell viability. As shown in Figure 4, the concentrations of blank NPs were selected as 0.25, 0.5, 0.75 and 1.0 μg/mL. After 24 h of nanomaterial action, the different concentrations of blank NPs were not significantly toxic to MCF-7 and MDA-MB-231 BC cells, and the cell survival rates were above 95%. In conclusion, the nanomaterials selected for the study have proven to be safe as drug carriers and possess high biocompatibility.

3.4.2 Cytotoxicity of drug-loaded NPs

The results of the drug cytotoxicity assay are shown in Figure 5. The cytotoxic effects of different administration forms of the model

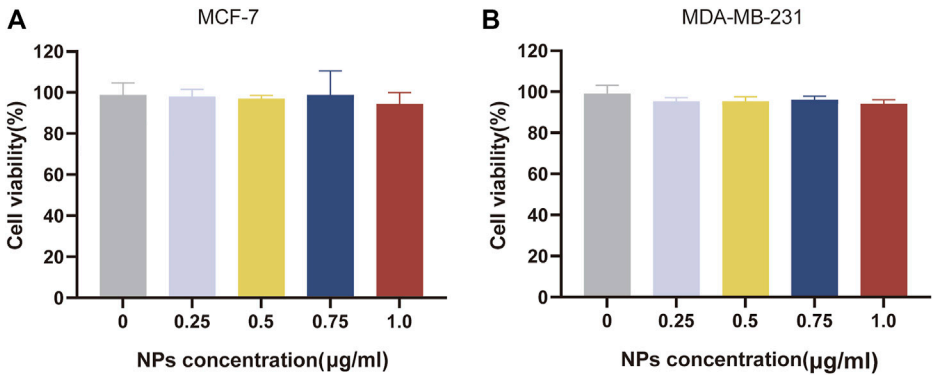

FIGURE 4
Biocompatibility evaluation of nanomaterials. *In vitro* cell viability of empty NPs at various concentrations for 24 h, respectively on MCF-7 cell **(A)** and MDA-MB-231 cell **(B)**.

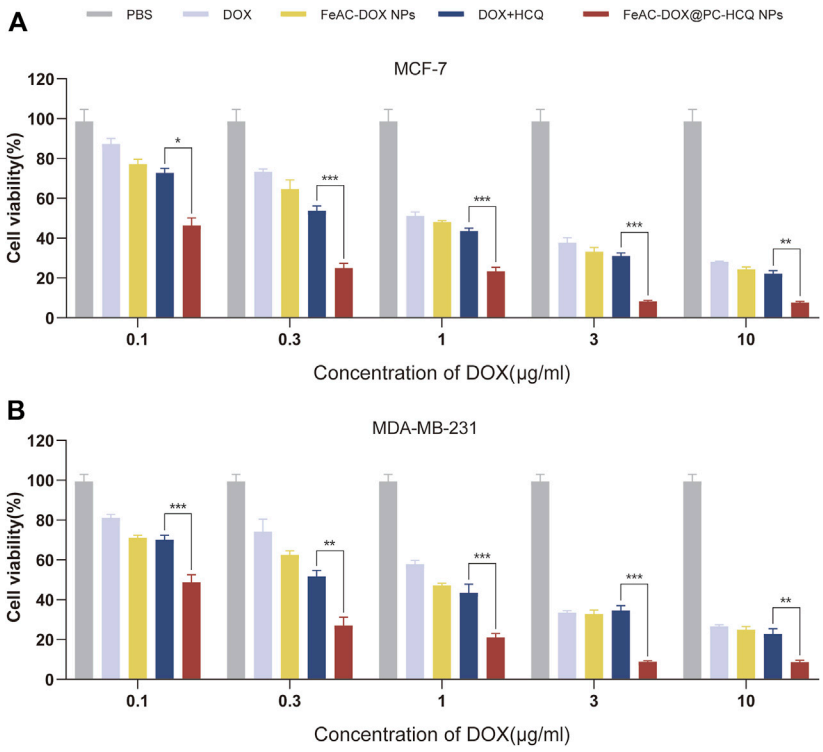

FIGURE 5
Cytotoxicity of drug-loaded NPs. The compare of *in vitro* cytotoxic between free drugs (DOX, DOX and HCQ) and drugs-loaded NPs (FeAC-DOX NPs, FeAC-DOX@PC-HCQ NPs) at various concentrations for 24 h, respectively on MCF-7 cell **(A)** and MDA-MB-231 cell **(B)**. Data represent as mean ± SD (n = 3). *$p < 0.05$, **$p < 0.01$ and ***$p < 0.001$.

drug (free DOX, FeAC-DOX NPs, free DOX + HCQ and FeAC-DOX@PC-HCQ NPs) on MCF-7 and MDA-MB-231 cells were examined at different DOX concentrations. The results showed that NPs containing different concentrations of DOX (FeAC-DOX NPs) had a higher cytotoxic effect on both BC cells than the free DOX group. Nanopreparations containing lower concentrations of DOX (0.1–1.0 μg/mL) had significantly higher cytotoxic effects on BC cells than the free drug ($p < 0.05$), while nanopreparations containing higher concentrations of DOX (10 μg/mL) had comparable cytotoxic effects to the free DOX group. The cytotoxic effects of nanopreparations with almost all concentrations of DOX (0.1–10 μg/mL) were significantly higher than those of the free drug group for both BC cells ($p < 0.05$). Notably, the combination drug group at different concentrations (DOX + HCQ) was more potent in killing both BC cells than the chemotherapeutic drug DOX alone, and this aspect was more pronounced for MCF-7 cells.

TABLE 3 IC50 values of different formulations at 24 h.

Formulation	IC50(μg/mL)	
	MCF-7	MDA-MB-231
DOX	0.62	1.24
FeAC-DOX NPs	0.46	0.95
DOX + HCQ	0.32	0.59
FeAC-DOX@PC-HCQ NPs	0.16	0.13

In addition, the IC50 values of different free drug and drug-loaded NPs were compared for MCF-7 cells and MDA-MB-231 cells. From the experimental results (Table 3), it can be seen that the nanoformulation of DOX (FeAC-DOX NPs) showed lower IC50 values than free DOX in both cell lines. The NDDS increased the killing effect of DOX on MCF-7 and MDA-MB-231 cells by 25.80% and 23.39%, respectively. For the co-administration of DOX and HCQ, the cytotoxic effect of co-loaded nano-x on both BC cells also reached 2 and 4.54 times that of the two free drugs, respectively, and this killing effect was even more pronounced for MDA-MB-231 cells.

3.4.3 Effect of drug-loaded NPs on cell migration

The migration of tumour cells is closely related to tumour metastasis, which is a major factor contributing to high mortality (Ko et al., 2021). Figures 6A, C demonstrate the effects of different model drugs on the migration of MCF-7 cells and MDA-MB-231 cells *in vitro*, respectively. Compared to the control group, each drug treatment group inhibited the migration of BC cells to different degrees ($p < 0.01$ or $p < 0.001$), with the most pronounced inhibition occurring in the co-loaded NPs (FeAC-DOX@PC-HCQ NPs) treated group. In the cell migration assay, control cells gradually migrated towards the nutrient-rich and low survival pressure scratches, which recovered significantly after 48 h incubation. For MCF-7 cells, cell migration rates were 34.1%, 30.6%, 17.1% and 11.7% after 48 h incubation by medium containing the same drug loading of free DOX, DOX nanoformulation (FeAC-DOX NPs), free DOX + HCQ, DOX and HCQ co-loaded nanoformulation (FeAC-DOX@PC-HCQ NPs), respectively. In contrast, for MDA-MB-231 cells, the cell migration rates after the same treatment were 38.6%, 31.4%, 14.5% and 6.9%, respectively (Figures 6B, D). The results indicated that the nanoformulation enabled the drugs to inhibit BC cell migration more significantly than the free drugs, while the combined drug group was more able to inhibit tumour cell migration than the group treated with chemotherapeutic drugs alone.

3.4.4 Cellular uptake of NPs

Whether NPs can be effectively taken up by cells is a major requirement for evaluating their therapeutic efficacy. To investigate the detailed uptake of drugs in cancer cells, free DOX and FeAC-DOX@PC-HCQ NPs were co-incubated with MCF-7 and MDA-MB-231 BC cells for 0 h, 6 h, 12 h and 24 h, respectively (Figure 7).

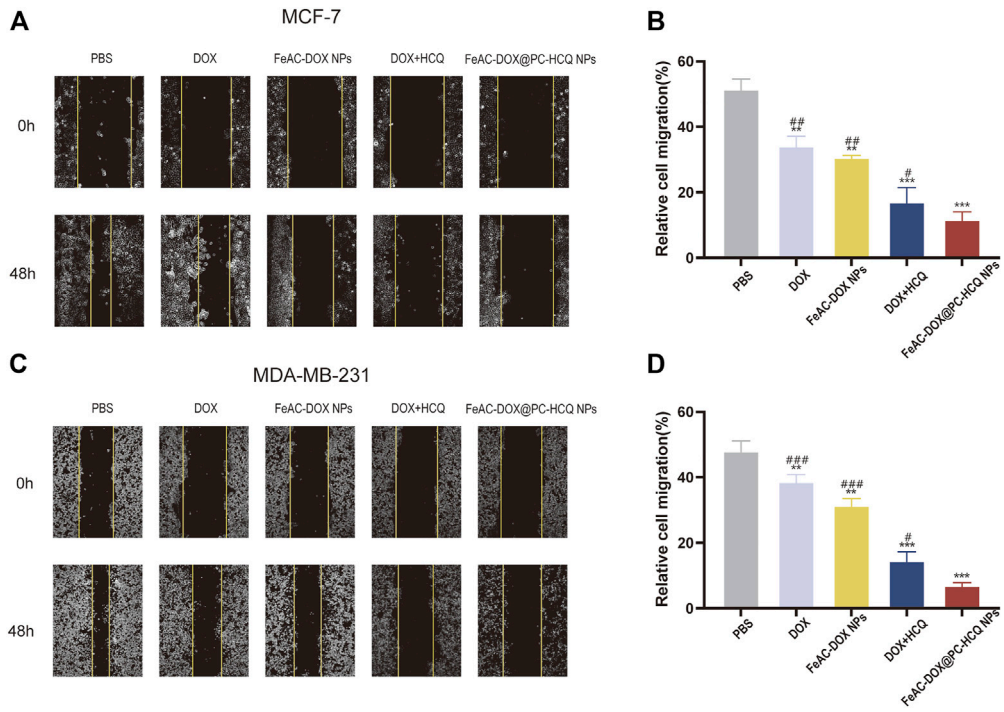

FIGURE 6
Effect of drug-loaded NPs on cell migration. Representative images and relative cell migration treated with PBS, free drugs (DOX, DOX and HCQ) and drugs-loaded NPs (FeAC-DOX NPs, FeAC-DOX@PC-HCQ NPs) for 48 h, respectively on MCF-7 cell **(A, B)** and MDA-MB-231 cell **(C, D)**. Data represent as mean ± SD ($n = 3$). *$p < 0.05$, **$p < 0.01$ and ***$p < 0.001$. *vs.* PBS. #$p < 0.05$, ##$p < 0.01$ and ###$p < 0.001$. *vs* FeAC-DOX@PC-HCQ NPs.

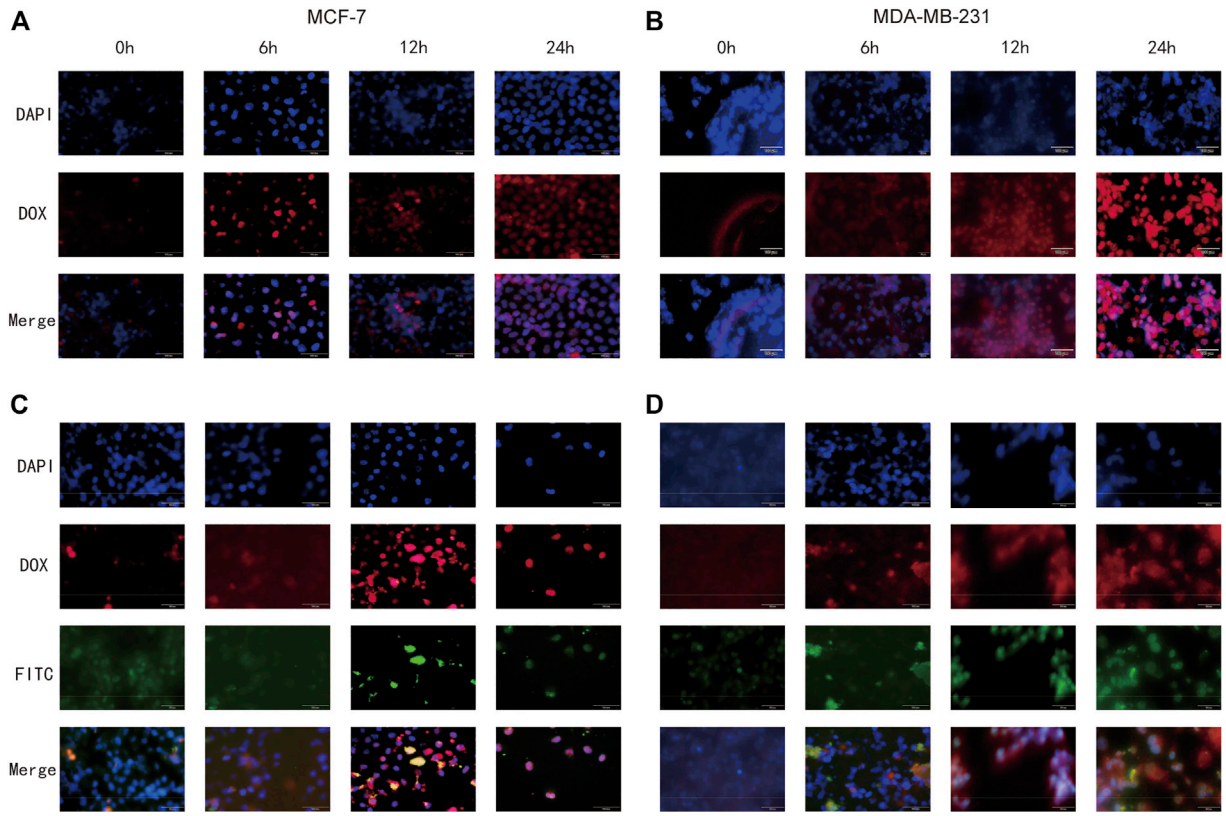

FIGURE 7
Cellular uptake of free DOX and FeAC-DOX@PC-FITC-HCQ NPs by MCF-7 cells and MDA-MB-231 cells, respectively. MCF-7 cells **(A)** and MDA-MB-231 cells **(B)** were treated with free DOX (red) for 0, 6, 12 and 24 h, and the fixed cells were stained with DAPI to observe the nucleus (blue). MCF-7 cells **(C)** and MDA-MB-231 cells **(D)** were treated with FeAC-DOX@PC-FITC-HCQ NPs for 0, 6, 12 and 24 h. Red fluorescence indicates DOX loaded in NPs, green fluorescence indicates FITC loaded in NPs, and blue fluorescence indicates the region of the nucleus stained with DAPI.

Figures 7A, B show the uptake of free DOX by both cell lines, with blue fluorescence representing the DAPI-stained nucleus, red fluorescence representing DOX and purple fluorescence representing the overlapping area between the two. As the results show, when the cells were treated with free DOX for 0 h, no overlap between blue and red fluorescence was seen, indicating that no free DOX was entering the cells at this time. After 6 h of co-incubation, red fluorescence appeared near the nucleus, and as the time was extended to 12 h, the blue fluorescence and red fluorescence came further together and even partially overlapped. At 24 h, the overlapping purple fluorescence continued to increase, indicating that the free drug had effectively entered the nucleus at this time, and this phenomenon was more fully expressed in MCF-7 cells.

The internalization process and intracellular localisation of the FeAC-DOX@PC-HCQ nanoparticle drug in two BC cell lines was then proceeded to be examined using fluorescent tracer techniques (Figures 7C, D). Since HCQ is loaded in larger NPs without fluorescent properties, FeAC-DOX@PC-FITC-HCQ NPs were prepared for fluorescent tracing for this purpose. In this fluorescent tracer system, DOX and FITC exhibit red and green fluorescence, respectively, and blue fluorescence remains representative of the DAPI-stained nuclei. Thus, under fluorescence microscopy, the yellow fluorescence is an overlap of red (DOX) and green (FITC) fluorescence, and the purple fluorescence represents a fusion of blue (DAPI) and red (DOX) fluorescence. From 0 h to 12 h, yellow fluorescence gradually accumulated around the nucleus as the incubation time increased, demonstrating that the co-administered NDDS had been effectively delivered to the pericellular area. For the cellular uptake of DOX, from 0 h to 6 h, the purple fluorescence around the nucleus gradually increased in density as the incubation time increased, demonstrating the presence of DOX in the nucleus, while from 12 h to 24 h, the purple fluorescence was clearly visible in the nucleus and continued to increase in density, indicating that DOX had accumulated in the nucleus of tumour cells and exerted anti-cancer effects. This phenomenon was also evident in both BC cell lines. This demonstrates that the NDDS can deliver the drug to the nucleus more efficiently than the free DOX, thus exerting anti-cancer effects.

3.5 Autophagy analysis

3.5.1 LC3-II and LC3-II/LC3-I protein expression assay

It is well known that autophagy is strongly linked to the conversion of LC3-I proteins to autophagosome-associated LC3-II proteins in the cytoplasm, and that an increase in the LC3-II to

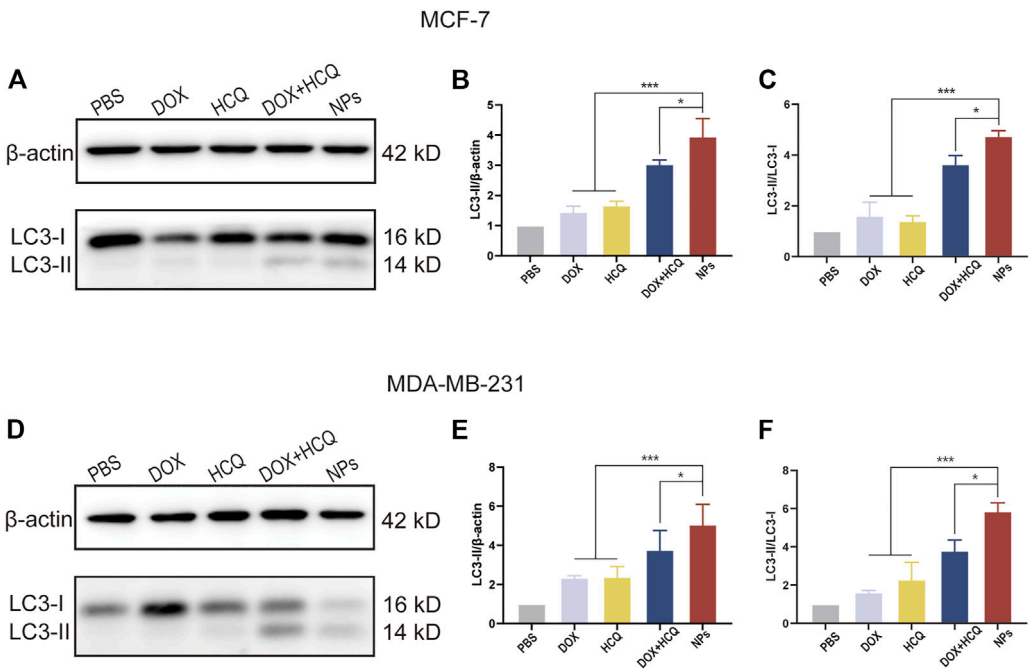

FIGURE 8
WB analysis of cellular autophagy inhibition levels in different treatment groups. The expression level of LC3-I and LC3-II, and the ratio of LC3-II/β-actin and LC3-II/LC3-I treated with PBS, free drugs (DOX, DOX and HCQ) and drugs-loaded NPs (FeAC-DOX NPs, FeAC-DOX@PC-HCQ NPs) for 24 h and their quantitative analysis, respectively on MCF-7 cell **(A–C)** and MDA-MB-231 cell **(D–F)**. Protein levels are normalized to βactin. Data represent as mean ± SD (n = 3). *p < 0.05, **p < 0.01 and ***p < 0.001.

LC3-I ratio indicates inhibition of autophagy (Song et al., 2019). To evaluate autophagy inhibition, western blotting was utilized to detect the level of LC3, an essential molecule of autophagy. Figure 8 shows the protein expression of LC3-I and LC3-II and interpretation of LC3-II/β-actin and LC3-II/LC3-I after 24 h treatment of MCF-7 and MDA-MB-231 cells with different groups of model drugs. For both BC cell lines, western blot results showed that the LC3-II and LC3-II/LC3-Iwas significantly increased in the DOX and HCQ combination administration group compared to free DOX or free HCQ alone (p < 0.001). The chemotherapeutic drug DOX induced autophagy, while HCQ prevented the fusion of endosomes with lysosomes, leading to the accumulation of LC3-II and thus the cessation of autophagy at a later stage. In contrast, the LC3-II and LC3-II/LC3-I was significantly higher in the co-administered nanodrug group (FeAC-DOX@PC-HCQ NPs) than in all other groups (p < 0.05), indicating that the accumulation of LC3-II was the highest in all groups, thus demonstrating that co-administered NPs inhibited autophagy best.

3.5.2 Autophagic vesicles assay

After a series of experiments to demonstrate the effectiveness of the NDDS against BC *in vitro*, to further demonstrate whether the NDDS in this experiment achieved better efficacy due to autophagy inhibition, an MDC kit was used to stain autophagic vesicles. The autophagy inhibition was observed by comparing the amount of autophagic vesicles in the cells after treatment with the model drugs in each group. The results showed that after treatment with free DOX alone, autophagic vesicles continued to increase in two different BC cell lines, indicating that the cells had started to produce autophagosomes at this point, a situation that was a hindrance to better tumour killing. In contrast, the fluorescence intensity increased significantly after DOX combined with HCQ treatment, indicating that autophagy inhibition was occurring at this point and that the destroyed organelles within the cells could not be cleared, thus improving drug efficacy. Furthermore, the intracellular fluorescence intensity after treatment with co-administered nanodrugs (FeAC-DOX@PC-HCQ NPs) was significantly higher (p < 0.05) than in all other groups, as demonstrated in both BC cell lines. Taken together, this further confirms that the nano-loaded system in this experiment can enhance tumour killing through autophagy inhibition Figure 9.

4 Discussion

In the treatment of BC, traditional chemotherapy has been gradually replaced by combination chemotherapy in order to achieve better treatment outcomes (Hu et al., 2010; Tilekar et al., 2020). Trastuzumab in combination with paclitaxel chemotherapy for the treatment of BC was first reported by Slamon et al. (2001). In recent years, Co-NDDSs have been combined with chemotherapy to counter the drawbacks of low bioavailability and poor targeting of chemotherapeutic drugs, thereby enhancing the anti-cancer effects (Xiao et al., 2012). However, they require further research to address

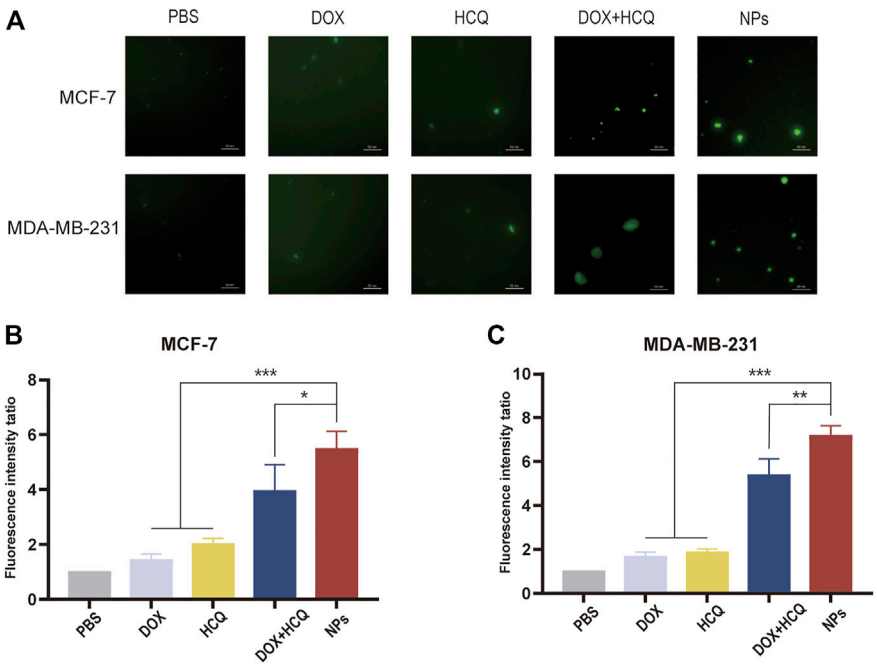

FIGURE 9
Autophagic vacuoles staining by MDC. **(A)** Fluorescence microscopy images of MDC staining of PBS, free drug (DOX, DOX, HCQ) and drug-loaded NPs (FeAC-DOX NPs, FeAC-DOX@PC-HCQ NPs) after 24 h treatment on MCF-7 cells and MDA-MB-231 cells, respectively. Quantification of MDC staining by fluorescent intensity analysis, respectively on MCF-7 cell **(B)** and MDA-MB-231 cell **(C)**. Data represent as mean ± SD (n = 3). *$p < 0.05$, **$p < 0.01$ and ***$p < 0.001$.

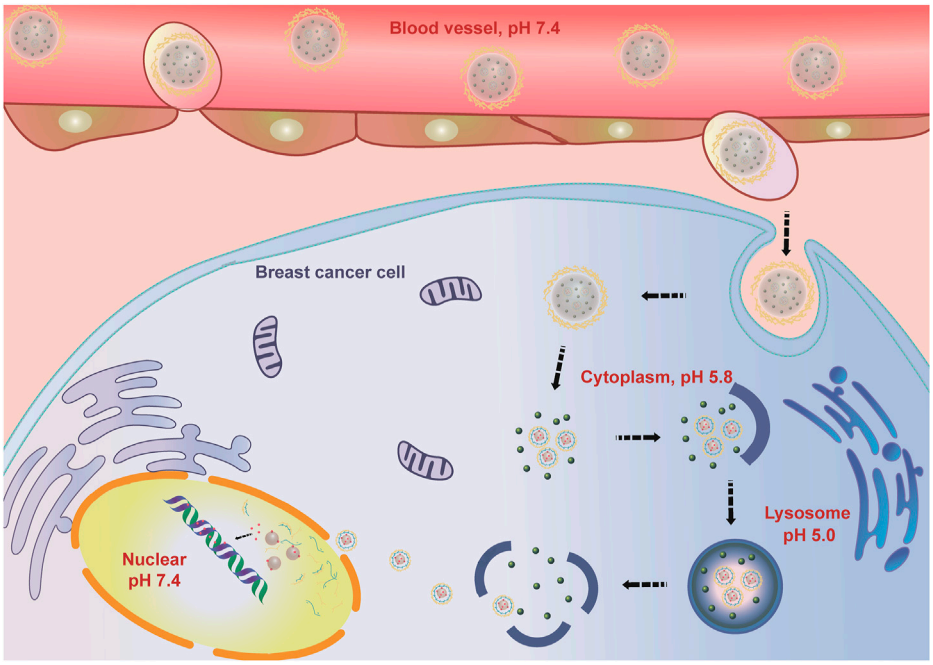

FIGURE 10
Schematic illustration of action of Co-NDDS.

the problem of enhanced autophagy levels in tumour cells by chemotherapeutic drugs and thus reduced drug utilisation.

Based on the above background, we successfully prepared a Co-NDDS loaded with the chemotherapeutic drug DOX and the autophagy inhibitor HCQ. The smaller NPs FeAC-DOX NPs was encapsulated with the chemotherapeutic drug DOX, and then FeAC-DOX NPs and the autophagy inhibitor HCQ were co-encapsulated in the larger NPs FeAC-DOX@PC-HCQ NPs. The Co-NDDS is highly biocompatible and effectively improves the bioavailability of the drug, and the prepared NDDS was verified by various assays to have good physicochemical properties and morphological characteristics to compensate for these drawbacks. Among them, FeAC-DOX@PC-HCQ NPs were observed to be uniformly dispersed with a diameter of approximately 200 nm under transmission electron microscopy (TEM); the particle size of the NPs was measured by DLS to be 255.7 ± 18.45 nm, which is similar to the results obtained under TEM, and NPs with this size distribution have enhanced permeability and retention effect (EPR), resulting in accumulation at cancer sites more (Ngoune et al., 2016). Smaller NPs loaded with the chemotherapeutic drug DOX alone measured a particle size of 59.3 ± 7.1 nm, a size suitable for entry into the nucleus through the nuclear pores of BC cells (Fan et al., 2015). The results of the infrared spectroscopy and fluorescence tracing experiments also provide ample evidence that both drugs were successfully encapsulated in the final NPs.

In addition, the release pattern of FeAC-DOX@PC-HCQ NPs was examined by simulating the neutral blood environment and acidic tumour cell environment pH *in vivo*, which showed that the outermost CS and PLGA nanoshells could protect HCQ from releasing less in the blood environment and more in the acidic tumour environment, which might be related to the fact that CS undergoes high dissolution under acidic conditions (Milosavljevic et al., 2020). We also verified that FeAC-DOX NPs is less likely to release drug in the simulated acidic cytoplasmic environment as well as in the lysosomal environment and more in the neutral environment of the nucleus, which may be due to the enhanced binding between CS and ALG in the acidic environment, thus protecting the chemotherapeutic drug DOX inside (Du et al., 2013). In summary, our NDDS effectively avoids the release of drugs at normal physiological sites, instead concentrating on tumour sites, and further enables the release of chemotherapeutic drugs acting on the nucleus of tumour cells in the nucleus rather than in the cytoplasmic environment.

To investigate the *in vitro* cytotoxicity of the drug delivery system, two different human BC cell lines were selected as model cells, including MCF-7 cells representing an *in-situ* ER-positive BC cell line with low malignancy and MDA-MB-231 cells representing a triple negative BC cell with high malignancy (Nordin et al., 2018). By testing the *in vitro* cytotoxicity of the blank nanomaterials at different concentrations, it was well demonstrated that our selected materials have excellent biocompatibility and can be safely used as drug delivery carriers. These results are closely related to the good biocompatibility and low toxicity of materials such as CS and ALG (Li et al., 2022). On the other hand, NDDSs containing the same concentration of the target drug were able to inhibit the survival of BC cells more effectively than free drugs. The autophagy inhibitor HCQ affects the degradation of autophagosomes in the late stages of autophagy by inhibiting the fusion of autophagosomes with lysosomes, thereby enhancing the killing of tumour cells by chemotherapeutic drugs (Dragowska et al., 2013). Equally importantly, the efficient tumour cell killing effect of our designed co-loaded nanosystems is closely related to the reasonable particle size and pH-responsive drug release, thus coping with the complex tumour cell environment. This is further corroborated by the wound healing assay, which also demonstrates that the NDDS can inhibit tumour cell proliferation.

Finally, we examined the expression of autophagy-related proteins by western blotting assay and MDC fluorescence staining of autophagic vesicles to demonstrate that the NDDS can better inhibit autophagy in tumour cells. HCQ affects the degradation of autophagosomes at the late stage of autophagy by inhibiting the fusion of autophagosomes with lysosomes, thus improving the chemotherapeutic effect of tumours (Zhang et al., 2014).

Due to the time and conditions of the study, we have not yet conducted *in vivo* experiments in a tumour-bearing animal model. We will continue to improve and innovate by using *in vivo* tumour-bearing animal models to further validate the efficiency and safety of the *in vivo* antitumour effect and to reduce the side effects of chemotherapy drugs, such as the cardiotoxicity of DOX (Shafei et al., 2017).

5 Conclusion

In this study, a Co-NDDS, FeAC-DOX@PC-HCQ NPs, which can encapsulate the chemotherapeutic drug DOX and the autophagy inhibitor HCQ into their respective domains, was successfully prepared and characterized based on the idea of anti-cancer sensitization. The NDDS consists of smaller internal NPs carrying the chemotherapeutic drug DOX (FeAC-DOX NPs) and the autophagy inhibitor HCQ, with the smaller NPs being loaded into FeAC-DOX@PC-HCQ NPs are released less in the neutral blood environment and more in the acidic tumour environment. release. The drug HCQ prevented late nuclear endosomes from binding to lysosomes and blocked the cellular autophagy process, thus protecting the chemotherapeutic drug DOX from being degraded and destroyed by autophagy. FeAC-DOX NPs entered the nucleus of BC cells through the nuclear pore, and the smaller NPs could release DOX and target DNA in the nucleus under the alkaline environment (pH 7.4), thus exerting pharmacological effects to kill cancer cells (Figure 10). The results show that the Co-NDDS has excellent physicochemical characteristics, and its pH-sensitive property enables precise drug release in BC cells, thus increasing drug delivery to the cytoplasm and nucleus, effectively inhibiting autophagic degradation of tumour cells, and enhancing the cytotoxic effect of anti-cancer drugs on tumour cells. In conclusion, this Co-NDDS could be a promising platform for the treatment of BC.

Data availability statement

The original contributions presented in the study are included in the article/supplementary material further inquiries can be directed to the corresponding authors.

Author contributions

CZ, SL, and NH conceived and designed the experiments. HZ and ZZ performed the experiments and obtained the data. HZ and QX analyzed the data. HZ, QX, and ZZ wrote the manuscript. SL revised the manuscript. CZ supervised and coordinated the project. All authors read and approved the manuscript.

Funding

This work was supported by Shandong Provincial Natural Science Foundation (ZR2021MH403) and Innovation Capability Improvement Project of Science and Technology for Small and Medium-sized Enterprises in Shandong Province (2021TSGC1295).

Conflict of interest

NH was employed by Sino Genomics Technology Co., Ltd.

The remaining authors declare that the research was conducted in the absence of any commercial or financial relationships that could be construed as a potential conflict of interest.

Publisher's note

All claims expressed in this article are solely those of the authors and do not necessarily represent those of their affiliated organizations, or those of the publisher, the editors and the reviewers. Any product that may be evaluated in this article, or claim that may be made by its manufacturer, is not guaranteed or endorsed by the publisher.

References

Aiello, P., Consalvi, S., Poce, G., Raguzzini, A., Toti, E., Palmery, M., et al. (2021). Dietary flavonoids: Nano delivery and nanoparticles for cancer therapy. *Semin Cancer Biol.* 69, 150–165. doi:10.1016/j.semcancer.2019.08.029

Amaravadi, R. K., Kimmelman, A. C., and Debnath, J. (2019). Targeting autophagy in cancer: Recent advances and future directions. *Cancer Discov.* 9, 1167–1181. doi:10.1158/2159-8290.CD-19-0292

Bao, L., Hazari, S., Mehra, S., Kaushal, D., Moroz, K., and Dash, S. (2012). Increased expression of P-glycoprotein and doxorubicin chemoresistance of metastatic breast cancer is regulated by miR-298. *Am. J. Pathol.* 180, 2490–2503. doi:10.1016/j.ajpath.2012.02.024

Biswas, S., Chattopadhyay, M., Sen, K. K., and Saha, M. K. (2015). Development and characterization of alginate coated low molecular weight chitosan nanoparticles as new carriers for oral vaccine delivery in mice. *Carbohydr. Polym.* 121, 403–410. doi:10.1016/j.carbpol.2014.12.044

Dong, Y., and Feng, S. S. (2005). Poly(d,l-lactide-co-glycolide)/montmorillonite nanoparticles for oral delivery of anticancer drugs. *Biomaterials* 26, 6068–6076. doi:10.1016/j.biomaterials.2005.03.021

Dragowska, W. H., Weppler, S. A., Wang, J. C., Wong, L. Y., Kapanen, A. I., Rawji, J. S., et al. (2013). Induction of autophagy is an early response to gefitinib and a potential therapeutic target in breast cancer. *PLoS One* 8, e76503. doi:10.1371/journal.pone.0076503

Du, C., Zhao, J., Fei, J., Gao, L., Cui, W., Yang, Y., et al. (2013). Alginate-based microcapsules with a molecule recognition linker and photosensitizer for the combined cancer treatment. *Chem. Asian J.* 8, 736–742. doi:10.1002/asia.201201088

Du, J. Z., Du, X. J., Mao, C. Q., and Wang, J. (2011). Tailor-made dual pH-sensitive polymer-doxorubicin nanoparticles for efficient anticancer drug delivery. *J. Am. Chem. Soc.* 133, 17560–17563. doi:10.1021/ja207150n

Fan, W., Shen, B., Bu, W., Zheng, X., He, Q., Cui, Z., et al. (2015). Design of an intelligent sub-50 nm nuclear-targeting nanotheranostic system for imaging guided intranuclear radiosensitization. *Chem. Sci.* 6, 1747–1753. doi:10.1039/c4sc03080j

Farooq, M. A., Aquib, M., Farooq, A., Haleem Khan, D., Joelle Maviah, M. B., Sied Filli, M., et al. (2019). Recent progress in nanotechnology-based novel drug delivery systems in designing of cisplatin for cancer therapy: An overview. *Artif. Cells Nanomed Biotechnol.* 47, 1674–1692. doi:10.1080/21691401.2019.1604535

Global Burden of Disease Cancer, C., Fitzmaurice, C., Akinyemiju, T. F., Al Lami, F. H., Alam, T., Alizadeh-Navaei, R., et al. (2018). Global, regional, and national cancer incidence, mortality, years of life lost, years lived with disability, and disability-adjusted life-years for 29 cancer groups, 1990 to 2016: A systematic analysis for the global burden of Disease study. *JAMA Oncol.* 4, 1553–1568. doi:10.1001/jamaoncol.2018.2706

Hu, C. M., Aryal, S., and Zhang, L. (2010). Nanoparticle-assisted combination therapies for effective cancer treatment. *Ther. Deliv.* 1, 323–334. doi:10.4155/tde.10.13

Hu, X., Zhai, S., Liu, G., Xing, D., Liang, H., and Liu, S. (2018). Concurrent drug unplugging and permeabilization of polyprodrug-gated crosslinked vesicles for cancer combination chemotherapy. *Adv. Mater* 30, e1706307. doi:10.1002/adma.201706307

Huang, P., Wang, X., Liang, X., Yang, J., Zhang, C., Kong, D., et al. (2019). Nano-micro-and macroscale drug delivery systems for cancer immunotherapy. *Acta Biomater.* 85, 1–26. doi:10.1016/j.actbio.2018.12.028

Irvine, D. J., and Dane, E. L. (2020). Enhancing cancer immunotherapy with nanomedicine. *Nat. Rev. Immunol.* 20, 321–334. doi:10.1038/s41577-019-0269-6

Jin, M., Li, S., Wu, Y., Li, D., and Han, Y. (2021). Construction of chitosan/alginate nano-drug delivery system for improving dextran sodium sulfate-induced colitis in mice. *Nanomater. (Basel)* 11, 1884. doi:10.3390/nano11081884

Karagounis, I. V., Kalamida, D., Mitrakas, A., Pouliliou, S., Liousia, M. V., Giatromanolaki, A., et al. (2016). Repression of the autophagic response sensitises lung cancer cells to radiation and chemotherapy. *Br. J. Cancer* 115, 312–321. doi:10.1038/bjc.2016.202

Ko, J., Winslow, M. M., and Sage, J. (2021). Mechanisms of small cell lung cancer metastasis. *EMBO Mol. Med.* 13, e13122. doi:10.15252/emmm.202013122

Li, L., Wang, J., Kong, H., Zeng, Y., and Liu, G. (2018). Functional biomimetic nanoparticles for drug delivery and theranostic applications in cancer treatment. *Sci. Technol. Adv. Mater* 19, 771–790. doi:10.1080/14686996.2018.1528850

Li, S., Zhang, H., Chen, K., Jin, M., Vu, S. H., Jung, S., et al. (2022). Application of chitosan/alginate nanoparticle in oral drug delivery systems: Prospects and challenges. *Drug Deliv.* 29, 1142–1149. doi:10.1080/10717544.2022.2058646

Li, Y., Atkinson, K., and Zhang, T. (2017a). Combination of chemotherapy and cancer stem cell targeting agents: Preclinical and clinical studies. *Cancer Lett.* 396, 103–109. doi:10.1016/j.canlet.2017.03.008

Li, Y., Lei, Y. H., Yao, N., Wang, C. R., Hu, N., Ye, W. C., et al. (2017b). Autophagy and multidrug resistance in cancer. *Chin. J. Cancer* 36, 52. doi:10.1186/s40880-017-0219-2

Milosavljevic, V., Jamroz, E., Gagic, M., Haddad, Y., Michalkova, H., Balkova, R., et al. (2020). Encapsulation of doxorubicin in furcellaran/chitosan nanocapsules by layer-by-layer technique for selectively controlled drug delivery. *Biomacromolecules* 21, 418–434. doi:10.1021/acs.biomac.9b01175

Molinaro, R., Martinez, J. O., Zinger, A., De Vita, A., Storci, G., Arrighetti, N., et al. (2020). Leukocyte-mimicking nanovesicles for effective doxorubicin delivery to treat breast cancer and melanoma. *Biomater. Sci.* 8, 333–341. doi:10.1039/c9bm01766f

Moussa, S. H., Tayel, A. A., and Al-Turki, A. I. (2013). Evaluation of fungal chitosan as a biocontrol and antibacterial agent using fluorescence-labeling. *Int. J. Biol. Macromol.* 54, 204–208. doi:10.1016/j.ijbiomac.2012.12.029

Muxika, A., Etxabide, A., Uranga, J., Guerrero, P., and De La Caba, K. (2017). Chitosan as a bioactive polymer: Processing, properties and applications. *Int. J. Biol. Macromol.* 105, 1358–1368. doi:10.1016/j.ijbiomac.2017.07.087

Natrajan, D., Srinivasan, S., Sundar, K., and Ravindran, A. (2015). Formulation of essential oil-loaded chitosan-alginate nanocapsules. *J. Food Drug Anal.* 23, 560–568. doi:10.1016/j.jfda.2015.01.001

Ngoune, R., Peters, A., Von Elverfeldt, D., Winkler, K., and Putz, G. (2016). Accumulating nanoparticles by EPR: A route of no return. *J. Control Release* 238, 58–70. doi:10.1016/j.jconrel.2016.07.028

Nordin, M. L., Abdul Kadir, A., Zakaria, Z. A., Abdullah, R., and Abdullah, M. N. H. (2018). *In vitro* investigation of cytotoxic and antioxidative activities of Ardisia crispa against breast cancer cell lines, MCF-7 and MDA-MB-231. *BMC Complement. Altern. Med.* 18, 87. doi:10.1186/s12906-018-2153-5

O'grady, S., and Morgan, M. P. (2021). Calcium transport and signalling in breast cancer: Functional and prognostic significance. *Semin. Cancer Biol.* 72, 19–26. doi:10.1016/j.semcancer.2019.12.006

Oh, Y., Je, J. Y., Moorthy, M. S., Seo, H., and Cho, W. H. (2017). pH and NIR-light-responsive magnetic iron oxide nanoparticles for mitochondria-mediated apoptotic cell death induced by chemo-photothermal therapy. *Int. J. Pharm.* 531, 1–13. doi:10.1016/j.ijpharm.2017.07.014

Onorati, A. V., Dyczynski, M., Ojha, R., and Amaravadi, R. K. (2018). Targeting autophagy in cancer. *Cancer* 124, 3307–3318. doi:10.1002/cncr.31335

Piao, S., Ojha, R., Rebecca, V. W., Samanta, A., Ma, X. H., Mcafee, Q., et al. (2017). ALDH1A1 and HLTF modulate the activity of lysosomal autophagy inhibitors in cancer cells. *Autophagy* 13, 2056–2071. doi:10.1080/15548627.2017.1377377

Qi, S. S., Sun, J. H., Yu, H. H., and Yu, S. Q. (2017). Co-delivery nanoparticles of anti-cancer drugs for improving chemotherapy efficacy. *Drug Deliv.* 24, 1909–1926. doi:10.1080/10717544.2017.1410256

Rastogi, P., and Kandasubramanian, B. (2019). Review of alginate-based hydrogel bioprinting for application in tissue engineering. *Biofabrication* 11, 042001. doi:10.1088/1758-5090/ab331e

Rizeq, B. R., Younes, N. N., Rasool, K., and Nasrallah, G. K. (2019). Synthesis, bioapplications, and toxicity evaluation of chitosan-based nanoparticles. *Int. J. Mol. Sci.* 20, 5776. doi:10.3390/ijms20225776

Ryu, J. H., Yoon, H. Y., Sun, I. C., Kwon, I. C., and Kim, K. (2020). Tumor-targeting glycol chitosan nanoparticles for cancer heterogeneity. *Adv. Mater* 32, e2002197. doi:10.1002/adma.202002197

Shafei, A., El-Bakly, W., Sobhy, A., Wagdy, O., Reda, A., Aboelenin, O., et al. (2017). A review on the efficacy and toxicity of different doxorubicin nanoparticles for targeted therapy in metastatic breast cancer. *Biomed. Pharmacother.* 95, 1209–1218. doi:10.1016/j.biopha.2017.09.059

Slamon, D. J., Leyland-Jones, B., Shak, S., Fuchs, H., Paton, V., Bajamonde, A., et al. (2001). Use of chemotherapy plus a monoclonal antibody against HER2 for metastatic breast cancer that overexpresses HER2. *N. Engl. J. Med.* 344, 783–792. doi:10.1056/NEJM200103153441101

Smith, A. G., and Macleod, K. F. (2019). Autophagy, cancer stem cells and drug resistance. *J. Pathol.* 247, 708–718. doi:10.1002/path.5222

Song, P., Li, Y., Dong, Y., Liang, Y., Qu, H., Qi, D., et al. (2019). Estrogen receptor beta inhibits breast cancer cells migration and invasion through CLDN6-mediated autophagy. *J. Exp. Clin. Cancer Res.* 38, 354. doi:10.1186/s13046-019-1359-9

Sun, L., Legood, R., Sadique, Z., Dos-Santos-Silva, I., and Yang, L. (2018). Cost-effectiveness of risk-based breast cancer screening programme, China. *Bull. World Health Organ* 96, 568–577. doi:10.2471/BLT.18.207944

Sun, T., Zhang, Y. S., Pang, B., Hyun, D. C., Yang, M., and Xia, Y. (2014). Engineered nanoparticles for drug delivery in cancer therapy. *Angew. Chem. Int. Ed. Engl.* 53, 12320–12364. doi:10.1002/anie.201403036

Tilekar, K., Upadhyay, N., Iancu, C. V., Pokrovsky, V., Choe, J. Y., and Ramaa, C. S. (2020). Power of two: Combination of therapeutic approaches involving glucose transporter (GLUT) inhibitors to combat cancer. *Biochim. Biophys. Acta Rev. Cancer* 1874, 188457. doi:10.1016/j.bbcan.2020.188457

Tun, J. O., Salvador-Reyes, L. A., Velarde, M. C., Saito, N., Suwanborirux, K., and Concepcion, G. P. (2019). Synergistic cytotoxicity of renieramycin M and doxorubicin in MCF-7 breast cancer cells. *Mar. Drugs* 17, 536. doi:10.3390/md17090536

Vyas, A., Gomez-Casal, R., Cruz-Rangel, S., Villanueva, H., Sikora, A. G., Rajagopalan, P., et al. (2022). Lysosomal inhibition sensitizes TMEM16A-expressing cancer cells to chemotherapy. *Proc. Natl. Acad. Sci. U. S. A.* 119, e2100670119. doi:10.1073/pnas.2100670119

Wang, B., Huang, X., Liang, H., Yang, H., Guo, Z., Ai, M., et al. (2021). PLK1 inhibition sensitizes breast cancer cells to radiation via suppressing autophagy. *Int. J. Radiat. Oncol. Biol. Phys.* 110, 1234–1247. doi:10.1016/j.ijrobp.2021.02.025

Wang, H., Zhao, Y., Wu, Y., Hu, Y. L., Nan, K., Nie, G., et al. (2011). Enhanced anti-tumor efficacy by co-delivery of doxorubicin and paclitaxel with amphiphilic methoxy PEG-PLGA copolymer nanoparticles. *Biomaterials* 32, 8281–8290. doi:10.1016/j.biomaterials.2011.07.032

Wong, K. K. (2021). DNMT1: A key drug target in triple-negative breast cancer. *Semin. Cancer Biol.* 72, 198–213. doi:10.1016/j.semcancer.2020.05.010

Xiao, H., Li, W., Qi, R., Yan, L., Wang, R., Liu, S., et al. (2012). Co-delivery of daunomycin and oxaliplatin by biodegradable polymers for safer and more efficacious combination therapy. *J. Control Release* 163, 304–314. doi:10.1016/j.jconrel.2012.06.004

Yang, Z., Zhang, Q., Yu, L., Zhu, J., Cao, Y., and Gao, X. (2021). The signaling pathways and targets of traditional Chinese medicine and natural medicine in triple-negative breast cancer. *J. Ethnopharmacol.* 264, 113249. doi:10.1016/j.jep.2020.113249

Zhang, M., Xu, C., Liu, D., Han, M. K., Wang, L., and Merlin, D. (2018). Oral delivery of nanoparticles loaded with ginger active compound, 6-shogaol, attenuates ulcerative colitis and promotes wound healing in a murine model of ulcerative colitis. *J. Crohns Colitis* 12, 217–229. doi:10.1093/ecco-jcc/jjx115

Zhang, X., Yang, Y., Liang, X., Zeng, X., Liu, Z., Tao, W., et al. (2014). Enhancing therapeutic effects of docetaxel-loaded dendritic copolymer nanoparticles by co-treatment with autophagy inhibitor on breast cancer. *Theranostics* 4, 1085–1095. doi:10.7150/thno.9933

Frontiers in Oncology

Advances knowledge of carcinogenesis and tumor progression for better treatment and management

The third most-cited oncology journal, which highlights research in carcinogenesis and tumor progression, bridging the gap between basic research and applications to imrpove diagnosis, therapeutics and management strategies.

Discover the latest Research Topics

See more →

Frontiers

Avenue du Tribunal-Fédéral 34
1005 Lausanne, Switzerland
frontiersin.org

Contact us

+41 (0)21 510 17 00
frontiersin.org/about/contact